COMBATING CANCER WITH NATURAL PRODUCTS: WHAT WOULD NON-CODING RNAS BRING?

EDITED BY: Yongye Huang, Yue Hou, Peng Qu and Yong Cai

PUBLISHED IN: Frontiers in Oncology and Frontiers in Pharmacology

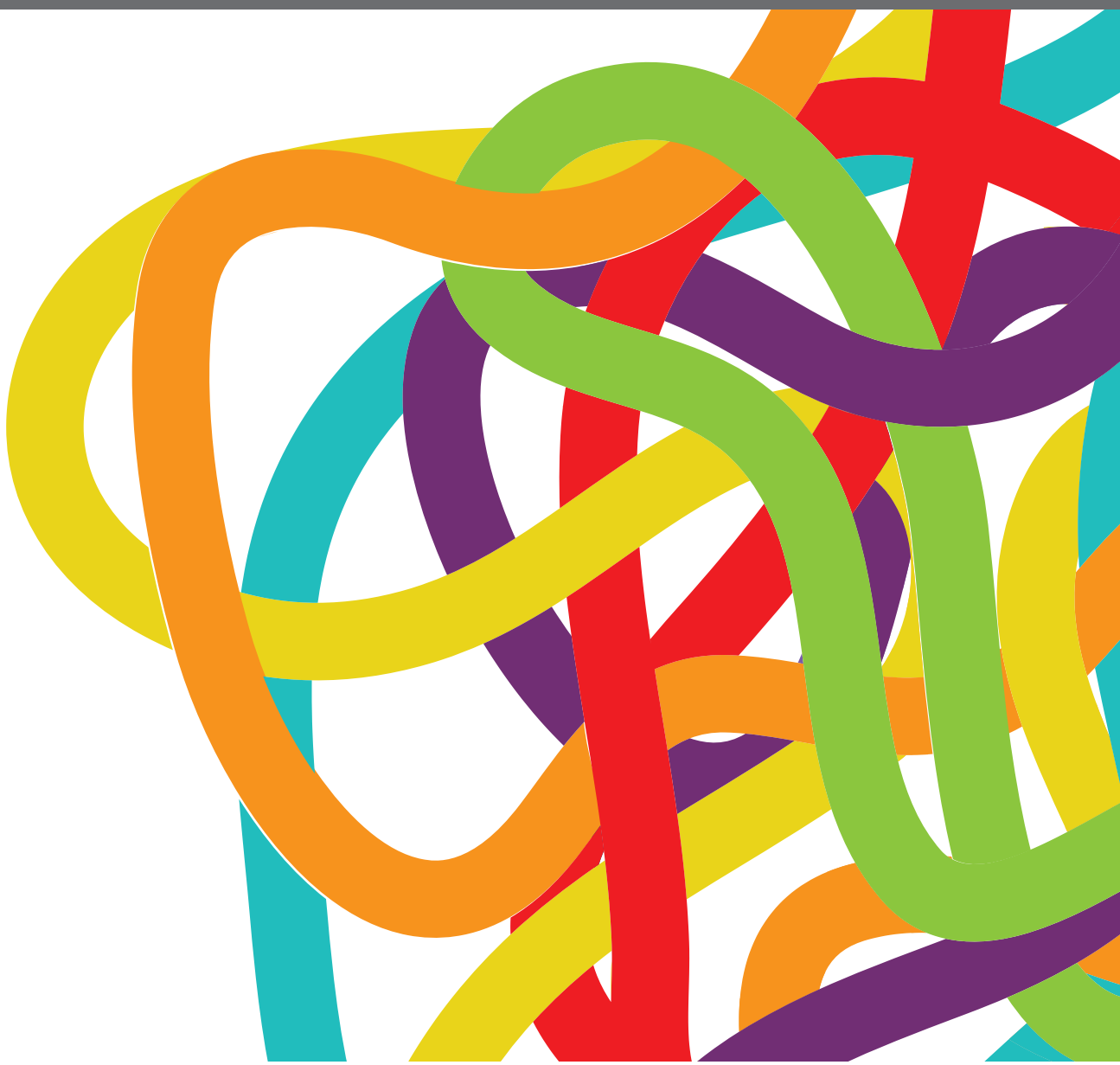

frontiers Research Topics

frontiers

ISSN 1664-8714
ISBN 978-2-88971-596-1
DOI 10.3389/978-2-88971-596-1

About Frontiers

Frontiers is more than just an open-access publisher of scholarly articles: it is a pioneering approach to the world of academia, radically improving the way scholarly research is managed. The grand vision of Frontiers is a world where all people have an equal opportunity to seek, share and generate knowledge. Frontiers provides immediate and permanent online open access to all its publications, but this alone is not enough to realize our grand goals.

Frontiers Journal Series

The Frontiers Journal Series is a multi-tier and interdisciplinary set of open-access, online journals, promising a paradigm shift from the current review, selection and dissemination processes in academic publishing. All Frontiers journals are driven by researchers for researchers; therefore, they constitute a service to the scholarly community. At the same time, the Frontiers Journal Series operates on a revolutionary invention, the tiered publishing system, initially addressing specific communities of scholars, and gradually climbing up to broader public understanding, thus serving the interests of the lay society, too.

Dedication to Quality

Each Frontiers article is a landmark of the highest quality, thanks to genuinely collaborative interactions between authors and review editors, who include some of the world's best academicians. Research must be certified by peers before entering a stream of knowledge that may eventually reach the public - and shape society; therefore, Frontiers only applies the most rigorous and unbiased reviews.
Frontiers revolutionizes research publishing by freely delivering the most outstanding research, evaluated with no bias from both the academic and social point of view. By applying the most advanced information technologies, Frontiers is catapulting scholarly publishing into a new generation.

What are Frontiers Research Topics?

Frontiers Research Topics are very popular trademarks of the Frontiers Journals Series: they are collections of at least ten articles, all centered on a particular subject. With their unique mix of varied contributions from Original Research to Review Articles, Frontiers Research Topics unify the most influential researchers, the latest key findings and historical advances in a hot research area! Find out more on how to host your own Frontiers Research Topic or contribute to one as an author by contacting the Frontiers Editorial Office: frontiersin.org/about/contact

COMBATING CANCER WITH NATURAL PRODUCTS: WHAT WOULD NON-CODING RNAS BRING?

Topic Editors:
Yongye Huang, Northeastern University, China
Yue Hou, Northeastern University, China
Peng Qu, National Institutes of Health (NIH), United States
Yong Cai, Jilin University, China

Citation: Huang, Y., Hou, Y., Qu, P., Cai, Y., eds. (2021). Combating Cancer with Natural Products: What Would Non-Coding RNAs Bring?. Lausanne: Frontiers Media SA. doi: 10.3389/978-2-88971-596-1

Table of Contents

frontiers in Oncology

EDITORIAL
published: 17 September 2021
doi: 10.3389/fonc.2021.747586

Editorial: Combating Cancer With Natural Products: What Would Non-Coding RNAs Bring?

Yongye Huang[1]*, *Yue Hou*[1]*, *Peng Qu*[2]* and *Yong Cai*[3]*

[1] College of Life and Health Sciences, Northeastern University, Shenyang, China, [2] Cancer and Inflammation Program, National Cancer Institute (NCI), Frederick, MD, United States, [3] School of Life Sciences, Jilin University, Changchun, China

Keywords: natural products, cancer, microRNA, lncRNA, circRNA

Editorial on the Research Topic

Combating Cancer With Natural Products: What Would Non-Coding RNAs Bring?

OPEN ACCESS

Edited and reviewed by:
Olivier Feron,
Université catholique de Louvain, Belgium

***Correspondence:**
Yongye Huang
huangyongye88@163.com
Yue Hou
houy20002000@163.com
Peng Qu
peng.qu@nih.gov
Yong Cai
caiyong62@jlu.edu.cn

Specialty section:
This article was submitted to Pharmacology of Anti-Cancer Drugs, a section of the journal Frontiers in Oncology

Received: *26 July 2021*
Accepted: *17 August 2021*
Published: *17 September 2021*

Citation:
Huang Y, Hou Y, Qu P and Cai Y (2021) Editorial: Combating Cancer With Natural Products: What Would Non-Coding RNAs Bring? Front. Oncol. 11:747586. doi: 10.3389/fonc.2021.747586

Natural products are innumerably diverse and exhibit different biological characteristics. Natural products have long been used as medicine for different applications. Chemotherapy is ranked as one of the leading cancer treatments, and a wide range of natural products are currently undergoing clinical evaluation for cancer treatment. However, there is still a large proportion of natural products that are not being used in a clinical setting. We have pointed out that managing factors in genetics, epigenetics, cancer stem cells, and the tumor microenvironment have the potential to broaden the application of natural products in cancer therapy (1, 2). Non-coding RNAs (ncRNAs) are an important component of epigenetics. Therefore, the present Research Topic aims to collect articles that evaluate the anti-tumor effect of natural products in relation to regulating ncRNAs.

The major types of ncRNAs include rRNA, tRNA, snRNA, snoRNA, siRNA, microRNA, lncRNA, and circRNA. The crosstalk among lncRNA, microRNA, and circRNA plays a key regulatory role in the progression of cancer. They can also affect cancer development and progression *via* regulating chromatin remodeling, RNA polymerase II binding to the promoter, mRNA splicing, RNA interference, protein stability and location, and more. In the Research Topic, the natural products chrysin (Chen et al.), cucurbitacin B (Tao et al.), ailanthone (Chen et al.), baicalein (Ma et al.), fucoidan (Ma et al.), casearlucin A (Li et al.), Wan-Nian-Qing prescription, bruceine D (Li et al.), and cinnamaldehyde (Chen et al.) were evaluated for their capacity to regulate ncRNAs to treat cancer (**Figure 1**). Through gathering these papers, many significant findings and implications were found.

NATURAL PRODUCTS REGULATE A CERTAIN TYPE OF ONCOGENES AND TUMOR SUPPRESSOR GENES

For example, p53 is shown to be upregulated by cucurbitacin B treatment to suppress cell proliferation in tongue cancer. It is well known that p53, which is of vital importance in tumor inhibition, modulates cell death and survival processes *via* regulating the expression of many anti and pro-apoptotic genes (3). Besides the p53 signaling pathway, the PI3K-Akt, JAK-STAT, Wnt/β-

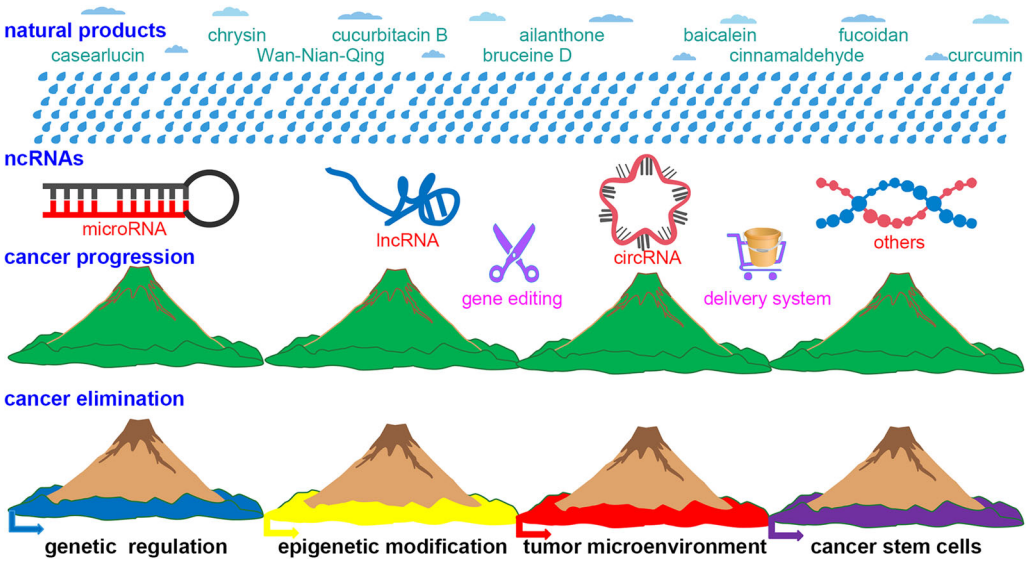

FIGURE 1 | The schematic diagram of this Research Topic. Similar to the phenomenon in which rain with different chemical compositions can alter soil fertility to affect vegetation coverage, natural products with ncRNAs regulation can alter cancer cell survival rates by modulating genetics, epigenetics, the tumor microenvironment, and cancer stem cells. The gene-editing technique (i.e., Crispr/Cas9) and delivery system (i.e., exosomes) can enhance the application of natural products in cancer treatment.

catenin, MAPK, and NF-κB signaling pathways can be regulated by curcumin, another natural product (Wang et al.). In addition, authors screened differentially expressed genes using an RNA-seq technique in cancer cells with chrysin (Chen et al.), ailanthone (Chen et al.), and fucoidan (Ma et al.) treatment to find many more potential target genes to expand the application of natural products.

EPIGENETIC FACTORS ARE CENTRAL FOR DEVELOPING ANTI-TUMOR APPLICATIONS OF NATURAL PRODUCT

Epigenetics includes DNA methylation, chromatin remodeling, histone modification, expression of ncRNAs and RNA modification (4). As mentioned above, ncRNAs are critically important in tumorigenesis and cancer therapy. In addition, the competing endogenous RNAs (ceRNAs) network has been found to modulate gene expression, thus regulating the physical or pathological process. In this Research Topic, studies have revealed that lncRNA or circRNA functions as ceRNA with microRNAs and interacts directly with oncogenes and tumor-suppressor genes. In gastric cancer, chrysin is reported to trigger apoptosis *via* the H19/let-7a/COPB2 axis to suppress tumor growth (Chen et al.). COPB2, responsible for vesicular trafficking between the Golgi apparatus and endoplasmic reticulum, is involved in tumorigenesis in various kinds of cancer (5). In tongue cancer, cucurbitacin B inhibits cell survival *via* modulating the Xist/miR-29b/p53 axis (Tao et al.). In addition, bruceine D inhibits gastric cancer cell proliferation and chemoresistance by regulating the LINC01667/miR-138-5p/cyclin E1 axis (Li et al.). DNA methylation is another important type of epigenetic modification. The DNA methylation profile of the H19 differentially methylated region (DMR) in gastric cancer was also investigated by Chen et al. However, there are to date only a few papers addressing DNA methylation with the treatment of natural products. It would be helpful to employ precision medicine using natural products in cancer therapy by targeting such epigenetic modifications.

NATURAL PRODUCTS COULD BE APPLIED TO REMODEL THE TUMOR MICROENVIRONMENT

The tumor microenvironment is one of the key elements supporting cancer progression and is also a major obstacle to cancer therapy. The tumor microenvironment can modulate drug metabolism and is considered a crucial contributor to the known differential response of patients to chemotherapy (6). Natural products, such as curcumin, resveratrol, epigallocatechin gallate, phloretin, and shikonin, have shown promise in modulating tumor microenvironment (7). In addition, ncRNAs may play a critical role in this process. As revealed by Xia et al., tumor-cell and non-tumor-cell-derived exosomes carrying ncRNAs are able to modulate cancerous derivations of target cells and remodel the tumor microenvironment. As an area of concern for cancer research, the targeting of the tumor

microenvironment in clinical cancer therapy should be performed by applying natural products to determine their usefulness.

CANCER STEM CELLS COULD ALSO BE A POTENTIAL TARGET FOR TREATMENT WITH NATURAL PRODUCTS

Cancer stem cells represent a minority subpopulation of cancer cells that possess self-renewal and differentiation abilities that drive tumorigenesis, cancer progression, and chemoresistance (8). Growing evidence has documented the close relationship between cancer stem cells and the tumor microenvironment, and many researchers have tried to determine the underlying mechanism of cancer stem cell plasticity to prevent cancer development, recurrence, and drug resistance. It is unfortunate that we did not gather papers addressing natural products targeting cancer stem cells in this Research Topic. In our previous investigation, we found that studies on this topic are not widespread (1). Some chemical modifications or techniques should be developed to improve natural products to target cancer stem cells directly and precisely in the future.

Besides obtaining theoretical advancement in this Research Topic, it also provides some useful strategies to enhance the application of natural products in cancer therapy. Exosomes are a kind of small extracellular vesicle secreted by various cell types. Exosomes are generated from late endosomes through several pathways. Most importantly, exosomes deliver various kinds of molecules, including proteins, lipids, iron, and nucleic acid. Research has indicated that exosomal ncRNAs are promising for early diagnosis and precise therapy of hepatocellular carcinoma (Xia et al.). Thus, combination with an exosomal delivery system would greatly enhance the effectiveness of natural products. Furthermore, applying gene-editing techniques in natural products-based cancer therapy could become an important strategy for anti-tumor treatment. In this Research Topic, the CRISPR/Cas9 system was used to knockout Xist in SCC9 cells to investigate the relationship between cucurbitacin B treatment and Xist expression (Tao et al.). Besides CRISPR/Cas9, A-to-I RNA editing is another advanced gene-editing technique that could be implemented in cancer treatment and investigation (Wang et al.). It would be possible to improve the anti-tumor function of natural products by applying A-to-I RNA editing to edit microRNA, lncRNA, and circRNA. Generally, the diverse research on this Research Topic provides important information for applying natural products to cancer therapy and indicates a promising direction for the future study of natural products for combating cancer in the realms of genetics, epigenetics, cancer stem cells, and the microenvironment.

AUTHOR CONTRIBUTIONS

All authors listed have made a substantial, direct and intellectual contribution to the work, and approved it for publication.

FUNDING

YH is supported by Natural Science Foundation of Liaoning Province (2021-MS-104), and National Natural Science Foundation of China (Nos.81502582).

REFERENCES

1. Xiang Y, Guo Z, Zhu P, Chen J, Huang Y. Traditional Chinese Medicine as a Cancer Treatment: Modern Perspectives of Ancient But Advanced Science. *Cancer Med* (2019) 8(5):1958–75. doi: 10.1002/cam4.2108
2. Huang Y, Yuan K, Tang M, Yue J, Bao L, Wu S, et al. Melatonin Inhibiting the Survival of Human Gastric Cancer Cells Under ER Stress Involving Autophagy and Ras-Raf-MAPK Signalling. *J Cell Mol Med* (2021) 25(3):1480–92. doi: 10.1111/jcmm.16237
3. Zuckerman V, Wolyniec K, Sionov RV, Haupt S, Haupt Y. Tumour Suppression by P53: The Importance of Apoptosis and Cellular Senescence. *J Pathol* (2009) 219(1):3–15. doi: 10.1002/path.2584
4. Wang X, Xie H, Ying Y, Chen D, Li J. Roles of N(6) -Methyladenosine (M(6) A) RNA Modifications in Urological Cancers. *J Cell Mol Med* (2020) 24 (18):10302–10. doi: 10.1111/jcmm.15750
5. Bhandari A, Zheng C, Sindan N, Sindan N, Quan R, Xia E, et al. COPB2 Is Up-Regulated in Breast Cancer and Plays a Vital Role in the Metastasis *via* N-Cadherin and Vimentin. *J Cell Mol Med* (2019) 23(8):5235–45. doi: 10.1111/jcmm.14398
6. Ozkan A, Stolley DL, Cressman ENK, McMillin M, DeMorrow S, Yankeelov TE, et al. Tumor Microenvironment Alters Chemoresistance of Hepatocellular Carcinoma Through CYP3A4 Metabolic Activity. *Front Oncol* (2021) 11:662135. doi: 10.3389/fonc.2021.662135
7. Dias AS, Helguero L, Almeida CR, Duarte IF. Natural Compounds as Metabolic Modulators of the Tumor Microenvironment. *Molecules* (2021) 26(12):3494. doi: 10.3390/molecules26123494
8. Zheng X, Yu C, Xu M. Linking Tumor Microenvironment to Plasticity of Cancer Stem Cells: Mechanisms and Application in Cancer Therapy. *Front Oncol* (2021) 11:678333. doi: 10.3389/fonc.2021.678333

Conflict of Interest: The authors declare that the research was conducted in the absence of any commercial or financial relationships that could be construed as a potential conflict of interest.

Publisher's Note: All claims expressed in this article are solely those of the authors and do not necessarily represent those of their affiliated organizations, or those of the publisher, the editors and the reviewers. Any product that may be evaluated in this article, or claim that may be made by its manufacturer, is not guaranteed or endorsed by the publisher.

frontiers in Pharmacology

ORIGINAL RESEARCH
published: 24 November 2020
doi: 10.3389/fphar.2020.584960

Bruceine D inhibits Cell Proliferation Through Downregulating LINC01667/MicroRNA-138-5p/Cyclin E1 Axis in Gastric Cancer

Lin Li[1,2,3,4,5†], *Zhen Dong*[1,3,4,5,6†], *Pengfei Shi*[1,3,4,5], *Li Tan*[1,3,4,5], *Jie Xu*[1,3,4,5], *Pan Huang*[1,3,4,5], *Zhongze Wang*[1,3,4,5], *Hongjuan Cui*[1,3,4,5,6*] and *Liqun Yang*[1,3,4,5*]

[1] State Key Laboratory of Silkworm Genome Biology, Institute of Sericulture and Systems Biology, College of Sericulture and Textile and Biomass Science, Southwest University, Chongqing, China, [2] Department of Immunology, School of Basic Medicine, Southwest Medical University, Luzhou, China, [3] Cancer Center, Reproductive Medicine Center, Medical Research Institute, Southwest University, Chongqing, China, [4] Engineering Research Center for Cancer Biomedical and Translational Medicine, Southwest University, Chongqing, China, [5] Chongqing Engineering and Technology Research Center for Silk Biomaterials and Regenerative Medicine, Southwest University, Chongqing, China, [6] NHC Key Laboratory of Birth Defects and Reproductive Health (Chongqing Key Laboratory of Birth Defects and Reproductive Health, Chongqing Population and Family Planning Science and Technology Research Institute), Chongqing, China

OPEN ACCESS

Edited by:
Yue Hou,
Northeastern University, China

Reviewed by:
Yanlong Liu,
Wenzhou Medical University, China
Guangyun Tan,
The First Hospital of Jilin University, China

***Correspondence:**
Hongjuan Cui
hcui@swu.edu.cn
Liqun Yang
cysylq@swu.edu.cn

[†]*These authors have contributed equally to this work*

Specialty section:
This article was submitted to Pharmacology of Anti-Cancer Drugs, a section of the journal Frontiers in Pharmacology

Received: *19 July 2020*
Accepted: *13 October 2020*
Published: *24 November 2020*

Citation:
Li L, Dong Z, Shi P, Tan L, Xu J, Huang P, Wang Z, Cui H and Yang L (2020) Bruceine D inhibits Cell Proliferation Through Downregulating LINC01667/MicroRNA-138-5p/Cyclin E1 Axis in Gastric Cancer. Front. Pharmacol. 11:584960. doi: 10.3389/fphar.2020.584960

Objective: Gastric cancer is one of the most common malignant tumors. Bruceine D (BD) is one of the extracts of *Brucea javanica*. In recent years, it has been reported that BD has anti-tumor activity in some human cancers through different mechanisms. Here, this study try to explore the effect of BD on gastric cancer and its regulatory mechanism.

Methods: Cell proliferation ability was detected by 3-(4,5-dimethylthiazol-2-yl)-2,5-diphenyl tetrazolium bromide (MTT) assays, 5-bromo-2-deoxyuridine (BrdU) staining and soft agar colony formation assay, respectively. The tumor xenograft model was used to verify the effect of BD on the tumorigenicity of gastric cancer cells *in vivo*. Flow cytometry analysis and Western blot assay were performed to detect cell cycle and apoptosis. Gastric cancer cells were analyzed by transcriptome sequencing. The interaction between LINC01667, microRNA-138-5p (miR-138-5p) and Cyclin E1 was verified by dual luciferase experiment and RT-PCR assays.

Results: We found that BD significantly inhibited cell proliferation and induced cell cycle arrest at S phase in gastric cancer cells. Transcriptome analysis found that the expression of a long non-coding RNA, LINC01667, were significantly down-regulated after BD treatment. Mechanically, it was discovered that LINC01667 upregulated the expression of Cyclin E1 by sponging miR-138-5p. Furthermore, BD enhanced the chemosensitivity of gastric cancer cells to doxorubicin, a clinically used anti-cancer agent.

Conclusion: BD inhibit the growth of gastric cancer cells by downregulating the LINC01667/miR-138-5p/Cyclin E1 axis. In addition, BD enhances the chemosensitivity of gastric cancer cells to doxorubicin. This study indicates that BD may be used as a candidate drug for the treatment of patients with gastric cancer.

Keywords: bruceine D, gastric cancer, LINC01667, microRNA-138-5p, cell proliferation

INTRODUCTION

Gastric cancer is a malignant tumor originating from gastric mucosal epithelium. Despite the decline in the incidence and mortality of gastric cancer in the past 50 years, gastric cancer is still the fifth most commonly diagnosed cancer and the third largest cause of cancer-related death (Ferlay et al., 2010). In 2018, there are more than 1,033,701 new cases and 782,685 deaths of gastric cancer. On average, the incidence of gastric cancer in men is two to three times higher than that in women (Bray et al., 2018; Thrift and El-Serag, 2019). Although great progress has been made in a variety of treatments, including surgery, radiotherapy and chemotherapy, the prognosis of gastric cancer is still very poor (Lazar et al., 2016; Ilson, 2019). Therefore, screening or developing an effective drug is very important for the treatment of gastric cancer.

Brucea javanica (L.) Merr. is an herb which can play the similar role as artemisinin in anti-malaria and anti-cancer. *Brucea javanica* oil has been used in clinic, mainly for adjuvant treatment of digestive system tumors and lung cancer (Zhang et al., 2011; Wu et al., 2018; Zhu et al., 2018). The content of fatty oil in *Brucea javanica* seed is about 56.23%, including linoleic acid, oleic acid, etc. The chemical substances of *Brucea javanica* mainly include alkaloids, glycosides and flavonoids (Yu and Li, 1990). The seeds of *Brucea javanica* contain a variety of bitter ingredients similar to bitter lignin, including *Brucea javanica* bitter alcohol, bruceine A, B, C, D, E, F, G, H and so on. However, research on the bitter components of *Brucea javanica* is still in the primary initiation stage. At present, it has been confirmed that bruceine A has a certain inhibitory effect on the proliferation of non-small cell lung cancer cells, and induces apoptosis by causing DNA damage and activating mitochondrial apoptosis. In addition, bruceine A and D have antiparasite activity in goldfish (Wang et al., 2011). Bruceine D (BD) has anti-inflammatory activity and can be used as an effective leukocyte-endothelial cell adhesion inhibitor (Utoguchi et al., 1997).

BD is also one of these natural compounds extracted from *Brucea javanica* (Zhang et al., 1980; Shen et al., 2008). Previous studies have demonstrated that BD inhibits the proliferation of non-small cell lung cancer and induces apoptosis mediated by ROS mitochondria and JNK phosphorylation (Tan et al., 2019; Xie et al., 2019). BD inhibits the growth of hepatocellular carcinoma cells by targeting miR-95 (Xiao et al., 2014). Recent studies indicated that BD inhibits tumor growth and stem cell-like characteristics of osteosarcoma by inhibiting STAT3 (Wang et al., 2019). In chronic myeloid leukemia K562 cells, BD exerts its anti-tumor activity by inhibiting the phosphorylation of AKT and ERK and induces cellular apoptosis through mitochondrial pathway (Zhang et al., 2016). In addition, BD induces apoptosis in pancreatic cancer cells through inhibiting the anti-apoptotic activity of NF-κB, reducing mitochondrial membrane potential and activating redox sensitive p38-MAPK pathway (Lau et al., 2009; Yang et al., 2012).

However, the effect of BD in gastric cancer has not been explored. Based on previous findings, we hypothesize that BD may inhibit gastric cancer cell proliferation. This study firstly proves that BD has an anti-tumor activity in gastric cancer cells, which underpins a theoretical basis for the development and application of BD for the treatment of gastric cancer.

MATERIALS AND METHODS

Cell Culture

The human gastric cancer cell lines HGC27, MKN45 and SGC7901, the human normal gastric epithelial cell line GES-1 and the human embryonic renal cell line 293FT were purchased from the American Type Culture Collection (ATCC, Rockville, MD, United States). Gastric cancer cell lines and GES-1 were cultured in Roswell Park Memorial Institute-1640 (RPMI-1640, Gibco) with 10% fetal bovine serum (FBS) and 1% penicillin-streptomycin (P/S, Invitrogen). 293FT cells were cultured in Dulbecco's modified Eagle's medium (DMEM, Gibco) containing 10% FBS, 1% P/S, 1% Geneticin 418 (G418, Invitgen), 1% non-essential amino acids (Invitgen), 1% sodium pyruvate (Invitgen) and 2% L-glutamine (Invitgen). 293FT transfection medium did not contain P/S or G418. All cells were cultured in a humidified incubator containing 5% CO_2 at 37°C.

Drug Treatment

BD was purchased from Chengdu Herbpurify (Chengdu, China) and then was dissolved in dimethyl sulfoxide (DMSO). The mother liquor concentration was 100 mM, and stored at −80°C. Human gastric cancer cells were treated with different concentrations of BD for different time. Cell morphology was photographed by an inverted microscope (Olympus, Japan).

Cell Proliferation Assays

Cell proliferation was determined by 3-(4,5-dimethylthiazol-2-yl)-2,5-diphenyl tetrazolium bromide (MTT) assay. The cells were seeded to 96-well plates with 1,000 cells/well and cultured overnight in the incubator. The medium mixed with specified concentration of BD or DMSO. After a specific time, 20 μl MTT was added to each well and cells were cultured in the incubator for 2 h. The medium was sucked and 150 μl DMSO was added. The absorbance was measured at 560 nm using a microboard reader (Thermo Fisher, Waltham, MA, United States). The change of cell viability was calculated by formula (1-average absorbance/control group average absorbance) × 100%.

5-Bromo-2-Deoxyuridine Staining

The cells were seeded to a 24-well plate with 20,000 cells/well and cultured overnight in the incubator. Then they were cultured in the incubator for 48 h after the medium containing DMSO or BD was added to each well. After incubated with BrdU (Abcam, United States, 30 μg/ml) for 45 min, the cells were washed with phosphate buffered saline (PBS) and fixed in 4% paraformaldehyde (PFA) for 15 min. Subsequently, 200 μl 2 M hydrochloric acid was added to each well at 37°C for 20 min. After washing with PBS for three times, 10% goat serum containing 0.5% Triton X-100 (ZSGB-Bio, Beijing, China) was used for blocking at room temperature (RT) for 2 h. The cells were

incubated with anti-BrdU monoclonal rat first antibody (1: 1,000) overnight at 4°C. The samples were incubated at RT for 2 h with Alexa FluorR®488 goat anti-mouse IgG second antibody (HG L; 1: 10,000, antioxidant). The nuclei were stained with DAPI (1: 1,000). The percentage of BrdU staining was calculated from at least five microscopic visual fields.

Soft Agar Colony Formation Assay

The colony forming ability of gastric cancer cells was detected by soft agar colony formation assay (Hu et al., 2016). Briefly, 1 ml RPMI-1640 (Gibco) medium containing 0.6% agarose (Sigma-Aldrich, United States) was added to the 6-well plate as the basic agar. Then 1.5 ml RPMI-1640 (Gibco) medium containing 1,000 logarithmic cells, 0.3% agar mixed with a specific concentration of BD was added onto the basic agar. After cultured at 37°C for 2–3 weeks, the colonies were captured under microscope and counted after MTT staining.

Flow Cytometry Analysis

Cells were treated with DMSO or BD for 48 h, and then collected for flow cytometry analysis. DMSO was used as control. Cell cycle and apoptosis analysis were performed as previously reported (Dong et al., 2017). For cell cycle assay, the cells were washed with cold PBS and then fixed with 75% ethanol at 4°C for 24 h. After washing with PBS, the cells were incubated in 200 μl PBS containing 1 μl 5 mg/ml propidium iodide (PI, BD, San Jose, CA, United States) and 2 μl 4 mg/ml RNaseA (Sigma Aldrich, Sigma Aldrich) at 37°C for 30 min. The cells were analyzed by a BD Accuri C6 flow cytometry (BD, United States). For the determination of cell apoptosis, the cells were incubated in 100 μl binding buffer containing 5 μl 50 μg/ml PI (BD, United States) and 5 μl Annexin-V (BD, San Jose, CA, United States) at room temperature for 20 min. The cells were analyzed by a BD Accuri C6 flow cytometry. All samples were analyzed by the FlowJo 7.6 software (BD, United States).

Tumor Xenografts

Twelve 4-week-old female BALB/c nude mice (Beijing Laboratory Animal Research Center, China) were purchased and housed in the specific pathogen free room to acclimate for a week. The gastric cancer cells SGC7901 and MKN45 cells (1×10^6) in 100 μl PBS were subcutaneously injected into both sides of each mouse. Seven days after cell injection, the mice were randomly divided into two groups. One group was intraperitoneally injected with BD (1.5 mg/kg), and the other group was injected with DMSO as control every two days for 14 days. The tumor growth was measured by caliper every day, and the tumor volume was calculated by formula (volume = length × width ^{2} × π/6). At the end of the experiment, the tumor was removed and weighed. All animal experiments were pre-approved by the Animal Ethics Committee of Southwest University. H&E and immunohistochemical (IHC) staining were performed as previous report (Yang L. et al., 2019).

Western Blot Assay

Cells were collected and lyzed by using the RIPA lysis buffer (Beyotime, China) containing the complete protease inhibitor cocktail (Roche) and phosphatase inhibitors (Sigma Aldrich, St. Louis, MO, United States). Cell lysates were degenerated at 100°C for 15 min. Proteins were isolated with 8, 10 or 12% SDS-PAGE and transferred to the polyvinylidene fluoride (PVDF) membranes. The membrane was blocked with 5% bovine serum albumin (BSA) at RT for 2 h. The PVDF membrane was incubated with specific primary antibody against CDK2, Cyclin E1, Cyclin E2, PARP and Caspase3 (1: 1,000, cell Signal Technology, United States), α-tubulin (1: 1,000, Beyotime, China, United States) at 4°C overnight. The membrane was incubated with secondary antibodies (goat anti-mouse IgG and goat anti-rabbit IgG, 1:10,000, Beyotime, China) at RT for 2 h. The high sensitivity substrate of SuperSignal West Femto (Thermo Fisher, Waltham, MA, United States) was used to display protein bands, and Chemiscope 6000 chemiluminescence gel imaging system (Clinx Science, China) was used to capture proteins.

TABLE 1 | Primers used in the quantity real-time PCR assay.

GAPDH-F	5′ AACGGATTTGGTCGTATTGGG3′
GAPDH-R	5′ CCTGGAAGATGGTGATGGGAT3′
LINC01002- F-1	5′TCCTAGCCTCCAGTTTTACCCT3′
LINC01002- R-1	5′CTAATAACCATCAACGTCTTCTGTG3′
LINC01667- F-1	5′ GATGACAGCAGTCGCAAAGG3′
LINC01667- R-1	5′ ATGACAGTGACCCAACCAACA3′
LINC01671- F-2	5′GTATCAGACGTGGGAAAGCAAT3′
LINC01671- R-2	5′CAGGAGCACATCAACAGGGA3′
LINC01001- F-1	5′CCCACTGATTCTACATTATGCTCC3′
LINC01001- R-1	5′TGCCGTGACGTAGGGTATGG3′
LINC00958- F-1	5′AAATTAGCCGGGCGTTGT3′
LINC00958- R-1	5′TGGAGTTTCGCTCTTGTTGC3′
LINC01278- F-1	5′GTGAGAACCTGGGGACGCTA3′
LINC01278- R-1	5′CGCCACGGTCTGAACTCTT3′
LINC00969- F-1	5′AAAGCAGATCCGTGGTTCCC3′
LINC00969- R-1	5′TCCGTCCCAAGACAGCAAA3′
LINC01089- F-1	5′CCAAGCCCAAGGACTCACA3′
LINC01089- R-1	5′CACGTTCTGCTCCTTCCACTT3′
CyclinE1-F-1	5′GTCCAAGTGGCCTACGTCAA3′
CyclinE1-R-1	5′AAGCAGCGAGGACACCATAA3′
U6-F	5′CTCGCTTCGGCAGCACA3′
U6-R	5′AACGCTTCACGAATTTGGGT3′
hsa-microRNA-138-5p	5′AGCTGGTGTTGTGAATCAGGCCG3′
MicroRNA unified reverse primer	5′TGGTGTCGTGGAGTCG3′

RNA-Seq

MKN45 cells were treated with 1.2 μM BD or isometric DMSO for 48 h. Each group consisted of three biological repeats. Then the total RNA of each sample was extracted by using the RNAiso Plus (Total RNA extraction reagent) (TaKaRa, Dalian, China). Afterward, the samples were shipped with enough dry ice to Sangon Biotech Co., Ltd. (Shanghai, China) The quality and quantity of total RNA were confirmed by agarose gel electrophoresis. cDNA was prepared by using the cDNA Synthesis Kit (Illumina Inc., San Diego, CA, United States) and then was used for library construction and further Illumina deep sequencing. The tool package SOAP2 was used for alignments for short oligo nucleotide analysis, and only up to two mismatches with reference sequences were allowed. The quality of the original sequencing data was evaluated by

FastQC. Through Trimmomatic for mass shearing, relatively accurate and effective data can be obtained. The ENSEMBL database (Homo_sapiens.GRCh37.55.cdna.all.fa) were used for the alignment of the sequenced reads to analyze the transcript levels. HISAT2 was used to compare the effective data of the samples to the reference genome and count the mapping information. RSeQC was used to perform redundant sequence analysis and insert fragment distribution analysis based on the comparison results. Qualimap was used to perform uniform distribution check and genome structure distribution analysis based on the comparison results. BEDTools were used to perform statistical analysis of gene coverage and analysis of sequence distribution on chromosomes. Heml 1.0: Heatmap Illustrator was used to draw a heatmap.

Quantitative Real-Time PCR

After treated with DMSO or BD for 48 h, the cells were collected. Total RNA was extracted from cells using TRIzol™ reagent (Invitrogen) according to the manufacturer's instructions. quantity real-time PCR (qRT-PCR) was conducted as previous report (Dong et al., 2020). Briefly, the total RNA was reversely transcribed to cDNA by using the M-MLV reverse transcriptase (Promega). SYBR PreMix Ex Taq II (Vazyme Biotech, Nanjing, China) was used to carry out qRT-PCR in 20 μL reaction system. RT-qPCR reaction was carried out by using a LightCycle96 real-time PCR system (Roche). The relative mRNA expression level was calculated by $2^{-\Delta\Delta CT}$ method. The primers used in this study are listed in **Table 1**.

Transfection and Infection

Human full-length LINC01667 RNA (NR_038377.1) and CCNE1 (NM_001238) were downloaded from the National Center for Biotechnology Information and ligated into a pCDH-CMV-MCS-EF1-GFP-puro vector by Changsha Youbao Biotechnology Co., Ltd. (Changsha, China). The packaging plasmid (pLP1, pLP2, pLP/VSVG) and overexpression plasmid were co-transfected into 293FT cell line by lipofectamine 2000 (Invitrogen, Carlsbad, CA, United States). At 48 h after transfection, the supernatant of the virus was collected and infected with gastric cancer cells by adding with polybrene. Drug resistant cell lines were selected with 2 mg/ml puromycin for subsequent experiments.

Luciferase Reporter Assay

According to the predicted sites of TargetScanHuman 7.0 database (Agarwal et al., 2015), we constructed LINC01667 wild type and mutant double luciferase vectors (purchased from the Genecreate Biological Engineering Co., Ltd., Wuhan, China). 3×10^5 cells were placed in each well and placed in a 24-well plate for cell transfection. 600 ng PRL-TK and 600 ng LINC01667-WT/MUT, 50 nM miRNA NC/microRNA-138-5p (miR-138-5p) mimics were co-transfected into 293FT and MKN45 cells in Opti-MEM serum-lowering medium (Life Technologies). After 8 h, 3 ml medium was refreshed in each well. After 48 h, luciferase reporter assay was carried out according to Promega production instructions. Luciferase activity was normalized to PRL-TK activity.

Statistical Analysis

All experiments were confirmed by at least three technical and biological replicates. Quantitative data are expressed as the mean ± SD. Two-tailed Student's t-test was performed for paired samples. p value < 0.05 was considered statistically significant.

RESULTS

Bruceine D Inhibits Cell Growth and Proliferation in Gastric Cancer Cells

To explore the biological function of BD in gastric cancer cells, the viability of cells treated with increasing doses of BD for 48 h was detected by MTT assay. The results showed that the IC_{50} of HGC27 and MKN45 cells were 0.32 and 1.11 μM, respectively (**Figure 1A**). According to the IC_{50} value, we selected the appropriate concentration of BD to treat gastric cancer cells (0.4 μM for HGC27 and 1.2 μM for MKN45). Observed by microscopy, HGC27 and MKN45 cells treated with BD showed significant morphological changes, and cell numbers decreased in a dose-dependent manner (**Figures 1B–D**). To confirm this result, MTT and BrdU staining assays were performed. MTT assay showed that gastric cancer cells treated with BD showed a sharp decline in the growth curve, compared to the DMSO group (**Figures 1E,F**). BrdU staining analysis also showed that the percentage of BrdU-positive cells treated with BD for 48 h was significantly lower than that in the DMSO group (**Figures 1G,H**). These results demonstrate that BD dramatically inhibits cell growth and proliferation in gastric cancer cells.

Bruceine D Inhibits Cell Proliferation by Inducing Cell Cycle Arrest at the S Phase

Cell proliferation is usually regulated by the procession of cell cycle. In order to understand the mechanism of BD in the inhibition of the proliferation of gastric cancer cells, we used flow cytometry to analyze the cell cycle of gastric cancer cells treated with BD for 48 h. The results showed that BD induced cell cycle arrest at the S phase (**Figures 2A,B**). To confirm this result, we detected the expression of CDK2, Cyclin E1 and Cyclin E2 that promoted cells to go through the G1 checkpoint by Western blot analysis. We found that the expression levels of CDK2, Cyclin E1 (CCNE1) and Cyclin E2 (CCNE2) were decreased in BD-treated cells in a dose- and time- dependent manner (**Figures 2C,D**). These results suggest that BD induces cell cycle arrest at the S phase in gastric cancer cells.

Bruceine D Inhibits Clonogenicity and Tumorigenecity of Human Gastric Cancer Cells

In order to study the effect of BD on tumor growth in gastric cancer cells, soft agar colony formation assay *in vitro* and subcutaneously xenograft *in vivo* were carried out. In the soft agar colony formation assay, it was revealed that fewer and smaller cell colonies were produced in the BD-treated group,

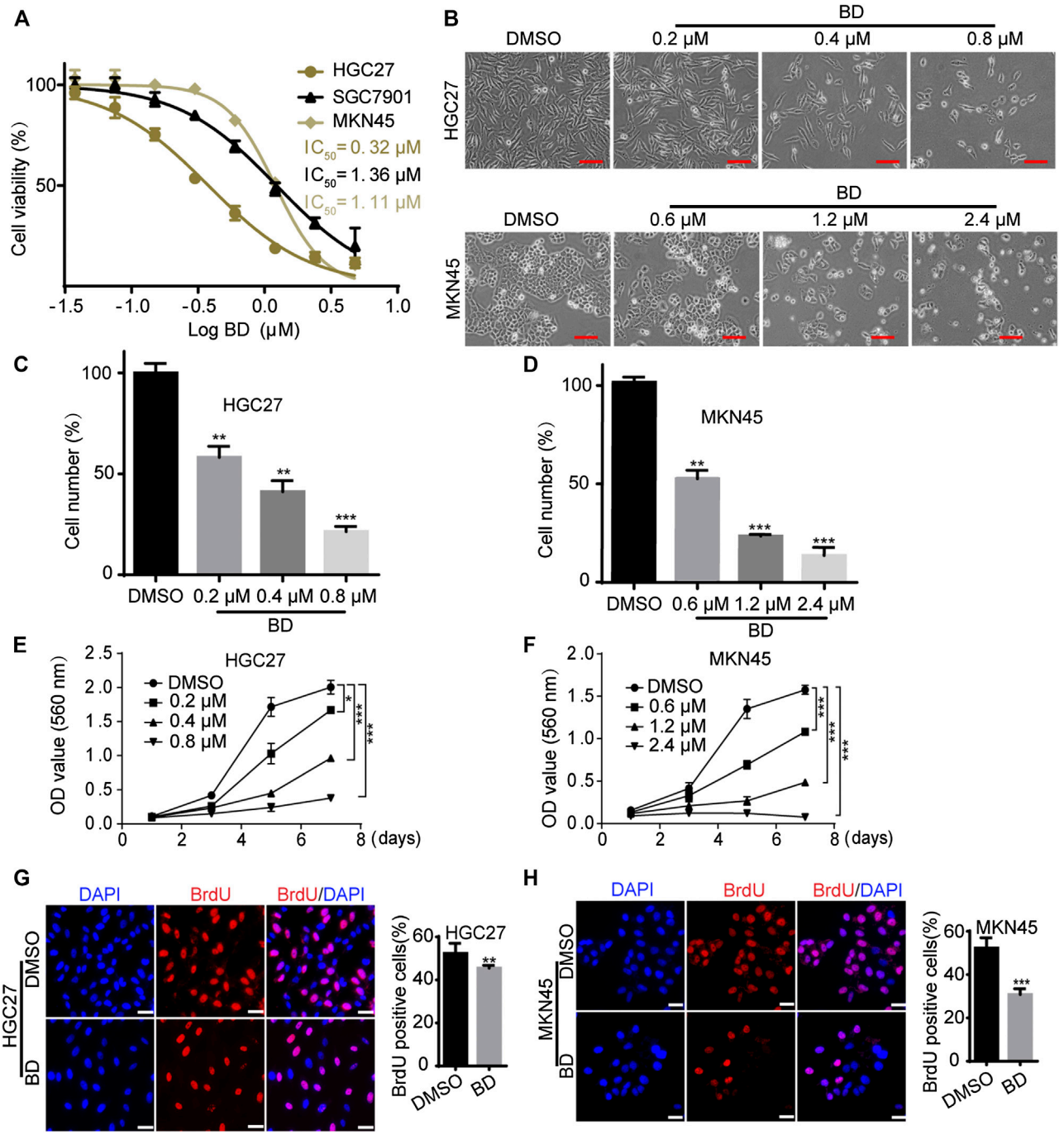

FIGURE 1 | Bruceine D (BD) inhibits cell proliferation in gastric cancer cells. **(A)** HGC27, SGC7901 and MKN45 cells were treated with increasing concentrations of BD. After 48 h of BD treatment, cellular viability was determined by 3-(4,5-dimethylthiazol-2-yl)-2,5-diphenyl tetrazolium bromide (MTT) assay. Non-linear regression analysis was performed to determine IC_{50} values. **(B)** The morphology of HGC27 and MKN45 cells. HGC27 cells were treated with BD in different concentrations of 0.2, 0.4, and 0.8 μM for 48 h. MKN45 cells were treated with BD in different concentrations of 0.6, 1.2, and 2.4 μM for 48 h. Dimethyl sulfoxide (DMSO) was used as control. Scale bar = 50 μm. **(C,D)** Counting the number of cells treated as in **(B)**, and the histogram showed the quantity of cell proliferation rate. Cell numbers of DMSO-treated group were regarded as 100%. **(E,F)** Cell growth was monitored using MTT assays in cells treated with BD at the indicated times and concentrations. **(G,H)** Immunofluorescence staining for 5-bromo-2-deoxyuridine (BrdU) was performed. DAPI was used for nuclear staining. DMSO was used as control. Scale bar = 20 μm. The histogram shows the quantification of BrdU-positive HGC27 and MKN45 cells. All experiments were repeated at least three times. All data were used as mean ± SD, significant difference was tested by the two tailed and unpaired student's t-test. Error bars, $^{*}p < 0.05$, $^{**}p < 0.01$, and $^{***}p < 0.001$.

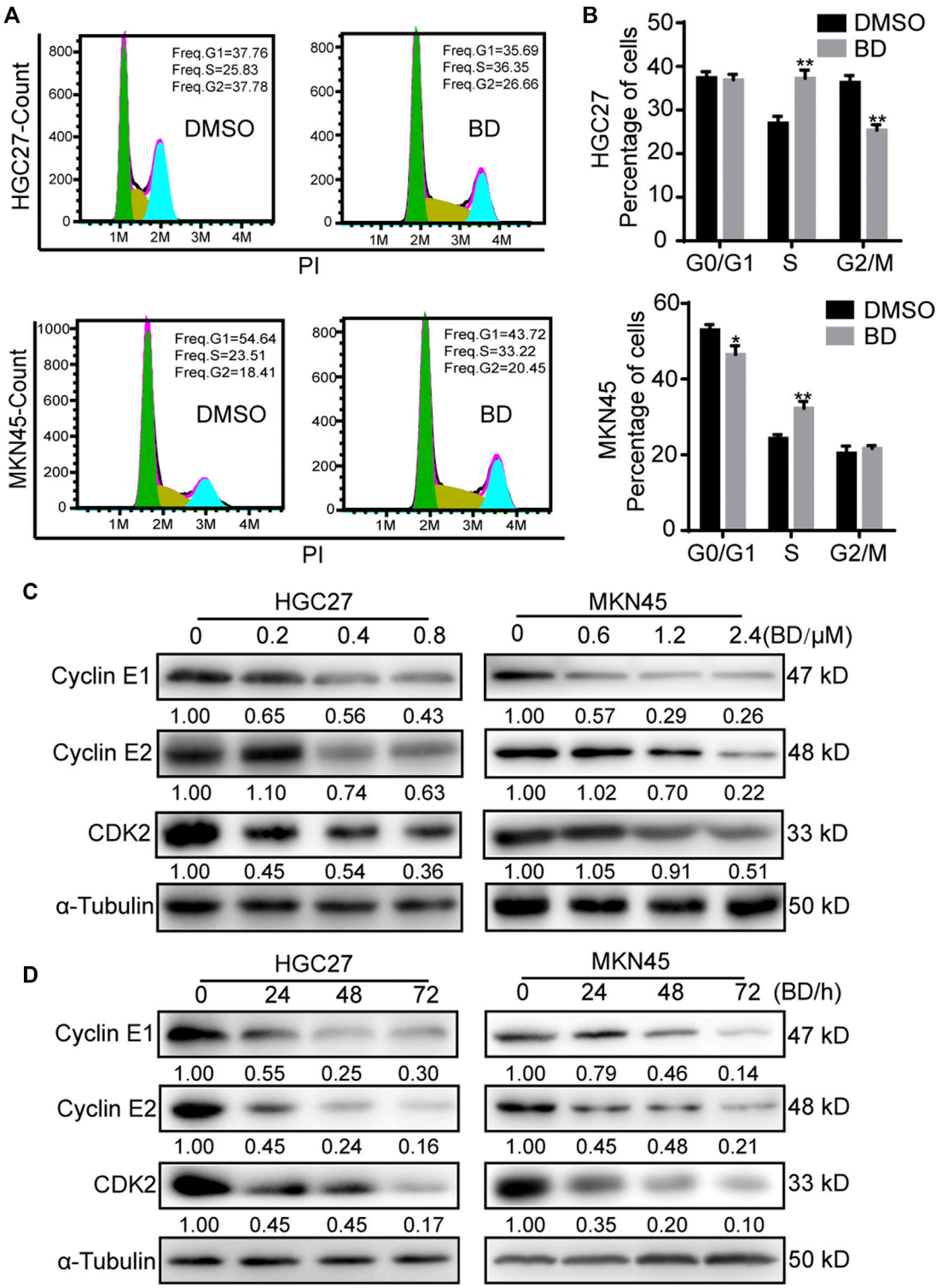

FIGURE 2 | Bruceine D (BD) induces cell cycle arrest at S phase. **(A)** The cell cycle of gastric cancer cells were performed using flow cytometry. HGC27 and MKN45 cells were treated with BD at concentrations of 0.4 and 1.2 μM for 48 h, respectively. DMSO was used as control. **(B)** The histogram demonstrates the quantification of percentage of indicated HGC27 and MKN45 cells in different phase. **(C,D)** The expression of Cyclin E1, Cyclin E2 and CDK2 were determined using Western blot analysis after cells were treated with BD at different concentrations **(C)** or at different time points **(D)**. α-Tubulin was used as control. The gray ratio of Cyclin E1/α-Tubulin, Cyclin E2/α-Tubulin and CDK2/α-Tubulin was calculated. All experiments were repeated at least three times. All data were used as mean ± SD, significant difference was tested by the two tailed and unpaired student's t-test. Error bars, $^{*}p < 0.05$, $^{**}p < 0.01$, and $^{***}p < 0.001$.

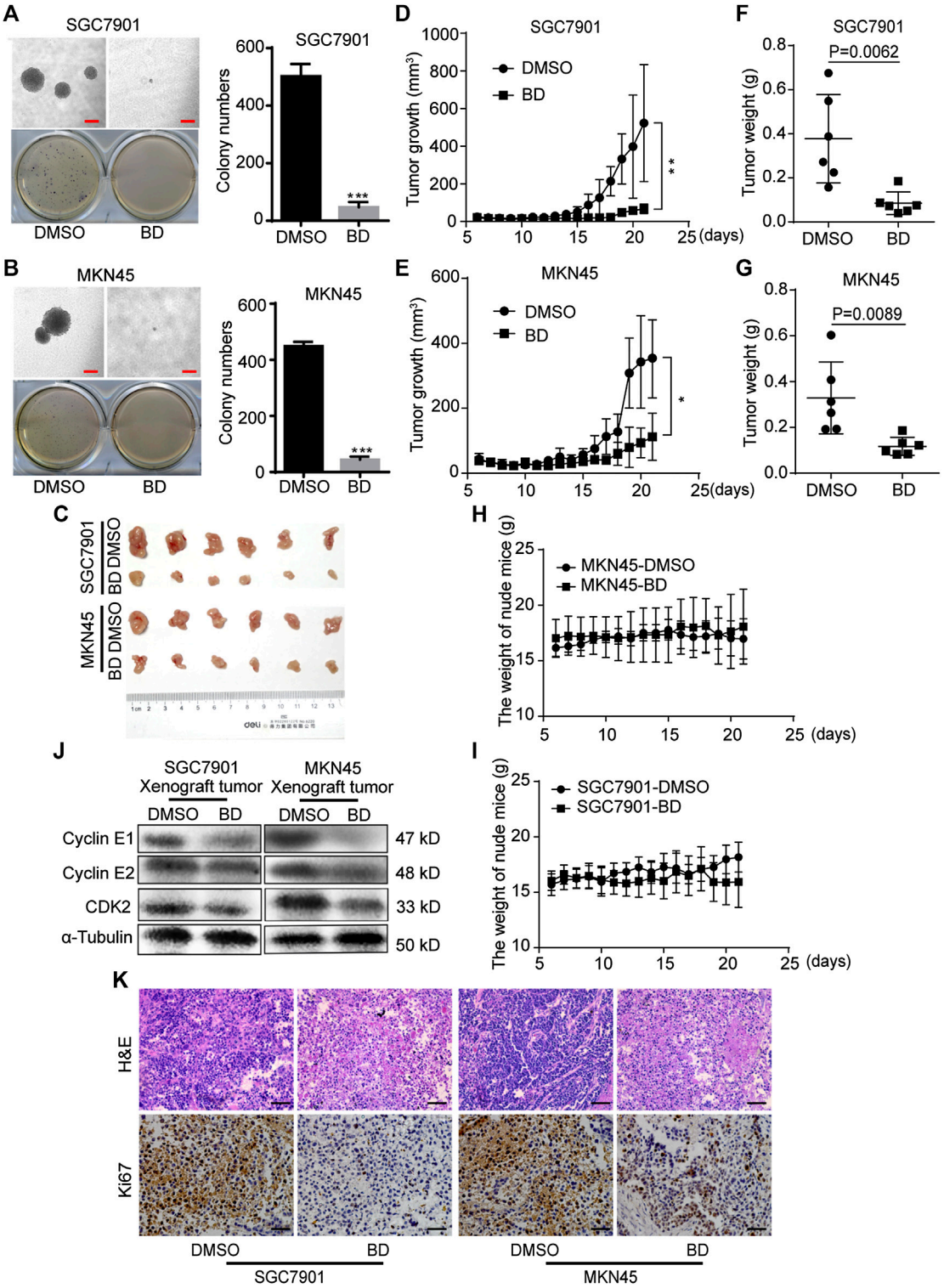

FIGURE 3 | Bruceine D (BD) inhibits clonogenicity and tumorigenecity of human gastric cancer cells. **(A,B)** Soft agar assays were performed, and the results were quantitated in SGC7901 **(A)** and MKN45 **(B)** cells treated with 1.2 μM BD for two weeks. DMSO was used as control. Scale bar = 100 μm. **(C)** Image of xenograft tumors from mice. **(D,E)** Tumor growth curves in mice were calculated **(F,G)** Tumor weight removed from mice were measured. **(H,I)** The body weight of nude mice were measured. **(J)** The expression levels of CDK2, Cyclin E1 and Cyclin E2 were determined using Western blot assays in xenograft tumors. α-Tubulin was used as control. **(K)** H&E staining and immunohistochemical staining for Ki67 were performed in xenograft tumors. Scale bar = 50 μm. All data were used as mean ± SD, significant difference was tested by the two tailed and unpaired student's t-test. Error bars, $^{*}p < 0.05$, $^{**}p < 0.01$, and $^{***}p < 0.001$.

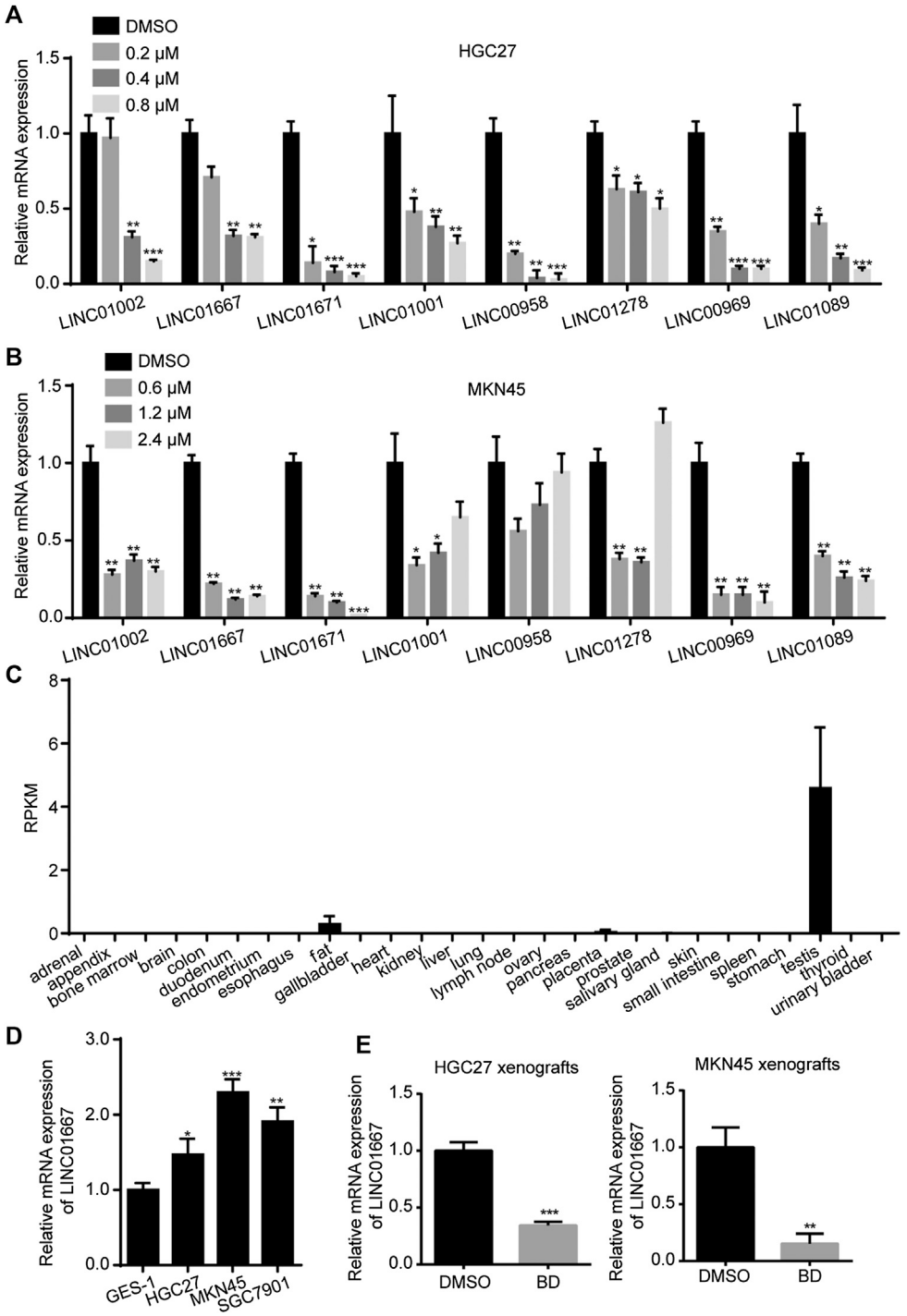

FIGURE 4 | Bruceine D inhibits the expression of LINC01667. **(A,B)** The mRNA expression levels of several differential long non-coding RNAs weres detected by quantity real-time PCR (qRT-PCR) experiment. **(C)** The expression of LINC01667 in various parts of the human body. **(D)** The mRNA expression levels of LINC01667 in GES-1 and gastric cancer cell lines were detected by qRT-PCR experiment. **(E)** The mRNA expression levels of LINC01667 in HGC27 and MKN45 xenografts were detected by qRT-PCR experiment. All data were used as mean ± SD, significant difference was tested by the two tailed and unpaired student's t-test. Error bars, $^{*}p < 0.05$, $^{**}p < 0.01$, and $^{***}p < 0.001$.

compared with the DMSO control group (**Figures 3A,B**). Next, we examined the effect of BD on tumor growth in the nude mice. The results showed that BD significantly inhibited tumor growth (**Figure 3C**), and the tumor weight in the BD-treated group was significantly lighter than those in the control group (**Figures 3D–G**). There was no significant change in body weight and

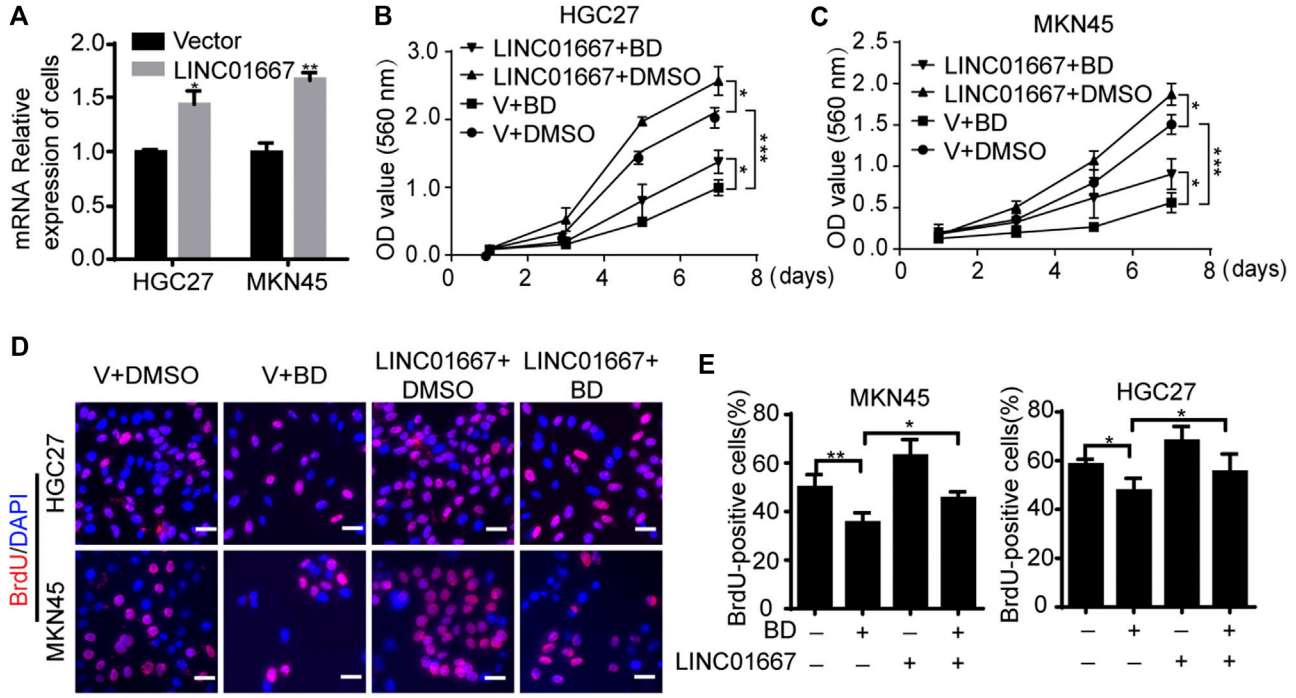

FIGURE 5 | Bruceine D (BD) inhibits the proliferation of gastric cancer cells by inhibiting LINC01667. **(A)** The expression of LINC01667 in gastric cancer cell line was detected by quantity real-time PCR (qRT-PCR) assays. **(B,C)** Growth curve of LINC01667 overexpressing HGC27 and MKN45 cells after treating with BD at concentrations of 0.4 and 1.2 μM for the indicated time, respectively. Dimethyl sulfoxide (DMSO) and empty vector were used as control. **(D)** 5-bromo-2-deoxyuridine (BrdU)-positive cells in LINC01667-overexpressed HGC27 and MKN45 cells after treating with BD at concentrations of 0.4 and 1.2 μM for 48 h, respectively. DMSO and empty vector were used as control. Scale bar = 20 μm. **(E)** Quantification of BrdU-positive HGC27 and MKN45 cells in **C**. All data were used as mean ± SD, significant difference was tested by the two tailed and unpaired student's t-test. Error bars, $^{*}p < 0.05$, $^{**}p < 0.01$, and $^{***}p < 0.001$.

behavior of mice treated with BD (**Figures 3H,I**). In addition, we detected cell cycle-related proteins expressed in the xenograft tumors obtained from mice by using the Western blot. The results showed that the expressions of these cell cycle-related proteins CDK2, Cyclin E1 and Cyclin E2 were significantly down-regulated after BD treatment (**Figure 3J**). H&E and IHC staining further supported the above results. H&E staining showed that the number of cells was decreased and the nucleus became smaller in BD-treated group. IHC staining showed that the expression of Ki67, a marker of cell proliferation, was significantly reduced in BD-treated group (**Figure 3K**). These results suggest that BD significantly inhibits the tumorigenecity of gastric cancer cells.

Bruceine D Inhibits the Proliferation of Gastric Cancer Cells by Inhibiting LINC01667

In order to reveal how BD inhibits cell proliferation, a transcriptome analysis was performed on gastric cancer cells treated with BD or DMSO. In recent years, long non-coding RNA (lncRNAs) has been proved to play an important role in epigenetic regulation, cell cycle regulation and cell differentiation regulation (Geisler and Coller, 2013; Cech and Steitz, 2014). Besides, lncRNAs are emerging as a kind of new prognostic, diagnostic and therapeutic targets for cancer (Huarte, 2015), especially are important in gastric cancer (Wei et al., 2020). Through the analysis of the transcriptome data, we screened 89 lncRNA with significant changes in expression level (**Supplementary Figure S1**). Then we further screened out LINC01667, which may be a potential differential expressed lncRNA, through qRT-PCR analysis (**Figures 4A,B**) and database (https://www.ncbi.nlm.nih.gov/Gene/) (**Figure 4C**). LINC01667 was rarely expressed in gastric cell GES-1, but it was highly expressed in gastric cancer cell lines (**Figure 4D**). Importantly, LINC01667 mRNA expression was also significantlt decreased in both HGC27 and MKN45 xenografts treated by BD (**Figure 4E**). These data suggested that LINC01667 could play an oncogenic role in gastric cancer. In order to verify whether LINC01667 has an effect on the proliferation of gastric cancer cells, we constructed LINC01667 overexpression vector (**Figure 5A**). Then MTT (**Figures 5B,C**) and BrdU assays (**Figures 5D,E**) were carried out. The results showed that overexpression of LINC01667 could rescue the inhibition of cell activity induced by BD treatment. In summary, these results suggest that BD inhibits cell proliferation by inhibiting LINC01667.

LINC01667 Sponges MicroRNA-138-5p and Upregulates Cyclin E1 Expression

Results above suggested that overexpression of LINC01667 could restore the inhibition of BD on the proliferation of gastric cancer

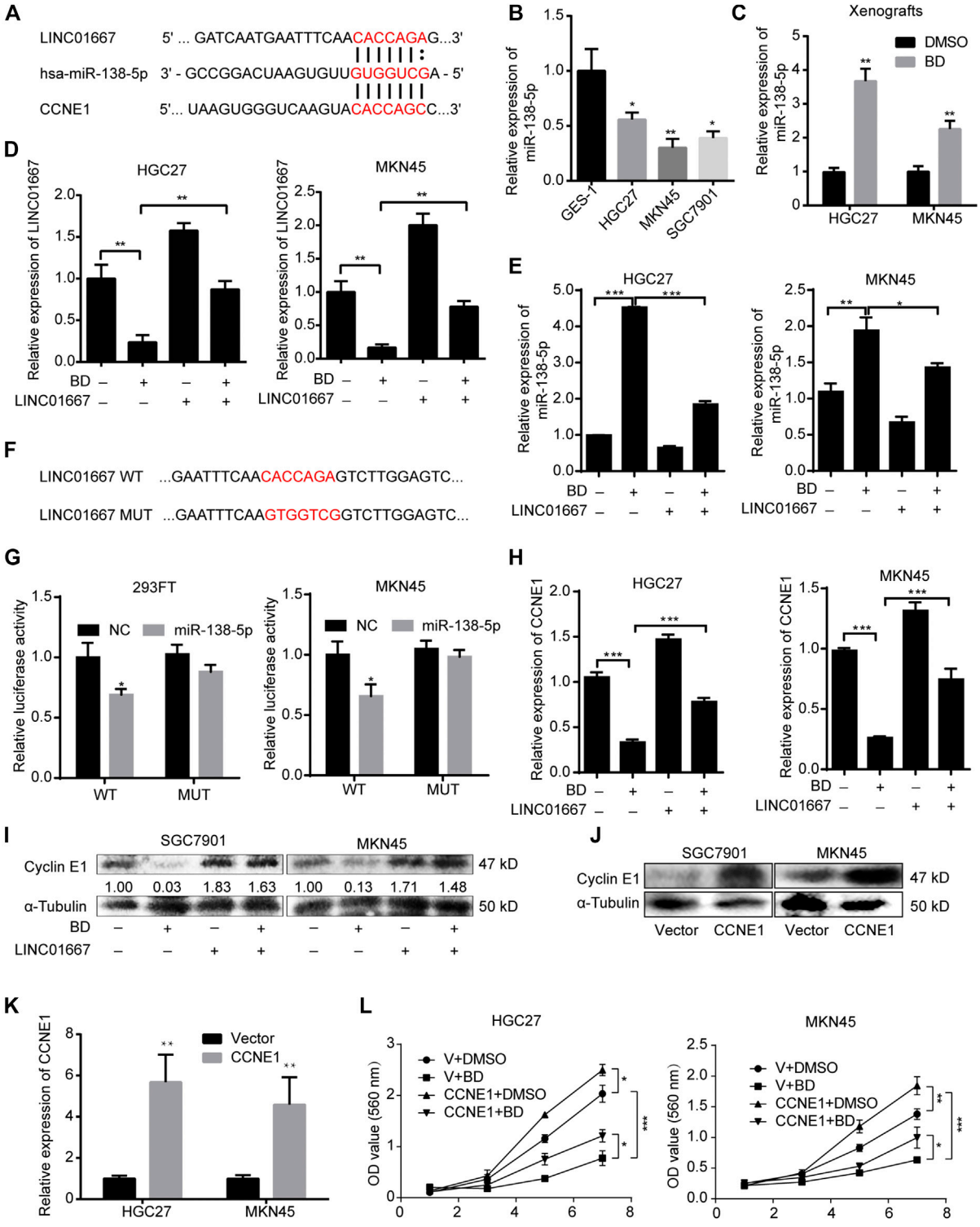

FIGURE 6 | LINC01667 sponges microRNA-138-5p (miR-138-5p) and regulates Cyclin E1 expression. **(A)** The schematic diagram of the binding sites between miR-138-5p and LINC01667 or Cyclin E1 predicted by the TargetScanHuman 7.0. **(B)** The mRNA expression levels of miR-138-5p in GES-1 and gastric cancer cell lines were detected by quantity real-time PCR (qRT-PCR) experiment. **(C)** The mRNA expression levels of miR-138-5p in HGC27 and MKN45 xenografts were detected by

(*Continued*)

cells. Next, we explored the potential molecular mechanism of this phenomenon. A lncRNA may have many modes of actions via interacting with both proteins, nucleic acids and even metabolites, but the role of sponging microRNAs is the most well studied functions. Therefore, we tried to analyze whether LINC01667-regulated miRNAs also have the potential to regulate cell cycle and cell proliferation in human beings. Interstingly, the binding sites between miR-138-5p and LINC01667 or Cyclin E1 can be predicted by the TargetScanHuman 7.0 (**Figure 6A**). Importantly, from the database of TargetScanHuman 7.0, the binding site of CACCAGC in the 3′UTR of human are conserved in chimp, rhesus, squirrel, mouse, rat, rabbit, pig, cow, cat, dog, brown bat, elephant and lizard and microRNA-138-5p is the only conserved microRNA that targeted CCNE1 (**Supplementary Figure S2**; **Supplementary Table S1**).

As expected, miR-138-5p is downregulated in gastric cancer cell lines, compared with that of the GES-1 cells (**Figure 6B**). Besides, miR-138-5p was also significantly upregulated after BD treatment in HGC27 and MKN45 xenografts (**Figure 6C**). To further confirm the relationship between LINC01667 and miR-138-5p, LINC01667 was overexpressed (**Figure 6D**) and the results revealed that the expression of miR-138-5p was significantly upregulated in gastric cancer cells treated with BD, while overexpression of LINC01667 could inhibit the expression of miR-138-5p (**Figure 6E**). In order to verify the binding between LINC01667 and miR-138-5p, we constructed the luciferase reporter gene plasmid of LINC01667 wild-type or mutant-type (**Figure 6F**). Dual-luciferase reporter assays showed that miR-138-5p mimics considerably reduced the luciferase activity of LINC01667-WT, compared with LINC01667-MUT group (**Figure 6G**).

Since we have showed that Cyclin E1, an important cell cycle regulator, was significantly decreased after BD treatment, we thought that Cyclin E1, one of the potential target genes of miR-138-5p, might be the probable mechanism for regulating cell proliferation in gastric cancer. The results revealed that the expression of Cyclin E1 was remarkably decreased in both mRNA and protein levels after BD treatment in gastric cancer cells, but was recovered in some extent after LINC01667 restoration (**Figures 6H,I**). To confirm that Cyclin E1 is the downstream target of BD, we overexpressed it (**Figures 6J,K**) and the results showed that CCNE1 overexpression could rescued the inhibition of cell proliferation induced by BD treatment (**Figure 6L**).

These results confirm that LINC01667 could sponge miR-138-5p, thereby promoting the expression of Cyclin E1.

Bruceine D Enhances the Chemosensitivity of Gastric Cancer Cells to Doxorubicin

Next, we explored whether BD can induce apoptosis of gastric cancer cells. Flow cytometry analysis showed that BD did not induce apoptosis of gastric cancer cells (**Figure 7C**). Doxorubicin is a commonly chemotherapeutic drug in the treatment of gastric cancer. Therefore, we evaluated whether BD can enhance the chemosensitivity of gastric cancer cells to doxorubicin. Firstly, we used CompuSyn software to judge the combination index of BD and doxorubicin (**Figures 7A,B**). HGC27 cells were treated with BD (0.4 μM) and doxorubicin (0.4 μM) alone or in combination for 48 h, and MKN45 cells were treated with BD (1.2 μM) and doxorubicin (0.4 μM) alone or in combination for 48 h. The cells were collected for flow cytometry analysis. The results showed that BD significantly increased the cell apoptosis induced by doxorubicin (**Figures 7C,D**). Western blot analysis confirmed this discovery, and the results showed that the expression of cleaved fragments of PARP and caspase-3 were significantly increased after combination treatment of BD and doxorubicin (**Figure 7E**). These results suggest that BD can enhance the chemosensitivity of gastric cancer cells to doxorubicin.

DISCUSSION

Although the incidence has declined over the past few decades, gastric cancer remains as the third leading cause of cancer-related death (Ferlay et al., 2010; Thrift and El-Serag, 2019). Patients with advanced or recurrent gastric cancer have a low survival rate due to drug resistance to chemotherapy (Hu et al., 2015; Chang et al., 2019). Therefore, screening or developing effective therapeutic drugs is one of keys to the treatment of gastric cancer. At present, the treatment of diseases with traditional Chinese medicine has been shown great potential. BD is a quassinoid isolated from the seeds of *Brucea javanica*, which has been used as a traditional Chinese herb to treat a variety of diseases (Zhang et al., 1980; Shen et al., 2008). Recent studies showed that BD had anti-cancer effect in multiple tumor types, including non-small cell lung cancer (Tan et al., 2019), leukemia (Zhang et al., 2016), osteosarcoma (Wang et al., 2019), hepatocellular carcinoma (Cheng et al., 2017) and pancreatic adenocarcinoma (Lau et al., 2009; Yang et al., 2012). However, as far as we know, the effect of BD in gastric cancer still remains unclear.

In this study, we evaluated the anti-tumor activity of BD in gastric cancer. First of all, we demonstrated that BD significantly inhibited tumor growth *in vivo* and *in vitro*. MTT and BrdU

FIGURE 6 | qRT-PCR experiment **(D,E)** qRT-PCR assays were performed to evaluate the expression of LINC01667 and miR-138-5p in LINC01667-overexpressed HGC27 and MKN45 cells after treating with bruceine D (BD) at concentrations of 0.4 and 1.2 μM for 48 h, respectively. **(F)** The schematic diagram of LINC01667 wild-type and mutant **(G)** The relative luciferase activity detected by the dual-luciferase reporter assay. **(H)** Cyclin E1 mRNA expression of LINC01667 overexpressing HGC27 and MKN45 cells after treating with BD at concentrations of 0.4 and 1.2 μM for 48 h, respectively. **(I)** The expression levels of Cyclin E1 were determined using the Western blot assay in HGC27 and MKN45 cells after treating with BD at concentrations of 0.4 and 1.2 μM for 48 h, respectively. α-Tubulin was used as control. The gray ratio of Cyclin E1/α-Tubulin was calculated. **(J)** The expression levels of Cyclin E1 were determined using Western blot assay in HGC27 and MKN45 cells after CCNE1 overexpression. **(K)** The relative mRNA expression levels of Cyclin E1 were determined using qRT-PCR in HGC27 and MKN45 cells after CCNE1 overexpression. **(L)** Cell viability was detected by using the MTT assay in HGC27 and MKN45 cells after CCNE1 overexpression and BD treatment. All data were used as mean ± SD, significant difference was tested by the two tailed and unpaired student's t-test. Error bars, $^{*}p < 0.05$, $^{**}p < 0.01$, and $^{***}p < 0.001$.

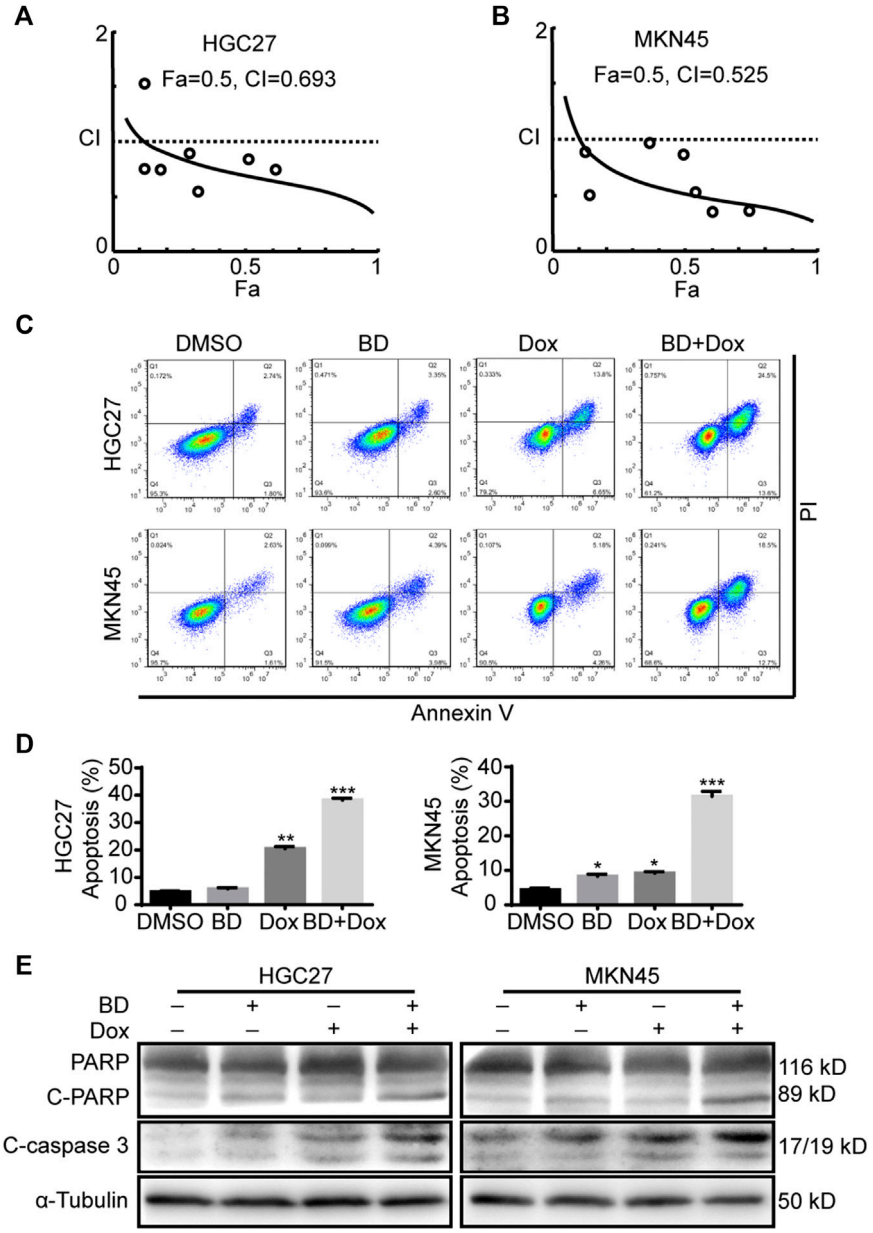

FIGURE 7 | Bruceine D (BD) enhances the chemosensitivity of gastric cancer cells to doxorubicin. **(A,B)** The combined index of BD and doxorubicin were calculated using the CompuSyn software in HGC27 **(A)** and MKN45 **(B)** cells. Fa = 0.5 and combination index (CI) < 1 represents synergy. **(C,D)** The apoptosis of cells was detected by flow cytometry. HGC27 and MKN45 cells were treated with BD and doxorubicin alone or in combination for 48 h, respectively. Dimethyl sulfoxide (DMSO) was used as control. Apoptotic rate of HGC27 and MKN45 cells was quantified. **(E)** The expression of apoptotic proteins, cleaved-PARP and cleaved-caspase3 in cells treated with BD and doxorubicin alone or in combination for 48 h, respectively. α-Tubulin was used as internal reference. All data were used as mean ± SD, significant difference was tested by the two tailed and unpaired student's t-test. Error bars, $^{*}p < 0.05$, $^{**}p < 0.01$, and $^{***}p < 0.001$.

assays indicated that BD inhibited the proliferation of gastric cancer cells in a dose-dependent manner. Soft agar assay showed that the colony size became lesser and smaller after BD treatment. Xenograft experiment showed that the tumors formed in nude mice were slower and smaller, and the weight and size of the tumor were significantly reduced after BD treatment. These results suggest that BD can inhibit the growth of gastric cancer cells *in vitro* and *in vivo*.

In recent years, lncRNAs has become a hot spot in tumor research. LncRNAs could be used as a key regulator of epigenetic regulation, transcription and translation to participate in a variety of physiological and pathological processes (Geisler and Coller, 2013; Cech and Steitz, 2014). In this experiment, transcriptome analysis showed that the expression of LINC01667 decreased significantly after BD treatment. LINC01667 is hardly expressed in gastric tissue, but LINC01667 is highly expressed in gastric

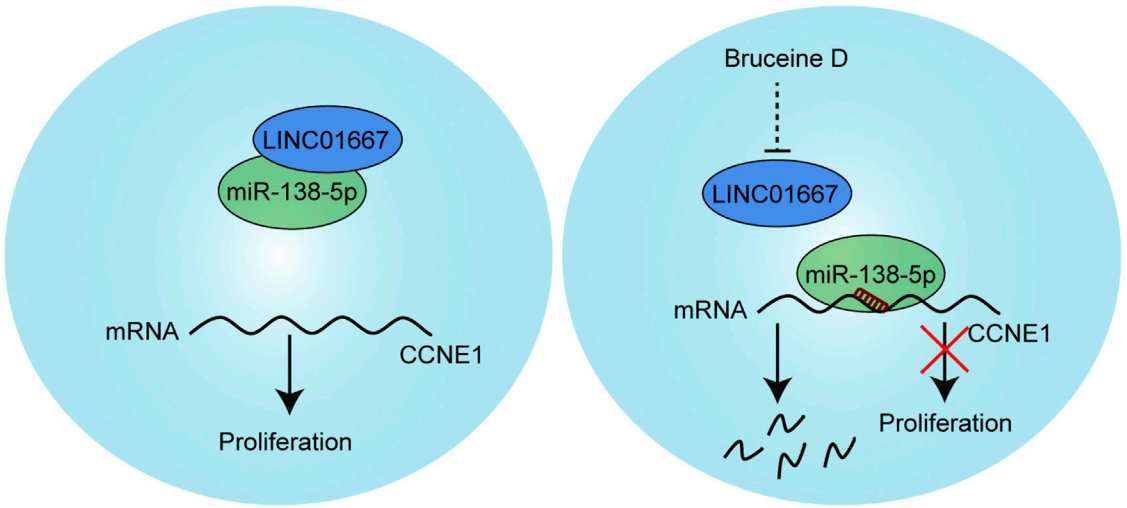

FIGURE 8 | Model of action for the BD/LINC01667/microRNA-138-5p (miR-138-5p)/Cyclin E1 regulatory axis in the modulation of cell proliferation in gastric cancer cells. Briefly, under normal conditions, LINC01667 can competitively adsorb miR-138-5p. When treated with bruceine D (BD), the expression of LINC01667 was down-regulated, and miR-138-5p combined with CCNE1 mRNA, which inhibited the expression of Cyclin E1 and inhibited the proliferation of cells.

cancer cells, which suggested that LINC01667 might play an oncogenic role in gastric cancer. MTT and BrdU assays further proved that LINC01667 could restore the inhibition of cell proliferation induced by BD treatment.

Recently, competitive endogenous RNA model has been proved to play a key role in tumorigenesis. In this model, lncRNA can influence other mRNA or lncRNA transcripts by competitively binding to miRNA response element (MRE) to affect post-transcriptional regulation (Cesana et al., 2011; Salmena et al., 2011). In order to explore the potential mechanism, we found that miR-138-5p targeted the mRNA of LINC01667 or Cyclin E1 through the TargetScanHuman 7.0 database. According to previous research reports, miR-138-5p plays an important role in cancer progress. MiR-138 can influence the progression of gastric cancer by regulating EGFR (Wang et al., 2018). LncRNA H19 sponges miR-138-5p, which directly targets SIRT1, and then affects progression of cervical cancer cells (Ou et al., 2018). Long non-coding RNA MCM3AP-AS1 promotes growth and migration through modulating FOXK1 by sponging miR-138-5p in pancreatic cancer (Yang M. et al., 2019). According to the target binding sites, we constructed LINC01667-WT and LINC01667-MUT double luciferase vectors. Next, dual-luciferase reporter assays showed that miR-138-5p could significantly reduce the luciferase activity of LINC01667-WT, compared with LINC01667-MUT. These experimental results showed that LINC01667 could target miR-138-5p.

Unlimited cell proliferation is one of the most distinctive features of tumor. Cell cycle is closely related to cell proliferation. Some studies have confirmed that the catalytic activity of CDK is regulated by Cyclins and CDK inhibitor (CKI), and the close cooperation between them is very important for the normal advancement of the cell cycle. Based on the above results from the cell cycle and Western blotting assays, we found that BD arrested gastric cancer cells in S phase by down-regulating Cyclin E1, Cyclin E2 and CDK2. CCNE1 (cyclin E1) mRNAs are significantly higher in GC tissues than in normal tissues in both Oncomine and The Cancer Genome Atlas (TCGA) datasets (Zhang et al., 2018) and this was also confirmed by the multiplex ligation-dependent probe amplification and fluorescence *in situ* hybridization (Ooi et al., 2017). Besides, it was also revealed that upregulated Cyclin E1 is highly associated gastric cancer development (Gu et al., 2010) and liver metastasis (Chang et al., 2009; Kim et al., 2019). In our study, qRT-PCR experiments showed that BD treatment could significantly reduce the expression of Cyclin E1, while overexpression of LINC01667 could restore the expression of Cyclin E1 to some extent. Besides, overexpression of CCNE1 also recovered cell proliferation inhibition induced by BD treatment to some extent. These results indicated that BD could inhibit the proliferation of gastric cancer cells through LINC01667/miR-138-5p/Cyclin E1 pathway. However, the binding activity and the association between miR-138-5p and CCNE1 mRNA should be further confirmed.

Cyclin E2 are also shown to be upregulated at the early stage of gastric cancer (Kumari et al., 2016). CDK2 may also contributes to gastric progression via promoting gluycolysis (Tang et al., 2018). In our study, these two factors were also significantly inhibited by BD treatment, indicating Cyclin E2 and CDK2 might also be the potential target genes. However, we did not found their connections with LINC01667. They might be affected by BD through other unknown mechanisms. Besides, whether there were other mechanisms except for LINC01667/miR-138-3p/CCNE1 needs to be explored in the future research.

Drug resistance to therapeutic drugs is one of the main reasons for the low efficacy of cancer treatment. Some studies have shown

that the extraction of traditional Chinese medicine can improve the drug sensitivity of cancer cells. Such as, scutellarin enhanced the sensitivity of prostate cancer cells to cisplatin (Gao et al., 2017). Corilagin sensitized epithelial ovarian cancer cells to paclitaxel and carboplatin treatment by inhibiting snail-glycolysis pathways (Jia et al., 2017). Triptolide enhanced the sensitivity of breast cancer cells to doxorubicin (Deng et al., 2018). Doxorubicin is one of the commonly used chemotherapeutic drugs in the treatment of gastric cancer (Murad et al., 1993). Therefore, we evaluated whether BD could enhance the chemosensitivity of gastric cancer cells to doxorubicin. We found that the apoptosis of cells treated with BD and doxorubicin was significantly higher than that treated with BD or doxorubicin alone. At the same time, the Western blot assay were carried out. The results showed that the expression of apoptotic proteins PARP and caspase-3 were significantly increased after combination treatment with BD and doxorubicin. Therefore, these results confirm that BD can enhance the chemosensitivity of gastric cancer cells to doxorubicin.

In summary, we identify that BD inhibits the proliferation of gastric cancer cells through the LINC01667/miR-138-5p/Cyclin E1 pathway (**Figure 8**). More importantly, BD can enhance the chemosensitivity of gastric cancer cells to doxorubicin. Our results provide a new perspective for the molecular pathogenesis of gastric cancer and initially suggest that BD may be a promising drug for the treatment of gastric cancer.

DATA AVAILABILITY STATEMENT

The original contributions presented in the study are included in the article/**Supplementary Material**, further inquiries can be directed to the corresponding authors.

ETHICS STATEMENT

The animal study was reviewed and approved by Animal Ethics Committee of Southwest University.

AUTHOR CONTRIBUTIONS

LL, ZD, LY, and HC study design; LL, PS, LT, JX, PH, and ZW acquisition of data; LL and ZD analysis and interpretation of data; LL and ZD drafting of the manuscript; LL and ZD statistical analysis; LY and HC funding and study supervision. All authors read and approved the final manuscript.

FUNDING

We are grateful for funding support from the National Natural Science Foundation of China (Nos. 31672496, 81201551, 81902664, 81872071, and 81672502), the Fundamental Research Funds for the Central Universities (Nos. XDJK2020B006 and SWU120009), the Research and Innovation Project of Graduate Students in Chongqing (No. CYS19136), the Eyas Program of the Youth Innovative Talents Cultivation in Chongqing (No. CY200237), the National Key Research and Development Program of China (Nos. 2017YFC1308600 and 2016YFC1302204), and the Natural Science Foundation of Chongqing (No. cstc2019jcyj-zdxmX0033).

SUPPLEMENTARY MATERIAL

The Supplementary Material for this article can be found online at: https://www.frontiersin.org/articles/10.3389/fphar.2020.584960/full#supplementary-material

REFERENCES

Agarwal, V., Bell, G. W., Nam, J. W., and Bartel, D. P. (2015). Predicting effective microRNA target sites in mammalian mRNAs. *Elife* 4, e05005. doi:10.7554/eLife.05005

Bray, F., Ferlay, J., Soerjomataram, I., Siegel, R. L., Torre, L. A., and Jemal, A. (2018). Global cancer statistics 2018: GLOBOCAN estimates of incidence and mortality worldwide for 36 cancers in 185 countries. *CA A Cancer J. Clin.* 68 (6), 394–424. doi:10.3322/caac.21492

Cech, T. R., and Steitz, J. A. (2014). The noncoding RNA revolution-trashing old rules to forge new ones. *Cell* 157 (1), 77–94. doi:10.1016/j.cell.2014.03.008

Cesana, M., Cacchiarelli, D., Legnini, I., Santini, T., Sthandier, O., Chinappi, M., et al. (2011). A long noncoding RNA controls muscle differentiation by functioning as a competing endogenous RNA. *Cell* 147 (2), 358–369. doi:10.1016/j.cell.2011.09.028

Chang, H. J., Choi, M. Y., Cho, M. H., Lee, K. E., and Lee, S. N. (2019). Molecular mechanism of chemoresistance and restoration in human gastric cancer cells. *J. Clin. Oncol.* 37 (15), e15544. doi:10.1200/Jco.2019.37.15_Suppl.E15544

Chang, W., Ma, L., Lin, L., Gu, L., Liu, X., Cai, H., et al. (2009). Identification of novel hub genes associated with liver metastasis of gastric cancer. *Int. J. Cancer* 125 (12), 2844–2853. doi:10.1002/ijc.24699

Cheng, Z., Yuan, X., Qu, Y., Li, X., Wu, G., Li, C., et al. (2017). Bruceine D inhibits hepatocellular carcinoma growth by targeting beta-catenin/jagged1 pathways. *Canc. Lett.* 403, 195–205. doi:10.1016/j.canlet.2017.06.014

Deng, Y., Li, F., He, P., Yang, Y., Yang, J., Zhang, Y., et al. (2018). Triptolide sensitizes breast cancer cells to Doxorubicin through the DNA damage response inhibition. *Mol. Carcinog.* 57 (6), 807–814. doi:10.1002/mc.22795

Dong, Z., Lei, Q., Yang, R., Zhu, S., Ke, X.-X., Yang, L., et al. (2017). Inhibition of neurotensin receptor 1 induces intrinsic apoptosis via let-7a-3p/Bcl-w axis in glioblastoma. *Br. J. Canc.* 116 (12), 1572–1584. doi:10.1038/bjc.2017.126

Dong, Z., Yang, J., Li, L., Tan, L., Shi, P., Zhang, J., et al. (2020). FOXO3a-SIRT6 axis suppresses aerobic glycolysis in melanoma. *Int. J. Oncol.* 56 (3), 728–742. doi:10.3892/ijo.2020.4964

Ferlay, J., Shin, H. R., Bray, F., Forman, D., Mathers, C., and Parkin, D. M. (2010). Estimates of worldwide burden of cancer in 2008: globocan 2008. *Int. J. Cancer* 127 (12), 2893–2917. doi:10.1002/ijc.25516

Gao, C., Zhou, Y., Jiang, Z., Zhao, Y., Zhang, D., Cong, X., et al. (2017). Cytotoxic and chemosensitization effects of Scutellarin from traditional Chinese herb *Scutellaria altissima* L. in human prostate cancer cells. *Oncol. Rep.* 38 (3), 1491–1499. doi:10.3892/or.2017.5850

Geisler, S., and Coller, J. (2013). RNA in unexpected places: long non-coding RNA functions in diverse cellular contexts. *Nat. Rev. Mol. Cell Biol.* 14 (11), 699–712. doi:10.1038/nrm3679

Gu, L.-q., Chang, W.-j., Han, Y.-f., Cai, H., Ma, L.-y., and Cao, G. (2010). Up-regulated expression of cyclin E1 is associated with gastric cancer development. *Acad. J. Second Mil. Med. Univ.* 30, 508–512. doi:10.3724/SP.J.1008.2010.00508

Hu, H., Dong, Z., Tan, P., Zhang, Y., Liu, L., Yang, L., et al. (2016). Antibiotic drug tigecycline inhibits melanoma progression and metastasis in a p21CIP1/Waf1-dependent manner. *Oncotarget* 7 (3), 3171–3185. doi:10.18632/oncotarget.6419

Huarte, M. (2015). The emerging role of lncRNAs in cancer. *Nat. Med.* 21 (11), 1253–1261. doi:10.1038/nm.3981

Hu, M., Li, K., Maskey, N. N., Xu, Z. G., Peng, C. W., Tian, S. F., et al. (2015). 15-PGDH expression as a predictive factor response to neoadjuvant chemotherapy in advanced gastric cancer. *Int. J. Clin. Exp. Pathol.* 8 (6), 6910–6918

Ilson, D. H. (2019). Advances in the treatment of gastric cancer: 2019. *Curr. Opin. Gastroenterol.* 35 (6), 551–554. doi:10.1097/MOG.0000000000000577

Jia, L., Zhou, J., Zhao, H., Jin, H., Lv, M., Zhao, N., et al. (2017). Corilagin sensitizes epithelial ovarian cancer to chemotherapy by inhibiting Snailglycolysis pathways. *Oncol. Rep.* 38 (4), 2464–2470. doi:10.3892/or.2017.5886

Kim, B., Shin, H. C., Heo, Y. J., Ha, S. Y., Jang, K.-T., Kim, S. T., et al. (2019). CCNE1 amplification is associated with liver metastasis in gastric carcinoma. *Pathol. Res. Pract.* 215 (8), 152434. doi:10.1016/j.prp.2019.152434

Kumari, S., and Puneet, Prasad, S. B., Yadav, S. S., Kumar, M., Khanna, A. K., et al. (2016). Cyclin D1 and cyclin E2 are differentially expressed in gastric cancer. *Med. Oncol.* 33, 40. doi:10.1007/s12032-016-0754-8

Lau, S. T., Lin, Z. X., Liao, Y., Zhao, M., Cheng, C. H., and Leung, P. S. (2009). Bruceine D induces apoptosis in pancreatic adenocarcinoma cell line PANC-1 through the activation of p38-mitogen activated protein kinase. *Canc. Lett.* 281 (1), 42–52. doi:10.1016/j.canlet.2009.02.017

Lazar, D. C., Taban, S., Cornianu, M., Faur, A., and Goldis, A. (2016). New advances in targeted gastric cancer treatment. *World J. Gastroenterol.* 22 (30), 6776–6799. doi:10.3748/wjg.v22.i30.6776

Murad, A. M., Santiago, F. F., Petroianu, A., Rocha, P. R., Rodrigues, M. A., and Rausch, M. (1993). Modified therapy with 5-fluorouracil, doxorubicin, and methotrexate in advanced gastric cancer. *Cancer* 72 (1), 37–41. doi:10.1002/1097-0142(19930701)72:1<37::aid-cncr2820720109>3.0.co

Ooi, A., Oyama, T., Nakamura, R., Tajiri, R., Ikeda, H., Fushida, S., et al. (2017). Gene amplification of CCNE1, CCND1, and CDK6 in gastric cancers detected by multiplex ligation-dependent probe amplification and fluorescence *in situ* hybridization. *Hum. Pathol.* 61, 58–67. doi:10.1016/j.humpath.2016.10.025

Ou, L., Wang, D., Zhang, H., Yu, Q., and Hua, F. (2018). Decreased expression of miR-138-5p by lncRNA H19 in cervical cancer promotes tumor proliferation. *Oncol. Res.* 26 (3), 401–410. doi:10.3727/096504017X15017209042610

Salmena, L., Poliseno, L., Tay, Y., Kats, L., and Pandolfi, P. P. (2011). A ceRNA hypothesis: the rosetta stone of a hidden RNA language? *Cell* 146 (3), 353–358. doi:10.1016/j.cell.2011.07.014

Shen, J. G., Zhang, Z. K., Wu, Z. J., Ouyang, M. A., Xie, L. H., and Lin, Q. Y. (2008). Antiphytoviral activity of where science meets business bruceine-D from *Brucea javanica* seeds. *Pest Manag. Sci.* 64 (2), 191–196. doi:10.1002/ps.1465

Tan, B., Huang, Y., Lan, L., Zhang, B., Ye, L., Yan, W., et al. (2019). Bruceine D induces apoptosis in human non-small cell lung cancer cells through regulating JNK pathway. *Biomed. Pharmacother.* 117, 109089. doi:10.1016/j.biopha.2019.109089

Tang, Z., Li, L., Tang, Y., Xie, D., Wu, K., Wei, W., et al. (2018). CDK2 positively regulates aerobic glycolysis by suppressing SIRT5 in gastric cancer. *Canc. Sci.* 109 (8), 2590–2598. doi:10.1111/cas.13691

Thrift, A. P., and El-Serag, H. B. (2019). Burden of gastric cancer. *Clin. Gastroenterol. Hepatol.* 18 (3), 534–542. doi:10.1016/j.cgh.2019.07.045

Utoguchi, N., Nakata, T., Cheng, H. H., Ikeda, K., Makimoto, H., Mu, Y., et al. (1997). Bruceine B, a potent inhibitor of leukocyte-endothelial cell adhesion. *Inflammation* 21 (2), 223–233. doi:10.1023/a:1027374321718

Wang, S., Hu, H., Zhong, B., Shi, D., Qing, X., Cheng, C., et al. (2019). Bruceine D inhibits tumor growth and stem cell-like traits of osteosarcoma through inhibition of STAT3 signaling pathway. *Cancer Med.* 8 (17), 7345–7358. doi:10.1002/cam4.2612

Wang, Y., Wu, Z. F., Wang, G. X., Wang, F., Liu, Y. T., Li, F. Y., et al. (2011). *In vivo* anthelmintic activity of bruceine A and bruceine D from brucea javanica against dactylogyrus intermedius (Monogenea) in goldfish (*Carassius auratus*). *Vet. Parasitol.* 177 (1-2), 127–133. doi:10.1016/j.vetpar.2010.11.040

Wang, Y., Zhang, H., Ge, S., Fan, Q., Zhou, L., Li, H., et al. (2018). Effects of miR1385p and miR2045p on the migration and proliferation of gastric cancer cells by targeting EGFR. *Oncol. Rep.* 39 (6), 2624–2634. doi:10.3892/or.2018.6389

Wei, L., Sun, J., Zhang, N., Zheng, Y., Wang, X., Lv, L., et al. (2020). Noncoding RNAs in gastric cancer: implications for drug resistance. *Mol. Canc.* 19 (1), 62. doi:10.1186/s12943-020-01185-7

Wu, J. R., Liu, S. Y., Zhu, J. L., Zhang, D., and Wang, K. H. (2018). Efficacy of *Brucea javanica* oil emulsion injection combined with the chemotherapy for treating gastric cancer: a systematic review and meta-analysis. *Evid. Based Comple. Alternat. Med.* 2018, 6350782. doi:10.1155/2018/6350782

Xiao, Z., Ching Chow, S., Han Li, C., Chun Tang, S., Tsui, S. K., Lin, Z., et al. (2014). Role of microRNA-95 in the anticancer activity of Brucein D in hepatocellular carcinoma. *Eur. J. Pharmacol.* 728, 141–150. doi:10.1016/j.ejphar.2014.02.002

Xie, J. H., Lai, Z. Q., Zheng, X. H., Xian, Y. F., Li, Q., Ip, S. P., et al. (2019). Apoptosis induced by bruceine D in human nonsmallcell lung cancer cells involves mitochondrial ROS mediated death signaling. *Int. J. Mol. Med.* 44 (6), 2015–2026. doi:10.3892/ijmm.2019.4363

Yang, J., Wei, X., Xu, J., Yang, D., Liu, X., Yang, J., et al. (2012). A sigma-class glutathione S-transferase from Solen grandis that responded to microorganism glycan and organic contaminants. *Fish Shellfish Immunol.* 32 (6), 1198–1204. doi:10.1016/j.fsi.2012.03.010

Yang, L., Lei, Q., Li, L., Yang, J., Dong, Z., and Cui, H. (2019). Silencing or inhibition of H3K79 methyltransferase DOT1L induces cell cycle arrest by epigenetically modulating c-Myc expression in colorectal cancer. *Clin. Epigenet.* 11 (1), 199. doi:10.1186/s13148-019-0778-y

Yang, M., Sun, S., Guo, Y., Qin, J., and Liu, G. (2019). Long non-coding RNA MCM3AP-AS1 promotes growth and migration through modulating FOXK1 by sponging miR-138-5p in pancreatic cancer. *Mol. Med.* 25 (1), 55. doi:10.1186/s10020-019-0121-2

Yu, Y. N., and Li, X. (1990). Studies on the chemical constituents of *Brucea javanica* (L.) Merr. *Yao Xue Xue Bao* 25 (5), 382–386 [in Chinese].

Zhang, H., Yang, J. Y., Zhou, F., Wang, L. H., Zhang, W., Sha, S., et al. (2011). Seed oil of *Brucea javanica* induces apoptotic death of acute myeloid leukemia cells via both the death receptors and the mitochondrial-related pathways. *Evid. Based Complement Alternat. Med.* 2011, 965016. doi:10.1155/2011/965016

Zhang, H. P., Li, S. Y., Wang, J. P., and Lin, J. (2018). Clinical significance and biological roles of cyclins in gastric cancer. *OncoTargets Ther.* 11, 6673–6685. doi:10.2147/ott.S171716

Zhang, J., Lin, L., Chen, Z., and Xu, R. (1980). Studies on the chemical-components of *Brucea-javanica*. *Planta Med.* 39 (3), 265.

Zhang, J. Y., Lin, M. T., Tung, H. Y., Tang, S. L., Yi, T., Zhang, Y. Z., et al. (2016). Bruceine D induces apoptosis in human chronic myeloid leukemia K562 cells via mitochondrial pathway. *Am. J. Cancer Res.* 6 (4), 819–826.

Zhu, S., Dong, Z., Ke, X., Hou, J., Zhao, E., Zhang, K., et al. (2018). The roles of sirtuins family in cell metabolism during tumor development. *Semin. Canc. Biol.* 57, 59–71. doi:10.1016/j.semcancer.2018.11.003

Conflict of Interest: The authors declare that the research was conducted in the absence of any commercial or financial relationships that could be construed as a potential conflict of interest.

frontiers in Pharmacology

REVIEW
published: 27 January 2021
doi: 10.3389/fphar.2020.613464

MicroRNAs and Natural Compounds Mediated Regulation of TGF Signaling in Prostate Cancer

Zeeshan Javed[1], Khushbukhat Khan[2], Amna Rasheed[3], Haleema Sadia[4], Shahid Raza[1], Bahare Salehi[5], William C. Cho[6]*, Javad Sharifi-Rad[7,8]*, Wojciech Koch[9]*, Wirginia Kukula-Koch[10], Anna Głowniak-Lipa[11] and Paweł Helon[12]*

[1]Office for Research Innovation and Commercialization, Lahore Garrison University, Lahore, Pakistan, [2]Atta-ur-Rahman School of Applied Biosciences (ASAB), National University of Sciences and Technology (NUST), Islamabad, Pakistan, [3]School of Basic Medical Sciences, Lanzhou University, Lanzhou, China, [4]Department of Biotechnology, Balochistan University of Information Technology, Engineering and Management Sciences, Quetta, Pakistan, [5]Medical Ethics and Law Research Center, Shahid Beheshti University of Medical Sciences, Tehran, Iran, [6]Department of Clinical Oncology, Queen Elizabeth Hospital, Hong Kong, China, [7]Phytochemistry Research Center, Shahid Beheshti University of Medical Sciences, Tehran, Iran, [8]Facultad de Medicina, Universidad del Azuay, Cuenca, Ecuador, [9]Chair and Department of Food and Nutrition, Medical University of Lublin, Lublin, Poland, [10]Department of Pharmacognosy, Medical University of Lublin, Lublin, Poland, [11]Department of Cosmetology, University of Information Technology and Management in Rzeszów, Rzeszów, Poland, [12]Branch in Sandomierz, Jan Kochanowski University in Kielce, Sandomierz, Poland

OPEN ACCESS

Edited by:
Yue Hou,
Northeastern University, China

Reviewed by:
Zhaoli Meng,
Jilin University, China
Yanqiang Wang,
Shanxi Medical University, China

***Correspondence:**
Bahare Salehi
bahar.salehi007@gmail.com
William C. Cho
chocs@ha.org.hk
Javad Sharifi-Rad
javad.sharifirad@gmail.com
Wojciech Koch
kochw@interia.pl

Specialty section:
This article was submitted to Pharmacology of Anticancer Drugs, a section of the journal Frontiers in Pharmacology

Received: *02 October 2020*
Accepted: *24 November 2020*
Published: *27 January 2021*

Citation:
Javed Z, Khan K, Rasheed A, Sadia H, Raza S, Salehi B, Cho WC, Sharifi-Rad J, Koch W, Kukula-Koch W, Głowniak-Lipa A and Helon P (2021) MicroRNAs and Natural Compounds Mediated Regulation of TGF Signaling in Prostate Cancer. Front. Pharmacol. 11:613464. doi: 10.3389/fphar.2020.613464

Prostate cancer (PCa) is with rising incidence in male population globally. It is a complex anomaly orchestrated by a plethora of cellular processes. Transforming growth factor-beta (TGF-β) signaling is one of the key signaling pathways involved in the tumorigenesis of PCa. TGF-β signaling has a dual role in the PCa, making it difficult to find a suitable therapeutic option. MicroRNAs (miRNAs) mediated regulation of TGF-β signaling is responsible for the TGF-*β* paradox. These are small molecules that modulate the expression of target genes and regulate cancer progression. Thus, miRNAs interaction with different signaling cascades is of great attention for devising new diagnostic and therapeutic options for PCa. Natural compounds have been extensively studied due to their high efficacy and low cytotoxicity. Here, we discuss the involvement of TGF-*β* signaling in PCa with the interplay between miRNAs and TGF-β signaling and also review the role of natural compounds for the development of new therapeutics for PCa.

Keywords: prostate cancer, miRNAs, transforming growth factor-beta signaling, natural compounds, therapeutics, biomarkers

INTRODUCTION

Prostate cancer (PCa) is the fifth leading cancer cause of death worldwide. The mortality associated with PCa is strongly related to age. The highest incidence of PCa is observed in men over age 65 years. The recent advances in the field of genetic technologies have enabled us to delineate the genomic complexity of PCa (Rawla, 2019). It is a multifaceted disease orchestrated by a plethora of both intrinsic and extrinsic factors (Prasad et al., 2020). The complex molecular landscape of PCa renders it to escape cellular defenses and continue proliferation. Tumor development and progression is regulated by a number of cellular signaling pathways (Javed et al., 2020). Transforming growth factor-beta (TGF-β) has emerged as an essential modulator and mediator of the key steps of development of cancer such as the epithelial–mesenchymal transition (EMT), migration, and invasion (Behbahani et al., 2017). The TGF-β has a dual role in cancer. It has recently been

shown that the dual nature of TGF-β can be due to its interaction with microRNAs (miRNAs) (Hao et al., 2019). These are small noncoding RNA in 21–25 nt that are crucial for the plethora of cellular processes (Javed et al., 2015). TGF-β signaling has been reported to regulate the formation of microprocessor complex *via* recruitment of mother against decapentaplegic homolog (SMADs) and influence the processing of pri-miRNAs (Miscianinov et al., 2018). PCa is the second most prevalent cancer in men after lung cancer, at which the cancer biomarker, that is, prostate specific antigen (PSA), is most commonly used for the PCa diagnosis. It has recently come to limelight that TGF-β signaling has broader implications in PCa. Both *in vitro* and *in vivo* approaches have shown the importance of TGF-β signaling as a new therapeutic approach for PCa (Hamidi et al., 2017). It is known that traditional medicines have been employed for centuries to treat cancers (Li and Weng, 2017). Interestingly, in recent times, the natural products and their derivatives have shown a tremendous potential for the treatment of PCa. (Leichter et al., 2017; Li et al., 2018a; Lu et al., 2018). Here, we discuss the interaction between TGF-β signaling and miRNAs in PCa, and also review the importance of natural compounds as a new therapeutic intervention in PCa.

PCA TREATMENT AND PROGNOSIS

PCa is an androgen-dependent cancer; it originates from the peripheral zone of the prostate. Alterations in the genetic framework of PCa lead to variations in the tumor physiology, including different tumor grades, aggressiveness of the tumor, and various treatment options (Hayes and Barry, 2014). Treatment options for PCs include prostatectomy, chemotherapy, hormonal therapy and radiation therapy. For low-volume and low-grade cancers, palliative therapy is also an option while androgen deprivation therapy (ADT) which includes the bilateral orchiectomy with androgen antagonist or agonist of GnRH is used for advanced grade prostate tumors. In high-grade metastatic prostate tumors, a combination of ADT and chemotherapy is used. Castration-resistant PCas involve different second-line treatments which include chemotherapy, antiandrogen therapy, steroid inhibitors, immunotherapy, and radioactive treatments (Mottet et al., 2017). Tumor grades and stage of disease determine the prognosis of PCa patients. Majority of the people suffering from PCa undergo organ-confined surgery and radiation therapy (Donovan et al., 2016). The survival frequency of PCa patients over the span of five years has been reported to be 27–53%. In patients with advanced grade prostate tumor, the survival and recurrence of diseases is measured by the relative decrease in PSA levels and response to ADT (Matulewicz et al., 2017).

TGF-β SIGNALING IN CANCER

The TGF-β superfamily involve in development and differentiation of various mammalian cells. It consists of a broad range of proteins, such as the bone morphogenetic proteins (BMPs), anti-muellerian hormones (AMH), activins, growth factors, differentiation factors, and isoforms of TGF-β (TGF-β1, TGF-β2, and TGF-β3) that act as regulators of diverse cellular processes. This superfamily has been reported to orchestrate the key cellular processes and interactions (development, differentiation, migration, invasion, apoptosis, and immune responses) (Nacif and Shaker, 2014). TGF-β signaling has been reported for the tissue homeostasis (Xu et al., 2018). The role of TGF-β in cancer is debatable as it can either be tumor suppressor or oncogenic (Drabsch and Ten Dijke, 2011). The complex molecular landscape of cells along with the varied extrinsic and intrinsic factors determines TGF-β role. During the early stages of development, the TGF-β signaling plays a constructive role and facilitates differentiation and development of cells; however, with the passage of time, TGF-β signaling plays a destructive role through promulgation of metastasis and invasiveness in various tissues. This complex behavior of TGF-β signaling has been referred to as TGF-β paradox (Tian and Schiemann, 2009; Gong et al., 2015). Abrogation in the TGF-β signaling cascade triggers the development of PCa (Barrett et al., 2017) during the later stages of life. This has led scientists to focus on the intricate behavior of TGF-β in the progression of PCa and other tumors. Recent technological advances enabled us to target TGF-β signaling for possible therapeutic intervention. Inhibiting TGF-β seems to be a promising strategy for the treatment of PCa.

Three isoforms of TGF-β are having distinctive functions and play a crucial role in cellular growth (Akhurst, 2017). The latency associated protein (LAP) regulates the activation of TGF-β receptor through formation of latent TGF-β–binding protein (LTBP) (Nickel et al., 2018). The activated TGF-β then triggers either canonical or noncanonical TGF-β signaling, which involves activation of Smads (Smads 2,3 and 4) in case of canonical TGF-β signaling, while the non-canonical TGF-β signaling does not involve the activation of Smads (Massagué, 1998; Lodyga and Hinz, 2020). The noncanonical TGF-β signaling mechanistically promotes the activation of phosphatidylinositol-3-kinase/AKT/mammalian target of rapamycin (PI3K/AKT/mTOR), Janus kinase and p38 (JNK/P38), Rho-GTPase, and mitogen-activating protein kinases (MAPK).

The noncanonical signaling pathway is triggered by the same TβRI and TβRII complex that mechanistically promotes the activation of the broad range of molecular cascades such that the conjointly canonical and noncanonical signaling regulates a myriad of cellular functions ranging from posttranslational modifications to the binding of proteins to the target genes. TGF-β signaling plays a crucial role in the cellular development *via* inhibiting cellular growth. Loss of function mutations in TGF-β pathway has been reported to trigger uncontrolled cellular growth that ultimately leads to the development of tumor. Abnormal TGF-β signaling has been reported to accelerate carcinogenesis (Zhang et al., 2013). miRNAs contribute to the transcriptional activity of the TGF-β pathway, indicating functional links between short noncoding RNAs and TGF-β pathway. (**Figure 1**)

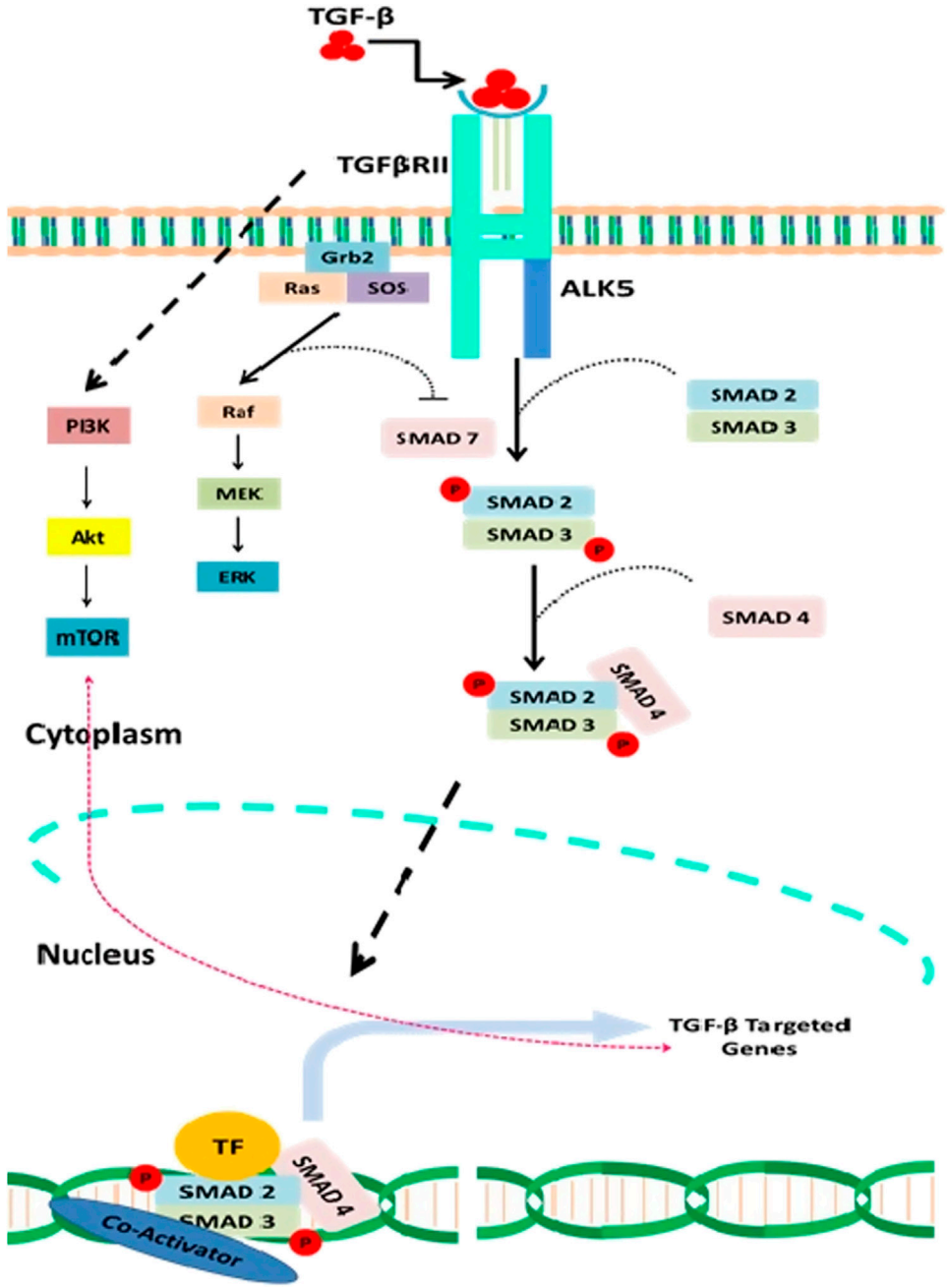

FIGURE 1 | A detail description of both canonical and noncanonical TGF-β signaling and interaction of natural compounds in the regulation of this signaling cascade at various levels. Natural compounds such as the resveratrol modulate TGF-β pathway by inhibiting the receptor activity such as the attachment of TGF-β to TGF-βRII and thus prevent the downstream activation of Smads. Curcumin and Nobilitin both modulate Smad2/3/4 and prevent the activation of TGF-β pathway signaling genes such as the TWIST1, SNAIL, and SLUG. Caricoside E blocks the formation of Smad complex and their translocation to the nucleus. Arctigenin inhibits the TGF-β–mediated activation of ERK and thus triggers apoptosis. Baicalin has also been reported that inhibit TGF-βRII expression and thus downstream signaling of TGF-β pathway.

ALTERED TGF-β SIGNALING IN PCa

TGF-β signaling is responsible for growth, proliferation, differentiation, metastasis, invasion, and apoptosis of both stromal and epithelial cells of prostate tissue (Barrack, 1997). Alterations in TGF-β signaling result in the development of PCa. TGF-β1 has been documented to be overexpressed in PCa. There was an increased level of TGF-β1 protein in tissue, serum, and urine of PCa patients (Reis et al., 2011; Liu et al., 2014). TGF-β1 increased levels curtail the grade, stage, invasiveness,

angiogenesis, and metastasis of PCa (Reis et al., 2011). In addition, TGF-β1 expression also correlates with the survival rates of the patients. Loss or downregulation of TGF-β receptors is the most frequent alteration observed in PCa. Nearly 30% of PCa have altered or downregulated the expression of TGF-β receptors (Yumoto et al., 2016). Furthermore, expression of TGFβR1 and TGFβR2 was low in PCa with metastatic potential as compared to localized primary tumors. TGFβR2 upregulation promotes apoptosis and inhibits metastasis in PCa cells *via* activation of caspase-1 (Pu et al., 2009). TGFβR2 activates the expression of TGF-β1, a precursor for the activation of caspase-mediated apoptosis. However, downregulation of TGFβR2 promotes malignant transformation in PCa cells (Pu et al., 2009). These findings suggest that TGFβR2 downregulation plays a pivotal role in the progression of resistant PCa cells. TGFβR2 has proven to be a tumor suppressor gene. Hypoxic activation of DNA methyltransferases is the key enzyme responsible for the downregulation of TGFβR2 in PCa cells. DNA methyltransferases triggers the hypermethylation of the promoter region of TGFβR2 which in turn inhibits gene activation (Brattain et al., 1996). Prior to this, it was reported that mutations in the promoter region of TGFβR2 led to the downregulation of this apoptosis-inducing gene. In addition to TGFβR2, downregulation of TGFβR3 is the most prevalent modification of the TGF-β cascade in PCa (Brattain et al., 1996). Downregulation of TGFβR3 promotes invasiveness, motility, and metastasis of PCa cells both *in vitro* and *in vivo* (Turley et al., 2007). It is reported that in normal prostate epithelial cells, downregulation of TGFβR3 expression resulted in the development of cancer stem cell phenotype and impeded cell to cell contact (Sharifi et al., 2007). Testosterone and dihydrotestosterone (DHT) are the activators of androgen receptor (AR) signaling. AR is a nuclear receptor whose activations result in its translocation to the nucleus where it modulates the expression of the target genes directly or indirectly. AR-mediated direct expression of target genes includes binding to AR–binding elements (AREs) and genes, while the indirect expression involves the regulation of various transcription factors. TGF-β signaling interacts with AR signaling and regulates it to certain extent. In PCa, the expression of TGF-β–targeted genes is influenced by AR signaling. SMAD3 interacts with AR and impedes SMAD3 binding to the SBEs (SMAD-binding elements) (Chipuk et al., 2002). DHT has been reported to inhibit the expression of TGFβR2. The DHT-mediated attenuation of the expression of TGFβR2 in turn decreases the binding of SP1 to the promoter genes. The downregulation of TGFβR2 promotes the apoptosis in prostate adenocarcinoma cells *via* upregulation of TGFβR2-targeted genes such as the cyclin Ds, Bcl-xL, and caspase-3 (Song et al., 2008). Abrogation in the AR signaling leads to cell survival, growth, and motility in PCa cells. The differentiation of the PCa cells is affected by the defected AR signaling which increases the overexpression of TGF-β and triggers growth, viability, aggressiveness, and invasiveness of the androgen-resistant PCa cells. TGF-β and AR synergistically stimulate apoptosis in PCa cells overexpressing TGFβR2 (Steiner and Barrack, 1992). The interplay between AR and SMAD4 proteins synergistically stimulates apoptosis in PCa cells with overexpressed TGFβR2 (Zhu and Kyprianou, 2010). It has been documented that administration of DHT to PC-3 cells, can lead to activation of EMT through interaction with SNAIL protein. The DHT administration increases the expression of N-cadherin which in turn inhibits the expression of E-cadherin and beta catenin and stimulates the activation of EMT. In addition, TGF-β signaling interacts with AR signaling pathway to facilitate the expression of TWIST1 that triggers the activation of EMT in PCa cells (Shiota et al., 2012). These findings indicate that TGF-β signaling has a decisive role in promoting invasiveness of PCa cells. The tumor cells employ a vast range of strategies to escape apoptosis and retain progressive growth and invasiveness (Hu et al., 2014). The tumorigenic prostate epithelial cells escape the apoptotic TGF-β signaling *via* constitutive activation of Akt pathway. The activated Akt pathway prevents the nuclear translocation of TGF-β–regulated Smad3 and arrest the growth of proteins such as the p21. The PI3K/Akt/mTOR pathway activates EMT in PCa cells through modulating the expression of TGF-β (Ao et al., 2006). Downregulation of PI3K/Akt/mTOR results in the inhibition of TGF-β–induced expression of vimentin. These in turn promote the downregulation of keratin and thus increase invasiveness of the tumor cells. Nuclear factor-kappa B (NF-κβ) has also been reported to activate EMT in PCa cells through its interplay with TGF-β signaling. It has been reported that overexpression of NF-κβ is modulated by the overexpression of TGF-β. The NF-κβ expression elevates the synthesis of vimentin and increases metastasis and invasion in PCa cells (Ao et al., 2006). Inhibition of either TGF-β or NF-κβ suppressed the invasion of cancer cells and the EMT process.

INTERPLAY BETWEEN TGF-β PATHWAY AND MIRNAS IN PCa

miRNAs form a class of endogenous, small (19–25 nucleotides), single-stranded, noncoding RNA molecules (Finotti et al., 2019), which progressively contribute to a vast range of critically important biological events such as development (Wienholds and Plasterk, 2005; Cho et al., 2019), proliferation (Zhuang et al., 2018), differentiation (Li et al., 2018b), apoptosis (Slattery et al., 2018), signal transduction (Barbu et al., 2020), and many more. Expression patterns of miRNAs are linked with a wide range of anomalies; thus, screening and characterization of miRNAs can serve as a potential diagnostic and therapeutic tool (Dwivedi et al., 2019). Till date, more than 25,000 miRNA sequences have been identified, and this number is expected to grow. According to an estimation, 3–4% of human genome comprises miRNAs (Valinezhad Orang et al., 2014). These miRNAs interfere with numerous key regulators of cellular processes by binding with posttranscriptional products. For this reason, miRNAs are considered as important biomarkers for many cancers, including PCa. Here, we shall focus on the interplay between various miRNAs and TGF-β signaling regulators with a focus on PCa.

Growing bodies of evidence have revealed multiple miRNAs–TGF-β checkpoints that control TGF-β signaling in different manners and intrinsically control the progression of PCa. For instance, SMAD family appeared to be the major target of miRNAs. The miRNAs can affect progression of PCa in individual or in combination with other miRNAs. Moreover, many miRNAs may interact in direct or indirect manners. Overexpression of miR-486-5p downregulates the expression of SMAD2 to promote cell pre-filtration in PCa which was reversed by knocking miR-486-5p (Yang et al., 2017). Another miRNA named miR-505-3p has the ability to interact with both SMAD2 and SMAD3 to contribute in PCa progression (Tang et al., 2019). MiR-19a-3p is a tumor suppressor miRNA that targets the SMAD2 and SMAD4 resulting in inactivation of TGF-β and suppression of PCa (Wa et al., 2018). Interactions of miRNAs with TGF-β pathways also indirectly controlled by other key players as well. For instance, TR4, a transcription regulator, can suppress the expression of miR-373-3p which otherwise would inhibite SMAD3 through inhibition of TGF-βR2 (Qiu et al., 2015). Interestingly, miRNAs can work in clusters to regulate tumor progression as well. For instance, a cluster of miR-15a/16 controls TGF-β signaling by downregulation of *p*-SMAD3, ACVR2A, Snail, and Twist, resulting in attenuated expression of TGF-β–dependent genes MMP2 and E-cadherin. This condition leads to the inhibition of EMT and invasion of PCa in LNCaP cells (Jin et al., 2018). Similarly, another miRNA cluster i.e., miR-122/132 downregulates SOX4 and disrupts the EMT process to suppress PCa (Fu et al., 2016). On the other hand, single miRNAs are also capable of controlling progression of PCa by interacting with TGF-*ß*. For example, miR-34 interacts with TGF-*ß* signaling through SMAD3 and suppresses PCa (Fang et al., 2017). Just like SMAD3, SMAD4 is also a vital target of many miRNAs. A study has shown that overexpression of miR-1260b suppressed SMAD4 and promoted PC progression, whereas genistein-induced downregulation of miR-120b resulted in increased expression of SMAD4 and sFRP1, hence promoting apoptosis (Hirata et al., 2014b). Hyperglycemia-induced overexpression of miR-301a also suppresses p21 and SMAD4 which result in G1/S cell cycle transition and cell proliferation ultimately (Li et al., 2018c). Another miR-205 targets 3′UTR of SMAD4 and downregulates its expression to promote PCa (Zeng et al., 2016).

Apart from the SMAD family, miRNAs also interact with TGF-β receptors. Hypoxia-induced elevated levels of miR-93 promote PCa through degradation of TGFβR2 (Zhou et al., 2018). miR-133b plays its role in the suppression of PCa by downregulation of TGFβR1 and TGFβR2. Attenuated expressions of miR-133b lead to activation of TGF-β signaling and progression of PCa (Huang et al., 2018). TGFRβR2 is down regulated by a number of miRNAs, resulting in the progression of PCa. For example, miR-21 in positive feedback loop with AR downregulates TGFRβR2 and promotes PCa (Mishra et al., 2014). miR-212 has been reported to down regulate the expression of heterogenous nuclear ribonuclear protein H1 (hnRNPH1), a splicing protein vital for the growth and progression of PCa. Ectopic expression of miR-212 mimic directly modulated the expression of hnRNPH1 transrcipts which in turn reduced the expression of AR splice variant AR-V7 in PCa cells. The hnRNPH1 protein in conjunction with AR promotes the expression of steroid receptor coactivator-2 (SRC-3) vital for the activation of AR–regulated genes (Yang et al., 2016). Another miRNA named miR-2909 promotes PCa by interacting with 3′-UTR of sequence of TGFRβR2 and resulting in its downregulation. Moreover, overexpression of miR-2909 also results in decreased expression of SMAD3, further verifying its role in tumor progression (Ayub et al., 2017). Recent advances in the field of phytochemistry have begun to scratch the surface of molecular oncology. The natural compounds pose a wide range of therapeutic benefits that can help in culminating cancer. Interaction among miRNAs, natural compounds, and TGF-β signaling cascade is an emerging avenue for devising precision medicines for various cancers. The miRNAs and natural compounds can modulate the expression of TGF-β–associated signaling molecules.

Carnosol (CAR) is the main compound derived from the rosemary plant. It is a phenolic diterpene with strong antiproliferative ability both *in vitro* and *in vivo*. Data have suggested that carnosol can be implemented as a therapeutic option for the glioblastoma cells (Giacomelli et al., 2016). CAR can regulate a broad range of cellular processes affiliated with cancer proliferation, stemness, invasion, and metastasis through its interaction with key signaling pathways and miRNAs. Accumulating evidences have suggested that CAR has the ability to regulate the expression of miR-200c. miR-200c has been investigated for its role in modulation of TNF-α/TGF-β signaling and upregulated the expression of key downstream genes responsible for EMT (Snail, Slug, Twist, and ZEB1) *in vitro* (Giacomelli et al., 2017). Osthole is a natural coumarin obtained from the *Cnidium* plant. It has tremendous antiproliferative ability as it can reduce the tumor aggressiveness and metastasis. Osthole has the ability to suppress growth, metastasis, and EMT in PCa *via* modulating the expression of TGF-β/AkT/MAPK. Osthole-mediated downregulation of EMT promoter genes Snail, and miRNA-23a-3p triggers growth arrest and apoptosis in PCa cells (Wen et al., 2015). The data regarding the interplay between miRNA/TGF-β/natural compounds in PCa are scarce and require more research to be done. **Table 1** shows the miRNAs and their interplay with TGF-β signaling and their effect on PCa status.

NATURAL COMPOUNDS IN PCa

The effectiveness of natural compounds in curbing various diseases including cancers has been proven experimentally (Salehi et al., 2019). In recent years, there are more attentions in elucidating therapeutic efficacy of natural compounds in PCa (Bayala et al., 2020; Zhang et al., 2020). These compounds target different pathways in cancer cells that are being exploited by such cells to ensure survival, growth, and also acquisition of metastatic capabilities. Inhibition of these pathways results in metastatic reversal, tumor growth regression, and apoptosis (Lajis et al., 2020) (**Table 2**).

TABLE 1 | List of miRNAs and TGFβ signaling to control PCa.

miRNA	Target	Effect on PCa	References
miR-486-5p	SMAD2	Upregulate	(Yang et al., 2017)
miR-505-3p	SMAD2 and SMAD3	Upregulate	(Tang et al., 2019)
miR-19a-3p	SMAD2 and SMAD4	Downregulate	(Wa et al., 2018)
miR-373-3p	TR4 and SMAD3	Downregulate	(Qiu et al., 2015)
miR-15a/16	pSMAD3	Upregulate	(Jin et al., 2018)
miR122/132	SOX	Downregulate	(Fu et al., 2016)
miR-34	SMAD3	Downregulate	(Fang et al., 2017)
miR1260b	SMAD4	Upregulate	(Hirata et al., 2014b)
miR301a	SMAD4	Upregulate	(Li et al., 2018c)
miR-205	SMAD4	Upregulate	(Zeng et al., 2016)
miR-93	TGFβR2	Upregulate	(Xu et al., 2018)
miR-133b	TGFβR1 and TGFβR2	Upregulate	(Huang et al., 2018)
miR-21	TGFβR2	Upregulate	(Mishra et al., 2014)
miR-2909	TGFβR2 and SMAD3	Upregulate	(Ayub et al., 2017)
miR-539	SMAD4 and DLX1	Downregulate	(Sun et al., 2019)
miR-582-3p and miR-582-5p	SMAD2, SMAD4, TGFβR1, and TGFβR2	Downregulate	(Huang et al., 2019)
miR-181a	TGFβR2	Upregulate	(Zhiping et al., 2017)
miR-221-5p	EMT (E-Cadherin, N-Cadherin, vimentin, Zinc finger homeobox 2 (ZEB2), SNAIL1/2, and TWIST	Downregulate	(Kiener et al., 2019)
miR-96	TGFβR2	Upregulate	(Siu et al., 2015)
miR-1 and miR-200	EMT (SLUG)	Downregulate	(Liu et al., 2013)
miR-183	SMAD4 and Dkk-3	Upregulate	(Ueno et al., 2013)
miR-485	Smurf-2 and TGFβR1	Downregulate	(Wang et al., 2018a)
miR-155	SMAD2	Downregulate	(Ji et al., 2014)

TABLE 2 | List of natural compounds, their sources, and pathway modulated in PCa.

Natural compound	Source	Pathway	References
Nobiletin	Citrus peels	TLR4 pathway	(Deveci Ozkan et al., 2020)
Curcumin	*Curcumin longa*	NF-Kb pathway and AR pathway	(Lajis et al., 2020)
Resveratrol	Grapes and berries	NF-Kb pathway	(Khusbu et al., 2020)
Daucosterol	*Crateva adansonii* DC	PI3K/Akt pathway	(Zingue et al., 2020)
Silibinin	*Silybum marianum*	PI3K/Akt pathway, ERK pathway, and JAK/STAT pathway	(Sherman et al., 2020)
Plectranthoic acid	*Ficus microcarpa*	TGF-β signaling and RAC1 signaling pathway	(Akhtar et al., 2018)
Osthole	*Cnidium monnieri*	TGF-β signaling and PI3k/AkT/mTOR pathway	(Wen et al., 2015)
Genistein	Soyabeans	TGF-β signaling, Smad4, and p38 MAPK	(Chen et al., 2018)
Oxymatrine	*Sophora japonica*	TGF-β signaling and Smad signaling	(Liu et al., 2016)
Tannic acid	Oak tree	TGF-β signaling, Smad signaling, SNAIL, and vimentin	(Pattarayan et al., 2018)
Paeoniflorin	*Paeonia lactiflora*	TGF-β signaling, Smad2/3 signaling inhibition, SNAIL, e-cadherin, and MMP-9 expression	(Wang et al., 2018b)

Natural compounds have been employed for the treatment of various human diseases for centuries. They have been found to be experimentally effective against different cancers. A plethora of studies have been conducted to delineate the complex interaction of natural compounds with molecular landscape of tumor cells both *in vitro* and *in vivo*. This has enabled researchers to determine novel compounds which can inhibit tumor growth, invasiveness, and metastasis. PCa is a complex disease orchestrated by a wide range of intrinsic and extrinsic factors. In PCa, the tumor growth is slow and has a persistently long latency period. These characteristics make PCa suitable for integration of natural compounds with other existing therapies for managing disease progression and mortality. The imbalance between abrupt cellular growth and apoptosis is the hallmark of PCa. Several oncogenes are overexpressed in PCa that lead to transformation of benign tumors to more aggressive metastatic PCa through suppression of the proapoptotic proteins. These changes trigger resistance to chemotherapy and radiotherapy. Natural compounds have been employed as adjuvants in combination with chemotherapy and radiotherapy to resensitize tumor cells toward treatment and also reduce drug resistance. There are a number of medicinal plants and their derivatives that have been reported to hold great therapeutic potential for PCa treatment. A phytochemical (amygdalin) present in the kernals of the member Rosaceae and prunasin has been found effective to reduce proliferation in PCa cell lines LnCaP and DU-145. Further insight into the tumor suppressor potential of amygdalin revealed that it reduced Bcl-2 and α6 integrin expression, and increased the cell cycle proteins (cyclin A, cyclin B, and cdk1) at G1-phase, resulting in the inhibition of growth, metastasis, adhesion, and chemotaxis (Saleem et al., 2018). Despite this, there are several cytotoxic effects caused

by amygdalin. Leaf extracts of *Withania coagulans*, with anolides, were also reported to have antiproliferative, anti-migratory, and pro-apoptotic activities in DU-145 and PC-3 cells (Rehman et al., 2019). Caspase-dependent apoptosis is induced by ethanol extracts of *Hizikia fusiforme* in PC-3 cells where it downregulated c-Flip and promoted reactive oxygen species (ROS) production (Choi et al., 2020). Daucosterol obtained from *Crateva adansonii* has been reported to suppress growth, proliferation, and metastasis in LNCaP, DU-145, and PC-3 cell lines through upregulation of Bax protein and modulation of PI3K/AkT/mTOR pathway (Zingue et al., 2020). Daucosterol also phosphorylates JNK and elicits autophagy-induced apoptotic response (Gao et al., 2019). Phenols, coumaric acid and ascorbic acid, found in *Rosa canina*, bring about G1-phase growth arrest and induce intrinsic apoptosis by significantly reducing mitochondrial membrane potential (90%) and caspase-3 and caspase-7 activation in PC-3 cells (Kilinc et al., 2020). The extracts derived from *Lespedeza bicolor* induced G1-phase growth arrest *in vitro* inhibiting CDKs at the posttranscriptional or posttranslational level (Dyshlovoy et al., 2020). Cytotoxicity is one major stumbling block regarding the treatment of the PCa. Several natural compounds in combination with chemotherapy have been proven effective to reduce cytotoxicity and chemo-driven side effects. Licorice obtained from *Glycyrrhiza glabra* prevented tumor proliferation in PC-3 cell when administrated along with adriamycin (Gioti et al., 2020). Licorice also induced chemosensitivity in cisplatin-resistant DU-I45 and PC-3 cells (Martínez-Martínez et al., 2019). Docetaxel and thymoquinone reduced chemoprevention *in vitro*. A combination of the above reduced chemoresistance in C4-2B and DU-145 cells through modulation of PIK2/Akt axis (Singh et al., 2019). Neferine obtained from *Nelumbo nucifera* triggered apoptosis in DU-145 cell through enhancement of apoptosis *via* modulation of TRAIL and phosphorylation of JNK (Nazim et al., 2020). Excelsanone, an isoflavonoid found in the bark of *Erythrina excelsa*, has been tested for its anticancer properties in PCa cell lines DU-145 and PC-3 cells, and enhanced cytotoxicity (Gbaweng et al., 2020). Phytoalexin resveratrol, abundantly present in grapes and berries, halts EMT in PCa. It induces the lysosomal degradation of TRAF6 and indirectly suppresses NF-κB signaling and the transcription of SLUG which are among the main drivers of metastasis. Exposure of resveratrol in PC-3 and DU-145 cells reduced cell proliferation and viability (Khusbu et al., 2020). Another compound, ellagic acid, found in black raspberries prevented tumor growth in mice but at very high dose. Rest of the raspberry compounds such as protocatechuic acid and anthocyanin cyanidin-3-rutinoside did not have any recuperative effect on carcinogenesis both *in vivo* and *in vitro* (Eskra et al., 2020).

NATURAL COMPOUNDS ON THE BASIS OF ANDROGEN STATUS OF THE CANCER

The effectiveness of natural compounds is also evaluated on the basis of androgen status of the cancer. A nonpolar flavonoid, nobiletin, present in citrus peels has been reported to curb PCa growth by suppressing inflammation. The efficacy of its therapeutic influence is dependent on androgen status of PCa. Androgen-dependent LNCaP cell line is reported to be more sensitive to nobiletin than androgen-independent, metastatic PC-3 cell line. Mechanistically, it targets TLR4/TRIF/IRF3 and TLR9/IRF7 pathways by inhibiting TLR4, IRF3, TLR9, and IRF7 expression at the transcriptional level. Also, it reduces the mRNA and protein levels of IFN-α and IFN-β, which are downstream targets of TLR4 signaling cascade (Deveci Ozkan et al., 2020). Similarly, *Aegiceras corniculatum*–derived sakurasosaponin is reported as AR inhibitor. In sakurasosaponin-treated cell lines (LNCaP, C4-2, and 22Rv1), the rate of androgen receptor expression, along with few target genes (PSA, NKX3.1, and TMPRSS2), was decreased with increased dose and time. Furthermore, its treatment also induced intrinsic apoptosis by reducing mitochondrial membrane potential and Bcl-Lx expression. *In vivo* analysis revealed that it significantly attenuated tumor growth in AR-positive xenografted mice than in AR-negative xenografted mice (Song et al., 2020). Total saponins from *Paris forrestii* (PST3) constituting polyphillin D, dioscin, ophiopogonin C′, polyphyllin F, formosanin C, and glucopyranoside are isolated by Xia and team. They treated PC-3 and LNCaP cells with PST3 and found that it significantly reduced cell proliferation and promoted anti-invasiveness at minimum 1 μg/mL in LNCaP cells and 2 μg/mL in PC-3 cells. Its proapoptotic influence was in a dose-dependent manner in both cells lines (Xia et al., 2020). Resveratrol induces apoptosis in androgen-independent prostate cells by enhancing the expression of DUSP-1 which further suppresses NF-κB signaling and COX-2 expression (Martínez-Martínez et al., 2019). Curcumin is a widely studied natural compound in numerous cancers. In PCa, it induces cell proliferation inhibition, reversion of metastatic capability and cell death by inhibiting AR signaling *via* downregulating receptor transcription and translation or by inhibiting AR coactivators NF-κB, AP-1, and CBP. In LNCaP-xenografted mice (Tsui et al., 2008), its treatment halted signal transduction through AR *via* modulation of Wnt/β-catenin pathway (Hong et al., 2015; Lajis et al., 2020). In PC-3 cells, it decreased surface availability of AR by suppressing the expression of Hsp90 (Rivera et al., 2017) and promoted cell apoptosis through reducing mitochondrial membrane potential, promoting Bax expression and suppressing Bcl-2 expression (Yang et al., 2015). Synthetic derivatives of curcumin, cinnamaldehyde and dimethylamino derivative, were reported to improve sensitization of LNCaP cells for photodynamic therapy at concentration of 3 μM. Curcuminoid dimethylamino derivative reduced cell survivability in a dose-dependent manner (Kazantzis et al., 2020). Performing curcumin derivatives and photodynamic therapy together on other PCa cell lines and in animal models might give a novel method for curbing this disease. Triterpenes (trinordammaranolactone triterpene and dihydroxyoxodammarane triterpene) from *C. khorassanica* are reported effective against PCa, irrespective of hormone status (Sajjadi et al., 2020).

NATURAL COMPOUNDS FOR THE TREATMENT OF OBESITY EXPOSED PCa

Significance of natural compounds is also evaluated in obesity-exposed PCa cells. Studies have demonstrated that obesity promotes PCa proliferation and metastasis by inducing aberrant signaling through PI3K/Akt pathway, ERK pathway, and JAK/STAT pathway and by upregulating expression of pro-inflammatory COX-2 expression. Silibinin is a compound derived from *Silybum marianum*. Its *in vitro* treatment reported to cause reduction in signal transduction through all these pathways and downregulation of COX-2, leading to cell proliferation inhibition and reduced metastasis (Sherman et al., 2020). Silibinin is suggested as an effective therapeutic option for obese individuals suffering from PCa. Yet, the *in vivo* evidences are scarce to further validate its significance.

NATURAL COMPOUNDS AS MODULATOR OF TGF SIGNALING IN PCa

TGF-β signaling role in cancers is in dual manner: it acts both as oncogene and tumor suppressor. Very few investigations have focused on therapeutically targeting this pathway in PCa. Thus, understanding TGF-β pathway tumor suppressive or oncogenic role at different stages of cancer is very important (Colak and ten Dijke, 2017). In PCa, TGF-β pathway is aberrantly activated which mostly involves mutated downstream targets or mutation in TGF-β receptor (Seoane and Gomis, 2017; Grover et al., 2018). Many evidences are reported in which natural compounds acted as antagonist for this pathway in PCa. For instance, the dried powdered extract of *Ganoderma lucidum* inhibits angiogenesis of PC-3 cells. It induces this effect by hindering the phosphorylation of Akt and Erk1/2 which then fails to activate their downstream target AP-1, hence indirectly silencing the expression of TGF-β1 (Stanley et al., 2005). Resveratrol treatment to PCa cells also inhibits Akt activation by regulating miR-21 (Sheth et al., 2012), which can also lead to TGF-β1 expression downregulation and suppression of cancer cell proliferation. Compounds EGCG and myricetin halt TGF-β signaling in PC-3 cells by downregulating expression of TGFβR1 at the transcriptional level at a dose of ~80 μM (Singh et al., 2016). TGFβR1 expression is reciprocal to the expression of miR-34c/b. In PC-3 cells, miR-34b/c expression is downregulated, which promotes TGFβR1 transcription and translation (Fang et al., 2017). It is possible that EGCG and myricetin might promote miR-34c/b expression that further inhibits TGFβR1posttranscriptionally. TGF-β and BMP pathway crosstalk is associated with PCa metastasis (Chen et al., 2012). Phenethyl isothiocyanate (PIT) treatment to PC-3 cells promoted miR-194 expression which downregulated BMP1 expression. PIT treatment also inhibited MMP2 and three expression which led to decreased invasiveness and metastatic capabilities (Zhang et al., 2016). Osthole, a bioactive coumarin, prevents EMT by simultaneously suppressing miR-23a-3p and TGF-β expression. TGF-β directly activates miR-23a-3p which then targets E-cadharin (Wen et al., 2015). Cairicoside E obtained from *Ipomoea cairica* has been investigated both *in vitro and in vivo*. It has been reported that Cairicoside E targets phosphorylation of Smads 2/3 triggered by TGF-β and prevents EMT in various tumors (Chen et al., 2017). Baicalin and baicalein are the two molecules that have been reported to modulate TGF-β signaling. These two compounds have been found effective both *in vitro* and *in vivo* in suppressing the proliferative potential via modulation of SLUG and NF-κβ signaling (Chung et al., 2015). Baicalin has also been demonstrated to inhibit the phosphorylation of Smads and promoted apoptosis and cell death *in vitro* (Zheng et al., 2016). Recent pharmacological evidences have shed light on paeoniflorin obtained from *Paenoia lactiflora* as a potential inhibitor of proliferation, metastasis, and invasion both *in vivo* and *in vitro*. In the mice model, it has been reported that paeoniflorin downregulated the expression of TGF-β, Snail, e-cadherin, vimentin, and MMP-9 (Ji et al., 2016) (Wang et al., 2018b). Altogether, downregulation of these molecules prevented proliferation and invasiveness in lung cancer. From these findings, it can be concluded that paeoniflorin could be a promising candidate to be tested for PCa. Evidence reported that tumor progression in early stages of PCa involves reduced signal transduction through TGF-β pathway. *Racemic gossypol*, present in cotton seeds, is reported to decrease cell proliferation and prolong the doubling time of PC-3 cells. Gossypol exerted its effects by promoting TGF-β1 expression at the transcriptional and translational levels (JIANG et al., 2004). Another compound, genistein inhibits invasiveness and promotes TGF-β signaling by suppressing onco-miR-1260b expression and removing smad4 from its regulatory control. Genistein also induces epigenetic modification (DNA demethylation) of smad4 gene to promote its transcription (Hirata et al., 2014a). Its treatment also induces miR-574-3p (tumor suppressor miRNA) expression (Chiyomaru et al., 2013), but its association with TGF-β signaling is yet to be determined. Berberine, a natural compound obtained from barberry, has been reported to have extensive antiproliferative, anti-microbial, and anti-inflammatory properties (Tillhon et al., 2012). The role of berberine as a potential inhibitor of metastasis has been well documented. A study conducted by Kou et al. demonstrated that berberine prevented cell adhesion *via* modulating the expression of E-cadherin, vimentin, and fibronectin in cell lines. Berberine downregulates the expression of several EMT genes *via* regulating the PI3K/AkT signaling axis and retinoic acid receptor signaling in various cancers (Kou et al., 2016). Arctigenin is another natural liganin obtained from the plants of Asteraceae family. Arctigenin possesses tremendous antiviral and antiproliferative properties *in vitro*. Recent studies have demonstrated that arctigenin modulated the expression of TGF-β expression and inhibited the phosphorylation of the Smad2/3, and thus prevented the downstream activation of EMT in lung cancer cell lines. Moreover, overexpression of E-cadherin in a dose-dependent manner increased the expression of ERK and ß-catenin that in turn facilitated the expression of TGF-β and triggered EMT (Xu et al., 2017). All together, these findings shed light that arctigenin may be implemented as a potential therapeutic approach for culminating PCa cancer as well. Alpha-solanine is another natural compound that has been reported to

prevent invasiveness, EMT, and proliferation of the PCa *via* modulation of ERK and PI3K/Akt axis. Alpha-solanine prevents phosphorylation of these molecules that in turn prevents the activation of EMT target genes and thus inhibit growth of PCa cell *in vitro* (Shen et al., 2014). Plectranthoic acid (PA) has been investigated for its role in inhibiting cell proliferation and invasiveness in PCa *via* modulation of the TGF-β signaling. Recent findings suggest that PA triggers growth arrest and inhibition of metastasis *via* regulation of RAC1 signaling (Akhtar et al., 2018). A phytochemical obtained from *Solanum nigrum Linn* (α-solanum) has been found active against TGF-β–mediated EMT transition in PCa cells *in vitro*. α-solanum suppressed MMP expression *via* modulation of ERK/AkT axis and thus prevented EMT in PCa (Shen et al., 2014). Sulforaphane is a natural compound found abundant in broccoli and other cruciferous vegetables. This phytochemical has tremendous anti-oxidant properties. Sulforaphane has been documented to prevent growth and proliferation in various tumors including PCa. It directly targets TGF-β signaling and *via* suppression of SLUG (Amjad et al., 2015). Sulforaphane has also been shown to prevent metastasis through interplay among miR-616-5p, beta-catenin, and GSK-3β signaling cascade (Wang et al., 2017). Osthole derived from *Cnidium monnieri* has been found effective in the prevention of metastasis and invasion in different cancers. Osthole blocks EMT *via* modulation/suppression of TGF-β/AkT/MAPK axis, downregulation of Snail, and upregulation of E-cadherin both *in vitro* and *in vivo* (Wen et al., 2015). However, few compounds discussed above have potential to curb PCa progression, but none of these compounds are validated in animal models. Also, the influence of these compounds according to androgen-dependent or independent status also needs to be determined. Finally, with progressing cancer status of TGF-β pathway activation changes, so with further understanding of actors involved in switching on/off in this pathway, the development of natural compound-based therapy is warrant to pursue.

PERSPECTIVES

PCa is a serious anomaly that affects male population in the world. A number of studies over the years provide strong evidence of the involvement of both TGF-β signaling and miRNAs in the development and progression of PCa. The interplay between miRNAs and TGF-β signaling is so crucial that it may aid in resolving the dual behavior of TGF-β signaling in various cancers. miRNAs have a dual role in regulating TGF-β signaling. They can either modulate the expression of the key components of TGF-β signaling machinery such as the receptors, SMADs, and antiapoptotic behavior of the TGF-β–mediated oncogenes. This results in decreased cellular growth and metastasis. However, during proliferation of PCa, expression of these tiny molecules is downregulated, causing direct activation of downstream TGF-β effectors. The miRNAs can also directly act on genes which are activated by TGF-β signaling, thus either inhibiting or promoting the proliferation of PCa. The oncogenic miRNAs are upregulated in highly metastatic PCa cells. They achieve this by downregulating the expression of tumor suppressor miRNAs in a variety of ways leading to cancer progression. From these findings, it can be observed that the switching of miRNAs expression is a pivotal mechanism to understand the dual role of TGF-β signaling in PCa. TGF-β signaling is renowned for regulating molecular landscape of tumor cells and immune responses. Therefore, understanding the interplay between miRNAs and TGF-β signaling could help in the development of diagnostic and prognostic biomarkers. In addition, the interplay between miRNAs and TGF-β signaling is emerging as platform for therapeutic interventions. This will lead to the inclusion of miRNAs that specifically target TGF-β signaling pathway in to clinical trials for the new therapeutic intervention in PCa. Given the prospect, miRNA-mediated regulation of TGF-β signaling in PCa may be promising for the treatment of aggressive prostate tumors.

Phytochemicals have recently emerged as a promising field that can help in prevention and even treatment of PCa. It has been reported that several medicinal plants, herbs, and phytochemicals have tremendous potential in preventing various cancers. The chemical constituents of various plant species have a preponderant role in the production of bioactive phytochemicals. The phenolic extracts of several plants prevented the proliferative potential of the PCa followed by alkaloids and terepnoids. Despite these encouraging results, only few of the phytochemicals have undergone clinical trials. More clinical evidences are required to validate the *in vitro* and *in vivo* studies conducted on natural compounds and their interplay with miRNAs and TGF-β signaling in PCa. Combining natural compounds, miRNAs and TGF-β signaling will ensure better chemoprevention and advanced therapeutic strategies for PCa.

AUTHOR CONTRIBUTIONS

Conceptualization: JS-R, ZJ, KK, AR, AS, SR, BS, WC, WK, WK-K, AG-L, and PH. Validation investigation, resources, data curation, writing: all authors. Review and editing: WC, JS-R, WK, and BS. All authors contributed to the article and approved the submitted version.

REFERENCES

Akhtar, N., Syed, D. N., Lall, R. K., Mirza, B., and Mukhtar, H. (2018). Targeting epithelial to mesenchymal transition in prostate cancer by a novel compound, plectranthoic acid, isolated from Ficus microcarpa. *Mol. Carcinog.* 57 (5), 653–663. doi:10.1002/mc.22790

Akhurst, R. J. (2017). Targeting TGF-β signaling for therapeutic gain. *Cold Spring Harb. Perspect. Biol.* 9 (10), a022301. doi:10.1101/cshperspect.a022301

Amjad, A. I., Parikh, R. A., Appleman, L. J., Hahm, E. R., Singh, K., and Singh, S. V. (2015). Broccoli-derived sulforaphane and chemoprevention of prostate cancer: from bench to bedside. *Curr. Pharmacol. Rep*. 1 (6), 382–390. doi:10.1007/s40495-015-0034-x

Ao, M., Williams, K., Bhowmick, N. A., and Hayward, S. W. (2006). Transforming growth factor-beta promotes invasion in tumorigenic but not in nontumorigenic human prostatic epithelial cells. *Canc. Res*. 66 (16), 8007–8016. doi:10.1158/0008-5472.can-05-4451

Ayub, S. G., Kaul, D., and Ayub, T. (2017). An androgen-regulated miR-2909 modulates TGFβ signalling through AR/miR-2909 axis in prostate cancer. *Gene*. 631, 1–9. doi:10.1016/j.gene.2017.07.037

Barbu, M. G., Condrat, C. E., Thompson, D. C., Bugnar, O. L., Cretoiu, D., Toader, O. D., et al. (2020). MicroRNA involvement in signaling pathways during viral infection. *Front. Cell Dev. Biol*. 8, 143. doi:10.3389/fcell.2020.00143

Barrack, E. R. (1997). TGF beta in prostate cancer: a growth inhibitor that can enhance tumorigenicity. *Prostate*. 31 (1), 61–70. doi:10.1002/(sici)1097-0045(19970401)31:1<61::aid-pros10>3.0.co;2-m

Barrett, C. S., Millena, A. C., and Khan, S. A. (2017). TGF-β effects on prostate cancer cell migration and invasion require FosB. *Prostate*. 77 (1), 72–81. doi:10.1002/pros.23250

Bayala, B., Zoure, A. A., Baron, S., de Joussineau, C., Simpore, J., and Lobaccaro, J.-M. A. (2020). Pharmacological modulation of steroid activity in hormone-dependent breast and prostate cancers: effect of some plant extract derivatives. *Int. J. Mol. Sci*. 21 (10), 3690. doi:10.3390/ijms21103690

Behbahani, G. D., Ghahhari, N. M., Javidi, M. A., Molan, A. F., Feizi, N., and Babashah, S. (2017). MicroRNA-mediated post-transcriptional regulation of epithelial to mesenchymal transition in cancer. *Pathol. Oncol. Res*. 23 (1), 1–12. doi:10.1007/s12253-016-0101-6

Brattain, M. G., Markowitz, S. D., and Willson, J. K. (1996). The type II transforming growth factor-beta receptor as a tumor-suppressor gene. *Curr. Opin. Oncol*. 8 (1), 49–53. doi:10.1097/00001622-199601000-00009

Chen, C., Ma, T., Zhang, C., Zhang, H., Bai, L., Kong, L., et al. (2017). Down-regulation of aquaporin 5-mediated epithelial-mesenchymal transition and anti-metastatic effect by natural product Cairicoside E in colorectal cancer. *Mol. Carcinog*. 56 (12), 2692–2705. doi:10.1002/mc.22712

Chen, C., Wang, Y. Y., Wang, Y. X., Cheng, M. Q., Yin, J. B., Zhang, X., et al. (2018). Gentiopicroside ameliorates bleomycin-induced pulmonary fibrosis in mice via inhibiting inflammatory and fibrotic process. *Biochem. Biophys. Res. Commun*. 495 (4), 2396–2403. doi:10.1016/j.bbrc.2017.12.112

Chen, G., Deng, C., and Li, Y. P. (2012). TGF-β and BMP signaling in osteoblast differentiation and bone formation. *Int. J. Biol. Sci*. 8 (2), 272. doi:10.7150/ijbs.2929

Chipuk, J. E., Cornelius, S. C., Pultz, N. J., Jorgensen, J. S., Bonham, M. J., Kim, S. J., Danielpour, D., et al. (2002). The androgen receptor represses transforming growth factor-beta signaling through interaction with Smad3. *J. Biol. Chem*. 277 (2), 1240–1248. doi:10.1074/jbc.M108855200

Chiyomaru, T., Yamamura, S., Fukuhara, S., Hidaka, H., Majid, S., Saini, S., et al. (2013). Genistein up-regulates tumor suppressor microRNA-574-3p in prostate cancer. *PloS One*. 8 (3), e58929. doi:10.1371/journal.pone.0058929

Cho, K. H. T., Xu, B., Blenkiron, C., and Fraser, M. (2019). Emerging roles of miRNAs in brain development and perinatal brain injury. *Front. Physiol*. 10, 227. doi:10.3389/fphys.2019.00227

Choi, E. O., Lee, H., Park, C., Kim, G.-Y., Cha, H.-J., Kim, S., et al. (2020). Ethanol extracts of Hizikia fusiforme induce apoptosis in human prostate cancer PC3 cells via modulating a ROS-dependent pathway. *Asian Pac. J. Trop. Biomed*. 10 (2), 78. doi:10.4103/2221-1691.275422

Chung, H., Choi, H. S., Seo, E. K., Kang, D. H., and Oh, E. S. (2015). Baicalin and baicalein inhibit transforming growth factor-β1-mediated epithelial-mesenchymal transition in human breast epithelial cells. *Biochem. Biophys. Res. Commun*. 458 (3), 707–713. doi:10.1016/j.bbrc.2015.02.032

Colak, S., and ten Dijke, P. (2017). Targeting TGF-β signaling in cancer. *Trends Canc*. 3 (1), 56–71. doi:10.1016/j.trecan.2016.11.008

Deveci Ozkan, A., Kaleli, S., Onen, H. I., Sarihan, M., Guney Eskiler, G., Kalayci Yigin, A., et al. (2020). Anti-inflammatory effects of nobiletin on TLR4/TRIF/IRF3 and TLR9/IRF7 signaling pathways in prostate cancer cells. *Immunopharmacol. Immunotoxicol*. 42 (2), 93–100. doi:10.1080/08923973.2020.1725040

Donovan, J. L., Hamdy, F. C., Lane, J., Mason, M., Metcalfe, C., Walsh, E., et al. (2016). Patient-reported outcomes after monitoring, surgery, or radiotherapy for prostate cancer. *N. Engl. J. Med*. 375, 1425–1437. doi:10.1056/NEJMoa1606221

Drabsch, Y., and Ten Dijke, P. (2011). TGF-β signaling in breast cancer cell invasion and bone metastasis. *J. Mammary Gland Biol. Neoplasia*. 16 (2), 97–108. doi:10.1007/s10911-011-9217-1

Dwivedi, S., Purohit, P., and Sharma, P. (2019). MicroRNAs and diseases: promising biomarkers for diagnosis and therapeutics. *Indian J. Clin. Biochem*. 34 (3), 243–245. doi:10.1007/s12291-019-00844-x

Dyshlovoy, S. A., Tarbeeva, D., Fedoreyev, S., Busenbender, T., Kaune, M., Veselova, M., et al. (2020). Polyphenolic compounds from Lespedeza bicolor root bark inhibit progression of human prostate cancer cells via induction of apoptosis and cell cycle arrest. *Biomolecules* 10 (3), 451. doi:10.3390/biom10030451.

Eskra, J. N., Dodge, A., Schlicht, M. J., and Bosland, M. C. (2020). Effects of black raspberries and their constituents on rat prostate carcinogenesis and human prostate cancer cell growth *in vitro*. *Nutr. Canc*. 72 (4), 672–685. doi:10.1080/01635581.2019.1650943

Fang, L.-l., Sun, B.-f., Huang, L.-r., Yuan, H.-b., Zhang, S., Chen, J., et al. (2017). Potent inhibition of miR-34b on migration and invasion in metastatic prostate cancer cells by regulating the TGF-β pathway. *Int. J. Mol. Sci*. 18 (12), 2762. doi:10.3390/ijms18122762.

Finotti, A., Fabbri, E., Lampronti, I., Gasparello, J., Borgatti, M., and Gambari, R. (2019). MicroRNAs and long non-coding RNAs in genetic diseases. *Mol. Diagn. Ther*. 23 (2), 155–171. doi:10.1007/s40291-018-0380-6

Fu, W., Tao, T., Qi, M., Wang, L., Hu, J., Li, X., et al. (2016). MicroRNA-132/212 upregulation inhibits TGF-β-mediated epithelial-mesenchymal transition of prostate cancer cells by targeting SOX4. *Prostate*. 76 (16), 1560–1570. doi:10.1002/pros.23241

Gao, P., Huang, X., Liao, T., Li, G., Yu, X., You, Y., et al. (2019). Daucosterol induces autophagic-dependent apoptosis in prostate cancer via JNK activation. *Biosci. Trends*. 13 (2), 160–167. doi:10.5582/bst.2018.01293

Gbaweng, A. J. Y., Daïrou, H., Zingué, S., Emmanuel, T., Tchinda, A. T., Frédérich, M., et al. (2020). Excelsanone, a new isoflavonoid from Erythrina excelsa (Fabaceae), with *in vitro* antioxidant and *in vitro* cytotoxic effects on prostate cancer cells lines. *Nat. Prod. Res*. 34 (5), 659–667. doi:10.1080/14786419.2018.1495639

Giacomelli, C., Daniele, S., Natali, L., Iofrida, C., Flamini, G., Braca, A., et al. (2017). Carnosol controls the human glioblastoma stemness features through the epithelial-mesenchymal transition modulation and the induction of cancer stem cell apoptosis. *Sci. Rep*. 7 (1), 1–17. doi:10.1038/s41598-017-15360-2

Giacomelli, C., Natali, L., Trincavelli, M. L., Daniele, S., Bertoli, A., Flamini, G., et al. (2016). New insights into the anticancer activity of carnosol: p53 reactivation in the U87MG human glioblastoma cell line. *Int. J. Biochem. Cell Biol*. 74, 95–108. doi:10.1016/j.biocel.2016.02.019

Gioti, K., Papachristodoulou, A., Benaki, D., Beloukas, A., Vontzalidou, A., Aligiannis, N., et al. (2020). Glycyrrhiza glabra-enhanced extract and adriamycin antiproliferative effect on PC-3 prostate cancer cells. *Nutr. Canc*. 72 (2), 320–332. doi:10.1080/01635581.2019.1632357

Gong, C., Qu, S., Liu, B., Pan, S., Jiao, Y., Nie, Y., et al. (2015). MiR-106b expression determines the proliferation paradox of TGF-β in breast cancer cells. *Oncogene*. 34 (1), 84–93. doi:10.1038/onc.2013.525

Grover, P., Nath, S., Nye, M. D., Zhou, R., Ahmad, M., and Mukherjee, P. (2018). SMAD4-independent activation of TGF-β signaling by MUC1 in a human pancreatic cancer cell line. *Oncotarget*. 9 (6), 6897. doi:10.18632/oncotarget.23966

Hamidi, A., Song, J., Thakur, N., Itoh, S., Marcusson, A., Bergh, A., et al. (2017). TGF-β promotes PI3K-AKT signaling and prostate cancer cell migration through the TRAF6-mediated ubiquitylation of p85α. *Sci. Signal*. 10 (486), eaal4186. doi:10.1126/scisignal.aal4186

Hao, Y., Baker, D., and ten Dijke, P. (2019). TGF-β-mediated epithelial-mesenchymal transition and cancer metastasis. *Int. J. Mol. Sci*. 20 (11), 2767. doi:10.3390/ijms20112767

Hayes, J. H., and Barry, M. J. (2014). Screening for prostate cancer with the prostate-specific antigen test: a review of current evidence. *Jama*. 311 (11), 1143–1149. doi:10.1001/jama.2014.2085

Hirata, H., Hinoda, Y., Shahryari, V., Deng, G., Tanaka, Y., Tabatabai, Z., et al. (2014a). Genistein downregulates onco-miR-1260b and upregulates sFRP1 and

Smad4 via demethylation and histone modification in prostate cancer cells. *Br. J. Canc*. 110 (6), 1645–1654. doi:10.1038/bjc.2014.48

Hirata, H., Hinoda, Y., Shahryari, V., Deng, G., Tanaka, Y., Tabatabai, Z. L., et al. (2014b). Genistein downregulates onco-miR-1260b and upregulates sFRP1 and Smad4 via demethylation and histone modification in prostate cancer cells. *Br. J. Canc*. 110 (6), 1645–1654. doi:10.1038/bjc.2014.48

Hong, J. H., Lee, G., and Choi, H. Y. (2015). Effect of curcumin on the interaction between androgen receptor and Wnt/β-catenin in LNCaP xenografts. *Korean J. Urol*. 56 (9), 656–665. doi:10.4111/kju.2015.56.9.656

Hu, S., Yu, W., Lv, T. J., Chang, C. S., Li, X., and Jin, J. (2014). Evidence of TGF-β1 mediated epithelial-mesenchymal transition in immortalized benign prostatic hyperplasia cells. *Mol. Membr. Biol*. 31 (2–3), 103–110. doi:10.3109/09687688.2014.894211

Huang, S., Zou, C., Tang, Y., Wa, Q., Peng, X., Chen, X., et al. (2019). miR-582-3p and miR-582-5p suppress prostate cancer metastasis to bone by repressing TGF-β signaling. *Mol. Ther. Nucleic Acids*. 16, 91–104. doi:10.1016/j.omtn.2019.01.004

Huang, S., Wa, Q., Pan, J., Peng, X., Ren, D., Li, Q., et al. (2018). Transcriptional downregulation of miR-133b by REST promotes prostate cancer metastasis to bone via activating TGF-β signaling. *Cell Death Dis*. 9 (7), 779. doi:10.1038/s41419-018-0807-3

Javed, Z., Ahmed Shah, F., Rajabi, S., Raza, Q., Iqbal, Z., Ullah, M., et al. (2020). LncRNAs as potential therapeutic targets in thyroid cancer. *Asian Pac. J. Cancer Prev. APJCP*. 21 (2), 281–287. doi:10.31557/APJCP.2020.21.2.281

Javed, Z., Iqbal, M. Z., Latif, M. U., Yaqub, H. M. F., and Qadri, Q. R. (2015). Potent implications of miRNA in cancer biology–a brief review. *Adv. Life Sci*. 2 (3), 106–109.

Ji, H., Li, Y., Jiang, F., Wang, X., Zhang, J., Shen, J., et al. (2014). Inhibition of transforming growth factor beta/SMAD signal by MiR-155 is involved in arsenic trioxide-induced anti-angiogenesis in prostate cancer. *Canc. Sci*. 105 (12), 1541–1549. doi:10.1111/cas.12548

Ji, Y., Dou, Y. N., Zhao, Q. W., Zhang, J. Z., Yang, Y., Wang, T., et al. (2016). Paeoniflorin suppresses TGF-β mediated epithelial-mesenchymal transition in pulmonary fibrosis through a Smad-dependent pathway. *Acta Pharmacol. Sin*. 37 (6), 794–804. doi:10.1038/aps.2016.36

Jiang, J., Sugimoto, Y., Liu, S., Chang, H. L., Park, K. Y., Kulp, S. K., et al. (2004). The inhibitory effects of gossypol on human prostate cancer cells-PC3 are associated with transforming growth factor beta1 (TGFbeta1) signal transduction pathway. *Anticancer Res*. 24 (1), 91–100.

Jin, W., Chen, F., Wang, K., Song, Y., Fei, X., and Wu, B. (2018). miR-15a/miR-16 cluster inhibits invasion of prostate cancer cells by suppressing TGF-β signaling pathway. *Biomed. Pharmacother*. 104, 637–644. doi:10.1016/j.biopha.2018.05.041

Kazantzis, C., Koutsonikoli, K., Mavroidi, B., Zachariadis, M., Alexiou, P., Pelecanou, M., et al. (2020). Curcumin derivatives as photosensitizers in photodynamic therapy: photophysical properties and *in vitro* studies with prostate cancer cells. Photochemical & Photobiological Sciences 19, 193–206. 10.1039/C9PP00375D.

Khusbu, F. Y., Zhou, X., Roy, M., Chen, F.-Z., Cao, Q., and Chen, H.-C. (2020). Resveratrol induces depletion of TRAF6 and suppresses prostate cancer cell proliferation and migration. *Int. J. Biochem. Cell Biol*. 118, 105644. doi:10.1016/j.biocel.2019.105644

Kiener, M., Chen, L., Krebs, M., Grosjean, J., Klima, I., Kalogirou, C., et al. (2019). miR-221-5p regulates proliferation and migration in human prostate cancer cells and reduces tumor growth *in vivo*. *BMC Canc*. 19 (1), 627. doi:10.1186/s12885-019-5819-6

Kilinc, K., Demir, S., Turan, I., Mentese, A., Orem, A., Sonmez, M., et al. (2020). Rosa canina extract has antiproliferative and proapoptotic effects on human lung and prostate cancer cells. *Nutr. Canc*. 72(2), 273–282. doi:10.1080/01635581.2019.1625936

Kou, Y., Li, L., Li, H., Tan, Y., Li, B., Wang, K., et al. (2016). Berberine suppressed epithelial mesenchymal transition through cross-talk regulation of PI3K/AKT and RARα/RARβ in melanoma cells. *Biochem. Biophys. Res. Commun*. 479 (2), 290–296. doi:10.1016/j.bbrc.2016.09.061

Lajis, N. H., Abas, F., Othman, I., and Naidu, R. (2020). Mechanism of anti-cancer activity of curcumin on androgen-dependent and androgen-independent prostate cancer. *Nutrients* 12 (3), 679. doi:10.3390/nu12030679

Leichter, A. L., Sullivan, M. J., Eccles, M. R., and Chatterjee, A. (2017). MicroRNA expression patterns and signalling pathways in the development and progression of childhood solid tumours. *Mol. Canc*. 16 (1), 15. doi:10.1186/s12943-017-0584-0

Li, F., Liang, J., and Bai, L. (2018a). MicroRNA-449a functions as a tumor suppressor in pancreatic cancer by the epigenetic regulation of ATDC expression. *Biomed. Pharmacother*. 103, 782–789. doi:10.1016/j.biopha.2018.04.101

Li, F. S., and Weng, J. K. (2017). Demystifying traditional herbal medicine with modern approach. *Native Plants*. 3 (8), 1–7. doi:10.1038/nplants.2017.109

Li, L., Miu, K. K., Gu, S., Cheung, H. H., and Chan, W. Y. (2018b). Comparison of multi-lineage differentiation of hiPSCs reveals novel miRNAs that regulate lineage specification. *Sci. Rep*. 8 (1), 9630. doi:10.1038/s41598-018-27719-0

Li, X., Li, J., Cai, Y., Peng, S., Wang, J., Xiao, Z., et al. (2018c). Hyperglycaemia-induced miR-301a promotes cell proliferation by repressing p21 and Smad4 in prostate cancer. *Canc. Lett*. 418, 211–220. doi:10.1016/j.canlet.2018.01.031

Liu, G. L., Yang, H. J., Liu, T., and Lin, Y. Z. (2014). Expression and significance of E-cadherin, N-cadherin, transforming growth factor-β1 and Twist in prostate cancer. *Asian Pac. J. Trop. Med*. 7 (1), 76–82. doi:10.1016/s1995-7645(13)60196-0

Liu, L., Wang, Y., Yan, R., Li, S., Shi, M., Xiao, Y., et al. (2016). Oxymatrine inhibits renal tubular EMT induced by high glucose via upregulation of SnoN and inhibition of TGF-β1/smad signaling pathway. *PloS One*. 11 (3), e0151986. doi:10.1371/journal.pone.0151986

Liu, Y. N., Yin, J. J., Abou-Kheir, W., Hynes, P. G., Casey, O. M., Fang, L., et al. (2013). MiR-1 and miR-200 inhibit EMT via slug-dependent and tumorigenesis via slug-independent mechanisms. *Oncogene*. 32 (3), 296–306. doi:10.1038/onc.2012.58

Lodyga, M., and Hinz, B. (2020). TGF-β1—a truly transforming growth factor in fibrosis and immunity. *Semin. Cell Dev. Biol*. 101, 123–139. doi:10.1016/j.semcdb.2019.12.010

Lu, Y., Tang, L., Zhang, Q., Zhang, Z., and Wei, W. (2018). MicroRNA-613 inhibits the progression of gastric cancer by targeting CDK9. *Artificial cells, nanomedicine, and biotechnology*. 46 (5), 980–984. doi:10.1080/21691401.2017.1351983.

Martínez-Martínez, D., Soto, A., Gil-Araujo, B., Gallego, B., Chiloeches, A., and Lasa, M. (2019). Resveratrol promotes apoptosis through the induction of dual specificity phosphatase 1 and sensitizes prostate cancer cells to cisplatin. *Food Chem. Toxicol*. 124, 273–279. doi:10.1016/j.fct.2018.12.014

Massagué, J. (1998). "TGF-β signal transduction," in *Annual reviews 4139 el camino way*.. 10139. Palo Alto, CA: PO Box.

Matulewicz, R. S., Weiner, A. B., and Schaeffer, E. M. (2017). Active surveillance for prostate cancer. *Jama*. 318 (21), 2152. doi:10.1001/jama.2017.17222

Miscianinov, V., Martello, A., Rose, L., Parish, E., Cathcart, B., Mitić, T., et al. (2018). MicroRNA-148b targets the TGF-β pathway to regulate angiogenesis and endothelial-to-mesenchymal transition during skin wound healing. *Mol. Ther*. 26 (8), 1996–2007. doi:10.1016/j.ymthe.2018.05.002

Mishra, S., Deng, J. J., Gowda, P. S., Rao, M. K., Lin, C. L., Chen, C. L., et al. (2014). Androgen receptor and microRNA-21 axis downregulates transforming growth factor beta receptor II (TGFBR2) expression in prostate cancer. *Oncogene*. 33 (31), 4097–4106. doi:10.1038/onc.2013.374

Mottet, N., Bellmunt, J., Bolla, M., Briers, E., Cumberbatch, M. G., De Santis, M., et al. (2017). EAU-ESTRO-SIOG guidelines on prostate cancer. Part 1: screening, diagnosis, and local treatment with curative intent. *Eur. Urol*. 71 (4), 618–629. doi:10.1016/j.eururo.2016.08.003

Nacif, M., and Shaker, O. (2014). Targeting transforming growth factor-β (TGF-β) in cancer and non-neoplastic diseases. *J. Canc. Ther*. 5, 735–745.

Nazim, U., Yin, H., and Park, S. Y. (2020). Neferine treatment enhances the TRAIL-induced apoptosis of human prostate cancer cells via autophagic flux and the JNK pathway. *Int. J. Oncol*. 56 (5), 1152–1161. doi:10.3892/ijo.2020.5012

Nickel, J., ten Dijke, P., and Mueller, T. D. (2018). TGF-β family co-receptor function and signaling. *Acta Biochim. Biophys. Sin*. 50 (1), 12–36. doi:10.1093/abbs/gmx126

Pattarayan, D., Sivanantham, A., Krishnaswami, V., Loganathan, L., Palanichamy, R., Natesan, S., et al. (2018). Tannic acid attenuates TGF-β1-induced epithelial-to-mesenchymal transition by effectively intervening TGF-β signaling in lung epithelial cells. *J. Cell. Physiol*. 233 (3), 2513–2525. doi:10.1002/jcp.26127

Prasad, S., Ramachandran, S., Gupta, N., Kaushik, I., and Srivastava, S. K. (2020). Cancer cells stemness: a doorstep to targeted therapy. *Biochim. Biophys. Acta (BBA) - Mol. Basis Dis.* 1866 (4), 165424. doi:10.1016/j.bbadis.2019.02.019

Pu, H., Collazo, J., Jones, E., Gayheart, D., Sakamoto, S., Vogt, A., et al. (2009). Dysfunctional transforming growth factor-beta receptor II accelerates prostate tumorigenesis in the TRAMP mouse model. *Canc. Res.* 69 (18), 7366–7374. doi:10.1158/0008-5472.CAN-09-0758

Qiu, X., Zhu, J., Sun, Y., Fan, K., Yang, D. R., Li, G., et al. (2015). TR4 nuclear receptor increases prostate cancer invasion via decreasing the miR-373-3p expression to alter TGFβR2/p-Smad3 signals. *Oncotarget.* 6 (17), 15397–15409. doi:10.18632/oncotarget.3778

Rawla, P. (2019). Epidemiology of prostate cancer. *World J. Oncol.* 10 (2), 63. doi:10.14740/wjon1191

Rehman, S., Keefover-Ring, K., Haq, I., Dilshad, E., Khan, M. I., Akhtar, N., et al. (2019). Drier climatic conditions increase withanolide content of withania coagulans enhancing its inhibitory potential against human prostate cancer cells. *Appl. Biochem. Biotechnol.* 188 (2), 460–480. doi:10.1007/s12010-018-02933-8

Reis, S. T., Pontes-Júnior, J., Antunes, A. A., Sousa-Canavez, J. M., Abe, D. K., Cruz, J. A., et al. (2011). Tgf-β1 expression as a biomarker of poor prognosis in prostate cancer. *Clinics.* 66 (7), 1143–1147. doi:10.1590/s1807-59322011000700004

Rivera, M., Ramos, Y., Rodríguez-Valentín, M., López-Acevedo, S., Cubano, L. A., Zou, J., et al. (2017). Targeting multiple pro-apoptotic signaling pathways with curcumin in prostate cancer cells. *PloS One.* 12 (6), e0179587. doi:10.1371/journal.pone.0179587

Sajjadi, S.-E., Ghanadian, M., Aghaei, M., and Salehi, A. (2020). Two new dammarane triterpenes isolated from Cleome khorassanica Bunge & Bien with cytotoxicity against DU-145 and LNCaP prostate cancer cell lines. *J. Asian Nat. Prod. Res.* 22 (1), 38–46. doi:10.1080/10286020.2018.1538211

Saleem, M., Asif, J., Asif, M., and Saleem, U. (2018). Amygdalin from apricot kernels induces apoptosis and causes cell cycle arrest in cancer cells: an updated review. *Anti Canc. Agents Med. Chem.* 18 (12), 1650–1655. doi:10.2174/1871520618666180105161136

Salehi, B., Ata, A., Kumar, N. V. A., Sharopov, F., Ramírez-Alarcón, K., Ruiz-Ortega, A., et al. (2019). Antidiabetic potential of medicinal plants and their active components. *Biomolecules.* 9 (10), 551. doi:10.3390/biom9100551

Seoane, J., and Gomis, R. R. (2017). TGF-β family signaling in tumor suppression and cancer progression. *Cold Spring Harb. Perspect. Biol.* 9 (12), a022277. doi:10.1101/cshperspect.a022277

Sharifi, N., Hurt, E. M., Kawasaki, B. T., and Farrar, W. L. (2007). TGFBR3 loss and consequences in prostate cancer. *Prostate.* 67 (3), 301–311. doi:10.1002/pros.20526

Shen, K.-H., Liao, A. C.-H., Hung, J.-H., Lee, W.-J., Hu, K.-C., Lin, P.-T., et al. (2014). α-Solanine inhibits invasion of human prostate cancer cell by suppressing epithelial-mesenchymal transition and MMPs expression. *Molecules.* 19 (8), 11896–11914. doi:10.3390/molecules190811896

Sherman, B., Hernandez, A. M., Alhado, M., Menge, L., and Price, R. S. (2020). Silibinin differentially decreases the aggressive cancer phenotype in an in vitro model of obesity and prostate cancer. *Nutr. Canc.* 72 (2), 333–342. doi:10.1080/01635581.2019.1633363

Sheth, S., Jajoo, S., Kaur, T., Mukherjea, D., Sheehan, K., Rybak, L. P., et al. (2012). Resveratrol reduces prostate cancer growth and metastasis by inhibiting the Akt/MicroRNA-21 pathway. *PloS One.* 7 (12), e51655. doi:10.1371/journal.pone.0051655

Shiota, M., Zardan, A., Takeuchi, A., Kumano, M., Beraldi, E., Naito, S., et al. (2012). Clusterin mediates TGF-β-induced epithelial-mesenchymal transition and metastasis via Twist1 in prostate cancer cells. *Canc. Res.* 72 (20), 5261–5272. doi:10.1158/0008-5472.can-12-0254

Singh, P., Bast, F., and Singh, R. (2016). Natural compounds targeting transforming growth factor-β. *Elect. J. Biol.* 13, 6–13.

Singh, S. K., Apata, T., Gordetsky, J. B., and Singh, R. (2019). Docetaxel combined with thymoquinone induces apoptosis in prostate cancer cells via inhibition of the PI3K/AKT signaling pathway. *Cancers.* 11 (9), 1390. doi:10.3390/cancers11091390.

Siu, M. K., Tsai, Y. C., Chang, Y. S., Yin, J. J., Suau, F., Chen, W. Y., et al. (2015). Transforming growth factor-β promotes prostate bone metastasis through induction of microRNA-96 and activation of the mTOR pathway. *Oncogene.* 34 (36), 4767–4776. doi:10.1038/onc.2014.414

Slattery, M. L., Mullany, L. E., Sakoda, L. C., Wolff, R. K., Samowitz, W. S., and Herrick, J. S. (2018). Dysregulated genes and miRNAs in the apoptosis pathway in colorectal cancer patients. *Apoptosis.* 23 (3–4), 237–250. doi:10.1007/s10495-018-1451-1

Song, I.-S., Jeong, Y. J., Kim, J., Seo, K.-H., Baek, N.-I., Kim, Y., et al. (2020). Pharmacological inhibition of androgen receptor expression induces cell death in prostate cancer cells. *Cell. Mol. Life Sci.* 77, 4663–4673. doi:10.1007/s00018-019-03429-2

Song, K., Wang, H., Krebs, T. L., Kim, S. J., and Danielpour, D. (2008). Androgenic control of transforming growth factor-beta signaling in prostate epithelial cells through transcriptional suppression of transforming growth factor-beta receptor II. *Canc. Res.* 68 (19), 8173–8182. doi:10.1158/0008-5472.can-08-2290

Stanley, G., Harvey, K., Slivova, V., Jiang, J., and Sliva, D. (2005). Ganoderma lucidum suppresses angiogenesis through the inhibition of secretion of VEGF and TGF-beta1 from prostate cancer cells. *Biochem. Biophys. Res. Commun.* 330 (1), 46–52. doi:10.1016/j.bbrc.2005.02.116

Steiner, M. S., and Barrack, E. R. (1992). Transforming growth factor-beta 1 overproduction in prostate cancer: effects on growth *in vivo* and *in vitro*. *Mol. Endocrinol.* 6 (1), 15–25. doi:10.1210/mend.6.1.1738367

Sun, B., Fan, Y., Yang, A., Liang, L., and Cao, J. (2019). MicroRNA-539 functions as a tumour suppressor in prostate cancer via the TGF-β/Smad4 signalling pathway by down-regulating DLX1. *J. Cell Mol. Med.* 23 (9), 5934–5948. doi:10.1111/jcmm.14402

Tang, Y., Wu, B., Huang, S., Peng, X., Li, X., Huang, X., et al. (2019). Downregulation of miR-505-3p predicts poor bone metastasis-free survival in prostate cancer. *Oncol. Rep.* 41 (1), 57–66. doi:10.3892/or.2018.6826

Tian, M., and Schiemann, W. P. (2009). The TGF-β paradox in human cancer: an update. *Future Oncol.* 5, 259–271. doi:10.2217/14796694.5.2.259

Tillhon, M., Guamán Ortiz, L. M., Lombardi, P., and Scovassi, A. I. (2012). Berberine: new perspectives for old remedies. *Biochem. Pharmacol.* 84 (10), 1260–1267. doi:10.1016/j.bcp.2012.07.018

Tsui, K. H., Feng, T. H., Lin, C. M., Chang, P. L., and Juang, H. H. (2008). Curcumin blocks the activation of androgen and interlukin-6 on prostate-specific antigen expression in human prostatic carcinoma cells. *J. Androl.* 29 (6), 661–668. doi:10.2164/jandrol.108.004911

Turley, R. S., Finger, E. C., Hempel, N., How, T., Fields, T. A., and Blobe, G. C. (2007). The type III transforming growth factor-beta receptor as a novel tumor suppressor gene in prostate cancer. *Canc. Res.* 67 (3), 1090–1098. doi:10.1158/0008-5472.CAN-06-3117

Ueno, K., Hirata, H., Shahryari, V., Deng, G., Tanaka, Y., Tabatabai, Z. L., et al. (2013). microRNA-183 is an oncogene targeting Dkk-3 and SMAD4 in prostate cancer. *Br. J. Canc.* 108 (8), 1659–1667. doi:10.1038/bjc.2013.125

Valinezhad Orang, A., Safaralizadeh, R., and Kazemzadeh-Bavili, M. (2014). Mechanisms of miRNA-mediated gene regulation from common downregulation to mRNA-specific upregulation. *Int. J. Genomics.* 2014, 970607. doi:10.1155/2014/970607

Wa, Q., Li, L., Lin, H., Peng, X., Ren, D., Huang, Y., et al. (2018). Downregulation of miR-19a-3p promotes invasion, migration and bone metastasis via activating TGF-β signaling in prostate cancer. *Oncol. Rep.* 39 (1), 81–90. doi:10.3892/or.2017.6096

Wang, D. X., Zou, Y. J., Zhuang, X. B., Chen, S. X., Lin, Y., Li, W. L., et al. (2017). Sulforaphane suppresses EMT and metastasis in human lung cancer through miR-616-5p-mediated GSK3β/β-catenin signaling pathways. *Acta Pharmacol. Sin.* 38 (2), 241–251. doi:10.1038/aps.2016.122

Wang, J., Li, H. Y., Wang, H. S., and Su, Z. B. (2018a). MicroRNA-485 modulates the TGF-β/smads signaling pathway in chronic asthmatic mice by targeting Smurf2. *Cell. Physiol. Biochem.* 51 (2), 692–710. doi:10.1159/000495327

Wang, Z., Liu, Z., Yu, G., Nie, X., Jia, W., Liu, R. E., et al. (2018b). Paeoniflorin inhibits migration and invasion of human glioblastoma cells via suppression transforming growth factor β-induced epithelial-mesenchymal transition. *Neurochem. Res.* 43 (3), 760–774. doi:10.1007/s11064-018-2478-y

Wen, Y.-C., Lee, W.-J., Tan, P., Yang, S.-F., Hsiao, M., Lee, L.-M., et al. (2015). By inhibiting snail signaling and miR-23a-3p, osthole suppresses the EMT-mediated metastatic ability in prostate cancer. *Oncotarget.* 6 (25), 21120. doi:10.18632/oncotarget.4229

Wienholds, E., and Plasterk, R. H. (2005). MicroRNA function in animal development. *FEBS Lett*. 579 (26), 5911–5922. doi:10.1016/j.febslet.2005.07.070

Xia, C., Chen, L., Sun, W., Yan, R., Xia, M., Wang, Y., et al. (2020). Total saponins from Paris forrestii (Takht) H. Li. show the anticancer and RNA expression regulating effects on prostate cancer cells. *Biomed. Pharmacother*. 121, 109674. doi:10.1016/j.biopha.2019.109674

Xu, X., Zheng, L., Yuan, Q., Zhen, G., Crane, J. L., Zhou, X., et al. (2018). Transforming growth factor-β in stem cells and tissue homeostasis. *Bone Res*. 6 (1), 1–31. doi:10.1038/s41413-017-0005-4

Xu, Y., Lou, Z., and Lee, S.-H. (2017). Arctigenin represses TGF-β-induced epithelial mesenchymal transition in human lung cancer cells. *Biochem. Biophys. Res. Commun*. 493 (2), 934–939. doi:10.1016/j.bbrc.2017.09.117

Yang, J., Ning, J., Peng, L., and He, D. (2015). Effect of curcumin on Bcl-2 and Bax expression in nude mice prostate cancer. *Int. J. Clin. Exp. Pathol*. 8 (8), 9272–9278.

Yang, Y., Ji, C., Guo, S., Su, X., Zhao, X., Zhang, S., et al. (2017). The miR-486-5p plays a causative role in prostate cancer through negative regulation of multiple tumor suppressor pathways. *Oncotarget*. 8 (42), 72835–72846. doi:10.18632/oncotarget.20427

Yang, Y., Jia, D., Kim, H., Abd Elmageed, Z. Y., Datta, A., Davis, R., et al. (2016). Dysregulation of miR-212 promotes castration resistance through hnRNPH1-mediated regulation of AR and AR-V7: implications for racial disparity of prostate cancer. *Clin. Canc. Res*. 22 (7), 1744–1756. doi:10.1158/1078-0432.ccr-15-1606

Yumoto, K., Eber, M. R., Wang, J., Cackowski, F. C., Decker, A. M., Lee, E., et al. (2016). Axl is required for TGF-β2-induced dormancy of prostate cancer cells in the bone marrow. *Sci. Rep*. 6, 36520. doi:10.1038/srep36520

Zeng, Y., Zhu, J., Shen, D., Qin, H., Lei, Z., Li, W., et al. (2016). Repression of Smad4 by miR-205 moderates TGF-β-induced epithelial-mesenchymal transition in A549 cell lines. *Int. J. Oncol*. 49 (2), 700–708. doi:10.3892/ijo.2016.3547

Zhang, C., Shu, L., Kim, H., Khor, T. O., Wu, R., Li, W., et al. (2016). Phenethyl isothiocyanate (PEITC) suppresses prostate cancer cell invasion epigenetically through regulating microRNA-194. *Mol. Nutr. Food Res*. 60 (6), 1427–1436. doi:10.1002/mnfr.201500918

Zhang, L., Zhou, F., and ten Dijke, P. (2013). Signaling interplay between transforming growth factor-β receptor and PI3K/AKT pathways in cancer. *Trends Biochem. Sci*. 38 (12), 612–620. doi:10.1016/j.tibs.2013.10.001

Zhang, Z.-B., Ip, S.-P., Cho, W. C. S., Hu, Z., Huang, Y.-F., Luo, D.-D., et al. (2020). Evaluation of the effects of androgenic Chinese herbal medicines on androgen receptors and tumor growth in experimental prostate cancer models. *J. Ethnopharmacol*. 260, 113058. doi:10.1016/j.jep.2020.113058

Zheng, J., Son, D. J., Gu, S. M., Woo, J. R., Ham, Y. W., Lee, H. P., et al. (2016). Piperlongumine inhibits lung tumor growth via inhibition of nuclear factor kappa B signaling pathway. *Sci. Rep*. 6 (1), 26357–26413. doi:10.1038/srep26357

Zhiping, C., Shijun, T., Linhui, W., Yapei, W., Lianxi, Q., and Qiang, D. (2017). MiR-181a promotes epithelial to mesenchymal transition of prostate cancer cells by targeting TGIF2. *Eur. Rev. Med. Pharmacol. Sci*. 21 (21), 4835–4843.

Zhou, H., Wu, G., Ma, X., Xiao, J., Yu, G., Yang, C., et al. (2018). Attenuation of TGFBR2 expression and tumour progression in prostate cancer involve diverse hypoxia-regulated pathways. *J. Exp. Clin. Canc. Res*. 37 (1), 89. doi:10.1186/s13046-018-0764-9

Zhu, M. L., and Kyprianou, N. (2010). Role of androgens and the androgen receptor in epithelial-mesenchymal transition and invasion of prostate cancer cells. *Faseb. J*. 24 (3), 769–777. doi:10.1096/fj.09-136994

Zhuang, M., Qiu, X., Cheng, D., Zhu, C., and Chen, L. (2018). MicroRNA-524 promotes cell proliferation by down-regulating PTEN expression in osteosarcoma. *Canc. Cell Int*. 18 (1), 114. doi:10.1186/s12935-018-0612-1

Zingue, S., Gbaweng Yaya, A. J., Michel, T., Ndinteh, D. T., Rutz, J., Auberon, F., et al. (2020). Bioguided identification of daucosterol, a compound that contributes to the cytotoxicity effects of Crateva adansonii DC (capparaceae) to prostate cancer cells. *J. Ethnopharmacol*. 247, 112251. doi:10.1016/j.jep.2019.112251

Conflict of Interest: The authors declare that the research was conducted in the absence of any commercial or financial relationships that could be construed as a potential conflict of interest.

frontiers in Pharmacology

ORIGINAL RESEARCH
published: 09 February 2021
doi: 10.3389/fphar.2020.611060

Systematic Transcriptome Analysis Reveals the Inhibitory Function of Cinnamaldehyde in Non-Small Cell Lung Cancer

Ru Chen[1†], Juan Wu[1†], Chang Lu[2], Ting Yan[3], Yu Qian[3], Huiqing Shen[1], Yujing Zhao[1], Jianzhen Wang[1], Pengzhou Kong[3]* and Xinri Zhang[1]**

[1]Department of Respiratory and Critical Care Medicine, The First Hospital of Shanxi Medical University, Taiyuan, China, [2]College of Animal Science, Shanxi Agricultural University, Taigu, China, [3]Department of Pathology and Shanxi Key Laboratory of Carcinogenesis and Translational Research on Esophageal Cancer, Shanxi Medical University, Taiyuan, China

OPEN ACCESS

Edited by:
Yongye Huang,
Northeastern University, China

Reviewed by:
Boshi Wang,
Shanghai Cancer Institute, China
Yang Han,
RWTH Aachen University, Germany

***Correspondence:**
Jianzhen Wang
wjzzjw@126.com
Pengzhou Kong
kongpengzhou@sxmu.edu.cn
Xinri Zhang
ykdzxr61@163.com

[†]These authors have contributed equally to this work and share first authorship

Specialty section:
This article was submitted to Pharmacology of Anti-Cancer Drugs, a section of the journal Frontiers in Pharmacology

Received: 28 September 2020
Accepted: 29 December 2020
Published: 09 February 2021

Citation:
Chen R, Wu J, Lu C, Yan T, Qian Y, Shen H, Zhao Y, Wang J, Kong P and Zhang X (2021) Systematic Transcriptome Analysis Reveals the Inhibitory Function of Cinnamaldehyde in Non-Small Cell Lung Cancer. Front. Pharmacol. 11:611060. doi: 10.3389/fphar.2020.611060

Cinnamaldehyde (CA) is the main component extracted from the traditional Chinese medicine cinnamon. Recent studies revealed that CA has antiviral and anti-tumor effects. However, the effect and mechanism of CA on non-small cell lung cancer (NSCLC) through whole transcriptome sequencing integrated analysis have not been systematically investigated. In this study, whole transcriptome sequencing was used to identify differentially expressed messenger RNAs (mRNAs), micro RNAs (miRNAs), and long non-coding RNAs (lncRNAs) that were influenced by CA and screen regulatory pathways. The results showed that CA significantly inhibited proliferation, invasion, and migration, whereas it induced the apoptosis of NSCLC cells. CA inhibited tumor growth *in vivo*. Gene ontology and Kyoto Encyclopedia of Genes and Genomes analysis revealed that these differentially expressed mRNAs were potentially implicated in the CA-suppressing malignant phenotypes of NSCLC. According to the competing endogenous RNA (ceRNA) hypothesis, a ceRNA network was constructed, including 13 mRNAs, 6 miRNAs, and 11 lncRNAs. Kyoto Encyclopedia of Genes and Genomes analysis of the 13 mRNAs in the ceRNA network showed that suppressors of cytokine signaling 1 (SOCS1), BTG anti-proliferation factor 2 (BTG2), and Bruton tyrosine kinase (BTK) were significantly enriched in the JAK/STAT signaling pathway, RNA degradation, and nuclear factor-κB (NF-κB) signaling pathway related to cancer. These findings indicated that SOCS1, BTG2, and BTK play an essential role in CA against NSCLC. Meanwhile, based on the ceRNA network, three lncRNAs (long intergenic non-protein coding RNA 1504 [LINC01504], LINC01783, and THUMPD3 antisense RNA 1 [THUMPD3-AS1]) and three miRNAs (has-miR-155-5p, has-miR-7-5p, and has-miR-425-5p) associated with SOCS1, BTG2, and BTK may be important in CA against NSCLC. Taken together, the present study demonstrated the activity of CA against lung cancer and its potential use as a therapeutic agent.

Keywords: cinnamaldehyde, long non-coding RNAs, micro RNAs, non-small cell lung cancer, messenger RNAs

INTRODUCTION

Lung cancer is the most common type of cancer and the leading cause of cancer-related death. It is expected that its incidence rate will continue to increase (Chen et al., 2016). Approximately 85% of patients with lung cancer have non-small cell lung cancer (NSCLC). Lung adenocarcinoma and lung squamous cell carcinoma are the major types of NSCLC (Molina et al., 2008; Herbst et al., 2018). Although the development of drugs has greatly improved the therapy of patients with advanced NSCLC, the 5 years survival rates of these patients remain low (Minguet et al., 2016). Therefore, it is urgent to identify effective drugs for combating the malignant phenotype of lung cancer and elucidate the anti-tumor molecular mechanism.

Cinnamaldehyde (CA; C9H80, MW 132.16), the main component of the essential oil isolated from cinnamon, is a traditional Chinese medicine (Wu et al., 2017). Studies have demonstrated that CA can exert significant anti-cancer effects through multiple mechanisms. In human hepatocarcinoma cells, CA induces cell apoptosis by downregulating the expression of BCL-(XL) and upregulating that of CD95 and p53 (Ng and Wu 2011). Moreover, CA exerts an effective chemo-preventive effect by activating the JNK, ERK, and AKT signaling pathways, resulting in NRF2 nuclear translocation, eventually upregulating the expression of the phase II enzyme (Huang et al., 2011). CA could induce apoptosis and inhibit invasion and adhesion in colorectal cancer cells by antagonizing the activation of the PI3K/AKT signaling pathway (Li et al., 2016). In NSCLC, CA could induce apoptosis and reverse epithelial-mesenchymal transition through inhibition of the Wnt/β-catenin signaling pathway (Wu et al., 2017). In addition, CA could induce cell apoptosis by a novel circular RNA hsa_circ_0043256 (Tian et al., 2017).

Noncoding RNAs (ncRNAs) comprise rRNAs and others that can be further classified into short ncRNAs (micro RNAs [miRNAs], small interfering RNAs, small nucleolar RNAs, transfer RNAs, and piwi-interacting RNAs) and long ncRNAs (lncRNAs) (Chan and Tay. 2018). miRNAs are an abundant class of small ncRNAs with 20–24 nucleotides (Wang et al., 2020), which negatively regulate the gene expression of messenger RNAs (mRNAs) and translation inhibition involved in cell death and cell proliferation (Ambros 2004). lncRNAs are longer than 200 nucleotides, and play essential roles in the proliferation, metastasis, drug sensitivity, and progression of tumors (Xie et al., 2019). In 2011, Salmena et al. proposed a regulatory mechanism between ncRNAs and mRNA, namely the competing endogenous RNA (ceRNA) hypothesis (Salmena et al., 2011). According to this hypothesis, miRNAs could regulate the expression of target mRNAs and ncRNAs by binding to the miRNA response elements. It has been reported that ncRNAs serve as miRNA sponges to decrease miRNA abundance, thus relieving the inhibitory effect of miRNA on downstream target mRNAs (Guttman et al., 2009; Prensner and Chinnaiyan. 2011; Salmena et al., 2011). An increasing body of evidence has demonstrated that the ncRNAs play an important role in multiple cancers, such as breast cancer (Fan et al., 2018), liver cancer (Yan et al., 2018), and lung cancer (Sui et al., 2016).

The aim of this study was to unveil the regulatory effect of CA in NSCLC and investigate its regulatory mechanism, as well as identify key mediator molecules for the effect of CA on NSCLC.

MATERIALS AND METHODS

Cell Culture

A549 and NCI-H1650 cell lines (lung adenocarcinoma), and SK-MES-1 and NCI-H226 cell lines (lung squamous cell carcinoma) were purchased from the Type Culture Collection of the Chinese Academy of Sciences (Shanghai, China). Cancer cells were cultured in RPMI1640 supplemented with 10% fetal bovine serum (FBS) and 1% penicillin (100 U/ml)/streptomycin (100 μg/ml) at 37°C with 5% CO_2.

Drugs and Reagents

The CA (purity 99.41% as measured by high-performance liquid chromatography) was purchased from the Shanghai BS Bio-Tech Co., Ltd (Shanghai, China) and dissolved in dimethyl sulfoxide. A total of 7.6 μL of CA was dissolved in 92.4 μL of dimethyl sulfoxide, and the final concentration of CA was 80 mg/ml. The 3-(4,5-Dimethylthiazol-2-thiazolyl)-2,5-diphenyltetrazolium bromide (MTT) was obtained from the Sigma Chemical Corporation (St. Louis, MO, United States). The annexin V/propidium iodide apoptosis detection kit was obtained from BD Biosciences (Franklin Lake, NJ, United States). The Matrigel was purchased from Corning (Wujiang, China). The TRIzol reagent was purchased from Invitrogen (Carlsbad, CA, United States). The RT reagent Kit and SYBR Green polymerase chain reaction (PCR) Master Mix were purchased from Promega (Madison, WI, United States). The primary antibodies against phospho-NF-κB (p-NF-κB) p65, *p*-JAK, phospho-signal transducer and activator of transcription 3 (p-STAT3), peroxisome proliferator-activated receptor gamma (PPARγ), and β-actin (1:1,000) were purchased from the Cell Signaling Technology Co., Ltd (Danvers, MA, United States).

Cell Proliferation Assay

Cell viability was assessed using the MTT assay (Hao et al., 2020). Briefly, A549 (3,000 cells/well), NCI-H1650 (8,000 cells/well), SK-MES-1 (5,000 cells/well), and NCI-H226 (5,000 cells/well) cells were seeded in 96-well plates in the presence of various concentrations of CA. After treatment with CA for 24, 48, and 72 h, the cells were incubated with MTT (0.25 mg/ml) for 4 h at 37°C. Subsequently, the supernatant was discarded, and the formazan crystals were dissolved by adding dimethyl sulfoxide. The plates were analyzed at 490 nm to determine cell viability.

Cell Apoptosis Assay

Cells were resuspended in 500 μl of binding buffer after treatment with various concentrations of CA for 24 h. Subsequently, 5 μl of annexin V-fluorescein isothiocyanate (FITC) and propidium iodide (PI) were added, and the cells were incubated for 15 min in the dark. Flow cytometry was employed to analyze the apoptosis of lung cancer cells.

Cell Migration and Invasion Assay

For the migration assay, NSCLC cells were resuspended in 200 μL of FBS-free RPMI1640 medium that contained various concentrations of CA and placed in the upper chambers. The lower chambers were filled with 600 μL of RPMI1640 medium containing 10% FBS. At 24 h following the treatment with CA, the cells were fixed using 4% paraformaldehyde and stained with 0.25% crystal violet. The stained cells were imaged and counted to detect cell migration.

For the invasion assay, the membrane was coated with Matrigel (1:10 dilution) to form a matrix barrier. NSCLC cells were resuspended in 200 μL of RPMI1640 medium containing 5% FBS and various concentrations of CA and placed in the upper chambers. The lower chambers were filled with 600 μL of RPMI1640 medium containing 20% FBS. At 48 h after treatment with CA, the cells were fixed using 4% paraformaldehyde and stained with 0.25% crystal violet. The stained cells were imaged and counted to detect cell migration.

In vivo Tumor Xenograft Experiments

Five-week-old female BALB/c nude mice were purchased from the Beijing Charles River Laboratory Animal Technology Co., Ltd. (Beijing, China) and used for the xenograft model. A549 cells were dissociated using trypsin and washed with sterilized phosphate-buffered saline (PBS). Subsequently, 0.1 ml of PBS containing 5×10^6 cells was subcutaneously injected into the left flank of all mice. Mice were randomly separated into the vehicle group (PBS; $n = 5$) and CA group (100 mg/kg; $n = 5$). Both PBS and CA were intraperitoneally delivered once daily, and the mean tumor volumes were calculated using the following formula: volume = (length × width^2)/2. The weight of mice was monitored and the tumor volume was measured once every 3 days. The mice were sacrificed 24 h after the last dose, and tumors were excised for weight and volume computation. All experiments were performed in accordance with the Guide for the Care and Use of Laboratory Animals, with the approval of Shanxi Medical University (Taiyuan, China).

Whole Transcriptome Sequencing

A549 cells (control and 80 μg/ml CA groups) and SK-MES-1 cells (control and 40 μg/ml CA groups) were sent to Beijing Novogene (Beijing, China) to extract RNA, establish a cDNA library, and perform whole transcriptome sequencing. A total amount of 3 μg of RNA per sample was used as the input material for the preparation of the RNA samples. Sequencing libraries were generated using the NEBNext® Ultra™ RNA Library Prep Kit for Illumina® (NEB, United States). Gene expression was quantified using fragments per kilobase of transcript per million reads mapped (FPKM).

Identification of Differentially Expressed (DE) Genes

The volcano plot was visualized using the R ggplot2 packages between the control and 80 μg/ml CA groups of the A549 cell line (including all genes), and the control and 40 μg/ml CA groups of the SK-MES-1 cell line (including all genes). Next, genes with an FPKM of any group >1, $|\log_2\text{FoldChange}| > 1$, and adjusted p-value < 0.05 were considered as DE genes. The DE-mRNAs, DE-miRNAs, and DE-lncRNAs with the same expression trend intersecting from the 80 μg/ml CA group of A549 cells and the 40 μg/ml CA group of SK-MES-1 cells were regarded as common DE-mRNAs (CDE-mRNAs), CDE-miRNAs, and CDE-lncRNAs compared with control. Venn diagrams were plotted by VENNY 2.1.0 (https://bioinfogp.cnb.csic.es/tools/venny/index.html). The pheatmap package in R was used to plot the heatmap of the CDE-mRNAs, CDE-miRNAs, and CDE-lncRNAs.

Functional Enrichment Analysis

Gene ontology (GO) functional enrichment was conducted using Metascape (https://metascape.org/gp/index.html) and Kyoto Encyclopedia of Genes and Genomes (KEGG) pathway enrichment analysis was performed using KOBAS 3.0 (http://kobas.cbi.pku.edu.cn/kobas3/genelist/) to investigate the possible functions of the CDE-mRNAs. The top 20 enriched GO categories and KEGG pathways were considered statistically significant and shown. The pathway. plot package in R was used to draw the GO term and KEGG pathway. The protein-protein interaction (PPI) network of the CDE-mRNAs was constructed to evaluate the interactive relationships by employing the STRING online database (https://string-db.org). The PPI pairs with a combined confidence score ≥0.4 were visualized in the network using the Cytoscape software.

Prediction of miRNA-targeted mRNA and miRNA-mRNA network construction, prediction of miRNA-targeted lncRNA and ceRNA network construction

The lncRNA-miRNA-mRNA ceRNA network was constructed according to the miRNAs that can negatively regulate the expression of mRNAs and lncRNAs. Firstly, target mRNAs of the CDE-miRNAs were screened through the online mirtarbase (http://mirtarbase.cuhk.edu.cn/php/index.php) and Targetscan (http://www.targetscan.org/vert_72/). Only the miRNA-mRNA relationship pairs found in both databases were selected as candidate genes to construct the ceRNA network. Secondly, target lncRNAs of the CDE-miRNAs were screened through the online LncBase (http://carolina.imis.athena-innovation.gr/). Thirdly, the intersection of target mRNAs of the CDE-miRNAs and CDE-mRNAs was selected for further analysis. The intersection of target lncRNAs of the CDE-miRNAs and CDE-lncRNAs was also selected for further analysis. Finally, the miRNAs that were negatively regulated by the lncRNAs and mRNAs were selected to construct the miRNA-mRNA network and ceRNA network. Cytoscape (version 3.5.1) was used to visualize the miRNA-mRNA and lncRNA-miRNA-mRNA ceRNA networks.

Validation by Real-Time PCR

Total RNA was extracted with TRIzol and converted to cDNA according to the instructions provided by the manufacturer. The cDNA was subjected to quantitative real-time PCR to detect

TABLE 1 | The list of gene primer.

gene	Forward primer	Reverse primer
CREBRF	GTCTCCGACAACTTGGGTGAACAG	GCCGAATCCTTCATCATGGTCCTC
BTK	CCCTGAGCTCATTAACTACCAT	CCCATACTTCACTACCCCAAAT
MXD1	ACAAGGACAGAGATGCCTTAAA	TAAACTCAACGTAGTGTGTCGA
BTG2	CACTCACAGAGCACTACAAACA	CATCTTGTGGTTGATGCGAATG
SOCS1	ACACGCACTTCCGCACATT	TAGAATCCGCAGGCGTCCA
LINC01504	GAGAGCGTGGCTTTAACGTCT	TCCCTGGCCCAAGCTATCTC
LINC01783	CCAACAAGGACAGCAGGTGG	GTGCGCAAGTGCTTGGTAGA
LINC01484	GCCTTAGTGCTGCCATGCTGAG	GTGCCTGATGAGTCCTGGGAAATG
LUCAT1	CACCACACCCAGGAATCCAACTTG	GTACAGGCACGCTAAGTCTCATCC
THUMPD3-AS1	GAGACAAGCCCGACCTGCTA	CTCTGTGCTTACGCAACGGATA

mRNA expression using the GoTaq one-step real-time PCR kit with SYBR green; glyceraldehyde-3-phosphate dehydrogenase was used as an internal control. The gene primer list is shown in **Table 1**.

Western Blotting Analysis

Total protein from cells was extracted using cell lysis buffer supplemented with protease inhibitors and phosphatase inhibitors. Equal amounts of protein were separated on 10% sodium dodecyl sulfate-polyacrylamide gel electrophoresis gels and transferred to nitrocellulose filter membranes. The membranes were blocked with 5% skim milk to block antigens at room temperature for 1 h and probed overnight at 4°C with primary antibodies. This was followed by further incubation with fluorescent secondary antibody for 2 h at room temperature. After washing, proteins were visualized with Odyssey (Licor, United States). The quantitative analysis was performed using the ImageJ software (National Institute of Mental Health, Bethesda, MD, United States).

Statistical Analysis

One-way ANOVA followed by Fisher's least significant difference (LSD) or Dunnett's T3 were used to evaluate the differences between the groups when more than two groups and the independent sample *t*-test was used to analysis the differences of two groups using the SPSS 26.0 software (SPSS Inc., Chicago, IL, United States). Bioinformatics analysis was conducted using the aforementioned bioinformatics tools.

RESULTS

CA Suppresses NSCLC Cell Proliferation

The chemical structure of CA is shown in **Figure 1A**. A549, NCI-H1650, SK-MES-1, and NCI-H226 cell viability was significantly inhibited after treatment with CA for 24, 48, and 72 h. The observed inhibition rates were both dose- and time-dependent (**Figure 1B–E**). The IC_{50} values of the A549, NCI-H1650, SK-MES-1, and NCI-H226 cells were 47.44, 23.37, 27.63, and 28.13 μg/ml after treatment with CA for 24 h, respectively. According to the IC_{50} values, the 24 h treatment timepoint was selected for subsequent experiments.

CA Induces Apoptosis and Inhibits Invasion and Migration in NSCLC Cells

Annexin V-FITC analysis was performed to detect the apoptosis of cells after treatment with CA for 24 h. CA significantly induced apoptosis of A549, NCI-H1650, SK-MES-1, and NCI-H226 cells in a dose-dependent manner (**Figure 2A–D**). The results suggested that CA may suppress NSCLC cell proliferation via induction of apoptosis.

To clarify whether CA could inhibit the invasion and migration of NSCLC cells, we conducted Transwell invasion and migration assays. The results showed that CA significantly inhibited cell invasion and migration in a dose-dependent manner (**Figure 3A–H**).

CA Inhibits Tumor Growth in Mice

To study the effect of CA *in vivo*, a model of subcutaneous tumor implantation was established. The detailed protocol is shown in **Figure 4A**. The volume and weight of the tumors of mice treated with CA were smaller than those observed in the vehicle group (**Figures 4B–E**). In addition, there were no significant differences in body weight between CA-treated mice and vehicle mice (**Figure 4F**), indicating that CA may not induce physiological toxicity at the tested dose. The results of this experiment suggesting that CA could inhibit tumor growth.

Identification of CDE-mRNAs, CDE-miRNAs, and CDE-lncRNAs

To elucidate the anti-cancer mechanism of CA, we used doses of 80 μg/ml and 40 μg/ml to treat A549 and SK-MES-1 cells, respectively. Subsequently, we carried out whole transcriptome sequencing to analyze the gene expression patterns in the CA-treated and -untreated cells.

The volcano plot displayed all altered mRNAs, miRNAs, and lncRNAs in A549 and SK-MES-1 cells (**Figures 5A–C**). As shown in the Venn diagram, 528 and 1,620 DE-mRNAs (**Figure 6A**), 43 and 127 DE-miRNAs (**Figure 6B**), and 267 and 1,254 DE-lncRNAs (**Figure 6C**) were identified in A549 and SK-MES-1 cells, respectively. Furthermore, 152 CDE-mRNAs (82 upregulated and 70 downregulated), 21 CDE-miRNAs (11 upregulated and 10 downregulated), and 78 CDE-lncRNAs (67 upregulated and 11

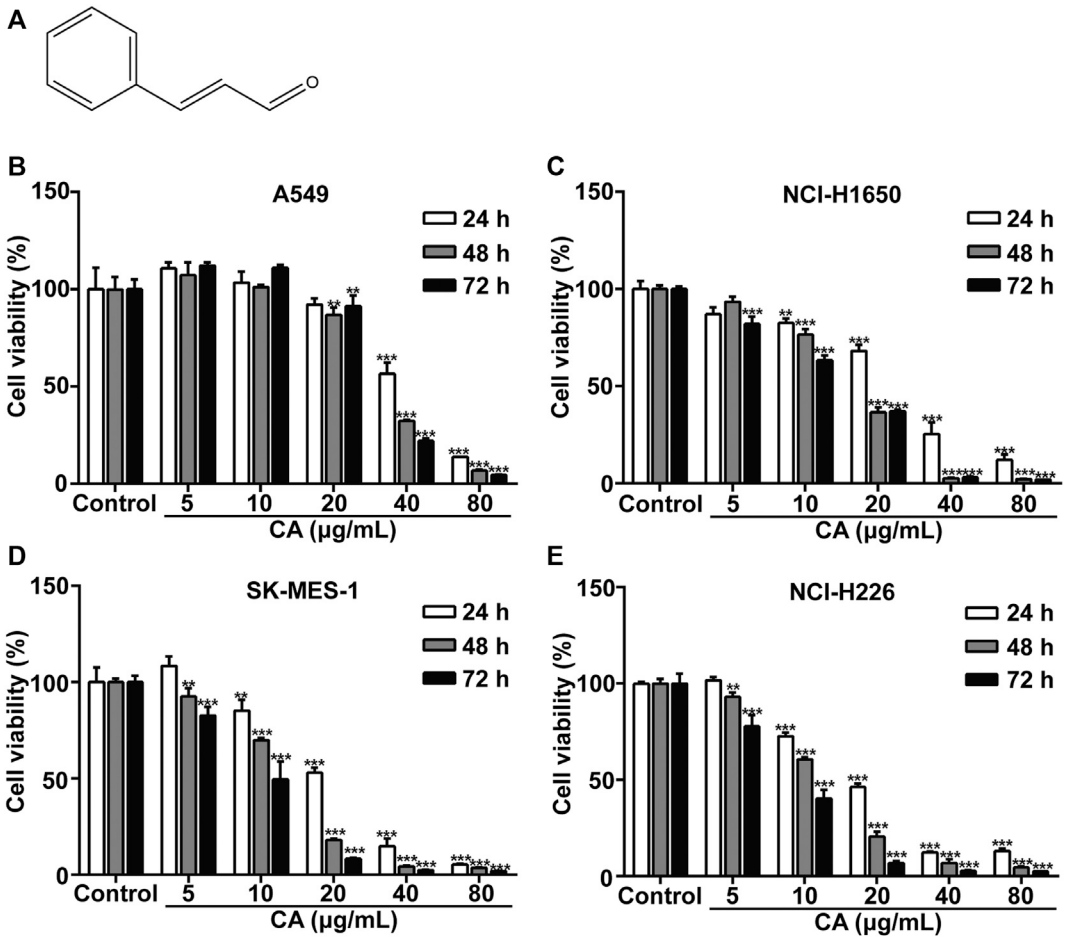

FIGURE 1 | Cinnamaldehyde (CA) inhibits the proliferation of NSCLC cells. **(A)** Chemical structure of CA. **(B–E)** A549, NCI-H1650, SK-MES-1, and NCI-H226 cells were treated with various concentrations of CA for 24, 48, and 72 h, cell proliferation was measured using the MTT assay. Data are expressed as the mean ± SD of three independent experiments. $^{**}p < 0.01$ and $^{***}p < 0.001$ vs. the control group. NSCLC, non-small cell lung cancer; SD, standard deviation.

downregulated) were detected in two cell line (**Figures 6A–C** and **Supplementary Table S1**). The heatmap of CDE-mRNAs, CDE-miRNAs, and CDE-lncRNAs showed that after treatment with CA, gene expression was significantly changed compared with the control group (**Figures 6A–C**).

Functional Analysis of the CDE-mRNAs

To investigate the biological functions of the identified CDE-mRNAs, we performed GO term enrichment analysis and KEGG pathway analysis. The result of GO annotation indicated that CDE-mRNAs were significantly enriched in terms associated with cell apoptosis and proliferation, such as the apoptotic signaling pathway, the regulation of the neuron apoptotic process, the intrinsic apoptotic signaling pathway in response to endoplasmic reticulum stress, the negative regulation of growth, and the negative regulation of cell proliferation (**Figure 7A**). KEGG pathway analysis showed that CDE-mRNAs were significantly enriched in some cancer-associated pathways, including transcriptional misregulation in cancer, the MAPK signaling pathway, pathways in cancer, the PI3K/AKT signaling pathway, the Ras signaling pathway, apoptosis - multiple species, and the FOXO signaling pathway (**Figure 7B**). Taken together, these results indicated that CDE-mRNAs were closely related to apoptosis and cancer. To explore the relationship between these CDE-mRNAs, the PPI network was constructed using the STRING online database and visualized using Cytoscape (**Figure 7C**). The subnetwork (highly correlated module) was extracted from the whole PPI network using the Molecular COmplex DEtection (MCODE) algorithm. Highly correlated module analysis showed that CA affected histone genes, indicating that CA may play a central role in the regulation of transcription, DNA repair, DNA replication, and chromosomal stability (**Figure 7D**).

Target mRNAs of CDE-miRNAs and Construction of the miRNA-mRNA Network

To further investigate the anti-cancer molecular mechanism involved in the effect of CA, target genes of CDE-miRNAs

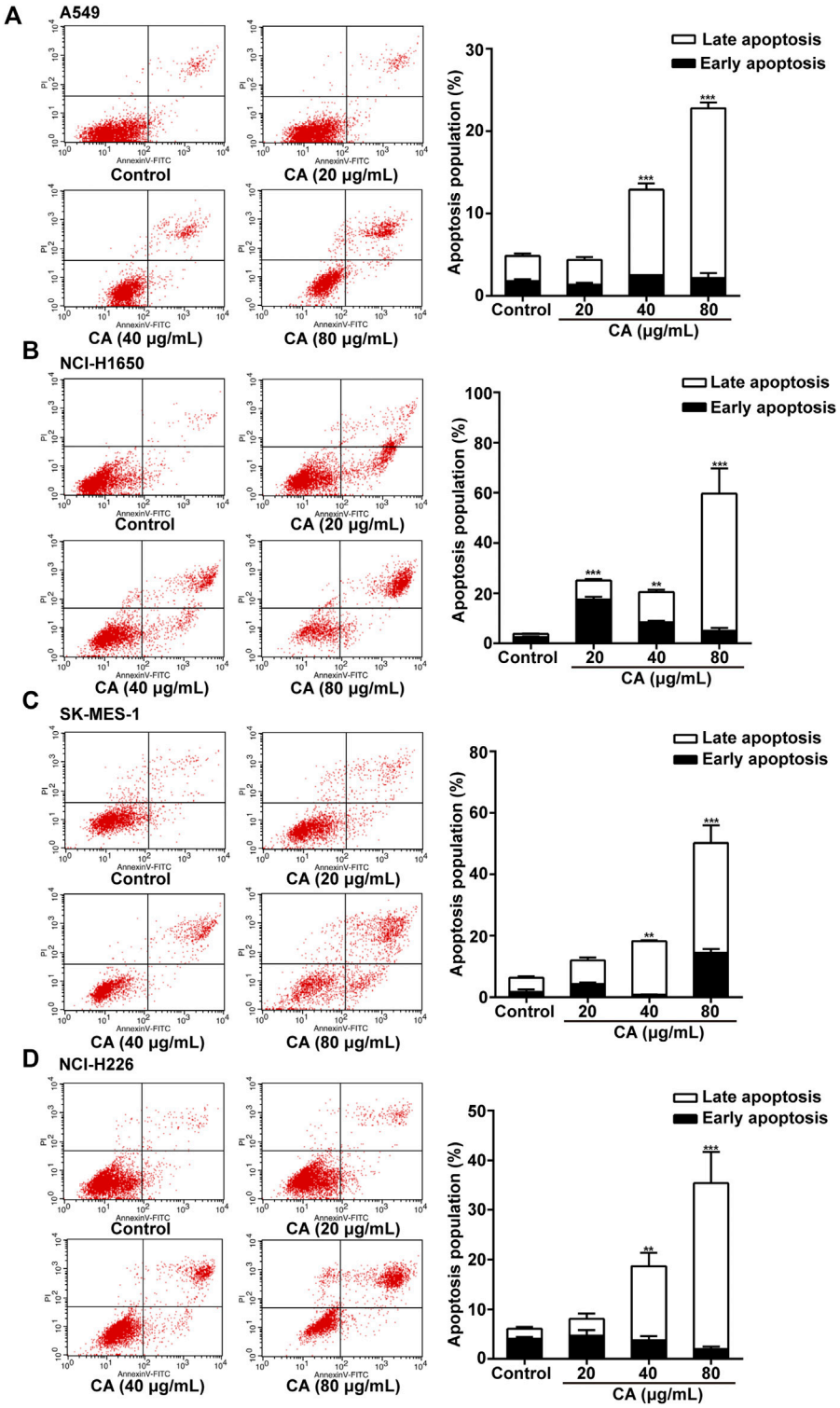

FIGURE 2 | Cinnamaldehyde (CA) induces the apoptosis of NSCLC cells. **(A)** A549 cells were treated with 20, 40, and 80 μg/ml of CA for 24 h and stained with FITC-conjugated annexin V and PI to detect cell apoptosis through flow cytometry. **(B–D)** NCI-H1650, SK-MES-1, and NCI-H226 cells were treated with 10, 20, and 40 μg/ml of CA for 24 h and stained with FITC-conjugated annexin V and PI to detect cell apoptosis through flow cytometry. The quantitative results are shown in the right panel, and data are expressed as the mean ± SD of three independent experiments. $^{**}p < 0.01$ and $^{***}p < 0.001$ vs. the control group. FITC, fluorescein isothiocyanate; NSCLC, non-small cell lung cancer; PI, propidium iodide; SD, standard deviation.

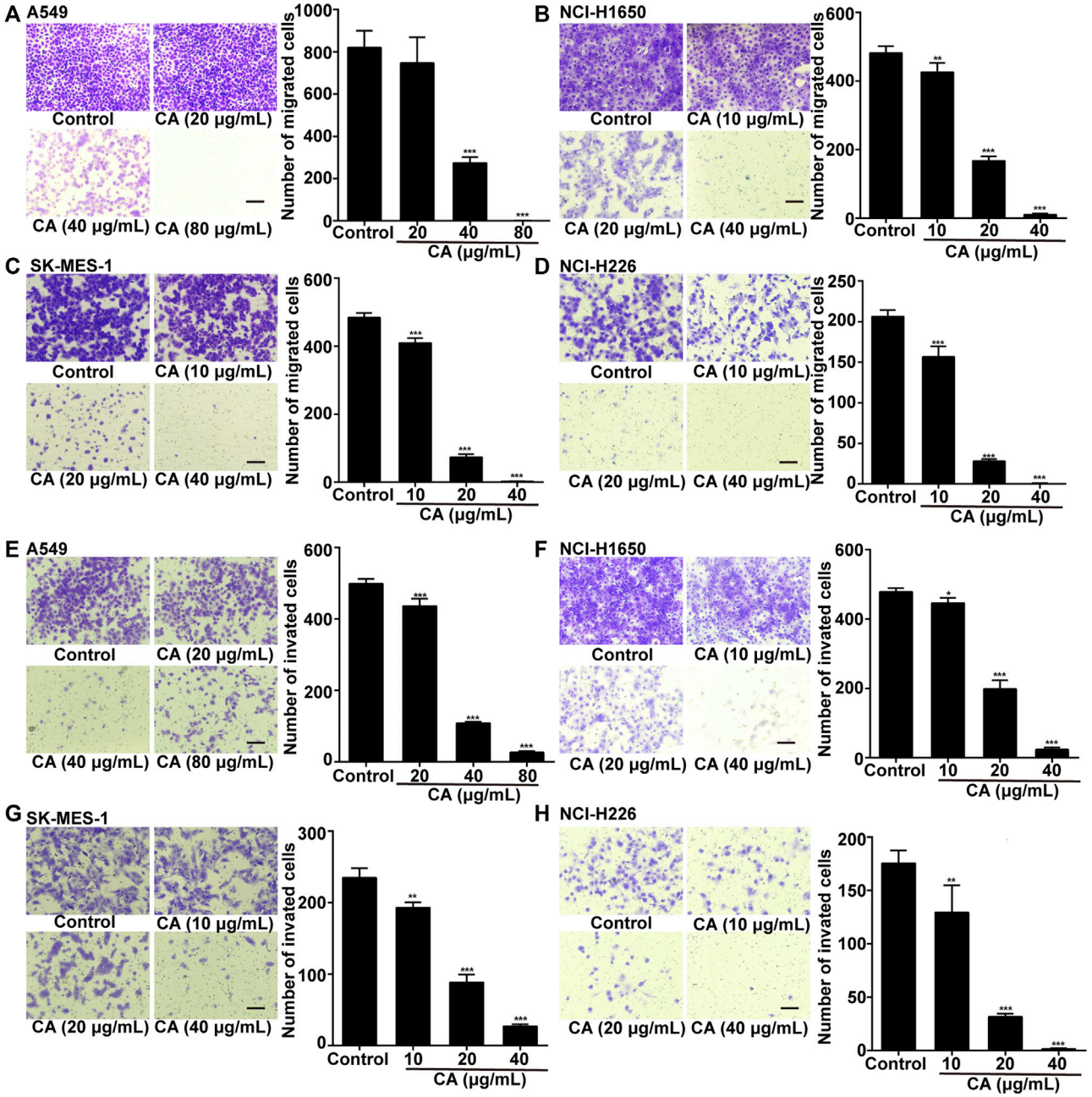

FIGURE 3 | Cinnamaldehyde (CA) inhibits the invasion and migration of NSCLC cells. **(A)** A549 cells were treated with 20, 40, and 80 μg/ml of CA for 24 h to detect cell migration. **(B–D)** NCI-H1650, SK-MES-1, and NCI-H226 cells were treated with 10, 20, and 40 μg/ml of CA for 24 h to detect cell migration; **(E)** A549 cells were treated with 20, 40, and 80 μg/ml of CA for 48 h to detect cell invasion; **(F–H)** NCI-H1650, SK-MES-1, and NCI-H226 cells were treated with 10, 20, and 40 μg/ml of CA for 48 h to detect cell invasion. The quantitative results are shown in the right panel, and data are expressed as the mean ± SD of three independent experiments. $^{*}p < 0.05$, $^{**}p < 0.01$, and $^{***}p < 0.001$ vs. the control group. NSCLC, non-small cell lung cancer; SD, standard deviation.

were predicted using the miRTarBase and Targetscan databases. A total of 24 mRNAs, such as a suppressor of cytokine signaling 1 (SOCS1), CREB3 regulatory factor (CREBRF), Bruton tyrosine kinase (BTK), BTG anti-proliferation factor 2 (BTG2), zinc finger and BTB domain containing 46 (ZBTB46), and M-phase specific PLK1 interacting protein (MPLKIP) overlapped with the CDE-mRNAs (**Supplementary Table S2**). According to the inverse regulatory relationship between miRNA and its target gene, a regulated miRNA-mRNA network was constructed using Cytoscape, which included 7 CDE-miRNAs and 15 target CDE-mRNAs (**Figure 8A**). Those CDE-miRNAs were selected for further analysis.

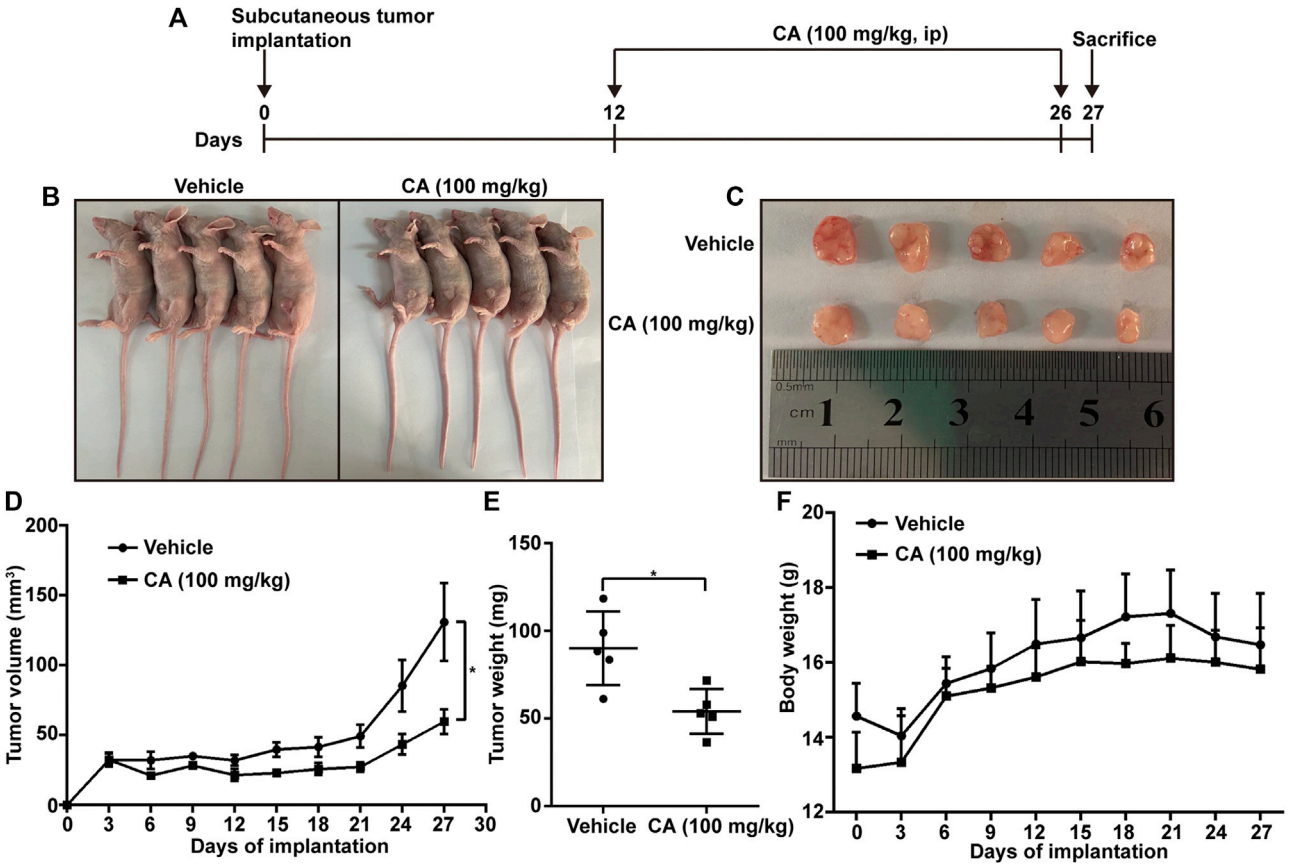

FIGURE 4 | Cinnamaldehyde (CA) inhibits tumor growth in mice. **(A)** Diagram of the animal study protocol. **(B)** A549 cells (5×10^6) were implanted into nude mice ($n = 5$). Representative images show the tumor xenografts. **(C,D)** Tumor volumes and weight were measured, and the volume of the tumors was calculated ((length × width^2)/2). **(E)** Body weight was calculated every 3 days after implantation. Data are expressed as the mean ± SD of five independent experiments. *$p < 0.05$ vs. the vehicle group. ip, intraperitoneal injection; SD, standard deviation.

Target lncRNAs of CDE-miRNAs and Construction of the ceRNA Regulatory Network

It is widely acknowledged that lncRNA can function as a sponge to competitively bind to miRNA. Hence, we predicted upstream lncRNAs that could potentially bind to those seven key CDE-miRNAs using an online LncBase database. A total of 14 lncRNAs, such as PARD6G antisense RNA 1 (PARD6G-AS1), BNC2-AS1, THUMPD3-AS1, lung cancer associated transcript 1 (LUCAT1), AC015813.1, long intergenic non-protein coding RNA 1504 (LINC01504), and LINC01484 overlapped with the CDE-lncRNAs (**Supplementary Table S3**). Based on the ceRNA hypothesis, the miRNAs were negatively regulated by the lncRNAs and mRNAs. The ceRNA network was constructed, including 6 CDE-miRNAs, 13 target CDE-mRNAs, and 11 target CDE-lncRNAs (**Figure 8B**).

KEGG Analysis of the mRNAs in the ceRNA Network

The KEGG pathway analysis showed that mRNAs in the ceRNA network were significantly enriched in the JAK/STAT signaling pathway (Owen et al., 2019), RNA degradation (Chang and Huang 2019), and NF-κB signaling pathway (Khan et al., 2020) related to cancer. SOCS1, BTK, and BTG2 were significantly enriched in these pathways (**Figure 9**).

Among lncRNAs in the ceRNA, LINC01504, LINC01783, and THUMPD3-AS1 were related to prognosis, indicating their important role in the development of cancer. Thus, based on the ceRNA network, three key lncRNAs (LINC01504, LINC01783, and THUMPD3-AS1) and miRNAs (has-miR-155–5p, has-miR-7-5p, and has-425–5p) that regulate SOCS1, BTG2, and BTK were identified.

Gene Expression Verification via Quantitative PCR (qPCR)

We also determined the accuracy and reliability of the present bioinformatics analysis. For this purpose, qPCR was used to evaluate gene expression in the A549 and SK-MES-1 cells. Genes in the ceRNA network were selected to verify the reliability of the sequencing results. Consistent with the sequencing results, the expression levels of five mRNAs

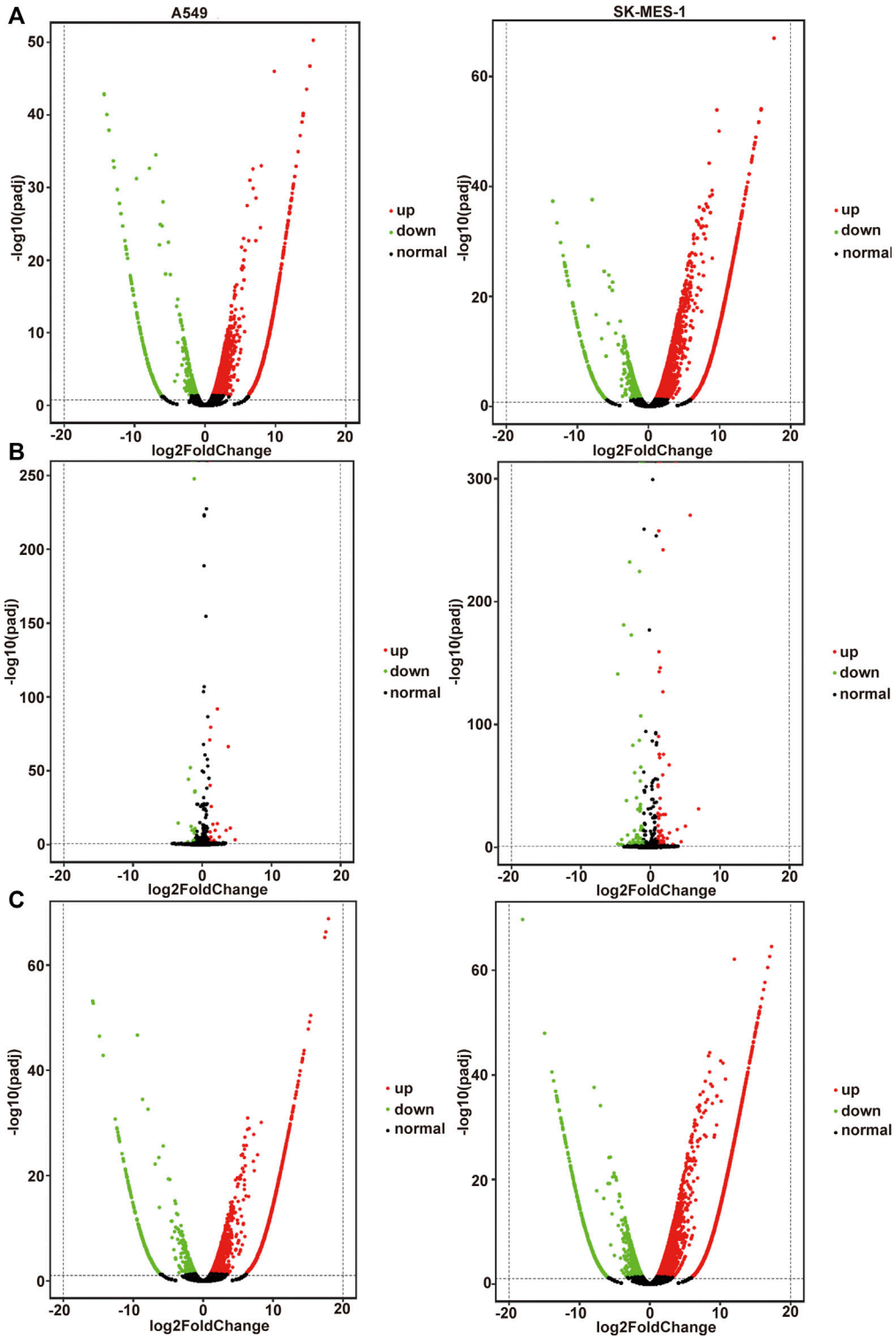

FIGURE 5 | All genes affected by cinnamaldehyde (CA). **(A–C)** Volcano plot showing all altered mRNAs, miRNAs, and lncRNAs in A549 cells and SK-MES-1 cells. A549 cells are shown on the left, SK-MES-1 cells are shown on the right. mRNAs, messenger RNAs; miRNAs, micro RNAs; lncRNAs, long noncoding RNAs.

(i.e., SOCS1, CREBRF, MAX dimerization protein 1 [MXD1], BTK, and BTG2), and three lncRNAs (i.e., LINC01504, LINC01783, and LUCAT1) were significantly elevated after the A549 cells were treated with CA (**Figures 10A**). The expression levels of five mRNAs (i.e., SOCS1, CREBRF, MXD1, BTK, and BTG2) and five lncRNAs (i.e., LINC01504,

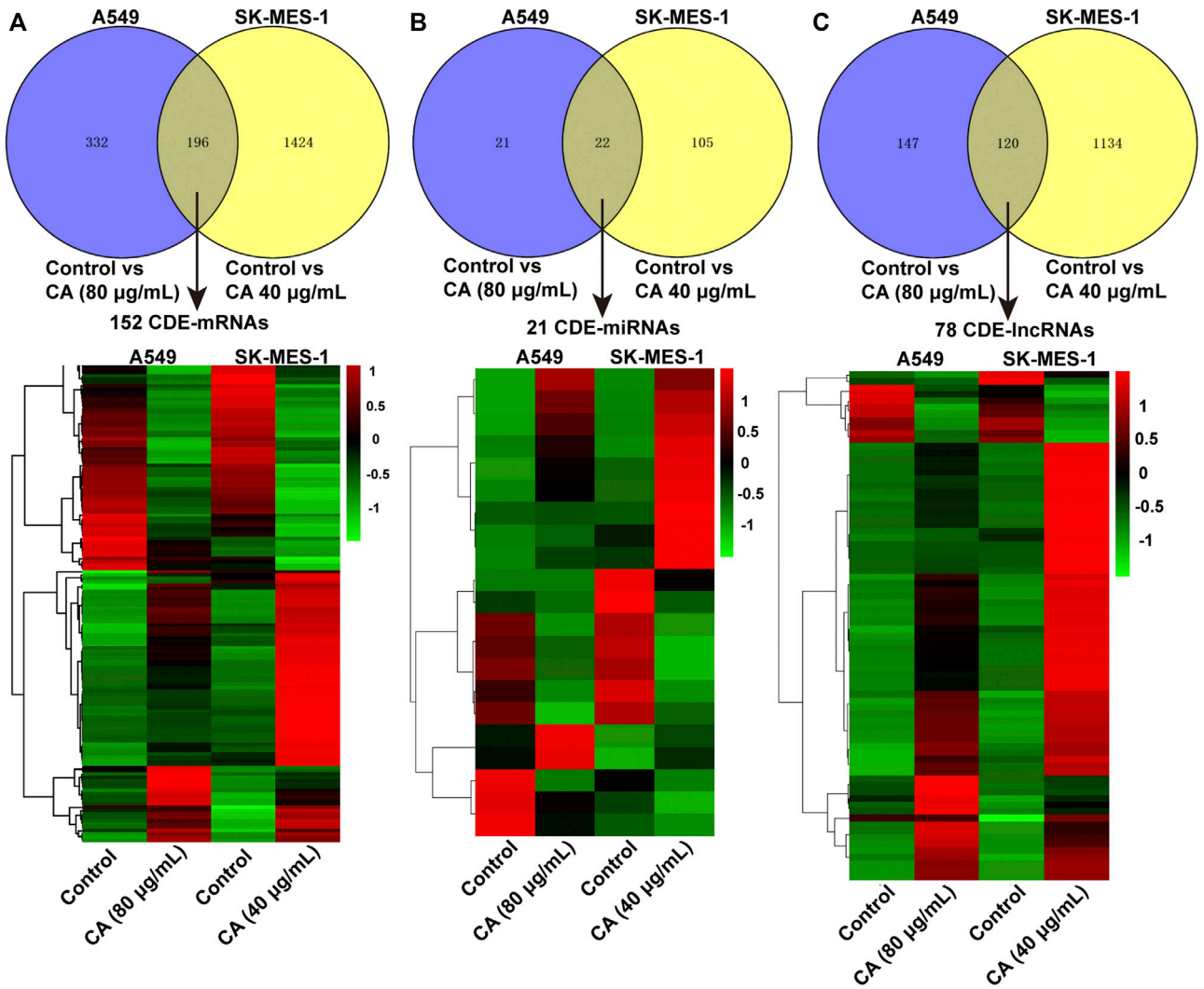

FIGURE 6 | The expression profiles of DE-mRNAs were influenced by cinnamaldehyde (CA). **(A–C)** Venn diagram showing CDE-mRNAs, CDE-miRNAs, and CDE-lncRNAs in A549 cells and SK-MES-1 cells. Heatmap of CDE-mRNAs, CDE-miRNAs, and CDE-lncRNAs in A549 cells and SK-MES-1 cells. DE, differentially expressed; CDE, common differentially expressed; lncRNAs, long noncoding RNAs; mRNAs, messenger RNAs; miRNAs, micro RNAs.

LUCAT1, LINC01484, THUMPD3-AS1, and LINC01783) were significantly elevated after the SK-MES-1 cells were treated with CA (**Figures 10C**).

CA inhibits the JAK/STAT3 signaling pathway, NF-κB signaling pathway, and RNA degradation signaling pathway

The involvement of key pathways, such as the JAK/STAT3 signaling pathway, NF-κB signaling pathway, and RNA degradation pathway, in the inhibitory effects of CA on NSCLC was analyzed. The phosphorylation levels of JAK, STAT3, and NF-κB p65 were significantly suppressed by CA in A549 and SK-MES-1 cells (**Figures 11A,B**). Moreover, the expression of PPARγ was also inhibited by CA (**Figures 11A,B**). These results suggested that CA could inhibit multiple pathways, including the JAK/STAT3, NF-κB, and RNA degradation signaling pathway.

DISCUSSION

Natural products against cancer have been considered in numerous studies. After experimental and clinical verification, agents such as vincristine, camptothecin, and paclitaxel have been approved for medical use and have become essential drugs for the treatment and prevention of tumors. Research has demonstrated that CA can exert an anti-tumor effect. In this study, it could inhibit proliferation, induce apoptosis, and inhibit the migration and invasion of NSCLC cells *in vitro*. Moreover, it could efficiently suppress NSCLC progression *in vivo*. In the present study, we used whole transcriptome sequencing to reveal the anti-

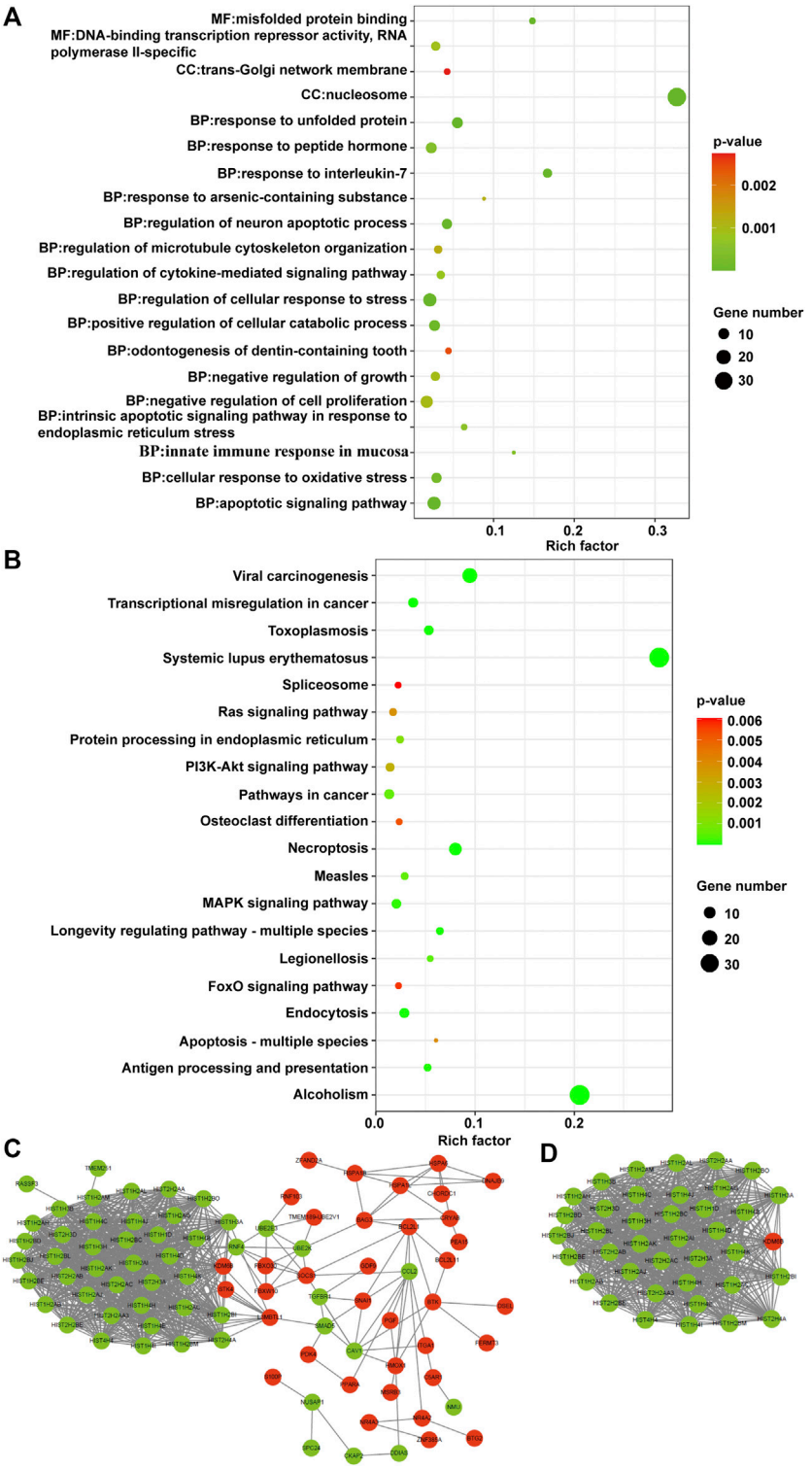

FIGURE 7 | Functional analysis of the CDE-mRNAs. **(A)** The top 20 GO enrichment terms. **(B)** The top 20 KEGG enrichment terms. **(C)** The PPI network contains 88 nodes and 830 edges. **(D)** The subnetwork from the PPI network contains 39 nodes and 732 edges. The genes in red and green represent upregulation and downregulation, respectively. CDE-mRNAs, common differentially expressed-messenger RNAs; GO, Gene ontology; KEGG, Kyoto Encyclopedia of Genes and Genomes; PPI, protein-protein interaction.

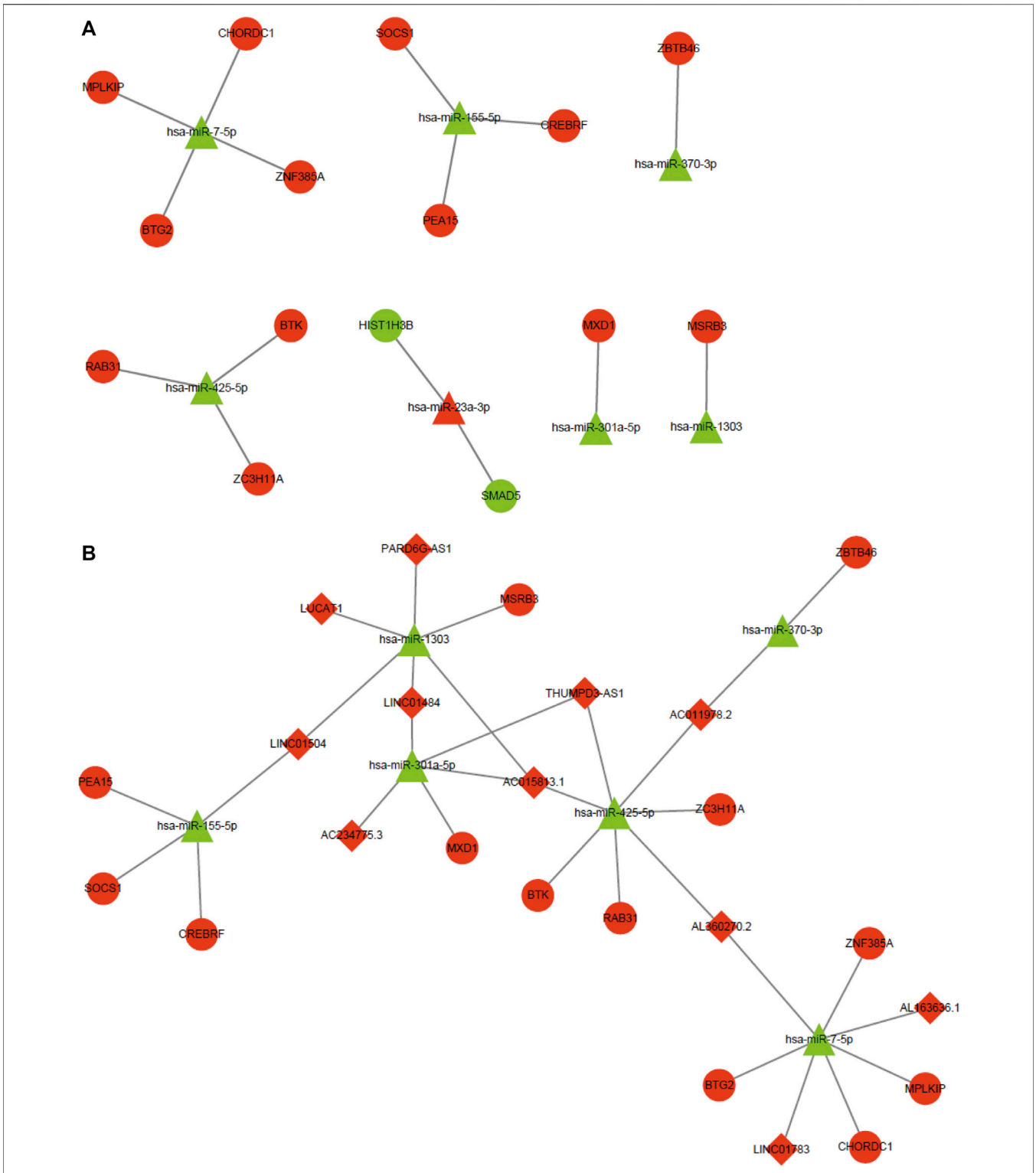

FIGURE 8 | MiRNA-mRNA regulatory network and ceRNA network. **(A)** miRNA-mRNA regulatory network. Red and green represent upregulation and downregulation, respectively. Triangles and circles represent CDE-miRNAs and CDE-mRNAs, respectively. **(B)** ceRNA network. Red and green represent upregulation and downregulation, respectively. Triangles, circles, and diamonds represent CDE-miRNAs, CDE-mRNAs, and CDE-lncRNAs, respectively. CDE, common differentially expressed; ceRNA, competing endogenous RNA; lncRNAs, long noncoding RNAs; mRNAs, messenger RNAs; miRNAs, micro RNAs.

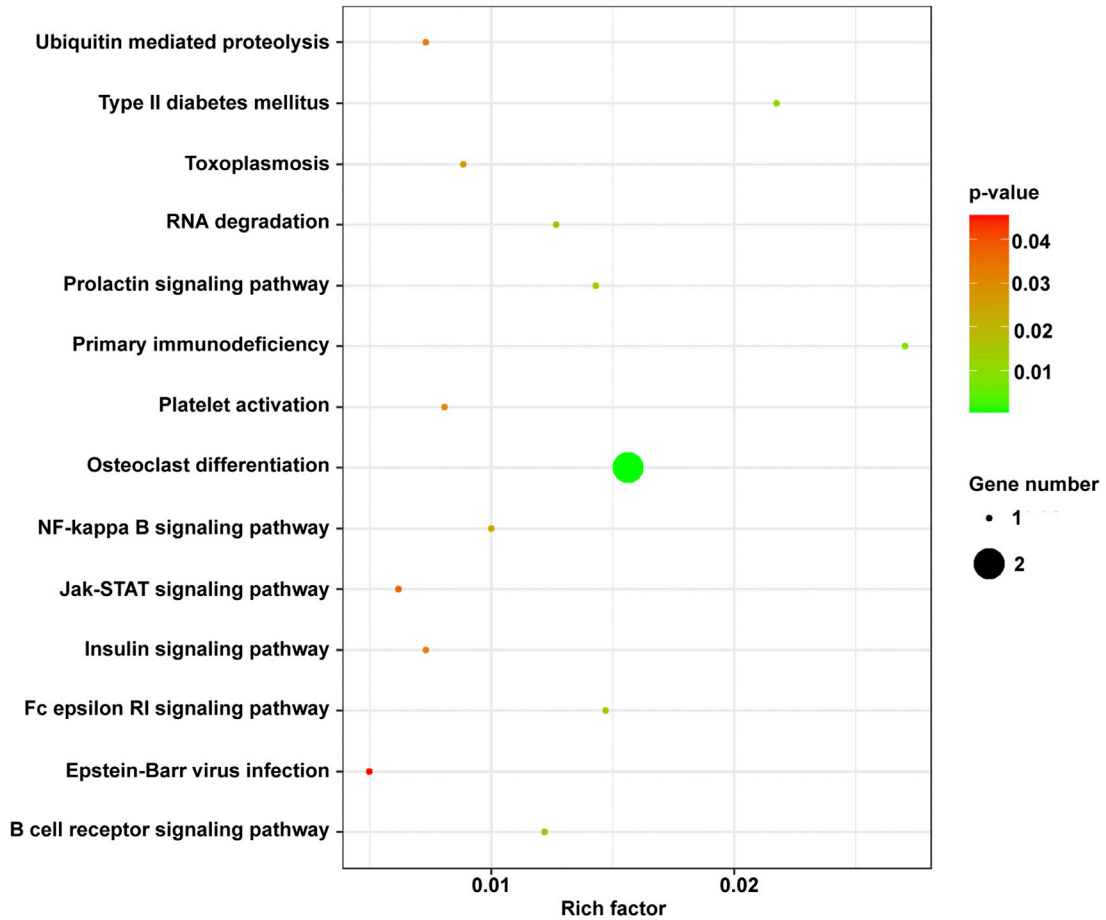

FIGURE 9 | The KEGG enrichment terms of mRNAs in the ceRNA network. ceRNA, competing endogenous RNA; KEGG, Kyoto Encyclopedia of Genes and Genomes; mRNA, messenger RNA.

tumor mechanism involved in the effects of CA and identify novel prognostic indicators of lung cancer.

In the present study, we successfully constructed an lncRNA-miRNA-mRNA regulatory network. Firstly, we screened 152 dysregulated CDE-mRNAs; GO analysis revealed that those CDE-mRNAs were significantly enriched in some cancer-related GO items, such as the regulation of the neuron apoptotic process (Hollville et al., 2019), the intrinsic apoptotic signaling pathway in response to endoplasmic reticulum stress (Ghobrial et al., 2005), the negative regulation of growth, and the negative regulation of cell proliferation (Giordano and Tommonaro 2019). Subsequent KEGG pathway enrichment analysis also highlighted various pathways involved in cancer progression, including transcriptional misregulation in cancer, the MAPK signaling pathway (Davis 2000), pathways in cancer, the PI3K/AKT signaling pathway (Martini et al., 2014), the Ras signaling pathway (Fang 2016), apoptosis across multiple species, and the FOXO signaling pathway (Farhan et al., 2017). The PPI network was constructed to exhibit complicated associations among these CDE-mRNAs. Therefore, these CDE-mRNAs interact with each other and may play important roles in the effect of CA on cancer.

The ceRNA network was constructed according to the expression analysis of sequencing data and the ceRNA hypothesis. Among the identified three-lncRNA signature, LINC01504 is involved in nontranslocation-related sarcomas (Delespaul et al., 2017). The specific anti-cancer mechanism of LINC01504 is unclear; however, it is lowly expressed in NSCLC and associated with the prognosis of NSCLC. A recent study reported that LINC01783 was associated with the proliferation, migration, and invasion of cervical cancer cells, indicating its important role in cancer (Chen et al., 2020). It was also discovered that THUMPD3-AS1 is involved in many tumors, and affects the proliferation and self-renewal of NSCLC cells (Hu et al., 2019). In our study, LINC01504 and SOCS1 in the ceRNA network were upregulated after treatment with CA, whereas has-miR-155–5p was downregulated. Moreover, CA could inhibit the activation of the JAK/STAT3 signaling pathway. Previous studies have shown that hsa-miR-155–5p functions as an oncogene to promote the progression of hepatocellular carcinoma (Fu et al., 2017) and affect cell proliferation and apoptosis (Zhao et al., 2019). SOCS1 could reduce inflammation within the tumor microenvironment to contribute to tumor suppression in a cancer cell-intrinsic manner (Villalobos-Hernandez et al., 2017). In addition, SOCS1 could inhibit cell growth and attenuate MET signaling, thereby inhibiting hepatocyte growth factor-induced migration

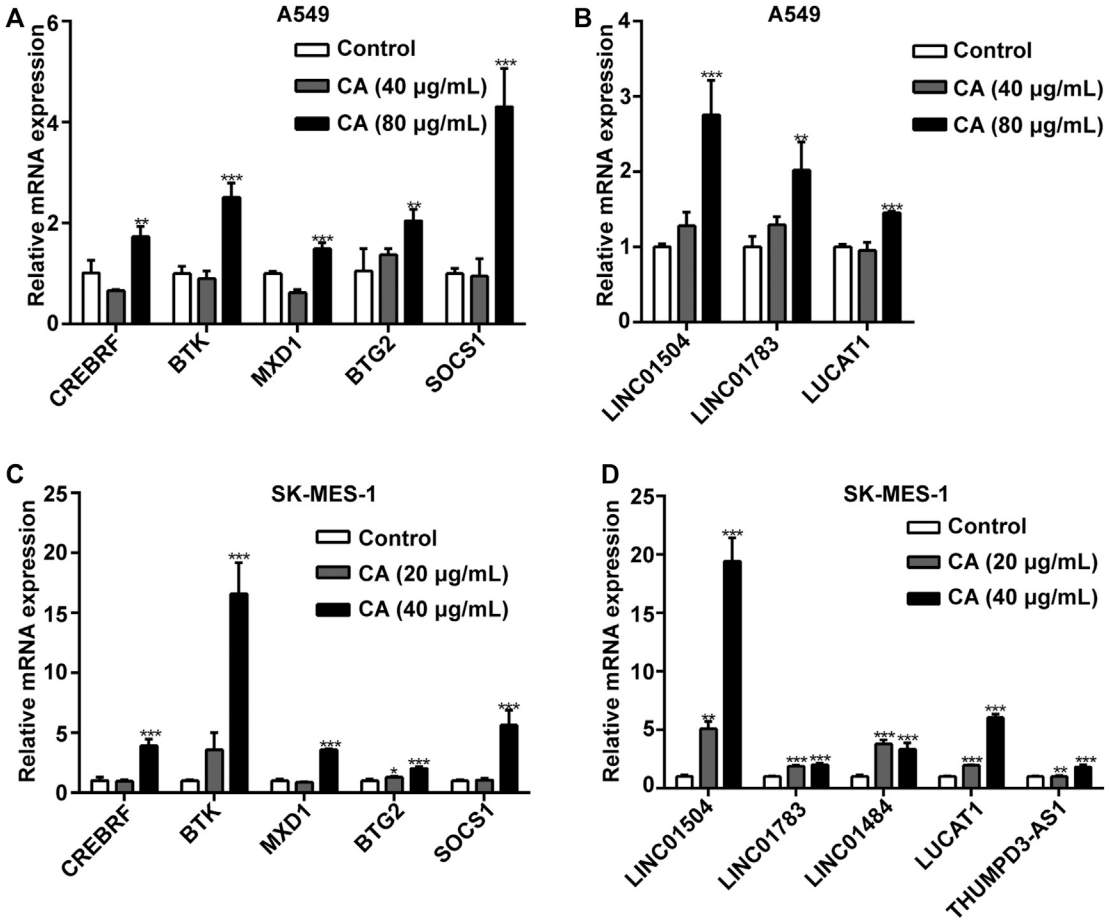

FIGURE 10 | The effects of cinnamaldehyde (CA) on the expression of CDE-mRNAs and CDE-lncRNAs in the ceRNA network. **(A, B)** After treatment with CA for 24 h, the expression of CDE-mRNAs and CDE-lncRNAs in A549 cells was determined by RT-qPCR. **(C, D)** After treatment with CA for 24 h, the expression of CDE-mRNAs and CDE-lncRNAs in SK-MES-1 cells was determined by RT-qPCR. Data are expressed as the mean ± SD of three independent experiments. $^{**}p < 0.01$ and $^{***}p < 0.001$ vs. the control group. CDE, common differentially expressed; ceRNA, competing endogenous RNA; lncRNAs, long noncoding RNAs; mRNAs, messenger RNAs; RT-qPCR, reverse transcription-quantitative polymerase chain reaction; SD, standard deviation.

and invasion (Flowers et al., 2005). After treatment with CA, LINC01783 and BTG2 in the ceRNA network were upregulated, whereas hsa-miR-7-5p was downregulated. Also, CA could modulate PPARγ expression in the RNA degradation pathway. In colorectal cancer, has-miR-7 is significantly upregulated and correlates with venous invasion, tumor depth, lymph node metastasis, lymphatic invasion, liver metastasis, and poor overall survival (Nagano et al., 2016). miR-7-5p was significantly upregulated in neuroendocrine neoplasms (Heverhagen et al., 2018). Inhibition of miR-7 expression could inhibit migration and proliferation, as well as induce apoptosis in renal cell carcinoma (Yu et al., 2013). BTG2 is a member of the BTG/TOB family, and its encoded proteins have antiproliferative properties. BTG2-encoded protein products have been associated with transcriptional regulation, DNA repair, cell division, and mRNA stability (Yuniati et al., 2019). After treatment with CA, THUMPD3-AS1 and BTK in the ceRNA network were upregulated, whereas hsa-miR-425–5p was downregulated. In addition, CA could inhibit the activation of the NF-κB signaling pathway. Downregulation of miR-425–5p expression inhibited the proliferation, invasion, and migration of gastric cancer cells (Yan et al., 2017). BTK is a non-receptor kinase that plays an essential role in the proliferation of numerous B cell malignancies and is also an important component of the tumor microenvironment (Pal Singh et al., 2018). Traditionally, BTK was considered oncogenic in B cell malignancies. However, recent data have shown that it can also act as a tumor suppressor in other types of cancer, as an essential member of the p53 and p73 damage response (Rada et al., 2018). The present findings indicate that LINC01504, LINC01783, and THUMPD3-AS1 may play roles as NSCLC suppressors.

The current study had some limitations. Firstly, we only focused on the negative regulation of miRNA-mRNA and miRNA-lncRNA of the ceRNA hypothesis and its prognostic value, which may exclude more complex regulatory mechanisms. Secondly, experiments should have been performed to verify the specific mechanism involved in the effects of CA on lung cancer, and experimental validation will be carried out in the future. However, this study aimed

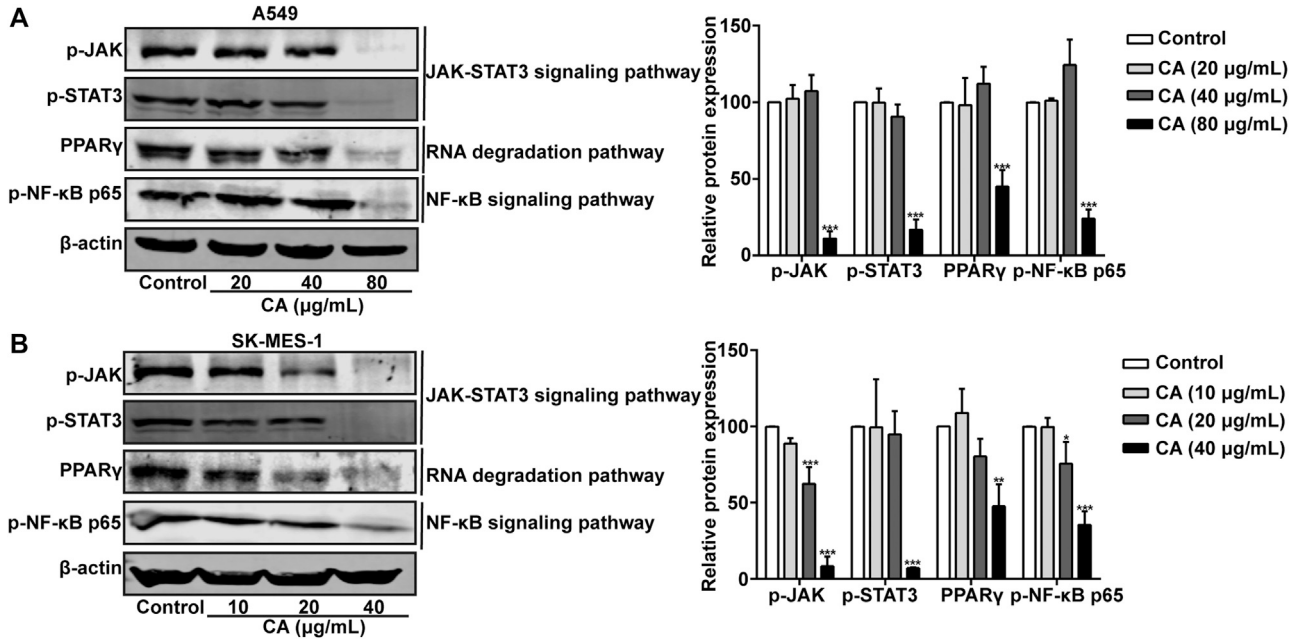

FIGURE 11 | Cinnamaldehyde (CA) inhibits the activation of the JAK/STAT3 signaling pathway, RNA degradation, and NF-κB signaling pathway. **(A)** A549 cells were treated with 20, 40, and 80 μg/ml of CA for 24 h. The protein expression of p-JAK, p-STAT3, PPARγ, and p-NF-κB p65 was determined using western blotting and the quantitative results are shown in the right panel. **(B)** SK-MES-1 cells were treated with 10, 20, and 40 μg/ml of CA for 24 h. The protein expression of p-JAK, p-STAT3, PPARγ, and p-NF-κB p65 was determined using western blotting and the quantitative results are shown in the right panel. Data are expressed as the mean ± SD of three independent experiments. $^{*}p < 0.05$, $^{**}p < 0.01$, and $^{***}p < 0.001$ vs. the control group. NF-κB, nuclear factor-κB; p-JAK, phospho-JAK; p-STAT3, phospho-signal transducer and activator of transcription 3; PPARγ, peroxisome proliferator-activated receptor gamma; SD, standard deviation.

to build a regulatory ceRNA network and screen key lncRNAs that can provide a basis for further experimental and clinical studies.

CONCLUSION

In summary, CA is effective against lung cancer. LINC01504, LINC01783, THUMPD3-AS1, has-miR-155–5p, has-miR-425–5p, and has-miR-7-5p may be key ncRNAs in the suppression of malignant phenotypes of NSCLC by CA. The JAK/STAT signaling pathway, RNA degradation, and NF-κB signaling pathway may be key regulatory pathways involved in the effect of CA against NSCLC. These data highlight CA as a potential therapeutic agent for the clinical treatment of lung cancer.

DATA AVAILABILITY STATEMENT

The original contributions presented in the study are publicly available. This data can be found here: https://dataview.ncbi.nlm.nih.gov/object/PRJNA686481?reviewer=270idd6itbb0hvlr1siot1i4lh.

ETHICS STATEMENT

The animal study was reviewed and approved by Shanxi Medical University.

AUTHOR CONTRIBUTIONS

RC and JW—Assisted in designing the research, performed the research, analyzed the data, and participated in writing the manuscript. CL, TY, YQ, HQS, and YJZ—Performed the research and assisted in data analysis. JZW, PZK, and XRZ—Designed the study, analyzed the data, and drafted the manuscript. All authors approved the final version of the manuscript.

FUNDING

This study was funded by The Special Fund Project for Guiding Local Science and Technology Development by the Central Government (YDZX20191400002737) and the Key R&D Program of Shanxi Province (Social Development) (201803D31093).

ACKNOWLEDGMENTS

We thank Yongping Cui, PZK, and XRZ for their technical assistance.

SUPPLEMENTARY MATERIAL

The Supplementary Material for this article can be found online at: https://www.frontiersin.org/articles/10.3389/fphar.2020.611060/full#supplementary-material.

REFERENCES

Ambros, V. (2004). The functions of animal microRNAs. *Nature* 431, 350–355. doi:10.1038/nature02871

Chan, J. J., and Tay, Y. (2018). Noncoding RNA:RNA Regulatory Networks in cancer. *Int. J. Mol. Sci.* 19. doi:10.3390/ijms19051310

Chang, N. W., and Huang, Y. P. (2019). The RNA degradation pathway is involved in PPARalpha-modulated anti-oral tumorigenesis. *Biomedicine* 9, 27. doi:10.1051/bmdcn/2019090427

Chen, W. J., Xiong, L., Yang, L., Yang, L. J., Li, L., Huang, L., et al. (2020). Long non-coding RNA LINC01783 promotes the progression of cervical cancer by sponging miR-199b-5p to mediate GBP1 expression. *Cancer Manag. Res.* 12, 363–373. doi:10.2147/CMAR.S230171

Chen, W., Zheng, R., Baade, P. D., Zhang, S., Zeng, H., Bray, F., et al. (2016). Cancer statistics in China, 2015. *CA Cancer J. Clin.* 66, 115–132. doi:10.3322/caac.21338

Davis, R. J. (2000). Signal transduction by the JNK group of MAP kinases. *Cell* 103, 239–252. doi:10.1016/s0092-8674(00)00116-1

Delespaul, L., Lesluyes, T., Perot, G., Brulard, C., Lartigue, L., Baud, J., et al. (2017). Recurrent TRIO fusion in nontranslocation-related sarcomas. *Clin. Cancer Res.* 23, 857–867. doi:10.1158/1078-0432.CCR-16-0290

Fan, C. N., Ma, L., and Liu, N. (2018). Systematic analysis of lncRNA-miRNA-mRNA competing endogenous RNA network identifies four-lncRNA signature as a prognostic biomarker for breast cancer. *J. Transl. Med.* 16, 264. doi:10.1186/s12967-018-1640-2

Fang, B. (2016). RAS signaling and anti-RAS therapy: lessons learned from genetically engineered mouse models, human cancer cells, and patient-related studies. *Acta Biochim. Biophys. Sin.* 48, 27–38. doi:10.1093/abbs/gmv090

Farhan, M., Wang, H., Gaur, U., Little, P. J., Xu, J., and Zheng, W. (2017). FOXO signaling pathways as therapeutic targets in cancer. *Int. J. Biol. Sci.* 13, 815–827. doi:10.7150/ijbs.20052

Flowers, L. O., Subramaniam, P. S., and Johnson, H. M. (2005). A SOCS-1 peptide mimetic inhibits both constitutive and IL-6 induced activation of STAT3 in prostate cancer cells. *Oncogene* 24, 2114–2120. doi:10.1038/sj.onc.1208437

Fu, X., Wen, H., Jing, L., Yang, Y., Wang, W., Liang, X., et al. (2017). MicroRNA-155-5p promotes hepatocellular carcinoma progression by suppressing PTEN through the PI3K/Akt pathway. *Cancer Sci.* 108, 620–631. doi:10.1111/cas.13177

Ghobrial, I. M., Witzig, T. E., and Adjei, A. A. (2005). Targeting apoptosis pathways in cancer therapy. *CA Cancer J. Clin.* 55, 178–194. doi:10.3322/canjclin.55.3.178

Giordano, A., and Tommonaro, G. (2019). Curcumin and cancer. *Nutrients* 11, 2376. doi:10.3390/nu11102376

Guttman, M., Amit, I., Garber, M., French, C., Lin, M. F., Feldser, D., et al. (2009). Chromatin signature reveals over a thousand highly conserved large non-coding RNAs in mammals. *Nature* 458, 223–227. doi:10.1038/nature07672

Hao, T., Yang, Y., Li, N., Mi, Y., Zhang, G., Song, J., et al. (2020). Inflammatory mechanism of cerebral ischemia-reperfusion injury with treatment of stepharine in rats. *Phytomedicine* 76, 153353. doi:10.1016/j.phymed.2020.153353

Herbst, R. S., Morgensztern, D., and Boshoff, C. (2018). The biology and management of non-small cell lung cancer. *Nature* 553, 446–454. doi:10.1038/nature25183

Heverhagen, A. E., Legrand, N., Wagner, V., Fendrich, V., Bartsch, D. K., and Slater, E. P. (2018). Overexpression of microRNA miR-7-5p is a potential biomarker in neuroendocrine neoplasms of the small intestine. *Neuroendocrinology* 106, 312–317. doi:10.1159/000480121

Hollville, E., Romero, S. E., and Deshmukh, M. (2019). Apoptotic cell death regulation in neurons. *FEBS J.* 286, 3276–3298. doi:10.1111/febs.14970

Hu, J., Chen, Y., Li, X., Miao, H., Li, R., Chen, D., et al. (2019). THUMPD3-AS1 is correlated with Non-small cell lung cancer and Regulates self-Renewal through miR-543 and ONECUT2. *Onco. Targets Ther.* 12, 9849–9860. doi:10.2147/OTT.S227995

Huang, T. C., Chung, Y. L., Wu, M. L., and Chuang, S. M. (2011). Cinnamaldehyde enhances Nrf2 nuclear translocation to upregulate phase II detoxifying enzyme expression in HepG2 cells. *J. Agric. Food Chem.* 59, 5164–5171. doi:10.1021/jf200579h

Khan, H., Ullah, H., Castilho, P., Gomila, A. S., D'Onofrio, G., Filosa, R., et al. (2020). Targeting NF-kappaB signaling pathway in cancer by dietary polyphenols. *Crit. Rev. Food Sci. Nutr.* 60, 2790–2800. doi:10.1080/10408398

Li, J., Teng, Y., Liu, S., Wang, Z., Chen, Y., Zhang, Y., et al. (2016). Cinnamaldehyde affects the biological behavior of human colorectal cancer cells and induces apoptosis via inhibition of the PI3K/Akt signaling pathway. *Oncol. Rep.* 35, 1501–1510. doi:10.3892/or.2015.4493

Martini, M., De Santis, M. C., Braccini, L., Gulluni, F., and Hirsch, E. (2014). PI3K/AKT signaling pathway and cancer: an updated review. *Ann. Med.* 46, 372–383. doi:10.3109/07853890.2014.912836

Minguet, J., Smith, K. H., and Bramlage, P. (2016). Targeted therapies for treatment of non-small cell lung cancer--Recent advances and future perspectives. *Int. J. Cancer* 138, 2549–2561. doi:10.1002/ijc.29915

Molina, J. R., Yang, P., Cassivi, S. D., Schild, S. E., and Adjei, A. A. (2008). Non-small cell lung cancer: epidemiology, risk factors, treatment, and survivorship. *Mayo Clin. Proc.* 83, 584–594. doi:10.4065/83.5.584

Nagano, Y., Toiyama, Y., Okugawa, Y., Imaoka, H., Fujikawa, H., Yasuda, H., et al. (2016). MicroRNA-7 is associated with malignant potential and poor prognosis in human colorectal cancer. *Anticanc. Res.* 36, 6521–6526. doi:10.21873/anticanres.11253

Ng, L. T., and Wu, S. J. (2011). Antiproliferative activity of Cinnamomum cassia constituents and effects of pifithrin-alpha on their apoptotic signaling pathways in Hep G2 cells. *Evid. Based Compl. Alternat. Med.* 2011, 492148. doi:10.1093/ecam/nep220

Owen, K. L., Brockwell, N. K., and Parker, B. S. (2019). JAK-STAT signaling: a double-edged sword of immune regulation and cancer progression. *Cancers* 11, 2002. doi:10.3390/cancers11122002

Pal Singh, S., Dammeijer, F., and Hendriks, R. W. (2018). Role of Bruton's tyrosine kinase in B cells and malignancies. *Mol. Cancer* 17, 57. doi:10.1186/s12943-018-0779-z

Prensner, J. R., and Chinnaiyan, A. M. (2011). The emergence of lncRNAs in cancer biology. *Cancer Discov.* 1, 391–407. doi:10.1158/2159-8290.CD-11-0209

Rada, M., Barlev, N., and Macip, S. (2018). BTK: a two-faced effector in cancer and tumour suppression. *Cell Death Dis.* 9, 1064. doi:10.1038/s41419-018-1122-8

Salmena, L., Poliseno, L., Tay, Y., Kats, L., and Pandolfi, P. P. (2011). A ceRNA hypothesis: the Rosetta Stone of a hidden RNA language? *Cell* 146, 353–358. doi:10.1016/j.cell.2011.07.014

Sui, J., Li, Y. H., Zhang, Y. Q., Li, C. Y., Shen, X., Yao, W. Z., et al. (2016). Integrated analysis of long non-coding RNAassociated ceRNA network reveals potential lncRNA biomarkers in human lung adenocarcinoma. *Int. J. Oncol.* 49, 2023–2036. doi:10.3892/ijo.2016.3716

Tian, F., Yu, C. T., Ye, W. D., and Wang, Q. (2017). Cinnamaldehyde induces cell apoptosis mediated by a novel circular RNA hsa_circ_0043256 in non-small cell lung cancer. *Biochem. Biophys. Res. Commun.* 493, 1260–1266. doi:10.1016/j.bbrc.2017.09.136

Villalobos-Hernandez, A., Bobbala, D., Kandhi, R., Khan, M. G., Mayhue, M., Dubois, C. M., et al. (2017). SOCS1 inhibits migration and invasion of prostate cancer cells, attenuates tumor growth and modulates the tumor stroma. *Prost. Cancer Prost. Dis.* 20, 36–47. doi:10.1038/pcan.2016.50

Wang, C., Feng, Y., Li, B., Zhou, D., Ma, J., Chen, G., et al. (2020). CircRNAsin lung-intestinal axis cancer. *Curr. Mol. Med.* 20, 1. doi:10.2174/1566524020999200831122219

Wu, C., Zhuang, Y., Jiang, S., Tian, F., Teng, Y., Chen, X., et al. (2017). Cinnamaldehyde induces apoptosis and reverses epithelial-mesenchymal transition through inhibition of Wnt/beta-catenin pathway in non-small cell lung cancer. *Int. J. Biochem. Cell Biol.* 84, 58–74. doi:10.1016/j.biocel.2017.01.005

Xie, Y., Dang, W., Zhang, S., Yue, W., Yang, L., Zhai, X., et al. (2019). The role of exosomal noncoding RNAs in cancer. *Mol. Cancer* 18, 37. doi:10.1186/s12943-019-0984-4

Yan, H., Wang, Q., Shen, Q., Li, Z., Tian, J., Jiang, Q., et al. (2018). Identification of potential transcription factors, long noncoding RNAs, and microRNAs

associated with hepatocellular carcinoma. *J. Cancer Res. Therapeut.* 14, S622–S627. doi:10.4103/0973-1482.204846

Yan, Y. F., Gong, F. M., Wang, B. S., and Zheng, W. (2017). MiR-425-5p promotes tumor progression via modulation of CYLD in gastric cancer. *Eur. Rev. Med. Pharmacol. Sci.* 21, 2130–2136

Yu, Z., Ni, L., Chen, D., Zhang, Q., Su, Z., Wang, Y., et al. (2013). Identification of miR-7 as an oncogene in renal cell carcinoma. *J. Mol. Histol.* 44, 669–677. doi:10.1007/s10735-013-9516-5

Yuniati, L., Scheijen, B., van der Meer, L. T., and van Leeuwen, F. N. (2019). Tumor suppressors BTG1 and BTG2: beyond growth control. *J. Cell. Physiol.* 234, 5379–5389. doi:10.1002/jcp.27407

Zhao, X. S., Han, B., Zhao, J. X., Tao, N., and Dong, C. Y. (2019). MiR-155-5p affects Wilms' tumor cell proliferation and apoptosis via targeting CREB1. *Eur. Rev. Med. Pharmacol. Sci.* 23, 1030–1037. doi:10.26355/eurrev_201902_16990

Conflict of Interest: The authors declare that the research was conducted in the absence of any commercial or financial relationships that could be construed as a potential conflict of interest.

frontiers in Oncology

REVIEW
published: 11 February 2021
doi: 10.3389/fonc.2020.632187

A-to-I RNA Editing in Cancer: From Evaluating the Editing Level to Exploring the Editing Effects

Heming Wang[1,2,3†], *Sinuo Chen*[2,3†], *Jiayi Wei*[2,3], *Guangqi Song*[2,3*] *and Yicheng Zhao*[1*]

[1] Clinical Medical College, Changchun University of Chinese Medicine, Changchun, China, [2] Department of Gastroenterology and Hepatology, Zhongshan Hospital of Fudan University, Shanghai, China, [3] Shanghai Institute of Liver Diseases, Shanghai, China

As an important regulatory mechanism at the posttranscriptional level in metazoans, adenosine deaminase acting on RNA (ADAR)-induced A-to-I RNA editing modification of double-stranded RNA has been widely detected and reported. Editing may lead to non-synonymous amino acid mutations, RNA secondary structure alterations, pre-mRNA processing changes, and microRNA-mRNA redirection, thereby affecting multiple cellular processes and functions. In recent years, researchers have successfully developed several bioinformatics software tools and pipelines to identify RNA editing sites. However, there are still no widely accepted editing site standards due to the variety of parallel optimization and RNA high-seq protocols and programs. It is also challenging to identify RNA editing by normal protocols in tumor samples due to the high DNA mutation rate. Numerous RNA editing sites have been reported to be located in non-coding regions and can affect the biosynthesis of ncRNAs, including miRNAs and circular RNAs. Predicting the function of RNA editing sites located in non-coding regions and ncRNAs is significantly difficult. In this review, we aim to provide a better understanding of bioinformatics strategies for human cancer A-to-I RNA editing identification and briefly discuss recent advances in related areas, such as the oncogenic and tumor suppressive effects of RNA editing.

Keywords: ADAR, RNA editing, cancer, non-coding RNA, circular RNAs

OPEN ACCESS

Edited by:
Yue Hou,
Northeastern University, China

Reviewed by:
Jun-Hao Li,
University of California, San Diego, United States
Giovanni Nigita,
The Ohio State University, United States

***Correspondence:**
Guangqi Song
song_guangqi@fudan.edu.cn
Yicheng Zhao
yichengzhao@live.cn

[†]These authors have contributed equally to this work

Specialty section:
This article was submitted to Pharmacology of Anti-Cancer Drugs, a section of the journal Frontiers in Oncology

Received: *22 November 2020*
Accepted: *21 December 2020*
Published: *11 February 2021*

Citation:
Wang H, Chen S, Wei J, Song G and Zhao Y (2021) A-to-I RNA Editing in Cancer: From Evaluating the Editing Level to Exploring the Editing Effects. Front. Oncol. 10:632187. doi: 10.3389/fonc.2020.632187

INTRODUCTION

In mammals, ADAR-induced adenine to inosine (A-to-I) is a widespread primary type of RNA editing (1). As adenosine deaminases, ADAR proteins are able to bind to both intracellular and extranuclear double-stranded RNA (dsRNA), producing inosine (I) from adenosine (A) by deamination on RNA coding and non-coding regions. Since inosine prefers to pair with cytidine (C), researchers have also recognized A-to-I RNA editing as A-to-G (guanine) editing (2). ADAR proteins include three types in mammals, ADAR1, ADAR2 (ADARB1), and ADAR3 (ADARB2) (**Figure 1A**). ADAR1 and ADAR2 reside in most human tissues and are the major mediators of A-to-I RNA editing. Without deaminase activity, ADAR3 is mainly expressed in the brain. Recent research has indicated that ADAR3 may disturb ADAR2 function by acting as a competitive inhibitor (3). Moreover, ADAR1 has two isoforms resulting from the alternative promoters ADAR1 p110 and ADAR1 p150. ADAR1 p110 is constitutively expressed, while ADAR1 p150 is inducible

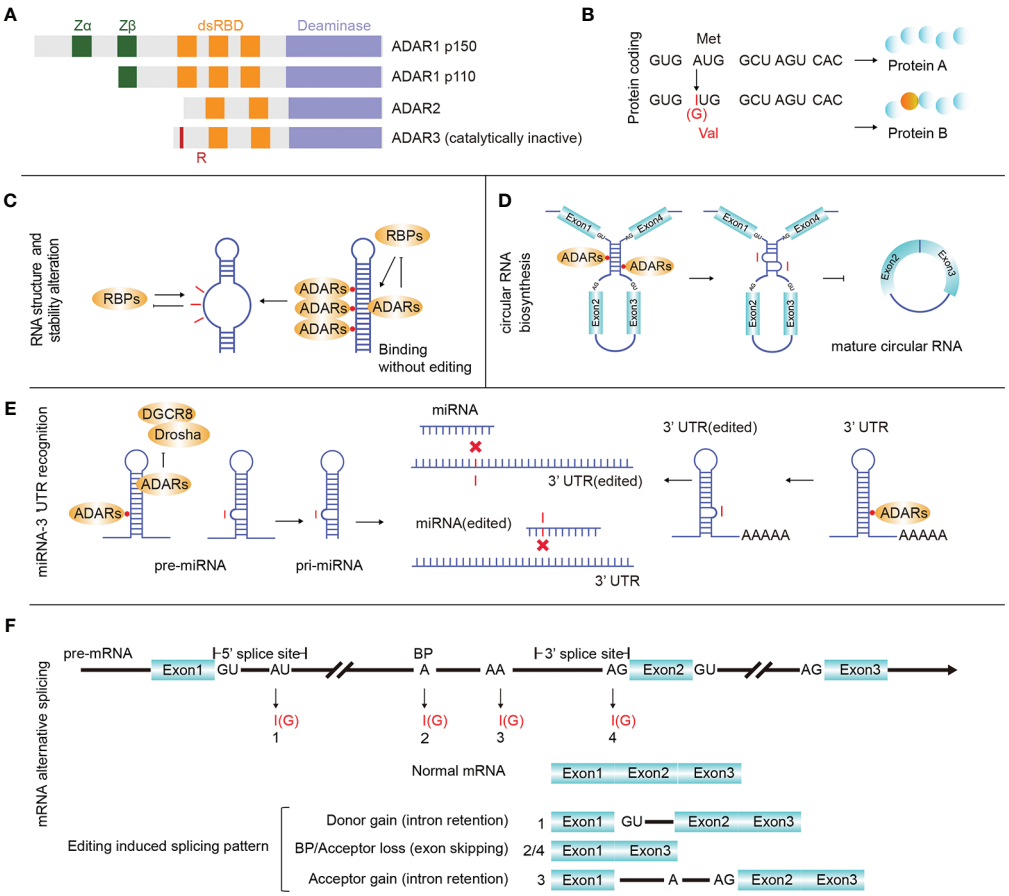

FIGURE 1 | ADARs and RNA editing effects. **(A)** There are three main proteins of ADAR enzymes, ADAR1 (p110 and p150), ADAR2, and ADAR3. Vertebrate ADARs share a conserved deaminase domain and two to three dsRNA-binding domains (dsRBDs). In addition, ADAR1 p110 and p150 have similar Z-DNA-binding domains. ADAR3 is unique since its deaminase domain is catalytically inactive, and it also has an arginine-rich domain (R). **(B)** RNA editing in gene coding regions may introduce protein mutations. **(C)** Binding ADARs to certain dsRNAs may affect the RNA structure, thereby altering RNA biological processing and stability. **(D)** ADAR1 binds and inhibits the generation of circular RNAs. **(E)** microRNA (miRNA) or 3' UTR editing may change or redirect the interactive relationship between certain UTRs and miRNAs. **(F)** RNA editing sites were identified in all three main regions involved with pre-mRNA alternative splicing (donor: 5' splicing site, acceptor: 3' splicing site and branch site), and pre-mRNA intron editing may contribute to pre-mRNA alternative splicing.

by interferons (IFNs). When dsRNA sensors (such as MDA5 and PKR) in cells sense the presence of exogenous nucleic acids, they can induce the generation of IFNs and activate ADAR1 p150 (4).

Although past research has indicated that ADARs and A-to-I RNA editing are essential for multiple biological processes, abnormal expression or editing levels can trigger various diseases (5, 6). ADAR1 is required for mammalian early development (7–10), null ADAR1 expression causes embryonic death in mice (11, 12), and knocking out MDA5 can rescue the ADAR$^{-/-}$ embryonic phenotype because MDA5 is responsible for distinguishing and helping remove exogenous dsRNA, except for ADAR-edited dsRNA (13). ADAR1 is a suppressor of interferon signaling (7) and controls innate immune responses to exogenous RNA (14). Abnormal expression of ADAR1 results in IFN production, which may take part in enhancing autoimmunity and inducing systemic lupus erythematosus to a certain degree (15). ADAR1&2 expression is positively correlated with the proliferative activity of most cells and inflammatory responses, especially playing a vital role in the occurrence and development of several cancers (16).

RNA editing affects many basic biological processes. When editing occurs in the mRNA coding region, it may cause mutations that increase the regulation diversity at both the transcriptional and proteomic levels (**Figure 1B**). When editing occurs in the non-coding RNA region, it can affect the RNA secondary structure (**Figure 1C**), circular RNA biosynthesis (**Figure 1D**), microRNA (miRNA)-mRNA targeting (**Figure 1E**) and mRNA alternative splicing (**Figure 1F**). Editing-induced RNA secondary structure alterations may affect the related protein abundance by changing the RNA stability (17–19). Therefore, accurate identification of RNA editing sites in cancer is important for investigating cancer development. Currently, many RNA editing identification bioinformatics strategies and software tools have been developed. Using these tools and algorithms, researchers have

systematically identified RNA editing sites (20–22) on a large scale. At present, these identified human RNA editing sites are mainly summarized in four databases, REDIportal (http://srv00.recas.ba.infn.it/atlas/index.html) (21), DARNED (https://darned.ucc.ie/) (23), RADAR (http://rnaedit.com/) (24), and CLAIRE (http://srv00.recas.ba.infn.it/atlas/claire.html) (25). There are about 15.6 million editing sites in REDIportal, 0.2 million in DARNED, 2 million in RADAR, and 1,147 in CLAIRE, and REDIportal almost covered all human RNA editing sites of these four databases. Statistical analysis of these RNA editing site gene regions showed that most sites resided in non-coding RNA regions. In fact, protein-coding RNA regions account for only 2% of the human genome (26), while a large number of regions are non-coding regions, and most of the known RNAs are non-coding RNAs (ncRNAs). ncRNAs come from a wide range of sources and are abundantly expressed. While many rRNAs and tRNAs have high abundance, some ncRNAs, such as miRNAs, circular RNAs, long non-coding RNAs (lncRNAs), and Piwi-interacting RNAs (piRNAs), have low abundance (27). ncRNAs play a vital role in tumor regulation (28), and multiple ncRNAs interact in tumors, forming a competing endogenous RNA (ceRNA) network in cancer formation (29). Abnormal expression of some ncRNAs, such as miRNAs and lncRNAs, can affect cancer occurrence and progression. Moreover, the level of RNA editing in non-coding regions was identified to be significantly associated with cancer patient survival (30). As a special ring-shaped ncRNA, circular RNA is usually produced during the back-splicing of exons. Because of its circular structure property, it is more stable than linear RNA. Current studies have shown that circular RNAs mainly function by acting as miRNA sponges and interacting with RNA-binding proteins and lncRNAs. Circular RNA also plays an important role in multiple cancer types and can be used as a cancer biomarker (31). Due to its unique formation mechanism, the generation of circular RNA is easily affected by the expression of ADARs. Many studies have shown that ADARs can inhibit the synthesis of circular RNAs (32–34).

As a novel characteristic of tumors, certain genes display different expression patterns in cancer patients and show distinct RNA editing levels that vary within the same patient in different tissues. Interestingly, high RNA editing levels posttranscriptionally increase the heterogeneity of genes, including both oncogenes and tumor suppressors, in cancer. Researchers have previously investigated the RNA editing levels between tumor and paracarcinoma tissues from the TCGA database (35–38), including sites in coding regions and non-coding regions (miRNAs, intergenic regions, etc.) and have analyzed functional RNA editing events (16, 39, 40). Furthermore, ADARs were found to be highly expressed in $Lgr5^+$ cells (controversial cancer stem cells) (41). In addition to DNA mutations, RNA editing caused by ADARs significantly increases the RNA abundance, which could increase the protein heterogeneity in tumor cells and induce tumor drug resistance (39). The identification of RNA editing sites in tumors will help us study the mechanism of tumorigenesis and identify some tumor-specific molecular markers. However, because of the high DNA mutation in tumors, it is a challenge to identify RNA editing sites accurately.

It is difficult to predict the function of RNA editing sites located in non-coding regions owing to their diversity and interactions with various ncRNAs. Moreover, except for typical RNA editing sites (such as those resulting in proteins and microRNA seed region alterations) that can be intuitively selected according to their locations, many other potentially functional RNA editing sites residing in non-coding regions still need to be explored and validated (42). This problem is complicated by the lack of effective judging and predicting tools.

This review outlines the existing bioinformatics strategies for identifying editing sites in tumors, which can be used for further experimental verification of downstream effects and clinical relevance. Simultaneously, we provide some suggestions for ncRNA editing research and the potential application of ADAR inhibitors in the treatment of cancer.

RNA EDITING SITE IDENTIFICATION

In 1991, the first A-to-I RNA editing report was published when researchers detected RNA editing events on GluR mRNA (43). At the same time, four editing sites on 5-HT(2c) mRNA were identified (44). As DNA/RNA sequencing technology has developed, abundant high-seq data have made it possible to search RNA editing sites and analyze RNA editing levels by comparing RNA-seq data to related DNA-seq data, even using RNA-seq data alone (45–47). In addition, there are several experimental methods that directly detect inosine, including ICE-seq (48), EndoVIPER-seq (49), and other methods for capturing inosine (50–52). However, these methods also have obvious defects. (1) The effects of enzymatic or chemical treatments are usually incomplete, and RNase T1 will also induce RNA degradation. (2) RNA modifications could directly disturb reverse transcription (53), such as m1A (54, 55), and this effect induces many false-positive results that must be corrected with complex bioinformatics methods.

Lateral Computational A-to-G RNA Editing Site Calling Strategy

Editing site calling is a complicated process involving many aspects and requiring appropriate optimization and high accuracy in each step. Therefore, researchers have summarized some functionally integrated pipelines (56–59). Currently, there are two popular analysis methods targeting A-to-I RNA editing, including comparing the RNA-seq data with its DNA-seq data and directly analyzing the RNA-seq data alone. In 2012, several groups separately reported their optimized RNA editing calling methods by directly comparing the RNA-seq data with its corresponding DNA-seq data (60–62). Since there is no need to delete SNPs (single-nucleotide polymorphisms), the editing identification accuracy will be improved in theory. At present, it is acknowledged that directly comparing RNA-seq data with the original DNA-seq data is the most ideal strategy by which to perform RNA editing calling. Unfortunately, matched DNA and RNA sequencing data from the same sample are not always available. To decrease costs and reduce processing times, researchers prefer to adopt RNA-seq alone to search for

editing events. Until 2013, detection methods using tissue- and cell-specific RNA-seq alone were reported by several different groups (46, 63). This strategy has substantially promoted research in related fields, and it is thought to be useful in other organisms carrying suitable reference genomes.

As mentioned above, the two popular strategies share a common calling strategy that includes the following four steps: (1) preprocessing sequencing data, (2) sequencing read mapping, (3) RNA editing calling, and (4) RNA editing site annotation. When analyzing RNA editing levels, studies usually employ certain common mapping tools, such as BWA (64), Bowtie (65), HISAT2 (66), GSNAP (67), and STAR (68). Interestingly, the same high-seq data usually display low repeatability when processed by different mapping tools; therefore, some specific tools for RNA editing calling have been developed, such as RASER (69). However, recent integrated pipelines for RNA editing analysis usually require specific mapping tools according to each developer's optimization. RNA editing calling is the key step that identifies true RNA editing events according to DNA-RNA mismatches. A conventional identification method is to identify DNA/RNA mismatches in samples using the tools HaplotypeCaller in GATK, Samtools (70), VarScan 2 (71), etc., followed by removing SNPs and DNA mutations. Researchers have also developed a large number of tools for accurate identification of RNA editing. For instance, to filter out these false-positive events, REDItools provided a threshold according to an empirically observed distribution (47). We summarize the popular RNA editing bioinformatics tools in **Table 1**.

Current Situation and Challenge of RNA Editing Calling

Sequencing errors, DNA mutations, and a lack of a suitable SNP database will result in false-positive results that affect RNA editing detection. These sequencing errors are mainly caused by reverse transcription, homopolymers, low-quality sequences, etc. An important factor resulting in sequencing errors is RNA modification, such as m1A and m6A. The reverse transcriptase will likely misidentify modified nucleotides as other types of nucleotides (91) [e.g., m1A is usually recognized as G instead of A (92)], which will produce many false-positive editing sites in the final results. In addition, tumor tissues are usually stored in paraffin or formalin for further research, and chemical reagents may damage DNA and RNA in these samples and ultimately affect the quality of the DNA/RNA library. To acquire high-quality sequencing reads, researchers usually perform several corrective processes. Pinto et al. summarized the related progress and provided several necessary remarks in their review (57). The processes mainly included adjusting the read quality (QC) threshold value to over 20, removing low-quality reads and using the random sequencing primer adaptor.

Upon removing SNPs, several tools, such as REDItools (47) and RNAEditor (74), automatically compare the data with the SNP databases. Researchers have established several SNP datasets, including dbSNP and HapMap (93). Plainly, the SNP database quality and selection are important determinants for analyzing the editing level using RNA-seq alone. Interestingly, it appears that a problem is caused by the accuracy of the dbSNP database remaining uncertain, since some SNP cases reported in past experimental results have recently been reclassified as RNA editing (94). For this reason, researchers have developed many other tools that remove SNPs better. GIREMI includes a mutual information (MI) model that is able to directly remove SNPs without comparing the data to a reference SNP database (45), and SPRINT is capable of directly identifying RNA editing events *via* a novel SNP-free algorithm (77).

TABLE 1 | Main bioinformatics tools for RNA editing detection.

Tools	Required sequencing data	URL	Ref
REDItools	RNA-seq or RNA and DNA-seq	https://github.com/BioinfoUNIBA/REDItools	(47)
RES-Scanner	RNA-seq and DNA-seq	https://github.com/ZhangLabSZ/RES-Scanner	(72)
JACUSA	RNA-seq or RNA and DNA-seq	https://github.com/dieterich-lab/JACUSA	(73)
GIREMI	RNA-seq	https://github.com/zhqingit/giremi	(45)
RNAEditor	RNA-seq	http://rnaeditor.uni-frankfurt.de/	(74)
DeepRed	RNA-seq	https://github.com/wenjiegroup/DeepRed	(75)
RED-ML	RNA-seq or RNA and DNA-seq	https://github.com/BGIRED/RED-ML	(76)
SPRINT	RNA-seq	https://sprint.tianlab.cn/	(77)
RDDpred	RNA-seq	http://epigenomics.snu.ac.kr/RDDpred/	(78)
Rcare	RNA-seq or RNA and DNA-seq	http://www.snubi.org/software/rcare/	(79)
DREAM	miRNA-seq	http://www.cs.tau.ac.il/~mirnaed/	(80)
RASER	RNA-seq	https://www.ibp.ucla.edu/research/xiao/RASER.html	(69)
InosinePredict	RNA-seq	http://hci-bio-app.hci.utah.edu:8081/Bass/InosinePredict	(81)
VIRGO	RNA-seq	https://github.com/InfOmics/VIRGO	(82)
AIRLINER	RNA-seq	http://alpha.dmi.unict.it/airliner/	(83)
PAI	RNA-seq	N/A	(84)
iRNA-AI	RNA-seq	N/A	(85)
EPAI-NC	RNA-seq	N/A	(86)
isoTar	RNA-seq	https://ncrnaome.osumc.edu/isotar/	(87)
REP	RNA-seq or RNA and DNA-seq	http://www.rnaeditplus.net/	(88)
RED	RNA-seq or RNA and DNA-seq	https://github.com/REDetector/RED	(89)
PRESa2i	RNA sequences	http://brl.uiu.ac.bd/presa2i/index.php	(90)

Improvements in Editing Site Calling for Cancer Research

Although the detection of editing sites with high-seq data is widely accepted and utilized, systematic optimization for accurately measuring RNA editing is still insufficient. Here, we offer several suggestions for applications using next-generation RNA sequencing for cancer RNA editing research (**Figure 2**).

1. Perform DNA-seq sequencing of the same sample if available. Tumor tissues generally have a high DNA mutation rate, and the filtration of DNA mutations is very difficult without DNA-seq sequencing. The method commonly used is to refer to previously reported DNA mutation data, such as the COSMIC database (35, 95).
2. Adapt the strand-specific and ribosome-free strategy for preparing the RNA-seq library. This will improve the accuracy of editing calling, yield more editing events on unspliced pre-mRNA fragments, and obtain more information from non-coding RNAs. Generally, the abundance of some ncRNAs, such as circular RNAs, is low, so we can obtain more circular RNAs or improve the depth of sequencing by removing linear RNAs through RNase R treatment.
3. Using hg38 as a reference genome and repeatable mapping is feasible for improving the fault-tolerant ability for hyperediting reads. Recent research indicates that the RNA editing site location usually displays a clustering pattern (96), and sequencing reads containing multiple mismatches are considered to be hyperediting. Porath et al. developed a specific method that recognized all A as G in unmapped reads before the mapping process to avoid the excessive deletion of hyperediting reads (97). Subsequently, Picardi et al. analyzed human hyperediting levels from different tissues *via* this method (22). Therefore, we recommend referring to Porath's strategy to analyze hyperediting reads.
4. Employ the Alu editing index (AEI) to measure the global editing levels in different samples. Erez Y. Levanon and Eli Eisenberg et al. provided the Alu editing index (AEI) to measure the global editing levels in different samples. The AEI ratio weighted by A-to-G mismatches within Alu repeats relative to the total number of adenosines within Alu elements represents the average Alu editing levels, indirectly showing the overall RNA editing levels (36, 98).
5. For the identification of RNA editing in tumor samples with both DNA-seq and RNA-seq data, we suggest BWA (DNA and RNA-seq) or BWA (DNA-seq) + STAR (RNA-seq) for mapping the sequencing data and REDITools for RNA editing calling. Maria et al. compared some commonly used alignment tools, including BWA, GSNAP, HISAT, and STAR, and RNA identification tools, such as RNAEditor, GIREMI, REDItools, RES, and JACUSA, and analyzed the ability of these tools to identify RNA editing (59). In their findings, BWA and STAR achieved the best alignment. REDItools is a more comprehensive RNA editing identification tool with high accuracy that can analyze the data obtained from various strategies of library construction (stranded or non-stranded RNA-seq) and provide additional options, allowing researchers to filter (SNP or DNA mutations) and annotate (genomic region or Alu region) the editing sites with their own files. To our delight, Picardi shares their updated protocol, which is a relatively systematic and detailed RNA editing identification process, for identifying RNA editing sites (99). The protocol explains how to analyze the original DNA/RNA sequencing data and obtain the candidate RNA editing sites in detail. Taking Huntington disease (HD) as an example, it also introduces how to compare the differences in RNA editing levels in different tissues. Moreover, they also developed high-performance HPC-REDItools for large-scale samples, which greatly improves the speed of operation (100). For the

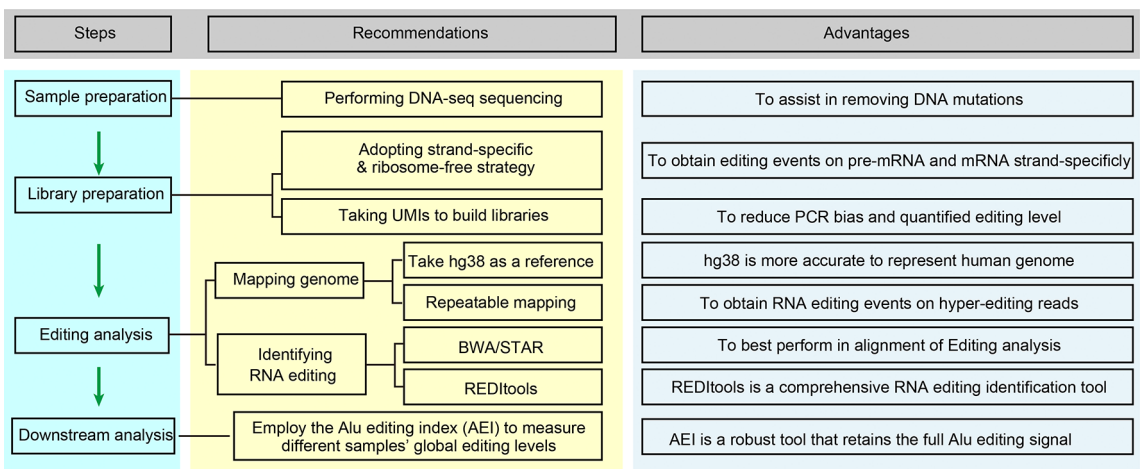

FIGURE 2 | Optimized editing sites identification strategies for cancer research. This flow chart is briefly regarding the content of *Improvements in Editing Site Calling for Cancer Research*.

identification of RNA editing in tumor samples with only RNA-seq, we recommend HISAT2 to handle RNA-seq data and REDITools to conduct RNA editing calling. We compared several RNA editing identification processes using YH's RNA-seq data and concluded that this combination is better in terms of speed and accuracy (88). At present, some researchers only focus on the known editing sites in existing RNA editing databases, such as RADAR and REDIportal. In our opinion, especially for cancer RNA editing research, *de novo* identification of these unknown RNA editing sites is necessary.

6. We suggest selecting unique molecular identifiers (UMIs) when building RNA-seq libraries, which will bring many advantages (101): PCR mutations will be directly removed, the editing levels will be absolutely quantified according to the accurate number of edited RNAs, and the computational operational process will be simplified. However, this novel method requires further refined algorithms and processing flows.

THE EFFECTS OF ADARS INDUCED A-TO-I RNA EDITING IN CANCER

Based on tens of thousands of potential RNA editing sites reported from bioinformatics methods, many experimentally validated A-to-I editing sites and their regulatory mechanisms have been demonstrated. As shown in **Figure 1B**, editing in mRNA may results in missense mutations and alterations in the beginning and terminating translation (102). Multiple editing sites located in certain coding regions, such as AZIN1 (103, 104), GABRA3 (105, 106), and COPA (40, 107, 108), have been shown to affect tumor progression. According to the reported databases, most editing sites reside within non-coding regions (>90%), and RNA editing has been detected in many types of ncRNAs, including piRNAs (109). Here, we briefly summarize the mechanisms of several typical editing effects in non-coding regions. (1) Editing occurs in the 5' splice site, branch point, and 3' splice site and is able to affect pre-mRNA alternative splicing. (2) When combined with pre-miRNA or pri-miRNA, ADARs inhibit Drosha and Dicer1 functions, affecting miRNA maturation and expression. The editing-induced sequence changes in mature miRNAs (especially in the seed sequence) or in the 3' UTR can disturb their specific interactions. (3) For long non-coding RNAs, several reports analyzing editing levels have been published (110–112), and partial editing sites having direct effects have been reported (113). (4) Since circular RNAs are byproducts of RNA splicing, editing effects on RNA splicing theoretically affect circular RNA expression. Researchers have observed high levels of A-to-I editing in circular RNA precursors and have confirmed that ADAR is related to its formation (32, 33). (5) Editing sites occurring in the 3' UTR or intron region are able to affect the RNA structure and stability (17–19). For convenience, we list recently reported tumor-effectible RNA editing sites in **Supplementary Table S1**.

RNA Editing Events in Non-Coding Regions Are Involved With Cancer

There are a large number of RNA editing phenomena in ncRNAs (114), and researchers have identified many RNA editing sites located in ncRNAs, such as lncRNAs (112). In addition, several specific databases aimed at ncRNAs have been built, including MiREDiBase (https://ncrnaome.osumc.edu/miredibase/) (for miRNA) (115) and LNCediting (http://bioinfo.life.hust.edu.cn/LNCediting/) (for lncRNA) (110). Several typical editing effects that occur on ncRNAs are listed below. (1) ADAR1-mediated miR-200 overediting affects an oncogene in thyroid cancer (116). The overediting of miR-200 weakens its interaction with and targeting of ZEB1, resulting in inhibition of epithelial-mesenchymal transition (EMT). (2) In prostate cancer, ADAR1 promotes cell proliferation by editing lncRNAs and PCA3 and improving the stability and expression of PCA3, thereby inhibiting the tumor suppressor PRUNE2 (113). (3) In glioma tumors, ADAR2 inhibits cell migration and invasion by editing miR-376a-1 and shifting the targeted gene from RAP2A to AMFR (117). (4) In melanoma, ADAR1 attenuates the inhibition of CPEB1 by miR-455-5p by editing miR-455-5p, which promotes the proliferation and metastasis of melanoma (118). (5) Zipeto et al. found that the edited miRNA Let-7 is a main factor promoting leukemia cell self-renewal (119). (6) Hepatocellular carcinoma (HCC) and the android receptor (AR) promote the expression of ADAR1 p110, while ADAR1 p110 inhibits circular RNA (hsa_circ_0085154) expression and finally inhibits the proliferation of HCC tumors (120).

Search Strategies for Effective RNA Editing Events in Cancer

Tumor and adjacent tissue samples are suitable subjects for studying RNA editing—a large number of non-cancer-specific RNA editing sites can be excluded by comparing RNA editing in cancer and adjacent tissue. The investigation range of essential RNA editing sites affecting cancer occurrence and development can be effectively narrowed by comparing the editing levels in cancer and adjacent tissue. Most cancers are accompanied by detailed clinical data, from which the characteristics of RNA editing in different cancers can be summarized and the range of key targets can be further streamlined.

ADAR1&2 expression is different in various cancers. ADAR1 expression increases in most cancer types, such as breast invasive carcinoma and liver hepatocellular carcinoma, but decreases in a few cancers, such as kidney chromophobe. Some researchers found that the expression of ADAR1 and ADAR2 in the same cancer can be totally opposite. For example, some studies show that ADAR1 is a potential tumor enhancer with high levels, and ADAR2 is recognized as a tumor suppressor in HCC (40, 108).

The role of specific RNA editing level changes mediated by different ADAR enzymes in tumors has been partially discovered. To further determine which RNA editing site is closely related to tumor development and maintenance, researchers can select paired samples from cancer patients and identify these tumor-related RNA editing sites using statistical methods such as Fisher's exact test and Wilcoxon rank sum and signed rank test. Studies

have shown that certain site editing levels are greatly associated with patient survival (30). Therefore, we can link the editing level of RNA editing sites with clinical data such as the tumor clinical stage, cancer subtype and patient survival. In addition, Han et al. showed that editing levels of certain genes are associated with tumor drug sensitivity, which could be used as a potential screening strategy in clinical medication (35).

Based on the initial selection strategies mentioned above, a large number of candidate editing sites related to cancer could be identified, and we can further narrow the range according to previously reported important tumor-related genes. Additionally, since the level of RNA editing is regulated by ADAR1 and/or ADAR2, we can determine which enzyme acts on a specific editing site by analyzing the correlation between the expression levels of ADAR1/2 and editing sites. Moreover, RNA editing affects the gene expression level in various ways, so we were able to analyze whether there was a correlation between the change in the editing level of RNA editing sites and the expression level of the gene in which RNA editing sites were located. Finally, a necessary confirmation step should be performed for the newly identified editing sites *via* Sanger sequencing (121), mmPCR-seq (122), or RESSq-PCR (123).

Predicting the Function of RNA Editing Events in Cancer

Predicting the capabilities of editing is challenging. Before carrying out experiments to verify the abovementioned tumor-related editing sites, we can roughly analyze the impact of these RNA editing sites by *in silico* prediction to guide subsequent experiments. RNA editing sites are distributed in different regions of the gene, such as CDS, introns, and UTRs, so it is vital to distinguish different locations of these editing sites when predicting their functions. RNA editing sites occurring in CDS may cause non-synonymous amino acids or lead to early termination of mRNAs, and many tools, such as ANNOVAR (124), VEP (125), SnpEff (126), and SnpSift, can predict these sites. Julie et al. compared the three tools and discovered that VEP and SnpEff can better annotate the mutations of different transcripts, which is helpful for the functional prediction of RNA editing sites (127). In fact, 95% of nascent pre-mRNA could be influenced by RNA editing (128). Some predictable RNA editing sites are involved in splicing, and the conventional way of detecting these sites is predicting the conserved 5' splice site and 3' splice site and then analyzing the proportion between variant RNAs after editing occurs and the original RNAs, which is also called the percent spliced in index (PSI) (129). For RNA editing sites that occur in 3' UTR, a large number of current studies have revealed miRNA interactions, and there are also multiple tools that can analyze the relationship between mutant RNAs and the corresponding miRNAs (130). In addition, a few RNA editing events lead to alterations of the RNA structure, and these editing cases that change the free energy of RNAs can be predicted by platforms such as RNAfold (131) and STRUM (132).

To predict functional editing sites with high efficiency, we took the lead in developing an *in silico* online analysis system, RNA Editing Plus (REP), that effectively calls and annotates human A-to-I RNA editing events, predicting their downstream effects on pre-mRNA alternative splicing and miRNA-3' UTR targeting *via* human high-seq data (88). We believe that our platform governing multiple optimized prediction methods will assist more scientific groups in investigating their targets of interest in cancer.

Effects of ADARs Induced A-to-I Editing on Circular RNAs

ADARs can significantly affect the biosynthesis of circular RNAs (32–34). We summarize that ADARs affect circular RNAs in two ways. In the first effect, despite the lack of direct evidence, theoretically, RNA editing sites located in the recognition region of 5' splice site and 3' splice site could directly affect the generation of circular RNAs. When RNA editing takes place in the 5' splice site and 3' splice site regions, it not only affects pre-mRNA splicing but also further changes the splicing mode of mRNA, which may directly affect the generation of circular RNAs. In addition, it has been pointed out that approximately 99.2% of circular RNAs require 5' splice sites and 3' splice sites simultaneously (133), so if RNA editing occurs in these regions, most of the circular RNAs will be directly affected. On the other hand, the formation of dsRNA structures is accompanied by the formation of circular RNAs. Since ADARs can act on these regions and produce A-to-I RNA editing, the structure of dsRNA is destroyed, and the biosynthesis of circular RNAs is affected. In conclusion, changes in ADAR1 expression could directly influence the biosynthesis of circular RNAs.

Interestingly, mutations resulting from RNA editing occurring in pre-mRNA could be transmitted into mature circular RNAs. For instance, Hosaka et al. reported a circular RNA edited by ADAR2 named circGRIA2 (hsa_circ_0125620) in mouse spinal motor neurons and human SH-SY5Y cells, and circGRIA2 editing level alteration is a potential marker for early serum diagnosis of amyotrophic lateral sclerosis (ALS) since it can be secreted out of the cell (134). They claimed that circular RNA can be used as a marker for the early diagnosis of neoplastic diseases because it can be excluded from extracellular properties. However, the clinical feasibility of blood tests for measuring circular RNAs needs to be further validated. As mentioned earlier, in cancer, various types of ncRNAs, such as circular RNAs, miRNAs, mRNAs, and lncRNAs, can work together to form a ceRNA regulatory network. miRNA plays a vital role in this process. As sponges of miRNAs, circular RNAs can inhibit the function of miRNAs. In addition, we can use the aforementioned splicing prediction tools to analyze the changes in RNA editing at 5' splice site and 3' splice site through RNA-seq sequencing data (128), thus directly predicting the changes in circular RNAs.

Application of ADARs Induced A-to-I Editing in Cancer Therapy

Since the ability of ADARs to deaminate has also been applied to the field of gene editing, they also have great potential in cancer therapy (135, 136). Nevertheless, recent findings have pointed us toward new avenues to identify the posttranscriptional regulatory mechanisms in cancer research. The editing of endogenous dsRNA by ADARs was found to be required to prevent innate immune system activation (14, 137, 138). Two groups also showed that knockdown of ADAR1 reduced the sensitivity of

several tumor cells to antitumor drugs by activating interferons (IFNs), meaning that ADAR1 is able to enhance the effects of certain tumor immune drugs (139, 140). In addition, it has been shown that RNA editing is associated with drug resistance in tumors, and some clinically relevant RNA editing sites occurring on ncRNAs have also been demonstrated (30). Overall, ADAR1 and RNA editing can be used as targets in cancer immunotherapy (141) to treat cancer together with tumor immune drugs.

It has been found that some chemically synthesized small-molecule drugs can inhibit the expression of ADAR1. Ding et al. reported that 8-chloro-adenosine can inhibit the ADAR1/p53 pathway, inhibiting the proliferation of breast cancer (142). Erythro-9-(2-hydroxy-3-nonyl) adenine hydrochloride (EHNA) has also been proven to be an inhibitor of ADARs (143). Targeted inhibitors are considered to be effective in cancer treatment, and these small-molecular drugs are currently mainly divided into artificial drugs and natural products. There are some effective components in natural drugs that can inhibit cancers and have been used in clinical treatments. For example, paclitaxel extracted from plants is an effective antitumor drug (144). This is also why some researchers have used a variety of methods to identify the ingredients of important natural products to treat cancer (145). However, there are few studies on the active components of natural products as inhibitors of ADARs. Natural compounds may change the level of ADAR-mediated editing in tumors or play an anticancer role by virtue of the non-editing function of ADARs, which will provide a new research direction for the potential of ADARs in cancer therapy.

CONCLUSIONS AND FUTURE PERSPECTIVES

To date, great efforts have been made to develop computational methods alongside the advancement of sequencing technologies to detect RNA editing events, and millions of editing sites have been reported, allowing researchers to gain growing information on different tissues. However, many aspects could be optimized to explore tissue-specific editing levels in the future. In addition, the advent of third-generation long-read sequencing technologies such as Pacific Biosciences and Oxford Nanopore brings about more facilities for editing calling since it will theoretically circumvent the current technical bottlenecks, such as PCR errors and hyperediting read loss (96, 146, 147). On the other hand, more high-seq data from single cells have been made public, providing necessary information for unraveling RNA editing effects on cell diversity at the single-cell level. Interpreting the level of RNA editing at the single-cell level in cancer has a great promoting effect on our further understanding of tumor heterogeneity and the development of tumor heterogeneity. Although initial research has been reported on the human brain (148), reads with low abundance and coverage have restricted the application of these data (57). As mentioned earlier, RNA editing located in the non-coding region is most abundant in cancer. It is also urgent to clarify the functions of RNA editing sites and apply them to the treatment of tumors. RNA editing could dramatically increase ncRNA abundance, while ncRNAs such as lncRNAs are able to affect the drug resistance of tumors (149). Therefore, in-depth mining of the mechanism of RNA editing in lncRNAs facilitates our in-depth understanding of tumor heterogeneity, helping us treat cancer. There is a link between RNA editing and drug sensitivity—for example, the levels of RNA editing of COG3 and COPA have a strong correlation with drug sensitivity (37), which indicates that RNA editing has great potential in cancer therapy and drug development.

AUTHOR CONTRIBUTIONS

Conceptualization: YZ and GS. Writing—original draft preparation: YZ, HW, and SC. Writing—review and editing: all authors. Visualization and table collection: HW and JW. Funding acquisition: YZ and GS. All authors contributed to the article and approved the submitted version.

FUNDING

This research was funded by National Natural Science Foundation of China, grant number 31502030 to YZ and grant number 81700550 to GS.

SUPPLEMENTARY MATERIAL

The Supplementary Material for this article can be found online at: https://www.frontiersin.org/articles/10.3389/fonc.2020.632187/full#supplementary-material

REFERENCES

1. Eisenberg E, Levanon EY. A-to-I RNA editing - immune protector and transcriptome diversifier. *Nat Rev Genet* (2018) 19:473–90. doi: 10.1038/s41576-018-0006-1
2. Nishikura K. A-to-I editing of coding and non-coding RNAs by ADARs. *Nat Rev Mol Cell Biol* (2016) 17:83–96. doi: 10.1038/nrm.2015.4
3. Oakes E, Anderson A, Cohen-Gadol A, Hundley HA. Adenosine Deaminase That Acts on RNA 3 (ADAR3) Binding to Glutamate Receptor Subunit B Pre-mRNA Inhibits RNA Editing in Glioblastoma. *J Biol Chem* (2017) 292:4326–35. doi: 10.1074/jbc.M117.779868
4. Gannon HS, Zou T, Kiessling MK, Gao GF, Cai D, Choi PS, et al. Identification of ADAR1 adenosine deaminase dependency in a subset of cancer cells. *Nat Commun* (2018) 9:5450. doi: 10.1038/s41467-018-07824-4
5. Khermesh K, D'Erchia AM, Barak M, Annese A, Wachtel C, Levanon EY, et al. Reduced levels of protein recoding by A-to-I RNA editing in Alzheimer's disease. *RNA* (2016) 22:290–302. doi: 10.1261/rna.054627.115
6. Kung CP, Maggi LBJr, Weber JD. The Role of RNA Editing in Cancer Development and Metabolic Disorders. *Front Endocrinol (Lausanne)* (2018) 9:762. doi: 10.3389/fendo.2018.00762
7. Hartner JC, Walkley CR, Lu J, Orkin SH. ADAR1 is essential for the maintenance of hematopoiesis and suppression of interferon signaling. *Nat Immunol* (2009) 10:109–15. doi: 10.1038/ni.1680
8. Moore Iv JB, Sadri G, Fischer A, Weirick T, Militello G, Wysoczynski M, et al. The A-to-I RNA Editing Enzyme Adar1 Is Essential for

NormalEmbryonic Cardiac Growth and Development. *Circ Res* (2020) 127:550–2. doi: 10.1161/CIRCRESAHA.120.316932
9. Xufeng R, Nie D, Yang Q, Wang W, Cheng T, Wang Q. RNA editing enzyme ADAR1 is required for early T cell development. *Blood Sci* (2020) 2:27–32. doi: 10.1097/bs9.0000000000000039
10. Vongpipatana T, Nakahama T, Shibuya T, Kato Y, Kawahara Y. ADAR1 Regulates Early T Cell Development via MDA5-Dependent and -Independent Pathways. *J Immunol* (2020) 204:2156–68. doi: 10.4049/jimmunol.1900929
11. Hartner JC, Schmittwolf C, Kispert A, Muller AM, Higuchi M, Seeburg PH. Liver disintegration in the mouse embryo caused by deficiency in the RNA-editing enzyme ADAR1. *J Biol Chem* (2004) 279:4894–902. doi: 10.1074/jbc.M311347200
12. Wang Q, Miyakoda M, Yang W, Khillan J, Stachura DL, Weiss MJ, et al. Stress-induced apoptosis associated with null mutation of ADAR1 RNA editing deaminase gene. *J Biol Chem* (2004) 279:4952–61. doi: 10.1074/jbc.M310162200
13. Liddicoat BJ, Piskol R, Chalk AM, Ramaswami G, Higuchi M, Hartner JC, et al. RNA editing by ADAR1 prevents MDA5 sensing of endogenous dsRNA as nonself. *Science* (2015) 349:1115–20. doi: 10.1126/science.aac7049
14. Mannion NM, Greenwood SM, Young R, Cox S, Brindle J, Read D, et al. The RNA-editing enzyme ADAR1 controls innate immune responses to RNA. *Cell Rep* (2014) 9:1482–94. doi: 10.1016/j.celrep.2014.10.041
15. Roth SH, Danan-Gotthold M, Ben-Izhak M, Rechavi G, Cohen CJ, Louzoun Y, et al. Increased RNA Editing May Provide a Source for Autoantigens in Systemic Lupus Erythematosus. *Cell Rep* (2018) 23:50–7. doi: 10.1016/j.celrep.2018.03.036
16. Xu X, Wang Y, Liang H. The role of A-to-I RNA editing in cancer development. *Curr Opin Genet Dev* (2018) 48:51–6. doi: 10.1016/j.gde.2017.10.009
17. Stellos K, Gatsiou A, Stamatelopoulos K, Perisic Matic L, John D, Lunella FF, et al. Adenosine-to-inosine RNA editing controls cathepsin S expression in atherosclerosis by enabling HuR-mediated post-transcriptional regulation. *Nat Med* (2016) 22:1140–50. doi: 10.1038/nm.4172
18. Anantharaman A, Tripathi V, Khan A, Yoon JH, Singh DK, Gholamalamdari O, et al. ADAR2 regulates RNA stability by modifying access of decay-promoting RNA-binding proteins. *Nucleic Acids Res* (2017) 45:4189–201. doi: 10.1093/nar/gkw1304
19. Amin EM, Liu Y, Deng S, Tan KS, Chudgar N, Mayo MW, et al. The RNA-editing enzyme ADAR promotes lung adenocarcinoma migrationand invasion by stabilizing FAK. *Sci Signal* (2017) 10:3941. doi: 10.1126/scisignal.aah3941
20. Tan MH, Li Q, Shanmugam R, Piskol R, Kohler J, Young AN, et al. Dynamic landscape and regulation of RNA editing in mammals. *Nature* (2017) 550:249–54. doi: 10.1038/nature24041
21. Picardi E, D'Erchia AM, Lo Giudice C, Pesole G. REDIportal: a comprehensive database of A-to-I RNA editing events in humans. *Nucleic Acids Res* (2017) 45:D750–7. doi: 10.1093/nar/gkw767
22. Picardi E, Manzari C, Mastropasqua F, Aiello I, D'Erchia AM, Pesole G. Profiling RNA editing in human tissues: towards the inosinome Atlas. *Sci Rep* (2015) 5:14941. doi: 10.1038/srep14941
23. Kiran A, Baranov PV. DARNED: a DAtabase of RNa EDiting in humans. *Bioinformatics* (2010) 26:1772–6. doi: 10.1093/bioinformatics/btq285
24. Ramaswami G, Li JB. RADAR: a rigorously annotated database of A-to-I RNA editing. *Nucleic Acids Res* (2014) 42:D109–13. doi: 10.1093/nar/gkt996
25. Schaffer AA, Kopel E, Hendel A, Picardi E, Levanon EY, Eisenberg E. The cell line A-to-I RNA editing catalogue. *Nucleic Acids Res* (2020) 48:5849–58. doi: 10.1093/nar/gkaa305
26. Wells A, Heckerman D, Torkamani A, Yin L, Sebat J, Ren B, et al. Ranking of non-coding pathogenic variants and putative essential regions of the human genome. *Nat Commun* (2019) 10:5241. doi: 10.1038/s41467-019-13212-3
27. Cech TR, Steitz JA. The noncoding RNA revolution-trashing old rules to forge new ones. *Cell* (2014) 157:77–94. doi: 10.1016/j.cell.2014.03.008
28. Slack FJ, Chinnaiyan AM. The Role of Non-coding RNAs in Oncology. *Cell* (2019) 179:1033–55. doi: 10.1016/j.cell.2019.10.017
29. Anastasiadou E, Jacob LS, Slack FJ. Non-coding RNA networks in cancer. *Nat Rev Cancer* (2018) 18:5–18. doi: 10.1038/nrc.2017.99
30. Gu T, Fu AQ, Bolt MJ, White KP. Clinical Relevance of Noncoding Adenosine-to-Inosine RNA Editing in Multiple Human Cancers. *JCO Clin Cancer Inform* (2019) 3:1–8. doi: 10.1200/cci.18.00151
31. Su M, Xiao Y, Ma J, Tang Y, Tian B, Zhang Y, et al. Circular RNAs in Cancer: emerging functions in hallmarks, stemness, resistance and roles as potential biomarkers. *Mol Cancer* (2019) 18:90. doi: 10.1186/s12943-019-1002-6
32. Ivanov A, Memczak S, Wyler E, Torti F, Porath HT, Orejuela MR, et al. Analysis of intron sequences reveals hallmarks of circular RNA biogenesis in animals. *Cell Rep* (2015) 10:170–7. doi: 10.1016/j.celrep.2014.12.019
33. Rybak-Wolf A, Stottmeister C, Glazar P, Jens M, Pino N, Giusti S, et al. Circular RNAs in the Mammalian Brain Are Highly Abundant, Conserved, and Dynamically Expressed. *Mol Cell* (2015) 58:870–85. doi: 10.1016/j.molcel.2015.03.027
34. Jakobi T, Siede D, Glembotski CC, Doroudgar S, Dieterich C. Abstract 14952: Dynamic Expression of Cardiac CircRNAs May Be Regulated by Stress-Induced ADAR1-Mediated RNA Editing in Human Induced Pluripotent Stem Cell-Derived Cardiac Myocytes and in Mouse Hearts In Vivo. *Circulation* (2018) 138:A14952–2. doi: 10.1161/circ.138.suppl_1.14952
35. Han L, Diao L, Yu S, Xu X, Li J, Zhang R, et al. The Genomic Landscape and Clinical Relevance of A-to-I RNA Editing in Human Cancers. *Cancer Cell* (2015) 28:515–28. doi: 10.1016/j.ccell.2015.08.013
36. Paz-Yaacov N, Bazak L, Buchumenski I, Porath HT, Danan-Gotthold M, Knisbacher BA, et al. Elevated RNA Editing Activity Is a Major Contributor to Transcriptomic Diversity in Tumors. *Cell Rep* (2015) 13:267–76. doi: 10.1016/j.celrep.2015.08.080
37. Peng X, Xu X, Wang Y, Hawke DH, Yu S, Han L, et al. A-to-I RNA Editing Contributes to Proteomic Diversity in Cancer. *Cancer Cell* (2018) 33:817–28.e7. doi: 10.1016/j.ccell.2018.03.026
38. Wang Y, Xu X, Yu S, Jeong KJ, Zhou Z, Han L, et al. Systematic characterization of A-to-I RNA editing hotspots in microRNAs across human cancers. *Genome Res* (2017) 27:1112–25. doi: 10.1101/gr.219741.116
39. Ben-Aroya S, Levanon EY. A-to-I RNA Editing: An Overlooked Source of Cancer Mutations. *Cancer Cell* (2018) 33:789–90. doi: 10.1016/j.ccell.2018.04.006
40. Fritzell K, Xu LD, Lagergren J, Ohman M. ADARs and editing: The role of A-to-I RNA modification in cancer progression. *Semin Cell Dev Biol* (2018) 79:123–30. doi: 10.1016/j.semcdb.2017.11.018
41. Qiu W, Wang X, Buchanan M, He K, Sharma R, Zhang L, et al. ADAR1 is essential for intestinal homeostasis and stem cell maintenance. *Cell Death Dis* (2013) 4:e599. doi: 10.1038/cddis.2013.125
42. Chan T, Fu T, Bahn JH, Jun H-I, Lee J-H, Quinones-Valdez G, et al. Differential RNA editing between epithelial and mesenchymal tumorsimpacts mRNA abundance in immune response pathways. *bioRxiv* (2020) 21:2020.03.06.981191:21. doi: 10.1101/2020.03.06.981191
43. Sommer B, Kohler M, Sprengel R, Seeburg PH. RNA editing in brain controls a determinant of ion flow in glutamate-gated channels. *Cell* (1991) 67:11–9. doi: 10.1016/0092-8674(91)90568-j
44. Burns CM, Chu H, Rueter SM, Hutchinson LK, Canton H, Sanders-Bush E, et al. Regulation of serotonin-2C receptor G-protein coupling by RNA editing. *Nature* (1997) 387:303–8. doi: 10.1038/387303a0
45. Zhang Q, Xiao X. Genome sequence-independent identification of RNA editing sites. *Nat Methods* (2015) 12:347–50. doi: 10.1038/nmeth.3314
46. Ramaswami G, Zhang R, Piskol R, Keegan LP, Deng P, O'Connell MA, et al. Identifying RNA editing sites using RNA sequencing data alone. *Nat Methods* (2013) 10:128–32. doi: 10.1038/nmeth.2330
47. Picardi E, Pesole G. REDItools: high-throughput RNA editing detection made easy. *Bioinformatics* (2013) 29:1813–4. doi: 10.1093/bioinformatics/btt287
48. Sakurai M, Yano T, Kawabata H, Ueda H, Suzuki T. Inosine cyanoethylation identifies A-to-I RNA editing sites in the human transcriptome. *Nat Chem Biol* (2010) 6:733–40. doi: 10.1038/nchembio.434
49. Knutson SD, Arthur RA, Johnston HR, Heemstra JM. Selective Enrichment of A-to-I Edited Transcripts from Cellular RNA Using Endonuclease V. *J Am Chem Soc* (2020) 142:5241–51. doi: 10.1021/jacs.9b13406
50. Li Y, Gohl M, Ke K, Vanderwal CD, Spitale RC. Identification of Adenosine-to-Inosine RNA Editing with Acrylonitrile Reagents. *Org Lett* (2019) 21:7948–51. doi: 10.1021/acs.orglett.9b02929
51. Knutson SD, Ayele TM, Heemstra JM. Chemical Labeling and Affinity Capture of Inosine-Containing RNAs Using Acrylamidofluorescein. *Bioconjug Chem* (2018) 29:2899–903. doi: 10.1021/acs.bioconjchem.8b00541
52. Knutson SD, Korn MM, Johnson RP, Monteleone LR, Dailey DM, Swenson CS, et al. Chemical Profiling of A-to-I RNA Editing Using a Click-

CompatiblePhenylacrylamide. *Chemistry* (2020) 26:9874–8. doi: 10.1002/chem.202001667
53. Motorin Y, Muller S, Behm-Ansmant I, Branlant C. Identification of Modified Residues in RNAs by ReverseTranscription-Based Methods, RNA Modification. *Methods Enzymol* (2007) 425:21–53. doi: 10.1016/S0076-6879(07)25002-5
54. Hauenschild R, Tserovski L, Schmid K, Thuring K, Winz ML, Sharma S, et al. The reverse transcription signature of N-1-methyladenosine in RNA-Seq is sequence dependent. *Nucleic Acids Res* (2015) 43:9950–64. doi: 10.1093/nar/gkv895
55. Schwartz S, Motorin Y. Next-generation sequencing technologies for detection of modified nucleotides in RNAs. *RNA Biol* (2017) 14:1124–37. doi: 10.1080/15476286.2016.1251543
56. Ramaswami G, Li JB. Identification of human RNA editing sites: A historical perspective. *Methods* (2016) 107:42–7. doi: 10.1016/j.ymeth.2016.05.011
57. Pinto Y, Levanon EY. Computational approaches for detection and quantification of A-to-I RNA-editing. *Methods* (2019) 156:25–31. doi: 10.1016/j.ymeth.2018.11.011
58. Guo Y, Yu H, Samuels DC, Yue W, Ness S, Zhao YY. Single-nucleotide variants in human RNA: RNA editing and beyond. *Brief Funct Genomics* (2019) 18:30–9. doi: 10.1093/bfgp/ely032
59. Diroma MA, Ciaccia L, Pesole G, Picardi E. Elucidating the editome: bioinformatics approaches for RNA editing detection. *Brief Bioinform* (2019) 20:436–47. doi: 10.1093/bib/bbx129
60. Ramaswami G, Lin W, Piskol R, Tan MH, Davis C, Li JB. Accurate identification of human Alu and non-Alu RNA editing sites. *Nat Methods* (2012) 9:579–81. doi: 10.1038/nmeth.1982
61. Peng Z, Cheng Y, Tan BC, Kang L, Tian Z, Zhu Y, et al. Comprehensive analysis of RNA-Seq data reveals extensive RNA editing in a human transcriptome. *Nat Biotechnol* (2012) 30:253–60. doi: 10.1038/nbt.2122
62. Bahn JH, Lee JH, Li G, Greer C, Peng G, Xiao X. Accurate identification of A-to-I RNA editing in human by transcriptome sequencing. *Genome Res* (2012) 22:142–50. doi: 10.1101/gr.124107.111
63. Zhu S, Xiang JF, Chen T, Chen LL, Yang L. Prediction of constitutive A-to-I editing sites from human transcriptomes in the absence of genomic sequences. *BMC Genomics* (2013) 14:206. doi: 10.1186/1471-2164-14-206
64. Li H, Durbin R. Fast and accurate short read alignment with Burrows-Wheeler transform. *Bioinformatics* (2009) 25:1754–60. doi: 10.1093/bioinformatics/btp324
65. Langmead B, Trapnell C, Pop M, Salzberg SL. Ultrafast and memory-efficient alignment of short DNA sequences to the human genome. *Genome Biol* (2009) 10:R25. doi: 10.1186/gb-2009-10-3-r25
66. Kim D, Langmead B, Salzberg SL. HISAT: a fast spliced aligner with low memory requirements. *Nat Methods* (2015) 12:357–60. doi: 10.1038/nmeth.3317
67. Wu TD, Nacu S. Fast and SNP-tolerant detection of complex variants and splicing in short reads. *Bioinformatics* (2010) 26:873–81. doi: 10.1093/bioinformatics/btq057
68. Dobin A, Davis CA, Schlesinger F, Drenkow J, Zaleski C, Jha S, et al. STAR: ultrafast universal RNA-seq aligner. *Bioinformatics* (2013) 29:15–21. doi: 10.1093/bioinformatics/bts635
69. Ahn J, Xiao X. RASER: reads aligner for SNPs and editing sites of RNA. *Bioinformatics* (2015) 31:3906–13. doi: 10.1093/bioinformatics/btv505
70. Li H, Handsaker B, Wysoker A, Fennell T, Ruan J, Homer N, et al. The Sequence Alignment/Map format and SAMtools. *Bioinformatics* (2009) 25:2078–9. doi: 10.1093/bioinformatics/btp352
71. Koboldt DC, Zhang Q, Larson DE, Shen D, McLellan MD, Lin L, et al. VarScan 2: somatic mutation and copy number alteration discovery in cancer by exome sequencing. *Genome Res* (2012) 22:568–76. doi: 10.1101/gr.129684.111
72. Wang Z, Lian J, Li Q, Zhang P, Zhou Y, Zhan X, et al. RES-Scanner: a software package for genome-wide identification of RNA-editing sites. *Gigascience* (2016) 5:37. doi: 10.1186/s13742-016-0143-4
73. Piechotta M, Wyler E, Ohler U, Landthaler M, Dieterich C. JACUSA: site-specific identification of RNA editing events from replicate sequencing data. *BMC Bioinf* (2017) 18:7. doi: 10.1186/s12859-016-1432-8
74. John D, Weirick T, Dimmeler S, Uchida S. RNAEditor: easy detection of RNA editing events and the introduction of editing islands. *Brief Bioinform* (2017) 18:993–1001. doi: 10.1093/bib/bbw087
75. Ouyang Z, Liu F, Zhao C, Ren C, An G, Mei C, et al. Accurate identification of RNA editing sites from primitive sequence with deep neural networks. *Sci Rep* (2018) 8:6005. doi: 10.1038/s41598-018-24298-y
76. Xiong H, Liu D, Li Q, Lei M, Xu L, Wu L, et al. RED-ML: a novel, effective RNA editing detection method based on machine learning. *Gigascience* (2017) 6:1–8. doi: 10.1093/gigascience/gix012
77. Zhang F, Lu Y, Yan S, Xing Q, Tian W. SPRINT: an SNP-free toolkit for identifying RNA editing sites. *Bioinformatics* (2017) 33:3538–48. doi: 10.1093/bioinformatics/btx473
78. Kim MS, Hur B, Kim S. RDDpred: a condition-specific RNA-editing prediction model from RNA-seq data. *BMC Genomics* (2016) 17 Suppl 1:5. doi: 10.1186/s12864-015-2301-y
79. Lee SY, Joung JG, Park CH, Park JH, Kim JH. RCARE: RNA Sequence Comparison and Annotation for RNA Editing. *BMC Med Genomics* (2015) 8 Suppl 2:S8. doi: 10.1186/1755-8794-8-s2-s8
80. Alon S, Erew M, Eisenberg E. DREAM: a webserver for the identification of editing sites in mature miRNAs using deep sequencing data. *Bioinformatics* (2015) 31:2568–70. doi: 10.1093/bioinformatics/btv187
81. Eggington JM, Greene T, Bass BL. Predicting sites of ADAR editing in double-stranded RNA. *Nat Commun* (2011) 2:319. doi: 10.1038/ncomms1324
82. Distefano R, Nigita G, Macca V, Lagana A, Giugno R, Pulvirenti A, et al. VIRGO: visualization of A-to-I RNA editing sites in genomic sequences. *BMC Bioinf* (2013) 14 Suppl 7:S5. doi: 10.1186/1471-2105-14-s7-s5
83. Nigita G, Alaimo S, Ferro A, Giugno R, Pulvirenti A. Knowledge in the Investigation of A-to-I RNA Editing Signals. *Front Bioeng Biotechnol* (2015) 3:18. doi: 10.3389/fbioe.2015.00018
84. Chen W, Feng P, Ding H, Lin H. PAI: Predicting adenosine to inosine editing sites by using pseudo nucleotide compositions. *Sci Rep* (2016) 6:35123. doi: 10.1038/srep35123
85. Chen W, Feng P, Yang H, Ding H, Lin H, Chou KC. iRNA-AI: identifying the adenosine to inosine editing sites in RNA sequences. *Oncotarget* (2017) 8:4208–17. doi: 10.18632/oncotarget.13758
86. Ahmad A, Shatabda S. EPAI-NC: Enhanced prediction of adenosine to inosine RNA editing sites using nucleotide compositions. *Anal Biochem* (2019) 569:16–21. doi: 10.1016/j.ab.2019.01.002
87. Distefano R, Nigita G, Veneziano D, Romano G, Croce CM, Acunzo M. isoTar: Consensus Target Prediction with Enrichment Analysis for MicroRNAs Harboring Editing Sites and Other Variations. *Methods Mol Biol* (2019) 1970:211–35. doi: 10.1007/978-1-4939-9207-2_12
88. Yao L, Wang H, Song Y, Dai Z, Yu H, Yin M, et al. Large-scale prediction of ADAR-mediated effective human A-to-I RNA editing. *Brief Bioinform* (2019) 20:102–9. doi: 10.1093/bib/bbx092
89. Sun Y, Li X, Wu D, Pan Q, Ji Y, Ren H, et al. RED: A Java-MySQL Software for Identifying and Visualizing RNA Editing Sites Using Rule-Based and Statistical Filters. *PLoS One* (2016) 11:e0150465. doi: 10.1371/journal.pone.0150465
90. Choyon A, Rahman A, Hasanuzzaman M, Farid DM, Shatabda S. PRESa2i: incremental decision trees for prediction of Adenosine toInosine RNA editing sites. *F1000Research* (2020) 9:16–21. doi: 10.12688/f1000research.22823.1
91. Potapov V, Fu X, Dai N, Correa IR Jr., Tanner NA, Ong JL. Base modifications affecting RNA polymerase and reverse transcriptase fidelity. *Nucleic Acids Res* (2018) 46:5753–63. doi: 10.1093/nar/gky341
92. Safra M, Sas-Chen A, Nir R, Winkler R, Nachshon A, Bar-Yaacov D, et al. The m1A landscape on cytosolic and mitochondrial mRNA at single-base resolution. *Nature* (2017) 551:251–5. doi: 10.1038/nature24456
93. Phillips C, databases SNP. *Methods Mol Biol* (2009) 578:43–71. doi: 10.1007/978-1-60327-411-1_3
94. Eisenberg E. Identification of RNA editing sites in the SNP database. *Nucleic Acids Res* (2005) 33:4612–7. doi: 10.1093/nar/gki771
95. Tate JG, Bamford S, Jubb HC, Sondka Z, Beare DM, Bindal N, et al. COSMIC: the Catalogue Of Somatic Mutations In Cancer. *Nucleic Acids Res* (2019) 47:D941–7. doi: 10.1093/nar/gky1015
96. Reich DP, Bass BL. Mapping the dsRNA World. *Cold Spring Harb Perspect Biol* (2019) 11. doi: 10.1101/cshperspect.a035352
97. Porath HT, Carmi S, Levanon EY. A genome-wide map of hyper-edited RNA reveals numerous new sites. *Nat Commun* (2014) 5:4726. doi: 10.1038/ncomms5726

98. Roth SH, Levanon EY, Eisenberg E. Genome-wide quantification of ADAR adenosine-to-inosine RNA editing activity. *Nat Methods* (2019) 16:1131–8. doi: 10.1038/s41592-019-0610-9
99. Lo Giudice C, Tangaro MA, Pesole G, Picardi E. Investigating RNA editing in deep transcriptome datasets with REDItools and REDIportal. *Nat Protoc* (2020) 15:1098–131. doi: 10.1038/s41596-019-0279-7
100. Flati T, Gioiosa S, Spallanzani N, Tagliaferri I, Diroma MA, Pesole G, et al. HPC-REDItools: a Novel HPC-aware Tool for Improved Large ScaleRNA-editing Analysis. *bioRxiv* (2020) 21:2020.04.30.069732. doi: 10.1101/2020.04.30.069732
101. Kivioja T, Vaharautio A, Karlsson K, Bonke M, Enge M, Linnarsson S, et al. Counting absolute numbers of molecules using unique molecular identifiers. *Nat Methods* (2011) 9:72–4. doi: 10.1038/nmeth.1778
102. Lev-Maor G, Sorek R, Levanon EY, Paz N, Eisenberg E, Ast G. RNA-editing-mediated exon evolution. *Genome Biol* (2007) 8:R29. doi: 10.1186/gb-2007-8-2-r29
103. Takeda S, Shigeyasu K, Okugawa Y, Yoshida K, Mori Y, Yano S, et al. Activation of AZIN1 RNA editing is a novel mechanism that promotes invasive potential of cancer-associated fibroblasts in colorectal cancer. *Cancer Lett* (2019) 444:127–35. doi: 10.1016/j.canlet.2018.12.009
104. Chen L, Li Y, Lin CH, Chan TH, Chow RK, Song Y, et al. Recoding RNA editing of AZIN1 predisposes to hepatocellular carcinoma. *Nat Med* (2013) 19:209–16. doi: 10.1038/nm.3043
105. Gumireddy K, Li A, Kossenkov AV, Sakurai M, Yan J, Li Y, et al. The mRNA-edited form of GABRA3 suppresses GABRA3-mediated Akt activation and breast cancer metastasis. *Nat Commun* (2016) 7:10715. doi: 10.1038/ncomms10715
106. Ohlson J, Pedersen JS, Haussler D, Ohman M. Editing modifies the GABA (A) receptor subunit alpha3. *RNA* (2007) 13:698–703. doi: 10.1261/rna.349107
107. Song Y, An O, Ren X, Man Chan TH, Tai Tay DJ, Tang SJ, et al. RNA editing mediates the functional switch of COPA in a novelmechanism of hepatocarcinogenesis. *J Hepatol* (2020) 74:135–47. doi: 10.1016/j.jhep.2020.07.021
108. Chan TH, Lin CH, Qi L, Fei J, Li Y, Yong KJ, et al. A disrupted RNA editing balance mediated by ADARs (Adenosine DeAminases that act on RNA) in human hepatocellular carcinoma. *Gut* (2014) 63:832–43. doi: 10.1136/gutjnl-2012-304037
109. Yang XZ, Chen JY, Liu CJ, Peng J, Wee YR, Han X, et al. Selectively Constrained RNA Editing Regulation Crosstalks with piRNA Biogenesis in Primates. *Mol Biol Evol* (2015) 32:3143–57. doi: 10.1093/molbev/msv183
110. Gong J, Liu C, Liu W, Xiang Y, Diao L, Guo AY, et al. LNCediting: a database for functional effects of RNA editing in lncRNAs. *Nucleic Acids Res* (2017) 45:D79–84. doi: 10.1093/nar/gkw835
111. Picardi E, D'Erchia AM, Gallo A, Montalvo A, Pesole G. Uncovering RNA Editing Sites in Long Non-Coding RNAs. *Front Bioengineering Biotechnol* (2014) 2:64. doi: 10.3389/fbioe.2014.00064
112. Silvestris DA, Scopa C, Hanchi S, Locatelli F, Gallo A. De Novo A-to-I RNA Editing Discovery in lncRNA.*Cancers (Basel)* (2020) 12:2959. doi: 10.3390/cancers12102959
113. Salameh A, Lee AK, Cardo-Vila M, Nunes DN, Efstathiou E, Staquicini FI, et al. PRUNE2 is a human prostate cancer suppressor regulated by the intronic long noncoding RNA PCA3. *Proc Natl Acad Sci USA* (2015) 112:8403–8. doi: 10.1073/pnas.1507882112
114. Liao Y, Jung SH, Kim T. A-to-I RNA editing as a tuner of noncoding RNAs incancer. *Cancer Lett* (2020) 494:88–93. doi: 10.1016/j.canlet.2020.08.004
115. Marceca GP, Distefano R, Tomasello L, Lagana' A, Russo F, Calore F, et al. MiREDiBase: a manually curated database of editing events inmicroRNAs. *bioRxiv* (2020) 37:2020.09.04.283689. doi: 10.1101/2020.09.04.283689
116. Ramirez-Moya J, Baker AR, Slack FJ, Santisteban P. ADAR1-mediated RNA editing is a novel oncogenic process in thyroid cancer and regulates miR-200 activity. *Oncogene* (2020) 39:3738–53. doi: 10.1038/s41388-020-1248-x
117. Choudhury Y, Tay FC, Lam DH, Sandanaraj E, Tang C, Ang BT, et al. Attenuated adenosine-to-inosine editing of microRNA-376a* promotes invasiveness of glioblastoma cells. *J Clin Invest* (2012) 122:4059–76. doi: 10.1172/JCI62925
118. Shoshan E, Mobley AK, Braeuer RR, Kamiya T, Huang L, Vasquez ME, et al. Reduced adenosine-to-inosine miR-455-5p editing promotes melanoma growth and metastasis. *Nat Cell Biol* (2015) 17:311–21. doi: 10.1038/ncb3110
119. Zipeto MA, Court AC, Sadarangani A, Delos Santos NP, Balaian L, Chun HJ, et al. ADAR1 Activation Drives Leukemia Stem Cell Self-Renewal by Impairing Let-7 Biogenesis. *Cell Stem Cell* (2016) 19:177–91. doi: 10.1016/j.stem.2016.05.004
120. Shi L, Yan P, Liang Y, Sun Y, Shen J, Zhou S, et al. Circular RNA expression is suppressed by androgen receptor (AR)-regulated adenosine deaminase that acts on RNA (ADAR1) in human hepatocellular carcinoma. *Cell Death Dis* (2017) 8:e3171. doi: 10.1038/cddis.2017.556
121. Oakes E, Vadlamani P, Hundley HA. Methods for the Detection of Adenosine-to-Inosine Editing Events in Cellular RNA. *Methods Mol Biol* (2017) 1648:103–27. doi: 10.1007/978-1-4939-7204-3_9
122. Zhang R, Li X, Ramaswami G, Smith KS, Turecki G, Montgomery SB, et al. Quantifying RNA allelic ratios by microfluidic multiplex PCR and sequencing. *Nat Methods* (2014) 11:51–4. doi: 10.1038/nmeth.2736
123. Crews LA, Jiang Q, Zipeto MA, Lazzari E, Court AC, Ali S, et al. An RNA editing fingerprint of cancer stem cell reprogramming. *J Transl Med* (2015) 13:52. doi: 10.1186/s12967-014-0370-3
124. Wang K, Li M, Hakonarson H. ANNOVAR: functional annotation of genetic variants from high-throughput sequencing data. *Nucleic Acids Res* (2010) 38:e164. doi: 10.1093/nar/gkq603
125. McLaren W, Gil L, Hunt SE, Riat HS, Ritchie GR, Thormann A, et al. The Ensembl Variant Effect Predictor. *Genome Biol* (2016) 17:122. doi: 10.1186/s13059-016-0974-4
126. Cingolani P, Platts A, Wang le L, Coon M, Nguyen T, Wang L, et al. A program for annotating and predicting the effects of single nucleotide polymorphisms, SnpEff: SNPs in the genome of Drosophila melanogaster strain w1118; iso-2; iso-3. *Fly (Austin)* (2012) 6:80–92. doi: 10.4161/fly.19695
127. Wertz J, Liao Q, Bair TB, Chimenti MS. PyVar: An Extensible Framework for Variant Annotator Comparison. *bioRxiv* (2016) 078386. doi: 10.1101/078386
128. Hsiao YE, Bahn JH, Yang Y, Lin X, Tran S, Yang EW, et al. RNA editing in nascent RNA affects pre-mRNA splicing. *Genome Res* (2018) 28:812–23. doi: 10.1101/gr.231209.117
129. Tang SJ, Shen H, An O, Hong H, Li J, Song Y, et al. Cis- and trans-regulations of pre-mRNA splicing by RNA editing enzymes influence cancer development. *Nat Commun* (2020) 11:799. doi: 10.1038/s41467-020-14621-5
130. Schafer M, Ciaudo C. Prediction of the miRNA interactome - Established methods and upcoming perspectives. *Comput Struct Biotechnol J* (2020) 18:548–57. doi: 10.1016/j.csbj.2020.02.019
131. Lorenz R, Bernhart SH, Höner zu Siederdissen C, Tafer H, Flamm C, Stadler PF, et al. ViennaRNA Package 2.0. *Algorithms Mol Biol* (2011) 6:26. doi: 10.1186/1748-7188-6-26
132. Quan L, Lv Q, Zhang Y. STRUM: structure-based prediction of protein stability changes upon single-point mutation. *Bioinformatics* (2016) 32:2936–46. doi: 10.1093/bioinformatics/btw361
133. Vo JN, Cieslik M, Zhang Y, Shukla S, Xiao L, Zhang Y, et al. The Landscape of Circular RNA in Cancer. *Cell* (2019) 176:869–81.e13. doi: 10.1016/j.cell.2018.12.021
134. Hosaka T, Yamashita T, Teramoto S, Hirose N, Tamaoka A, Kwak S. ADAR2-dependent A-to-I RNA editing in the extracellular linear and circular RNAs. *Neurosci Res* (2019) 147:48–57. doi: 10.1016/j.neures.2018.11.005
135. Cox DBT, Gootenberg JS, Abudayyeh OO, Franklin B, Kellner MJ, Joung J, et al. RNA editing with CRISPR-Cas13. *Science* (2017) 358:1019–27. doi: 10.1126/science.aaq0180
136. Aquino-Jarquin G. Novel Engineered Programmable Systems for ADAR-Mediated RNA Editing. *Mol Ther Nucleic Acids* (2020) 19:1065–72. doi: 10.1016/j.omtn.2019.12.042
137. George CX, Ramaswami G, Li JB, Samuel CE. Editing of Cellular Self-RNAs by Adenosine Deaminase ADAR1 Suppresses Innate Immune Stress Responses. *J Biol Chem* (2016) 291:6158–68. doi: 10.1074/jbc.M115.709014
138. Pestal K, Funk CC, Snyder JM, Price ND, Treuting PM, Stetson DB. Isoforms of RNA-Editing Enzyme ADAR1 Independently Control Nucleic Acid Sensor MDA5-Driven Autoimmunity and Multi-organ Development. *Immunity* (2015) 43:933–44. doi: 10.1016/j.immuni.2015.11.001
139. Ishizuka JJ, Manguso RT, Cheruiyot CK, Bi K, Panda A, Iracheta-Vellve A, et al. Loss of ADAR1 in tumours overcomes resistance to immune

checkpoint blockade. *Nature* (2019) 565:43–8. doi: 10.1038/s41586-018-0768-9
140. Liu H, Golji J, Brodeur LK, Chung FS, Chen JT, deBeaumont RS, et al. Tumor-derived IFN triggers chronic pathway agonism and sensitivity to ADAR loss. *Nat Med* (2019) 25:95–102. doi: 10.1038/s41591-018-0302-5
141. Bhate A, Sun T, Li JB. ADAR1: A New Target for Immuno-oncology Therapy. *Mol Cell* (2019) 73:866–8. doi: 10.1016/j.molcel.2019.02.021
142. Ding HY, Yang WY, Zhang LH, Li L, Xie F, Li HY, et al. 8-Chloro-Adenosine Inhibits Proliferation of MDA-MB-231 and SK-BR-3 Breast Cancer Cells by Regulating ADAR1/p53 Signaling Pathway. *Cell Transplant* (2020) 29:963689720958656. doi: 10.1177/0963689720958656
143. Pham NT, Tohda M, Tezuka Y, Matsumoto K. Influence of an adenosine deaminase inhibitor, erythro-9-(2-hydroxy-3-nonyl) adenine hydrochloride, on 5-HT2CR mRNA editing in primary cultured cortical cells. *Biol Pharm Bull* (2010) 33:527–9. doi: 10.1248/bpb.33.527
144. Li FS, Weng JK. Demystifying traditional herbal medicine with modern approach. *Nat Plants* (2017) 3:17109. doi: 10.1038/nplants.2017.109
145. Harvey AL, Edrada-Ebel R, Quinn RJ. The re-emergence of natural products for drug discovery in the genomics era. *Nat Rev Drug Discovery* (2015) 14:111–29. doi: 10.1038/nrd4510
146. Weirather JL, de Cesare M, Wang Y, Piazza P, Sebastiano V, Wang XJ, et al. Comprehensive comparison of Pacific Biosciences and Oxford Nanopore Technologies and their applications to transcriptome analysis. *F1000Res* (2017) 6:100. doi: 10.12688/f1000research.10571.2
147. Garalde DR, Snell EA, Jachimowicz D, Sipos B, Lloyd JH, Bruce M, et al. Highly parallel direct RNA sequencing on an array of nanopores. *Nat Methods* (2018) 15:201–6. doi: 10.1038/nmeth.4577
148. Picardi E, Horner DS, Pesole G. Single-cell transcriptomics reveals specific RNA editing signatures in the human brain. *RNA* (2017) 23:860–5. doi: 10.1261/rna.058271.116
149. Liu K, Gao L, Ma X, Huang JJ, Chen J, Zeng L, et al. Long non-coding RNAs regulate drug resistance in cancer. *Mol Cancer* (2020) 19:54. doi: 10.1186/s12943-020-01162-0

Conflict of Interest: The authors declare that the research was conducted in the absence of any commercial or financial relationships that could be construed as a potential conflict of interest.

frontiers in Oncology

REVIEW
published: 18 February 2021
doi: 10.3389/fonc.2020.634936

Anti-Tumor Mechanisms Associated With Regulation of Non-Coding RNA by Active Ingredients of Chinese Medicine: A Review

Tian-Jia Liu, Shuang Hu, Zhi-Dong Qiu and Da Liu**

School of Pharmacy, Changchun University of Chinese Medicine, Changchun, China

Cancer has become the second leading cause of death worldwide; however, its complex pathogenesis remains largely unclear. Previous research has shown that cancer development and progression are closely associated with various non-coding RNAs, including long non-coding RNAs and microRNAs, which regulate gene expression. Target gene abnormalities are regulated and engaged in the complex mechanism underlying tumor formation, thereby controlling apoptosis, invasion, and migration of tumor cells and providing potentially effective targets for the treatment of malignant tumors. Chemotherapy is a commonly used therapeutic strategy for cancer; however, its effectiveness is limited by general toxicity and tumor cell drug resistance. Therefore, increasing attention has been paid to developing new cancer treatment modalities using traditional Chinese medicines, which exert regulatory effects on multiple components, targets, and pathways. Several active ingredients in Chinese medicine, including ginsenoside, baicalin, and matrine have been found to regulate ncRNA expression levels, thus, exerting anti-tumor effects. This review summarizes the scientific progress made regarding the anti-tumor mechanisms elicited by various active ingredients of Chinese medicine in regulating non-coding RNAs, to provide a theoretical foundation for treating tumors using traditional Chinese medicine.

Keywords: microRNA, lncRNA, non-coding RNA, active ingredients of Chinese medicine, anti-cancer

OPEN ACCESS

Edited by:
Peng Qu,
National Institutes of Health (NIH), United States

Reviewed by:
Hanming Jiang,
Shandong First Medical University, China
Guohao Wang,
National Institutes of Health (NIH), United States

****Correspondence:***
Zhi-Dong Qiu
qzd_ccucm@163.com
Da Liu
liuda_1986@163.com

Specialty section:
This article was submitted to Pharmacology of Anti-Cancer Drugs, a section of the journal Frontiers in Oncology

Received: *29 November 2020*
Accepted: *31 December 2020*
Published: *18 February 2021*

Citation:
Liu T-J, Hu S, Qiu Z-D and Liu D (2021) Anti-Tumor Mechanisms Associated With Regulation of Non-Coding RNA by Active Ingredients of Chinese Medicine: A Review. Front. Oncol. 10:634936. doi: 10.3389/fonc.2020.634936

INTRODUCTION

The incidence of cancer has tripled over the past three decades and is expected to increase five-fold by 2030 (1). Nevertheless, the precise mechanism associated with cancer pathogenesis remains largely unclear as it is highly complex and diverse. Since the 1970s, gene therapy has become an increasingly attractive strategy for the treatment of various diseases. Accordingly, more recently, the focus has shifted toward identifying specific genetic etiologies of cancer to design effective gene

Abbreviations: ncRNA, non-coding RNA; lncRNA, long non-coding RNA; miRNA, microRNA; siRNA, small interfering RNA; piRNA, Piwi-interacting RNA; rRNA, ribosomal RNA; tRNA, transfer RNA; snRNA, small nuclear RNA; EMT, epithelial-mesenchymal transition; ceRNA, competing endogenous RNA; T-ALL, T-cell acute lymphoblastic leukemia; B-ALL, B-cell acute lymphoblastic leukemia; PKM2, pyruvate kinase M2; MMPs, Matrix metalloproteinases; circRNA, circular RNA.

therapies to overcome the challenges associated with traditional cancer treatment modalities. As the human genome is gradually deciphered, RNA has been shown to play an auxiliary role as an intermediate vector of genetic information, and an increasing number of regulatory functions have been ascribed to this class of molecules. In particular, non-coding sequences, which account for 99% of the total human genome, have received greater attention (2). Most of the identified non-coding RNAs (ncRNAs), including long non-coding (lnc)RNAs, micro (mi) RNAs, small interfering (si)RNAs, Piwi-interacting (pi)RNAs, ribosomal (r)RNAs, transfer (t)RNAs, and small nuclear (sn) RNAs, participate in the translation, modification, and other cellular functions. Among these molecules, lncRNAs and miRNAs have been researched more intensively to decipher their fundamental roles in many diseases, including cancer (3). In fact, lncRNAs were initially believed to be the "noise" of genome transcription, a by-product of RNA polymerase II transcription, and were considered biologically non-functional (4). However, recent studies have shown that lncRNAs play an essential role in cancer signal transduction pathways by interacting with proteins and RNA (5) and are reportedly associated with various cancers, including those of the stomach (6–8), lung (9, 10), breast (11, 12), and prostate (13, 14). Specifically, inhibition of lncRNA H19 and lncRNA *PVT1* expression can effectively inhibit the cancerization, metastasis (15), and angiogenesis (7) of gastric cancer.

miRNA is a class of small (18–22 nucleotides) ncRNA molecules; it is present in all eukaryotic cells, with over 2,000 of these RNAs being identified in humans (3). However, ncRNAs have also been described in insects, plants, fungi, bacteria, and viruses (16, 17). Compared with lncRNA, the regulatory mechanism of miRNA is relatively simple and clear. It regulates gene expression by either suppressing mRNA translation or degrading mRNA molecules (18). Previous studies have found that the abnormal expression of miRNAs can disrupt many signaling pathways resulting in reduced proliferation, migration, and invasion of cancer cells and the promotion of apoptosis (19–21). Numerous carcinogenic miRNAs, including miR-638, miR-155, miR-31, miR-21, miR-221, miR-222, and miR-294 among others, are overexpressed in various malignant tumors (22–24), whereas others, including miR-429, miR-211, miR-1271, and miR-34a, exert anti-cancer effects and are under-expressed in cancer cells (25, 26).

The emergence of ncRNA provides new alternatives for cancer treatment, but its effective application in clinical cancer treatment remains challenging. At present, chemotherapy is one of the most important means of treating malignant tumors. However, its efficacy is limited by systemic toxicity and tumor cell resistance (27). Traditional Chinese medicine has been practiced for thousands of years because of its safety and minimal side effects. To date, many cancer patients have used traditional Chinese medicine as an alternative therapy for cancer treatment (28). Moreover, some of the active ingredients of Chinese medicine have been shown to exert anti-cancer effects by regulating ncRNAs and acting on various signaling pathways and cancer-related molecular targets, thus, inhibiting tumor proliferation, metastasis, and invasion and inducing cancer cell apoptosis (29). For instance, the isoflavone calycosin inhibits nasopharyngeal carcinoma cell growth by regulating the lncRNA *EWSAT1* and its downstream *TRAF6* pathways (30). Additionally, curcumin upregulates miR-145 expression to inhibit cell proliferation and invasion *in vitro*, while inducing cell cycle arrest (31). These reports suggested that ncRNA have anti-tumor abilities that regulate cancer cell apoptosis, proliferation, resistance, metastasis, and invasion.

ACTIVE INGREDIENTS OF TRADITIONAL CHINESE MEDICINE REGULATE THE ANTI-TUMOR MECHANISM OF MIRNA

Over the past decades, miRNA has been shown to play a regulatory role in many cancer signaling pathways (32). The active ingredients in traditional Chinese medicine act through different mechanisms to upregulate the expression of tumor-suppressing miRNAs and downregulate the expression of oncogenic miRNAs (33). They also inhibit tumor occurrence and development by inducing cell apoptosis to inhibit tumor metastasis, enhancing cell cycle arrest to reduce drug resistance, and by downregulating other pathways (34) (**Table 1**).

ACTIVE INGREDIENTS OF CHINESE MEDICINE TARGETING MIRNA INDUCE TUMOR APOPTOSIS

Apoptosis is a basic biological phenomenon, that involves the activation, expression, and regulation of a series of genes. The active ingredients of traditional Chinese medicine regulate target genes by influencing an abnormal expression of miRNAs and inducing tumor cell apoptosis (**Figure 1**). miR-21 inhibits apoptosis in various tumor cells (71–73). Ginsenoside Rh2 is a natural monosome of ginseng total saponin, and its anti-cancer effects have been demonstrated in various tumors. A former report showed that ginsenoside Rh2 inhibited Bcl-2 by increasing miR-21 levels, which induced apoptosis and significantly decreased leukemia cell viability (35). PTEN is a classical anti-oncogene, the inhibition of PTEN is key for cell apoptosis, mainly relying on the phosphorylation and dephosphorylation of Akt. In FTC-133 human follicular thyroid cells, the alkaloid Chinese medicine active ingredient matrine is induced by upregulating the *PTEN/Akt* signaling pathway *via* the downregulating miR-21 (39) it induces apoptosis of TPC-1 human thyroid cancer cells (40). Similarly, the reverse quantitative polymerase chain reaction of an extract of *Magnolia officinalis* revealed that magnolol could induce abnormal expression of miRNA in human osteosarcoma cells, with miR-21 showing a very strong ability to downregulate mRNAs. Recent evidence has suggested that Honokiol is able to suppress the *PI3K/AKT* signaling pathway; however, it was reactivated by miR-21 overexpression. Honokiol inhibits proliferation and induces apoptosis by regulating the *miR-21/*

TABLE 1 | Detailed information on Chinese medicine active ingredients targeting miRNAs.

Active Compound	Types of cancer	miRNA	Target Genes	Related Hallmark	Reference
Ginsenoside Rh2	Acute myeloid leukemia	miR-21	Bcl-2	Induce apoptosis	(35)
Ginsenoside Rh2	Human liver cancer	miR-21	MCL1/Nrf2/Bcl-2	Induce apoptosis	(36)
Ginsenoside Rh2	Prostate cancer	miR-4295	CDKN1A	Anti-proliferation	(37)
Ginsenoside Rh2	Lung adenocarcinoma	miR-491	MMP-9	Anti-metastasis	(38)
Matrine	Human thyroid cancer	miR-21	PTEN/p-Akt	Induce apoptosis	(39, 40)
Honokiol	Osteosarcoma	miR-21	PTEN/PI3K/AKT	Induce apoptosis	(41)
Berberine	Non-small cell lung cancer	miR-19a	TF/MAPK	Induce apoptosis	(42)
Baicalin	Colon cancer	miR-217	DKK1	Induce apoptosis	(33)
Baicalin	Hepatoma	miR-3127-5p	PI3K/Akt	Cell cycle arrest Anti-proliferation	(43)
Resveratrol	Breast cancer	miR-122-5p/miR-542-3p	XIAP/Bcl-2	Induce apoptosis	(44)
Resveratrol	Acute lymphoblastic leukemia	miR-196b/miR-1290	Caspase-3	Induce apoptosis/anti-migration/cycle arrest	(45)
Resveratrol	Cancer	miR-326	PKM2	Induce apoptosis	(46)
Resveratrol	Breast cancer	miR-34a/miR-424/miR-503	Bcl2/p53	Anti-proliferation	(47)
Triacetyl resveratrol	Pancreatic cancer	miR-200	Shh	Anti-MET process/Anti-metastasis	(48)
Resveratrol	Low invasive breast cancer	miR-122-5p	Bcl2/CDKs	Enhance chemosensitivity	(49)
Resveratrol	Colorectal cancer	miR-200c	Vimentin/ZEB1	Anti-MET process/anti-metastasis	(50)
Ginsenoside Rg3	Oral squamous cell carcinoma	miR-221	PI3K/AKT, MAPK/ERK	Anti-EMT process	(51)
Ginsenoside Rg3	Ovarian cancer	miR-145	DNMT3A/FSCN1	Anti-EMT process	(52)
Camptothecin	Cancer	miR-125b	Bak1/Mcl1/p53	Induce apoptosis	(53)
Camptothecin	Cervical cancer	miR-15a/16	Rictor	Enhance chemosensitivity	(54)
Paeoniflorin	Gastric carcinoma	miR-124	PI3K/Akt/STAT3	Anti-proliferation	(55)
Paeoniflorin	Human glioma cells	miR-16	MMP-9	Anti-proliferation/induce apoptosis	(56)
Paeoniflorin	Multiple myeloma	miR-29b	MMP-2	Anti-proliferation/induce apoptosis	(57)
Shikonin	Glioblastoma	miR-143	BAG3	Induce apoptosis	(58)
Shikonin	Endometrioid endometrial cancer	miR-106b	AKT/mTOR	Anti-proliferation/Induce apoptosis	(59)
Shikonin	Gastric carcinoma	miR-195	PI3K/AKT	Anti-migration/anti-invasion	(60)
Shikonin	Cervical Cancer	miR-183-5p	E-cadherin	Anti-migration/anti-invasion	(61)
Shikonin	Retinoblastoma	miR-34a/miR-202	MYCN	Anti-proliferation	(62)
Celastrol	Ovarian carcinoma	miR-21	PI3K/p-Akt/NF-κB	Induce apoptosis	(63)
Celastrol	Colon cancer	miR-21	PI3K/AKT/GSK-3β	Anti-proliferation	(64)
Celastrol	Gastric cancer	miR-21	MMP9/Vimentin Cyclin D1/CDK6	Anti-migration/induces cell cycle arrest	(65)
Celastrol	Gastric cancer	miR-21	P27/mTOR	Induces cell cycle arrest	(66)
Celastrol	Prostate cancer	miR-101	NA	Induces autophagy	(67)
Celastrol	Prostate cancer	miR-17-92a	NA	Induces autophagy	(68)
Celastrol	Lung adenocarcinoma	miR-24/miR-181b	STAT3	Anti-proliferation	(69)
Celastrol	Lung adenocarcinoma	miR-33a-5p	mTOR/p-p70S6K/p-4EBP1	Enhance chemosensitivity	(70)

PTEN/PI3K/AKT signaling pathway in human osteosarcoma cells (41).

A previous report described that Rh2 reduces the expression levels of MCL1 and Nrf2, suppresses colony formation, and induces HepG2 cell apoptosis by inhibiting miR-146a-5p in HepG2 cells (36). Berberine is a quaternary ammonium alkaloid isolated from *Coptis chinensis*. It inhibits the growth of non-small-cell lung cancer *via* the *miR-19a/TF/MAPK* axis and promotes apoptosis. A previous study of the mechanism of anti-tumor baicalin in human colon cancer showed that baicalin induced colon cancer cell apoptosis *via* the Wnt signaling pathway mediated by *miR-217/DDK1*, in which *DDK1* was identified as a direct downstream target gene of miR-217 (33). A previous study showed that resveratrol regulated the apoptosis and cell cycle of breast cancer cells by regulating miRNAs such as miR-125b-5p, miR-200C-3p, miR-409-3p, miR-122-5p, and miR-542-3p. Resveratrol-mediated miRNA modulation regulates key anti-apoptotic and cell cycle proteins, including *Bcl-2*, X-linked inhibitor of apoptosis protein, and CDKs, which are critical for its activity. Among these, miR-542-3p and miR-122-5P play key roles in resveratrol-mediated apoptosis of MCF-7 and MDA-MB-231 breast cancer cells, respectively (44). Resveratrol significantly reduced miR-196b/miR-1290 expression in the T-ALL (T-cell acute lymphoblastic leukemia) TTL-104 and B-ALL (B-cell acute lymphoblastic leukemia) SUP-B15 cell lines and upregulated the expression of IGFBP3. As a miR-196b/miR-1290 inhibitor, resveratrol was further demonstrated to exert antitumor effects on ALL cells including antiproliferation, cell cycle arrest, apoptosis and inhibition of migration (45). Pyruvate kinase *PKM2* is highly expressed in various tumors. The expression of miR-326 was

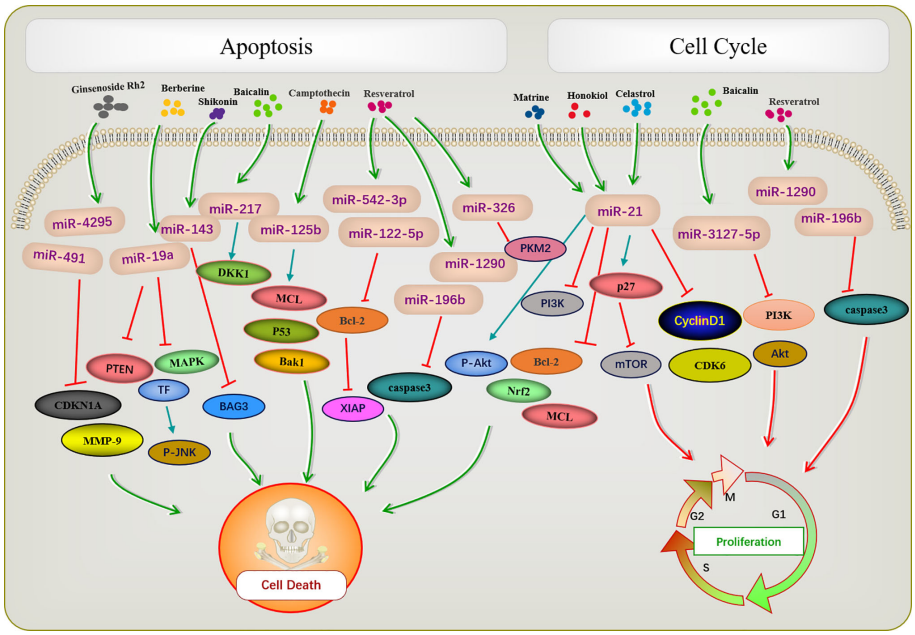

FIGURE 1 | Active ingredients of Chinese medicine targeting miRNAs induce tumor apoptosis and cell cycle blocking.

increased after resveratrol treatment, and *miR-326/PKM2*-mediated stress and mitochondrial dysfunction were involved in apoptosis induced by resveratrol (46). Camptothecin, a cytotoxic quinoline alkaloid, is an anti-cancer compound found in plants. Deep sequencing analysis of miRNA expression profiles during the camptothecin-induced apoptosis showed that 79 miRNAs were downregulated post-treatment (74). A study of camptothecin verified that miR-125b was down-regulated in camptothecin induced apoptosis in cancer cells. Camptothecin induced apoptosis in cancer cells through miR-125b-mediated mitochondrial pathways by targeting the 3'-untranslated (UTR) regions of Bak1, Mcl1, and p53 (53). In glioblastoma stem cells, miR-143 expression was downregulated after shikonin administration, whereas the regulation factor BAG3 was upregulated. Notably, miR-143 overexpression reversed this phenomenon and enhanced the anti-tumor activity of shikonin in glioblastoma stem cells (58). Celastrol is found in the root of *Celastrus orbiculatus*, belonging to the family Celastraceae. It can regulate apoptosis-promoting signaling pathways (75). Celastrol suppresses cellular proliferation and induces apoptosis of ovarian cancer OVCAR3 cells by downregulating miR-21 to inhibit the *PI3K/P-Akt-NF-κB* signaling pathway, thereby revealing a potential therapeutic approach (63).

ACTIVE INGREDIENTS OF CHINESE MEDICINE TARGET MIRNAS TO BLOCK TUMOR CELL CYCLE

The occurrence of most tumors is related to the disruption of cell cycle regulation, leading to uncontrolled cell growth. Many active ingredients of Chinese medicine play an anti-tumor role by blocking the tumor cell cycle and inhibiting cell proliferation (**Figure 1**). For instance, in patients with acute lymphoblastic leukemia (ALL), a study demonstrated that the expression of IGFBP3 was decreased in ALL patients. The authors further identified that miR-196b and miR-1290 were overexpressed in T-ALL TALL-104 and B-ALL SUP-B15 cell lines, respectively. As an miR-196b/miR-1290 inhibitor, resveratrol was further demonstrated to exert antitumor effects on ALL cells including cell cycle arrest. Resveratrol blocks T-ALL T-ALL-104 cells during the G1 phase and the B-ALL SUP-B15 cells in the S phase by inhibiting miR-196b/miR-1290 (45). Baicalin upregulates miR-3127-5p, which increases *p21/CDKN1A* and *P27/CDKN1B* expression to inhibit cell proliferation arresting the cell cycle in S and G2/M phases in Bel-7402 cells (43). Celastrol caused G2/M cell cycle arrest that was accompanied by the down-regulation of miR-21 expression. Further study showed that celastrol inhibited p27 protein degradation by inhibiting the miR-21 and mTOR signaling pathways in BGC-823 and MGC-803 cells. The effect of celastrol on cell cycle arrest of gastric cancer cells was due to an increase in the p27 protein level *via* inhibition of the miR-21-mTOR signaling pathway (66).

ACTIVE INGREDIENTS OF CHINESE MEDICINE TARGETING MIRNA INHIBIT TUMOR CELL PROLIFERATION

Many traditional Chinese medicines regulate cell proliferation through miRNAs (**Figure 2**). Paeoniflorin is a monoterpene glycoside with various anti-cancer activities and is derived

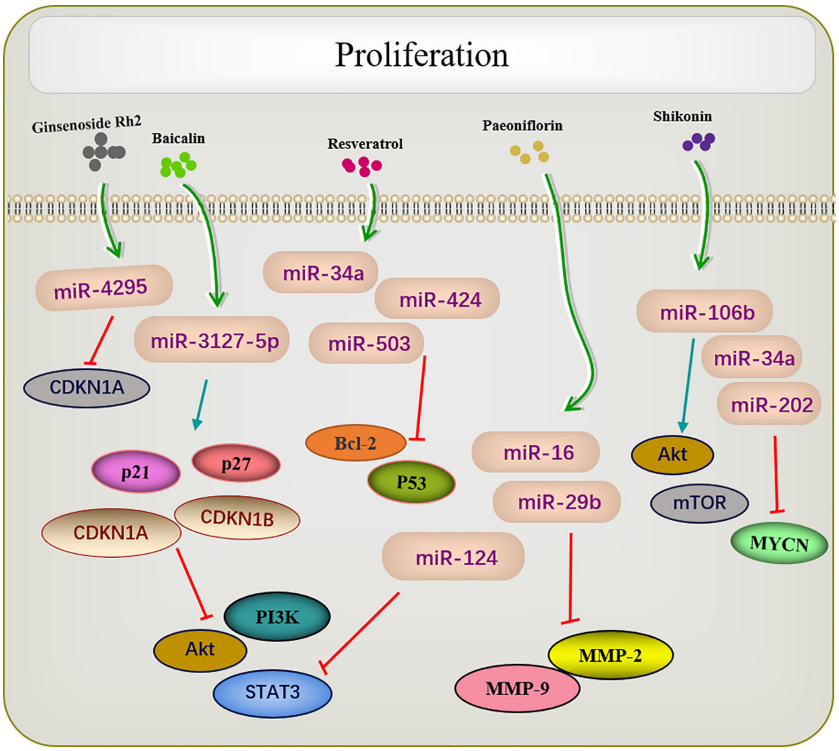

FIGURE 2 | Active ingredients of Chinese medicine targeting miRNAs inhibit tumor cell proliferation.

from *Paeonia lactiflora*. Studies have shown that paeoniflorin has broad-spectrum anti-tumor activities against various cancers (76), including those of liver (77), lungs (78), breast (79), and pancreas (80). miR-124 levels are significantly increased in paeoniflorin-treated MGC-803 cells, which inhibits *PI3K/Akt* and *p-STAT3* expression. A PI3K agonist or *STAT3* overexpression can reverse effects of paeoniflorin on MGC-803 cell proliferation (55).

Shikonin, a natural naphthoquinone isolated from traditional Chinese herbs. miR-106b is one of the most significantly downregulated miRNAs among the several miRNAs dysregulated by shikonin. miR-106b targets the tumor suppressor gene phosphatase and tensin homolog (*PTEN*), thereby modulating *AKT/mTOR* signaling pathway and ultimately inhibiting the proliferation of endometrial cancer cells (59). An earlier report investigated changes in the proliferation of the retinoblastoma cell lines Y-79 and Weri-RB-1 after shikonin administration. The results revealed that shikonin upregulated miR-34a and miR-202 expression and directly targeted the oncogene *MYCN* to degrade its mRNA while inhibiting the proliferation of retinoblastoma cells (62).

Several studies have shown that celastrol can inhibit tumor cell proliferation in several types of cancers. For example, in colon cancer cells, the overexpression of miR-21 enhanced cell viability, inhibited apoptosis, increase Bcl-2 expression, and decreased Bax levels; these effects were reversed by celastrol. As enzymes are involved in cell survival, the PI3K/AKT/GSK-3β pathway provides important signals for tumor cell proliferation Clastrol may inhibit colon cancer cell proliferation by negatively regulating the PI3K/AKT/GSK-3 pathways *via* miR-21 (64). Similar results were reported in lung adenocarcinoma, in which celastrol inhibited cell proliferation and induced apoptosis by regulating the expression levels of miR-24 and miR-181b (69).

Another study showed that ginsenoside Rh2 inhibited the proliferation of prostate cancer cells in a dose-dependent manner, and no *CDKN1A* cell cycle inhibitor was observed in the increased protein of ginsenoside Rh2. Screening all candidate miRNAs for binding to the 3′-untranslated region of *CDKN1A* showed that miR-4295 was dose-dependently inhibited by ginsenoside Rh2. Therefore, comprehensive experimental investigations revealed that ginsenoside Rh2 inhibits prostate cancer cell growth by inhibiting miRNA-4295, which activates *CDKN1A* (37).

ACTIVE INGREDIENTS OF CHINESE MEDICINE TARGETING MIRNA INHIBIT TUMOR CELL METASTASIS AND INVASION

The metastasis and invasion are essential feature characterizing the biological behavior of malignant tumors. The active

ingredients of traditional Chinese medicine can inhibit the invasion and metastasis of tumors by regulating miRNA (**Figure 3**). EMT is an important prerequisite for tumor cell metastasis. The miR-200 family inhibits EMT, thereby inhibiting tumor metastasis. A previous study reported that triacetyl resveratrol, a derivative of resveratrol, inhibited pancreatic cancer growth and EMT by upregulating the expression of the members of the miR-200 family and targeting the Shh pathway (48). Moreover, resveratrol increased the expression of miR-200c to inhibit cell proliferation and invasion in HCT116 cells (50). Ginseng saponin Rg3 suppressed EMT in oral squamous cell carcinoma and ovarian cancer *via* miR-221 (51) and miR-145 (52). E-cadherin, the most common EMT protein, plays an important role in tumor invasion, and the loss of E-cadherin expression promotes tumor and EMT. In the cervical cancer cell lines HeLa and C33a, Shikonin inhibits EMT by inducing miR-183-5p expression *via* E-cadherin (61). Similarly, miR-17-5p expression was upregulated in triple-negative breast cancer. The *PTEN* is a direct target of miR-17-5p. Studies have shown that increased expression of *PTEN* can inhibit miR-17-5p and reduce the expression of *Akt* and *P-Akt*, thereby inhibiting EMT and the migration and invasion of triple-negative breast cancer cells (81).

Shikonin can inhibit tumor migration and invasion *via* modulating miRNA-mediated regulation of multiple pathways. miR-195 is an important member of the micro-15/16/195/424/497 family and can be used as a diagnostic biomarker in breast cancer (82). In NCI-N87 cells, shikonin inhibited the proliferation, migration, and invasion by regulating miR-195 to inhibit the *PI3K/AKT* signaling pathway (60). Matrix metalloproteinases (MMPs) play important roles in mediating angiogenesis, metastasis, and invasion. *MMP-2/9* expression is related to the progression of many tumors, such as colon cancer (83), neuroblastoma (84), and bladder cancer (85). Paeoniflorin regulated miR-16/29b, which targeted *MMP-9/2* (56) to inhibit the growth and invasion of multiple myeloma cells (57). Celastrol can downregulate miR-21 and *MMP9* and regulate the expression of the cell migration protein vimentin; this reduces the migration and invasion ability of MKN45 gastric cancer cells (65). Resveratrol significantly inhibited cell migration in T-cell ALL T-ALL-104 and B-cell ALL SUP-B15 cells by inhibiting miR-196b/miR-1290 (45).

ACTIVE INGREDIENTS OF CHINESE MEDICINE TARGETING MIRNA REVERSE TUMOR CELL RESISTANCE

Increasing evidence has revealed that dysfunctional miRNAs significantly affect chemotherapy resistance. Active ingredients of Chinese medicine play an important role in reducing the toxic and side effects of chemotherapy and improving resistance to chemotherapy (**Figure 3**). A previous study showed that low-invasive breast cancer cells were resistant to amycin and this resistance was reversed by resveratrol, which also targeted the regulatory inhibitor miR-122-5p to influence the cell cycle and apoptosis (49). Increased autophagy during chemotherapy can promote tumor apoptosis or mediate autophagy-related apoptosis. miR-15a and miR-16 effectively induce autophagy,

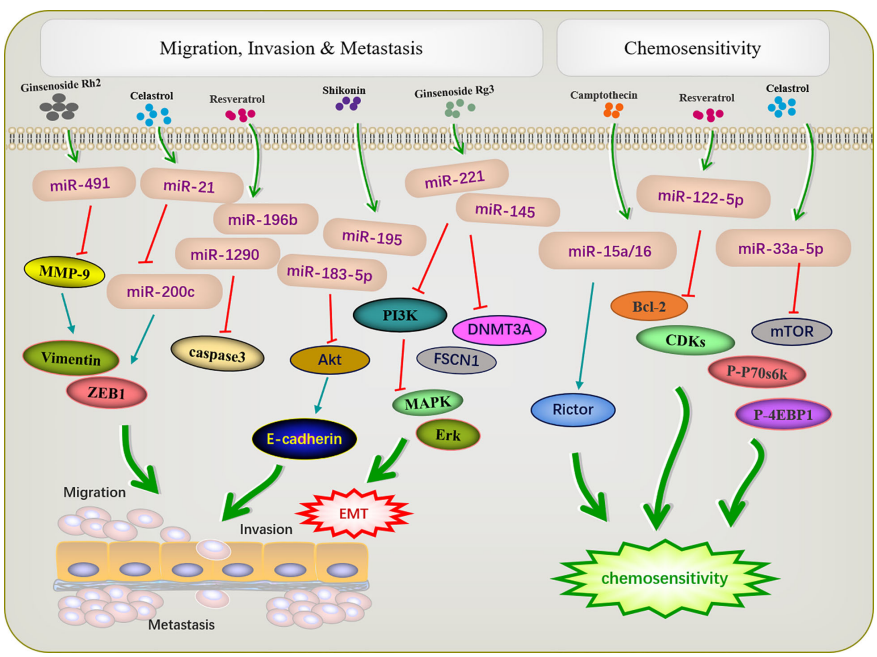

FIGURE 3 | Active ingredients of Chinese medicine targeting miRNAs inhibit tumor cell metastasis and invasion, and reverse tumor cell resistance.

enhancing the therapeutic effect of camptothecin (54). Celastrol reduced *mTOR, P-P70S6K*, and *p-4EBP1* expression by increased miR33a-5p to inhibited tumor growth (70).

THE ACTIVE INGREDIENTS OF TRADITIONAL CHINESE MEDICINE REGULATE THE ANTI-TUMOR MECHANISM OF LNCRNAS

Generally, lncRNAs are defined as molecules comprising more than 200 nucleotides lacking protein-coding capacity. However, more recently, lncRNAs have been reported to regulate gene expression (86). Meanwhile, various active ingredients in Chinese medicines, such as curcumin and resveratrol, modulate tumor development *via* lncRNA expression regulation *in vitro* and *in vivo* (**Table 2**). In gemcitabine-resistant pancreatic ductal adenocarcinoma cell, a phenolic compound extracted from turmeric, curcumin, desensitizes chemotherapy-resistant pancreatic ductal adenocarcinoma *via* inhibiting the *PRC2-PVT1-c-Myc* axis. Hence, emerging evidence suggested that curcumin may be an effective sensitizing agent for chemotherapeutic drugs (96). Moreover, curcumin induces the expression of the lncRNA *PINT* to inhibit acute lymphoblastic leukemia cell growth (88).

Resveratrol is a non-flavonoid polyphenol compound with a wide pharmacological spectrum of anti-cancer, anti-inflammatory, anti-microbial, and antioxidant activity (97). One study on lung cancer reported the upregulation of 21 lncRNAs and downregulation of 19 lncRNAs resveratrol treated A549 cells. Among these, decreased levels of the lncRNA *AK001796* weakened the inhibitory effect of resveratrol on cell proliferation (91). Resveratrol inhibits cell proliferation, migration, and invasion by downregulating *AK001796* and *NEAT1* in lung cancer and multiple myeloma (91, 92). Similarly, triptolide and isoflavone calycosin inhibit tumor cell growth by inhibiting specific lncRNAs in nasopharyngeal cancer. Triptonide inhibits human nasopharyngeal carcinoma cell growth *via* disrupting lncRNA *THOR-IGF2BP1* signaling. Conversely, ectopic lncRNA *THOR* overexpression inhibits Triptonide-induced cytotoxicity in NPC cells (95).

One of the representative lncRNAs, *H19*, is recognized as a cancer biomarker and is associated with the occurrence of esophageal cancer (98), colorectal cancer (99), liver cancer (100), breast cancer (101), bladder cancer (102), and stomach cancer. Furthermore, reduced expression of H19 can inhibit cancer development (103, 104). Specifically, curcumin inhibited cell proliferation *via c-Myc/H19* pathway, which reduced the expression of H19 in stomach cancer cells. This indicated that curcumin is a potential drug for gastric cancer (87). Moreover, microarray data identified *H19* as a potential target of Huaier (a fungal parasite on locust trees), the extract from which reduced the expression of *H19*, while also reducing the viability of breast cancer cells by inducing apoptosis *via* regulation of the *H19-miR-675-5p-CBL* axis (105). Besides, certain lncRNAs and miRNAs mutually restrict and regulate target genes to achieve tumor inhibition. For example, in bladder cancer, *H19* can directly bind miR-29b-3p to derepress the target *DNMT3B*. Further, upregulating H19 antagonizes miR-29b-3p-mediated proliferation, migration, and epithelial-mesenchymal transition (EMT) suppression in bladder cells. This evidence demonstrated, for the first time, that *H19* may function as a competing endogenous RNA (ceRNA) for miR-29b-3p and relieve the suppression of *DNMT3B*, leading to EMT and metastasis of bladder cancer (106). In 2011, a new theory was proposed that ceRNAs and miRNA response elements could mediate the interactions between mRNA pseudogenes and some ncRNAs to form a large-scale regulatory network in the transcriptome and serve as a "new language" for "mutual conversation" (107) (**Figure 4**). These networks are characterized by sponge activity, in which ncRNA interacts with the target gene to competitively bind or inhibit. In addition, ceRNAs have been identified as key regulatory factors in cancer (108, 109). *PVT1*, located downstream of the proto-oncogene *Myc* in chromosome 8q24, was used as a ceRNA of miR-216b and miR-152 in non-small-cell lung cancer and osteosarcoma to promote the tumor resistance to anti-cancer drugs (110, 111). In prostate cancer cells, *lncRNA-ROR* and the stem cell marker *Oct4* mRNA contain binding regions for miR-145 and directly compete with this microRNA. Curcumin reduced the expression of endogenous *lncRNA-ROR* and effectively increased the available concentration of miR-145 in human prostate cancer stem cells,

TABLE 2 | Detailed information on Chinese medicine active ingredients targeting lncRNAs.

Active Compound	LncRNA	Cancer	Related Hallmark	Reference
Curcumin	H19	Gastric cancer	Proliferation	(87)
Curcumin	GAS5	Breast cancer	Apoptosis	(12)
Curcumin	PINT	Acute lymphoblastic leukemia	Proliferation	(88)
Curcumin	ROR	Prostate cancer	Proliferation	(31)
Curcumin	PANDAR	Colorectal cancer	Apoptosis	(89)
Curcumin	MEG3	Ovarian cancer	Drug resistance	(90)
Resveratrol	AK001796	Lung cancer	Proliferation/cycle arrest	(91)
Resveratrol	NEAT1	Multiple myeloma	Proliferation/migration	(92)
Matrine	LINC00472	Bladder carcinoma	Growth/metastasis	(93)
Artesunate	UCA1	Prostate cancer	Apoptosis/migration	(94)
Triptolide	THOR	Nasopharyngeal carcinoma	Growth	(95)
Calycosin	EWSAT1	Nasopharyngeal carcinoma	Growth	(30)

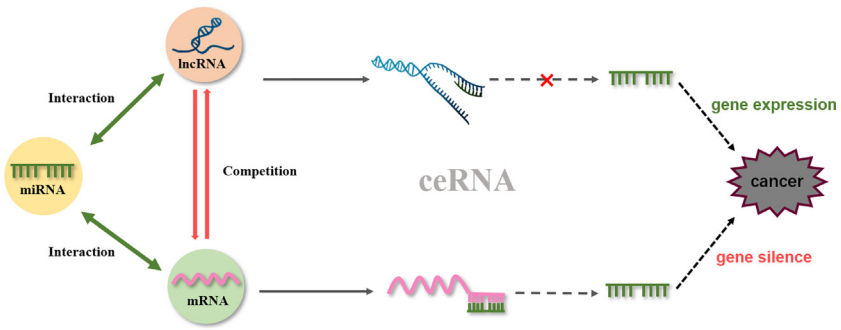

FIGURE 4 | ceRNA network.

where miR-145 prevented cell proliferation by decreasing *Oct4* expression (31). The ceRNA hypothesis has revealed new mechanisms of RNA interactions, which incentivized the analysis of ncRNA role in cancer development.

REGULATION OF THE ANTI-TUMOR MECHANISM BY CIRCRNA AND OTHER NCRNAS

As potential targets for the active ingredients of Chinese medicine, circRNA, siRNA, rRNA, and other non-coding RNAs are involved in tumor development. Some circRNAs affect cancer biogenesis in diverse manners, such as by functioning as miRNA sponges, combining with RNA-binding proteins, acting as transcription factors, and affecting protein translation (112). Matrine decreased circRNA-104075 and Bcl-9 expression significantly *via* inhibition of PI3K/AKT and Wnt-β-catenin pathways,it suppressed cell viability while induceing apoptosis and autophagy in glioma cell line U251 (113). Another study shows that matrine down-regulated the levels of circ_0027345 and HOXD3, and up-regulated miR-345-5p expression. Meanwhile, matrine restrained tumor growth, invasion and promoted autophagy of HCC by regulating the circ_0027345/miR-345-5p/HOXD3 axis *in vivo* (114). Curcumin has antioxidant and anti-cancer properties, and it has also been used as a radiosensitizer. A study compared the differences in circRNA levels in NPC cell lines after radiotherapy and after treatment with curcumin, using a high-throughput microarray. Finally, it was demonstrated by reverse transcription-quantitative polymerase chain reaction assay and wound healing assay that curcumin could enhance radiosensitization of NPC cell lines *via* mediating regulation of tumor stem-like cells by the "hsa_circRNA_102115"-"hsa-miR-335-3p"-"MAPK1" interaction network (115). At present, although circRNA has shown significant activity in the treatment of cancer, there are few reports on the regulation of circRNA by Active Ingredients of Chinese Medicine, which is also an important direction for future researchers to concern and research. circRNA has been expected to become a new molecular biomarker for the clinical diagnosis, treatment and prognosis, and the potential target for targeted therapy. siRNAs are double-stranded RNAs of 20-25 nucleotides and are involved in RNA interference; they regulate gene expression in a specific manner. Multiple synthetic siRNAs can achieve long-term silencing of target genes without interfering with endogenous microRNA pathways. Ginsenoside Rh2 downregulated P-STAT3/STAT3 and intracellular oxidative stress by upregulating PPAR. In response to siRNA-mediated knockdown of PPAR, STAT3 and intracellular oxidative stress were increased (116). rRNA is the most abundant type of RNA in cells. In lung cancer cells, triptolide interrupts rRNA synthesis by inhibiting transcriptional activation of *RNA Pol I* and *UBF*, thereby activating the apoptosis regulators *caspase 9* and *caspase 3* to inhibit *BCL2* and induce apoptosis and cell cycle arrest (117).

DISCUSSION

During cancer development, abnormal ncRNAs modulate cell proliferation, migration, and invasion by regulating the expression of proto-oncogenes and tumor suppressor genes. Many active ingredients of traditional Chinese medicine, such as resveratrol, matrine, and berberine, have been evaluated *in vivo* and *in vitro* to target specific ncRNA and shown to play anti-cancer roles. This review summarized the finding regarding 16 active ingredients of traditional Chinese medicine that can target miRNAs, lncRNAs, and other ncRNAs, thereby playing an effective role in suppressing cancer growth. Among the ncRNAs regulated by Chinese medicine active ingredients, miR-21 is the most reported ncRNA and is extensively studied in various cancers. It is involved in most of the cancer-related processes, such as cell apoptosis, proliferation, migration, and cell cycle. These findings indicate that miR21 is one of the promising ncRNAs to develop targeted therapeutic agents for many types of cancer. Some active ingredients of traditional Chinese medicine, such as Ginsenoside Rh2 and Resveratrol, promote apoptosis by regulating ncRNAs to target common apoptosis-related target genes, such as *BCL2* and *Caspase3*.

In conclusion, traditional Chinese medicine's active ingredients significantly ameliorate malignant neoplasms *via* ncRNA regulation, suggesting that active ingredients of traditional Chinese medicine may become alternative therapeutic agents for cancer in the future. At present, most studies have reported that the active ingredients of traditional Chinese medicine mainly target one kind of ncRNA for cancer treatment. However, ceRNA mechanism suggests that several kinds of ncRNA have complex interactions in cancer treatment. Therefore, we need to further explore the detailed anti-cancer mechanism and clinical safety of each of the active ingredients of traditional Chinese medicine. We hope that this review on the regulation of ncRNA by active ingredients of traditional Chinese medicine on tumor will be helpful for future research studies on anti-cancer of traditional Chinese medicine and provide a reference for their clinical application.

AUTHOR CONTRIBUTIONS

TL and SH participated in writing, editing, and making figures. ZQ and DL read and approved the final manuscript. All authors contributed to the article and approved the submitted version.

FUNDING

This work was supported by the National Natural Science Foundation of China (grant 81973712,81803680,82003985), China Postdoctoral Science Foundation (grant 2020M670825, 2020T130568), Jilin Province Science and Technology Development Project in China (grant 20170309005YY, 20200504005YY), Jilin Province TCM science and technology project (grant 2020041).

REFERENCES

1. Sohyla R, Shahram S, Alireza Z, Arash Z, Fariba S. Cancer CMJJoG. a comparative study of spatial distribution of gastrointestinal cancers in poverty and affluent strata (kermanshah metropolis, iran). *J Gastrointest Cancer* (2018) 50(4):838–47. doi: 10.1007/s12029-018-0163-7
2. Hong M, Wang N, Tan HY, Tsao SW, Feng Y. MicroRNAs and chinese medicinal herbs: new possibilities in cancer therapy. *Cancers* (2015) 7 (3):1643–57. doi: 10.3390/cancers7030855
3. Romano G, Veneziano D, Acunzo M, Croce CM. Small non-coding RNA and cancer. *Carcinogenesis* (2017) 38(5):485–91. doi: 10.1093/carcin/bgx026
4. Long J, Xiong J, Bai Y, Mao J, Lin J, Xu W, et al. Construction and investigation of a lncrna-associated cerna regulatory network in cholangiocarcinoma. *Front Oncol* (2019) 9:649. doi: 10.3389/fonc.2019.00649
5. Lin C, Yang L. Long noncoding RNA in cancer: wiring signaling circuitry. *Trends Cell Biol* (2018) 28(4):287–301. doi: 10.1016/j.tcb.2017.11.008
6. Hao NB, He YF, Li XQ, Wang K, Wang RL. The role of miRNA and lncRNA in gastric cancer. *Oncotarget* (2017) 8(46):81572–82. doi: 10.18632/oncotarget.19197
7. Zhao J, Du P, Cui P, Qin Y, Hu C, Wu J, et al. LncRNA PVT1 promotes angiogenesis via activating the STAT3/VEGFA axis in gastric cancer. *Oncogene* (2018) 37(30):4094–109. doi: 10.1038/s41388-018-0250-z
8. Wei GH, Wang X. lncRNA MEG3 inhibit proliferation and metastasis of gastric cancer via p53 signaling pathway. *Eur Rev Med Pharmacol Sci* (2017) 21(17):3850–6.
9. Nie W, Ge HJ, Yang XQ, Sun X, Huang H, Tao X, et al. LncRNA-UCA1 exerts oncogenic functions in non-small cell lung cancer by targeting miR-193a-3p. *Cancer Lett* (2016) 371(1):99–106. doi: 10.1016/j.canlet.2015.11.024
10. Fang Z, Chen W, Yuan Z, Liu X, Jiang H. LncRNA-MALAT1 contributes to the cisplatin-resistance of lung cancer by upregulating MRP1 and MDR1 via STAT3 activation. *Biomed Pharmacother* (2018) 101:536–42. doi: 10.1016/j.biopha.2018.02.130
11. Chen F, Chen J, Yang L, Liu J, Zhang X, Zhang Y, et al. Extracellular vesicle-packaged HIF-1α-stabilizing lncRNA from tumour-associated macrophages regulates aerobic glycolysis of breast cancer cells. *Nat Cell Biol* (2019) 21 (4):498–510. doi: 10.1038/s41556-019-0299-0
12. Gu J, Wang Y, Wang X, Zhou D, Shao C, Zhou M, et al. Downregulation of lncRNA GAS5 confers tamoxifen resistance by activating miR-222 in breast cancer. *Cancer Lett* (2018) 434:1–10. doi: 10.1016/j.canlet.2018.06.039
13. Zhang Y, Pitchiaya S, Cieślik M, Niknafs YS, Tien JC, Hosono Y, et al. Analysis of the androgen receptor-regulated lncRNA landscape identifies a role for ARLNC1 in prostate cancer progression. *Nat Genet* (2018) 50 (6):814–24. doi: 10.1038/s41588-018-0120-1
14. Mitobe Y, Takayama KI, Horie-Inoue K, Inoue S. Prostate cancer-associated lncRNAs. *Cancer Lett* (2018) 418:159–66. doi: 10.1016/j.canlet.2018.01.012
15. Li H, Yu B, Li J, Su L, Yan M, Zhu Z, et al. Overexpression of lncRNA H19 enhances carcinogenesis and metastasis of gastric cancer. *Oncotarget* (2014) 5(8):2318–29. doi: 10.18632/oncotarget.1913
16. Hammond SM. An overview of microRNAs. *Adv Drug Deliver Rev* (2015) 87:3–14. doi: 10.1016/j.addr.2015.05.001
17. Ashrafizadeh M, Ahmadi Z, Mohammadinejad R, Farkhondeh T, Samarghandian S. MicroRNAs mediate the anti-tumor and protective effects of ginsenosides. *Nutr Cancer* (2020) 72(8):1264–75. doi: 10.1080/01635581.2019.1675722
18. Solomon MC, Radhakrishnan RA. MicroRNA's - The vibrant performers in the oral cancer scenario. *Japanese Dental Sci Rev* (2020) 56(1):85–9. doi: 10.1016/j.jdsr.2020.04.001
19. Yan S, Wang H, Chen X, Liang C, Shang W, Wang L, et al. MiR-182-5p inhibits colon cancer tumorigenesis, angiogenesis, and lymphangiogenesis by directly downregulating VEGF-C. *Cancer Lett* (2020) 488:18–26. doi: 10.1016/j.canlet.2020.04.021
20. Zhang X, Zhang L, Chen M, Liu D. miR-324-5p inhibits gallbladder carcinoma cell metastatic behaviours by downregulation of transforming growth factor beta 2 expression. *Artif cells Nanomed Biotechnol* (2020) 48 (1):315–24. doi: 10.1080/21691401.2019.1703724
21. Xia H, Zhao Y. miR-155 is high-expressed in polycystic ovarian syndrome and promotes cell proliferation and migration through targeting PDCD4 in KGN cells. *Artif cells Nanomed Biotechnol* (2020) 48(1):197–205. doi: 10.1080/21691401.2019.1699826
22. Mackenzie NC, Staines KA, Zhu D, Genever P, Macrae VE. miRNA-221 and miRNA-222 synergistically function to promote vascular calcification. *Cell Biochem Funct* (2014) 32(2):209–16. doi: 10.1002/cbf.3005
23. Li M, Zhang D, Cheng J, Liang J, Yu F. Ginsenoside Rh2 inhibits proliferation but promotes apoptosis and autophagy by down-regulating microRNA-638 in human retinoblastoma cells. *Exp Mol Pathol* (2019) 108:17–23. doi: 10.1016/j.yexmp.2019.03.004
24. Chen Y, Shang H, Zhang S, Zhang X. Ginsenoside Rh2 inhibits proliferation and migration of medulloblastoma Daoy by down-regulation of microRNA-31. *J Cell Biochem* (2018) 119(8):6527–34. doi: 10.1002/jcb.26716
25. Li N, Wang C, Zhang P, You S. Emodin inhibits pancreatic cancer EMT and invasion by up−regulating microRNA−1271. *Mol Med Rep* (2018) 18 (3):3366–74. doi: 10.3892/mmr.2018.9304
26. Zheng F, Li J, Ma C, Tang X, Tang Q, Wu J, et al. Novel regulation of miR-34a-5p and HOTAIR by the combination of berberine and gefitinib leading to inhibition of EMT in human lung cancer. *J Cell Mol Med* (2020) 24 (10):5578–92. doi: 10.1111/jcmm.15214
27. Ripani P, Delp J, Bode K, Delgado ME, Dietrich L, Betzler VM, et al. Thiazolides promote G1 cell cycle arrest in colorectal cancer cells by

targeting the mitochondrial respiratory chain. *Oncogene* (2020) 39 (11):2345–57. doi: 10.1038/s41388-019-1142-6
28. Xiang Y, Guo Z, Zhu P, Chen J, Huang YJCM. Traditional Chinese medicine as a cancer treatment: modern perspectives of ancient but advanced science. *Cancer Med* (2019) 8(5):1958–75. doi: 10.1002/cam4.2108
29. Yan Z, Lai Z, Lin J. Anticancer properties of traditional chinese medicine. *Combinatorial Chem High throughput screening* (2017) 20(5):423–9. doi: 10.2174/1386207320666170116141818
30. Kong L, Li X, Wang H, He G, Tang A. Calycosin inhibits nasopharyngeal carcinoma cells by influencing EWSAT1 expression to regulate the TRAF6-related pathways. *Biomed Pharmacother* (2018) 106:342–8. doi: 10.1016/j.biopha.2018.06.143
31. Liu T, Chi H, Chen J, Chen C, Huang Y, Xi H, et al. Curcumin suppresses proliferation and in vitro invasion of human prostate cancer stem cells by ceRNA effect of miR-145 and lncRNA-ROR. *Gene* (2017) 631:29–38. doi: 10.1016/j.gene.2017.08.008
32. Tang J, Ahmad A, Sarkar FH. MicroRNAs in breast cancer therapy. *Curr Pharm design* (2014) 20(33):5268–74. doi: 10.2174/1381612820666140128205239
33. Jia Y, Chen L, Guo S, Li Y. Baicalin induced colon cancer cells apoptosis through miR-217/DKK1-mediated inhibition of Wnt signaling pathway. *Mol Biol Rep* (2019) 46(2):1693–700. doi: 10.1007/s11033-019-04618-9
34. Farooqi AA, Khalid S, Ahmad A. Regulation of cell signaling pathways and miRNAs by resveratrol in different cancers. *Int J Mol Sci* (2018) 19(3):652. doi: 10.3390/ijms19030652
35. Wang X, Wang Y. Ginsenoside Rh2 mitigates pediatric leukemia through suppression of Bcl-2 in leukemia cells. *Cell Physiol Biochem Int J Exp Cell Physiol Biochem Pharmacol* (2015) 37(2):641–50. doi: 10.1159/000430383
36. Chen W, Chu S, Li H, Qiu Y. MicroRNA-146a-5p enhances ginsenoside Rh2-induced anti-proliferation and the apoptosis of the human liver cancer cell line HepG2. *Oncol Lett* (2018) 16(4):5367–74. doi: 10.3892/ol.2018.9235
37. Gao Q, Zheng J. Ginsenoside Rh2 inhibits prostate cancer cell growth through suppression of microRNA-4295 that activates CDKN1A. *Cell Proliferation* (2018) 51(3):e12438. doi: 10.1111/cpr.12438
38. Chen Y, Zhang Y, Song W, Zhang Y, Dong X, Tan M. Ginsenoside Rh2 Inhibits migration of lung cancer cells under hypoxia via mir-491. *Anti-cancer Agents Medicinal Chem* (2019) 19(13):1633–41. doi: 10.2174/1871520619666190704165205
39. Li Q, Zhang S, Wang M, Dong S, Wang Y, Liu S, et al. Downregulated miR-21 mediates matrine-induced apoptosis via the PTEN/Akt signaling pathway in FTC-133 human follicular thyroid cancer cells. *Oncol Lett* (2019) 18 (4):3553–60. doi: 10.3892/ol.2019.10693
40. Zhao L, Zhang X, Cui S. Matrine inhibits TPC-1 human thyroid cancer cells via the miR-21/PTEN/Akt pathway. *Oncol Lett* (2018) 16(3):2965–70. doi: 10.3892/ol.2018.9006
41. Yang J, Zou Y, Jiang D. Honokiol suppresses proliferation and induces apoptosis via regulation of the miR–21/PTEN/PI3K/AKT signaling pathway in human osteosarcoma cells. *Int J Mol Med* (2018) 41(4):1845–54. doi: 10.3892/ijmm.2018.3433
42. Chen QQ, Shi JM, Ding Z, Xia Q, Zheng TS, Ren YB, et al. Berberine induces apoptosis in non-small-cell lung cancer cells by upregulating miR-19a targeting tissue factor. *Cancer Manage Res* (2019) 11:9005–15. doi: 10.2147/cmar.S207677
43. Bie B, Sun J, Li J, Guo Y, Jiang W, Huang C, et al. Baicalein, a Natural Anti-Cancer Compound, Alters MicroRNA Expression Profiles in Bel-7402 Human Hepatocellular Carcinoma Cells. *Cell Physiol Biochem Int J Exp Cell Physiol Biochem Pharmacol* (2017) 41(4):1519–31. doi: 10.1159/000470815
44. Venkatadri R, Muni T, Iyer AK, Yakisich JS, Azad N. Role of apoptosis-related miRNAs in resveratrol-induced breast cancer cell death. *Cell Death Dis* (2016) 7(2):e2104. doi: 10.1038/cddis.2016.6
45. Zhou W, Wang S, Ying Y, Zhou R, Mao P. miR-196b/miR-1290 participate in the antitumor effect of resveratrol via regulation of IGFBP3 expression in acute lymphoblastic leukemia. *Oncol Rep* (2017) 37(2):1075–83. doi: 10.3892/or.2016.5321
46. Wu H, Wang Y, Wu C, Yang P, Li H, Li Z. Resveratrol induces cancer cell apoptosis through MiR-326/PKM2-Mediated ER stress and mitochondrial fission. *J Agric Food Chem* (2016) 64(49):9356–67. doi: 10.1021/acs.jafc.6b04549
47. Otsuka K, Yamamoto Y, Ochiya T. Regulatory role of resveratrol, a microRNA-controlling compound, in HNRNPA1 expression, which is associated with poor prognosis in breast cancer. *Oncotarget* (2018) 9 (37):24718–30. doi: 10.18632/oncotarget.25339
48. Fu J, Shrivastava A, Shrivastava SK, Srivastava RK, Shankar S. Triacetyl resveratrol upregulates miRNA–200 and suppresses the Shh pathway in pancreatic cancer: A potential therapeutic agent. *Int J Oncol* (2019) 54 (4):1306–16. doi: 10.3892/ijo.2019.4700
49. Zhang W, Jiang H, Chen Y, Ren F. Resveratrol chemosensitizes adriamycin-resistant breast cancer cells by modulating miR-122-5p. *J Cell Biochem* (2019) 120(9):16283–92. doi: 10.1002/jcb.28910
50. Karimi Dermani F, Saidijam M, Amini R, Mahdavinezhad A, Heydari K, Najafi R. Resveratrol inhibits proliferation, invasion, and epithelial-mesenchymal transition by increasing miR-200c expression in HCT-116 colorectal cancer cells. *J Cell Biochem* (2017) 118(6):1547–55. doi: 10.1002/jcb.25816
51. Cheng Z, Xing D. Ginsenoside Rg3 inhibits growth and epithelial-mesenchymal transition of human oral squamous carcinoma cells by down-regulating miR-221. *Eur J Pharmacol* (2019) 853:353–63. doi: 10.1016/j.ejphar.2019.03.040
52. Li J, Lu J, Ye Z, Han X, Zheng X, Hou H, et al. 20(S)-Rg3 blocked epithelial-mesenchymal transition through DNMT3A/miR-145/FSCN1 in ovarian cancer. *Oncotarget* (2017) 8(32):53375–86. doi: 10.18632/oncotarget.18482
53. Zeng CW, Zhang XJ, Lin KY, Ye H, Feng SY, Zhang H, et al. Camptothecin induces apoptosis in cancer cells via microRNA-125b-mediated mitochondrial pathways. *Mol Pharmacol* (2012) 81(4):578–86. doi: 10.1124/mol.111.076794
54. Huang N, Wu J, Qiu W, Lyu Q, He J, Xie W, et al. MiR-15a and miR-16 induce autophagy and enhance chemosensitivity of Camptothecin. *Cancer Biol Ther* (2015) 16(6):941–8. doi: 10.1080/15384047.2015.1040963
55. Zheng YB, Xiao GC, Tong SL, Ding Y, Wang QS, Li SB, et al. Paeoniflorin inhibits human gastric carcinoma cell proliferation through up-regulation of microRNA-124 and suppression of PI3K/Akt and STAT3 signaling. *World J Gastroenterol* (2015) 21(23):7197–207. doi: 10.3748/wjg.v21.i23.7197
56. Li W, Qi Z, Wei Z, Liu S, Wang P, Chen Y, et al. Paeoniflorin inhibits proliferation and induces apoptosis of human glioma cells via microRNA-16 upregulation and matrix metalloproteinase-9 downregulation. *Mol Med Rep* (2015) 12(2):2735–40. doi: 10.3892/mmr.2015.3718
57. Wang S, Liu W. Paeoniflorin inhibits proliferation and promotes apoptosis of multiple myeloma cells via its effects on microRNA–29b and matrix metalloproteinase–2. *Mol Med Rep* (2016) 14(3):2143–9. doi: 10.3892/mmr.2016.5498
58. Liu J, Qu CB, Xue YX, Li Z, Wang P, Liu YH. MiR-143 enhances the antitumor activity of shikonin by targeting BAG3 expression in human glioblastoma stem cells. *Biochem Biophys Res Commun* (2015) 468(1-2):105–12. doi: 10.1016/j.bbrc.2015.10.153
59. Huang C, Hu G. Shikonin suppresses proliferation and induces apoptosis in endometrioid endometrial cancer cells via modulating miR-106b/PTEN/AKT/mTOR signaling pathway. *Biosci Rep* (2018) 38(2):BSR20171546. doi: 10.1042/bsr20171546
60. Jia L, Zhu Z, Li H, Li Y. Shikonin inhibits proliferation, migration, invasion and promotes apoptosis in NCI-N87 cells via inhibition of PI3K/AKT signal pathway. *Artif cells Nanomed Biotechnol* (2019) 47(1):2662–9. doi: 10.1080/21691401.2019.1632870
61. Tang Q, Liu L, Zhang H, Xiao J, Hann SS. Regulations of miR-183-5p and snail-mediated shikonin-reduced epithelial-mesenchymal transition in cervical cancer cells. *Drug design Dev Ther* (2020) 14:577–89. doi: 10.2147/dddt.S236216
62. Su Y, Lu S, Li J, Deng L. Shikonin-mediated up-regulation of miR-34a and miR-202 inhibits retinoblastoma proliferation. *Toxicol Res* (2018) 7(5):907–12. doi: 10.1039/c8tx00079d
63. Zhang H, Li J, Li G, Wang S. Effects of celastrol on enhancing apoptosis of ovarian cancer cells via the downregulation of microRNA–21 and the suppression of the PI3K/Akt–NF–κB signaling pathway in an in vitro model of ovarian carcinoma. *Mol Med Rep* (2016) 14(6):5363–8. doi: 10.3892/mmr.2016.5894

64. Ni H, Han Y, Jin X. Celastrol inhibits colon cancer cell proliferation by downregulating miR-21 and PI3K/AKT/GSK-3β pathway. *Int J Clin Exp Pathol* (2019) 12(3):808–16.
65. Yao SS, Han L, Tian ZB, Yu YN, Zhang Q, Li XY, et al. Celastrol inhibits growth and metastasis of human gastric cancer cell MKN45 by down-regulating microRNA-21. *Phytother Res PTR* (2019) 33(6):1706–16. doi: 10.1002/ptr.6359
66. Sha M, Ye J, Luan ZY, Guo T, Wang B, Huang JX. Celastrol induces cell cycle arrest by MicroRNA-21-mTOR-mediated inhibition p27 protein degradation in gastric cancer. *Cancer Cell Int* (2015) 15:101. doi: 10.1186/s12935-015-0256-3
67. Guo J, Huang X, Wang H, Yang H. Celastrol induces autophagy by targeting AR/miR-101 in prostate cancer cells. *PLoS One* (2015) 10(10):e0140745. doi: 10.1371/journal.pone.0140745
68. Guo J, Mei Y, Li K, Huang X, Yang H. Downregulation of miR-17-92a cluster promotes autophagy induction in response to celastrol treatment in prostate cancer cells. *Biochem Biophys Res Commun* (2016) 478(2):804–10. doi: 10.1016/j.bbrc.2016.08.029
69. Yan YF, Zhang HH, Lv Q, Liu YM, Li YJ, Li BS, et al. Celastrol suppresses the proliferation of lung adenocarcinoma cells by regulating microRNA-24 and microRNA-181b. *Oncol Lett* (2018) 15(2):2515–21. doi: 10.3892/ol.2017.7593
70. Li YJ, Sun YX, Hao RM, Wu P, Zhang LJ, Ma X, et al. miR-33a-5p enhances the sensitivity of lung adenocarcinoma cells to celastrol by regulating mTOR signaling. *Int J Oncol* (2018) 52(4):1328–38. doi: 10.3892/ijo.2018.4276
71. Canfrán-Duque A, Rotllan N, Zhang X, Fernández-Fuertes M, Ramírez-Hidalgo C, Araldi E, et al. Macrophage deficiency of miR-21 promotes apoptosis, plaque necrosis, and vascular inflammation during atherogenesis. *EMBO Mol Med* (2017) 9(9):1244–62. doi: 10.15252/emmm.201607492
72. Xiao J, Pan Y, Li XH, Yang XY, Feng YL, Tan HH, et al. Cardiac progenitor cell-derived exosomes prevent cardiomyocytes apoptosis through exosomal miR-21 by targeting PDCD4. *Cell Death Dis* (2016) 7(6):e2277. doi: 10.1038/cddis.2016.181
73. Cheng X, Zhang G, Zhang L, Hu Y, Zhang K, Sun X, et al. Mesenchymal stem cells deliver exogenous miR-21 via exosomes to inhibit nucleus pulposus cell apoptosis and reduce intervertebral disc degeneration. *J Cell Mol Med* (2018) 22(1):261–76. doi: 10.1111/jcmm.13316
74. Erdoğan İ, Coşacak M, Nalbant A, Akgül B. Deep sequencing reveals two Jurkat subpopulations with distinct miRNA profiles during camptothecin-induced apoptosis. *Turkish J Biol = Turk biyoloji dergisi* (2018) 42(2):113–22. doi: 10.3906/biy-1710-62
75. Kashyap D, Sharma A, Tuli HS, Sak K, Mukherjee T, Bishayee A. Molecular targets of celastrol in cancer: recent trends and advancements. *Crit Rev Oncol/Hematol* (2018) 128:70–81. doi: 10.1016/j.critrevonc.2018.05.019
76. Xiang Y, Zhang Q, Wei S, Huang C, Li Z, Gao Y. Paeoniflorin: a monoterpene glycoside from plants of Paeoniaceae family with diverse anticancer activities. *J Pharm Pharmacol* (2020) 72(4):483–95. doi: 10.1111/jphp.13204
77. Liu H, Zang L, Zhao J, Wang Z, Li L. Paeoniflorin inhibits cell viability and invasion of liver cancer cells via inhibition of Skp2. *Oncol Lett* (2020) 19(4):3165–72. doi: 10.3892/ol.2020.11424
78. Wu Q, Chen GL, Li YJ, Chen Y, Lin FZ. Paeoniflorin inhibits macrophage-mediated lung cancer metastasis. *Chin J Natural Medicines* (2015) 13(12):925–32. doi: 10.1016/s1875-5364(15)30098-4
79. Zhang J, Yu K, Han X, Zhen L, Liu M, Zhang X, et al. Paeoniflorin influences breast cancer cell proliferation and invasion via inhibition of the Notch−1 signaling pathway. *Mol Med Rep* (2018) 17(1):1321–5. doi: 10.3892/mmr.2017.8002
80. Li Y, Gong L, Qi R, Sun Q, Xia X, He H, et al. Paeoniflorin suppresses pancreatic cancer cell growth by upregulating HTRA3 expression. *Drug Design Dev Ther* (2017) 11:2481–91. doi: 10.2147/dddt.S134518
81. Li J, Lai Y, Ma J, Liu Y, Bi J, Zhang L, et al. miR-17-5p suppresses cell proliferation and invasion by targeting ETV1 in triple-negative breast cancer. *BMC Cancer* (2017) 17(1):745. doi: 10.1186/s12885-017-3674-x
82. Liu Y, Tang D, Zheng S, Su R, Tang Y. Serum microRNA-195 as a potential diagnostic biomarker for breast cancer: a systematic review and meta-analysis. *Int J Clin Exp Pathol* (2019) 12(11):3982–91.
83. Hsu HH, Kuo WW, Day CH, Shibu MA, Li SY, Chang SH, et al. Taiwanin E inhibits cell migration in human LoVo colon cancer cells by suppressing MMP-2/9 expression via p38 MAPK pathway. *Environ Toxicol* (2017) 32(8):2021–31. doi: 10.1002/tox.22379
84. Li XY, Huang GH, Liu QK, Yang XT, Wang K, Luo WZ, et al. Porf-2 Inhibits Tumor Cell Migration Through the MMP-2/9 Signaling Pathway in Neuroblastoma and Glioma. *Front Oncol* (2020) 10:975. doi: 10.3389/fonc.2020.00975
85. Chen Z, Zhang F, Zhang S, Ma L. The down-regulation of SNCG inhibits the proliferation and invasiveness of human bladder cancer cell line 5637 and suppresses the expression of MMP-2/9. *Int J Clin Exp Pathol* (2020) 13(7):1873–9.
86. Peng WX, Koirala P, Mo YY. LncRNA-mediated regulation of cell signaling in cancer. *Oncogene* (2017) 36(41):5661–7. doi: 10.1038/onc.2017.184
87. Liu G, Xiang T, Wu QF, Wang WX. Curcumin suppresses the proliferation of gastric cancer cells by downregulating H19. *Oncol Lett* (2016) 12(6):5156–62. doi: 10.3892/ol.2016.5354
88. Garitano-Trojaola A, José-Enériz ES, Ezponda T, Unfried JP, Carrasco-León A, Razquin N, et al. Deregulation of linc-PINT in acute lymphoblastic leukemia is implicated in abnormal proliferation of leukemic cells. *Oncotarget* (2018) 9(16):12842–52. doi: 10.18632/oncotarget.24401
89. Chen T, Yang P, Wang H, He ZY. Silence of long noncoding RNA PANDAR switches low-dose curcumin-induced senescence to apoptosis in colorectal cancer cells. *OncoTargets Ther* (2017) 10:483–91. doi: 10.2147/ott.S127547
90. Zhang J, Liu J, Xu X, Li L. Curcumin suppresses cisplatin resistance development partly via modulating extracellular vesicle-mediated transfer of MEG3 and miR-214 in ovarian cancer. *Cancer Chemother Pharmacol* (2017) 79(3):479–87. doi: 10.1007/s00280-017-3238-4
91. Yang Q, Xu E, Dai J, Liu B, Han Z, Wu J, et al. A novel long noncoding RNA AK001796 acts as an oncogene and is involved in cell growth inhibition by resveratrol in lung cancer. *Toxicol Appl Pharmacol* (2015) 285(2):79–88. doi: 10.1016/j.taap.2015.04.003
92. Geng W, Guo X, Zhang L, Ma Y, Wang L, Liu Z, et al. Resveratrol inhibits proliferation, migration and invasion of multiple myeloma cells via NEAT1-mediated Wnt/β-catenin signaling pathway. *Biomed Pharmacother = Biomedecine Pharmacotherapie* (2018) 107:484–94. doi: 10.1016/j.biopha.2018.08.003
93. Li L, Qi F, Wang K. Matrine restrains cell growth and metastasis by up-regulating LINC00472 in bladder carcinoma. *Cancer Manage Res* (2020) 12:1241–51. doi: 10.2147/cmar.S224701
94. Zhou Y, Wang X, Zhang J, He A, Wang YL, Han K, et al. Artesunate suppresses the viability and mobility of prostate cancer cells through UCA1, the sponge of miR-184. *Oncotarget* (2017) 8(11):18260–70. doi: 10.18632/oncotarget.15353
95. Wang SS, Lv Y, Xu XC, Zuo Y, Song Y, Wu GP, et al. Triptonide inhibits human nasopharyngeal carcinoma cell growth via disrupting Lnc-RNA THOR-IGF2BP1 signaling. *Cancer Lett* (2019) 443:13–24. doi: 10.1016/j.canlet.2018.11.028
96. Yoshida K, Toden S, Ravindranathan P, Han H, Goel A. Curcumin sensitizes pancreatic cancer cells to gemcitabine by attenuating PRC2 subunit EZH2, and the lncRNA PVT1 expression. *Carcinogenesis* (2017) 38(10):1036–46. doi: 10.1093/carcin/bgx065
97. Amiri A, Tehran MM, Asemi Z, Shafiee A, Hajighadimi S, Moradizarmehri S, et al. Role of resveratrol in modulating microRNAs in human diseases: from cancer to inflammatory disorder. *Curr Medicinal Chem* (2019) 2(28):360–76. doi: 10.2174/0929867326666191212102407
98. Zhou YW, Zhang H, Duan CJ, Gao Y, Cheng YD, He D, et al. miR-675-5p enhances tumorigenesis and metastasis of esophageal squamous cell carcinoma by targeting REPS2. *Oncotarget* (2016) 7(21):30730–47. doi: 10.18632/oncotarget.8950
99. Li S, Hua Y, Jin J, Wang H, Du M, Zhu L, et al. Association of genetic variants in lncRNA H19 with risk of colorectal cancer in a Chinese population. *Oncotarget* (2016) 7(18):25470–7. doi: 10.18632/oncotarget.8330
100. Li X, Liu R. Long non-coding RNA H19 in the liver-gut axis: a diagnostic marker and therapeutic target for liver diseases. *Exp Mol Pathol* (2020) 115:104472. doi: 10.1016/j.yexmp.2020.104472

101. Collette J, Le Bourhis X, Adriaenssens E. Regulation of human breast cancer by the long non-coding RNA H19. *Int J Mol Sci* (2017) 18(11):2319. doi: 10.3390/ijms18112319
102. Taheri M, Omrani MD, Ghafouri-Fard S. Long non-coding RNA expression in bladder cancer. *Biophys Rev* (2018) 10(4):1205–13. doi: 10.1007/s12551-017-0379-y
103. Zhang L, Zhou Y, Huang T, Cheng AS, Yu J, Kang W, et al. The interplay of LncRNA-H19 and its binding partners in physiological process and gastric carcinogenesis. *Int J Mol Sci* (2017) 18(2):450. doi: 10.3390/ijms18020450
104. Ghafouri-Fard S, Esmaeili M, Taheri M. H19 lncRNA: Roles in tumorigenesis. *Biomed Pharmacother* (2020) 123:109774. doi: 10.1016/j.biopha.2019.109774
105. Wang J, Wang X, Chen T, Jiang L, Yang Q. Huaier extract inhibits breast cancer progression through a LncRNA-H19/MiR-675-5p pathway. *Cell Physiol Biochem Int J Exp Cell Physiol Biochem Pharmacol* (2017) 44 (2):581–93. doi: 10.1159/000485093
106. Lv M, Zhong Z, Huang M, Tian Q, Jiang R, Chen J. lncRNA H19 regulates epithelial-mesenchymal transition and metastasis of bladder cancer by miR-29b-3p as competing endogenous RNA. *Biochim Biophys Acta Mol Cell Res* (2017) 1864(10):1887–99. doi: 10.1016/j.bbamcr.2017.08.001
107. Salmena L, Poliseno L, Tay Y, Kats L. Pandolfi PP. A ceRNA hypothesis: the Rosetta Stone of a hidden RNA language? *Cell* (2011) 146(3):353–8. doi: 10.1016/j.cell.2011.07.014
108. Ogunwobi OO, Kumar A. Chemoresistance mediated by ceRNA networks associated with the PVT1 locus. *Front Oncol* (2019) 9:834. doi: 10.3389/fonc.2019.00834
109. Anastasiadou E, Jacob LS, Slack FJ. Non-coding RNA networks in cancer. *Nat Rev Cancer* (2018) 18(1):5–18. doi: 10.1038/nrc.2017.99
110. Chen L, Han X, Hu Z, Chen L. The PVT1/miR-216b/Beclin-1 regulates cisplatin sensitivity of NSCLC cells via modulating autophagy and apoptosis. *Cancer Chemother Pharmacol* (2019) 83(5):921–31. doi: 10.1007/s00280-019-03808-3
111. Sun ZY, Jian YK, Zhu HY, Li B. lncRNAPVT1 targets miR-152 to enhance chemoresistance of osteosarcoma to gemcitabine through activating c-MET/PI3K/AKT pathway. *Pathology Res Pract* (2019) 215(3):555–63. doi: 10.1016/j.prp.2018.12.013
112. Shang Q, Yang Z, Jia R, Ge S. The novel roles of circRNAs in human cancer. *Mol Cancer* (2019) 18(1):6. doi: 10.1186/s12943-018-0934-6
113. Chi G, Xu D, Zhang B, Yang F. Matrine induces apoptosis and autophagy of glioma cell line U251 by regulation of circRNA-104075/BCL-9. *Chemico Biological Interact* (2019) 308:198–205. doi: 10.1016/j.cbi.2019.05.030
114. Lin S, Zhuang J, Zhu L, Jiang Z. Matrine inhibits cell growth, migration, invasion and promotes autophagy in hepatocellular carcinoma by regulation of circ_0027345/miR-345-5p/HOXD3 axis. *Cancer Cell Int* (2020) 20:246. doi: 10.1186/s12935-020-01293-w
115. Zhu D, Shao M, Yang J, Fang M, Liu S, Lou D, et al. Curcumin enhances radiosensitization of nasopharyngeal carcinoma via mediating regulation of tumor stem-like cells by a CircRNA network. *J Cancer* (2020) 11(8):2360–70. doi: 10.7150/jca.39511
116. Tong-Lin Wu T, Tong YC, Chen IH, Niu HS, Li Y, Cheng JT. Induction of apoptosis in prostate cancer by ginsenoside Rh2. *Oncotarget* (2018) 9 (13):11109–18. doi: 10.18632/oncotarget.24326
117. Wang J, Zhang ZQ, Li FQ, Chen JN, Gong X, Cao BB, et al. Triptolide interrupts rRNA synthesis and induces the RPL23–MDM2–p53 pathway to repress lung cancer cells. *Oncol Rep* (2020) 43(6):1863–74. doi: 10.3892/or.2020.7569

Conflict of Interest: The authors declare that the research was conducted in the absence of any commercial or financial relationships that could be construed as a potential conflict of interest.

frontiers in Oncology

REVIEW
published: 26 March 2021
doi: 10.3389/fonc.2021.653846

Exosomal Non-Coding RNAs: Regulatory and Therapeutic Target of Hepatocellular Carcinoma

Haoming Xia[1], Ziyue Huang[1], Shuqiang Liu[1], Xudong Zhao[1], Risheng He[1], Zhongrui Wang[1], Wenguang Shi[1], Wangming Chen[1], Zhizhou Li[1], Liang Yu[1,2], Peng Huang[1,2], Pengcheng Kang[1], Zhilei Su[1], Yi Xu[1,2,3], Judy Wai Ping Yam[3]* and Yunfu Cui[1]**

[1] Department of Hepatopancreatobiliary Surgery, Second Affiliated Hospital of Harbin Medical University, Harbin, China, [2] The Key Laboratory of Myocardial Ischemia, Harbin Medical University, Ministry of Education, Harbin, China, [3] Department of Pathology, Li Ka Shing Faculty of Medicine, The University of Hong Kong, Hong Kong, Hong Kong

OPEN ACCESS

Edited by:
Yong Cai,
Jilin University, China

Reviewed by:
Peifeng Li,
Qingdao University, China
Jafar Rezaie,
Urmia University of Medical Sciences, Iran
Xiu-Yan Huang,
Shanghai Jiao Tong University, China

***Correspondence:**
Yunfu Cui
yfcui777@hotmail.com
Judy Wai Ping Yam
judyyam@pathology.hku.hk
Yi Xu
xuyihmu@163.com

Specialty section:
This article was submitted to Pharmacology of Anti-Cancer Drugs, a section of the journal Frontiers in Oncology

Received: 15 January 2021
Accepted: 01 March 2021
Published: 26 March 2021

Citation:
Xia H, Huang Z, Liu S, Zhao X, He R, Wang Z, Shi W, Chen W, Li Z, Yu L, Huang P, Kang P, Su Z, Xu Y, Yam JWP and Cui Y (2021) Exosomal Non-Coding RNAs: Regulatory and Therapeutic Target of Hepatocellular Carcinoma. Front. Oncol. 11:653846. doi: 10.3389/fonc.2021.653846

Exosomes are small extracellular vesicles secreted by most somatic cells, which can carry a variety of biologically active substances to participate in intercellular communication and regulate the pathophysiological process of recipient cells. Recent studies have confirmed that non-coding RNAs (ncRNAs) carried by tumor cell/non-tumor cell-derived exosomes have the function of regulating the cancerous derivation of target cells and remodeling the tumor microenvironment (TME). In addition, due to the unique low immunogenicity and high stability, exosomes can be used as natural vehicles for the delivery of therapeutic ncRNAs *in vivo*. This article aims to review the potential regulatory mechanism and the therapeutic value of exosomal ncRNAs in hepatocellular carcinoma (HCC), in order to provide promising targets for early diagnosis and precise therapy of HCC.

Keywords: exosomes, non-coding RNAs, hepatocellular carcinoma, tumor microenvironment, early diagnosis, precise therapy

INTRODUCTION

Hepatocellular carcinoma (HCC) is the third most common malignant tumor worldwide, accounting for 85–90% of primary liver cancer (1–3). Chronic liver inflammation and fibrosis mediated by viral hepatitis, alcohol and non-alcoholic fatty liver disease (NAFLD) have become the initiators of HCC (4, 5). Due to the lack of obvious early clinical symptoms and biomarkers, most patients have reached the advanced stage at the time of diagnosis, losing the opportunity of curative treatment (resection or transplantation) as a result of multiple intrahepatic and distant metastases. Palliative care has become the only option for advanced-stage patients (6, 7). The 5-year survival rate of less than 20%, the high resistance of palliative care and the frequent relapse make early diagnosis an inevitable requirement for prolonging the survival time of HCC patients (8). Relying on capturing humoral cells and nucleic acids including circulating tumor cells (CTC), circulating tumor DNA (ctDNA) and exosomes, liquid biopsy, an emerging minimally invasive technique, is helpful for the early diagnosis and monitoring of disease progression or treatment response of cancers (9). However, the low peripheral blood abundance of CTC and the short half-life of ctDNA make exosomes a better choice.

Extracellular vesicles (EVs) are submicron particles bounded by phospholipid bilayers with non-functional nuclei, which are naturally released by a variety of cells and have no replication function. "EV" is a term proposed by International Society for Extracellular Vesicles (ISEV) (10), covering exosomes, microparticles, apoptotic blebs and other EV subsets. Exosomes can mediate cross-linking between tumor cells/non-tumor cells and recipient cells by carrying a variety of biologically active substances (protein, RNA, cholesterol, lipids, etc.), as well as modifying the recipient cells phenotype and reshaping the TME through cargo transfer (11, 12). For example, exosomes derived by breast cancer cells can regulate multiple molecules and signaling pathways in receptor cells by carrying miR-155, miR-21, miR-1246 and other cargo, including TGF-β/Smad signaling, Mef2c-β-Catenin, etc., which mediate tumor cell proliferation, metastasis and radio/chemoresistance (13). Irradiation can induce the high secretion of irradiated cells and the pathological changes of its internal cargo, participating in the formation of the bystander effect of unirradiated cells, which is manifested by increasing the cell growth rate and inducing biological behaviors such as radioresistance by repairing damaged DNA (14). Annexin II, Heparanase, TGFβ, miR-126a and other angiogenic cargo can activate angiogenesis through targeted transport between tumor cells and endothelial cells (15). Moreover, exosomes are highly secreted in cancer patients. Benefit by their wide distribution in multiple body fluids (blood, urine, saliva, etc.) and the differential expression of cargo during the development of cancer, the isolation and acquisition of exosomes and the expression analysis of its cargo have become feasible, which are conducive to the early diagnosis, treatment and prognosis evaluation of cancers (16–18). For this reason, the high stability and low immunogenicity of exosomes make them a natural vehicle for targeted anti-tumor drug/nucleic acid delivery *in vivo*.

Non-coding RNAs (ncRNAs) are a kind of RNA subgroups without protein-coding ability or only have short peptide coding ability, including miRNAs, long ncRNAs (lncRNAs), circular RNAs (circRNAs), tRNA-derived small RNAs (tsRNAs), PIWI-interacting RNAs (piRNAs) and pseudogenes, etc. NcRNAs are widely and selectively enriched in exosomes, regulating gene expression at the transcriptional, post-transcriptional and epigenetic levels (19). Numerous studies have confirmed that the potential regulation of tumor metastasis, angiogenesis, immune escape, metabolic reprogramming and drug resistance make exosomal ncRNAs become endogenous tumor regulators in the body (20), and their dysregulation directly participates in the onset and progression of carcinogenesis (21, 22). This article aims to outline the potential regulatory mechanisms of exosomal ncRNAs in HCC, with a view towards providing options for the clinical application of HCC-related biomarkers and therapeutic targets.

OVERVIEW OF EXOSOME

Exosome Biogenesis

EVs, with lipid bilayer-enclosed membranous structures, are induced by cells to secrete under physiological conditions or specific biological instructions, which can be classified into different heterogeneous populations according to different sizes and subcellular origins (10). Since the specific biomarkers of different EVs have not been clearly defined yet, exosomes specifically refer to small EVs with a size of 40-160 nm (23). The process of exosome biogenesis includes three key steps: 1. The exosomes are initially formed as intraluminal vesicles (ILVs) from late endosomal membrane invagination. 2. ILVs form multivesicular bodies (MVBs) through endosome sorting complexes in an ESCRT-dependent or independent pathway. 3. MVB fuses with plasma membrane to release exosomes (24). **Figure 1** shows the biogenesis of exosomes

Exosomes Mediate Intercellular Communication

Since it was first discovered in mature reticulocytes in the 1980s (25), the extensive participation of exosomes in different pathophysiological processes such as viral infection, immune response, and tumor metastasis has been successively confirmed (26). Relying on the specific carrying of various biologically active substances (including protein, RNA, cholesterol, lipids, etc.), exosomes establish a contact-free substance exchange between cells in autocrine, endocrine, proximal, paracrine and remote communication (27). For example, myelin oligodendrocytes count on exosomal secretion to promote axon transport and long axon maintenance in adjacent neurons (28). Adipose stem cell-derived exosomes inhibit ischemia-reperfusion injury of cardiomyocytes by targeting miR-221/miR-222/PUMA/ETS proto-oncogene 1 (ETS-1) pathway (29). Exosomal Hic-5 regulates the proliferation and apoptosis of osteosarcoma *via* Wnt/β-catenin signal pathway (30).

Exosomes transmit signals *via* ligands/adhesion molecules expressed on the membrane surface or the cargo carried inside (31), establishing two crosslinking pathways with the recipient cells, either by membranous interactions or by payload release following cell uptake of exosomes (32). The exosome-mediated communication between donor cells and recipient cells has the following characteristics: 1. MVB-derived exosomal membranes contain ligands that can simultaneously bind to multiple cell surface receptors, therefore providing an information network in a way that highly mimics the direct contact between cells and cells (33). 2. The internalization of exosomes into recipient cells results in "novel" cell membrane loading part of the donor cell surface molecules, thereby changing the original adhesion or recruitment characteristics (34). 3. Exosomes provide an ideal medium for delivering genes or proteins to reprogram target cells (35). Additionally, as shown in **Table 1**, numerous studies have revealed the regulatory role of plentiful ncRNAs in HCC.

Exosomal NcRNAs Regulate Hepatocarcinogenesis

The discovery of non-coding RNA has drawn a new blueprint for the research of genome function: The nucleus has extensive transcription capacity (even introns and intergenic sites (55),

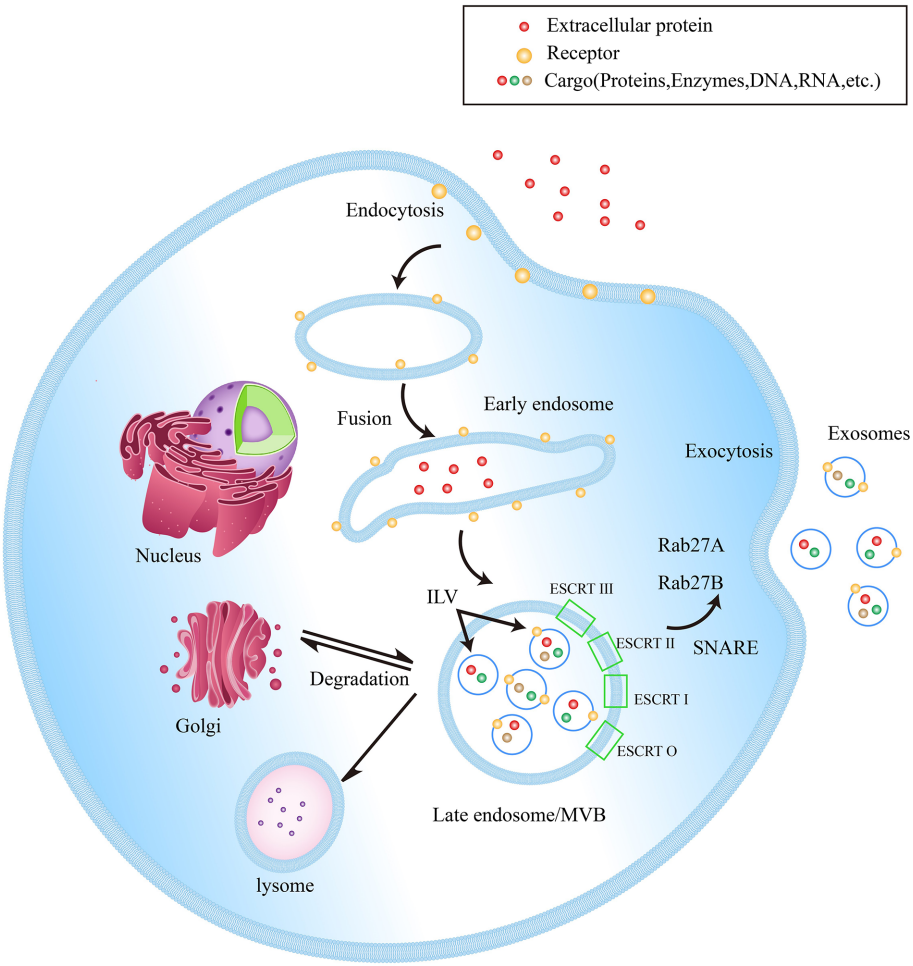

FIGURE 1 | Exosome biogenesis within endosomal system. Early endosomes are formed by the fusion of endocytic vesicles, further transformed into late endosomes/MVBs through inward budding of the membrane (packing the cargo into ILVs). ILVs protein sorting has two methods, ESCRT-dependent and ESCRT-independent. ESCRT-0, ESCRT-I, ESCRT-II and ESCRT-III are the four components of the ESCRT. They generalize the substrate on the inwardly budding endosomal membrane. Subsequently, a part of MVBs is fused with lysosomes to be degraded, while another part of MVBs can be fused with the plasma membrane to release ILVs into the extracellular space, now called exosomes. In addition, Rab27A and Rab27B are important mediators leading MVBs to the periphery of cells, and the SNARE complex helps MVBs fuse with the plasma membrane.

resulting in the production of short and long non-coding RNA with complex regulatory effects (56). As the most abundant biologically active substance in exosomes, ncRNAs play a pivotal role in intercellular communication. Growing evidences in recent years have revealed the regulatory effects of ncRNAs on the tumorigenesis and development of HCC: Exosomal circTMEM45A improves the proliferation and vascular invasion capacity of HCC cells through circTMEM45A/miR-665/IGF2 axis (41). Exosome-derived circ-0051443 suppresses the proliferation of HCC cells by upregulating the expression of BCL2 antagonist/killer 1 (BAK1), promoting apoptosis and G0/G1 cell cycle arrest (57). Cancer cells induce the ectopic expression of exosomal miR-1273f under hypoxia. The miR-1273f/LIM homeobox 6 (LHX6)/Wnt/β-catenin signaling pathway promotes the proliferation, movement, invasion and EMT of HCC cells even under normal oxygen conditions (58).

Exosome Therapeutic Applications

With the in-depth study of exosomal ncRNAs on the regulatory mechanisms of various cancers, gene-targeted therapies for related pathways have improved the prospective options for cancer cure. Since the cell membrane sets an insurmountable barrier to negatively charged nucleic acids, and the genetic material is difficult to transport freely in the body due to its own fragility, exosomes, as natural carriers for intercellular cross-linking, have been pushed to the forefront of drug delivery system. The natural ability to cross biological barriers (such as the blood-brain barrier), the transport capacity of areas without blood supply (such as dense cartilage matrix), the long residence time of target tissues, and the low clearance rate associated with high biocompatibility make exosomes become ideal carriers for gene targeted-therapy. In addition, exosomes have genetic engineering plasticity. The exogenous modification of their

TABLE 1 | Exosomal ncRNAs in HCC.

ncRNAs	Functions	Targets/Substrates	References
lncRNAs			
SENP3-EIF4A1	suppresses the proliferation and migration of HCC cells *via* SENP3-EIF4A1/miR-9-5p/ZFP36	miR-9-5p/ZFP36	(36)
FAM72D-3	promotes the proliferation and inhibits the apoptosis of HCC cells	EPC1-4	(37)
HULC	promotes secretion of exosomes from HCC cells, inducing cell invasion by targeting miR-372-3p/rab11a	miR-372-3p/rab11a	(38)
Linc-ROR	promotes the proliferation and prevents the apoptosis in condition of lacking nutrition	OCT4, NANOG, SOX2, P53 and CD133	(39)
FAL1	promotes cell growth and proliferation, cell migration and invasion in HCC cells.	miR-1236	(40)
circRNAs			
circTMEM45A	acts as the sponge of miR-665 to promote proliferation of HCC cells	miR-665	(41)
circZNF652	promotes cell proliferation, migration, invasion and glycolysis *via* miR-29a-3p/GUCD1 Axis	miR-29a-3p/GUCD1	(42)
circCdr1as	promotes proliferative and migratory abilities *via* targeting miR-1270/AFP	miR-1270/AFP	(43)
circPTGR1	increases the numbers of migrated cells, higher levels of apoptosis, and cell arrest at the S phase in the HCC cells	miR449a/MET	(44)
miRNAs			
miR-155	promotes the proliferation of HCC cells through miR-155/PTEN axis.	miR-155/PTEN	(45)
miR-296	attenuates the lymphatic vessel formation ability of HDLEC cells by upregulating EAG1 and stimulating VEGF signaling.	EAG1/VEGF signaling	(46)
miR-145	represses HCC cell proliferation, invasion, and migration, partially through downregulation of GOLM1.	GOLM1	(47)
let-7i-5p	inhibits TSP1/CD47-mediated Anti-tumorigenesis and Phagocytosis of HCC	TSP1/CD47	(48)
miRNA-21	converts HSCs to CAFs *via* down-regulating PTEN and activates PDK1/AKT signaling pathway to promote angiogenesis	PTEN, PDK1/AKT signaling pathway	(49)
miR-125	suppresses HCC cell proliferation, stem cell properties and migration *via* CD90	CD90	(50)
miR-93	promotes the stimulation in cell proliferation and invasion by targeting CDKN1A, TP53INP1 and TIMP2	CDKN1A, TP53INP1 and TIMP2	(51)
miR-25-5p	promotes tumor self-seeding in HCC to enhance cell motility by upregulating LRRC7	LRRC7	(52)
miR-103	attenuates the endothelial junction integrity by directly inhibiting the expression of VE-Cadherin, p120-catenin and ZO-1	VE-Cadherin, p120-catenin and ZO-1	(53)
miR-1247-3p	suppresses B4GALT3 expression to promote β1-integrin–NF-κB signaling in fibroblasts activation.	β1-integrin–NF-κB signaling/ B4GALT3	(54)

surface proteins can be used for many purposes. For example, the addition of tissue targeting peptides on the surface of exosomes can mediate selective targeting of cargo and reduce systemic pharmacological toxicity (59).

THE EFFECTS OF EXOSOMAL NCRNAS ON HEPATITIS

About 12% of cancer cases worldwide are induced by chronic infection of hepatitis virus pathogens (hepatitis B, hepatitis C, and hepatitis D) (60), of which HBV (54% of all HCCs) and HCV (31% of all HCCs) are clearly defined as risk factors for HCC (61). Persistent hepatitis and chronic viral infection cause both immune system and viral protein-mediated oxidative stress damage, directly participating in the tumorigenesis and development of HCC.

HBV, as the only DNA virus that induces genome instability through viral DNA integration, leads to the production of fusion gene products and changes in the expression of oncogenes or tumor suppressors. Ostm1 recruits RNA exosomal complexes by binding to HBV RNA to induce degradation of HBV RNA, resulting in HBV replication limit. Targeted excision of the RNA exosomal component Xonuclease 3 (Exosc3) can eliminate Ostm1-mediated HBV replication inhibition. C-terminal domain provides a targeted site for HBV-related treatments as the site of RNA exosomes (62). HBV X protein (HBx), a multifunctional viral regulator, participates in the regulation of the virus life cycle and the progress of HBV-related HCC. Deng et al. (63) confirm that peroxiredoxin 1 (Prdx1) as a cellular hydrogen peroxide scavenger can bind to HBx Cys and mediate the inhibition of HBx expression by interacting with the RNA exosomal complex component Exosc5, thereby inducing HBV RNA degradation. In another study, activating transcription factor 3 (ATF3) activates the transcriptional activity by interacting with the CRE motif (+164 to +171) in the Ski2 promoter. IL-1b acts as a positive regulator of ATF3 expression, mediating the upregulation of endogenous Ski2 mRNA and protein expression. Subsequently, Ski2/RNA exosome complex is formed to reduce the stability of HBx mRNA and induce the degradation of the transcript (64).

Myeloid-derived suppressor cells (MDSCs) maintain immune homeostasis by limiting excessive inflammatory response. Chronic HCV infection induces the accumulation of MDSCs in the peripheral blood. HCV-related exosomes mediate the upregulation of lncRNA RUNXOR and its downstream target RUNX family transcription factor 1 (RUNX1) in MDSCs, thereby promoting the differentiation and immunosuppression of MDSCs by activating the immunosuppressive molecule signal transducer and activator of transcription 3 (STAT3), negatively regulating the expression of miR-124 (65). Similar to the above research results, Thakuri et al. (66) have stated that HCV

exosomes upregulate lncRNA HOTAIRM1 and its target HOXA1 in MDSCs to achieve the activation of the expression of immunosuppressive molecules (Arg1, iNOS, STAT3 and ROS), and also mediate MDSCs-induced immune suppression by downregulating miR-124. In another study, HCV-related exosomes transfer immunomodulatory viral RNA from infected cells to adjacent immune cells, driving peripheral blood mononuclear cells (PBMCs) to differentiate into MDSCs. HCV-related exosomes further mediate the upregulation of peripheral blood TFR/TFH cell ratio and induce IL-10 production by inhibiting miR-124 in MDSCs, thereby antagonizing the differentiation and function of T cells during viral infection (67).

EXOSOMAL NCRNAS IN HCC PROGRESSION

Angiogenesis

The newly emerging sprouting microvessels or resident blood vessels next to the malignant tumor are important participants in the proliferation and metastasis of HCC cells (68). The interaction between endothelial cells and tumor microenvironment promotes the formation of new blood vessels through genetic or epigenetic mechanisms (69). Different from resting blood vessels (70), the rapid proliferation potential, high permeability and chaotic structure of new blood vessels (71) provide a convenient channel for the distant metastasis of tumor cells. Angiogenesis is also regarded as one of the hallmarks of solid (72, 73) and hematological malignancies (74), involved in tumorigenesis and development. Since Dr. Judah Folkman discovered the tumor-promoting effect of angiogenesis, targeted therapy for anti-angiogenesis has become a research hotspot for many scientists (75). However, different from the preclinical positive results obtained in animal models, the clinical application of anti-angiogenesis therapy has not achieved the desired effect yet (76). The potential drug resistance mechanism induced by vascular heterogeneity and tumor microenvironment has become the biggest shackle in this field (77, 78).

The core transcription regulator YAP1 of The Hippo pathway is highly correlated with the expression of tumor angiogenesis factor vascular endothelial growth factor A (VEGFA), and it has been confirmed to be recruited around HCC blood vessels, participating in mediating angiogenesis. The YAP1 inhibitor verteporfin has been used in anti-angiogenesis clinical trials for a variety of cancer treatments. Although the early therapeutic effect is ideal, the complicated distant metastasis with time has become the biggest factor limiting efficacy. Li et al. (79) confirm that the knockdown of YAP1 by verteporfin inhibits the proliferation, metastasis and angiogenesis of human umbilical vein endothelial cells (HUVECs), but verteporfin also induces the extracellular release of exosomes with lncRNA MALAT1 highly expressed. Internalized by HCC cells, MALAT1 promotes the metastasis and invasion of tumor cells by activating ERK1/2 signaling. The above mechanism provides a reasonable explanation for the concurrent distant metastasis after verteporfin treatment. Targeted inhibition of the exosomal MALAT1/ERK1/2 signaling axis may improve the long-term survival rate of patients with anti-vascular therapy. EIF3C, the C subunit of the translation initiation complex EIF3, has been confirmed to be abnormally highly expressed in HCC cells, which can stimulate the secretion of tumor cell exosomes, as well as carried into HUVECs and adjacent tissue cells with exosomes. Quantitative proteomics defines S100A11 as a cancer-related protein in HCC exosomes. Studies have shown that the activation of S100A11 expression by eukaryotic translation initiation factor 3 subunit C (EIF3C) promotes the proliferation of HCC cells and the growth of xenograft tumors in nude mice on the one hand. On the other hand, the activation of S100A11 by EIF3C induces tube formation of HUVECs and neovascularization in transplanted matrix gel plugs in nude mice (80). CircRNA-100,338 overexpressed in exosomes derived from highly metastatic HCC cells can activate the metastatic potential of ordinary HCC cells, and has been confirmed to be positively correlated with the metastatic ability of HCC. Mechanistically, exosomal circRNA-100,338 suppresses the formation of vasculogenic mimicry (VM) by negatively regulating Vascular endothelial cell cadherin (VE-cadherin) expression in HUEVCs, and increases the permeability of endothelial cells by destroying tight junctions between HUEVCs. The exogenous silencing of exosomal circRNA-100,338 significantly inhibits the invasion ability of HCC cells, as well as the growth of xenograft tumors in nude mice and the microvessel density in the tissues, meanwhile effectively reducing the number of lung metastatic nodules. In addition, the combined application of exosomal circRNA-100,338 knockdown and IFN-α shows a powerful synergistic effect in reversing exosome-mediated tumor development. Interestingly, further studies have found that the continuous high expression of serum exosomal circRNA-100,338 in HCC patients undergoing radical resection of HCC may be a risk indicator of HCC tissue proliferation, angiogenesis, lung metastasis and poor survival (81). Similar to the above studies, Yan et al. (82) confirm that circ_4911 and circ_4302 are low-expressed in HUVECs. The exogenous upregulation of both can inhibit the tumor formation capacity of HUVECs, increasing the proliferation activity and migration rate, as well as inducing G0/G1 arrest, along with the suppression of epidermal growth factor receptor (EGFR), p38 and cyclin D1. As a ceRNA, hsa_circ_0000092 can mediate the negative regulation of miR-338-3p by competitive combination, which further induces the deinhibition of the downstream target HN1. The oncogene HN1 subsequently participates in the activation of a variety of malignant biological behaviors of HUVECs, including improving the ability of vessel-like tube formation, proliferation, migration and invasion (83). In addition, circGFRA1 can also induce the proliferation and angiogenesis of HCC cells as a molecular sponge by targeted expression inhibition of miR-149 (84). CircASAP1 is clinically closely related to the pulmonary metastasis after radical resection in HCC patients, and is overexpressed in HCC cells with high metastatic potential. Studies have confirmed that it can indirectly induce the overexpression of downstream targets MAPK1 and

CSF-1 by acting as the ceRNA of miR-326 and miR-532-5p (both are tumor suppressor factors), thereby regulating miR-326/miR-532-5p/MAPK1 and miR-326/miR-532-5p/CSF-1 signaling pathway respectively to promote the proliferation/invasion of HCC cells and the infiltration of macrophages in the TME. Moreover, the highly expressed circASAP1 exhibits an ideal ability to promote the growth of xenograft tumors *in vivo*, as well as inducing the pulmonary metastasis of HCC cells (85). MiR-451a is abnormally downregulated in HCC pathological tissues and serum exosomes of patients. The co-incubation of HCC-derived exosomes highly expressed miR-451a and HUVECs mediates the transport of miR-451a towards endothelial cell, inhibiting the transfer and tube formation ability of HUVECs and inducing apoptosis. Located on the tight junctions between cells on the surface of the plasma membrane, zonula occludens 1 (ZO-1) serves as an indicator to assess vascular permeability. The overexpressed miR-451a in HUVECs reduces vascular permeability by inducing the transfer of ZO-1 from the cytoplasm to the cell membrane (86). In another study, miR-638 is also significantly downregulated in HCC tissues and serum exosomes. The exogenous upregulation of miR-638 not only antagonizes the proliferation and metastasis of HCC cells through the targeted inhibition of oncogene Sp1 transcription factor (SP1), but also regulates the endothelial function and inhibits angiogenesis *via* the internalization of miR-638 overexpressed exosomes by HUVECs (87).

Metabolic Reprogramming

Even in the aerobic state, tumor cells still have a tendency to transform from oxidative phosphorylation to glycolytic metabolism. This phenomenon is called the Warburg effect. The metabolic phenotype of aerobic glycolysis can induce tumor cells to form a state of high glucose uptake, providing ATP for tumor proliferation and intermediates/substrates for the synthesis of biological macromolecules (88–91). Meanwhile, pyruvate is converted into lactic acid, which lowers the pH value of the extracellular matrix (92), the acidic tumor microenvironment inducing tumor invasion and metastasis, as well as improving the resistance to ionizing radiation (93, 94). The unique metabolic reprogramming of tumor cells creates a favorable energy supply mode and survival soil for their own growth. Targeted inhibition of the Warburg effect may provide a breakthrough for tumor treatment.

Cytoplasmic Ski and nuclear TRAMP are the two main cofactor complexes involved in the recruitment of target RNA to nuclear exosomes, monitoring and degradation of RNA. RNA helicase MTR4 can mediate RNA insertion into exosomes by binding to TRMAP complex and take part in regulating the stability of exosomal RNA. Research by Yu (95) et al. confirm the mechanism of MTR4 participating in inducing the aerobic glycolysis phenotype of HCC cells: Ectopic expressed in HCC tissues and serum exosomes, MTR4 regulates coordinated alternative splicing by recruiting polypyrimidine tract binding protein 1 (PTBP1) to the intron region of target pre-mRNA. Exogenous knockdown of MTR4 can affect the correct alternative splicing of Glucose transporter 1 (GLUT1)/pyruvate kinase M2 (PKM2) pre-mRNA, thereby reducing the production of functional mRNA, and in turn produce new alternative splicing products GLUT1b and PKM1, both of which severely reduce the glycolysis of HCC. Consequently, the increased oxidative phosphorylation inhibits the rapid proliferation of HCC cells and the growth of xenograft tumors in nude mice. Further studies have found that the oncogenic factor c-Myc can bind to the MTR4 promoter and directly activate the transcription, indicating that MTR4, as a functional mediator of c-Myc, participates in the metabolic reprogramming of cancer cells. Another study confirms the overexpression of circFBLIM1 in the serum exosomes of HCC patients and HCC cell lines, and the co-incubation of isolated serum exosomes with tumor cells can mediate the latter's internalization of circFBLIM1. As a competitive endogenous RNA, circFBLIM1 deinhibits the expression of the downstream target gene LDL receptor related protein 6 (LRP6) by negatively regulating the expression of miR-338, thereby initiating tumor cell glycolytic metabolism phenotype transformation: High glucose consumption, increased production of lactic acid and ATP, upregulation of ECAR (reflecting the overall glycolytic flux) and downregulation of OCR (reflecting mitochondrial respiration). Additionally, circFBLIM1 also promotes the proliferation of HCC cells and the growth of xenograft tumors, as well as inducing cell apoptosis (96).

Obesity, high body weight, and high-fat diet have all been confirmed to be involved in the occurrence and development of non-alcoholic fatty liver disease (NAFLD), eventually leading to liver fibrosis, cirrhosis and HCC (97, 98). Studies have confirmed that the exogenous stimulation of different pathogenic factors can induce the transformation of healthy adipocytes into cancer-associated adipocytes (CAAs) (99, 100). CAAs can cause local vascular compression through its rapid expansion, forming a tissue hypoxic environment, and participate in inducing fibrosis and abnormal extracellular matrix remodeling, mediating changes in metabolic phenotype, local inflammatory response and neovascularization (101–103). There is a positive correlation between the body fat ratio (BFR) of HCC patients and the level of miR-23 in serum exosomes. Mature adipocytes can achieve targeted transport of miR-23 to HCC cells through exosomal secretion. As a tumor suppressor, von Hippel–Lindau tumor suppressor (VHL) protein participates in mediating the ubiquitination and proteasome degradation of hypoxia inducible factor-1α (HIF-1α), inhibiting the development of HCC. Exosomal miR-23 suppresses the expression of VHL to upregulate HIF-1α, GLUT-1, vascular endothelial growth factor (VEGF) and subsequently triggers the proliferation, metastasis, 5-FU resistance and other malignant biological behaviors of tumor cells (104). The deubiquitinating enzyme ubiquitin specific peptidase 7 (USP7) is overexpressed in a variety of tumor tissues and is closely related to the poor prognosis of patients. Research by Zhang et al. (105) confirms the extremely high expression of circ-DB in serum exosomes and mature adipocytes-derived exosomes of HCC patients with high BFR. The exosomal circ-DB internalized by HCC cells can be used as a molecular sponge to absorb miR-34a endogenously, thereby

deinhibiting the downstream target USP7, which inhibits the ubiquitination of cyclin A2 protein to maintain its stability. Both of USP7 and cyclin A2 synergistically promote the proliferation and metastasis of HCC cells, reducing intracellular DNA damage.

Drug Resistance

Due to the lack of significant clinical symptoms in the early stage of HCC, most patients lose the chance of radical resection. The clinical application of anti-tumor related drugs such as sorafenib, adriamycin (ADM), 5-fluorouracil (5-FU), platinum-containing anti-cancer drugs, camptothecin and gemcitabine has become an important means to extend the survival of patients with advanced HCC (106–108). However, the acquisition of multidrug resistance in tumor cells directly antagonizes the efficacy of the drug and leads to poor prognosis of patients. Existing studies have confirmed that a variety of pathophysiological processes are involved in mediation of tumor cell resistance, including upregulation of drug efflux transporter expression, intracellular agents accumulation and redistribution, inactivation of apoptotic signaling pathways, enhanced DNA damage repair capabilities, acceleration of drug metabolism and cancer stem cells (CSCs) activation (109–111). However, more molecular events related to drug resistance need to be further studied.

The intravenous anesthetic Propofol can inhibit the proliferation of HCC cells by activating the high mobility group AT-hook 2 (HMGA2) and Wnt/β-catenin signaling pathways (112). Co-incubation of the Propofol treated HCC cell-derived exosomes (Propofol-exo) with untreated HCC cells can mediate the inhibition of proliferation, metastasis and invasion of the latter, as well as inducing apoptosis. The exogenous transfection of lncRNA H19 overexpression vector to Propofol-exo can inhibit the expression of miR-520a-3p in HCC cells, so as to activate the expression of the downstream target oncogene LIM domain kinase 1 (LIMK1) and destroy the antagonistic effect of Propofol on the malignant biological behaviors of tumor cells (113).

Zhang et al. (114) and Lou et al. (115) respectively demonstrate the negative correlation between the expression level of miR-199a-3p and cisplatin (DDP)/doxorubicin (Dox) resistance in HCC cells. Internalization of exosomal miR-199a-3p in drug-resistant HCC cells mediates the high drug sensitivity by inhibiting the mTOR pathway, which is manifested as a significant inhibition of proliferation and metastasis after DDP/Dox treatment, accompanied by an increase in apoptotic cell ratio. Meanwhile, exogenous injection of exosomal miR-199a-3p into rats bearing transplantable tumors significantly reduces the size of xenograft tumors and the number of lung metastatic nodules. The expression of miR-744 in Sorafenib drug-resistant cell-derived exosomes is extremely downregulated. Overexpressed miR-744 in drug-resistant cell-derived exosomes can further act as a mediator to induce the upregulation of miR-744 in normal tumor cells, thereby increasing the sensitivity of Sorafenib by inhibiting the protein expression of the downstream target paired box 2 (PAX2) (116). Research by Li et al. (117) reveals the inducing effect of glucose regulates protein 78 (GRP78) on HCC Sorafenib resistance. Through the effective internalization of exosomes in HCC cells, siGRP78 modified exosomes significantly antagonize the Sorafenib resistance of tumor cells. Combination therapy with Sorafenib can inhibit the invasion ability of drug-resistant cells and the degradation of extracellular matrix, reducing the number of liver metastatic nodules in nude mice and inhibiting the liver metastasis of HCC cells. MiR-32-5p is overexpressed in HCC drug-resistant tissues. Exosomes from drug-resistant cells transfer oncogenic miR to sensitive cells and activate the PI3K/Akt pathway by negatively regulating the expression of the downstream target phosphatase and tensin homolog (PTEN), which induces VEGFA-mediated angiogenesis and increases microvessel density in the TME, mediating the multi-drug resistance of HCC (5-FU, OXA, GEM, and Sorafenib) (118).

Immunologic Escape

The human immune system plays a dual role in tumor progression: On the one hand, it can suppress tumorigenesis through innate and acquired immunity; On the other hand, a large number of immune cells and cytokines recruited in TME mediate the formation of immunosuppressive microenvironment through transformation and modification of a highly plastic system, which leads to immune escape of tumor cells and promotes tumor progression (119). As a negative co-receptor on the surface of activated T cells and B cells, PD-1 induces T cell anergy by binding to its ligand PD-L1, thereby maintaining the balance between autoimmunity and immune tolerance (120–122). Tumor cells inhibit the cytotoxicity of CD8+ T cells through the highly expressed PD-L1 to mediate immune escape.

As a highly plastic functional heterogeneous cell group, macrophages play an important role in the construction of TME. Exogenous stimulation of the microenvironment mediates the polarization of macrophages into two different phenotypes: M1 macrophages trigger a rapid pro-inflammatory response and eliminate pathogens, exhibiting anti-tumor activity, while M2 macrophages promote tumor development due to the activities of anti-inflammation and tissue repair. The polarization from M1 to M2 phenotype has become a driving factor for cancer development. HCC cells deliver ectopic expressed lnc TUC339 to nearby macrophages through exosomes, and participate in the repolarization of macrophages from M1 to M2. The exogenous silencing of lnc TUC339 by siRNA not only induces the upregulation of the pro-inflammatory cytokines IL-1β, TNF-α and the costimulatory molecule CD86 in macrophages, realizing the reactivation of macrophages, but also induces macrophages from M2 repolarizes to M1, thereby activating its cytotoxic effect on tumor cells (123). The abnormal high-expression of related markers GRP78, ATF6, PERK, IRE1α confirms the occurrence of endoplasmic reticulum stress events in HCC. The upregulation of ER-related proteins is not only closely related to the poor overall survival and pathological scores of HCC patients, but also indicates the high infiltration of CD68+ macrophages in the TME. The internalization of HCC-derived exosomal miR-23a-3p by macrophages mediates the inhibition of PTEN expression, while upregulating AKT phosphorylation and PD-L1 expression subsequently. Further studies have confirmed that the co-culture of macrophages activated by exosomes with T cells downregulates the ratio of CD8+ T cells and inhibits the production of interleukin 2, as well as inducing T cell apoptosis (124).

As one of the main inhibitory receptors of NK cells, TIM-3 realizes the imbalance of anti-tumor immunity of NK cells by binding to

tumor cells or ligands in the microenvironment. Carried by exosomes to NK cells, the overexpressed circUHRF1 achieves the same trend expression with TIM-3 by competitively binding miR-449c-5p, mediating the downregulation of active NK cell ratio in the microenvironment and the low secretion of IFN-γ and TNF-α through the induction of TIM-3. In addition, clinical pathological studies indicate that the expression level of serum circUHRF1 is significantly negatively correlated with the number of NKG2D-positive cells. Patients with overexpressed circUHRF1 have shown obvious PD1 resistance and poor clinical prognosis (125). HCC patients after living donor liver transplantation (LDLT) still have a high risk of recurrence (3–18%), while the underlying predisposing factors are still unknown yet. Nakano (126) et al. separately extract serum and exosome-free serum from orthotopic liver cancer rat models and inject them into nude mice intravenously. The former serum shows high levels of AFP and overexpressed miR-92b in tumorigenic tissues, while the latter shows no abnormalities of ATP levels. ROC curve confirms that the serum miR-92b level of patients after ADLT has an ideal predictability for the early (AUC = 0.925) and late (AUC = 0.761) recurrence of HCC. Mechanically, serum CD69 is not only involved in lymphocyte proliferation induction and signal transduction as one of the surface antigens of activated T cells, but also participates in NK cell-mediated cytotoxicity as an important mediator. The overexpressed miR-92b in HCC-derived exosomes actively infiltrates NK cells in the tumor microenvironment, participating in the inhibition of CD69 expression and antagonizing the cytotoxic effects of NK cells on HCC, thereby inducing immune escape of tumor cells. In summary, the regulatory effect of exosomal ncRNAs on HCC is shown in **Figure 2**.

EXOSOMAL NCRNAS AS EARLY DIAGNOSTIC BIOMARKERS

Ultrasound, as the preferred test for surveillance of HCC, limited by operator dependency and diagnostic accuracy, exhibits unsatisfactory clinical results (127). Alpha-fetoprotein (AFP), the most commonly used serological test, failed to show good diagnostic efficacy in retrospective case-control studies (Sensitivities: 60%, Specificities: 80%) (128, 129). Although the combined use of ultrasound and AFP can increase the detection rate, it may also increase false-positive suspicions and cost (130). Other tumor biomarkers, such as des-γ carboxyprothrombin, lectin-bound AFP, glypican 3, Golgi protein 73, and Dickkopf 1, also fail to effectively improve the accuracy of diagnosis (128, 129, 131, 132). Therefore, there is an urgent need for reliable inspection methods for early HCC diagnosis and tumor recurrence monitoring. The liquid biopsy technology applied to the analysis of human non-solid biological tissue samples (such as blood, cancerous ascites, feces, etc.) has received widespread attention in recent years (133). The collection of tumor genetic material in body fluids overcomes the invasive inconvenience of conventional biopsy and the limitations without being able to collect multiple times, providing an opportunity to systematically and dynamically tracking the evolution of the genome (134). As one of the cornerstones of liquid biopsy, exosomes have shown good diagnostic performance in growing HCC-related studies, which are expected to provide more detailed and personalized decisions for cancer management.

Cho et al. (135) comprehensively analyze the miR expression profiles of three different human liver cancer RNA sequencing datasets, and use logistic regression models to develop serum exo-miR panels. Four serum exo-miRs (miR-25-3p, miR-1269a, miR-4661-5p and miR-4746-5p) performed ideally in the test cohort (AUC >0.8). Noteworthily, serum exo-miR-4661-5p in all stages of HCC (AUC = 0.917), even early stage (AUC = 0.923), shows good diagnostic performance, whose accuracy is higher than other candidate serum exo-miRs and serum AFP. Furthermore, the exo-miR panel composed of exo-miR-4661-5p and exo-miR-4746-5p is considered to be the most accurate biomarker of early HCC (AUC = 0.947). The S fragment of RN7SL1 is enriched in HCC exosomes, with significantly higher expression level than that in the healthy donor group. ROC curve confirms that compared to the full-length transcript of RN7SL1 (AUC = 0.75), the S fragment of serum RN7SL1 is a better diagnostic marker for HCC (AUC = 0.87) (136). Ghosh et al. (137) validate that the expression level of miR-21-5p/miR-10b-5p/miR-221-3p/miR-223-3p in serum exosomes of HCC patients are significantly higher than that in patients with chronic hepatitis. The combination of miR-21-5p+miR-10b-5p+miR-221-3p+miR-223-3p can be used to distinguish HCC from chronic hepatitis and chronic hepatitis + liver cirrhosis (AUC = 0.86). Meanwhile, miR-10b-5p+miR-221-3p+miR-223-3p shows better efficacy in distinguishing low AFP-HCC from non-HCC hepatitis or liver cirrhosis patients compared to the combination of the four miRNAs (AUC = 0.84). Eight exosomal miRNAs (miR-122, miR-125b, miR-145, miR-192, miR-194, miR-29a, miR-17-5p and miR-106a) are overexpressed in the serum of HCC patients, ROC curve analysis confirms that the above exosomal miRNAs are potential biomarkers for distinguishing HCC patients from healthy controls (AUC = 0.535–0.850) (138). The expression of exosomal miR-212 in the serum of patients with chronic hepatitis B, liver cirrhosis and stage II/III HBV-HCC/Non-HBV-HCC are all significantly upregulated. Compared with AFP and CA125, miR-212 has a more significant correlation with Child-Pugh Classification, MELD score and MELD score, as well as associated with the progression of hepatitis B-related liver cancer, esophageal varices, ascites, and liver cirrhosis progress associated with HBV infection. The diagnostic value of miR-212 for HBV-HCC (AUC = 0.886) is higher than that of AFP (AUC = 0.849) and CA125 (AUC = 0.780), but for Non-HBV-HCC. The diagnostic value of miR-212 (AUC = 0.793) is slightly lower than AFP (AUC = 0.849) and higher than CA125 (AUC = 0.777) (139). Research by Huang et al. (140) reveals that serum exosomal lnc85 is highly expressed in both AFP-positive and negative HCC patients, and can distinguish AFP-negative HCC patients from healthy controls and liver cirrhosis patients (AUC = 0.869). The expression levels of miR-122, miR-148a and miR-1246 in HCC serum exosomes are higher than those in the liver cirrhosis and normal control groups, but fail to show significant differences compared with the chronic hepatitis group. MiR-148a

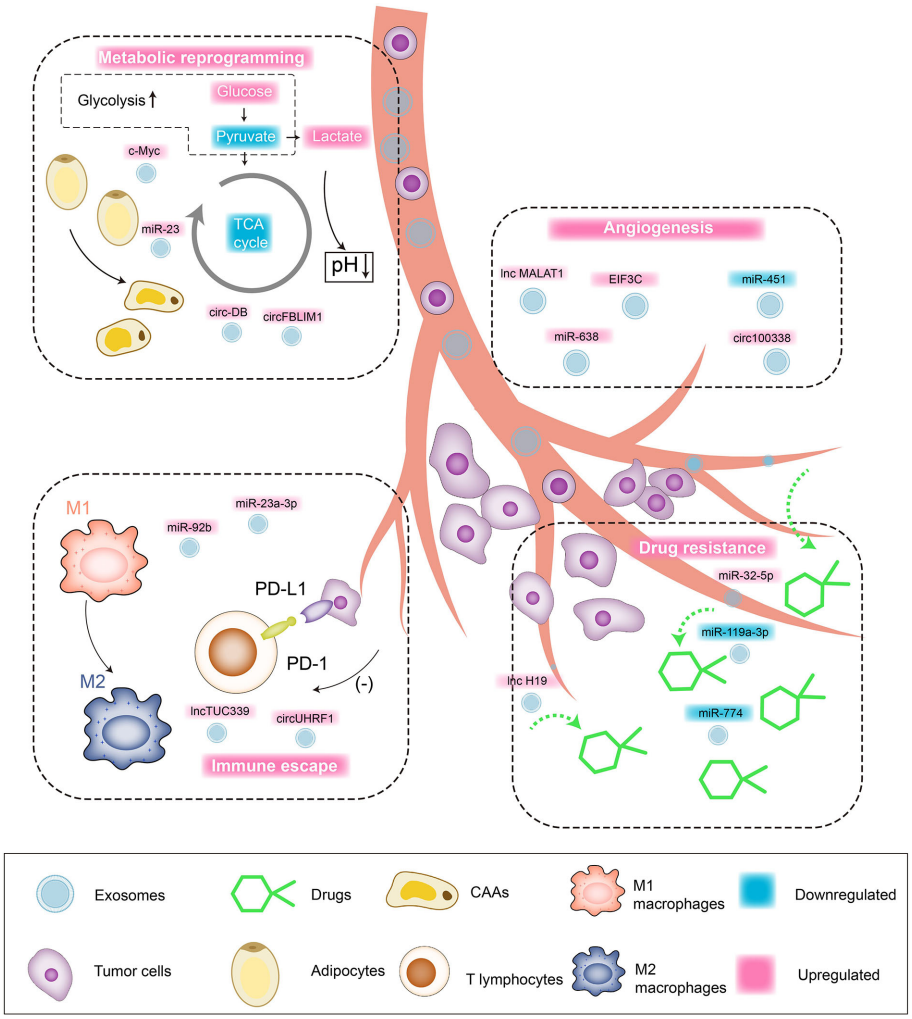

FIGURE 2 | Interaction network between exosomal ncRNAs and tumor microenvironment of HCC. Tumor cell/non-tumor cell-derived exosomes regulate the malignant biological behaviors of HCC through targeted cargo transportation. 1) Angiogenesis: upregulated lnc MALAT1, miR-638, EIF3C, circ100338 promote the angiogenesis in tumor microenvironment and HCC cell proliferation/blood-metastasis. 2) Drug resistance: upregulated miR-32-5p and lnc H19 are involved in mediating the drug resistance of HCC cells. 3) Metabolic reprogramming: upregulated c-Myc and circFBLIM1 induce aerobic glycolysis (Warburg Effect) of HCC cells. Upregulated miR-23 and circ-DB promote the transformation of fat cells into tumor-associated tumor cells (CAAs). 4) Immune escape: upregulated lnc TUC339 induces the repolarization of macrophages from M1 to M2, and the upregulation of miR-23a-3p can promote PD-L1/PD1 binding and induce T cell apoptosis.

shows good efficacy in identifying early HCC and liver cirrhosis (AUC = 0.891), which is significantly better than AFP (AUC = 0.712), and the combination of miR-122, miR-148a and AFP can further increase AUC to 0.931. Additionally, miR-122 is ideal for distinguishing HCC and NC (AUC = 0.990) (141). The multiple serum exosomal ncRNAs will undoubtedly open up a broad prospect for the clinical application of exosome-based liquid biopsy technology in the early diagnosis of HCC.

THERAPEUTIC FUNCTIONS OF EXOSOMAL NCRNAS ON HCC

Due to the lack of obvious clinical symptoms in the early stage and the high diagnosis rate at advanced stage, surgical resection and liver transplantation have become the main treatment methods for HCC (142). NcRNAs can shuttle between tissue cells with exosomes, regulating the biological behavior of recipient cells through intercellular communication. Abounding ncRNAs can be used as tumor suppressor regulators to participate in the rate-limiting step of tumor development. The targeted delivery of therapeutic ncRNAs carried by exosomes to tumor cells mediates its growth inhibition and achieves personalized treatment of different tumor cells (143).

As one of the key sources of adult stem cells, mesenchymal stem cells (MSCs) have become the ideal seed cells for tissue engineering due to self-renewal, multi-differentiation potential and low immunogenicity (144, 145). In addition, the high secretion properties of exosomes make MSCs a good place to cultivate therapeutic exosomal ncRNAs (146). MSCs-derived exosomes

pass through the blood tissue barrier due to the small size and are easily absorbed by tissue cells (147). They induce HCC cell apoptosis and cell cycle arrest *in vitro* and *in vivo* respectively (148), increasing the TME/systemic circulating NK cell ratio (149) to limit tumor progression. Cancer stem cells (CSCs) may be derived from the malignant transformation of tissue colonized stem cells (NSCs) (150). Exosomes secreted by CSCs are important mediators of chemotherapy resistance and tumor metastasis. The lncRNA H19 derived from CD90+CSC exosomes can induce angiogenesis, which limits the efficacy of anti-angiogenic therapy in HCC (151). In addition, CSCs-derived exosomes effectively increase the levels of serum tumor markers (AFP and GGT) and liver enzymes (ALT, AST and ALP) in DEN-induced HCC rats, as well as increasing the number of metastatic of cancer nodules. Meanwhile, CSCs-derived exosomes also significantly inhibit apoptosis, inducing angiogenesis, metastasis, invasion and EMT of HCC cells. MiR-21, lnc Tuc339, lnc HEIH and lnc HOTAIR are extremely upregulated in HCC exosomes affected by CSCs exosomes, while miR122, miR148a, miR16, and miR125b exhibit significant downregulation effect. Interestingly, MSC-derived exosomes reverse the above-mentioned effects and exhibit significant anti-tumor ability (152). The downregulation of miR-451a in HCC tissues indicates poor prognosis, and is closely related to malignant biological behaviors such as larger tumor diameter, no tumor capsule, advanced TNM stage, high differentiation and portal vein injury. Being transfected with an overexpression vector, miR-451a highly expressed in MSCs can be carried to HCC cells along with exosomes, inhibiting the paclitaxel resistance, proliferation, metastasis and EMT of tumor cells by negatively regulating the expression of ADAM metallopeptidase domain 10 (ADAM10) (153).

Oncogenic ncRNAs carried by tumor cell-derived exosomes (TDEs) can mediate their malignant biological behaviors through the internalization of different receptor cells. The suppression of TDEs dissemination from the primary tumor has become an important challenge in the treatment of cancer (154–156). Although therapeutic agents that block RAB family proteins, SNARE family proteins or p53 can reduce the secretion of TDEs (157, 158), the inhibitory effect on the secretion of exosomes in non-target tissues can also impair normal physiological functions (159). Liang et al. (160) prepare DC/CS-NP nanoparticles that can effectively encapsulate siRNA by thin-film hydration, which can rely on their own lipid bilayer structure to avoid siRNA degradation in the circulating or endosomal environment and ensure siRNA release at the targeted location. As a representative oncogenic exosomal miRNA, miRNA-21 is significantly upregulated in HCC cells. DC/CS NPs carrying Sphk2 siRNA induces miRNA-21 assembly to decrease in exosomes by inhibiting the expression of the cargo molecule packaging protein S1P, thereby destroying the carcinogenic efficacy of TDEs and avoiding the canceration of normal cells. Osteopontin (OPN), an important cell cancer assessment marker, shows no upregulation in the DC/CS-siSphk2 NPs treatment group, demonstrating the satisfying targeted therapeutic ability of nanoparticle.

The aerobic glycolysis of cancer cells (Warburg Effect) induces the acidification of the TME (161). Combined with abnormal blood perfusion and local hypoxia of tumors, a pH gradient is generated from the area inside the tumor to the normal tissues adjacent to the cancer, creating an ideal breeding ground for the metastasis of tumor cells (162, 163). Acidic conditions induce the upregulation of HIF-1α and HIF-2α in HCC cells, which bind to the miR-21 and miR-10b promoter regions to activate the transcription. The overexpressed miR-21 and miR-10b in HCC-derived exosomes induce metastasis, invasion and EMT of adjacent cells in a paracrine manner. Tian et al. (164) develop a nano-drug targeting exosomal miR-21 and miR-10b based on the PDCM system, and demonstrate obvious tumor growth inhibitory effects *in vivo*, effectively reducing the number of lung metastatic nodules. The low pH environment is conducive to the release of exosomes and the uptake of receptor cells (165). The neoplastic vacuolar H+ATPase (V-ATPases) overexpressed in cancer cells is very analogous with the H+/K+ATPase in parietal cells, which can rely on ATP to achieve H+ transport (166). The proton pump inhibitor pantoprazole effectively improves the liver function (ALT, albumin, T bilirubin, D bilirubin and AFP) in rats with precancerous lesions and the microstructure characteristics of the liver, reducing the exosomal abundance in the HCC tissues and serum of the rat liver. Meanwhile, pantoprazole also downregulates the serum exosomal RAB11A mRNA and lncRNA RP11-513I15.6, while upregulating exosomal miRNA-1262 in a dose-dependent manner (167).

Radiofrequency ablation (RFA) is one of the ideal treatments for advanced liver cancer besides surgical resection. However, many studies suggest that it is difficult for patients with liver cancer to achieve adequate ablation (168). Insufficient ablation area (169), heat loss of the tumor through blood vessels (170), or low temperature area in large tumors during ablation (171) may all be the inducing factors for insufficient ablation. The high recurrence and metastasis of residual tumors after RFA deficiency have always been a research hotspot in the academic field. Ma et al. (172) use heat-treated HCC cells to simulate the RFA environment. Studies confirm that heat-treated cells-derived exosomes mediate the upregulation of MYC expression in normal HCC cells, which bind to the ASMTL-AS1 promoter and positively activate its transcription. ASMTL-AS1 plays a role of carcinogen: As the disease stage progresses, ASMTL-AS1 in serum exosomes of HCC patients shows an increasing trend with further increasing after RFA; clinicopathological studies have confirmed that the expression level of ASMTL-AS1 is closely related to tumor volume, distant metastasis, and TNM staging. Meanwhile patients with highly expressed ASMTL-AS1 have significantly poor clinical prognosis. In terms of mechanism, as an endogenous molecular sponge, ASMTL-AS1 targets miR-342-3p and upregulates the expression level of downstream target nemo like kinase (NLK). Highly expressed NLK activates the malignant biological phenotypes of HCC cells by mediating Ser128 phosphorylation of Yes1 associated transcriptional regulator (YAP) and nuclear translocation, which are manifested in the promotion of proliferation, metastasis, invasion and the occurrence of EMT. The above studies reveal that the MYC/ASMTL-AS1/miR-342-3p/NLK/YAP regulatory axis plays a crucial role in mediating the malignant biological behaviors

of tumor cells after RFA deficiency, which indicates that the combination of targeted therapy against molecular targets can provide support for the prognosis of patients after RFA. The above and other therapeutic ncRNAs/drugs and related targets are summarized in **Table 2**.

CONCLUSION AND PERSPECTIVES

As small EVs, multi-cell-derived exosomes build a communication bridge between tissue cells. Intercellular signal transduction through cargo transportation induces the physiological or pathophysiological processes of different recipient cells. NcRNAs, the most abundant biologically active substances in exosomes, are involved in regulating the complex interaction between HCC cells and TME, as well as mediating HCC development through certain specific methods (tumor angiogenesis, metabolic reprogramming, drug resistance and immune escape). Relevant research on its specific regulatory mechanism can provide potential targets for precision treatment of HCC. Meanwhile, liquid biopsy technology based on exosomal ncRNAs also provides a non-invasive and promising option for early diagnosis and prognostic evaluation of multiple malignant tumors. What is more noteworthy is that due to its unique advantages, exosomes have developed into natural vehicles for the targeted delivery of therapeutic biologically active substances, bringing the gospel for precise treatment and effective survival of patients with advanced HCC. Its advantages are as follows: 1) As natural carriers produced by endogenous cells, exosomes have high stability and low immunogenicity, which can establish good biocompatibility with the body's immune system, and have low toxic/side effects. 2) Exosomes can avoid the phagocytosis of macrophages, penetrating blood vessels to enter the extracellular matrix, exhibiting efficient substance delivery capabilities. 3) Exosomes can break through biological barriers such as the blood-brain barrier to treat a variety of refractory diseases. However, although exosomes exhibit unique advantages in the delivery of numerous substances, their potential safety issues and industrialization issues are still stumbling blocks hindering their clinical application: 1) There is still a lack of standardized exosome separation technology. In view of the variability of biological fluids and exosome abundance, it is necessary to adopt standardized exosome isolation methods to ensure a consistent and reproducible supply of exosomes. 2) The development of exosomal biomarkers such as RNAs lacks large-scale prospective studies to provide evidences that liquid biopsy can replace tumor tissue biopsy. 3) Exosomal preparations should be based on the premise of high quality, uniform properties and no other cell vesicle contamination, and a complete quality control system needs to be established to improve the safety of their biological applications. However, in order to meet the above challenges, researchers have developed some engineering methods for magnetic separation or biotin separation to simplify the separation steps involved in the preparation of exosomes. Meanwhile, with the progress of nanomedicine and material manufacturing methods, many technologies will be used to design exosomes according to the specific characteristics of individual diseases to realize their large-scale production and rapid separation. Engineered exosomes may be developed as smart drugs for clinical diagnosis and treatment in the near future. In summary, with the continuous advancement of basic research on exosomes and the continuous development of modern biotechnology, engineered exosomes will have broad

TABLE 2 | Therapeutic target of exosomal ncRNAs for HCC.

Therapeutic substances	Functions	Targets/Substrates	References
ncRNAs			
miR-451a	Inhibiting paclitaxel resistance, proliferation, metastasis and EMT of tumor cells, as well as inducing apoptosis and cell cycle arrest	ADAM10	(153)
miR-145	Inhibiting the proliferation and metastasis of HCC cells, antagonizing the growth rate of xenograft tumors and the number of lung metastases in nude mice	GOLM1/GSK-3b/MMPs	(47)
miR-125	Inhibiting the proliferation and sphere formation of HCC cells	CD90	(50)
lncRNA H19	Inducing HCC cell apoptosis, inhibiting angiogenesis, invasion, metastasis and EMT, as well as reducing serum markers (AFP and GGT) and liver enzyme levels (AFP and GGT) in HCC rats	miR-21, lnc Tuc339, lnc HEIH, lnc HOTAIRmiR122, miR148a, miR16, miR125b	(151)
SENP3-EIF4A1	Inhibiting the proliferation and metastasis of tumor cells, and reducing the volume and weight of xenograft tumors in nude mice	miR-9-5p/ZFP36	(36)
circ-0051443	Inhibiting the proliferation of HCC cells, mediating G0/G1 cell cycle arrest and apoptosis, as well as reducing the weight and volume of xenograft tumors in nude mice	miR-331-3p/BAK1	(57)
Drugs			
nano-drugbased on the PDCM system	Inhibiting the growth rate of xenograft tumors, reducing the number of lung metastatic nodules, and improving the acidic environment of tumor microenvironment through targeted inhibition of exosomal miR-21 and miR-10b secreted by HCC cells	Exosomal miR-21, miR-10b	(164)
Pantoprazole	Improving liver functions (ALT, albumin, T bilirubin, D bilirubin, and Alfa Fetoprotein AFP) and liver microstructure characteristics of precancerous lesion rats, and improving the acidic tumor microenvironment.	Exosomal RAB11A mRNA, lncRNA RP11-513I15.6, miRNA-1262	(167)
Sphk2 RNAi nanoparticles	Inducing a reduced packaging of miRNA-21 in exosomes by inhibiting the expression of packaging protein S1P, subsequently inhibiting the carcinogenic efficacy of TDEs and avoiding normal cell canceration.	Exosomal miRNA-21	(160)

application prospects in the field of tumor treatment and regenerative medicine in the future.

AUTHOR CONTRIBUTIONS

HX wrote the manuscript. YX, JY and YC revised and approved the manuscript. All authors contributed to the article and approved the submitted version.

FUNDING

This study was funded by Natural Science Foundation of China (81902431), China Postdoctoral Science Foundation (2019T120279, 2018M641849), Foundation of Key Laboratory of Myocardial Ischemia, Ministry of Education (KF201810), Heilongjiang Postdoctoral Science Foundation (LBH-Z18107), Outstanding Youth Project of Natural Science Foundation of Heilongjiang (YQ2019H007).

REFERENCES

1. Torre LA, Bray F, Siegel RL, Ferlay J, Lortet-Tieulent J, Jemal A. Global cancer statistics, 2012. *CA Cancer J Clin* (2015) 65(2):87–108. doi: 10.3322/caac.21262
2. Qu Z, Wu J, Wu J, Luo D, Jiang C, Ding Y. Exosomes derived from HCC cells induce sorafenib resistance in hepatocellular carcinoma both in vivo and in vitro. *J Exp Clin Cancer Res* (2016) 35(1):159. doi: 10.1186/s13046-016-0430-z
3. Grohmann M, Wiede F, Dodd GT, Gurzov EN, Ooi GJ, Butt T, et al. Obesity Drives STAT-1-Dependent NASH and STAT-3-Dependent HCC. *Cell* (2018) 175(5):1289–1306.e20. doi: 10.1016/j.cell.2018.09.053
4. El-Serag HB. Epidemiology of viral hepatitis and hepatocellular carcinoma. *Gastroenterology* (2012) 142(6):1264–73.e1. doi: 10.1053/j.gastro.2011.12.061
5. Dyson J, Jaques B, Chattopadyhay D, Lochan R, Graham J, Das D, et al. Hepatocellular cancer: the impact of obesity, type 2 diabetes and a multidisciplinary team. *J Hepatol* (2014) 60(1):110–7. doi: 10.1016/j.jhep.2013.08.011
6. Forner A, Reig M, Bruix J. Hepatocellular carcinoma. *Lancet* (2018) 391(10127):1301–14. doi: 10.1016/S0140-6736(18)30010-2
7. Bruix J, Reig M, Sherman M. Evidence-Based Diagnosis, Staging, and Treatment of Patients With Hepatocellular Carcinoma. *Gastroenterology* (2016) 150(4):835–53. doi: 10.1053/j.gastro.2015.12.041
8. Allemani C, Matsuda T, Di Carlo V, Harewood R, Matz M, Nikšić M, et al. Global surveillance of trends in cancer survival 2000-14 (CONCORD-3): analysis of individual records for 37 513 025 patients diagnosed with one of 18 cancers from 322 population-based registries in 71 countries. *Lancet* (2018) 391(10125):1023–75. doi: 10.1016/S0140-6736(17)33326-3
9. De Rubis G, Rajeev Krishnan S, Bebawy M. Liquid Biopsies in Cancer Diagnosis, Monitoring, and Prognosis. *Trends Pharmacol Sci* (2019) 40(3):172–86. doi: 10.1016/j.tips.2019.01.006
10. Théry C, Witwer KW, Aikawa E, Alcaraz MJ, Anderson JD, Andriantsitohaina R, et al. Minimal information for studies of extracellular vesicles 2018 (MISEV2018): a position statement of the International Society for Extracellular Vesicles and update of the MISEV2014 guidelines. *Extracell Vesicles* (2018) 7(1):1535750. doi: 10.1080/20013078.2018.1535750
11. Ruivo CF, Adem B, Silva M, Melo SA. The Biology of Cancer Exosomes: Insights and New Perspectives. *Cancer Res* (2017) 77(23):6480–8. doi: 10.1158/0008-5472.CAN-17-0994
12. Kalra H, Simpson RJ, Ji H, Aikawa E, Altevogt P, Askenase P, et al. Vesiclepedia: a compendium for extracellular vesicles with continuous community annotation. *PloS Biol* (2012) 10(12):e1001450. doi: 10.1371/journal.pbio.1001450
13. Jabbari N, Akbariazar E, Feqhhi M, Rahbarghazi R, Rezaie J. Breast cancer-derived exosomes: Tumor progression and therapeutic agents. *J Cell Physiol* (2020) 235(10):6345–56. doi: 10.1002/jcp.29668
14. Jabbari N, Karimipour M, Khaksar M, Akbariazar E, Heidarzadeh M, Mojarad B, et al. Tumor-derived extracellular vesicles: insights into bystander effects of exosomes after irradiation. *Lasers Med Sci* (2020) 35(3):531–45. doi: 10.1007/s10103-019-02880-8
15. Ahmadi M, Rezaie J. Tumor cells derived-exosomes as angiogenenic agents: possible therapeutic implications. *J Transl Med* (2020) 18(1):249. doi: 10.1186/s12967-020-02426-5
16. Melo SA, Luecke LB, Kahlert C, Fernandez AF, Gammon ST, Kaye J, et al. Glypican-1 identifies cancer exosomes and detects early pancreatic cancer. *Nature* (2015) 523(7559):177–82. doi: 10.1038/nature14581
17. Manier S, Liu CJ, Avet-Loiseau H, Park J, Shi J, Campigotto F, et al. Prognostic role of circulating exosomal miRNAs in multiple myeloma. *Blood* (2017) 129(17):2429–36. doi: 10.1182/blood-2016-09-742296
18. Chen G, Huang AC, Zhang W, Zhang G, Wu M, Xu W, et al. Exosomal PD-L1 contributes to immunosuppression and is associated with anti-PD-1 response. *Nature* (2018) 560(7718):382–6. doi: 10.1038/s41586-018-0392-8
19. Holoch D, Moazed D. RNA-mediated epigenetic regulation of gene expression. *Nat Rev Genet* (2015) 16(2):71–84. doi: 10.1038/nrg3863
20. Fan Q, Yang L, Zhang X, Peng X, Wei S, Su D, et al. The emerging role of exosome-derived non-coding RNAs in cancer biology. *Cancer Lett* (2018) 414:107–15. doi: 10.1016/j.canlet.2017.10.040
21. Wang H, Hou L, Li A, Duan Y, Gao H, Song X. Expression of serum exosomal microRNA-21 in human hepatocellular carcinoma. *BioMed Res Int* (2014) 2014:864894. doi: 10.1155/2014/864894
22. Zhang C, Yang X, Qi Q, Gao Y, Wei Q, Han S. lncRNA-HEIH in serum and exosomes as a potential biomarker in the HCV-related hepatocellular carcinoma. *Cancer Biomark* (2018) 21(3):651–9. doi: 10.3233/CBM-170727
23. Théry C, Zitvogel L, Amigorena S. Exosomes: composition, biogenesis and function. *Nat Rev Immunol* (2002) 2(8):569–79. doi: 10.1038/nri855
24. van Niel G, D'Angelo G, Raposo G. Shedding light on the cell biology of extracellular vesicles. *Nat Rev Mol Cell Biol* (2018) 19(4):213–28. doi: 10.1038/nrm.2017.125
25. Johnstone RM, Adam M, Hammond JR, Orr L, Turbide C. Vesicle formation during reticulocyte maturation. Association of plasma membrane activities with released vesicles (exosomes). *J Biol Chem* (1987) 262(19):9412–20. doi: 10.1016/S0021-9258(18)48095-7
26. Shao H, Im H, Castro CM, Breakefield X, Weissleder R, Lee H. New Technologies for Analysis of Extracellular Vesicles. *Chem Rev* (2018) 118(4):1917–50. doi: 10.1021/acs.chemrev.7b00534
27. Andaloussi S EL, Mäger I, Breakefield XO, Wood MJ. Extracellular vesicles: biology and emerging therapeutic opportunities. *Nat Rev Drug Discovery* (2013) 12(5):347–57. doi: 10.1038/nrd3978
28. Frühbeis C, Kuo-Elsner WP, Müller C, Barth K, Peris L, Tenzer S, et al. Oligodendrocytes support axonal transport and maintenance via exosome secretion. *PloS Biol* (2020) 18(12):e3000621. doi: 10.1371/journal.pbio.3000621
29. Lai TC, Lee TL, Chang YC, Chen YC, Lin SR, Lin SW, et al. MicroRNA-221/222 Mediates ADSC-Exosome-Induced Cardioprotection Against Ischemia/Reperfusion by Targeting PUMA and ETS-1. *Front Cell Dev Biol* (2020) 8:569150:569150. doi: 10.3389/fcell.2020.569150
30. Sha L, Ma D, Chen C. Exosome-mediated Hic-5 regulates proliferation and apoptosis of osteosarcoma via Wnt/β-catenin signal pathway. *Aging (Albany NY)* (2020) 12(23):23598–608. doi: 10.18632/aging.103546
31. Syn NL, Wang L, Chow EK, Lim CT, Goh BC. Exosomes in Cancer Nanomedicine and Immunotherapy: Prospects and Challenges. *Trends Biotechnol* (2017) 35(7):665–76. doi: 10.1016/j.tibtech.2017.03.004
32. Farooqi AA, Desai NN, Qureshi MZ, Librelotto DRN, Gasparri ML, Bishayee A, et al. Exosome biogenesis, bioactivities and functions as new delivery systems of natural compounds. *Biotechnol Adv* (2018) 36(1):328–34. doi: 10.1016/j.biotechadv.2017.12.010

33. Maia J, Caja S, Strano Moraes MC, Couto N, Costa-Silva B. Exosome-Based Cell-Cell Communication in the Tumor Microenvironment. *Front Cell Dev Biol* (2018) 6:18. doi: 10.3389/fcell.2018.00018
34. Shi X, Cheng Q, Hou T, Han M, Smbatyan G, Lang JE, et al. Genetically Engineered Cell-Derived Nanoparticles for Targeted Breast Cancer Immunotherapy. *Mol Ther* (2020) 28(2):536–47. doi: 10.1016/j.ymthe.2019.11.020
35. Munoz JL, Bliss SA, Greco SJ, Ramkissoon SH, Ligon KL, Rameshwar P. Delivery of Functional Anti-miR-9 by Mesenchymal Stem Cell-derived Exosomes to Glioblastoma Multiforme Cells Conferred Chemosensitivity. *Mol Ther Nucleic Acids* (2013) 2(10):e126. doi: 10.1038/mtna.2013.60
36. Wang J, Pu J, Zhang Y, Yao T, Luo Z, Li W, et al. Exosome-transmitted long non-coding RNA SENP3-EIF4A1 suppresses the progression of hepatocellular carcinoma. *Aging (Albany NY)* (2020) 12(12):11550–67. doi: 10.18632/aging.103302
37. Yao Z, Jia C, Tai Y, Liang H, Zhong Z, Xiong Z, et al. Serum exosomal long noncoding RNAs lnc-FAM72D-3 and lnc-EPC1-4 as diagnostic biomarkers for hepatocellular carcinoma. *Aging (Albany NY)* (2020) 12(12):11843–63. doi: 10.18632/aging.103355
38. Cao SQ, Zheng H, Sun BC, Wang ZL, Liu T, Guo DH, et al. Long non-coding RNA highly up-regulated in liver cancer promotes exosome secretion. *World J Gastroenterol* (2019) 25(35):5283–99. doi: 10.3748/wjg.v25.i35.5283
39. He X, Yu J, Xiong L, Liu Y, Fan L, Li Y, et al. Exosomes derived from liver cancer cells reprogram biological behaviors of LO2 cells by transferring Linc-ROR. *Gene* (2019) 719:144044. doi: 10.1016/j.gene.2019.144044
40. Li B, Mao R, Liu C, Zhang W, Tang Y, Guo Z. LncRNA FAL1 promotes cell proliferation and migration by acting as a CeRNA of miR-1236 in hepatocellular carcinoma cells. *Life Sci* (2018) 197:122–9. doi: 10.1016/j.lfs.2018.02.006
41. Zhang T, Jing B, Bai Y, Zhang Y, Yu H. Circular RNA circTMEM45A Acts as the Sponge of MicroRNA-665 to Promote Hepatocellular Carcinoma Progression. *Mol Ther Nucleic Acids* (2020) 22:285–97. doi: 10.1016/j.omtn.2020.08.011
42. Li Y, Zang H, Zhang X, Huang G. Exosomal Circ-ZNF652 Promotes Cell Proliferation, Migration, Invasion and Glycolysis in Hepatocellular Carcinoma via miR-29a-3p/GUCD1 Axis. *Cancer Manag Res* (2020) 12:7739–51. doi: 10.2147/CMAR.S259424
43. Su Y, Lv X, Yin W, Zhou L, Hu Y, Zhou A, et al. CircRNA Cdr1as functions as a competitive endogenous RNA to promote hepatocellular carcinoma progression. *Aging (Albany NY)* (2019) 11(19):8182–203. doi: 10.18632/aging.102312
44. Wang G, Liu W, Zou Y, Wang G, Deng Y, Luo J, et al. Three isoforms of exosomal circPTGR1 promote hepatocellular carcinoma metastasis via the miR449a-MET pathway. *EBioMedicine* (2019) 40:432–45. doi: 10.1016/j.ebiom.2018.12.062
45. Sun JF, Zhang D, Gao CJ, Zhang YW, Dai QS. Exosome-Mediated MiR-155 Transfer Contributes to Hepatocellular Carcinoma Cell Proliferation by Targeting PTEN. *Med Sci Monit Basic Res* (2019) 25:218–28. doi: 10.12659/MSMBR.918134
46. Shi Y, Yang X, Xue X, Sun D, Cai P, Song Q, et al. HANR promotes lymphangiogenesis of hepatocellular carcinoma via secreting miR-296 exosome and regulating EAG1/VEGFA signaling in HDLEC cells. *J Cell Biochem* (2019) 120(10):17699–708. doi: 10.1002/jcb.29036
47. Gai X, Tang B, Liu F, Wu Y, Wang F, Jing Y, et al. mTOR/miR-145-regulated exosomal GOLM1 promotes hepatocellular carcinoma through augmented GSK-3β/MMPs. *J Genet Genomics* (2019) 46(5):235–45. doi: 10.1016/j.jgg.2019.03.013
48. Yang HD, Kim HS, Kim SY, Na MJ, Yang G, Eun JW, et al. HDAC6 Suppresses Let-7i-5p to Elicit TSP1/CD47-Mediated Anti-Tumorigenesis and Phagocytosis of Hepatocellular Carcinoma. *Hepatology* (2019) 70(4):1262–79. doi: 10.1002/hep.30657
49. Zhou Y, Ren H, Dai B, Li J, Shang L, Huang J, et al. Hepatocellular carcinoma-derived exosomal miRNA-21 contributes to tumor progression by converting hepatocyte stellate cells to cancer-associated fibroblasts. *J Exp Clin Cancer Res* (2018) 37(1):324. doi: 10.1186/s13046-018-0965-2
50. Wang Y, Wang B, Xiao S, Li Y, Chen Q. miR-125a/b inhibits tumor-associated macrophages mediated in cancer stem cells of hepatocellular carcinoma by targeting CD90. *J Cell Biochem* (2019) 120(3):3046–55. doi: 10.1002/jcb.27436
51. Xue X, Wang X, Zhao Y, Hu R, Qin L. Exosomal miR-93 promotes proliferation and invasion in hepatocellular carcinoma by directly inhibiting TIMP2/TP53INP1/CDKN1A. *Biochem Biophys Res Commun* (2018) 502(4):515–21. doi: 10.1016/j.bbrc.2018.05.208
52. Liu H, Chen W, Zhi X, Chen EJ, Wei T, Zhang J, et al. Tumor-derived exosomes promote tumor self-seeding in hepatocellular carcinoma by transferring miRNA-25-5p to enhance cell motility. *Oncogene* (2018) 37(36):4964–78. doi: 10.1038/s41388-018-0309-x
53. Fang JH, Zhang ZJ, Shang LR, Luo YW, Lin YF, Yuan Y, et al. Hepatoma cell-secreted exosomal microRNA-103 increases vascular permeability and promotes metastasis by targeting junction proteins. *Hepatology* (2018) 68(4):1459–75. doi: 10.1002/hep.29920
54. Fang T, Lv H, Lv G, Li T, Wang C, Han Q, et al. Tumor-derived exosomal miR-1247-3p induces cancer-associated fibroblast activation to foster lung metastasis of liver cancer. *Nat Commun* (2018) 9(1):191. doi: 10.1038/s41467-017-02583-0
55. ENCODE Project Consortium, Birney E, Stamatoyannopoulos JA, Dutta A, Guigó R, Gingeras TR, et al. Identification and analysis of functional elements in 1% of the human genome by the ENCODE pilot project. *Nature* (2007) 447(7146):799–816. doi: 10.1038/nature05874
56. Carninci P, Yasuda J, Hayashizaki Y. Multifaceted mammalian transcriptome. *Curr Opin Cell Biol* (2008) 20(3):274–80. doi: 10.1016/j.ceb.2008.03.008
57. Chen W, Quan Y, Fan S, Wang H, Liang J, Huang L, et al. Exosome-transmitted circular RNA hsa_circ_0051443 suppresses hepatocellular carcinoma progression. *Cancer Lett* (2020) 475:119–28. doi: 10.1016/j.canlet.2020.01.022
58. Yu Y, Min Z, Zhihang Z, Linhong M, Tao R, Yan L, et al. Hypoxia-induced exosomes promote hepatocellular carcinoma proliferation and metastasis via miR-1273f transfer. *Exp Cell Res* (2019) 385(1):111649. doi: 10.1016/j.yexcr.2019.111649
59. Duan L, Xu L, Xu X, Qin Z, Zhou X, Xiao Y, et al. Exosome-mediated delivery of gene vectors for gene therapy. *Nanoscale* (2021) 13(3):1387–97. doi: 10.1039/d0nr07622h
60. Plummer M, de Martel C, Vignat J, Ferlay J, Bray F, Franceschi S. Global burden of cancers attributable to infections in 2012: a synthetic analysis. *Lancet Glob Health* (2016) 4(9):e609–16. doi: 10.1016/S2214-109X(16)30143-7
61. Yang JD, Hainaut P, Gores GJ, Amadou A, Plymoth A, Roberts LR. A global view of hepatocellular carcinoma: trends, risk, prevention and management. *Nat Rev Gastroenterol Hepatol* (2019) 16(10):589–604. doi: 10.1038/s41575-019-0186-y
62. Ma C, Xu W, Yang Q, Liu W, Xiang Q, Chen J, et al. Osteopetrosis-Associated Transmembrane Protein 1 Recruits RNA Exosome To Restrict Hepatitis B Virus Replication. *J Virol* (2020) 94(11):e01800–19. doi: 10.1128/JVI.01800-19
63. Deng L, Gan X, Ito M, Chen M, Aly HH, Matsui C, et al. Peroxiredoxin 1, a Novel HBx-Interacting Protein, Interacts with Exosome Component 5 and Negatively Regulates Hepatitis B Virus (HBV) Propagation through Degradation of HBV RNA. *J Virol* (2019) 93(6):e02203–18. doi: 10.1128/JVI.02203-18
64. Shiromoto F, Aly HH, Kudo H, Watashi K, Murayama A, Watanabe N, et al. IL-1β/ATF3-mediated induction of Ski2 expression enhances hepatitis B virus x mRNA degradation. *Biochem Biophys Res Commun* (2018) 503(3):1854–60. doi: 10.1016/j.bbrc.2018.07.126
65. Thakuri BKC, Zhang J, Zhao J, Nguyen LN, Nguyen LNT, Schank M, et al. HCV-Associated Exosomes Upregulate RUNXOR and RUNX1 Expressions to Promote MDSC Expansion and Suppressive Functions through STAT3-miR124 Axis. *Cells* (2020) 9(12):2715. doi: 10.3390/cells9122715
66. Thakuri BKC, Zhang J, Zhao J, Nguyen LN, Nguyen LNT, Khanal S, et al. LncRNA HOTAIRM1 promotes MDSC expansion and suppressive functions through the HOXA1-miR124 axis during HCV infection. *Sci Rep* (2020) 10(1):22033. doi: 10.1038/s41598-020-78786-1
67. Wang L, Cao D, Wang L, Zhao J, Nguyen LN, Dang X, et al. HCV-associated exosomes promote myeloid-derived suppressor cell expansion via inhibiting

miR-124 to regulate T follicular cell differentiation and function. *Cell Discovery* (2018) 4:51. doi: 10.1038/s41421-018-0052-z
68. Kerbel RS. Tumor angiogenesis. *N Engl J Med* (2008) 358(19):2039–49. doi: 10.1056/NEJMra0706596
69. Baeriswyl V, Christofori G. The angiogenic switch in carcinogenesis. *Semin Cancer Biol* (2009) 19(5):329–37. doi: 10.1016/j.semcancer.2009.05.003
70. Ribatti D, Nico B, Crivellato E, Roccaro AM, Vacca A. The history of the angiogenic switch concept. *Leukemia* (2007) 21(1):44–52. doi: 10.1038/sj.leu.2404402
71. Ribatti D, Vacca A, Presta M. The discovery of angiogenic factors: a historical review. *Gen Pharmacol* (2000) 35(5):227–31. doi: 10.1016/s0306-3623(01)00112-4
72. Vermeulen PB, Gasparini G, Fox SB, Toi M, Martin L, McCulloch P, et al. Quantification of angiogenesis in solid human tumours: an international consensus on the methodology and criteria of evaluation. *Eur J Cancer* (1996) 32A(14):2474–84. doi: 10.1016/s0959-8049(96)00379-6
73. Hasan J, Byers R, Jayson GC. Intra-tumoural microvessel density in human solid tumours. *Br J Cancer* (2002) 86(10):1566–77. doi: 10.1038/sj.bjc.6600315
74. Leone P, Buonavoglia A, Fasano R, Solimando AG, De Re V, Cicco S, et al. Insights into the Regulation of Tumor Angiogenesis by Micro-RNAs. *J Clin Med* (2019) 8(12):2030. doi: 10.3390/jcm8122030
75. Galon J, Bruni D. Approaches to treat immune hot, altered and cold tumours with combination immunotherapies. *Nat Rev Drug Discovery* (2019) 18(3):197–218. doi: 10.1038/s41573-018-0007-y
76. Moserle L, Jiménez-Valerio G, Casanovas O. Antiangiogenic therapies: going beyond their limits. *Cancer Discovery* (2014) 4(1):31–41. doi: 10.1158/2159-8290.CD-13-0199
77. Argentiero A, Solimando AG, Krebs M, Leone P, Susca N, Brunetti O, et al. Anti-angiogenesis and Immunotherapy: Novel Paradigms to Envision Tailored Approaches in Renal Cell-Carcinoma. *J Clin Med* (2020) 9(5):1594. doi: 10.3390/jcm9051594
78. Sakariassen PØ, Prestegarden L, Wang J, Skaftnesmo KO, Mahesparan R, Molthoff C, et al. Angiogenesis-independent tumor growth mediated by stem-like cancer cells. *Proc Natl Acad Sci USA* (2006) 103(44):16466–71. doi: 10.1073/pnas.0607668103
79. Li Y, Zhang X, Zheng Q, Zhang Y, Ma Y, Zhu C, et al. YAP1 Inhibition in HUVECs Is Associated with Released Exosomes and Increased Hepatocarcinoma Invasion and Metastasis. *Mol Ther Nucleic Acids* (2020) 21:86–97. doi: 10.1016/j.omtn.2020.05.021
80. Lee HY, Chen CK, Ho CM, Lee SS, Chang CY, Chen KJ, et al. EIF3C-enhanced exosome secretion promotes angiogenesis and tumorigenesis of human hepatocellular carcinoma. *Oncotarget* (2018) 9(17):13193–205. doi: 10.18632/oncotarget.24149
81. Huang XY, Huang ZL, Huang J, Xu B, Huang XY, Xu YH, et al. Exosomal circRNA-100338 promotes hepatocellular carcinoma metastasis via enhancing invasiveness and angiogenesis. *J Exp Clin Cancer Res* (2020) 39(1):20. doi: 10.1186/s13046-020-1529-9
82. Yan K, Cheng W, Xu X, Cao G, Ji Z, Li Y. Circulating RNAs, circ_4911 and circ_4302, are novel regulators of endothelial cell function under a hepatocellular carcinoma microenvironment. *Oncol Rep* (2020) 44(4):1727–35. doi: 10.3892/or.2020.7702
83. Pu J, Wang J, Li W, Lu Y, Wu X, Long X, et al. hsa_circ_0000092 promotes hepatocellular carcinoma progression through up-regulating HN1 expression by binding to microRNA-338-3p. *J Cell Mol Med* (2020). doi: 10.1111/jcmm.15010
84. Yu YX, Ge TW, Zhang P. Circular RNA circGFRA1 promotes angiogenesis, cell proliferation and migration of hepatocellular carcinoma by combining with miR-149. *Eur Rev Med Pharmacol Sci* (2020) 24(21):11058–64. doi: 10.26355/eurrev_202011_23591
85. Hu ZQ, Zhou SL, Li J, Zhou ZJ, Wang PC, Xin HY, et al. Circular RNA Sequencing Identifies CircASAP1 as a Key Regulator in Hepatocellular Carcinoma Metastasis. *Hepatology* (2020) 72(3):906–22. doi: 10.1002/hep.31068
86. Zhao S, Li J, Zhang G, Wang Q, Wu C, Zhang Q, et al. Exosomal miR-451a Functions as a Tumor Suppressor in Hepatocellular Carcinoma by Targeting LPIN1. *Cell Physiol Biochem* (2019) 53(1):19–35. doi: 10.33594/000000118
87. Yang J, Li B, Zhao S, Du H, Du Y. Exosomal miR-638 Inhibits Hepatocellular Carcinoma Progression by Targeting SP1. *Onco Targets Ther* (2020) 13:6709–20. doi: 10.2147/OTT.S253151
88. Vander Heiden MG, Cantley LC, Thompson CB. Understanding the Warburg effect: the metabolic requirements of cell proliferation. *Science* (2009) 324(5930):1029–33. doi: 10.1126/science.1160809
89. Fantin VR, St-Pierre J, Leder P. Attenuation of LDH-A expression uncovers a link between glycolysis, mitochondrial physiology, and tumor maintenance. *Cancer Cell* (2006) 9(6):425–34. doi: 10.1016/j.ccr.2006.04.023
90. Altman BJ, Stine ZE, Dang CV. From Krebs to clinic: glutamine metabolism to cancer therapy. *Nat Rev Cancer* (2016) 16(11):749. doi: 10.1038/nrc.2016.114
91. DeBerardinis RJ, Mancuso A, Daikhin E, Nissim I, Yudkoff M, Wehrli S, et al. Beyond aerobic glycolysis: transformed cells can engage in glutamine metabolism that exceeds the requirement for protein and nucleotide synthesis. *Proc Natl Acad Sci USA* (2007) 104(49):19345–50. doi: 10.1073/pnas.0709747104
92. Held-Warmkessel J, Dell DD. Lactic acidosis in patients with cancer. *Clin J Oncol Nurs* (2014) 18(5):592–4. doi: 10.1188/14.CJON.592-594
93. Peppicelli S, Bianchini F, Calorini L. Extracellular acidity, a "reappreciated" trait of tumor environment driving malignancy: perspectives in diagnosis and therapy. *Cancer Metastasis Rev* (2014) 33(2-3):823–32. doi: 10.1007/s10555-014-9506-4
94. Shiraishi T, Verdone JE, Huang J, Kahlert UD, Hernandez JR, Torga G, et al. Glycolysis is the primary bioenergetic pathway for cell motility and cytoskeletal remodeling in human prostate and breast cancer cells. *Oncotarget* (2015) 6(1):130–43. doi: 10.18632/oncotarget.2766
95. Yu L, Kim J, Jiang L, Feng B, Ying Y, Ji KY, et al. MTR4 drives liver tumorigenesis by promoting cancer metabolic switch through alternative splicing. *Nat Commun* (2020) 11(1):708. doi: 10.1038/s41467-020-14437-3
96. Lai Z, Wei T, Li Q, Wang X, Zhang Y, Zhang S. Exosomal circFBLIM1 Promotes Hepatocellular Carcinoma Progression and Glycolysis by Regulating the miR-338/LRP6 Axis. *Cancer Biother Radiopharm* (2020). doi: 10.1089/cbr.2020.3564
97. Rinella ME. Nonalcoholic fatty liver disease: a systematic review. *JAMA* (2015) 313(22):2263–73. doi: 10.1001/jama.2015.5370
98. Manne V, Handa P, Kowdley KV. Pathophysiology of Nonalcoholic Fatty Liver Disease/Nonalcoholic Steatohepatitis. *Clin Liver Dis* (2018) 22(1):23–37. doi: 10.1016/j.cld.2017.08.007
99. Hefetz-Sela S, Scherer PE. Adipocytes: impact on tumor growth and potential sites for therapeutic intervention. *Pharmacol Ther* (2013) 138(2):197–210. doi: 10.1016/j.pharmthera.2013.01.008
100. Duong MN, Geneste A, Fallone F, Li X, Dumontet C, Muller C. The fat and the bad: Mature adipocytes, key actors in tumor progression and resistance. *Oncotarget* (2017) 8(34):57622–41. doi: 10.18632/oncotarget.18038
101. Sun K, Kusminski CM, Scherer PE. Adipose tissue remodeling and obesity. *J Clin Invest* (2011) 121(6):2094–101. doi: 10.1172/JCI45887
102. Fukumura D, Incio J, Shankaraiah RC, Jain RK. Obesity and Cancer: An Angiogenic and Inflammatory Link. *Microcirculation* (2016) 23(3):191–206. doi: 10.1111/micc.12270
103. Cao Y. Adipose tissue angiogenesis as a therapeutic target for obesity and metabolic diseases. *Nat Rev Drug Discovery* (2010) 9(2):107–15. doi: 10.1038/nrd3055
104. Liu Y, Tan J, Ou S, Chen J, Chen L. Adipose-derived exosomes deliver miR-23a/b to regulate tumor growth in hepatocellular cancer by targeting the VHL/HIF axis. *J Physiol Biochem* (2019) 75(3):391–401. doi: 10.1007/s13105-019-00692-6
105. Zhang H, Deng T, Ge S, Liu Y, Bai M, Zhu K, et al. Exosome circRNA secreted from adipocytes promotes the growth of hepatocellular carcinoma by targeting deubiquitination-related USP7. *Oncogene* (2019) 38(15):2844–59. doi: 10.1038/s41388-018-0619-z
106. Shen YC, Lin ZZ, Hsu CH, Hsu C, Shao YY, Cheng AL. Clinical trials in hepatocellular carcinoma: an update. *Liver Cancer* (2013) 2(3-4):345–64. doi: 10.1159/000343850
107. Grem JL. 5-Fluorouracil: forty-plus and still ticking. A review of its preclinical and clinical development. *Invest New Drugs* (2000) 18(4):299–313. doi: 10.1023/a:1006416410198
108. Kalyan A, Nimeiri H, Kulik L. Systemic therapy of hepatocellular carcinoma: current and promising. *Clin Liver Dis* (2015) 19(2):421–32. doi: 10.1016/j.cld.2015.01.009

109. Llovet JM, Villanueva A, Lachenmayer A, Finn RS. Advances in targeted therapies for hepatocellular carcinoma in the genomic era. *Nat Rev Clin Oncol* (2015) 12(7):408–24. doi: 10.1038/nrclinonc.2015.103
110. Butler EB, Zhao Y, Muñoz-Pinedo C, Lu J, Tan M. Stalling the engine of resistance: targeting cancer metabolism to overcome therapeutic resistance. *Cancer Res* (2013) 73(9):2709–17. doi: 10.1158/0008-5472.CAN-12-3009
111. Salehan MR, Morse HR. DNA damage repair and tolerance: a role in chemotherapeutic drug resistance. *Br J BioMed Sci* (2013) 70(1):31–40. doi: 10.1080/09674845.2013.11669927
112. Ou W, Lv J, Zou X, Yao Y, Wu J, Yang J, et al. Propofol inhibits hepatocellular carcinoma growth and invasion through the HMGA2-mediated Wnt/β-catenin pathway. *Exp Ther Med* (2017) 13(5):2501–6. doi: 10.3892/etm.2017.4253
113. Wang D, Xing N, Yang T, Liu J, Zhao H, He J, et al. Exosomal lncRNA H19 promotes the progression of hepatocellular carcinoma treated with Propofol via miR-520a-3p/LIMK1 axis. *Cancer Med* (2020) 9(19):7218–30. doi: 10.1002/cam4.3313
114. Zhang K, Shao CX, Zhu JD, Lv XL, Tu CY, Jiang C, et al. Exosomes function as nanoparticles to transfer miR-199a-3p to reverse chemoresistance to cisplatin in hepatocellular carcinoma. *Biosci Rep* (2020) 40(7): BSR20194026. doi: 10.1042/BSR20194026
115. Lou G, Chen L, Xia C, Wang W, Qi J, Li A, et al. MiR-199a-modified exosomes from adipose tissue-derived mesenchymal stem cells improve hepatocellular carcinoma chemosensitivity through mTOR pathway. *J Exp Clin Cancer Res* (2020) 39(1):4. doi: 10.1186/s13046-019-1512-5
116. Wang G, Zhao W, Wang H, Qiu G, Jiang Z, Wei G, et al. Exosomal MiR-744 Inhibits Proliferation and Sorafenib Chemoresistance in Hepatocellular Carcinoma by Targeting PAX2. *Med Sci Monit* (2019) 25:7209–17. doi: 10.12659/MSM.919219
117. Li H, Yang C, Shi Y, Zhao L. Exosomes derived from siRNA against GRP78 modified bone-marrow-derived mesenchymal stem cells suppress Sorafenib resistance in hepatocellular carcinoma. *J Nanobiotechnol* (2018) 16(1):103. doi: 10.1186/s12951-018-0429-z
118. Fu X, Liu M, Qu S, Ma J, Zhang Y, Shi T, et al. Exosomal microRNA-32-5p induces multidrug resistance in hepatocellular carcinoma via the PI3K/Akt pathway. *J Exp Clin Cancer Res* (2018) 37(1):52. doi: 10.1186/s13046-018-0677-7
119. Dunn GP, Old LJ, Schreiber RD. The three Es of cancer immunoediting. *Annu Rev Immunol* (2004) 22:329–60. doi: 10.1146/annurev.immunol.22.012703.104803
120. Freeman GJ, Long AJ, Iwai Y, Bourque K, Chernova T, Nishimura H, et al. Engagement of the PD-1 immunoinhibitory receptor by a novel B7 family member leads to negative regulation of lymphocyte activation. *J Exp Med* (2000) 192(7):1027–34. doi: 10.1084/jem.192.7.1027
121. Latchman Y, Wood CR, Chernova T, Chaudhary D, Borde M, Chernova I, et al. PD-L2 is a second ligand for PD-1 and inhibits T cell activation. *Nat Immunol* (2001) 2(3):261–8. doi: 10.1038/85330
122. Yang Y, Li CW, Chan LC, Wei Y, Hsu JM, Xia W, et al. Exosomal PD-L1 harbors active defense function to suppress T cell killing of breast cancer cells and promote tumor growth. *Cell Res* (2018) 28(8):862–4. doi: 10.1038/s41422-018-0060-4
123. Li X, Lei Y, Wu M, Li N. Regulation of Macrophage Activation and Polarization by HCC-Derived Exosomal lncRNA TUC339. *Int J Mol Sci* (2018) 19(10):2958. doi: 10.3390/ijms19102958
124. Liu J, Fan L, Yu H, Zhang J, He Y, Feng D, et al. Endoplasmic Reticulum Stress Causes Liver Cancer Cells to Release Exosomal miR-23a-3p and Up-regulate Programmed Death Ligand 1 Expression in Macrophages. *Hepatology* (2019) 70(1):241–58. doi: 10.1002/hep.30607
125. Zhang PF, Gao C, Huang XY, Lu JC, Guo XJ, Shi GM, et al. Cancer cell-derived exosomal circUHRF1 induces natural killer cell exhaustion and may cause resistance to anti-PD1 therapy in hepatocellular carcinoma. *Mol Cancer* (2020) 19(1):110. doi: 10.1186/s12943-020-01222-5
126. Nakano T, Chen IH, Wang CC, Chen PJ, Tseng HP, Huang KT, et al. Circulating exosomal miR-92b: Its role for cancer immunoediting and clinical value for prediction of posttransplant hepatocellular carcinoma recurrence. *Am J Transplant* (2019) 19(12):3250–62. doi: 10.1111/ajt.15490
127. Singal AG, Nehra M, Adams-Huet B, Yopp AC, Tiro JA, Marrero JA, et al. Detection of hepatocellular carcinoma at advanced stages among patients in the HALT-C trial: where did surveillance fail? *Am J Gastroenterol* (2013) 108 (3):425–32. doi: 10.1038/ajg.2012.449
128. Marrero JA, Feng Z, Wang Y, Nguyen MH, Befeler AS, Roberts LR, et al. Alpha-fetoprotein, des-gamma carboxyprothrombin, and lectin-bound alpha-fetoprotein in early hepatocellular carcinoma. *Gastroenterology* (2009) 137(1):110–8. doi: 10.1053/j.gastro.2009.04.005
129. Lok AS, Sterling RK, Everhart JE, Wright EC, Hoefs JC, Di Bisceglie AM, et al. Des-gamma-carboxy prothrombin and alpha-fetoprotein as biomarkers for the early detection of hepatocellular carcinoma. *Gastroenterology* (2010) 138(2):493–502. doi: 10.1053/j.gastro.2009.10.031
130. Singal A, Volk ML, Waljee A, Salgia R, Higgins P, Rogers MA, et al. Meta-analysis: surveillance with ultrasound for early-stage hepatocellular carcinoma in patients with cirrhosis. *Aliment Pharmacol Ther* (2009) 30 (1):37–47. doi: 10.1111/j.1365-2036.2009.04014.x
131. Capurro M, Wanless IR, Sherman M, Deboer G, Shi W, Miyoshi E, et al. Glypican-3: a novel serum and histochemical marker for hepatocellular carcinoma. *Gastroenterology* (2003) 125(1):89–97. doi: 10.1016/s0016-5085(03)00689-9
132. Shen Q, Fan J, Yang XR, Tan Y, Zhao W, Xu Y, et al. Serum DKK1 as a protein biomarker for the diagnosis of hepatocellular carcinoma: a large-scale, multicentre study. *Lancet Oncol* (2012) 13(8):817–26. doi: 10.1016/S1470-2045(12)70233-4
133. Corcoran RB, Chabner BA. Application of Cell-free DNA Analysis to Cancer Treatment. *N Engl J Med* (2018) 379(18):1754–65. doi: 10.1056/NEJMra1706174
134. Crowley E, Di Nicolantonio F, Loupakis F, Bardelli A. Liquid biopsy: monitoring cancer-genetics in the blood. *Nat Rev Clin Oncol* (2013) 10 (8):472–84. doi: 10.1038/nrclinonc.2013.110
135. Cho HJ, Baek GO, Seo CW, Ahn HR, Sung S, Son JA, et al. Exosomal microRNA-4661-5p-based serum panel as a potential diagnostic biomarker for early-stage hepatocellular carcinoma. *Cancer Med* (2020) 9(15):5459–72. doi: 10.1002/cam4.3230
136. Tan C, Cao J, Chen L, Xi X, Wang S, Zhu Y, et al. Noncoding RNAs Serve as Diagnosis and Prognosis Biomarkers for Hepatocellular Carcinoma. *Clin Chem* (2019) 65(7):905–15. doi: 10.1373/clinchem.2018.301150
137. Ghosh S, Bhowmik S, Majumdar S, Goswami A, Chakraborty J, Gupta S, et al. The exosome encapsulated microRNAs as circulating diagnostic marker for hepatocellular carcinoma with low alpha-fetoprotein. *Int J Cancer* (2020) 147(10):2934–47. doi: 10.1002/ijc.33111
138. Xue X, Zhao Y, Wang X, Qin L, Hu R. Development and validation of serum exosomal microRNAs as diagnostic and prognostic biomarkers for hepatocellular carcinoma. *J Cell Biochem* (2019) 120(1):135–42. doi: 10.1002/jcb.27165
139. Zhang Y, Xi H, Nie X, Zhang P, Lan N, Lu Y, et al. Assessment of miR-212 and Other Biomarkers in the Diagnosis and Treatment of HBV-infection-related Liver Diseases. *Curr Drug Metab* (2019) 20(10):785–98. doi: 10.2174/1389200220666191011120434
140. Huang X, Sun L, Wen S, Deng D, Wan F, He X, et al. RNA sequencing of plasma exosomes revealed novel functional long noncoding RNAs in hepatocellular carcinoma. *Cancer Sci* (2020) 111(9):3338–49. doi: 10.1111/cas.14516
141. Wang Y, Zhang C, Zhang P, Guo G, Jiang T, Zhao X, et al. Serum exosomal microRNAs combined with alpha-fetoprotein as diagnostic markers of hepatocellular carcinoma. *Cancer Med* (2018) 7(5):1670–9. doi: 10.1002/cam4.1390
142. Liu Y, Sun L, Gao F, Yang X, Li Y, Zhang Q, et al. A new scoring model predicting macroscopic vascular invasion of early-intermediate hepatocellular carcinoma. *Med (Baltimore)* (2018) 97(49):e13536. doi: 10.1097/MD.0000000000013536
143. Katakowski M, Buller B, Zheng X, Lu Y, Rogers T, Osobamiro O, et al. Exosomes from marrow stromal cells expressing miR-146b inhibit glioma growth. *Cancer Lett* (2013) 335(1):201–4. doi: 10.1016/j.canlet.2013.02.019
144. Uccelli A, Moretta L, Pistoia V. Mesenchymal stem cells in health and disease. *Nat Rev Immunol* (2008) 8(9):726–36. doi: 10.1038/nri2395
145. Aggarwal S, Pittenger MF. Human mesenchymal stem cells modulate allogeneic immune cell responses. *Blood* (2005) 105(4):1815–22. doi: 10.1182/blood-2004-04-1559
146. Yeo RW, Lai RC, Zhang B, Tan SS, Yin Y, Teh BJ, et al. Mesenchymal stem cell: an efficient mass producer of exosomes for drug delivery. *Adv Drug Delivery Rev* (2013) 65(3):336–41. doi: 10.1016/j.addr.2012.07.001
147. Katsuda T, Kosaka N, Takeshita F, Ochiya T. The therapeutic potential of mesenchymal stem cell-derived extracellular vesicles. *Proteomics* (2013) 13 (10-11):1637–53. doi: 10.1002/pmic.201200373

148. Bruno S, Collino F, Deregibus MC, Grange C, Tetta C, Camussi G. Microvesicles derived from human bone marrow mesenchymal stem cells inhibit tumor growth. *Stem Cells Dev* (2013) 22(5):758–71. doi: 10.1089/scd.2012.0304
149. Ko SF, Yip HK, Zhen YY, Lee CC, Lee CC, Huang CC, et al. Adipose-Derived Mesenchymal Stem Cell Exosomes Suppress Hepatocellular Carcinoma Growth in a Rat Model: Apparent Diffusion Coefficient, Natural Killer T-Cell Responses, and Histopathological Features. *Stem Cells Int* (2015) 2015:853506. doi: 10.1155/2015/853506
150. Wicha MS, Liu S, Dontu G. Cancer stem cells: an old idea–a paradigm shift. *Cancer Res* (2006) 66(4):1883–90. doi: 10.1158/0008-5472.CAN-05-3153 discussion 1895-6.
151. Conigliaro A, Costa V, Lo Dico A, Saieva L, Buccheri S, Dieli F, et al. CD90+ liver cancer cells modulate endothelial cell phenotype through the release of exosomes containing H19 lncRNA. *Mol Cancer* (2015) 14:155. doi: 10.1186/s12943-015-0426-x
152. Alzahrani FA, El-Magd MA, Abdelfattah-Hassan A, Saleh AA, Saadeldin IM, El-Shetry ES, et al. Potential Effect of Exosomes Derived from Cancer Stem Cells and MSCs on Progression of DEN-Induced HCC in Rats. *Stem Cells Int* (2018) 2018:8058979. doi: 10.1155/2018/8058979
153. Xu Y, Lai Y, Cao L, Li Y, Chen G, Chen L, et al. Human umbilical cord mesenchymal stem cells-derived exosomal microRNA-451a represses epithelial-mesenchymal transition of hepatocellular carcinoma cells by inhibiting ADAM10. *RNA Biol* (2020) 31:1–16. doi: 10.1080/15476286.2020.1851540
154. Antonyak MA, Li B, Boroughs LK, Johnson JL, Druso JE, Bryant KL, et al. Cancer cell-derived microvesicles induce transformation by transferring tissue transglutaminase and fibronectin to recipient cells. *Proc Natl Acad Sci USA* (2011) 108(12):4852–7. doi: 10.1073/pnas.1017667108
155. Balaj L, Lessard R, Dai L, Cho YJ, Pomeroy SL, Breakefield XO, et al. Tumour microvesicles contain retrotransposon elements and amplified oncogene sequences. *Nat Commun* (2011) 2:180. doi: 10.1038/ncomms1180
156. Tominaga N, Kosaka N, Ono M, Katsuda T, Yoshioka Y, Tamura K, et al. Brain metastatic cancer cells release microRNA-181c-containing extracellular vesicles capable of destructing blood-brain barrier. *Nat Commun* (2015) 6:6716. doi: 10.1038/ncomms7716
157. Bobrie A, Krumeich S, Reyal F, Recchi C, Moita LF, Seabra MC, et al. Rab27a supports exosome-dependent and -independent mechanisms that modify the tumor microenvironment and can promote tumor progression. *Cancer Res* (2012) 72(19):4920–30. doi: 10.1158/0008-5472.CAN-12-0925
158. Yu X, Harris SL, Levine AJ. The regulation of exosome secretion: a novel function of the p53 protein. *Cancer Res* (2006) 66(9):4795–801. doi: 10.1158/0008-5472.CAN-05-4579
159. Sung BH, Ketova T, Hoshino D, Zijlstra A, Weaver AM. Directional cell movement through tissues is controlled by exosome secretion. *Nat Commun* (2015) 6:7164. doi: 10.1038/ncomms8164
160. Liang J, Zhang X, He S, Miao Y, Wu N, Li J, et al. Sphk2 RNAi nanoparticles suppress tumor growth via downregulating cancer cell derived exosomal microRNA. *J Control Release* (2018) 286:348–57. doi: 10.1016/j.jconrel.2018.07.039
161. Amann T, Hellerbrand C. GLUT1 as a therapeutic target in hepatocellular carcinoma. *Expert Opin Ther Targets* (2009) 13(12):1411–27. doi: 10.1517/14728220903307509
162. Stock C, Schwab A. Protons make tumor cells move like clockwork. *Pflugers Arch* (2009) 458(5):981–92. doi: 10.1007/s00424-009-0677-8
163. Gatenby RA, Gawlinski ET, Gmitro AF, Kaylor B, Gillies RJ. Acid-mediated tumor invasion: a multidisciplinary study. *Cancer Res* (2006) 66(10):5216–23. doi: 10.1158/0008-5472.CAN-05-4193
164. Tian XP, Wang CY, Jin XH, Li M, Wang FW, Huang WJ, et al. Acidic Microenvironment Up-Regulates Exosomal miR-21 and miR-10b in Early-Stage Hepatocellular Carcinoma to Promote Cancer Cell Proliferation and Metastasis. *Theranostics* (2019) 9(7):1965–79. doi: 10.7150/thno.30958
165. Zhang X, Yuan X, Shi H, Wu L, Qian H, Xu W. Exosomes in cancer: small particle, big player. *J Hematol Oncol* (2015) 8:83. doi: 10.1186/s13045-015-0181-x
166. Forgac M. Vacuolar ATPases: rotary proton pumps in physiology and pathophysiology. *Nat Rev Mol Cell Biol* (2007) 8(11):917–29. doi: 10.1038/nrm2272
167. Matboli M, ElGwad AA, Hasanin AH, El-Tawdi A, Habib EK, Elmansy RA, et al. Pantoprazole attenuates tumorigenesis via inhibition of exosomal secretion in a rat model of hepatic precancerous lesion induced by diethylnitrosamine and 2-acetamidofluorene. *J Cell Biochem* (2019) 120(9):14946–59. doi: 10.1002/jcb.28757
168. Rajyaguru DJ, Borgert AJ, Smith AL, Thomes RM, Conway PD, Halfdanarson TR, et al. Radiofrequency Ablation Versus Stereotactic Body Radiotherapy for Localized Hepatocellular Carcinoma in Nonsurgically Managed Patients: Analysis of the National Cancer Database. *J Clin Oncol* (2018) 36(6):600–8. doi: 10.1200/JCO.2017.75.3228
169. Teng W, Liu KW, Lin CC, Jeng WJ, Chen WT, Sheen IS, et al. Insufficient ablative margin determined by early computed tomography may predict the recurrence of hepatocellular carcinoma after radiofrequency ablation. *Liver Cancer* (2015) 4(1):26–38. doi: 10.1159/000343877
170. Poch FG, Rieder C, Ballhausen H, Knappe V, Ritz JP, Gemeinhardt O, et al. The vascular cooling effect in hepatic multipolar radiofrequency ablation leads to incomplete ablation ex vivo. *Int J Hyperthermia* (2016) 32(7):749–56. doi: 10.1080/02656736.2016.1196395
171. Kim KW, Lee JM, Klotz E, Kim SJ, Kim SH, Kim JY, et al. Safety margin assessment after radiofrequency ablation of the liver using registration of preprocedure and postprocedure CT images. *AJR Am J Roentgenol* (2011) 196(5):W565–72. doi: 10.2214/AJR.10.5122
172. Ma D, Gao X, Liu Z, Lu X, Ju H, Zhang N. Exosome-transferred long non-coding RNA ASMTL-AS1 contributes to malignant phenotypes in residual hepatocellular carcinoma after insufficient radiofrequency ablation. *Cell Prolif* (2020) 53(9):e12795. doi: 10.1111/cpr.12795

Conflict of Interest: The authors declare that the research was conducted in the absence of any commercial or financial relationships that could be construed as a potential conflict of interest.

frontiers in Oncology

REVIEW
published: 12 April 2021
doi: 10.3389/fonc.2021.660712

Curcumin Regulates Cancer Progression: Focus on ncRNAs and Molecular Signaling Pathways

Haijun Wang[1,2], Ke Zhang[2], Jia Liu[2], Jie Yang[2], Yidan Tian[2], Chen Yang[2], Yushan Li[2], Minglong Shao[3], Wei Su[1] and Na Song[2,4]**

[1] Department of Pathology, Key Laboratory of Clinical Molecular Pathology, The First Affiliated Hospital of Xinxiang Medical University, Xinxiang, China, [2] School of Basic Medical Sciences, Xinxiang Medical University, Xinxiang, China, [3] Department of Mental Health, The Second Affiliated Hospital of Xinxiang Medical University, Xinxiang, China, [4] Institute of Precision Medicine, Xinxiang Medical University, Xinxiang, China

Curcumin [(1E,6E) -1,7-bis(4-hydroxy-3-methoxyphenyl) hepta-1,6-diene-3,5- dione] is a natural polyphenol derived from the rhizome of the turmeric plant *Curcuma longa*. Accumulated evidences have presented curcumin's function in terms of anti-inflammatory, antioxidant properties, and especially anti-tumor activities. Studies demonstrated that curcumin could exert anti-tumor activity *via* multiple biological signaling pathways, such as PI3K/Akt, JAK/STAT, MAPK, Wnt/β-catenin, p53, NF-κB and apoptosis related signaling pathways. Moreover, Curcumin can inhibit tumor proliferation, angiogenesis, epithelial-mesenchymal transition (EMT), invasion and metastasis by regulating tumor related non-coding RNA (ncRNA) expression. In this review, we summarized the roles of curcumin in regulating signaling pathways and ncRNAs in different kinds of cancers. We also discussed the regulatory effect of curcumin through inhibiting carcinogenic miRNA and up regulating tumor suppressive miRNA. Furthermore, we aim to illustrate the cross regulatory relationship between ncRNA and signaling pathways, further to get a better understanding of the anti-tumor mechanism of curcumin, thus lay a theoretical foundation for the clinical application of curcumin in the future.

Keywords: curcumin, cancer, ncRNA, miRNA, signaling pathway, review

OPEN ACCESS

Edited by:
Yue Hou,
Northeastern University, China

Reviewed by:
Jun Zhang,
The University of Texas Health Science Center at San Antonio, United States
Feilin Liu,
Mayo Clinic Florida, United States

****Correspondence:***
Na Song
sarah_song1986@163.com
Haijun Wang
wnavy200299@163.com

Specialty section:
This article was submitted to Pharmacology of Anti-Cancer Drugs, a section of the journal Frontiers in Oncology

Received: *29 January 2021*
Accepted: *24 March 2021*
Published: *12 April 2021*

Citation:
Wang H, Zhang K, Liu J, Yang J, Tian Y, Yang C, Li Y, Shao M, Su W and Song N (2021) Curcumin Regulates Cancer Progression: Focus on ncRNAs and Molecular Signaling Pathways. Front. Oncol. 11:660712. doi: 10.3389/fonc.2021.660712

INTRODUCTION

Malignant tumor is a tremendous threat to human health with high heterogeneity. Most cancer retain untreatable although the understanding of cancer on a molecular level has been improved in the past years. According to the latest data released by World Health Organization (WHO), the number of deaths due to malignant tumors is still increasing every year (1). In exploring the way to treat cancer, scientists have been constantly finding and developing new drugs to treat cancer, including chemotherapy, radiotherapy, targeted drugs, and immunotherapy, and so on. Accumulated studies have shown that some natural compounds have a good effect on anti-tumor therapy, which provides us an alternative way to treat and manage cancer.

Curcumin[(1E,6E)-1,7-bis(4-hydroxy-3-methoxyphenyl) hepta-1,6-diene-3,5-dione], an active component extracted from the rhizomes of *Curcuma longa* Linn (2), presents some favorable results in terms of anti-proliferation, anti-inflammation, anti-angiogenesis and anti-oxidation (3–8). Curcumin represents a promising phytochemicals in the field of anticancer to be used alone or combined with other drugs, which can affects multiple signaling pathways and molecular targets involved in cancer pathogenesis including NF-kB, MAPK, PTEN, p53, and ncRNA network (9).

A non-coding RNA (ncRNA) is a functional RNA molecule that is transcribed from DNA but not translated into proteins, which include microRNA (miRNA), small interfering RNA (siRNA), PIWI-interacting RNAs (piRNAs) and long noncoding RNAs (lncRNAs) (10–13). More and more studies have demonstrated that ncRNA plays an epigenetic regulatory role in the anti-cancer effect of curcumin, involving with histone modification, DNA methyltransferases, and regulation of microRNA (miRNA) expressions (14–18).

Although there have been reviews and talk about the role of curcumin in anti-tumor, it is mainly through explaining the regulation of curcumin in anti-tumor on related signal pathways, such as proliferation, invasion/migration, autophagy, apoptosis and other pathways (19–23), but there is no the relationship between ncRNA and pathway was clarified. In this review, we provide insights into the vital role and the signal pathways of curcumin in anti-cancer, and focus on the molecular mechanism of curcumin *via* ncRNA in regulating tumor development.

PI3K-AKT SIGNAL PATHWAY

The PI3K/AKT pathway is one of the major intracellular signaling pathways which has diverse downstream effects on basic intracellular functions, including cell proliferation, growth, apoptosis, epithelial-mesenchymal transition(ETM), metabolism and motility (24–26). The aberrant activation of the signaling pathway is often closely related to the occurrence and development of human cancers (27).

Studies show that miRNA-203,206 and miRNA-192-5p are very important tumor-inhibiting ncNRA. In a variety of tumors, they can inhibit tumor proliferation, invasion, migration, EMT, angiogenesis, *etc* (28–34). Curcumin could inhibit the cell proliferation and induce apoptosis of non-small cell lung cancer (NSCLC) cells *via* up-regulating the expression of miRNA-206/miRNA-192-5p and suppressing the PI3K/AKT/mTOR signaling pathway (35, 36). On the contrary, miR-206/miRNA-192-5p inhibitors could reverse the above results, following with the mTOR and Akt phosphorylation levels increase, which could promote cancer cell migration and invasion. Furthermore, miR-206/miRNA-192-5p mimics can also enhance curcumin inhibitory effect (37, 38). Curcumin might be a very effective agent for the treatment of NSCLC.

The most common genetic alteration activating PI3K is the genetic ablation of the tumor suppressor phosphatase and tensin homolog (PTEN), a negative regulator of PI3K-AKT signaling (39). miR-21 is one of the most frequently observed abnormal miRNAs in human cancers and is one of the first miRNAs described as oncogenic ncRNA (40–44). A large-scale miRNA analysis of 540 samples from six different types of solid tumors showed that miR-21 is the only up-regulated miRNA in all cancer types (45).

Curcumin can effectively repress the miR-21/PTEN/Akt molecular pathway to inhibit cell proliferation and induce apoptosis in gastric cancer cells. The p-Akt protein expression is negatively correlated with curcumin dose, with curcumin levels increase, PTEN expression increased and miR-21 levels decreased (46–48). Qiang et al.'s study showed that curcumin can play a synergistic role with other chemotherapy drugs. Curcumin could facilitate the apoptosis effect of PD98059, a potent and selective inhibitor of mitogen-activated protein kinase, *via* the miR-21/PTEN/Akt pathway (48). Diphenyl difluoroketone (EF24), curcumin analogue, function to enhance apoptosis by inhibiting miR-21 in DU145 human prostate cancer cells and B16 mouse melanoma cells (49).

Curcumin inhibits the proliferation of bladder cancer cells (50). Curcumin mediated the expression of miR-203 increase by inducing hypomethylation of miR-203 promoter. The target genes of miR-203, Akt2, Src, Jun, and Survivin, were repressed in mRNA and protein level, leading to proliferation decrease and apoptosis increase of bladder cancer cells.

Curcumin significantly enhanced the apoptosis of renal carcinoma Caki cells induced by dual PI3K/Akt and mTOR inhibitor NVP-BEZ235. Curcumin suppress Bcl-2 level and the stability of Mcl-1 protein with p53 dependent mode. It is noteworthy that NVP-BEZ235 alone has no effect on the death of human renal cell carcinoma Caki cells, but NVP-BEZ235 combined with curcumin contributed cell apoptosis significantly with Bcl-2 and Mcl-1 reduction (51).

JAK-STAT SIGNAL PATHWAY

Constitutive activation of the Janus kinase/signal transducers and activators of transcription (JAK/STAT) pathway was first recognized as being related with malignancy in the 1990's (52). JAK-STAT pathways can be activated and employed by diverse cytokines, growth factors, and related molecules, that in turn phosphorylates their targets STATs (53, 54). Activated STATs, as the form of dimerization, are translocated into the nucleus and initiated the gene transcription.

The effects of JAK/STAT signaling on tumor cell survival, proliferation and invasion have made the JAK/STAT pathway a hotspot target for tumor targeted therapy and drug development (55, 56). The expression of miR-99a has been studied in many human cancers. It has been reported to be down-regulated in several types of cancer, including non-small cell lung cancer (NSCLC), liver cancer, bladder cancer, *etc* (57–59). These findings indicate that miR-99a is widely down-regulated in human cancers, indicating the potential role of miR-99a as a tumor suppressor.

Curcumin can inhibit the proliferation, migration, invasion and promote apoptosis of retinoblastoma cells, which function

through up-regulating the miR-99a expression and then inhibiting JAK/STAT signaling pathway (60). In addition, curcumin can suppress the cell proliferation by down-regulations of cyclinD1 and up-regulations of p21 expression. In one of studies showed that curcumin could reduce the anti-apoptotic protein Bcl-2, enhance the pro-apoptotic protein Bax and cleaved-caspase-3/9 expression level, ultimately promoted the apoptosis of retinoblastoma cells. Furthermore, curcumin can synergistically enhance the anti-tumor activity of cisplatin on papillary thyroid cancer (PTC) cells and tumor stem cell like cells by inhibiting the activity of STAT3, suggesting that curcumin combined with chemotherapy drugs may play a better therapeutic effect *via* JAK/STAT signaling pathway (61).

WNT/β-CATENIN SIGNAL PATHWAY

Wnt/β-catenin signaling pathway, also called the canonical Wnt signaling pathway, is a highly conserved pathway in evolution. Activation of Wnt pathways can modulate cell proliferation, apoptosis, differentiation, migration, invasion, genetic stability, cell renewal. β-catenin is the core component of the cadherin complex and its stabilization is essential for the activation of Wnt/β-catenin signaling. T-cell factor/lymph enhancer factor-1 (TCF/LEF1) is a transcription complex that mediates the transcription of genes triggered by classic Wnt pathway. When the Wnt pathway is activated, β-catenin can bind to the TCF/LEF1 complex by translocating into the nucleus and bind to the target gene DNA to initiate the transcription of related genes, such as: cyclinD1, c-Myc, MMPs (62–66). Wnt/β-catenin plays a vital role in tumor occurrence and treatment response.

The anti-cancer effect of curcumin is released by inhibiting the Wnt/β-catenin pathway. In osteosarcoma, curcumin could promote the protein level of reversion-inducing cysteine-rich protein with kazal motifs (RECK) by reducing the expression of miR-21, further inhibited the Wnt pathway related proteins, such as: β-catenin, GSK-3β (67). Curcumin suppresses the NSCLC cell proliferation, migration, invasion and viability in a dose-dependent manner (68). Mechanistic analysis indicated that curcumin enhanced the expression level of miR−192−5p and decreased the expression of c−Myc. In addition, gene knockout miR-192-5p can rescue the curcumin-induced decrease of β-catenin, cyclin D1 and c-Myc expression levels. These findings indicate that the up-regulation of miR-192-5p, induced by curcumin, inhibits NSCLC cells with inactivation of Wnt/β-catenin signaling pathway and down-regulation of c-Myc transcription. Dou et al. documented that curcumin suppresses colon cancer by inhibiting Wnt/β-catenin pathway *via* down-regulating miR-130a, which may serve as a new target for colon cancer treatment (69).

As known, the lncRNA series (such as HOXA-AS2, HOTAIR and DANCR) function as oncogenes to promote cancer development and metastasis (70–72). Curcumin induced cell cycle arrest and apoptosis in hepatocellular carcinoma (HCC) by down-regulating lincROR which has been demonstrated to activate Wnt/β-catenin signaling (73). Shao et al. documented that curcumin may suppress cell proliferation of HCC cell line SMMC-7721, Huh-7, LO2 in a dose-dependent manner, the anti-proliferation effect of curcumin was partly caused by S phase arrest. The apoptosis rate of SMMC-7721 and Huh-7 cells with curcumin treatment was significantly higher than that in DMSO treatment group. Moreover, curcumin inhibits cell viability through lincROR/β-catenin regulatory pattern., Interestingly, the overexpression of lincROR partially reversed the inhibition of cell proliferation and rescue the inactivation of Wnt/β-catenin in curcumin-treated HCC cells (74). Liu et al. also found that curcumin suppressed the proliferation and tumorigenicity through a ceRNA effect of miR-145 and lncRNA-ROR in prostate cancer (75).

The cancer cells lose the characteristics of epithelial cells and acquire the mesenchymal phenotype, these changes are conducive to tumor cell invasion of surrounding tissues. The pathways associated with the EMT process have multiple signal cascades including the Wnt/β-catenin pathway. The curcumin analog EF24 shows effective anti-tumor activity by preventing the cell cycle and inducing cell apoptosis in melanoma (76). EF24 could inactivate the Wnt pathway *via* up-regulating the expression of miR-33b, which was able to inhibit EMT in melanoma cell lines through downregulation of the mesenchymal markers, Vimentin and N-cadherin. In addition, EF24 could decrease the phosphorylation of STAT3 and inhibit the HMGA2 expression, an oncological transcription factor, which promotes the proliferation of cancer cells and affect the progress of cell cycle in ovarian cancer cells and leukemia cells (77–79). In tamoxifen-resistant breast cancer cells, Curcumin attenuates lncRNA H19-induced epithelial-mesenchymal transition by the increase of N-cadherin and the decrease of E-cadherin (80).

MAPK SIGNAL PATHWAY

The mitogen-activated protein kinase (MAPK) cascade is a key signaling pathway that regulates various cellular processes (such as proliferation, differentiation, transformation, apoptosis and stress response) under normal and pathological conditions (81–84). Curcumin can inhibit proliferation and migration of human glioblastoma cells (85). miR-378 is considered to be a tumor suppressor miRNA, which has the ability to inhibit tumor cell proliferation, invasion and migration (86, 87). Li et al., proved that miR-378 is a downstream miRNA of glioblastoma multiforme, and it can enhance the inhibitory effect of curcumin on the growth of glioblastoma. Its inhibitory effect was enhanced in the stable U87 cells expressing miR-378 *in vitro* and *in vivo* compared with control cells. Moreover, it was found that curcumin can inhibit the expression of phosphorylated p38 at the protein level in U87 cells. miR-378 can counteract p38 inhibitory effect by increasing the phosphorylation of p38, further enhancing the sensitivity of cells to curcumin (85). Yu et al., showed that curcumin reduced the retinoblastoma cell viability and induced the apoptosis of Y79 cells through the activation of JNK and p38 MAPK pathways (88). Curcumin inhibits the growth and invasion of human monocytic leukemia SHI-1 cells *in vivo* by regulating MAPK and MMP signal transduction. The administration of curcumin significantly

inhibited tumor growth, which showed that the tumor weight significantly decreased from 0.67 g (control) to 0.47 g (15 mg/kg) and 0.35 g (30 mg/kg). Curcumin inhibits the expression of PCNA in tumor tissues, and increases the degree of TUNEL and the staining of cleaved caspase-3. Curcumin treatment can be involved in the downregulation of NF-κB and ERK signals, and simultaneously activate p38 and JNK. And curcumin would attenuate the expression levels of MMP2, MMP9 and vimentin to affect the EMT process (89). Curcumin has also been shown to inhibit the growth of human A549 lung adenocarcinoma cells and induce apoptosis with a dose-dependent manner. Treatment of A549 cells by curcumin causes the increase of cytosolic cytochrome c and loss of mitochondrial membrane potential. Curcumin-induced apoptosis was accompanied by alterations in intracellular oxidative stress-related enzymes, including decreased reactive oxygen species (ROS), malondialdehyde and 4-hydroxynonenal levels, increased superoxide dismutase (SOD), accompanied with the alteration of MAPK signaling pathway factors c-JNK, p38, ERK and apoptosis related protein, such as cleaved-caspase-3,9, Bcl-2, Bax, HSP70, and poly (ADP-ribose) polymerase (PARP) (90, 91). It may be owing to the biological activities of curcumin metabolites, which have cytotoxic effects represented by overhaul mutated DNA and remove free radicals, respectively (92, 93). Another study of NSCLC showed that curcumin strengthened the chemosensitivity of cisplatin the in A549 and H1703 cells *via* the downregulation of XRCC1. Breast cancer study revealed that the MAPK pathway mediated the down-regulation of EZH2, contributing to the anti-proliferative effects of curcumin against breast cancer (94). Taken together, curcumin exerts its anti-cancer role *via* MAPK signaling pathway in multiple types of cancer.

P53 SIGNAL PATHWAY

TP53 (p53), also described as the 'guardian of the genome', is the single most frequently altered gene in kinds of human cancers, the p53 mutations were observed in approximately 50% of all invasive tumors (95–98). p53 is a tumor suppressor gene involved in a variety of cellular mechanisms, including DNA repair, apoptosis, and cell cycle arrest. p53 mutations in breast cancer have been associated with lower survival rates and resistance to conventional therapies. Curcumin interferes with the proliferation of breast cancer by up-regulating pro-apoptotic proteins (such as p53 and Bax) and down-regulating anti-apoptotic proteins (such as MDM2 and Bcl-2). Studies showed that curcumin inhibited the proliferation of estrogen-receptor-positive MCF-7 human breast cancer cells from bisphenol A (BPA)-induced *via* modulating oncogenic miR-19 (99). Li et al., demonstrated that BPA exhibited estrogenic activity by increasing the proliferation of MCF-7 cells and triggering the cell transition from G1 to S phase. Curcumin inhibited the proliferation of BPA on MCF-7 cells. Meanwhile, BPA-induced upregulation of oncogenic miR-19a can be reversed by curcumin, including dysregulation of miR-19-related downstream proteins, such as PTEN, p-Akt, p-MDM2, p53, and proliferative nuclear antigen. These results indicate that curcumin can inhibit the proliferation of breast cancer mediated by BPA by regulating the miR-19/PTEN/AKT/p53 pathway (99).

It has been reported that curcumin leads to a markedly inhibition of cell growth, and promotes apoptosis in non-small cell lung cancer cells *via* p53-miR-192-5p/215-XIAP pathway (100). X-linked inhibitor of apoptosis (XIAP) is a member of the inhibitor of apoptosis family of proteins (IAP) and plays an important role in the process of resisting apoptosis (101, 102). More importantly, curcumin-induced increase in miR-192-5p/215 level was closely related to intracellular p53 status, only in wild-type cells (A549), while, curcumin does not cause an increase of miR-192-5p/215 in cells without p53 expression (H1299, p53-null). With miRBase, TargetScan, PicTar and miRDB target databases and luciferase assay, it was further discovered that XIAP is the direct target gene of miR-192-5p/215. Curcumin promotes cell apoptosis by increasing the level of miR-192-5p/215, which binds directly to resists apoptosis XIAP mRNA (100). Xu et al., demonstrated that curcumin mediates the sensitivity of bladder cancer cells to radiotherapy by activating p53. The combination of 10 μM curcumin and radiation was more effective in reducing miR-1246 expression, cell viability and colony formation than curcumin or radiation alone. Inhibition of miR-1246 significantly reduces the cell viability and colony formation of T24 and HT-1376 cells. Luciferase reporter assay showed that miR-1246 can directly inhibit the expression of p53 gene. Finally, miR-1246 participates in the anti-cancer effects of curcumin and radiation by targeting to inhibiting the translation of p53 gene in bladder cancer cells (103).

Furthermore, mechanism studies have shown that curcumin can inhibit the growth of gastric cancer cells by down-regulating lncRNA H19 which was proved to be a oncomir (104, 105). Gao et al. proved that curcumin inhibits the proliferation of SGC7901 gastric cancer cells by repressing the expression of lncRNA H19 and enhancing the expression of p53. Meantime, curcumin can enhance the expression ratio of Bax/Bcl-2, both of them are downstream molecules of p53, thereby promoting cell apoptosis. Additionally, curcumin can also reduce the expression of oncogene c-Myc which indicate that curcumin inhibits the proliferation of gastric cancer cells by down-regulating the c-Myc/lncRNA H19 pathway (106).

NF-κB SIGNAL PATHWAY

NF-κB (NF-κB) is a transcription factor involved in a wide variety of biological activity. Growing evidence support its pivotal role in many steps of tumorigenesis and chemoresistance. Aberrant or constitutive NF-kB activation has been detected in many human malignancies (107–109). Suppression of the NF-kB signaling pathway has turned out to be a potential therapeutic approach for cancer treatment.

Studies showed that curcumin inhibits invasion and proliferation of cervical cancer cells *via* impairment of NF-kB and Wnt/β-catenin pathways (110). Curcumin effectively

inhibits oncogenic NF-kB signaling and restrains stemness features in liver cancer (111). Under hypoxic conditions, curcumin would attenuate the malignancy of pancreatic cancer cell invasion and EMT by interfering with tumor–stromal crosstalk *via* the ERK/NF–κB axis. Li et al., demonstrated that curcumin inhibits the activation and migration of pancreatic stellate cells (PSC), which play an important role in pancreatic cancer progression. Moreover, curcumin inhibits pancreatic cancer cell invasion, EMT and alters the expression of E-cadherin, vimentin, and MMP-9. Furthermore, curcumin can counteract the increased levels of p-ERK and p-NF-κB (112). Xiang et al., documented that curcumin also can repress the proliferation, migration and apoptosis by regulating the NF-κB signaling pathway in human colorectal carcinoma HCT–116 cells (113). In T47D breast cancer cells, curcumin treatment for 48 h, prevented human autocrine growth hormone (GH) signaling mediated NF-kB activation and miR-183-96-182 cluster stimulated epithelial mesenchymal transition (114). Animal study showed that curcumin suppressed the paclitaxel-induced NF-kB in breast cancer cells and strengthened the growth inhibitory effect of paclitaxel in a breast cancer nude mice mode. Compared with either drug alone, the combined treatment of paclitaxel and curcumin can significantly suppress cell proliferation and reduce tumor size, increase cell apoptosis, and reduce the expression of matrix metalloproteinase 9 (MMP9) (115). Studies demonstrated that curcumin inhibits both cyclo-oxygenase-2 enzyme (COX-2) and NF-kB. Therefore, it decreases binding of NF-kB to DNA and overpasses chemoresistance phenomenon in cancer cells (92, 93, 116, 117).The targeting of the NF-κB signaling by curcumin might be a treatment option for cancer.

SUMMARY AND PROSPECT

Natural compounds have been well known for their potential effect on preventing cancer progression and as complementary or stand-alone therapies for cancer treatment (19, 118, 119). As a natural phenolic compound, curcumin is extracted from the dietary spice turmeric, showing an important significance in the adjuvant treatment of tumors with non-toxicity and tolerability (120–123). Curcumin participates in tumor control through multiple signaling pathways, including PI3K/Akt, JAK/STAT, MAPK, Wnt/β-catenin, p53, NF-κB and apoptosis related signaling pathways (**Table 1**). In addition, it is well known that ncRNA (including miRNA and lncRNA) plays an important role in the development of tumors. Curcumin regulates the expression of ncRNAs, which in turn affects the expression of related signaling pathway genes/proteins, and ultimately inhibits tumor cell proliferation, promotes cell apoptosis, and enhances sensitivity to chemotherapy drugs

TABLE 1 | Curcumin modulates cellular signaling pathway and ncRNAs in cancers.

Curcumin or analog	Signal Pathways	ncRNAs*	Downstream Targets	Cancer Type	Refs
Curcumin	PI3K/Akt	miR-206 (↑)	p-Akt (↓), p-mTOR (↓);	Non-small cell lung cancer	(23)
		miR-192-5p (↑)	Caspase-3 (↑), PI3K (↓), Akt (↓);	Non-small cell lung cancer	(24)
		miR-203 (↑)	Akt2 (↓), Src (↓), Jun (↓), Survivin (↓);	Bladder cancer	(30)
		miR-21 (↓)	PTEN (↑), PI3K (↓), Akt (↓), p-Akt (↓);	Gastric cancer	(27, 28)
			p21 (↑), MMP2 (↓), MMP9 (↓);	Gastric cancer	
Curcumin	JAK-STAT	miR-99a (↑)	p-JAK1 (↓), p-STAT1, 3 (↓), CyclinD1 (↓), p21 (↑), Bcl-2 (↓), Bax (↑), Cleaved-caspase-3,9 (↑), MMP2 (↓), RhoA (↓), ROCK1 (↓), Vimentin (↓);	Retinoblastoma	(37)
Analog	Wnt/β-catenin	miR-33b (↑)	HMGA2 (↓), E-cadherin (↑), N-cadherin (↓), Vimentin (↓), p-STAT3 (↓);	Melanoma	(53)
Curcumin		miR-192-5p (↑)	Cyclin D1 (↓), c-Myc (↓), β-catenin (↓);	Non-small cell lung cancer	(45)
		miR-21 (↓)	Bcl-2 (↓), Bax (↑), RECK (↑), MMP2 (↓), c-Myc (↓), β-catenin (↓), GSK-3β (↓);	Osteosarcoma	(44)
		miR-130 (↓)	Nkd2(↓), β-catenin (↓), TCF4 (↓);	Colon cancer	(46)
		lincROR (↓)	β-catenin (↓), CD44 (↓), Oct3/4 (↓), CyclinD1 (↓), c-Myc (↓);	Hepatocellular carcinoma	(51)
		lncRNA H19 (↓)	E-cadherin (↑), N-cadherin (↓), Vimentin (↓);	Breast cancer	(57)
Curcumin	MAPK	miR-378 (↑)	p-p38 (↑);	Glioblastoma	(62)
		/	p-JNK (↑), Cyclin D3 (↓), CDK2,6 (↓), p21 (↑), p27 (↑), Cleaved-caspase-3,9 (↑), p-p38 (↑);	Retinoblastoma	(63)
		/	p-JNK (↑), p-p38 (↑), p-ERK1,2 (↓), p-p65 (↓), MMP2 (↓), MMP9 (↓), Vimentin (↓);	Leukaemia	(64)
		/	p-p38 (↑), p-JNK (↑), Cleaved-caspase-3,9 (↑), Bcl-2 (↓), Bax (↑), HSP70 (↓);	Non-small cell lung cancer	(65)
			Cleaved-PARP (↑), ATF2 (↑), NF-κB (↓);	Colon cancer	(66)
Curcumin	p53	miR-19 (↓)	p53 (↑), p-MDM2 (↓), PCNA (↓), p-Akt (↓), PTEN (↑);	Breast cancer	(74)
		miR-1246 (↓)	p53 (↑);	Bladder cancer	(78)
		lncRNA H19 (↓)	p53 (↑), Bcl-2 (↓), Bax (↑), c-Myc (↓);	Gastric cancer	(79)
		miR-192-5p (↑)	p53 (↑), p21 (↑), Cleaved-PARP (↑), Cleaved-caspase-3 (↑), XIAP (↑);	Non-small cell lung cancer	(75)
		miR-215 (↑)			
Curcumin	NF-κB	/	p-ERK (↓), p-NF-κB (↓), MMP9 (↓), Vimentin (↓);	Pancreatic cancer	(85)
			Fas (↑), FADD (↑), Cleaved-caspase-3,8 (↑), MMP-9 (↓), NF-κB (↓), E-cadherin (↑), claudin-3 (↓),	Colon cancer	(86)

**ncRNAs expression altered under curcumin treatment.*

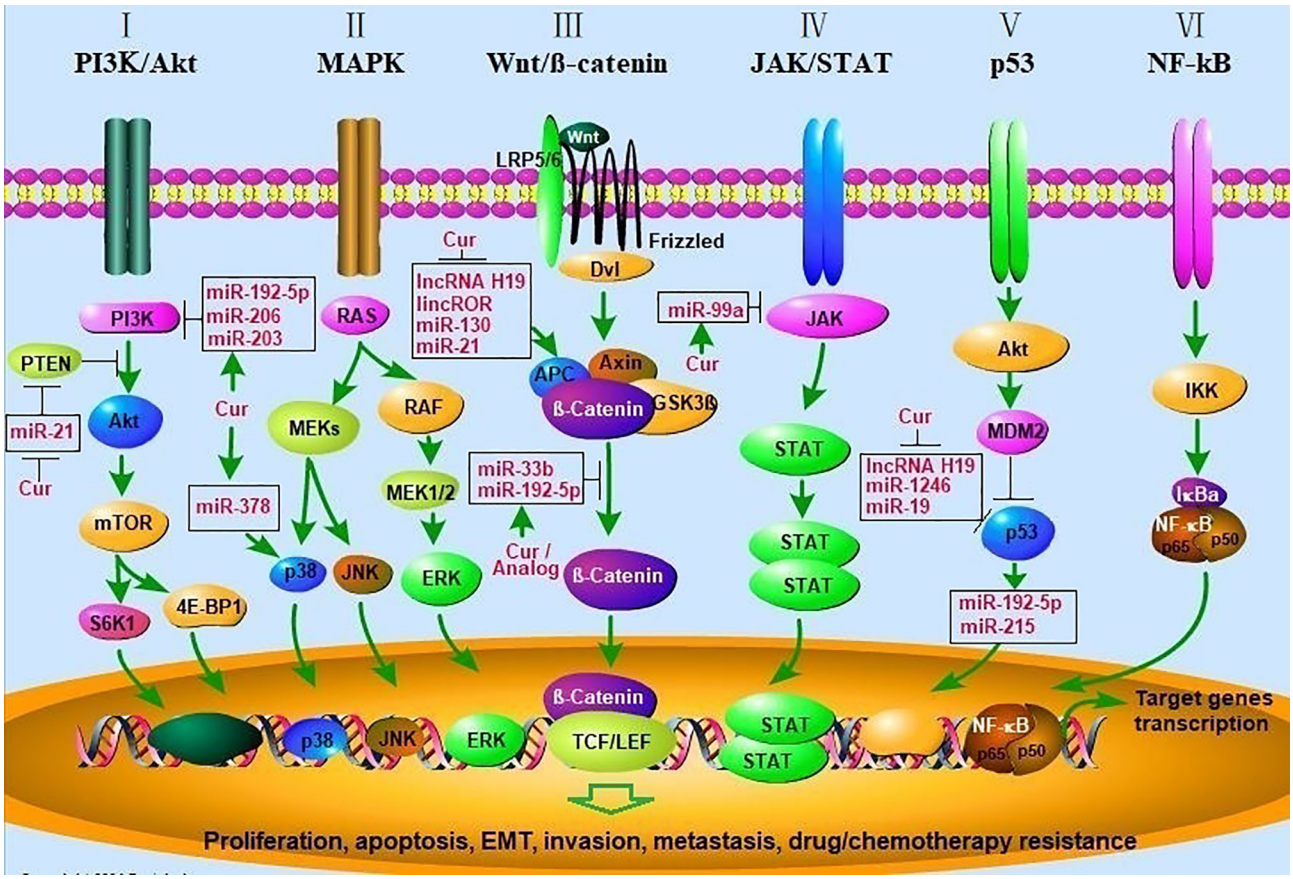

FIGURE 1 | Curcumin modulates cancer progression by regulating multiple signal transduction pathways. (I) Akt/PI3K/mTOR signaling pathway. PTEN inhibits the activation of Akt by PI3K, mTOR phosphorylates p70S6K1 (S6K1) and 4E-BP1 leading to activation of pathways involved in cell growth and survival. Curcumin inhibit the Akt/PI3K/mTOR pathway by enhancing the activity of PTEN *via* decreasing miR-21 and inhibiting the activity of PI3K *via* upregulating miR-192-5p, miR-206, miR-203; (II) MAPK signaling pathway. Signaling cascades leading to activation of the MEKs, which lead to activation of the ERK1/2, p38, and JNK cascades, and then initiate the gene transcription. Curcumin activated p38 MAPK *via* upregulating miR-378, leading to elevated p21/27, cleaved-caspase-3,9 expression, decreased Bcl-2, MMP2/9 expression. (III) Wnt/β-catenin pathway. Wnt binds both Frizzled and LRP5/6 receptors to initiate the dissociation of the Axin/APC/GSK3β complex. β-catenin phosphorylation and then translocates to the nucleus to bind TCF/LEF co-transcription factors, which induces the Wnt-response gene transcription. Curcumin inhibits the Wnt/β-catenin pathway by inhibiting lncRNA H19, lincROR, miR-130, 21 and upregulating miR-192-5p and miR-33b; (IV) JAK/STAT signaling. The pathway is activated by the binding of a ligand and then convey signals downstream STATs, whereas STATs are transcription factors that activate gene expression; (V) p53 signaling pathway. AKT-induced activation of MDM2, which can inhibit the antitumor activity of p53. Curcumin enhances the anti-tumor activity of p53 by inhibiting lncRNA H19, miR-1246, miR-19; (VI) NF-kB signaling pathway. Signaling cascade leads to the phosphorylation of IkBα resulting in degradation by the proteasome. This releases the NF-kB/p65/p50 complex and allows it to translocate to the nucleus for gene transcription. AKT, v-akt murine thymoma viral oncogene; PI3K, phosphatidylinositol 3-kinase; mTOR, mammalian target of rapamycin; PTEN, phosphatase and tensin homolog; MAPK, mitogen-activated protein kinase; MMP, matrix metalloprotinase), ERKs (extracellular regulated protein kinases), JNK (c-Jun N-terminal kinase; APC, adenomatous polyposis coli; Dvl, Disheveled; GSK3β, glycogen synthase kinase 3β; LRP5/6, low density lipoprotein receptor-related protein 5/6; TCF/LEF, T-cell factor/lymphoid enhancer-binding factor; JAK/STAT, janus kinase/signal transducers and activators of transcription; MDM2, murine double minute 2; NF-κB, nuclear factor kappa B; IKK, IκB kinase; IκBa, IkappaBa.

(**Figure 1**). These findings will help us better understand the molecular mechanism between curcumin and ncRNAs in anti-tumor, and the potentiality of clinical adjuvant treatment. Collectively, curcumin is a natural compound with potential drug value in adjuvant treatment of tumors.

AUTHOR CONTRIBUTIONS

All authors listed have made a substantial, direct, and intellectual contribution to the work, and approved it for publication.

FUNDING

This work was supported by National Natural Science Foundation of China (U1904133,81903688), Program for Young Key Teachers in Colleges and Universities in Henan Province (2020GGJS150), the Natural Science Foundation of Henan Province of China (212300410224), and Scientific Research Foundation of Xinxiang Medical University (XYBSKYZZ201512). This work was also supported by National Training Programs of Innovation and Entrepreneurship for Undergraduates (202010472011).

REFERENCES

1. Bray F, Ferlay J, Soerjomataram I, Siegel RL, Torre LA, Jemal A. Global cancer statistics 2018: GLOBOCAN estimates of incidence and mortality worldwide for 36 cancers in 185 countries. *CA Cancer J Clin* (2018) 68:394–424. doi: 10.3322/caac.21492
2. Zhang JY, Lin MT, Zhou MJ, Yi T, Tang YN, Tang SL, et al. Combinational Treatment of Curcumin and Quercetin against Gastric Cancer MGC-803 Cells in Vitro. *Molecules* (2015) 20:11524–34. doi: 10.3390/molecules200611524
3. .Zhao Y, Sun J, Dou W, Hu JH. Curcumin inhibits proliferation of interleukin-22-treated HaCaT cells. *Int J Clin Exp Med* (2015) 8:9580–4
4. Xu Y, Zhang J, Han J, Pan X, Cao Y, Guo H, et al. Curcumin inhibits tumor proliferation induced by neutrophil elastase through the upregulation of alpha1-antitrypsin in lung cancer. *Mol Oncol* (2012) 6:405–17. doi: 10.1016/j.molonc.2012.03.005
5. Chen L, Zhan CZ, Wang T, You H, Yao R. Curcumin Inhibits the Proliferation, Migration, Invasion, and Apoptosis of Diffuse Large B-Cell Lymphoma Cell Line by Regulating MiR-21/VHL Axis. *Yonsei Med J* (2020) 61:20–9. doi: 10.3349/ymj.2020.61.1.20
6. Siriviriyakul P, Chingchit T, Klaikeaw N, Chayanupatkul M, Werawatganon D. Effects of curcumin on oxidative stress, inflammation and apoptosis in L-arginine induced acute pancreatitis in mice. *Heliyon* (2019) 5:e02222. doi: 10.1016/j.heliyon.2019.e02222
7. Gaikwad D, Shewale R, Patil V, Mali D, Gaikwad U, Jadhav N. Enhancement in in vitro anti-angiogenesis activity and cytotoxicity in lung cancer cell by pectin-PVP based curcumin particulates. *Int J Biol Macromol* (2017) 104:656–64. doi: 10.1016/j.ijbiomac.2017.05.170
8. Yang L, Zheng Z, Qian C, Wu J, Liu Y, Guo S, et al. Curcumin-functionalized silk biomaterials for anti-aging utility. *J Colloid Interface Sci* (2017) 496:66–77. doi: 10.1016/j.jcis.2017.01.115
9. Liu Y SH, Makabel B, Cui Q, Li J, Su C, Ashby CRJr, et al. The targeting of non−coding RNAs by curcumin: Facts and hopes for cancer therapy (Review). *Oncol Rep* (2019) 42:20–34. doi: 10.3892/or.2019.7148
10. Romano G, Veneziano D, Acunzo M, Croce CM. Small non-coding RNA and cancer. *Carcinogenesis* (2017) 38:485–91. doi: 10.1093/carcin/bgx026
11. Slack FJ, Chinnaiyan AM. The Role of Non-coding RNAs in Oncology. *Cell* (2019) 179:1033–55. doi: 10.1016/j.cell.2019.10.017
12. Czech B, Munafo M, Ciabrelli F, Eastwood EL, Fabry MH, Kneuss E, et al. piRNA-Guided Genome Defense: From Biogenesis to Silencing. *Annu Rev Genet* (2018) 52:131–57. doi: 10.1146/annurev-genet-120417-031441
13. Liu Y, Dou M, Song X, Dong Y, Liu S, Liu H, et al. The emerging role of the piRNA/piwi complex in cancer. *Mol Cancer* (2019) 18:123. doi: 10.1186/s12943-019-1052-9
14. Wei JW, Huang K, Yang C, Kang CS. Non-coding RNAs as regulators in epigenetics (Review). *Oncol Rep* (2017) 37:3–9. doi: 10.3892/or.2016.5236
15. Mehta A, Dobersch S, Romero-Olmedo AJ, Barreto G. Epigenetics in lung cancer diagnosis and therapy. *Cancer Metastasis Rev* (2015) 34:229–41. doi: 10.1007/s10555-015-9563-3
16. Esteller M. Non-coding RNAs in human disease. *Nat Rev Genet* (2011) 12:861–74. doi: 10.1038/nrg3074
17. Stefanska B, MacEwan DJ. Epigenetics and pharmacology. *Br J Pharmacol* (2015) 172:2701–4. doi: 10.1111/bph.13136
18. Kaikkonen MU, Adelman K. Emerging Roles of Non-Coding RNA Transcription. *Trends Biochem Sci* (2018) 43:654–67. doi: 10.1016/j.tibs.2018.06.002
19. Giordano A, Tommonaro G. Curcumin and Cancer. *Nutrients* (2019) 11:2376. doi: 10.3390/nu11102376
20. Tomeh MA, Hadianamrei R, Zhao X. A Review of Curcumin and Its Derivatives as Anticancer Agents. *Int J Mol Sci* (2019) 20:1033. doi: 10.3390/ijms20051033
21. Shanmugam MK, Rane G, Kanchi MM, Arfuso F, Chinnathambi A, Zayed ME, et al. The multifaceted role of curcumin in cancer prevention and treatment. *Molecules* (2015) 20:2728–69. doi: 10.3390/molecules20022728
22. Mbese Z, Khwaza V, Aderibigbe BA. Curcumin and Its Derivatives as Potential Therapeutic Agents in Prostate, Colon and Breast Cancers. *Molecules* (2019) 24:4386. doi: 10.3390/molecules24234386
23. Baldi A, De Luca A, Maiorano P, D'Angelo C, Giordano A. Curcumin as an Anticancer Agent in Malignant Mesothelioma: A Review. *Int J Mol Sci* (2020) 21:1839. doi: 10.3390/ijms21051839
24. Noorolyai S, Shajari N, Baghbani E, Sadreddini S, Baradaran B. The relation between PI3K/AKT signalling pathway and cancer. *Gene* (2019) 698:120–8. doi: 10.1016/j.gene.2019.02.076
25. Xu W, Yang Z, Lu N. A new role for the PI3K/Akt signaling pathway in the epithelial-mesenchymal transition. *Cell Adh Migr* (2015) 9:317–24. doi: 10.1080/19336918.2015.1016686
26. Cheng J, Huang Y, Zhang X, Yu Y, Wu S, Jiao J, et al. TRIM21 and PHLDA3 negatively regulate the crosstalk between the PI3K/AKT pathway and PPP metabolism. *Nat Commun* (2020) 11:1880. doi: 10.1038/s41467-020-15819-3
27. Fresno Vara JA, Casado E, de Castro J, Cejas P, Belda-Iniesta C, Gonzalez-Baron M. PI3K/Akt signalling pathway and cancer. *Cancer Treat Rev* (2004) 30:193–204. doi: 10.1016/j.ctrv.2003.07.007
28. Chao P, Yongheng F, Jin Z, Yu Z, Shiyong Y, Kunxing Y, et al. lncRNA HOTAIR knockdown suppresses gastric cancer cell biological activities. *Food Sci Nutr* (2021) 9:123–34. doi: 10.1002/fsn3.1970
29. Park YR, Seo SY, Kim SL, Zhu SM, Chun S, Oh JM, et al. MiRNA-206 suppresses PGE2-induced colorectal cancer cell proliferation, migration, and invasion by targetting TM4SF1. *Biosci Rep* (2018) 38:BSR20180664. doi: 10.1042/BSR20180664
30. Chen XF, Guo JF, Xu JF, Yin SH, Cao WL. MiRNA-206 inhibits proliferation of renal clear cell carcinoma by targeting ZEB2. *Eur Rev Med Pharmacol Sci* (2019) 23:7826–34. doi: 10.26355/eurrev_201909_18992
31. Yang N, Wang L, Liu J, Liu L, Huang J, Chen X, et al. MicroRNA-206 regulates the epithelial-mesenchymal transition and inhibits the invasion and metastasis of prostate cancer cells by targeting Annexin A2. *Oncol Lett* (2018) 15:8295–302. doi: 10.3892/ol.2018.8395
32. Liang Z, Bian X, Shim H. Downregulation of microRNA-206 promotes invasion and angiogenesis of triple negative breast cancer. *Biochem Biophys Res Commun* (2016) 477:461–6. doi: 10.1016/j.bbrc.2016.06.076
33. Sun C, Liu Z, Li S, Yang C, Xue R, Xi Y, et al. Down-regulation of c-Met and Bcl2 by microRNA-206, activates apoptosis, and inhibits tumor cell proliferation, migration and colony formation. *Oncotarget* (2015) 6:25533–74. doi: 10.18632/oncotarget.4575
34. Yang L, Liang H, Wang Y, Gao S, Yin K, Liu Z, et al. MiRNA-203 suppresses tumor cell proliferation, migration and invasion by targeting Slug in gastric cancer. *Protein Cell* (2016) 7:383–7. doi: 10.1007/s13238-016-0259-4
35. Yan D, Dong Xda E, Chen X, Wang L, Lu C, Wang J, et al. MicroRNA-1/206 targets c-Met and inhibits rhabdomyosarcoma development. *J Biol Chem* (2009) 284:29596–604. doi: 10.1074/jbc.M109.020511
36. Zhang Y, He Y, Lu LL, Zhou ZY, Wan NB, Li GP, et al. miRNA-192-5p impacts the sensitivity of breast cancer cells to doxorubicin via targeting peptidylprolyl isomerase A. *Kaohsiung J Med Sci* (2019) 35:17–23. doi: 10.1002/kjm2.12004
37. Wang N, Feng T, Liu X, Liu Q. Curcumin inhibits migration and invasion of non-small cell lung cancer cells through up-regulation of miR-206 and suppression of PI3K/AKT/mTOR signaling pathway. *Acta Pharm* (2020) 70:399–409. doi: 10.2478/acph-2020-0029
38. Jin H, Qiao F, Wang Y, Xu Y, Shang Y. Curcumin inhibits cell proliferation and induces apoptosis of human non-small cell lung cancer cells through the upregulation of miR-192-5p and suppression of PI3K/Akt signaling pathway. *Oncol Rep* (2015) 34:2782–9. doi: 10.3892/or.2015.4258
39. Yin Y, Shen WH. PTEN: a new guardian of the genome. *Oncogene* (2008) 27:5443–53. doi: 10.1038/onc.2008.241
40. Qi R, Wang DT, Xing LF, Wu ZJ. miRNA-21 promotes gastric cancer growth by adjusting prostaglandin E2. *Eur Rev Med Pharmacol Sci* (2018) 22:1929–36. doi: 10.26355/eurrev_201804_14717
41. Markou A, Zavridou M, Lianidou ES. miRNA-21 as a novel therapeutic target in lung cancer. *Lung Cancer (Auckl)* (2016) 7:19–27. doi: 10.2147/LCTT.S60341
42. Yang Q, Yu H, Yin Q, Hu X, Zhang C. lncRNA-NEF is downregulated in osteosarcoma and inhibits cancer cell migration and invasion by downregulating miRNA-21. *Oncol Lett* (2019) 17:5403–8. doi: 10.3892/ol.2019.10276

43. Wang Y, Zhang P, Yuan M, Li X. Overexpression of miRNA-21 Promotes the Proliferation and Invasion in Hepatocellular Carcinoma Cells via Suppressing SMAD7. *Technol Cancer Res Treat* (2019) 18:1533033819878686. doi: 10.1177/1533033819878686
44. Wang Y, Zhou S, Fan K, Jiang C. MicroRNA-21 and its impact on signaling pathways in cervical cancer. *Oncol Lett* (2019) 17:3066–70. doi: 10.3892/ol.2019.10002
45. Volinia S, Calin GA, Liu CG, Ambs S, Cimmino A, Petrocca F, et al. A microRNA expression signature of human solid tumors defines cancer gene targets. *Proc Natl Acad Sci USA* (2006) 103:2257–61. doi: 10.1073/pnas.0510565103
46. Chen J, Xu T, Chen C. The critical roles of miR-21 in anti-cancer effects of curcumin. *Ann Transl Med* (2015) 3:330. doi: 10.3978/j.issn.2305-5839.2015.09.20
47. Liu W, Huang M, Zou Q, Lin W. Curcumin suppresses gastric cancer biological activity by regulation of miRNA-21: an in vitro study. *Int J Clin Exp Pathol* (2018) 11:5820–9.
48. Qiang Z, Meng L, Yi C, Yu L, Chen W, Sha W. Curcumin regulates the miR-21/PTEN/Akt pathway and acts in synergy with PD98059 to induce apoptosis of human gastric cancer MGC-803 cells. *J Int Med Res* (2019) 47:1288–97. doi: 10.1177/0300060518822213
49. Yang CH, Yue J, Sims M, Pfeffer LM. The curcumin analog EF24 targets NF-kappaB and miRNA-21, and has potent anticancer activity in vitro and in vivo. *PloS One* (2013) 8:e71130. doi: 10.1371/journal.pone.0071130
50. Saini S, Arora S, Majid S, Shahryari V, Chen Y, Deng G, et al. Curcumin modulates microRNA-203-mediated regulation of the Src-Akt axis in bladder cancer. *Cancer Prev Res (Phila)* (2011) 4:1698–709. doi: 10.1158/1940-6207.CAPR-11-0267
51. Seo BR, Min KJ, Cho IJ, Kim SC, Kwon TK. Curcumin significantly enhances dual PI3K/Akt and mTOR inhibitor NVP-BEZ235-induced apoptosis in human renal carcinoma Caki cells through down-regulation of p53-dependent Bcl-2 expression and inhibition of Mcl-1 protein stability. *PloS One* (2014) 9:e95588. doi: 10.1371/journal.pone.0095588
52. Leonard WJ, O'Shea JJ. Jaks and STATs: biological implications. *Annu Rev Immunol* (1998) 16:293–322. doi: 10.1146/annurev.immunol.16.1.293
53. Rawlings JS, Rosler KM, Harrison DA. The JAK/STAT signaling pathway. *J Cell Sci* (2004) 117:1281–3. doi: 10.1242/jcs.00963
54. Harrison DA. The Jak/STAT pathway. *Cold Spring Harb Perspect Biol* (2012) 4:a011205. doi: 10.1101/cshperspect.a011205
55. Thomas SJ, Snowden JA, Zeidler MP, Danson SJ. The role of JAK/STAT signalling in the pathogenesis, prognosis and treatment of solid tumours. *Br J Cancer* (2015) 113:365–71. doi: 10.1038/bjc.2015.233
56. Morris R, Kershaw NJ, Babon JJ. The molecular details of cytokine signaling via the JAK/STAT pathway. *Protein Sci* (2018) 27:1984–2009. doi: 10.1002/pro.3519
57. Yan HZ, Wang W, Du X, Jiang XD, Lin CY, Guo JL, et al. The expression and clinical significance of miRNA-99a and miRNA-224 in non-small cell lung cancer. *Eur Rev Med Pharmacol Sci* (2019) 23:1545–52. doi: 10.26355/eurrev_201902_17113
58. Tao C, Sun H, Sang W, Li S. miRNA-99a inhibits cell invasion and migration in liver cancer by directly targeting HOXA1. *Oncol Lett* (2019) 17:5108–14. doi: 10.3892/ol.2019.10199
59. Wu D, Zhou Y, Pan H, Zhou J, Fan Y, Qu P. microRNA-99a inhibiting cell proliferation, migration and invasion by targeting fibroblast growth factor receptor 3 in bladder cancer. *Oncol Lett* (2014) 7:1219–24. doi: 10.3892/ol.2014.1875
60. Li Y, Sun W, Han N, Zou Y, Yin D. Curcumin inhibits proliferation, migration, invasion and promotes apoptosis of retinoblastoma cell lines through modulation of miR-99a and JAK/STAT pathway. *BMC Cancer* (2018) 18:1230. doi: 10.1186/s12885-018-5130-y
61. Khan AQ, Ahmed EI, Elareer N, Fathima H, Prabhu KS, Siveen KS, et al. Curcumin-Mediated Apoptotic Cell Death in Papillary Thyroid Cancer and Cancer Stem-Like Cells through Targeting of the JAK/STAT3 Signaling Pathway. *Int J Mol Sci* (2020) 21:438. doi: 10.3390/ijms21020438
62. Pai SG, Carneiro BA, Mota JM, Costa R, Leite CA, Barroso-Sousa R, et al. Wnt/beta-catenin pathway: modulating anticancer immune response. *J Hematol Oncol* (2017) 10:101. doi: 10.1186/s13045-017-0471-6
63. Zhang Y, Wang X. Targeting the Wnt/beta-catenin signaling pathway in cancer. *J Hematol Oncol* (2020) 13:165. doi: 10.1186/s13045-020-00990-3
64. MacDonald BT, Tamai K, He X. Wnt/beta-catenin signaling: components, mechanisms, and diseases. *Dev Cell* (2009) 17:9–26. doi: 10.1016/j.devcel.2009.06.016
65. Song N, Zhong J, Hu Q, Gu T, Yang B, Zhang J, et al. FGF18 Enhances Migration and the Epithelial-Mesenchymal Transition in Breast Cancer by Regulating Akt/GSK3beta/Beta-Catenin Signaling. *Cell Physiol Biochem* (2018) 49:1019–32. doi: 10.1159/000493286
66. Pei J, Song N, Wu L, Qi J, Xia S, Xu C, et al. TCF4/beta-catenin complex is directly upstream of FGF21 in mouse stomach cancer cells. *Exp Ther Med* (2018) 15:1041–7. doi: 10.3892/etm.2017.5493
67. Zhou L, Lu Y, Liu JS, Long SZ, Liu HL, Zhang J, et al. The role of miR-21/RECK in the inhibition of osteosarcoma by curcumin. *Mol Cell Probes* (2020) 51:101534. doi: 10.1016/j.mcp.2020.101534
68. Pan Y, Sun Y, Liu Z, Zhang C. miR1925p upregulation mediates the suppression of curcumin in human NSCLC cell proliferation, migration and invasion by targeting cMyc and inactivating the Wnt/betacatenin signaling pathway. *Mol Med Rep* (2020) 22:1594–604. doi: 10.3892/mmr.2020.11213
69. Dou H, Shen R, Tao J, Huang L, Shi H, Chen H, et al. Curcumin Suppresses the Colon Cancer Proliferation by Inhibiting Wnt/beta-Catenin Pathways via miR-130a. *Front Pharmacol* (2017) 8:877. doi: 10.3389/fphar.2017.00877
70. Wang J, Su Z, Lu S, Fu W, Liu Z, Jiang X, et al. LncRNA HOXA-AS2 and its molecular mechanisms in human cancer. *Clin Chim Acta* (2018) 485:229–33. doi: 10.1016/j.cca.2018.07.004
71. Loewen G, Jayawickramarajah J, Zhuo Y, Shan B. Functions of lncRNA HOTAIR in lung cancer. *J Hematol Oncol* (2014) 7:90. doi: 10.1186/s13045-014-0090-4
72. Jin SJ, Jin MZ, Xia BR, Jin WL. Long Non-coding RNA DANCR as an Emerging Therapeutic Target in Human Cancers. *Front Oncol* (2019) 9:1225. doi: 10.3389/fonc.2019.01225
73. Feng L, Shi L, Lu YF, Wang B, Tang T, Fu WM, et al. Linc-ROR Promotes Osteogenic Differentiation of Mesenchymal Stem Cells by Functioning as a Competing Endogenous RNA for miR-138 and miR-145. *Mol Ther Nucleic Acids* (2018) 11:345–53. doi: 10.1016/j.omtn.2018.03.004
74. Shao J, Shi CJ, Li Y, Zhang FW, Pan FF, Fu WM, et al. LincROR Mediates the Suppressive Effects of Curcumin on Hepatocellular Carcinoma Through Inactivating Wnt/beta-Catenin Signaling. *Front Pharmacol* (2020) 11:847. doi: 10.3389/fphar.2020.00847
75. Liu T, Chi H, Chen J, Chen C, Huang Y, Xi H, et al. Curcumin suppresses proliferation and in vitro invasion of human prostate cancer stem cells by ceRNA effect of miR-145 and lncRNA-ROR. *Gene* (2017) 631:29–38. doi: 10.1016/j.gene.2017.08.008
76. Zhang P, Bai H, Liu G, Wang H, Chen F, Zhang B, et al. MicroRNA-33b, upregulated by EF24, a curcumin analog, suppresses the epithelial-to-mesenchymal transition (EMT) and migratory potential of melanoma cells by targeting HMGA2. *Toxicol Lett* (2015) 234:151–61. doi: 10.1016/j.toxlet.2015.02.018
77. Zhang S, Mo Q, Wang X. Oncological role of HMGA2 (Review). *Int J Oncol* (2019) 55:775–88. doi: 10.3892/ijo.2019.4856
78. Tan L, Wei X, Zheng L, Zeng J, Liu H, Yang S, et al. Amplified HMGA2 promotes cell growth by regulating Akt pathway in AML. *J Cancer Res Clin Oncol* (2016) 142:389–99. doi: 10.1007/s00432-015-2036-9
79. Malek A, Bakhidze E, Noske A, Sers C, Aigner A, Schafer R, et al. HMGA2 gene is a promising target for ovarian cancer silencing therapy. *Int J Cancer* (2008) 123:348–56. doi: 10.1002/ijc.23491
80. Cai J, Sun H, Zheng B, Xie M, Xu C, Zhang G, et al. Curcumin attenuates lncRNA H19induced epithelialmesenchymal transition in tamoxifenresistant breast cancer cells. *Mol Med Rep* (2021) 23:1. doi: 10.3892/mmr.2020.11651
81. Zhang W, Liu HT. MAPK signal pathways in the regulation of cell proliferation in mammalian cells. *Cell Res* (2002) 12:9–18. doi: 10.1038/sj.cr.7290105
82. Guo YJ, Pan WW, Liu SB, Shen ZF, Xu Y, Hu LL. ERK/MAPK signalling pathway and tumorigenesis. *Exp Ther Med* (2020) 19:1997–2007. doi: 10.3892/etm.2020.8454
83. Mirzaei H, Masoudifar A, Sahebkar A, Zare N, Sadri Nahand J, Rashidi B, et al. MicroRNA: A novel target of curcumin in cancer therapy. *J Cell Physiol* (2018) 233:3004–15. doi: 10.1002/jcp.26055

84. Huang Y, Yuan K, Tang M, Yue J, Bao L, Wu S, et al. Melatonin inhibiting the survival of human gastric cancer cells under ER stress involving autophagy and Ras-Raf-MAPK signalling. *J Cell Mol Med* (2020) 25:1480–92. doi: 10.1111/jcmm.16237
85. Li W, Yang W, Liu Y, Chen S, Chin S, Qi X, et al. MicroRNA-378 enhances inhibitory effect of curcumin on glioblastoma. *Oncotarget* (2017) 8:73938–46. doi: 10.18632/oncotarget.17881
86. Zeng M, Zhu L, Li L, Kang C. miR-378 suppresses the proliferation, migration and invasion of colon cancer cells by inhibiting SDAD1. *Cell Mol Biol Lett* (2017) 22:12. doi: 10.1186/s11658-017-0041-5
87. Guo XB, Zhang XC, Chen P, Ma LM, Shen ZQ. miR378a3p inhibits cellular proliferation and migration in glioblastoma multiforme by targeting tetraspanin 17. *Oncol Rep* (2019) 42:1957–71. doi: 10.3892/or.2019.7283
88. Yu X, Zhong J, Yan L, Li J, Wang H, Wen Y, et al. Curcumin exerts antitumor effects in retinoblastoma cells by regulating the JNK and p38 MAPK pathways. *Int J Mol Med* (2016) 38:861–8. doi: 10.3892/ijmm.2016.2676
89. Zhu G, Shen Q, Jiang H, Ji O, Zhu L, Zhang L. Curcumin inhibited the growth and invasion of human monocytic leukaemia SHI-1 cells in vivo by altering MAPK and MMP signalling. *Pharm Biol* (2020) 58:25–34. doi: 10.1080/13880209.2019.1701042
90. Yao Q, Lin M, Wang Y, Lai Y, Hu J, Fu T, et al. Curcumin induces the apoptosis of A549 cells via oxidative stress and MAPK signaling pathways. *Int J Mol Med* (2015) 36:1118–26. doi: 10.3892/ijmm.2015.2327
91. Collett GP, Campbell FC. Curcumin induces c-jun N-terminal kinase-dependent apoptosis in HCT116 human colon cancer cells. *Carcinogenesis* (2004) 25:2183–9. doi: 10.1093/carcin/bgh233
92. Khalid EB, Ayman EE, Rahman H, Abdelkarim G, Najda A. Natural products against cancer angiogenesis. *Tumour Biol* (2016) 37:14513–36. doi: 10.1007/s13277-016-5364-8
93. Awasthi M SS, Pandey VP, Dwivedi U. Curcumin: Structure-Activity Relationship Towards its Role as a Versatile Multi-Targeted Therapeutics. *Mini Rev Org Chem* (2017) 14:311–22. doi: 10.2174/1570193X14666170518112446
94. Hua WF, Fu YS, Liao YJ, Xia WJ, Chen YC, Zeng YX, et al. Curcumin induces down-regulation of EZH2 expression through the MAPK pathway in MDA-MB-435 human breast cancer cells. *Eur J Pharmacol* (2010) 637:16–21. doi: 10.1016/j.ejphar.2010.03.051
95. Toufektchan E, Toledo F. The Guardian of the Genome Revisited: p53 Downregulates Genes Required for Telomere Maintenance, DNA Repair, and Centromere Structure. *Cancers (Basel)* (2018) 10:135. doi: 10.3390/cancers10050135
96. Surget S, Khoury MP, Bourdon JC. Uncovering the role of p53 splice variants in human malignancy: a clinical perspective. *Onco Targets Ther* (2013) 7:57–68. doi: 10.2147/OTT.S53876
97. Isobe M, Emanuel BS, Givol D, Oren M, Croce CM. Localization of gene for human p53 tumour antigen to band 17p13. *Nature* (1986) 320:84–5. doi: 10.1038/320084a0
98. Bourdon JC, Fernandes K, Murray-Zmijewski F, Liu G, Diot A, Xirodimas DP, et al. p53 isoforms can regulate p53 transcriptional activity. *Genes Dev* (2005) 19:2122–37. doi: 10.1101/gad.1339905
99. Li X, Xie W, Xie C, Huang C, Zhu J, Liang Z, et al. Curcumin modulates miR-19/PTEN/AKT/p53 axis to suppress bisphenol A-induced MCF-7 breast cancer cell proliferation. *Phytother Res* (2014) 28:1553–60. doi: 10.1002/ptr.5167
100. Ye M, Zhang J, Zhang J, Miao Q, Yao L, Zhang J. Curcumin promotes apoptosis by activating the p53-miR-192-5p/215-XIAP pathway in non-small cell lung cancer. *Cancer Lett* (2015) 357:196–205. doi: 10.1016/j.canlet.2014.11.028
101. Holcik M, Korneluk RG. Functional characterization of the X-linked inhibitor of apoptosis (XIAP) internal ribosome entry site element: role of La autoantigen in XIAP translation. *Mol Cell Biol* (2000) 20:4648–57. doi: 10.1128/mcb.20.13.4648-4657.2000
102. Duckett CS, Li F, Wang Y, Tomaselli KJ, Thompson CB, Armstrong RC. Human IAP-like protein regulates programmed cell death downstream of Bcl-xL and cytochrome c. *Mol Cell Biol* (1998) 18:608–15. doi: 10.1128/mcb.18.1.608
103. Xu R, Li H, Wu S, Qu J, Yuan H, Zhou Y, et al. MicroRNA-1246 regulates the radio-sensitizing effect of curcumin in bladder cancer cells via activating P53. *Int Urol Nephrol* (2019) 51:1771–9. doi: 10.1007/s11255-019-02210-5
104. Li H, Yu B, Li J, Su L, Yan M, Zhu Z, et al. Overexpression of lncRNA H19 enhances carcinogenesis and metastasis of gastric cancer. *Oncotarget* (2014) 5:2318–29. doi: 10.18632/oncotarget.1913
105. Yang F, Bi J, Xue X, Zheng L, Zhi K, Hua J, et al. Up-regulated long non-coding RNA H19 contributes to proliferation of gastric cancer cells. *FEBS J* (2012) 279:3159–65. doi: 10.1111/j.1742-4658.2012.08694.x
106. Liu G, Xiang T, Wu QF, Wang WX. Curcumin suppresses the proliferation of gastric cancer cells by downregulating H19. *Oncol Lett* (2016) 12:5156–62. doi: 10.3892/ol.2016.5354
107. Xie C, Zhang LZ, Chen ZL, Zhong WJ, Fang JH, Zhu Y, et al. A hMTR4-PDIA3P1-miR-125/124-TRAF6 Regulatory Axis and Its Function in NF kappa B Signaling and Chemoresistance. *Hepatology* (2020) 71:1660–77. doi: 10.1002/hep.30931
108. Meng Q, Liang C, Hua J, Zhang B, Liu J, Zhang Y, et al. A miR-146a-5p/TRAF6/NF-kB p65 axis regulates pancreatic cancer chemoresistance: functional validation and clinical significance. *Theranostics* (2020) 10:3967–79. doi: 10.7150/thno.40566
109. Paciello F, Fetoni AR, Mezzogori D, Rolesi R, Di Pino A, Paludetti G, et al. The dual role of curcumin and ferulic acid in counteracting chemoresistance and cisplatin-induced ototoxicity. *Sci Rep* (2020) 10:1063. doi: 10.1038/s41598-020-57965-0
110. Ghasemi F, Shafiee M, Banikazemi Z, Pourhanifeh MH, Khanbabaei H, Shamshirian A, et al. Curcumin inhibits NF-kB and Wnt/beta-catenin pathways in cervical cancer cells. *Pathol Res Pract* (2019) 215:152556. doi: 10.1016/j.prp.2019.152556
111. Marquardt JU, Gomez-Quiroz L, Arreguin Camacho LO, Pinna F, Lee YH, Kitade M, et al. Curcumin effectively inhibits oncogenic NF-kappaB signaling and restrains stemness features in liver cancer. *J Hepatol* (2015) 63:661–9. doi: 10.1016/j.jhep.2015.04.018
112. Li W, Sun L, Lei J, Wu Z, Ma Q, Wang Z. Curcumin inhibits pancreatic cancer cell invasion and EMT by interfering with tumorstromal crosstalk under hypoxic conditions via the IL6/ERK/NFkappaB axis. *Oncol Rep* (2020) 44:382–92. doi: 10.3892/or.2020.7600
113. Xiang L, He B, Liu Q, Hu D, Liao W, Li R, et al. Antitumor effects of curcumin on the proliferation, migration and apoptosis of human colorectal carcinoma HCT116 cells. *Oncol Rep* (2020) 44:1997–2008. doi: 10.3892/or.2020.7765
114. Coker-Gurkan A, Bulut D, Genc R, Arisan ED, Obakan-Yerlikaya P, Palavan-Unsal N. Curcumin prevented human autocrine growth hormone (GH) signaling mediated NF-kappaB activation and miR-183-96-182 cluster stimulated epithelial mesenchymal transition in T47D breast cancer cells. *Mol Biol Rep* (2019) 46:355–69. doi: 10.1007/s11033-018-4479-y
115. Kang HJ, Lee SH, Price JE, Kim LS. Curcumin suppresses the paclitaxel-induced nuclear factor-kappaB in breast cancer cells and potentiates the growth inhibitory effect of paclitaxel in a breast cancer nude mice model. *Breast J* (2009) 15:223–9. doi: 10.1111/j.1524-4741.2009.00709.x
116. Anand P, Sundaram C, Jhurani S, Kunnumakkara AB, Aggarwal BB. Curcumin and cancer: an "old-age" disease with an "age-old" solution. *Cancer Lett* (2008) 267:133–64. doi: 10.1016/j.canlet.2008.03.025
117. Ferri C WK, Otero K, Kim YH. Effectiveness of curcumin for treating cancer during chemotherapy. *Altern Complement Ther* (2018) 24:13–8. doi: 10.1089/act.2017.29147.yhk
118. Abbas MN, Kausar S, Cui H. Therapeutic potential of natural products in glioblastoma treatment: targeting key glioblastoma signaling pathways and epigenetic alterations. *Clin Transl Oncol* (2020) 22:963–77. doi: 10.1007/s12094-019-02227-3
119. Xiang Y, Guo Z, Zhu P, Chen J, Huang Y. Traditional Chinese medicine as a cancer treatment: Modern perspectives of ancient but advanced science. *Cancer Med* (2019) 8:1958–75. doi: 10.1002/cam4.2108
120. Asadi S, Gholami MS, Siassi F, Qorbani M, Sotoudeh G. Beneficial effects of nano-curcumin supplement on depression and anxiety in diabetic patients with peripheral neuropathy: A randomized, double-blind, placebo-controlled clinical trial. *Phytother Res* (2020) 34:896–903. doi: 10.1002/ptr.6571

121. Hassaniazad M, Inchehsablagh BR, Kamali H, Tousi A, Eftekhar E, Jaafari MR, et al. The clinical effect of Nano micelles containing curcumin as a therapeutic supplement in patients with COVID-19 and the immune responses balance changes following treatment: A structured summary of a study protocol for a randomised controlled trial. *Trials* (2020) 21:876. doi: 10.1186/s13063-020-04824-y
122. Heshmati J, Golab F, Morvaridzadeh M, Potter E, Akbari-Fakhrabadi M, Farsi F, et al. The effects of curcumin supplementation on oxidative stress, Sirtuin-1 and peroxisome proliferator activated receptor gamma coactivator 1alpha gene expression in polycystic ovarian syndrome (PCOS) patients: A randomized placebo-controlled clinical trial. *Diabetes Metab Syndr* (2020) 14:77–82. doi: 10.1016/j.dsx.2020.01.002
123. Saghatelyan T, Tananyan A, Janoyan N, Tadevosyan A, Petrosyan H, Hovhannisyan A, et al. Efficacy and safety of curcumin in combination with paclitaxel in patients with advanced, metastatic breast cancer: A comparative, randomized, double-blind, placebo-controlled clinical trial. *Phytomedicine* (2020) 70:153218. doi: 10.1016/j.phymed.2020.153218

Conflict of Interest: The authors declare that the research was conducted in the absence of any commercial or financial relationships that could be construed as a potential conflict of interest.

frontiers in Oncology

ORIGINAL RESEARCH
published: 13 April 2021
doi: 10.3389/fonc.2021.653902

Fucoidan Inhibits the Progression of Hepatocellular Carcinoma *via* Causing lncRNA LINC00261 Overexpression

Danhui Ma[1,2†], *Jiayi Wei*[1,2†], *Sinuo Chen*[1,2†], *Heming Wang*[1,2], *Liuxin Ning*[1,2], *Shi-Hua Luo*[3], *Chieh-Lun Liu*[4], *Guangqi Song*[1,2*] *and Qunyan Yao*[1,2*]

[1] Department of Gastroenterology and Hepatology, Zhongshan Hospital of Fudan University, Shanghai, China, [2] Shanghai Institute of Liver Diseases, Shanghai, China, [3] Department of Traumatology, Rui Jin Hospital, School of Medicine, Shanghai Jiao Tong University, Shanghai, China, [4] Department of Clinical Research and Development, Hi-Q Marine Biotech International Ltd., Taipei, Taiwan

OPEN ACCESS

Edited by:
Yongye Huang,
Northeastern University, China

Reviewed by:
Yuchen Liu,
Shenzhen University, China
Wanhua Xie,
Shenyang Medical College, China
Xiangbao Yin,
Second Affiliated Hospital of Nanchang University, China

***Correspondence:**
Qunyan Yao
yao.qunyan@zs-hospital.sh.cn
Guangqi Song
song_guangqi@fudan.edu.cn

[†]These authors have contributed equally to this work and share first authorship

Specialty section:
This article was submitted to Pharmacology of Anti-Cancer Drugs, a section of the journal Frontiers in Oncology

Received: 15 January 2021
Accepted: 12 March 2021
Published: 13 April 2021

Citation:
Ma D, Wei J, Chen S, Wang H, Ning L, Luo S-H, Liu C-L, Song G and Yao Q (2021) Fucoidan Inhibits the Progression of Hepatocellular Carcinoma via Causing lncRNA LINC00261 Overexpression. Front. Oncol. 11:653902. doi: 10.3389/fonc.2021.653902

Hepatocellular carcinoma (HCC) as a main type of primary liver cancers has become one of the most deadly tumors because of its high morbidity and poor prognosis. Fucoidan is a family of natural, heparin-like sulfated polysaccharides extracted from brown algae. It is not only a widely used dietary supplement, but also participates in many biological activities, such as anti-oxidation, anti-inflammation and anti-tumor. However, the mechanism of fucoidan induced inhibition of HCC is elusive. In our study, we demonstrated that fucoidan contributes to inhibiting cell proliferation *in vivo* and *in vitro*, restraining cell motility and invasion and inducing cell cycle arrest and apoptosis. According to High-Throughput sequencing of long-non-coding RNA (lncRNA) in MHCC-97H cells treated with 0.5 mg/mL fucoidan, we found that 56 and 49 lncRNAs were correspondingly up- and down-regulated. LINC00261, which was related to the progression of tumor, was highly expressed in fucoidan treated MHCC-97H cells. Moreover, knocking down LINC00261 promoted cell proliferation by promoting the expression level of miR-522-3p, which further decreased the expression level of downstream SFRP2. Taken together, our results verified that fucoidan effectively inhibits the progression of HCC *via* causing lncRNA LINC00261 overexpression.

Keywords: fucoidan, hepatocellular carcinoma, long non-coding RNA, high-throughput sequencing, LINC00261

INTRODUCTION

As one of the most common types of cancer, hepatocellular carcinoma (HCC) is currently reported to be the third leading cause of cancer-related death worldwide (1) and accounts for 75% of all primary liver cancers (2). Epidemiology showed that the incidence rate of liver cancer has increased by nearly 4 times over the past 40 years (3). Surgical interventions are usually the main treatment for early HCC. However, the five-year recurrence rate after surgery reaches up to 50%-70% and only 15% of these cases could be resected repeatedly, which greatly limits the therapeutic effect of surgical resection (4). Interventional therapy such as transcatheter arterial chemoembolization (TACE) is

recommended as the standard treatment for patients with unresectable liver cancer. Although TACE prolongs the life of patients with advanced liver cancer to a certain extent, some patients develop TACE refractoriness after two cycles of treatment resulting in insufficient treatment effect and the mortality related to side effects of TACE reaches 0.5% (5, 6). Traditional cytotoxic drugs are limited in clinical application due to their high toxicity and side effects. While first-line recommended molecular targeted drugs, such as sorafenib and lenvatinib, are superior to traditional chemotherapy drugs in terms of safety and efficacy, which could only prolong the survival time of patients for several months due to the serious decline of liver function in patients with advanced HCC (7). The cell programmed death protein-1 (PD-1) inhibitors also showed definite efficacy only in 15%-20% of patients with advanced HCC (8). HCC has become one of the most malignant tumors with extremely difficulty to cure due to its high recurrence rate and strong drug resistance. Therefore, it is urgent to reveal the mechanism of HCC occurrence and development, develop new targets and effective targeted molecules.

Fucoidan is a family of natural, heparin-like sulfated polysaccharides extracted from brown algae. Its structure is highly dependent on the species of algae, but has common characteristics of the backbone of sulfated fucoidan (9). In the past few years, attention was paid to the research of fucoidan and large numbers of products containing fucoidan extract were developed. In 2003, a drug named "Haikun Shenxi Capsule" was approved for the treatment of chronic renal failure in China (10). In the United States and Europe, the use of fucoidan in supplements and cosmetics was also ratified by regulatory authorities (11). Till now, a series of studies have reported its effects on anti-oxidation, anti-coagulation, anti-thrombosis, immune regulation, anti-virus (12–16). Recent research demonstrated that fucoidan have certain therapeutic value for fatty liver and liver fibrosis in zebrafish (17). Fucoidan was also confirmed to have an anti-tumor effect, and as a natural product, it is considered to be safer than other classic chemotherapy drugs. This polymer could reduce the migration and metastasis ability of cancer cells (18), but also play an anti-tumor effect through arresting cell cycle, inducing apoptosis (19, 20), enhancing cancer immunity (21, 22) or inhibiting tumor angiogenesis (23). Since the mechanism of fucoidan in the treatment of HCC was not fully confirmed, our study will mainly explore the molecular mechanism of fucoidan in the occurrence, development and metastasis of HCC.

According to statistics, only about 2% of all the transcripted mammalian genomes are involved in protein coding (24). Of all the non-coding RNAs, those with length greater than 200 nucleotides were further identified as lncRNAs (25). At the very beginning, lncRNAs were regarded as the "garbage" of genome transcription, which was the by-product of RNA polymerase II transcription and had no biological function. With the development of High-Throughput sequencing technology, our understanding of lncRNAs was gradually improved. Through the progression of various studies in recent years, lncRNAs were observed to participate in complex biological activities. They serve as RNA scaffolds (26, 27), RNA guides (28), RNA decoys (29) or molecular sponges (30, 31) to regulate cell growth, differentiation, and establish cell identity, which are usually uncontrolled in cancer. Various studies already revealed that the aberrant expression and mutations of lncRNA are closely related to tumor occurrence and metastasis (32–35). H19 (36–38), HOTAIR (39–41), MALAT1 (42–44) and some other well-studied lncRNAs were proved to be able to influence the development of liver cancer through a variety of cellular regulatory mechanisms, such as regulating tumor suppressor genes (36), affecting cell cycle and apoptosis factors (45, 46), impacting the function of downstream microRNAs (miRNA) (30) and interrupting signaling pathways (35). Moreover, lncRNAs are also considered to be involved in regulating the characteristics of cancer stem cells (47) and may be related to the generation of drug resistance in some tumors (48, 49). Therefore, it is very promising to identify lncRNA functions, figure out their relationship with HCC and develop new strategies for diagnosis and trageted therapy based on lncRNAs.

Compared with small molecule chemical drugs, natural products have higher therapeutic safety. They also could affect the expression level of lncRNAs, which is crucial for tumor progression (50–53). In this research, we confirmed that fucoidan could effectively inhibit the progression of HCC. High-Throughput sequencing was used to detect and obtain the expression profile of lncRNAs in MHCC-97H cells treated with fucoidan. According to the analysis results, differentially expressed lncRNAs after fucoidan treatment, which are related to the occurrence and development of HCC, were selected to verify the effect of fucoidan. In this study, we demonstrated that fucoidan inhibits the proliferation and invasion of HCC cells by up-regulating LINC00261. Overexpression of LINC00261 regulates downstream miR-522-3p to play an anti-tumor role, which may provide potential new molecules and new targets for clinical treatment of HCC. The results demonstrated that LINC00261 inhibits proliferation and invasion of HCC cells by regulating miR-522-3p, which provided potential new molecules and new targets for clinical treatment of liver cancer.

MATERIALS AND METHODS

Cell Culture

The MHCC-97H and Hep3B cell lines were obtained from Zhongshan Hospital of Fudan University. MHCC-97H and Hep3B cells were cultured in complete DMEM supplemented with 10% fetal bovine serum, 1% penicillin and streptomycin. The cell culture environment was 37 °C with 5% CO2.

Reagents and Antibodies

Fucoidan powder was acquired from Hi-Q Marine Biotech International Ltd. Saline was used as solvent for fucoidan solutions. The storage concentration was 5 mg/mL, and then further diluted to the final required concentration (0.25 mg/mL and 0.5 mg/mL). The powder and solution are sealed and stored

at 4 °C. Antibody against SFRP2 was purchased from Proteintech (12189-1-AP).

Cell Morphological Examination

1×10^5 cells per well were seeded on the 12-well plate overnight. The adherent cells were then treated with saline, 0.25 mg/mL and 0.5 mg/mL fucoidan for 48 h. The cell morphology was recorded under microscope (Olympus, IX73) at 48 h after fucoidan treatment. All the pictures were taken under 20 times magnification. Each group had three independent duplications.

Cell Proliferation

1×10^5 cells per well were seeded on 6-well plate overnight. The adherent cells were treated with 0.25 mg/mL and 0.5 mg/mL fucoidan for 48 h. Cells are digested and resuspended after 48 h and counted by blood counting chamber and presented as the mean ± standard deviation (SD) from three independent duplications.

Cell Viability Assay (CCK-8 Assay)

We used the WST-8-based detection method to analyze the cell viability according to the instructions of a CCK-8 kit (Yeasen). 2000 cells were seeded to the 96-well plate overnight. The adherent cells were treated with 0.25 mg/mL and 0.5 mg/mL fucoidan for the indicated times (0, 24, 48 and 72 h). 10 μL CCK-8 reagent and 90 μL medium were added per well and incubated for 2 h. After incubation, a multifunctional reader (MD FlexStation3) was used to detect the absorbance of the cells at 450 nm. There were three repetitions in each group and values were presented as the mean ± standard deviation (SD).

Clone Formation Assay

2500 cells were seeded on 6-well plates overnight and were then treated with 0.5 mg/mL fucoidan for 7-10 days according to the cell condition. The cells were then fixed with 4% paraformaldehyde for 15 min. After that, the fixative was washed out, and 0.1 g/mL crystal violet was added for 15 min for staining. The clones were recorded by camera and was counted by ImageJ. Each group had three independent repetitions.

Wound Healing Assay

6×10^5 cells were seeded into the 6-well plate. The cells were cultured in complete DMEM for 12 h to 90%-95% density, sterile pipette tip was used to draw a line vertically in the middle of each well. Then, cell debris was removed with preheated PBS twice, and the cells were treated with 0.25 mg/mL and 0.5 mg/mL fucoidan in FBS-free DMEM. Images were collected 0 h and 48 h later to measure the distance of wound. The wound closure rate is equal to the distance of the wound at 48 h divided by the distance of the wound at 0 h. There were three independent repetitions in each group and values were presented as the mean ± standard deviation (SD).

Cell Invasion Assay

Transwell assay was carried out by using 8 μm transwell chamber according to the manual (BD Science). 1×10^5 cells per well were digested and washed with serum-free DMEM for three times before seeding into the upper chamber. Serum-free DMEM was used to dissolve fucoidan to 0.5 mg/mL and the cells were resuspended at a volume of 100 μL per well and planted into the upper chamber, while 600 μL DMEM supplemented with 20% FBS and 0.5 mg/mL fucoidan was added into the lower chamber. After 48 h, the films were removed, washed with PBS twice and fixed with 4% paraformaldehyde for 15 min. 0.1% crystal violet was used to stain the film for 15 min and then the upper side of the film was carefully wiped with cotton swabs. The cells were recorded with microscope and the total area of cells was counted by ImageJ and values were presented as the mean ± standard deviation (SD). Each group had three independent repetitions.

Cell Cycle Assay

After seeding 6-well plates with 8×10^5 cells per well, the cells were cultured in medium containing 0.25 mg/mL, 0.5 mg/mL fucoidan for 48 h. The cell cycle was detected by a cell cycle and apoptosis kit (Beyotime Biotechnology) and flow cytometry according to standard instructions.

Cell Apoptosis Assay

Cell apoptosis was analyzed by flow cytometry as per the FITC-conjugated Annexin V/PI method (Annexin V-FITC/PI apoptosis kit, Beyotime Biotechnology). 2×10^5 cells were seeded into the 6-well plates. After 48 h treatment of 0.25 mg/mL and 0.5 mg/mL fucoidan, the adherent and suspended cells in each well were collected and resuspended in 195 μL binding buffer, following which Annexin V-FITC (5 μL) and PI (10 μL) were added to each sample and mixed. Cells were incubated for 15 min in the dark at 4 °C and then analyzed by flow cytometry. Each group had three independent repetitions and values were presented as the mean ± standard deviation (SD).

RNA Extraction and qRT-PCR

Total RNA was extracted by TRIzol (Invitrogen) according to the manual. Then the RNA was reverse-transcribed to cDNA using the Hifair® III 1st Strand cDNA Synthesis SuperMix kit (Yeasen) following the manufacturer's instructions. The concentration and purity of each sample was tested by DS-11 Spectrophotometer (DeNovix). Equivalent amounts of cDNA were used for real-time PCR in a 20 μL reaction mixture using the Hieff® qPCR SYBR® Green Master Mix kit (Yeasen). Primers for qRT-PCR were as shown in **Supplementary Table S3**. The internal reference gene for lncRNA was GAPDH. QuantStudio5 (Applied Biosystems™) was used to perform the real-time fluorescent quantitative PCR, while ProFlex PCR system (Applied Biosystems™) was used to perform reverse-transcription. Relative levels in each sample were calculated based on their threshold cycle (Ct) values, $2^{-\Delta\Delta Ct}$ method was used. Each sample had three independent repetitions.

siRNA Interference

The siRNA for LINC00261 knockdown was customized from GenePharma. Before transfection, cells were plated in 60 mm dish and transfected with si-LINC00261 at the 60%-80%

confluence. The ribo FECT^{TM} CP Transfection kit (RiboBio) was used to perform the transfection according to the manufacturer's protocol. Every siRNA had a scrambled siRNA as negative control. The cells were incubated at 37 °C in a 5% CO2 incubator for 48 h, then the LINC00261 expression was examined by qRT-PCR.

High-Throughput Sequencing

To verify the change of lncRNA and mRNA expression after fucoidan treatment, High-Throughput sequencing was performed by GENEWIZ®. The cells were treated with saline and 0.5 mg/mL fucoidan for 48 h in T25 flasks. Cells were then digested and transferred into 1.5 mL tubes, the number of cells per tube is around 3×10^5. Total RNA was extracted by TRIzol (Invitrogen) according to the manual and was frozen to -80 °C. Ribosomal deletion RNA was used to build the sequencing library, thus the Illumina NovaSeq machine (Illumina) using a 2×150 paired-end (PE) configuration was used to perform the sequencing. Data with adapters and QCs less than 20 was removed using cutadapt (v1.9.1) to get the final clean record. Next, we used Hisat2 (v2.0.1) to analyze and map the clean data to the reference human genome. The count of each transcript was obtained by using rsem (v1.2.15) after quantification and annotation. Finally, the transcripts were standardized and analyzed for differential expression using DESeq2. The sequencing data was submitted to the Sequence Read Archive (SRA) data set with registration number PRJNA (PRJNA690771).

Differential Expression Analysis

Differential expression analysis used the DESeq2 or EdgeR Bioconductor package, a model based on the negative binomial distribution. The estimates of dispersion and logarithmic fold changes incorporate data-driven prior distributions, Padj of genes were setted <0.05 to detect differential expressed ones.

GO and KEGG Enrichment Analysis

GOSeq(v1.34.1) was used to identify Gene Ontology (GO) terms that annotate a list of enriched genes with a significant Padj less than 0.05. KEGG (Kyoto Encyclopedia of Genes and Genomes) is a collection of databases dealing with genomes, biological pathways, diseases, drugs, and chemical substances (http://en.wikipedia.org/wiki/KEGG). We used scripts in house to enrich significant differential expression gene in KEGG pathways.

Xenograft Tumor Model

All animal investigation in our study was conformed to the guidelines of Animal Care and Use Committee, Zhongshan Hospital of Fudan University. Balb/c nude mice were purchased from Vital River Laboratory Animal Technology Co., Ltd. 1×10^7 MHCC-97H cells were subcutaneously injected into 4 weeks old female mice. After two weeks, mice bearing tumors were randomly divided into two groups: the Ctrl group (saline) and the Fuc group (15 mg/kg per day). Each group consisted of five mice, which were orally fed for three weeks. Body weights of mice were measured every week. Tumor volume was measured by using the formula $V = (a \times b^2)/2$ (V is volume, a is the length of the tumor, b is the width of the tumor).

Statistical Analysis

Statistical analysis was performed using GraphPad 8.4.3. The analysis was carried out using Student's t test (N.S. means not significant, * means $P < 0.05$, ** means $P < 0.01$, *** means $P < 0.001$, **** means $P < 0.0001$).

RESULTS

Fucoidan Inhibits Proliferation of HCC *In Vitro* and *In Vivo*

The fucoidan we used contains a repetitive unit consisting of disaccharides including α-1,3-fucose and α-1,4-linked fucose with arms affixed to C2 position (54). To verify whether fucoidan could inhibit the proliferation of HCC, we treated MHCC-97H cells with saline (Ctrl), 0.25 and 0.5 mg/mL fucoidan (Fuc) for 48 h. Compared with the Ctrl group, fucoidan obviously restrained proliferation of MHCC-97H cells in a concentration-dependent manner and the morphological changes of cell apoptosis such as budding and vacuolation could be observed (**Figure 1A**). To further confirm this observation, we carried out cell proliferation experiment. Equal number of cells were treated with saline, 0.25 mg/mL and 0.5 mg/mL fucoidan respectively for 48 h. The results disclosed that the proliferation ability of the cells was slowed down after fucoidan treatment and the inhibitory effect was positively correlated with the dosages (**Figure 1B**). Similar results were obtained in the experiment repeated with Hep3B cells (**Figure 1C**). We additionally performed cell viability assay with both MHCC-97H and Hep3B cells respectively treated with saline, 0.25 mg/mL and 0.5 mg/mL fucoidan for 24 h, 48 h and 72 h. The results suggested that fucoidan suppressed cell viability and the inhibitory effect was manifested at 48 h (**Figures 1D, E**). The clone formation result further confirmed the inhibitory effect of fucoidan on HCC cell proliferation compared with the Ctrl group (**Figure 1F**).

To determine whether fucoidan inhibit HCC cell proliferation *in vivo*, we performed xenograft tumor model. 1×10^7 MHCC-97H cells were subcutaneously injected into 4 weeks old female Balb/c nude mice. After two weeks, 15 mg/kg Fuc were orally fed per day for three weeks. Body weights of mice were measured every week. Tumor weight and volume were recorded at the end of treatment. The results suggested that fucoidan not only is nearly no toxicity to mice (**Figure 2A**), but obviously decreased tumor weight and volume *in vivo* (**Figures 2B–D**).

Fucoidan Inhibits Motility and Invasion of HCC Cells

To determine whether fucoidan could affect cell motility in HCC, wound healing assay was performed. As shown in **Figure 3A**, the relative wound width of Ctrl group was significantly lower than that of fucoidan treatment group, while cells treated with 0.5 mg/mL fucoidan showed better performance than those treated

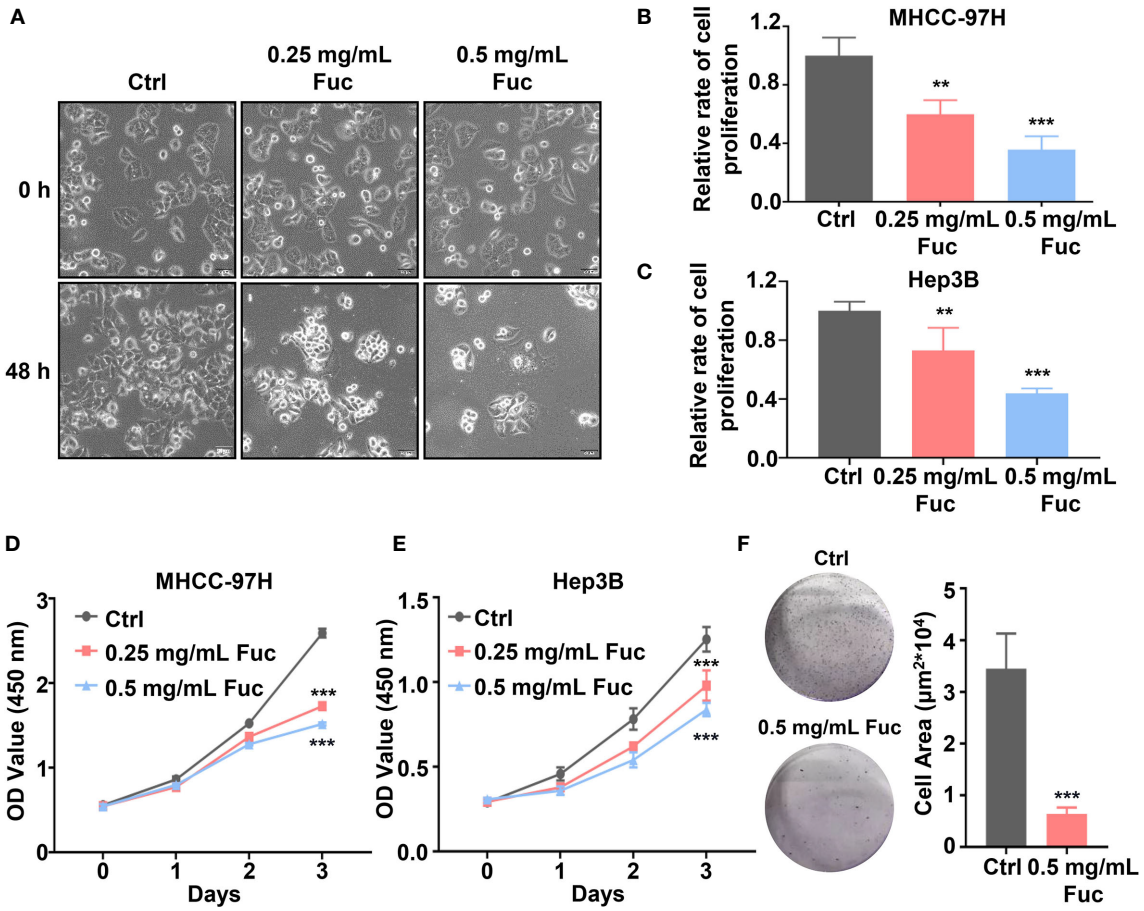

FIGURE 1 | Fucoidan inhibits proliferation of hepatocellular carcinoma *in vitro*. **(A)** Morphology of MHCC-97H cells treated with saline (Ctrl), 0.25 and 0.5 mg/mL Fuc. **(B, C)** Relative cell proliferation rate of MHCC-97H **(B)** and Hep3B **(C)** cells after treatment with saline (Ctrl), 0.25 and 0.5 mg/mL Fuc. ** means $P < 0.01$, *** means $P < 0.001$. **(D, E)** Cell viability of MHCC-97H **(D)** and Hep3B **(E)** cells treated with saline (Ctrl), 0.25 and 0.5 mg/mL Fuc. *** means $P < 0.001$. **(F)** Colony formation results of MHCC-97H cells treated with saline (Ctrl) and 0.5 mg/mL Fuc. *** means $P < 0.001$.

with 0.25 mg/mL, suggesting that fucoidan has inhibitory effect on cell motility and the effect is also dose-dependent (**Figures 3A, B**). Transwell assay was further conducted to verify the effect of fucoidan on the invasion ability of HCC cells. The results revealed that the number of cells penetrating the membrane decreased in the fucoidan treatment group, which confirmed that fucoidan decreased the invasion ability of the HCC cells (**Figure 3C**). Based on the above results, we preliminarily confirmed that fucoidan could inhibit the proliferation, motility and invasion of HCC cells.

Fucoidan Induces Apoptosis and Cell Cycle Arrest in HCC Cells

To gain further insight into the involvement of fucoidan in HCC development, we used flow cytometry to detect the cell cycle distribution and apoptosis rate of MHCC-97H cells treated with fucoidan. Similarly, we seeded the cells in medium with saline, 0.25 mg/mL and 0.5 mg/mL fucoidan for 48 h. As shown in **Figure 4A**, treatment of MHCC-97H cells with higher dosage of fucoidan increased the S phase distribution, which indicated that fucoidan could induce cell cycle arrest at S phase in a dose-dependent manner (**Figures 4A, B**). Meanwhile, higher apoptosis rate was observed in fucoidan treated group rather than that of the control group, which was positively correlated with the concentration of fucoidan. This result further prompts that fucoidan also promotes the apoptosis of HCC cells (**Figures 4C, D**). Therefore, our data demonstrated that fucoidan is able to arrest cell cycle and promote apoptosis of HCC cells.

Fucoidan Contributes to the Alteration of lncRNAs Profiling in HCC

To clarify the mechanism how fucoidan inhibits the development of HCC, we performed High-Throughput sequencing of lncRNAs in MHCC-97H cells with 0.5 mg/mL fucoidan treatment for 48 h. From the analysis of heatmap result, we could visually observe that large numbers of lncRNAs significantly altered. About 75% of all

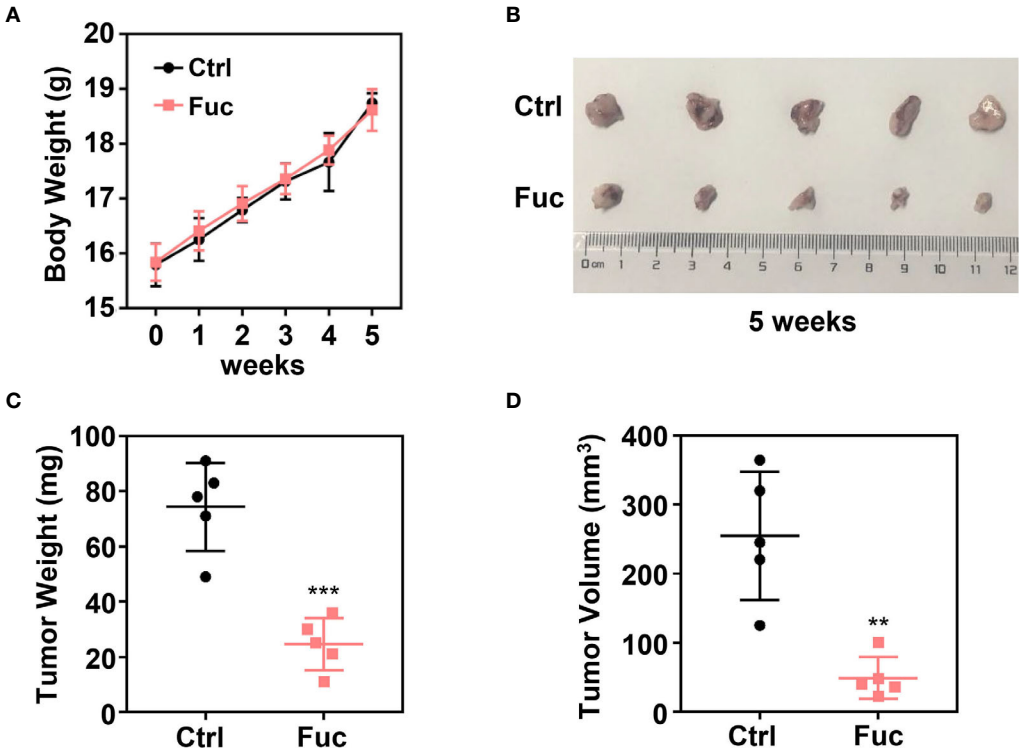

FIGURE 2 | Fucoidan inhibits proliferation of hepatocellular carcinoma *in vivo*. **(A)** Body weight of the Ctrl group and Fuc group (15 mg/kg Fuc per day, dissolved in saline). **(B)** Xenograft tumor formation of the Ctrl group and Fuc group. **(C)** Tumor weight of the Ctrl group and Fuc group. *** means $P < 0.001$. **(D)** Tumor volume of the Ctrl group and Fuc group. ** means $P < 0.01$.

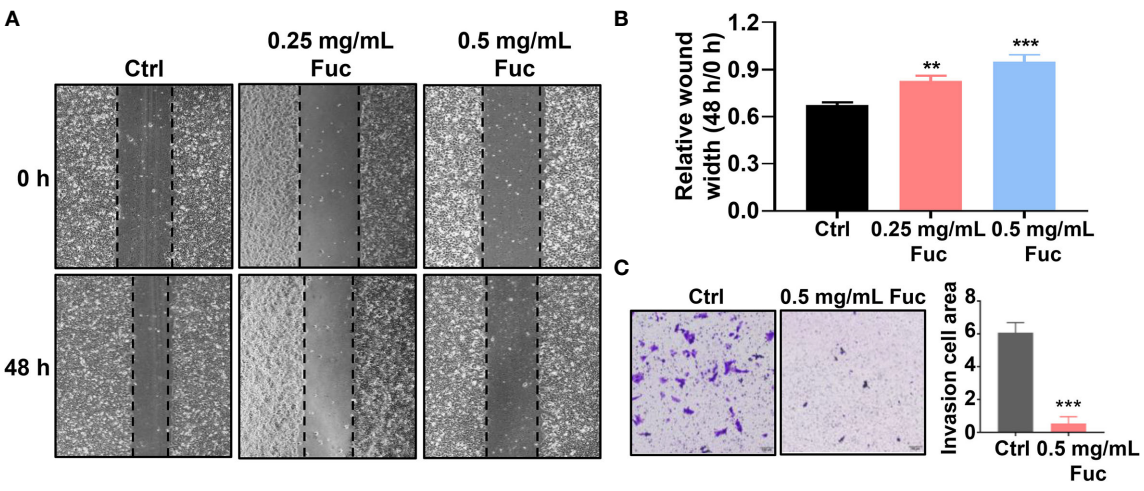

FIGURE 3 | Fucoidan inhibits motility and invasion of hepatocellular carcinoma cells. **(A, B)** Wound healing results of MHCC-97H treated with saline (Ctrl), 0.25 and 0.5 mg/mL Fuc. ** means $P < 0.01$, *** means $P < 0.001$. **(C)** Transwell results of MHCC-97H treated with saline (Ctrl) and 0.5 mg/mL Fuc. *** means $P < 0.001$.

lncRNAs detected were previously annotated, while the remaining 25% were novel (**Figure 5A**). The detailed lncRNA names were listed in **Supplementary Tables S1** and **S2** (as shown in **Supplementary Material**). A total of 105 differentially expressed lncRNAs (DElncRNA) was identified with thresholds of $\log_2$ (Fold Change)>1 and adjusted $P<0.05$, of which 49 were down-regulated and 56 were up-regulated as presented by Volcano Plot result (**Figures 5B, C**). To better comprehend the underlying

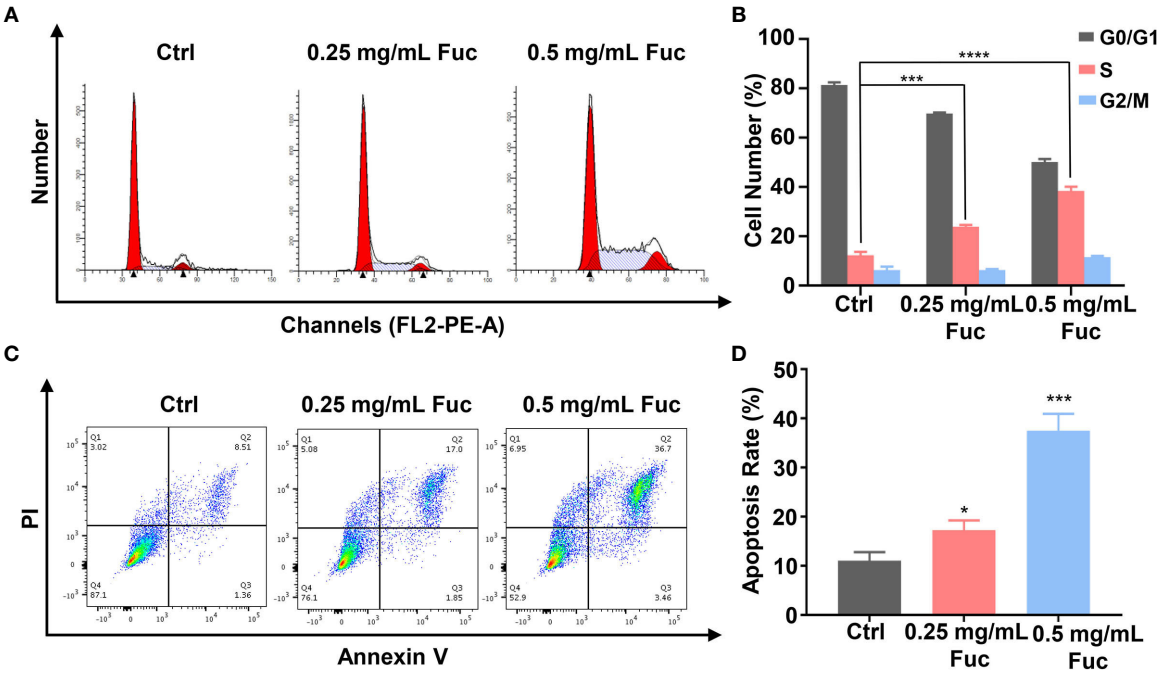

FIGURE 4 | Fucoidan arrests cell cycle and promotes apoptosis of MHCC-97H cells. **(A, B)** Cell cycle distribution was measured by flow cytometry in MHCC-97H cells induced by saline (Ctrl), 0.25 and 0.5 mg/mL Fuc. *** means $P < 0.001$, **** means $P < 0.0001$. **(C, D)** Percentage of apoptotic MHCC-97H cells after treatment with saline (Ctrl), 0.25 and 0.5 mg/mL Fuc. Q1 represents death cells, Q2 represents the late apoptosis cells, Q3 represents the ealry apoptosis cells, Q4 represents the normal cells. The apoptosis rate equals to the rate of late apoptosis cells (Q2) plus the rate of early apoptosis cells (Q3). * means $P < 0.05$, *** means $P < 0.001$.

mechanisms of these DElncRNAs in the tumorigenesis of HCC, we performed mRNA sequencing. Volcano plots diagram showed that 1633 mRNAs were down-regulated and 1737 mRNAs were up-regulated (**Figures 6A, B**). We further conducted KEGG pathway analysis, which suggested that downstream mRNAs regulated by lncRNA closely related to HCC. In addition, the apoptosis-relevant genes were significantly changed after treated with 0.5 mg/mL fucoidan in MHCC-97H cells (**Figure 6C**).

Fucoidan Obviously Increases the Expression Level of LINC00261 to Inhibit the Proliferation and Invasion of HCC Cells

To further verify whether these DElncRNAs play an important role in HCC tumorigenesis, we selected a lncRNA named LINC00261 from all the differentially expressed lncRNAs. LINC00261 was confirmed by other studies to act as a tumor suppressor gene in prostate cancer, breast cancer, pancreatic cancer and many other types of cancers. For example, LINC00261 was found to inhibit lung cancer cells by interfering with the expression of downstream miR-1269a (55). Another research also confirmed that LINC00261 could inhibit the transcription of c-Myc in pancreatic cancer, thereby inhibiting the proliferation and metastasis of pancreatic cancer cells (56). According to our sequencing results, LINC00261 was significantly up-regulated in fucoidan treated group ($\log_2$ (fold change)=3.45). Since the anti-tumor effect of LINC00261 in HCC was rarely reported, we chose LINC00261 as the target of our further study. To explore the role of LINC00261 in HCC tumorigenesis, si-LINC00261 (si-LINC00261-1, si-LINC00261-2 and si-LINC00261-3) were respectively transfected in MHCC-97H cells. Scramble siRNA transfection was used as negative control. Then we used qPCR to detect the relative mRNA expression level of LINC00261 in MHCC-97H cells. The results showed that the expression level of LINC00261 decreased after transfection of three kinds of siRNAs and the knockdown effect of si-LINC00261-2 was the most significant. Then si-LINC00261-2 was selected for the follow-up experiments (**Figure 7A**). To demonstrate the effect of LINC00261 on cell proliferation and viability, we conducted the cell proliferation and viability assay after si-LINC00261-2 transfection. As shown in **Figure 7B**, after LINC00261 was knocked down, the relative proliferation rate of MHCC-97H cells was significantly increased than that of negative control group, and CCK-8 experiment also proved that HCC cell viability was improved after si-LINC00261-2 was transfected (**Figure 7C**). In addition, wound healing assay was carried out in MHCC-97H cells transfected with scrambled siRNA and si-LINC00261-2 to investigate the effect of LINC00261 on the motility of HCC cells. Results revealed that LINC00261 also inhibit the motility of HCC cells (**Figures 7D, E**). Based on the above results, we testified that fucoidan is able to increase the expression level of LINC00261, which plays an anti-tumor role by inhibiting the proliferation, viability and motility of HCC cells.

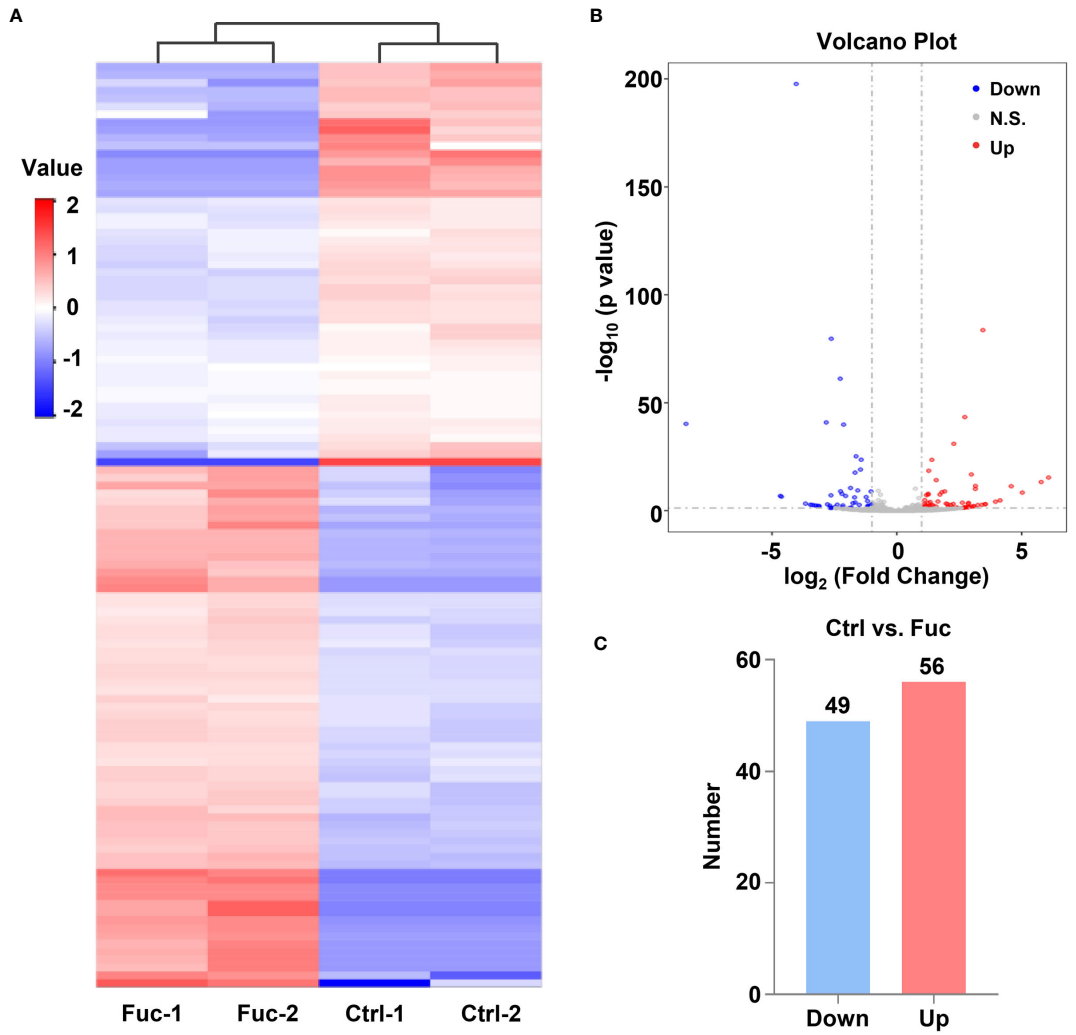

FIGURE 5 | Fucoidan contributes to the alteration of lncRNAs profiling in MHCC-97H cells. **(A)** Heatmap shows clustering analysis of differentially expressed lncRNAs treated with saline (Ctrl) and 0.5 mg/mL Fuc. Each group had two duplicated experiments. **(B)** Volcano plots presents significantly different expression profiles of lncRNAs in MHCC-97H cells treated with saline and 0.5 mg/mL Fuc. Vertical lines referred to 2-fold changes in up-regulation and down-regulation. Horizontal line corresponds to p=0.05. Blue and red points represent to down- and up-regulation with statistical significance. **(C)** Numbers of significantly down- and up-regulated lncRNAs in MHCC-97H cells treated with 0.5 mg/mL Fuc.

LINC00261 Inhibits Proliferation of MHCC-97H Cells *via* Regulating miR-522-3p

To explore whether LINC00261 could target miRNAs in MHCC-97H cells, we examined the expression level of miR-1296a, miR-105, miR-522-3p and miR-552-5p (55, 57–59), which were reported to bind LINC00261. The qPCR results suggested that miR-522-3p was remarkably decreased by comparing fucoidan treated group with the Ctrl group (**Figure 8A**). Then we added equivalent saline, 0.25 mg/mL fucoidan and 0.5 mg/mL fucoidan into MHCC-97H cells and examined the expression level of miR-522-3p by qPCR. The results showed that fucoidan down-regulated miR-522-3p in dose-dependent manner (**Figure 8B**). MiR-522-3p mimic and inhibitor synthesized from GenePharma were separately transfected in MHCC-97H cells (**Figure 8C**). The results suggested that miR-522-3p mimic increased and miR-522-3p inhibitor decreased the proliferation rate of MHCC-97H cells (**Figure 8D**). Besides, we also examined the cell viability by CCK-8 assay and discovered that miR-522-3p mimic promoted, miR-522-3p inhibitor inhibited the cell viability of HCC cells (**Figure 8E**). To further address the mechanism of fucoidan inhibiting the cell viability of HCC cells by regulating miR-522-3p. MHCC-97H cells were transfected with miR-522-3p mimic and exposed to 0.5 mg/mL fucoidan at the same time. Compared with the only 0.5 mg/mL fucoidan treated group, miR-522-3p effectively rescued

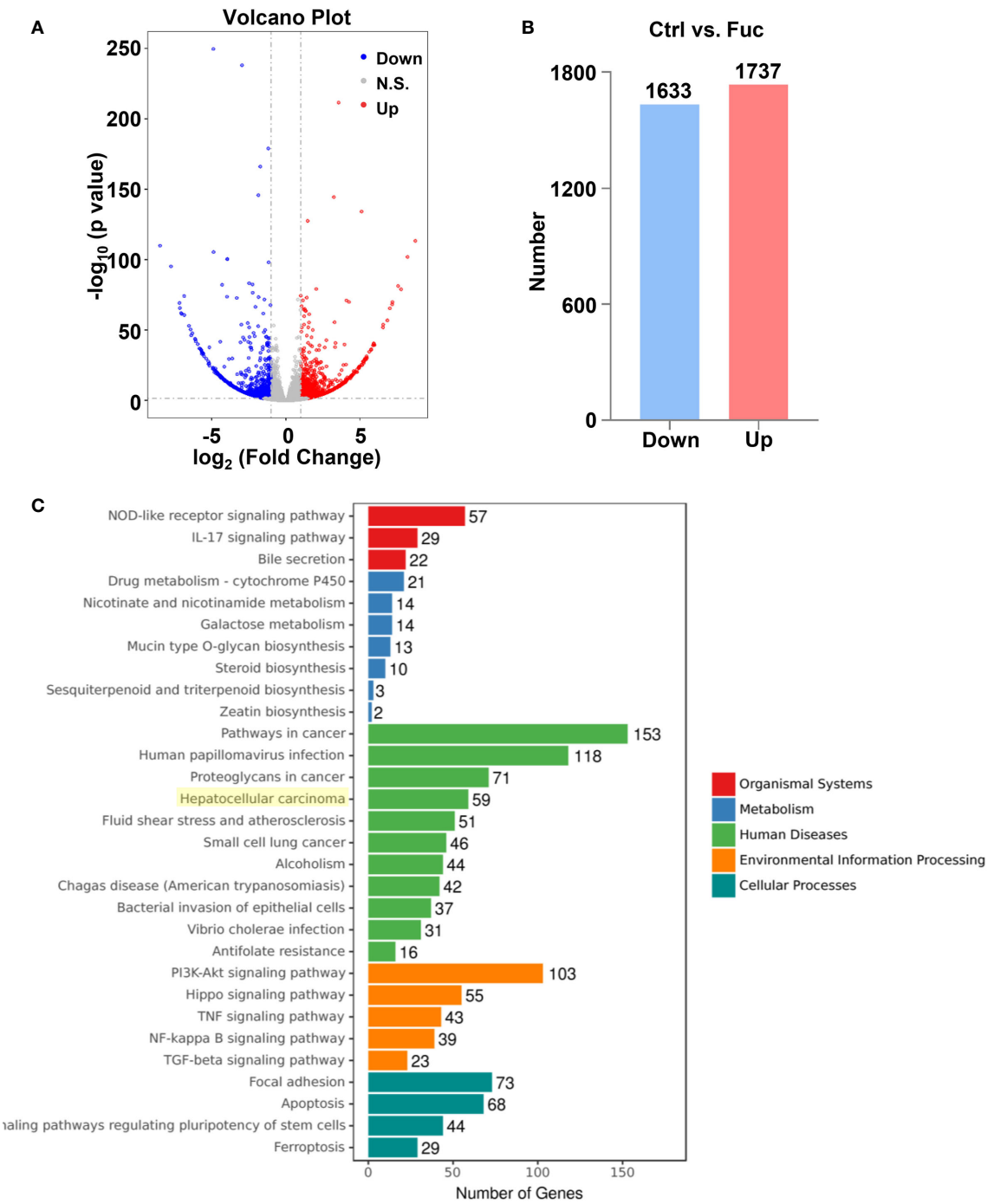

FIGURE 6 | The alteration of mRNAs profiling regulated by fucoidan in MHCC-97H cells. **(A)** Volcano plots presents significantly different expression profiles of mRNAs in MHCC-97H cells treated with 0.5 mg/mL Fuc. **(B)** Numbers of significantly down and up-regulated mRNAs in MHCC-97H cells treated with 0.5 mg/mL Fuc. **(C)** Enriched KEGG pathways of differentially expressed mRNAs after fucoidan treatment. p value < 0.05.

the inhibition of cell viability by fucoidan (**Figure 8F**). The transwell assay results further showed that overexpressing miR-522-3p promotes cell invasion of HCC and knocking down miR-522-3p inhibits cell invasion of HCC (**Figures 8G, H**). In conclusion, we demonstrated that fucoidan was able to increase the expression level of LINC00261, which inhibit cell proliferation and invasion of HCC *via* down-regulating miR-522-3p.

Previous studies (58) demonstrated that miR-522-3p binds to Wnt signaling related gene SFRP2 (secreted frizzled-related

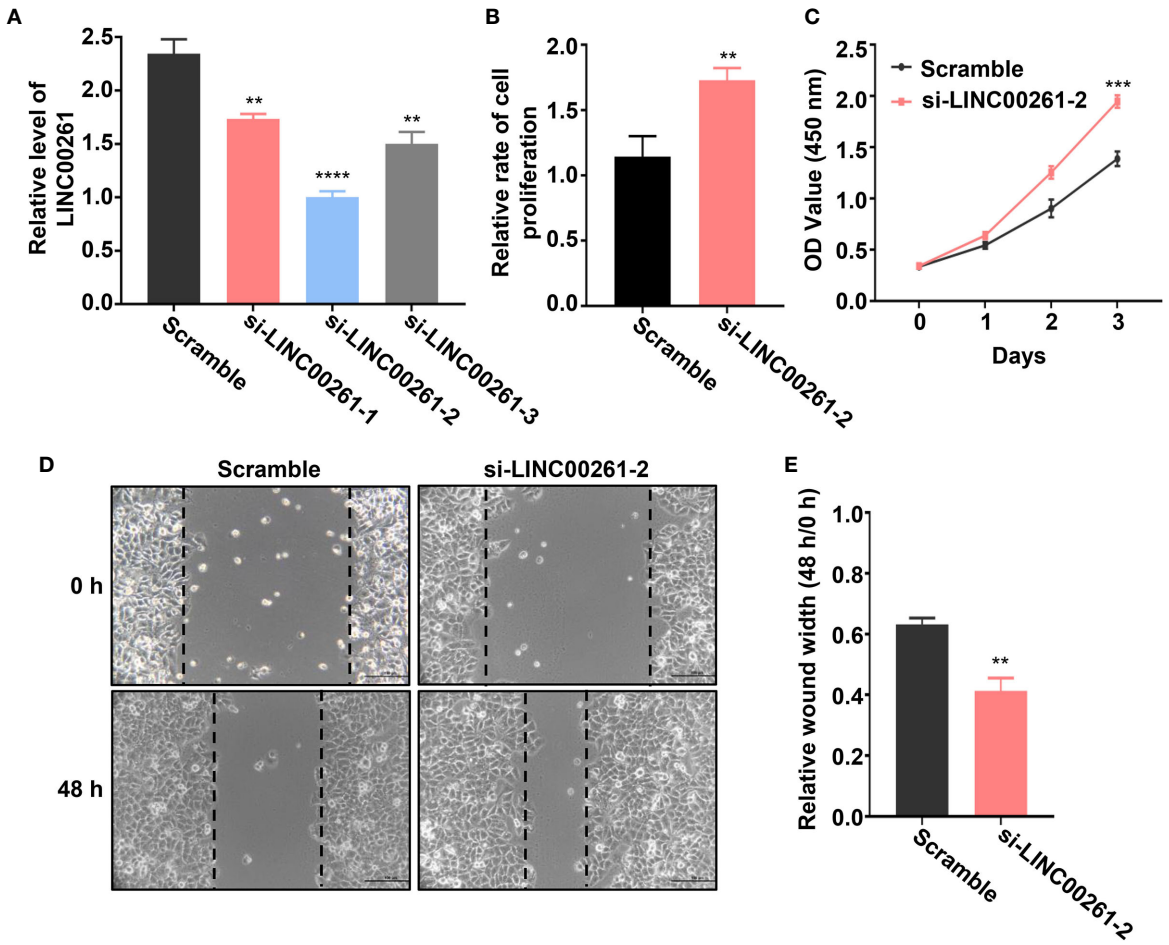

FIGURE 7 | **(A)** Relative LINC00261 expression level in MHCC-97H cells detected by qPCR after transfected with scramble siRNA, si-LINC00261-1, si-LINC00261-2 and si-LINC00261-3. ** means $P < 0.01$, **** means $P < 0.0001$. **(B)** Relative cell proliferation of MHCC-97H cells transfected with scramble siRNA and siLINC00261-2. ** means $P < 0.01$. **(C)** Cell viability of MHCC-97H transfected with scramble siRNA and si-LINC00261-2. *** means $P < 0.001$. **(D, E)** Wound healing results of MHCC-97H transfected with scramble siRNA and si-LINC00261-2. ** means $P < 0.01$.

protein 2) by base pairing. The qPCR result suggested that miR-522-3p could inhibit the expression level of SFRP2 (**Figure 9A**). Intriguingly, fucoidan increased the expression level of SFRP2 in a dose-dependent manner, which indicated that fucoidan up-regulates LINC00261 sponging miR-522-3p to increase the expression level of SFRP2 (**Figure 9B**). Western blots analysis also verified that fucoidan obviously increased the protein level of SFRP2 (**Figure 9C**).

DISCUSSION

Safe and effective treatment has always been a key issue in the field of clinical treatment. Although the research and development of various chemical and biological agents and immunotherapy already made some previously incurable diseases cured in recent years, therapeutic drugs with less side effects and toxicity still need to be further explored. Natural compounds were widely used in food, cosmetics and other industries for many years. Because of their high safety, many clinical and preclinical studies begun to pay attention to them (60–64). As a natural polysaccharide extracted from brown algae, fucoidan was proved to have many biological effects (12–16). The anti-tumor abilities of fucoidan were confirmed in pancreatic cancer, bladder cancer, ovarian cancer and other types of cancers (65–68). Fucoidan could inhibit the occurrence and development of tumor by regulating tumor immunity (21, 22), inhibiting angiogenesis (23), interfering with cell cycle and apoptosis (19, 20), which is considered to have a broad prospect in the field of tumor therapy.

HCC has become the leading cause of cancer-related death worldwide (2). In view of the high incidence rate and mortality rate of HCC, diagnosis and treatment have always been a hot topic (3). Currently, the main treatment of HCC includes

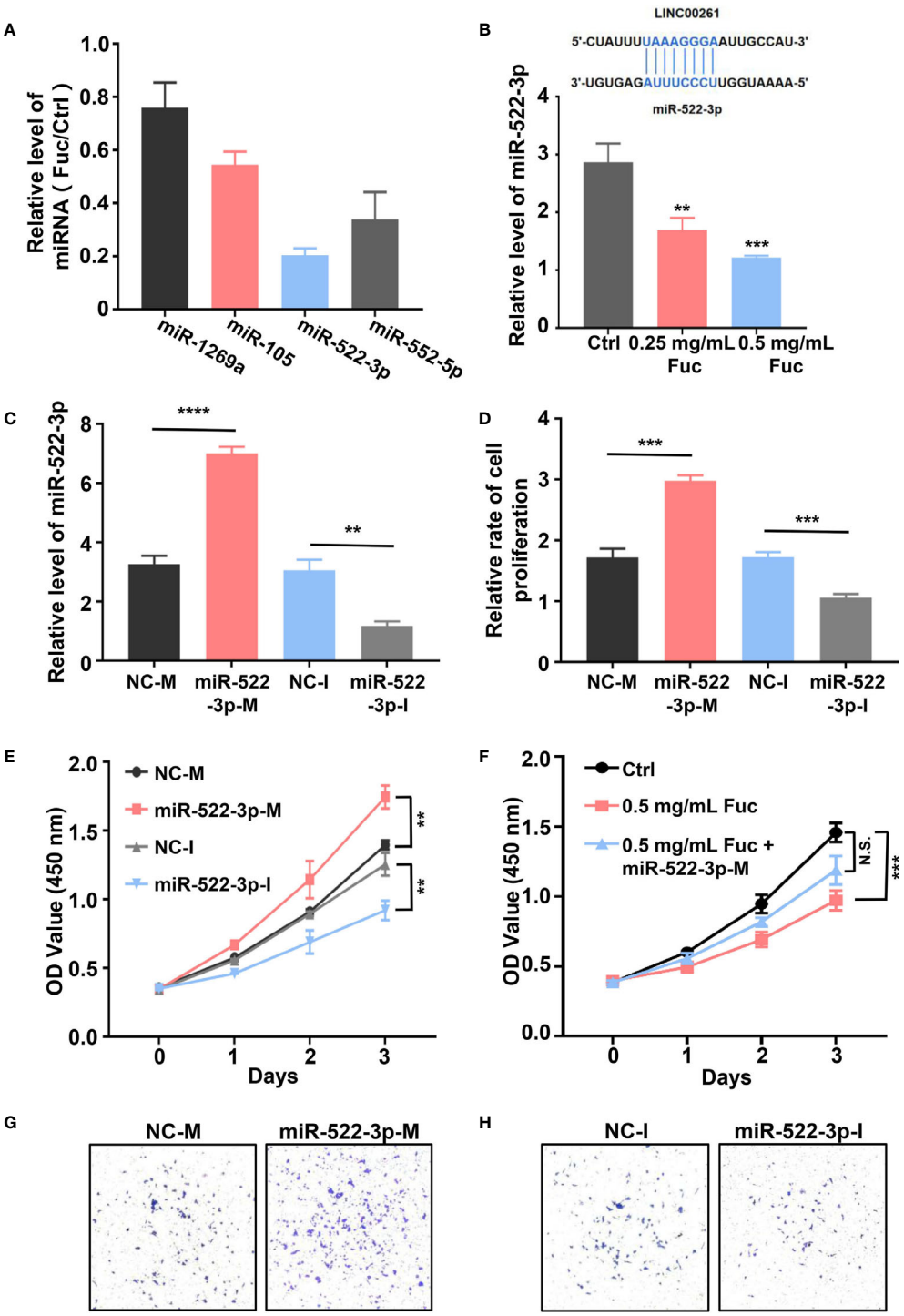

FIGURE 8 | **(A)** The relative level of miRNAs equals to the level of miRNAs in Fuc group divided by the level of miRNAs in Ctrl group. **(B)** The schematic of LINC00261 binds to miR-522-3p by base pairing. The examination of miR-522-3p level in MHCC-97H cells treated with saline (Ctrl), 0.25 mg/mL Fuc and 0.5 mg/mL Fuc. ** means $P < 0.01$, *** means $P < 0.001$. **(C)** The qPCR results of MHCC-97H cells transfected with miR-522-3p mimic and inhibitor. NC-M is short for negative control of miRNA mimic. NC-I is short for negative control of miRNA inhibitor. ** means $P < 0.01$, **** means $P < 0.0001$. **(D)** Relative cell proliferation rate of MHCC-97H cells transfected with miR-522-3p mimic and inhibitor. *** means $P < 0.001$. **(E)** Cell viability of MHCC-97H cells transfected with miR-522-3p mimic and inhibitor. ** means $P < 0.01$. **(F)** The cell viability of MHCC-97H cells in Ctrl group, 0.5 mg/mL Fuc treated group, 0.5 mg/mL Fuc treated and miR-522-3p mimic (miR-522-3p-M) transfected group. *** means $P < 0.001$. **(G)** Overexpression of miR-522-3p accelerates cell invasion of MHCC-97H cells. **(H)** Inhibition of miR-522-3p restrained cell invasion of MHCC-97H cells.

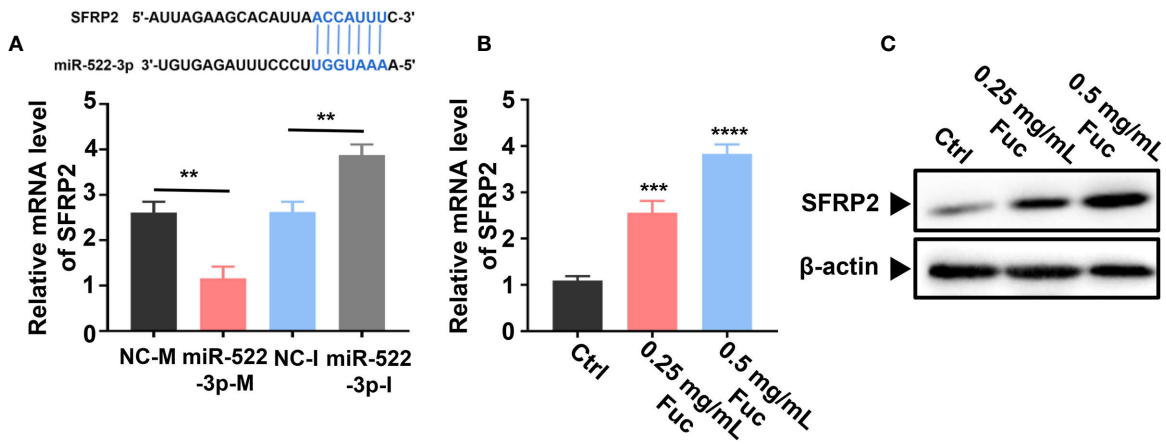

FIGURE 9 | Fucoidan regulates SFRP2 *via* miR-522-3p. **(A)** miR-522-3p binds to SFRP2 by base pairing. miR-522-3p-M down-, miR-522-3p-I up-regulates the expression level of SFRP2. ** means $P < 0.01$. **(B)** Fucoidan obviously increases the level of SFRP2. *** means $P < 0.001$, **** means $P < 0.0001$. **(C)** Western blots analysis of SFRP2 in MHCC-97H cells treated with different dosages of fucoidan (0, 0.25, 0.5 mg/mL).

surgery, traditional chemotherapy drugs and novel targeted drugs (4). Although these therapeutic methods improved the prognosis and survival rate of HCC patients to a certain extent, many patients still die of HCC due to the limited therapeutic effects. Therefore, further exploration of novel treatments is necessary. Since the application of fucoidan in the treatment of HCC is rarely reported, our study focused on the anti-tumor effect of fucoidan in HCC. According to the experimental results, fucoidan affects HCC tumorigenesis through inhibiting proliferation, motility and invasion of MHCC-97H cells and it also plays an important role in arresting cell cycle and promoting cell apoptosis in a dose-dependent manner.

lncRNAs were proved to be involved in a variety of biological activities, which is of great significance in regulating cell growth, differentiation and characteristics. They were also testified to play roles in the regulation of various types of tumors (50–53). In this paper, we took advantage of High-Throughout sequencing to reveal the changes of lncRNA expression profiles in HCC after fucoidan treatment. Among the detected lncRNAs, 75% of which were previously reported and the other lncRNAs were novel. Further KEGG analysis show that these up-regulated and down-regulated lncRNAs were involved in cellular biological functions and intracellular signal pathways in HCC development. Hence, we suggest that fucoidan play an anti-tumor effect by regulating the expression level of lncRNAs. In our study, we select a lncRNA named LINC00261, which was proved in other studies to play an anti-tumor role by regulating the expression of downstream microRNA (59, 69, 70). We proved that LINC00261 could inhibit the tumor characteristics of MHCC-97H cells by regulating miR-522-3p in HCC. Shi et al. reported that miR-522-3p interacted with SFRP2 to suppress Wnt signaling pathway in non–small cell lung cancer (58). In our study, we found miR-522-3p indeed down-regulated the expression level of SFRP2. We examined the mRNA and protein level of SFRP2 in MHCC-97H cells treated with saline, 0.25 and 0.5 mg/mL fucoidan. Interestingly, fucoidan markedly promoted the expression level of SFRP2, which indicated the LINC00261- miR-522-3p- SFRP2 interacting effects in HCC cells. Although some other novel lncRNAs were also detected, lncRNAs could also affect tumorigenesis by regulating the expression of tumor suppressor genes, activating intracellular signaling pathways, regulating cell cycle and other ways according to other studies (28, 36, 44, 46, 48), these lncRNAs involved in the fucoidan regulatory pathway and their underlying regulatory mechanisms require further study, which may contribute greatly to the future HCC therapy.

DATA AVAILABILITY STATEMENT

The datasets presented in this study can be found in online repositories. The names of the repository/repositories and accession number(s) can be found below: https://www.ncbi.nlm.nih.gov/, PRJNA690771.

ETHICS STATEMENT

The animal study was reviewed and approved by Animal Care and Use Committee, Zhongshan Hospital of Fudan University.

AUTHOR CONTRIBUTIONS

DM, JW, SC, and HW conducted the experiments, analyzed data, and wrote the manuscript. LN, and S-HL conducted the

experiments. C-LL contributed reagents. QY and GS provided the concept, designed the study, interpreted the results and wrote the manuscript. All authors contributed to the article and approved the submitted version.

FUNDING

This work was supported by the grant from the National Natural Science Foundation of China (No. 81700550 to GS and No. 81500460 to QY), by the Natural Science Foundation of Shanghai (No. 20ZR1411200 to GS), by the grant from the Zhongshan Hospital of Fudan University (No. H2020-064).

SUPPLEMENTARY MATERIAL

The Supplementary Material for this article can be found online at: https://www.frontiersin.org/articles/10.3389/fonc.2021.653902/full#supplementary-material

REFERENCES

1. Bray F, Ferlay J, Soerjomataram I, Siegel RL, Torre LA, Jemal A. Global cancer statistics 2018: GLOBOCAN estimates of incidence and mortality worldwide for 36 cancers in 185 countries. *CA Cancer J Clin* (2018) 68:394–424. doi: 10.3322/caac.21492
2. Sayiner M, Golabi P, Younossi ZM. Disease Burden of Hepatocellular Carcinoma: A Global Perspective. *Dig Dis Sci* (2019) 64:910–7. doi: 10.1007/s10620-019-05537-2
3. Petrick JL, Kelly SP, Altekruse SF, McGlynn KA, Rosenberg PS. Future of Hepatocellular Carcinoma Incidence in the United States Forecast Through 2030. *J Clin Oncol* (2016) 34:1787–94. doi: 10.1200/jco.2015.64.7412
4. Grandhi MS, Kim AK, Ronnekleiv-Kelly SM, Kamel IR, Ghasebeh MA, Pawlik TM. Hepatocellular carcinoma: From diagnosis to treatment. *Surg Oncol* (2016) 25:74–85. doi: 10.1016/j.suronc.2016.03.002
5. Li H, Wu F, Duan M, Zhang G. Drug-eluting bead transarterial chemoembolization (TACE) vs conventional TACE in treating hepatocellular carcinoma patients with multiple conventional TACE treatments history: A comparison of efficacy and safety. *Med (Baltimore)* (2019) 98:e15314. doi: 10.1097/md.0000000000015314
6. Tsurusaki M, Murakami T. Surgical and Locoregional Therapy of HCC: TACE. *Liver Cancer* (2015) 4:165–75. doi: 10.1159/000367739
7. Nault JC, Galle PR, Marquardt JU. The role of molecular enrichment on future therapies in hepatocellular carcinoma. *J Hepatol* (2018) 69:237–47. doi: 10.1016/j.jhep.2018.02.016
8. Heinrich B, Czauderna C, Marquardt JU. Immunotherapy of Hepatocellular Carcinoma. *Oncol Res Treat* (2018) 41:292–7. doi: 10.1159/000488916
9. Fitton HJ, Stringer DS, Park AY, Karpiniec SN. Therapies from Fucoidan: New Developments. *Mar Drugs* (2019) 17:571. doi: 10.3390/md17100571
10. Wang J, Geng L, Yue Y, Zhang Q. Use of fucoidan to treat renal diseases: A review of 15 years of clinic studies. *Prog Mol Biol Transl Sci* (2019) 163:95–111. doi: 10.1016/bs.pmbts.2019.03.011
11. Luthuli S, Wu S, Cheng Y, Zheng X, Wu M, Tong H. Therapeutic Effects of Fucoidan: A Review on Recent Studies. *Mar Drugs* (2019) 17:487. doi: 10.3390/md17090487
12. Wang Y, Xing M, Cao Q, Ji A, Liang H, Song S. Biological Activities of Fucoidan and the Factors Mediating Its Therapeutic Effects: A Review of Recent Studies. *Mar Drugs* (2019) 17:183. doi: 10.3390/md17030183
13. Wu L, Sun J, Su X, Yu Q, Yu Q, Zhang P. A review about the development of fucoidan in antitumor activity: Progress and challenges. *Carbohydr Polym* (2016) 154:96–111. doi: 10.1016/j.carbpol.2016.08.005
14. Palanisamy S, Vinosha M, Manikandakrishnan M, Anjali R, Rajasekar P, Marudhupandi T, et al. Investigation of antioxidant and anticancer potential of fucoidan from Sargassum polycystum. *Int J Biol Macromol* (2018) 116:151–61. doi: 10.1016/j.ijbiomac.2018.04.163
15. Mansour MB, Balti R, Yacoubi L, Ollivier V, Chaubet F, Maaroufi RM. Primary structure and anticoagulant activity of fucoidan from the sea cucumber Holothuria polii. *Int J Biol Macromol* (2019) 121:1145–53. doi: 10.1016/j.ijbiomac.2018.10.129
16. Elizondo-Gonzalez R, Cruz-Suarez LE, Ricque-Marie D, Mendoza-Gamboa E, Rodriguez-Padilla C, Trejo-Avila LM. In vitro characterization of the antiviral activity of fucoidan from Cladosiphon okamuranus against Newcastle Disease Virus. *Virol J* (2012) 9:307. doi: 10.1186/1743-422x-9-307
17. Wu SY, Yang WY, Cheng CC, Lin KH, Sampurna BP, Chan SM, et al. Low molecular weight fucoidan inhibits hepatocarcinogenesis and nonalcoholic fatty liver disease in zebrafish via ASGR/STAT3/HNF4A signaling. *Clin Transl Med* (2020) 10:e252. doi: 10.1002/ctm2.252
18. Atashrazm F, Lowenthal RM, Woods GM, Holloway AF, Dickinson JL. Fucoidan and cancer: a multifunctional molecule with anti-tumor potential. *Mar Drugs* (2015) 13:2327–46. doi: 10.3390/md13042327
19. Zhang Z, Teruya K, Eto H, Shirahata S. Fucoidan extract induces apoptosis in MCF-7 cells via a mechanism involving the ROS-dependent JNK activation and mitochondria-mediated pathways. *PloS One* (2011) 6:e27441. doi: 10.1371/journal.pone.0027441
20. Kim IH, Kwon MJ, Nam TJ. Differences in cell death and cell cycle following fucoidan treatment in high-density HT-29 colon cancer cells. *Mol Med Rep* (2017) 15:4116–22. doi: 10.3892/mmr.2017.6520
21. Zhang W, Oda T, Yu Q, Jin JO. Fucoidan from Macrocystis pyrifera has powerful immune-modulatory effects compared to three other fucoidans. *Mar Drugs* (2015) 13:1084–104. doi: 10.3390/md13031084
22. Cheng CC, Yang WY, Hsiao MC, Lin KH, Lee HW, Yuh CH. Transcriptomically Revealed Oligo-Fucoidan Enhances the Immune System and Protects Hepatocytes via the ASGPR/STAT3/HNF4A Axis. *Biomolecules* (2020) 10:898. doi: 10.3390/biom10060898
23. Rui X, Pan HF, Shao SL, Xu XM. Anti-tumor and anti-angiogenic effects of Fucoidan on prostate cancer: possible JAK-STAT3 pathway. *BMC Complement Altern Med* (2017) 17:378. doi: 10.1186/s12906-017-1885-y
24. Carninci P, Kasukawa T, Katayama S, Gough J, Frith MC, Maeda N, et al. The transcriptional landscape of the mammalian genome. *Science* (2005) 309:1559–63. doi: 10.1126/science.1112014
25. Jathar S, Kumar V, Srivastava J, Tripathi V. Technological Developments in lncRNA Biology. *Adv Exp Med Biol* (2017) 1008:283–323. doi: 10.1007/978-981-10-5203-3_10
26. Guo X, Gao L, Wang Y, Chiu DK, Wang T, Deng Y. Advances in long noncoding RNAs: identification, structure prediction and function annotation. *Brief Funct Genomics* (2016) 15:38–46. doi: 10.1093/bfgp/elv022
27. Sun TT, He J, Liang Q, Ren LL, Yan TT, Yu TC, et al. LncRNA GClnc1 Promotes Gastric Carcinogenesis and May Act as a Modular Scaffold of WDR5 and KAT2A Complexes to Specify the Histone Modification Pattern. *Cancer Discovery* (2016) 6:784–801. doi: 10.1158/2159-8290.Cd-15-0921
28. Mondal T, Subhash S, Vaid R, Enroth S, Uday S, Reinius B, et al. MEG3 long noncoding RNA regulates the TGF-β pathway genes through formation of RNA-DNA triplex structures. *Nat Commun* (2015) 6:7743. doi: 10.1038/ncomms8743
29. Kino T, Hurt DE, Ichijo T, Nader N, Chrousos GP. Noncoding RNA gas5 is a growth arrest- and starvation-associated repressor of the glucocorticoid receptor. *Sci Signal* (2010) 3:ra8. doi: 10.1126/scisignal.2000568
30. Thomson DW, Dinger ME. Endogenous microRNA sponges: evidence and controversy. *Nat Rev Genet* (2016) 17:272–83. doi: 10.1038/nrg.2016.20
31. Chan JJ, Tay Y. Noncoding RNA:RNA Regulatory Networks in Cancer. *Int J Mol Sci* (2018) 19:1310. doi: 10.3390/ijms19051310
32. Bartonicek N, Maag JL, Dinger ME. Long noncoding RNAs in cancer: mechanisms of action and technological advancements. *Mol Cancer* (2016) 15:43. doi: 10.1186/s12943-016-0530-6
33. Vitiello M, Tuccoli A, Poliseno L. Long non-coding RNAs in cancer: implications for personalized therapy. *Cell Oncol (Dordr)* (2015) 38:17–28. doi: 10.1007/s13402-014-0180-x

34. Bhan A, Soleimani M, Mandal SS. Long Noncoding RNA and Cancer: A New Paradigm. *Cancer Res* (2017) 77:3965–81. doi: 10.1158/0008-5472.Can-16-2634
35. Peng WX, Koirala P, Mo YY. LncRNA-mediated regulation of cell signaling in cancer. *Oncogene* (2017) 36:5661–7. doi: 10.1038/onc.2017.184
36. Barsyte-Lovejoy D, Lau SK, Boutros PC, Khosravi F, Jurisica I, Andrulis IL, et al. The c-Myc oncogene directly induces the H19 noncoding RNA by allele-specific binding to potentiate tumorigenesis. *Cancer Res* (2006) 66:5330–7. doi: 10.1158/0008-5472.Can-06-0037
37. Liu C, Chen L, You Z, Wu Y, Wang C, Zhang G, et al. Association between lncRNA H19 polymorphisms and cancer susceptibility based on a meta-analysis from 25 studies. *Gene* (2020) 729:144317. doi: 10.1016/j.gene.2019.144317
38. Ye Y, Shen A, Liu A. Long non-coding RNA H19 and cancer: A competing endogenous RNA. *Bull Cancer* (2019) 106:1152–9. doi: 10.1016/j.bulcan.2019.08.011
39. Bhan A, Mandal SS. LncRNA HOTAIR: A master regulator of chromatin dynamics and cancer. *Biochim Biophys Acta* (2015) 1856:151–64. doi: 10.1016/j.bbcan.2015.07.001
40. Loewen G, Jayawickramarajah J, Zhuo Y, Shan B. Functions of lncRNA HOTAIR in lung cancer. *J Hematol Oncol* (2014) 7:90. doi: 10.1186/s13045-014-0090-4
41. Tang Q, Hann SS. HOTAIR: An Oncogenic Long Non-Coding RNA in Human Cancer. *Cell Physiol Biochem* (2018) 47:893–913. doi: 10.1159/000490131
42. Gutschner T, Hämmerle M, Eissmann M, Hsu J, Kim Y, Hung G, et al. The noncoding RNA MALAT1 is a critical regulator of the metastasis phenotype of lung cancer cells. *Cancer Res* (2013) 73:1180–9. doi: 10.1158/0008-5472.Can-12-2850
43. Li ZX, Zhu QN, Zhang HB, Hu Y, Wang G, Zhu YS. MALAT1: a potential biomarker in cancer. *Cancer Manag Res* (2018) 10:6757–68. doi: 10.2147/cmar.S169406
44. Wu Q, Meng WY, Jie Y, Zhao H. LncRNA MALAT1 induces colon cancer development by regulating miR-129-5p/HMGB1 axis. *J Cell Physiol* (2018) 233:6750–7. doi: 10.1002/jcp.26383
45. Yao W, Bai Y, Li Y, Guo L, Zeng P, Wang Y, et al. Upregulation of MALAT-1 and its association with survival rate and the effect on cell cycle and migration in patients with esophageal squamous cell carcinoma. *Tumour Biol* (2016) 37:4305–12. doi: 10.1007/s13277-015-4223-3
46. Chen J, Wu D, Zhang Y, Yang Y, Duan Y, An Y. LncRNA DCST1-AS1 functions as a competing endogenous RNA to regulate FAIM2 expression by sponging miR-1254 in hepatocellular carcinoma. *Clin Sci (Lond)* (2019) 133:367–79. doi: 10.1042/cs20180814
47. Castro-Oropeza R, Melendez-Zajgla J, Maldonado V, Vazquez-Santillan K. The emerging role of lncRNAs in the regulation of cancer stem cells. *Cell Oncol (Dordr)* (2018) 41:585–603. doi: 10.1007/s13402-018-0406-4
48. Hu M, Zhang Q, Tian XH, Wang JL, Niu YX, Li G. lncRNA CCAT1 is a biomarker for the proliferation and drug resistance of esophageal cancer via the miR-143/PLK1/BUBR1 axis. *Mol Carcinog* (2019) 58:2207–17. doi: 10.1002/mc.23109
49. Yang Y, Jiang C, Yang Y, Guo L, Huang J, Liu X, et al. Silencing of LncRNA-HOTAIR decreases drug resistance of Non-Small Cell Lung Cancer cells by inactivating autophagy via suppressing the phosphorylation of ULK1. *Biochem Biophys Res Commun* (2018) 497:1003–10. doi: 10.1016/j.bbrc.2018.02.141
50. Yu X, Cao Y, Tang L, Yang Y, Chen F, Xia J. Baicalein inhibits breast cancer growth via activating a novel isoform of the long noncoding RNA PAX8-AS1-N. *J Cell Biochem* (2018) 119:6842–56. doi: 10.1002/jcb.26881
51. Wang M, Jiang S, Yu F, Zhou L, Wang K. Noncoding RNAs as Molecular Targets of Resveratrol Underlying Its Anticancer Effects. *J Agric Food Chem* (2019) 67:4709–19. doi: 10.1021/acs.jafc.9b01667
52. Liu G, Xiang T, Wu QF, Wang WX. Curcumin suppresses the proliferation of gastric cancer cells by downregulating H19. *Oncol Lett* (2016) 12:5156–62. doi: 10.3892/ol.2016.5354
53. Zhou B, Yu Y, Yu L, Que B, Qiu R. Sipi soup inhibits cancer–associated fibroblast activation and the inflammatory process by downregulating long non–coding RNA HIPK1–AS. *Mol Med Rep* (2018) 18:1361–8. doi: 10.3892/mmr.2018.9144
54. Hsu HY, Hwang PA. Clinical applications of fucoidan in translational medicine for adjuvant cancer therapy. *Clin Transl Med* (2019) 8:15. doi: 10.1186/s40169-019-0234-9
55. Guo C, Shi H, Shang Y, Zhang Y, Cui J, Yu H. LncRNA LINC00261 overexpression suppresses the growth and metastasis of lung cancer via regulating miR-1269a/FOXO1 axis. *Cancer Cell Int* (2020) 20:275. doi: 10.1186/s12935-020-01332-6
56. Liu S, Zheng Y, Zhang Y, Zhang J, Xie F, Guo S, et al. Methylation-mediated LINC00261 suppresses pancreatic cancer progression by epigenetically inhibiting c-Myc transcription. *Theranostics* (2020) 10:10634–51. doi: 10.7150/thno.44278
57. Chen T, Lei S, Zeng Z, Zhang J, Xue Y, Sun Y, et al. Linc00261 inhibits metastasis and the WNT signaling pathway of pancreatic cancer by regulating a miR–552–5p/FOXO3 axis. *Oncol Rep* (2020) 43:930–42. doi: 10.3892/or.2020.7480
58. Shi J, Ma H, Wang H, Zhu W, Jiang S, Dou R, et al. Overexpression of LINC00261 inhibits non-small cell lung cancer cells progression by interacting with miR-522-3p and suppressing Wnt signaling. *J Cell Biochem* (2019) 120:18378–87. doi: 10.1002/jcb.29149
59. Wang Z, Zhang J, Yang B, Li R, Jin L, Wang Z, et al. Long Intergenic Noncoding RNA 00261 Acts as a Tumor Suppressor in Non-Small Cell Lung Cancer via Regulating miR-105/FHL1 Axis. *J Cancer* (2019) 10:6414–21. doi: 10.7150/jca.32251
60. Cornejo A, Caballero J, Simirgiotis M, Torres V, Sánchez L, Díaz N, et al. Dammarane triterpenes targeting α-synuclein: biological activity and evaluation of binding sites by molecular docking. *J Enzyme Inhib Med Chem* (2021) 36:154–62. doi: 10.1080/14756366.2020.1851216
61. Huang Y, Yuan K, Tang M, Yue J, Bao L, Wu S, et al. Melatonin inhibiting the survival of human gastric cancer cells under ER stress involving autophagy and Ras-Raf-MAPK signalling. *J Cell Mol Med* (2020) 25:1480–92. doi: 10.1111/jcmm.16237
62. Mohammadian Haftcheshmeh S, Khosrojerdi A, Aliabadi A, Lotfi S, Mohammadi A, Momtazi-Borojeni AA. Immunomodulatory Effects of Curcumin in Rheumatoid Arthritis: Evidence from Molecular Mechanisms to Clinical Outcomes. *Rev Physiol Biochem Pharmacol* (2021). doi: 10.1007/112_2020_54
63. Wei C, Xiao Q, Kuang X, Zhang T, Yang Z, Wang L. Fucoidan inhibits proliferation of the SKM-1 acute myeloid leukaemia cell line via the activation of apoptotic pathways and production of reactive oxygen species. *Mol Med Rep* (2015) 12:6649–55. doi: 10.3892/mmr.2015.4252
64. Xiang Y, Guo Z, Zhu P, Chen J, Huang Y. Traditional Chinese medicine as a cancer treatment: Modern perspectives of ancient but advanced science. *Cancer Med* (2019) 8:1958–75. doi: 10.1002/cam4.2108
65. Etman SM, Mehanna RA, Bary AA, Elnaggar YSR, Abdallah OY. Undaria pinnatifida fucoidan nanoparticles loaded with quinacrine attenuate growth and metastasis of pancreatic cancer. *Int J Biol Macromol* (2020) 170:284–97. doi: 10.1016/j.ijbiomac.2020.12.109
66. Jafari M, Sriram V, Xu Z, Harris GM, Lee JY. Fucoidan-Doxorubicin Nanoparticles Targeting P-Selectin for Effective Breast Cancer Therapy. *Carbohydr Polym* (2020) 249:116837. doi: 10.1016/j.carbpol.2020.116837
67. Liu S, Yang J, Peng X, Li J, Zhu C. The Natural Product Fucoidan Inhibits Proliferation and Induces Apoptosis of Human Ovarian Cancer Cells: Focus on the PI3K/Akt Signaling Pathway. *Cancer Manag Res* (2020) 12:6195–207. doi: 10.2147/cmar.S254784
68. Miyata Y, Matsuo T, Ohba K, Mitsunari K, Mukae Y, Otsubo A, et al. Present Status, Limitations and Future Directions of Treatment Strategies Using Fucoidan-Based Therapies in Bladder Cancer. *Cancers (Basel)* (2020) 12:3776. doi: 10.3390/cancers12123776
69. Gao J, Qin W, Kang P, Xu Y, Leng K, Li Z, et al. Up-regulated LINC00261 predicts a poor prognosis and promotes a metastasis by EMT process in cholangiocarcinoma. *Pathol Res Pract* (2020) 216:152733. doi: 10.1016/j.prp.2019.152733
70. Zhou Z, Ma J. Expression and Clinical Significance of Long-chain Noncoding RNA LINC00261 in Colon Cancer. *Clin Lab* (2019) 65(12). doi: 10.7754/Clin.Lab.2019.190402

Conflict of Interest: C-LL is employee of Hi-Q Marine Biotech International Ltd.

The remaining authors declare that the research was conducted in the absence of any commercial or financial relationships that could be construed as a potential conflict of interest.

frontiers in Oncology

ORIGINAL RESEARCH
published: 30 April 2021
doi: 10.3389/fonc.2021.653061

Baicalein Induces Apoptosis of Pancreatic Cancer Cells by Regulating the Expression of miR-139-3p and miR-196b-5p

Danhui Ma[1,2†], Sinuo Chen[1,2†], Heming Wang[1,2†], Jiayi Wei[1,2], Hao Wu[1,2], Hong Gao[1,2], Xinlai Cheng[3], Taotao Liu[1,2], Shi-Hua Luo[4], Yicheng Zhao[5*] and Guangqi Song[1,2*]*

[1] Department of Gastroenterology and Hepatology, Zhongshan Hospital of Fudan University, Shanghai, China, [2] Shanghai Institute of Liver Diseases, Shanghai, China, [3] Buchmann Institute for Molecular Life Sciences, Goethe University Frankfurt, Frankfurt, Germany, [4] Department of Traumatology, Rui Jin Hospital, School of Medicine, Shanghai Jiao Tong University, Shanghai, China, [5] Clinical Medical College, Changchun University of Chinese Medicine, Changchun, China

OPEN ACCESS

Edited by:
Yue Hou,
Northeastern University, China

Reviewed by:
Guangchao Sui,
Northeast Forestry University, China
Yanbing Ding,
Yangzhou University, China

***Correspondence:**
Guangqi Song
song_guangqi@fudan.edu.cn
Yicheng Zhao
yichengzhao@live.cn
Shi-Hua Luo
jqab@163.com

†These authors have contributed equally to this work and share first authorship

Specialty section:
This article was submitted to Pharmacology of Anti-Cancer Drugs, a section of the journal Frontiers in Oncology

Received: 13 January 2021
Accepted: 18 March 2021
Published: 30 April 2021

Citation:
Ma D, Chen S, Wang H, Wei J, Wu H, Gao H, Cheng X, Liu T, Luo S-H, Zhao Y and Song G (2021) Baicalein Induces Apoptosis of Pancreatic Cancer Cells by Regulating the Expression of miR-139-3p and miR-196b-5p. Front. Oncol. 11:653061. doi: 10.3389/fonc.2021.653061

Pancreatic cancer is a common malignant tumor with a high incidence and mortality rate. The prognosis of patients with pancreatic cancer is considerably poor due to the lack of effective treatment in clinically. Despite numerous studies have revealed that baicalein, a natural product, is responsible for suppressing multiple cancer cells proliferation, motility and invasion. The mechanism by which baicalein restraining pancreatic cancer progression remains unclear. In this study, we firstly verified that baicalein plays a critical role in inhibiting pancreatic tumorigenesis *in vitro* and *in vivo*. Then we analyzed the alteration of microRNAs (miRNAs) expression levels in Panc-1 cells incubated with DMSO, 50 and 100 μM baicalein by High-Throughput sequencing. Intriguingly, we observed that 20 and 39 miRNAs were accordingly up- and down-regulated through comparing Panc-1 cells exposed to 100 μM baicalein with the control group. Quantitative PCR analysis confirmed that miR-139-3p was the most up-regulated miRNA after baicalein treatment, while miR-196b-5p was the most down-regulated miRNA. Further studies showed that miR-139-3p induced, miR-196b-5p inhibited the apoptosis of Panc-1 cells *via* targeting NOB1 and ING5 respectively. In conclusion, we demonstrated that baicalein is a potent inhibitor against pancreatic cancer by modulating the expression of miR-139-3p or miR-196b-5p.

Keywords: baicalein, pancreatic cancer, microRNA, high-throughput sequencing, apoptosis

INTRODUCTION

Pancreatic cancer is one of the most malignant cancers with relatively high incidence and mortality (1). According to the statistical data of GLOBOCAN 2012, there were about 300,000 pancreatic cancer patients in this single year, and almost the same number of deaths caused by this disease worldwide because of its high degree of malignant transformation and the difficulties in early diagnosis (2). Pancreatic cancer mainly includes two types, exocrine cancer (such as

adenocarcinoma) and neuroendocrine cancer. The former type accounts for the majority of cases and has always been emphasized in clinical and basic investigation (3). Although surgery, chemotherapy and radiotherapy have already been adopted for the treatment of pancreatic cancer, the prognosis of which was still extremely poor (4–6). Furthermore, the etiology and pathogenesis of pancreatic cancer have not been fully understood. In order to better treat pancreatic cancer, high curative-effect and low side-effect targeting drugs are urgent to be exploited as soon as possible.

Baicalein, a main active flavonoid ingredient purified from *Scutellaria baicalensis Georgi*, has been found to have significant therapeutic potentials in inflammatory diseases, neurological disorders and tumors (7–12). Several studies demonstrated that baicalein has the ability to inhibit the proliferation, invasion, migration and adhesion of various types of cancers (13–16). Yan et al. found that baicalein promoted cell apoptosis and autophagy through down-regulating PI3K/AKT pathway in breast cancer (17). Baicalein was also proved to cause PD-L1 suppression mediated by restraining STAT3 activity in hepatocellular carcinoma (18). Besides, another study in 2018 showed that baicalein was able to regulate the epithelial–mesenchymal transition (EMT) by targeting tumor associated macrophages (19). Although existing studies partially revealed the potential mechanism of baicalein inhibiting the progression of different cancers, the detailed function of baicalein performing in pancreatic cancer still remains unclear.

miRNAs are small endogenous non-coding RNAs with approximately 22 nts, which could regulate the translation and cleavage of mRNA (20–22). A single miRNA is able to bind to a variety of specific mRNAs and gives play to gene silencing and transcriptional inhibition (23). MiRNAs are responsible for many biological processes, such as cell proliferation, apoptosis, fat metabolism, migration and invasion (24–27). Previous studies found that the modulation of miRNAs expression level by baicalein was closely related to its obviously biological effects (28, 29). Baicalein decreased the expression level of miR-424-3p in lung cancer to suppress cell proliferation and improve cisplatin sensitivity (13). Baicalein activates p38-MAPK-JNK pathway *via* increasing the expression level of miR-29 to retard proliferation and collagen deposition (30). To date, few studies reported whether baicalein could alter several specific miRNAs expression pattern to further affect the progression of pancreatic cancer.

In our study, we firstly treated Panc-1 cells with equivalent DMSO, 50 and 100 μM baicalein. The results suggested that baicalein not only prominently inhibited cell proliferation, motility and invasion, but induced cell cycle arrest in S phase and promoted apoptosis. Through analyzing the High-Throughput sequencing results of miRNAs profiling between the DMSO group and 100 μM baicalein treated group, we discovered that the expression level of 20 miRNAs were up-regulated and 39 miRNAs were down-regulated. Intriguingly, the value of fold change was related to the concentration of baicalein. Furthermore, we verified that miR-139-3p, the most significant up-regulated miRNA, promotes apoptosis of Panc-1 cells *via* targeting NOB1. miR-196b-5p, the most significant down-regulated miRNA, restrains apoptosis of Panc-1 cells *via* targeting ING5. In brief, we demonstrated that the alteration of miRNAs profiling induced by baicalein is crucial for suppressing the progression of pancreatic cancer.

MATERIALS AND METHODS

Cell and Reagents

Panc-1 cells were preserved in our laboratory and were cultured in high-glucose Dulbecco's modified Eagle's medium (DMEM, Hyclone) containing 10% fetal bovine serum (FBS, Gibco) and 1% penicillin–streptomycin (Hyclone). All cells were cultured in a humidified incubator with 5% CO_2 at 37 °C. Trypsin (Hyclone) was used to dissociate cells. Baicalein (purity > 98%) was purchased from Institute for the Control of Pharmaceutical and Biological Products (Beijing, China). Dimethyl sulphoxide (DMSO) was purchased from SigmaAldrich (St. Louis, MO, USA). Antibodies against β-actin (ab8226), cleaved caspase-3 (ab49822), p21 (ab109520), CCND1 (ab16663), NOB1 (ab205718) and ING5 (ab259904) were purchased from Abcam.

RNA Extraction and Quantitative RT-PCR (qRT-PCR)

After Panc-1 cells grew to a certain confluency, they are treated with three concentrations of baicalein (0, 50, 100 μM) for 72 h. Cells were then collected after digestion and washed once with PBS. Total RNA was extracted using Trizol reagent (Invitrogen) according to the standard RNA isolation protocol. The concentration of RNA was measured by NanoDrop 8000 spectrophotometer (Thermo Fisher Scientific). Single-stranded complementary DNA was synthesized from per 500 ng RNA in a 10 μL reaction volume with reverse transcription kits (Takara), and the reaction was performed according to the manufacturer's protocol. qRT-PCR was carried out using a SYBR Green PCR kit (Thermo Fisher Scientific) following the protocol provided by the manufacturer and the cycle threshold (Ct) of each gene was recorded. The U6 small nuclear RNA was used as internal reference to calculate miRNAs expression and GAPDH was used as internal reference to calculate Caspase-3, p21, CCND1, NOB1 and ING5 expression. Data were analyzed by the comparative Ct method ($2^{-\Delta\Delta Ct}$) (31). The primers used in this study were shown in **Table S2** (shown in **Supplementary Material**).

Construction of MiRNAs Libraries and MiRNAs Expression Analysis

Total RNA was extracted by mirVana™ miRNAs Isolation Kit. After treatment with DNase I, 1 μg extracted RNA of each sample was taken to construct the small RNA library according to NEBNext® Multiplex Small RNA Library Prep Set for Illumina®. The concentration of each sample was determined

using NanoDrop 8000 spectrophotometer (Thermo Fisher). Then libraries of small RNAs were sequenced by Illumina Novaseq 6000 (2 × 150 bp paired-end). The sequencing raw data was submitted to Sequence Read Archive (SRA), and the accession number is PRJNA690773. To get clean data, we used Trim_galore (0.6.4) to remove the adapter sequences from the raw data and filtered out sequences with QC < 30. The clean data was mapped by Bowite (1.0.0) to miRBase (Release 22) (www.mirbase.org), and then used Samtools (1.7) to calculate the counts of miRNAs. Different miRNA analysis was analyzed by DESeq2. The target gene of miRNAs was derived from miRTarBase (http://mirtarbase.mbc.nctu.edu.tw/index.html) (32) and the network diagram of miRNA and target gene was drawn by Cytoscape. R-Package clusterProfiler (33) was used to analyze the target genes of miRNAs for KEGG and GO enrichment analysis.

MiRNA Transfection

When cell confluency met approximately 60–80%, cells in six-well plate were transfected with miRNA mimics or inhibitors as well as negative control miRNA using Lipo-fectamine^{TM} 2000 (Invitrogen). MiRNA mimics or inhibitors purchased from Shanghai GenePharma Co., Ltd. After transfection 6–8 h, medium was changed by fresh DMEM containing 10% FBS and cells were harvested after 24–72 h.

Cell Proliferation and Morphological Examination

After digestion, the cells were seeded in a six-well plate with a quantity of 2×10^5 per well. After overnight incubation, the medium containing with equivalent DMSO, 50 μM baicalein and 100 μM baicalein was added, and the cell morphology was photographed at 0 h. After that, the cell morphology in different groups were photographed at 48 h. At 72 h, all groups of cells were digested and then counted from three individual experiments to value the activity of cell proliferation.

CCK-8 Assay

The viability of cells treated with DMSO and different concentration of baicalein (50 and 100 μM) were obtained with Cell Counting Kit 8 (Beyotime Biotechnology). 2×10^3 cells per well were seeded in 96-well plates treated with different concentration of baicalein. All these cells were cultured for the indicated times (0, 24, 48 and 72h), and the cell viability was measured per 24 h stimulation by a multifunctional reader (MD FlexStation 3) to detect the absorbance of the cells at 450 nm according to the manufacturer's instructions.

Transwell Assay

2×10^4 cells were harvested in serum-free medium and then seeded in 200 μL serum-free DMEM onto transwell chambers (Corning) with the lower part filled with 600 μl DMEM containing 20% FBS. Meanwhile, DMSO and 100 μM baicalein were added to cells, which were cultured for 48 h at 37 °C and were fixed in 4% para-formaldehyde and stained with 0.1% crystal violet. Each group had three independent duplications.

Wound Healing Assay

8×10^5 cells per well were dissociated and seeded in 6-well plates. After overnight incubation, the cell monolayer in each well was scratched using a plastic tip vertically across the plate and then washed twice with PBS until no suspending cells were observed in the wound areas under the microscope. Subsequently, the cells were divided into three groups, each containing three replicates and were incubated in serum-free medium with different concentration of baicalein (0, 50, 100 μM) and images were taken at 0 and 48 h to measure the distance of wound.

Clone Formation Assay

2×10^3 cells per well were seeded onto 6-well plates and were cultured for 7–10 days until visible clone were formed and stained with crystal violet solution (0.1% crystal violet, 25% methanol in ddH_2O). The clones were recorded by camera and were counted by ImageJ. Each group had three independent repeats.

Apoptosis Assay

Apoptotic cells were determined with an Annexin V–fluorescein isothiocyanate (FITC)/PI apoptosis detection kit (Beyotime Biotechnology) according to the manufacturer's instructions. Cells were incubated with baicalein for 72 h and were measured by flow cytometry and each group had three repeats.

Cell Cycle

After laying 6-well plates with 8×10^5 cells per well, cells were cultured in medium containing three concentrations of baicalein (0, 50, 100 μM) for 72 h. Cell cycle were detected by a cell cycle and apoptosis kit (Beyotime Biotechnology) and were measured by flow cytometry according to standard instructions. The rates of cell cycle were computed by ModFit LT software.

Xenograft Tumor Model

All animal investigation in our study was conformed to the guidelines of Animal Care and Use Committee, Zhongshan Hospital of Fudan University. Balb/c nude mice were purchased from Vital River Laboratory Animal Technology Co., Ltd. 1×10^6 Panc-1 cells were subcutaneously injected into 4 weeks old female mice. After a week, mice bearing tumors were randomly divided into two groups and each group consisted of five mice. Then mice were administered *via* intraperitoneal injection control solvent (5% DMSO and 95% saline) or 10 mg/kg baicalein (dissolved in 5% DMSO and 95% saline) thrice a week for 4 weeks (34). Body weights of mice were

measured every week. Tumor volumes were measured by the formula $V = (a \times b^2)/2$ (V is the tumor volume, a is the length of the tumor, b is the width of the tumor).

Statistical Analysis

All data are showed as the mean ± SD (standard deviation). GraphPad 7.0 was used for data analysis. The unpaired, two-tailed Student's t test was used to compare the significance of differences between experimental groups and controls from at least three independent repeats. ****p <0.0001, ***p <0.001, **p <0.01, *p <0.05, N.S. means no significance.

RESULTS

Baicalein Inhibits Proliferation, Motility and Invasion of Pancreatic Cancer Cells

To verify whether baicalein (chemical formula as shown in **Figure 1A**, shortly BAI) functions in pancreatic cancer *in vitro*, equivalent DMSO, 50 μM baicalein and 100 μM baicalein was respectively added into Panc-1 cells for 48 h. The microscope records suggested that the density of Panc-1 cells in baicalein-treated group at 48 h was markedly less than the control group (**Figure 1B**). After treatment with baicalein for three days, the statistical result showed that baicalein significantly inhibited the proliferation of Panc-1 cells in a concentration dependent manner (**Figure 1C**). In addition, CCK-8 assay was performed to measure the cell viability of Panc-1 cells exposing to DMSO, 50 μM baicalein or 100 μM baicalein. The result also suggested that baicalein could restrain the viability of Panc-1 cells (**Figure 1D**). Then we performed colony formation experiment and measured the results by ImageJ, which indicated that baicalein decreased the ability of clone formation of Panc-1 cells (**Figures 1E, F**). Besides, wound healing assay demonstrated that baicalein indeed inhibited the ability of cell motility (**Figures 1G, H**). Transwell results showed that there was a significant difference in the number of migrated cells between the DMSO group and 100 μM baicalein group, which suggested baicalein was able to inhibit the invasion of Panc-1

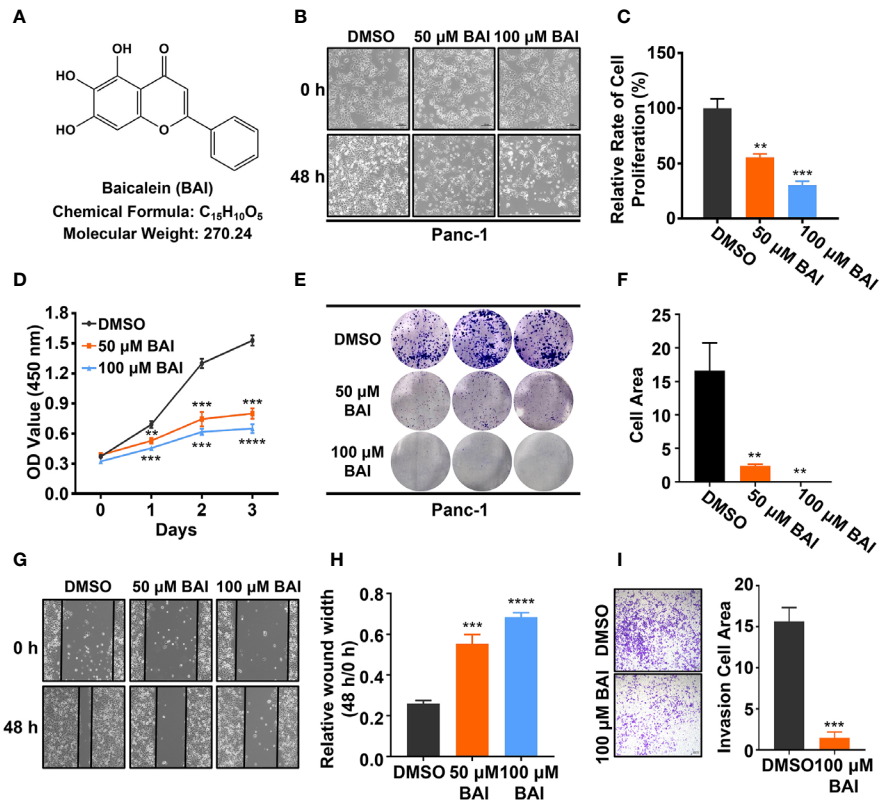

FIGURE 1 | Baicalein inhibits proliferation, motility and invasion of pancreatic cancer cells *in vitro*. **(A)** Structural formula of baicalein (BAI). **(B)** The morphology of Panc-1 cells treated with DMSO, 50 μM and 100 μM baicalein for 0 and 48 h. **(C)** The relative cell proliferation rate of Panc-1 cells treated with DMSO, 50 μM and 100 μM baicalein for 72 h. **(D)** The cell viability of Panc-1 cells treated with DMSO, 50 μM and 100 μM baicalein for 0, 24, 48 and 72 h. **(E, F)** The clone formation of Panc-1 cells treated with DMSO, 50 μM and 100 μM baicalein. Cell area was measured by ImageJ. **(G, H)** The wound healing assay of Panc-1 cells treated with DMSO, 50 μM and 100 μM baicalein for 48 h. The value of relative wound width was measured by ImageJ. **(I)** Transwell assay of Panc-1 cells treated with DMSO and 100 μM baicalein for 48 h. Cell area was measured by ImageJ. ** means $P < 0.01$, *** means $P < 0.001$, **** means $P < 0.0001$.

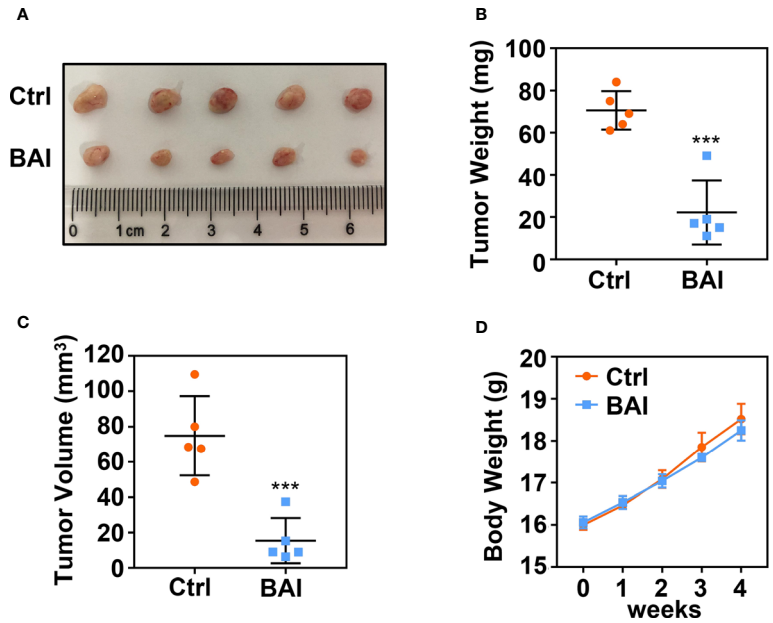

FIGURE 2 | Baicalein inhibits tumorigenesis of pancreatic cancer. **(A)** Xenograft tumor formation of the control (Ctrl) group (5% DMSO and 95% saline) and Baicalein (BAI) group (10 mg/kg BAI, dissolved in 5% DMSO and 95% saline). Each group consisted of five mice. **(B)** Tumor weights of the Ctrl group and BAI group. **(C)** Tumor volumes of the Ctrl group and BAI group. **(D)** Body weights of the Ctrl group and BAI group. *** means $P < 0.001$.

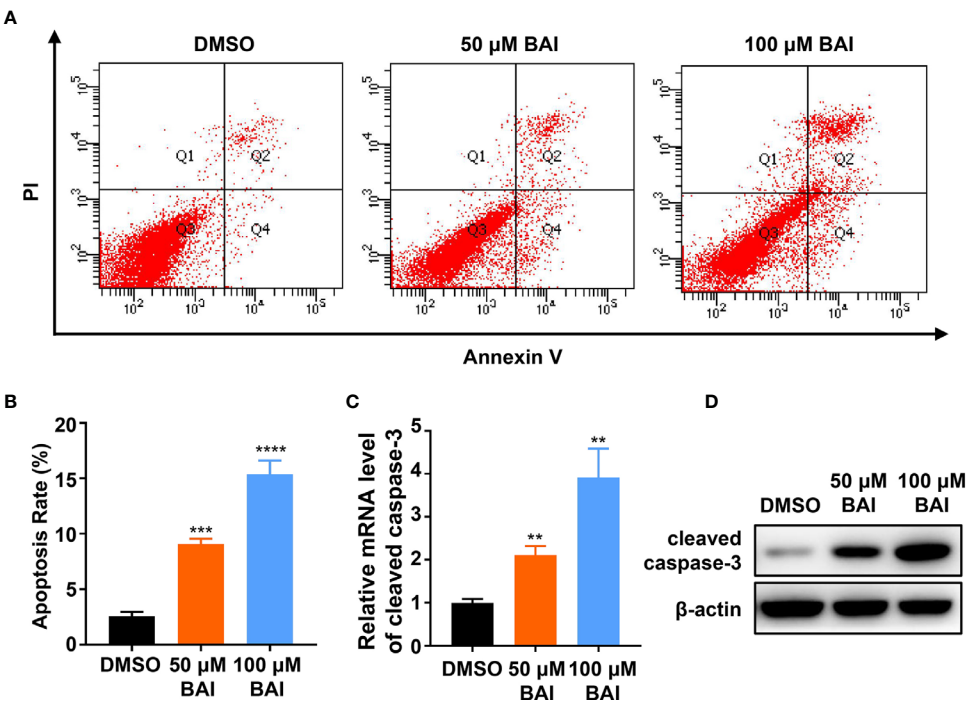

FIGURE 3 | Baicalein induces apoptosis in a concentration dependent manner. **(A)** Apoptosis results of Panc-1 cells treated with DMSO, 50 μM and 100 μM baicalein for 48 h by flow cytometry. Q1 represents death cells, Q2 represents the late apoptosis cells, Q3 represents the normal cells, Q4 represents the ealry apoptosis cells. **(B)** The statistical result of apoptosis rate, which equals to the rate of late apoptosis cells (Q2) plus the rate of early apoptosis cells (Q4). **(C, D)** The mRNA **(C)** and protein **(D)** level of apoptosis related protein cleaved caspase-3 in Panc-1 cells treated with DMSO, 50 μM and 100 μM baicalein. ** means $P < 0.01$, *** means $P < 0.001$, **** means $P < 0.0001$.

cells (**Figure 1I**). Taken together, these results showed that baicalein isolated from natural product obviously inhibits proliferation, motility and invasion of pancreatic cancer cells *in vitro*.

Baicalein Inhibits Tumorigenesis of Pancreatic Cancer *In Vivo*

To address whether baicalein could inhibit pancreatic cancer cell proliferation *in vivo*, we took advantage of xenograft tumor model in our study. 1×10^6 Panc-1 cells were subcutaneously injected into 4 weeks old female Balb/c nude mice. Mice bearing tumor were randomly divided into two groups, the control group (5% DMSO and 95% saline) and the baicalein group (10 mg/kg, dissolved in 5% DMSO and 95% saline). Baicalein and corresponding solvent were administered *via* intraperitoneal injection thrice a week for 4 weeks. Tumor weights and volumes were recorded at the end of treatment. The results suggested that baicalein obviously decreased pancreatic tumor weight and volume *in vivo* (**Figures 2A–C**). In addition, we found that there was no significant difference in mice body weights between the control group and baicalein treated group, which indicated that baicalein nearly has no toxicity to mice (**Figure 2D**).

Baicalein Induces Apoptosis and Cell Cycle Arrest in Panc-1 Cells

To determine the mechanism of how baicalein inhibits pancreatic cells proliferation, we treated Panc-1 cells with

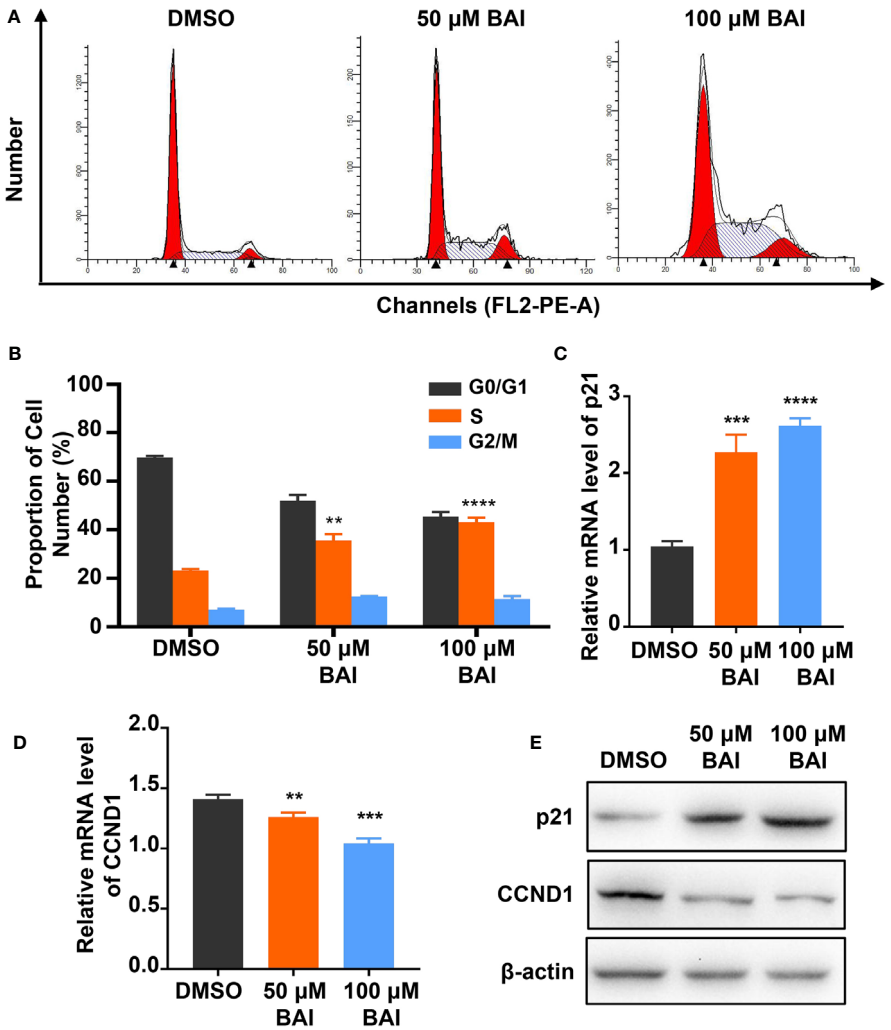

FIGURE 4 | Baicalein induces cell cycle arrest in S phase. **(A)** Cell cycle results of Panc-1 cells treated with DMSO, 50 μM and 100 μM BAI for 48 h by flow cytometry. **(B)** The statistical results of cell number measured by ModFit LT software. **(C, D)** The relative mRNA level of cell cycle related genes p21 **(C)** and CCND1 **(D)** measured by qPCR. **(E)** The protein level of p21 and CCND1 in Panc-1 cells treated with DMSO, 50 μM and 100 μM BAI measured by western blotting. ** means $P < 0.01$, *** means $P < 0.001$, **** means $P < 0.0001$.

DMSO, 50 μM baicalein or 100 μM baicalein for 48 h and performed Annexin V-FITC/PI assay to detect apoptosis rate by flow cytometry. The statistic result showed that the proportion of cells in early and late apoptosis was significantly increased after the treatment of baicalein and higher concentration of baicalein contributes to higher apoptosis rate (**Figures 3A, B**). We also examined the mRNA and protein level of Cleaved caspase-3 in Panc-1 cells treated with DMSO, 50 μM and 100 μM baicalein by qPCR and western blotting assay. Cleaved caspase-3 as the activated form of caspase-3 plays a key role in the pathway of apoptosis. The results suggested that baicalein significantly increases the expression of cleaved caspase-3 in a dosage dependent manner (**Figures 3C, D**).

To further confirm whether baicalein is able to affect cell cycle, we detected the proportion of cell phases through flow cytometry in Panc-1 cells treated with DMSO, 50 μM or 100 μM baicalein for 72 h. The results showed that baicalein induced S phase arrest in a concentration dependent manner (**Figures 4A, B**). Then we examined the mRNA and protein level of cell cycle related genes p21 and cyclinD 1 (CCND1) by qPCR and western blotting. We found that baicalein obviously increased p21 and decreased CCND1 levels in a dose-dependent manner (**Figures 4C–E**), which suggests that baicalein inhibit cell proliferation by extending duration of S phase. As a result, we concluded that baicalein inhibited pancreatic cells proliferation through promoting apoptosis and cell cycle arrest in S phase.

Alteration of MiRNAs Profiling in Panc-1 Cells Treated With Baicalein

Previous studies reported that miRNA could bind to mRNAs causing gene silencing and transcriptional inhibition and is

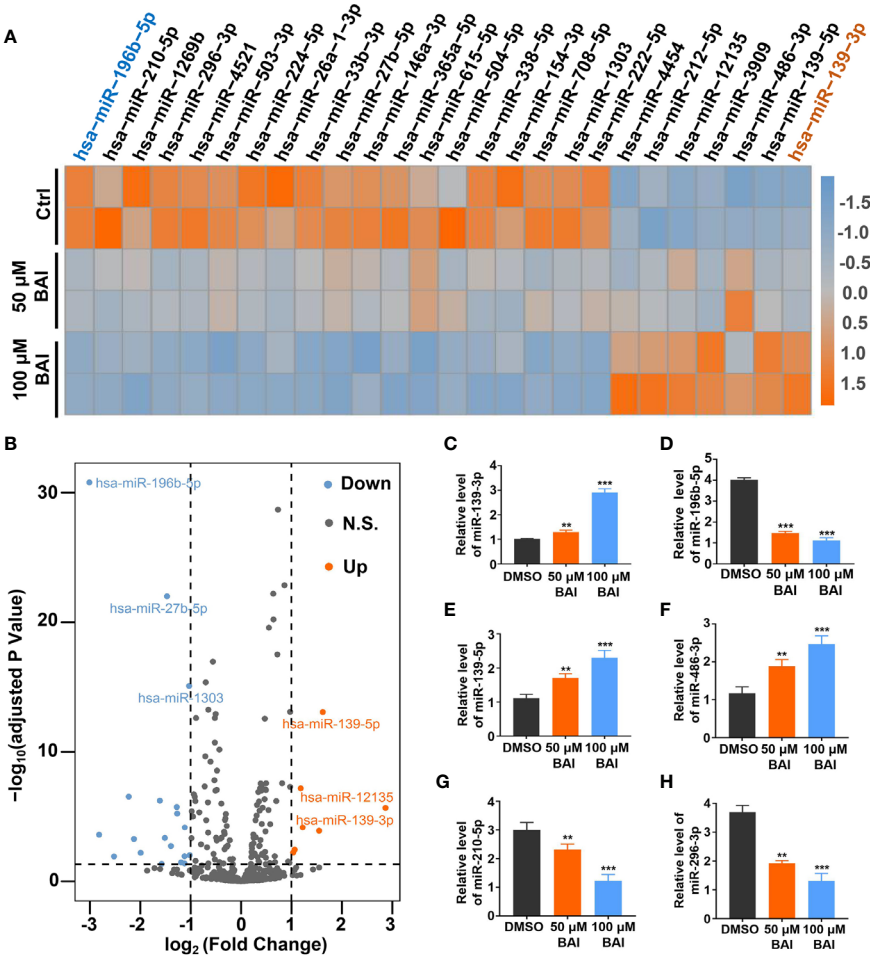

FIGURE 5 | Analysis of miRNAs profiling of Panc-1 cells treated with baicalein. **(A)** Heat map of deferentially expressed miRNAs in Panc-1 cells treated with different dosages of baicalein, $\log_2$ (Fold Change) >1. **(B)** The volcano plot of deferentially expressed miRNAs. Orange indicates up-regulated expression, grey means no significance and blue denotes down-regulated expression. **(C–H)** Identification of the miRNA level of hsa-miR-139-3p **(C)**, hsa-miR-196b-5p **(D)**, hsa-miR-139-5p **(E)**, hsa-miR-486-3p **(F)**, hsa-miR-210-5p **(G)** and hsa-miR-296-3p **(H)** by qPCR. N.S. means no significance, ** means $P < 0.01$, *** means $P < 0.001$.

responsible for inhibiting tumor cell proliferation, migration and invasion. However, whether baicalein is able to alter several specific miRNAs expression to further influence the progression of pancreatic cancer needs to be further exploited. To clarify the miRNAs pattern in Panc-1 cells after the treatment of baicalein (50 and 100 μM) for 48 h, the miRNA High-Throughput sequencing was performed. The volcano plot showed that 20 miRNAs were up-regulated and 39 miRNAs were down-regulated (**Figure 5B**). The detailed alteration results of miRNAs are shown in **Table S1**. From the heat-map result (**Figure 5A**), we could conclude that the alteration of miRNA expression level was closely related to the concentration of baicalein. Besides, the highest increased miRNA candidate is miR-139-3p (fold change = 7.283) and the highest decreased miRNA candidate is miR-196b-5p (fold change = 0.124) (**Figure 5A**), which were reconfirmed by qPCR (**Figures 5C, D**). Moreover, we also measured the relative miRNA expression of other up-regulated miRNAs (miR-139-5p and miR-486-3p) and down-regulated miRNAs (miR-210-5p and miR-296-3p) (**Figures 5E–H**). In addition, we utilized R-Package clusterProfiler to analyze all of the target genes of miRNAs and draw the diagrams of GO enrichment (**Figures S1A, B**) and KEGG (**Figures S1C, D**). The analysis results indicated that both miR-139-3p and miR-196b-5p participated in multiple essential pathways in pancreatic cancer cells.

Baicalein Alters the Expression Level of miR-139-3p and miR-196b-5p to Promote Apoptosis

Based on the above analysis data, we determined to clarify whether miR-139-3p and miR-196b-5p play a crucial role in the progression of pancreatic cancer. We firstly analyzed the association of miR-139-3p or miR-196b-5p expression level and the survival percentage of pancreatic cancer patients. Low level of miR-139-3p and high level of miR-196b-5p contribute to the poor survival according to the data from the TCGA (**Figures 6A, B**). To determine the function of miR-139-3p and miR-196b-5p in Panc-1 cells, cells were transfected with miRNA mimics or inhibitors (**Figures 6C, D**). After transfected, the apoptosis rate was measured. The results showed that miR-139-3p mimics (miR-139-3p-M) and miR-196b-5p inhibitor (miR-196b-5p-I) could promote apoptosis, while miR-139-3p inhibitor (miR-139-3p-I) and miR-196b-5p mimics (miR-196b-5p-M) function as inhibiting apoptosis (**Figures 6E–H**). To further explore whether baicalein promotes apoptosis through altering the expression level of miR-139-3p and miR-196b-5p, we performed rescue experiments by transfecting Panc-1 cells with miR-139-3p-I or miR-196b-5p-M after treated with 100 μM baicalein. qPCR results showed that miR-139-3p-I or miR-196b-5p-M partially rescued the alteration of the expression level of miR-139-3p or miR-196b-5p (**Figures 7A, B**). Then we measured the apoptosis rate by flow cytometry (**Figure 7C**), which showed that no matter miR-139-3p-I or miR-196b-5p-M could inhibited the acceleration of apoptosis caused by baicalein (**Figure 7D**).

We further severally analyzed the relationship between miR-139-3p (**Figure 8A**) or miR-196b-5p (**Figure 8B**) and its down-steamed target genes, which were derived from miRTarBase, and draw the network diagram by Cytoscape. Previous studies showed that miR-139-3p bind to the 3'UTR region of NOB1, which suppresses apoptosis in cancer cells (35). And miR-196b-5p bind to the 3'UTR region of ING5, which induces apoptosis in cancer cells (36). Therefore, we examined the mRNA level of NOB1 and ING5 in Panc-1 cells treated with different dosages of baicalein. Intriguingly, baicalein obviously decreased the expression of NOB1 and increased the expression of ING5 (**Figures 8C, E**). Further, the mRNA and protein level of NOB1 and ING5 were tested respectively after transfected with mimics or inhibitors. The results showed that miR-139-3p-M effectively decreased, whereas miR-139-3p-I increased NOB1 expression (**Figures 8D, G**). Meanwhile, MiR-196b-5p-M decreased, and miR-196b-5p-I increased ING5 expression (**Figures 8F, H**). In conclusion, baicalein plays a key role in promoting apoptosis by up-regulating miR-139-3p or down-regulating miR-196b-5p to alter the expression level of NOB1 and ING5.

DISCUSSION

In recent years, natural compounds were widely used in many fields including clinical treatment due to their safety and effectiveness. Many preclinical and clinical studies have confirmed that natural compounds have certain therapeutic effects in various diseases, especially cancers (12, 32, 37, 38). Baicalein purified from *Scutellaria baicalensis Georgi* is an active flavonoid ingredient, which was reported participating in inhibiting the progression of various cancers (13–19). However, the detailed mechanism of baicalein acting in pancreatic cancer still remains unclear. In this study, we demonstrated that baicalein plays a critical role in inhibiting pancreatic tumorigenesis *in vitro* and *in vivo*. Our results showed that 100 μM baicalein significantly suppressed the proliferation, motility and migration of pancreatic cancer cells. The Annexin V-FITC/PI assay indicated that baicalein is able to promote the apoptosis, which is similar to the previously reported in breast cancer (17). In order to further explore the mechanism of baicalein promoting apoptosis of pancreatic cancer cells, we analyzed the miRNAs High-Throughput sequencing data. As we expected, baicalein affect the profiling of miRNAs in pancreatic cancer cells. According to the analysis results, miR-139-3p or miR-196b-5p was increased or decreased the most in baicalein treated group. Further verification found that miR-139-3p induced, miR-196b-5p inhibited the apoptosis of Panc-1 cells *via* respectively targeting NOB1 and ING5. Although the concentrations of baicalein exposing to Panc-1 cells were relatively high comparing with some small molecule inhibitors of tumors, the result of *in vivo* experiments showed baicalein nearly has no toxicity to mice. In addition, we chose the

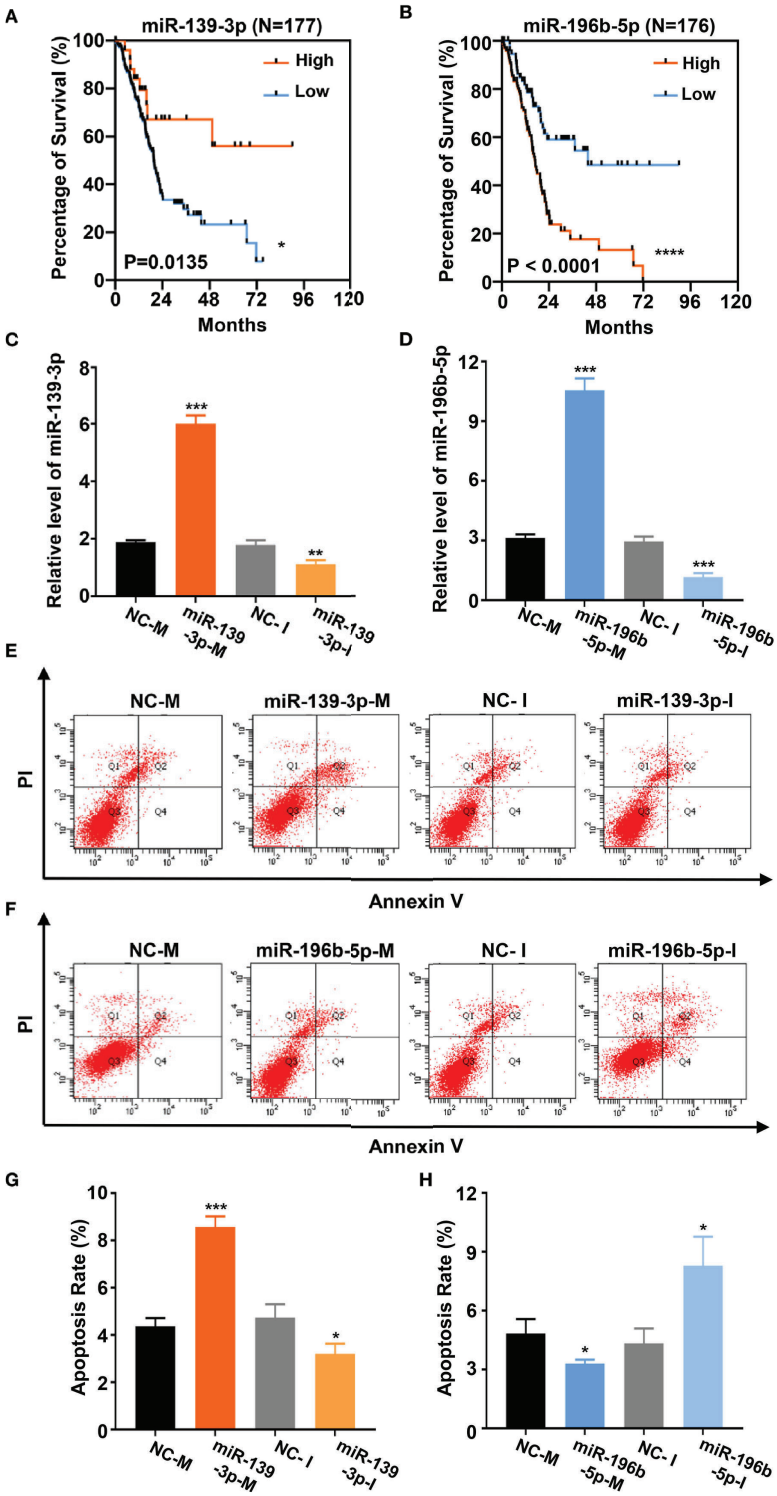

FIGURE 6 | Baicalein alters the expression level of miR-139-3p and miR-196b-5p to promote apoptosis. **(A, B)** Survival curves of 177 **(A)** or 176 **(B)** pancreatic adenocarcinoma samples in TCGA database. (miR-139-3p or miR-196b-5p high-expression group, orange line; miR-139-3p or miR-196b-5p low-expression group, blue line). The number of miR-139-3p or miR-196b-5p high-expression group is 25 or 100. The number of miR-139-3p or miR-196b-5p low-expression group is 152 or 76. **(C, D)** The relative mRNA level of miR-139-3p **(C)** and miR-196b-5p **(D)** transfected with corresponding mimics or inhibitors by qPCR. **(E–H)** The apoptosis rate of miR-139-3p **(E, G)** and miR-196b-5p **(F, H)** transfected with corresponding mimics and inhibitors by flow cytometry. The apoptosis rate equals to the rate of late apoptosis cells (Q2) plus the rate of early apoptosis cells (Q4). * means $P < 0.05$, ** means $P < 0.01$, *** means $P < 0.001$.

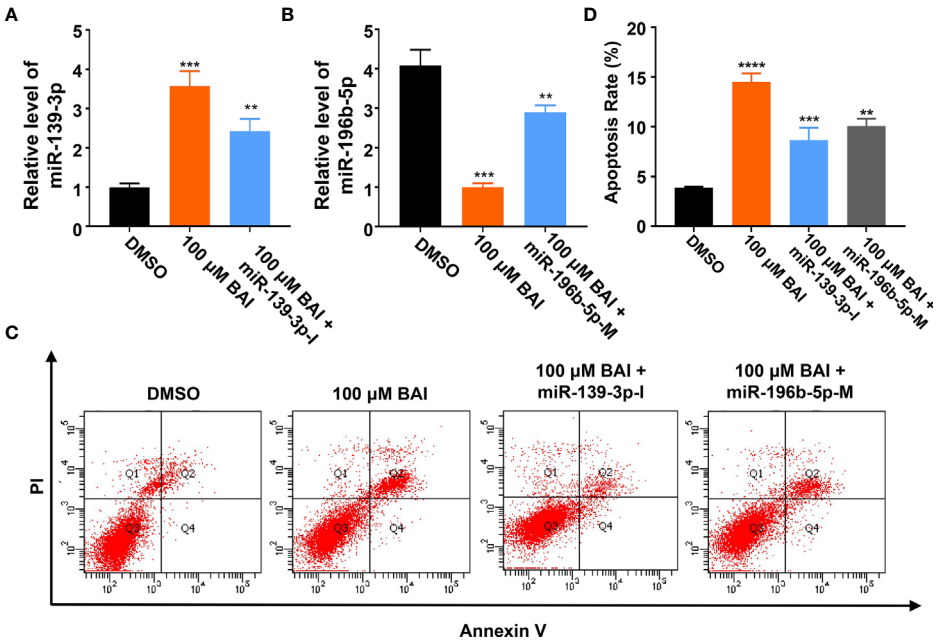

FIGURE 7 | MiR-139-3p-I or miR-196b-5p-M partially rescued the alteration of the expression level of miR-139-3p or miR-196b-5p from baicalein. **(A, B)** The relative mRNA level of miR-139-3p **(A)** and miR-196b-5p **(B)** by qPCR. **(C, D)** The relative apoptosis rate of miR-139-3p and miR-196b-5p in Panc-1 cells treated with DMSO, 100 μM baicalein, 100 μM baicalein and miR-139-3p-I, 100 μM baicalein and miR-196b-5p-M. The apoptosis rate equals to the rate of late apoptosis cells (Q2) plus the rate of early apoptosis cells (Q4). ** means $P < 0.01$, *** means $P < 0.001$.

appropriate concentrations of baicalein in *in vitro* experiments according to previous studies (11, 13–19, 30, 34, 39, 40).

miRNAs are small endogenous non-coding RNAs, which is able to bind to a variety of specific mRNAs to cause gene silencing. Numerous researchers found that the modulation of miRNAs expression in cancer cells is responsible for activate or inhibit tumorigenesis or metastasis (41). Firstly, miRNAs could directly bind to mRNA to suppress transcription activity of downstream oncogenes or tumor suppressor genes. In the second place, miRNAs also combine with long non-coding RNAs (lncRNAs) through base pairing, which influences transcription activity of downstream oncogenes or tumor suppressor gene (42). Previous studies have showed that baicalein inhibit the progression of lung cancer (13), hepatocellular carcinoma (40) and osteosarcoma (39, 43) by regulating miRNAs. In this study, we proved that baicalein promotes the apoptosis of pancreatic cancer cells by regulating the expression of miR-139-3p and miR-196b-5p. Further, we compared the expression levels of miR-139-3p and miR-196b-5p between normal tissues and pancreatic cancer tissues using TCGA database. Although there are very few miRNA expression data in normal tissues, the difference between the two groups still be seen (**Figures S2A, B**) which indicates that miR-139-3p and miR-196b-5p has a regulatory effect on pancreatic cancer. However, whether baicalein directly regulates the expression of miR-139-3p and miR-196b-5p still needs further exploration. Previously, Yu et al. reported that baicalein inhibits breast cancer growth *via* activating long noncoding RNA (lncRNA) PAX8-AS1-N (34), which indicated that baicalein may indirectly regulate miRNAs by affecting the expression of lncRNAs. In addition, more and more studies have confirmed that A-to-I RNA editing induced by ADARs family enzymes closely related to the tumorigenesis and progression of various types of cancers (44–47). Chen et al.reported that ADARs interact with Dicer to promote the processing of mature miR-27a, which targets a tumor suppressor gene METTL7A (48). Whether baicalein affects the expression of ADARs and regulates the processing of miRNAs is also worthy of further exploration.

In our study, we discovered that baicalein prominently induced cell cycle arrest and promoted apoptosis. Analysis of the High-Throughput sequencing data, we verified that miR-139-3p, the most significant up-regulated miRNA, promotes apoptosis of Panc-1 cells *via* suppressing NOB1 level. Meanwhile, miR-196b-5p, the most significant down-regulated miRNA, restrains apoptosis of Panc-1 cells *via* suppressing ING5 level. Based on existing studies, NOB1 was found to be associated with the 26S proteasome to inhibit apoptosis and ING5 may related to EGFR/PI3K/Akt pathway in colorectal cancer to induce apoptosis. We will further study NOB1 and ING5 participating in which downstream signaling pathways in the future. To sum up, this study not only further confirms the molecular mechanism of baicalein inhibiting pancreatic cancer but also provides a new possibility for the clinical treatment of pancreatic cancer.

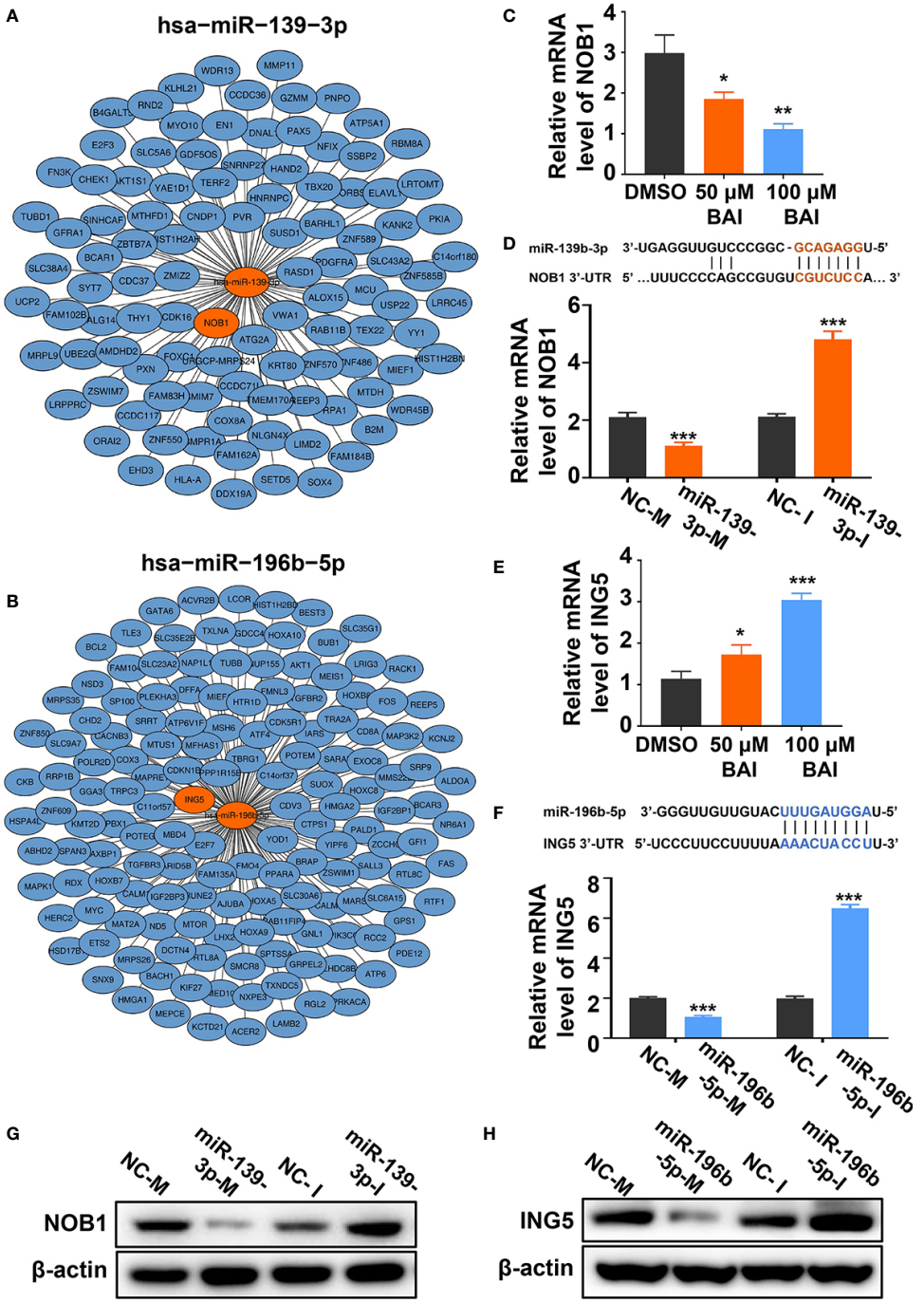

FIGURE 8 | Baicalein decreased the expression level of miR-139-3p downstream NOB1 and increased the expression level of miR-196b-5p downstream ING5. **(A, B)** Interactions between the top-ranked miRNA hsa-miR-139-3p **(A)** or hsa-miR-196b-5p **(B)** with corresponding downstream genes. The target gene of miRNAs was derived from miRTarBase and the network diagram was drawn by Cytoscape. **(C)** The relative mRNA level of NOB1 in Panc-1 cells treated with DMSO, 50 μM and 100 μM baicalein. **(D)** The relative mRNA level of NOB1 transfected with miR-139-3p mimics and inhibitors by qPCR. **(E)** The relative mRNA level of ING5 in Panc-1 cells treated with DMSO, 50 μM and 100 μM baicalein. **(F)** The relative mRNA level of ING5 transfected with miR-196b-5p mimics and inhibitors by qPCR. **(G)** The protein level of NOB1 transfected with miR-139-3p mimics and inhibitors by western blotting. **(H)** The protein level of ING5 transfected with miR-196b-5p mimics and inhibitors by western blotting. * means $P < 0.05$, ** means $P < 0.01$, *** means $P < 0.001$.

DATA AVAILABILITY STATEMENT

The datasets presented in this study can be found in online repositories. The names of the repository/repositories and accession number(s) can be found below: https://www.ncbi.nlm.nih.gov/sra, PRJNA690773.

ETHICS STATEMENT

The animal study was reviewed and approved by Animal Care and Use Committee, Zhongshan Hospital of Fudan University.

AUTHOR CONTRIBUTIONS

DM, SC, HWa and JW conducted the experiments, analyzed data, and wrote the manuscript. HWu, HG, XC and TL analyzed data. YZ and GS provided the concept, designed the study, interpreted the results, and wrote the manuscript. S-HL provided the concept and foundation for revision study, and revised the manuscript. All authors contributed to the article and approved the submitted version.

FUNDING

This work was supported by grants from the National Natural Science Foundation of China (No. 81700550 to GS, No. 31502030 to YZ), by the Natural Science Foundation of Shanghai (No. 20ZR1411200 to GS), by the Foundation of Shanghai Municipal Population and Family Planning Commission (No. 20174Y0151 to HW), by the Key Basic Research Program of Science and Technology Commission of Shanghai Municipality (20JC1415300 to HW), by the Foundation of Administration of Traditional Chinese Medicine for Innovative Key Talents of Traditional Chinese Medicine (to SL), by the LOEWE Center Frankfurt Cancer Institute (FCI) funded by the Hessen State Ministry for Higher Education, Research and the Arts (III L 5-519/03/03.001-(0015) to XC).

SUPPLEMENTARY MATERIAL

The Supplementary Material for this article can be found online at: https://www.frontiersin.org/articles/10.3389/fonc.2021.653061/full#supplementary-material

REFERENCES

1. Ilic M, Ilic I. Epidemiology of pancreatic cancer. *World J Gastroenterol* (2016) 22:9694–705. doi: 10.3748/wjg.v22.i44.9694
2. Ferlay J, Soerjomataram I, Dikshit R, Eser S, Mathers C, Rebelo M, et al. Cancer incidence and mortality worldwide: sources, methods and major patterns in GLOBOCAN 2012. *Int J Cancer* (2015) 136:E359–86. doi: 10.1002/ijc.29210
3. Vincent A, Herman J, Schulick R, Hruban RH, Goggins M. Pancreatic cancer. *Lancet* (2011) 378:607–20. doi: 10.1016/S0140-6736(10)62307-0
4. Gupta R, Amanam I, Chung V. Current and future therapies for advanced pancreatic cancer. *J Surg Oncol* (2017) 116:25–34. doi: 10.1002/jso.24623
5. Aroldi F, Zaniboni A. Immunotherapy for pancreatic cancer: present and future. *Immunotherapy* (2017) 9:607–16. doi: 10.2217/imt-2016-0142
6. Romiti A, Falcone R, Roberto M, Marchetti P. Tackling pancreatic cancer with metronomic chemotherapy. *Cancer Lett* (2017) 394:88–95. doi: 10.1016/j.canlet.2017.02.017
7. Lin CC, Shieh DE. The anti-inflammatory activity of Scutellaria rivularis extracts and its active components, baicalin, baicalein and wogonin. *Am J Chin Med* (1996) 24:31–6. doi: 10.1142/S0192415X96000050
8. Chen CH, Huang LL, Huang CC, Lin CC, Lee Y, Lu FJ. Baicalein, a novel apoptotic agent for hepatoma cell lines: a potential medicine for hepatoma. *Nutr Cancer* (2000) 38:287–95. doi: 10.1207/S15327914NC382_19
9. Cheng Y, He G, Mu X, Zhang T, Li X, Hu J, et al. Neuroprotective effect of baicalein against MPTP neurotoxicity: behavioral, biochemical and immunohistochemical profile. *Neurosci Lett* (2008) 441:16–20. doi: 10.1016/j.neulet.2008.05.116
10. Deng X, Liu J, Liu L, Sun X, Huang J, Dong J. Drp1-mediated mitochondrial fission contributes to baicalein-induced apoptosis and autophagy in lung cancer via activation of AMPK signaling pathway. *Int J Biol Sci* (2020) 16:1403–16. doi: 10.7150/ijbs.41768
11. He K, Yu X, Wang X, Tang L, Cao Y, Xia J, et al. Baicalein and Ly294002 induces liver cancer cells apoptosis via regulating phosphatidyl inositol 3-kinase/Akt signaling pathway. *J Cancer Res Ther* (2018) 14:S519–25. doi: 10.4103/0973-1482.235356
12. Xiang Y, Guo Z, Zhu P, Chen J, Huang Y. Traditional Chinese medicine as a cancer treatment: Modern perspectives of ancient but advanced science. *Cancer Med* (2019) 8:1958–75. doi: 10.1002/cam4.2108
13. Lu C, Wang H, Chen S, Yang R, Li H, Zhang G. Baicalein inhibits cell growth and increases cisplatin sensitivity of A549 and H460 cells via miR-424-3p and targeting PTEN/PI3K/Akt pathway. *J Cell Mol Med* (2018) 22:2478–87. doi: 10.1111/jcmm.13556
14. Yan X, Rui X, Zhang K. Baicalein inhibits the invasion of gastric cancer cells by suppressing the activity of the p38 signaling pathway. *Oncol Rep* (2015) 33:737–43. doi: 10.3892/or.2014.3669
15. Wang Z, Jiang C, Chen W, Zhang G, Luo D, Cao Y, et al. Baicalein induces apoptosis and autophagy via endoplasmic reticulum stress in hepatocellular carcinoma cells. *BioMed Res Int* (2014) 2014:732516. doi: 10.1155/2014/732516
16. Zhang X, Ruan Q, Zhai Y, Lu D, Li C, Fu Y, et al. Baicalein inhibits non-small-cell lung cancer invasion and metastasis by reducing ezrin tension in inflammation microenvironment. *Cancer Sci* (2020) 111:3802–12. doi: 10.1111/cas.14577
17. Yan W, Ma X, Zhao X, Zhang S. Baicalein induces apoptosis and autophagy of breast cancer cells via inhibiting PI3K/AKT pathway in vivo and vitro. *Drug Des Devel Ther* (2018) 12:3961–72. doi: 10.2147/DDDT.S181939
18. Ke M, Zhang Z, Xu B, Zhao S, Ding Y, Wu X, et al. Baicalein and baicalin promote antitumor immunity by suppressing PD-L1 expression in hepatocellular carcinoma cells. *Int Immunopharmacol* (2019) 75:105824. doi: 10.1016/j.intimp.2019.105824
19. Zhao X, Qu J, Liu X, Wang J, Ma X, Zhao X, et al. Baicalein suppress EMT of breast cancer by mediating tumor-associated macrophages polarization. *Am J Cancer Res* (2018) 8:1528–40.
20. Bartel DP. MicroRNAs: genomics, biogenesis, mechanism, and function. *Cell* (2004) 116:281–97. doi: 10.1016/s0092-8674(04)00045-5
21. Rocchi A, Moretti D, Lignani G, Colombo E, Scholz-Starke J, Baldelli P, et al. Neurite-Enriched MicroRNA-218 Stimulates Translation of the GluA2 Subunit and Increases Excitatory Synaptic Strength. *Mol Neurobiol* (2019) 56:5701–14. doi: 10.1007/s12035-019-1492-7
22. Park JH, Shin C. MicroRNA-directed cleavage of targets: mechanism and experimental approaches. *BMB Rep* (2014) 47:417–23. doi: 10.5483/bmbrep.2014.47.8.109
23. Vishnoi A, Rani S. MiRNA Biogenesis and Regulation of Diseases: An Overview. *Methods Mol Biol* (2017) 1509:1–10. doi: 10.1007/978-1-4939-6524-3_1

24. Brennecke J, Hipfner DR, Stark A, Russell RB, Cohen SM. bantam encodes a developmentally regulated microRNA that controls cell proliferation and regulates the proapoptotic gene hid in Drosophila. *Cell* (2003) 113:25–36. doi: 10.1016/s0092-8674(03)00231-9
25. Xu P, Vernooy SY, Guo M, Hay BA. The Drosophila microRNA Mir-14 suppresses cell death and is required for normal fat metabolism. *Curr Biol* (2003) 13:790–5. doi: 10.1016/s0960-9822(03)00250-1
26. Lima CR, Geraldo MV, Fuziwara CS, Kimura ET, Santos MF. MiRNA-146b-5p upregulates migration and invasion of different Papillary Thyroid Carcinoma cells. *BMC Cancer* (2016) 16:108. doi: 10.1186/s12885-016-2146-z
27. Sohn EJ, Park HT. MicroRNA Mediated Regulation of Schwann Cell Migration and Proliferation in Peripheral Nerve Injury. *BioMed Res Int* (2018) 2018:8198365. doi: 10.1155/2018/8198365
28. Zhang W, Xu J, Wang K, Tang X, He J. miR1393p suppresses the invasion and migration properties of breast cancer cells by targeting RAB1A. *Oncol Rep* (2019) 42:1699–708. doi: 10.3892/or.2019.7297
29. Jia AY, Castillo-Martin M, Domingo-Domenech J, Bonal DM, Sanchez-Carbayo M, Silva JM, et al. A common MicroRNA signature consisting of miR-133a, miR-139-3p, and miR-142-3p clusters bladder carcinoma in situ with normal umbrella cells. *Am J Pathol* (2013) 182:1171–9. doi: 10.1016/j.ajpath.2013.01.006
30. Yang X, Zhang C, Jiang J, Li Y. Baicalein retards proliferation and collagen deposition by activating p38MAPK-JNK via microRNA-29. *J Cell Biochem* (2019) 120:15625–34. doi: 10.1002/jcb.28829
31. Arocho A, Chen B, Ladanyi M, Pan Q. Validation of the 2-DeltaDeltaCt calculation as an alternate method of data analysis for quantitative PCR of BCR-ABL P210 transcripts. *Diagn Mol Pathol* (2006) 15:56–61. doi: 10.1097/00019606-200603000-00009
32. Zhong X, Huang S, Liu D, Jiang Z, Jin Q, Li C, et al. Galangin promotes cell apoptosis through suppression of H19 expression in hepatocellular carcinoma cells. *Cancer Med* (2020) 9:5546–57. doi: 10.1002/cam4.3195
33. Yu G, Wang LG, Han Y, He QY. clusterProfiler: an R package for comparing biological themes among gene clusters. *OMICS* (2012) 16:284–7. doi: 10.1089/omi.2011.0118
34. Yu X, Cao Y, Tang L, Yang Y, Chen F, Xia J. Baicalein inhibits breast cancer growth via activating a novel isoform of the long noncoding RNA PAX8-AS1-N. *J Cell Biochem* (2018) 119:6842–56. doi: 10.1002/jcb.26881
35. Huang P, Xi J, Liu S. MiR-139-3p induces cell apoptosis and inhibits metastasis of cervical cancer by targeting NOB1. *BioMed Pharmacother* (2016) 83:850–6. doi: 10.1016/j.biopha.2016.07.050
36. Xin H, Wang C, Chi Y, Liu Z. MicroRNA-196b-5p promotes malignant progression of colorectal cancer by targeting ING5. *Cancer Cell Int* (2020) 20:119. doi: 10.1186/s12935-020-01200-3
37. Zhong X, Liu D, Jiang Z, Li C, Chen L, Xia Y, et al. Chrysin Induced Cell Apoptosis and Inhibited Invasion Through Regulation of TET1 Expression in Gastric Cancer Cells. *Onco Targets Ther* (2020) 13:3277–87. doi: 10.2147/OTT.S246031
38. Huang Y, Yuan K, Tang M, Yue J, Bao L, Wu S, et al. Melatonin inhibiting the survival of human gastric cancer cells under ER stress involving autophagy and Ras-Raf-MAPK signalling. *J Cell Mol Med* (2020) 25(3):1480–92. doi: 10.1111/jcmm.16237
39. Zhang J, Yang W, Zhou YB, Xiang YX, Wang LS, Hu WK, et al. Baicalein inhibits osteosarcoma cell proliferation and invasion through the miR183/Ezrin pathway. *Mol Med Rep* (2018) 18:1104–12. doi: 10.3892/mmr.2018.9036
40. Bie B, Sun J, Li J, Guo Y, Jiang W, Huang C, et al. Baicalein, a Natural Anti-Cancer Compound, Alters MicroRNA Expression Profiles in Bel-7402 Human Hepatocellular Carcinoma Cells. *Cell Physiol Biochem* (2017) 41:1519–31. doi: 10.1159/000470815
41. Komoll RM, Hu Q, Olarewaju O, von Dohlen L, Yuan Q, Xie Y, et al. MicroRNA-342-3p is a potent tumour suppressor in hepatocellular carcinoma. *J Hepatol* (2021) 74:122–34. doi: 10.1016/j.jhep.2020.07.039
42. Zheng H, Wang T, Li X, He W, Gong Z, Lou Z, et al. LncRNA MALAT1 exhibits positive effects on nucleus pulposus cell biology in vivo and in vitro by sponging miR-503. *BMC Mol Cell Biol* (2020) 21:23. doi: 10.1186/s12860-020-00265-2
43. Orenlili Yaylagul E, Ulger C. The Effect of Baicalein On Wnt/ss-Catenin Pathway and MiR-25 Expression in Saos-2 Osteosarcoma Cell Line. *Turk J Med Sci* (2020) 50(44):1168–79. doi: 10.3906/sag-2001-161
44. Xu X, Wang Y, Liang H. The role of A-to-I RNA editing in cancer development. *Curr Opin Genet Dev* (2018) 48:51–6. doi: 10.1016/j.gde.2017.10.009
45. Lazzari E, Mondala PK, Santos ND, Miller AC, Pineda G, Jiang Q, et al. Alu-dependent RNA editing of GLI1 promotes malignant regeneration in multiple myeloma. *Nat Commun* (2017) 8:1922. doi: 10.1038/s41467-017-01890-w
46. Ramirez-Moya J, Baker AR, Slack FJ, Santisteban P. ADAR1-mediated RNA editing is a novel oncogenic process in thyroid cancer and regulates miR-200 activity. *Oncogene* (2020) 39:3738–53. doi: 10.1038/s41388-020-1248-x
47. Tang SJ, Shen H, An O, Hong H, Li J, Song Y, et al. Cis- and trans-regulations of pre-mRNA splicing by RNA editing enzymes influence cancer development. *Nat Commun* (2020) 11:799. doi: 10.1038/s41467-020-14621-5
48. Qi L, Song Y, Chan THM, Yang H, Lin CH, Tay DJT, et al. An RNA editing/dsRNA binding-independent gene regulatory mechanism of ADARs and its clinical implication in cancer. *Nucleic Acids Res* (2017) 45:10436–51. doi: 10.1093/nar/gkx667

Conflict of Interest: The authors declare that the research was conducted in the absence of any commercial or financial relationships that could be construed as a potential conflict of interest.

frontiers in Oncology

ORIGINAL RESEARCH
published: 24 May 2021
doi: 10.3389/fonc.2021.684627

Comparison of the Efficacy of S-1 Plus Oxaliplatin or Capecitabine Plus Oxaliplatin for Six and Eight Chemotherapy Cycles as Adjuvant Chemotherapy in Patients With Stage II-III Gastric Cancer After D2 Resection

Yuanyuan Yu[1,2†], Zicheng Zhang[2†], Qianhao Meng[1†], Yue Ma[1], Xiaona Fan[1], Jie Sun[2] and Guangyu Wang[1*]*

[1] Department of Gastrointestinal Medical Oncology, Harbin Medical University Cancer Hospital, Harbin, China, [2] School of Biomedical Engineering, School of Ophthalmology & Optometry and Eye Hospital, Wenzhou Medical University, Wenzhou, China

Objective: To compare the efficacy of adjuvant chemotherapy with six or eight cycles of S-1 plus oxaliplatin (SOX) or Capecitabine plus oxaliplatin (XELOX) after D2 resection of GC.

Design and participants: We collected 470 cases of patients with TNM stage II and III GC who underwent D2 gastrectomy in the Harbin Medical University Cancer Hospital from January 2007 to December 2017 and received six or eight cycles of SOX or XELOX regimen. This study was designed to evaluate the prognosis of patients receiving six or eight cycles of SOX or XELOX chemotherapy and identify the appropriate number of chemotherapy cycles.

Results: Among the 470 study participants [340 (72.3%) males; median age, 50 years (range, 24-76 years)], 355 and 115 received XELOX or SOX regimen chemotherapy, respectively. The number of 152 patients included in this study who received 6 and 8 cycles of chemotherapy in stage II and stage III without considering chemotherapy regimens were 125 and 27. The median DFS was, respectively, 14.9 months and 26.8 months (P = 0.08), the median OS was, respectively, 30.2 months and 30.8 months (P = 0.5), the difference was not statistically significant. Comprehensive survival analysis of XELOX and SOX group showed no significant difference for DFS (P = 0.29) and OS (P = 0.61). The total number of stage III GC patients who received six and eight cycles of chemotherapy was 92 and 19, respectively. The median DFS of patients who received six and eight cycles of chemotherapy was 14.6 and 23.2 months (P = 0.3), respectively. The median OS of patients who received six and eight cycles of chemotherapy was 26 and 30.6 months (P = 0.9), respectively. Comprehensive analysis of DFS (P=0.73) and OS (P=0.6) shows no difference between the XELOX group SOX groups. Subgroup analysis

OPEN ACCESS

Edited by:
Yongye Huang, Northeastern University, China

Reviewed by:
Yanhua Tian, University of Texas MD Anderson Cancer Center, United States
Yusheng Wang, Shanxi Provincial Cancer Hospital, China

***Correspondence:**
Guangyu Wang
Wangguangyu03@163.com
Jie Sun
suncarajie@wmu.edu.cn

†These authors have contributed equally to this work and share first authorship

Specialty section:
This article was submitted to Pharmacology of Anti-Cancer Drugs, a section of the journal Frontiers in Oncology

Received: *23 March 2021*
Accepted: *04 May 2021*
Published: *24 May 2021*

Citation:
Yu Y, Zhang Z, Meng Q, Ma Y, Fan X, Sun J and Wang G (2021) Comparison of the Efficacy of S-1 Plus Oxaliplatin or Capecitabine Plus Oxaliplatin for Six and Eight Chemotherapy Cycles as Adjuvant Chemotherapy in Patients With Stage II-III Gastric Cancer After D2 Resection. Front. Oncol. 11:684627. doi: 10.3389/fonc.2021.684627

revealed significant differences in the gender (P = 0.05) and histological classification (P < 0.05) distribution.

Conclusion: Regardless of the XELOX regimen or the SOX regimen, similar survival benefits are observed in patients receiving six or eight chemotherapy cycles irrespective of the regimen used. The XELOX and SOX regimens are well tolerated in patients undergoing D2 resection of GC.

Keywords: adjuvant chemotherapy, gastric cancer, chemotherapy cycles, S-1 plus oxaliplatin, capecitabine plus oxaliplatin

INTRODUCTION

Gastric cancer (GC) is the fifth most common cancer worldwide and the fourth leading cause of cancer-related death (1). GC disproportionally affects males, with the rate of affected males being almost twice that of affected females. In 2020, there will be an estimated 1.09 million new cases of GC worldwide and about 769,000 death (1). About 49.3% of new cancer cases and 58.3% of cancer deaths occur in Asia. In China, there were about 679,000 new cases of GC and 498,000 GC-related deaths in 2015, making makes GC the second to only lung cancer in terms of morbidity and mortality (2). In China, about 80% of patients with GC are at an advanced stage at the time of diagnosis, and the 5-year survival rate is less than 30% (3). Therefore, it is important to improve the prognosis of patients with stage II and stage III GC after surgery.

Postoperative adjuvant chemotherapy has become a routine treatment for patients with GC. Indications for adjuvant chemotherapy after resectable GC are: D2 gastrectomy and no preoperative treatment for postoperative patients with pathological stage II and III advanced GC. D2 gastrectomy is based on resectable GC. Four extensive clinical studies, the ACTS-GC, CLASSIC, JACCORGC-07 and ARTIST studies, have confirmed the value of postoperative adjuvant chemotherapy. The Japanese ACTS-GC trial confirmed that S-1 single-agent postoperative adjuvant chemotherapy could significantly improve the 5-year survival rate after D2 gastrectomy for locally advanced GC (4). However, this result has not been verified in other studies, and it is unclear whether patients with stage III GC can benefit from S-1 single-drug adjuvant chemotherapy. In response to this, the CLASSIC study, a randomized, open, parallel-controlled phase III clinical study involving patients from South Korea, China Mainland, and Taiwan, showed that GC patients who received XELOX adjuvant chemotherapy had a significantly higher 5-year disease-free survival (DFS) rate than did those who had surgery alone (68% vs. 53%; HR = 0.58; 95% CI: 0.47–0.72; P < 0.0001), and the overall survival (OS) rate was also significantly improved (78% vs. 69%; HR = 0.66; 95% CI: 0.51–0.85; P = 0.0015). These data confirm that XELOX regimen adjuvant chemotherapy can significantly reduce the risk of postoperative recurrence, and the benefits of prolonging DFS can then be translated into prolonging the OS of patients. As the first chemotherapy regimen validated by evidence-based medicine in the Chinese population, the classic study showed that the XELOX regimen is suitable for postoperative adjuvant chemotherapy for patients with stage II and II GC in China. It also further confirmed that postoperative adjuvant chemotherapy could play an essential role in treating locally advanced GC (5, 6). The Japanese JACCROGC-07 study is a randomized controlled study designed to evaluate the efficacy of S-1 combined with docetaxel in adjuvant treatment after surgery. The 3-year recurrence-free survival (RFS) of the S-1 combined with the docetaxel group was 7% higher than that of the control group. The 3-year RFS was significantly better in the treatment group than in the control group (65.9% vs. 49.6%, HR = 0.632, 99% CI: 0.400–0.998, P = 0.0007), and S-1 combined with docetaxel is recommended as the new standard for adjuvant treatment after D2 gastrectomy in patients with stage III GC (7). The Korean ARTIST study compared postoperative radiotherapy and chemotherapy after D2 surgery to postoperative adjuvant chemotherapy (Capecitabine combined with cisplatin). The results indicate that the DFS and OS of the two groups are similar. Subsequently, the ARTIST-II study, enrolling patients with GC and positive lymph nodes after D2, was designed. The results showed that compared with S-1 single-drug, the SOX regimen alone and in combination with radiotherapy can significantly prolong DFS. However, SOX regimen combined with radiotherapy did not improve survival when compared to SOX regimen alone (8–10). The results of these clinical studies indicate that surgery is the only possible cure for GC, and postoperative adjuvant chemotherapy is the main way to achieve long-term survival for patients with GC.

Based on the efficacy and safety of chemotherapy, the level I recommended choices for postoperative adjuvant chemotherapy for Chinese is XELOX and SOX. S-1 is a fluorouracil derivative, and the main components are tegafur, gemerazine, and otixiracet potassium. The curative effect of S-1 is equivalent to that of capecitabine. However, S-1 is superior to capecitabine in increasing the concentration and time of 5-FU in tumor tissue and blood and reducing side effects, including hand-foot syndrome (11, 12). In 2019, the RESOLVE study showed that eight cycles of SOX adjuvant chemotherapy after D2 radical resection of GC is not inferior to XELOX (13). Currently, eight chemotherapy cycles are recommended for patients with stage II and stage III GC, irrespective of whether they are undergoing the XELOX or SOX regimen. Individual differences in patients' tolerance to chemotherapy drugs mean that some patients

cannot tolerate the toxicity of chemotherapy drugs, leading to the early termination of chemotherapy. Therefore, for this group of patients, we aimed to compare the prognosis of patients who received six or eight cycles of XELOX or SOX adjuvant chemotherapy after radical resection of GC. These insights will allow practitioners to choose a suitable chemotherapy cycle for patients to avoid the occurrence of chemotherapy-related adverse reactions. Moreover, this data provides valuable evidence supporting the need for patients with advanced GC to receive standardized and individualized treatment, which can prolong their lives, improve their quality of life, and reduce the social burden on their families.

METHOD

Study Design

This is a retrospective study. In the real world, the proportion of people who can complete eight cycles of standard postoperative adjuvant chemotherapy for gastric cancer is not large. Most patients have completed six cycles of adjuvant chemotherapy. This research aims to compare whether six cycles are not inferior to eight cycles in the real world. We conducted a three-phase study. First, we compared the DFS and OS of patients with TNM stage II and III GC that received six or eight chemotherapy cycles without considering the chemotherapy regimen. Second, we compared the DFS and OS of patients who received six and eight chemotherapy cycles of XELOX and SOX. In the third step of the study design, the DFS and OS of patients with TNM stage III GC and 6 or 8 chemotherapy cycles were compared with and without considering the chemotherapy regimen.

Inclusion Criteria

Data were collected from patients who were pathologically diagnosed with GC (GC)/gastric junction adenocarcinoma (GEJC) and had undergone D2 radical resection and postoperative adjuvant chemotherapy at the Harbin Medical University Cancer Hospital from January 2007 to December 2017. This study was approved by the Ethics Committee of the Harbin Medical University Cancer Hospital. Patient data were confidential, and the study complied with the Declaration of Helsinki.

Case inclusion criteria were (1): preoperative endoscopic biopsy or postoperative pathological diagnosis of GC/GEJC; (2) having undergone D2 radical operation; (3) postoperative pathological staging of stage II and stage III disease based on the American Joint Committee on Cancer (AJCC) TNM staging (8th edition); (4) postoperative hematology and imaging evaluation of patients show that they meet the criteria of postoperative adjuvant chemotherapy, and tolerate chemotherapy drugs; and (5) their postoperative adjuvant chemotherapy is XELOX or SOX.

Case exclusion criteria were: (1) patient received chemotherapy regimens other than S-1, SOX, or XELOX after D2 radical surgery for GC; (2) patient was unable to complete the specified adjuvant chemotherapy cycle as required for any reason; (3) for any reason, the standard chemotherapy dose was reduced by more than 30%; (4) patients received neoadjuvant therapy; and (5) patients with distant metastasis or relapse within 6 months during operation and after the operation, were excluded.

Treatment Criteria

XELOX treatment regimen was: oxaliplatin 130 mg/m2 (intravenous drip) on day 1, repeated every three weeks and capecitabine 1000 mg/m2 (oral) on days 1-14, twice a day, repeated every three weeks. SOX treatment regimen was: oxaliplatin 130 mg/m2 (intravenous drip) on day 1, repeated every three weeks and S-1 40 mg/m2 (oral) on days 1-14, twice a day, repeated every three weeks. The two treatment groups were subject to 6 or 8 cycles of chemotherapy. During chemotherapy, symptomatic and supportive treatments including antiemetic, liver protection, and stomach protection were administered. B-ultrasound, CT and other imaging examinations were performed every three cycles to evaluate the treatment effect.

Research Targets

DFS is defined as the time from the date of GC D2 resection to the occurrence of recurrence, metastasis, or death. The OS is the time from the date of GC D2 resection to death due to any cause. The primary study endpoint was 5-year OS, and the secondary study endpoint was 3-year DFS. All patients were followed up for at least five years.

Statistical Methods

Clinicopathologic characteristics of patients receiving six and eight chemotherapy cycles were compared using the Chi-square test. The univariate Cox regression analysis to measure the association between treatment regimens and prognosis. The DFS and OS survival curves were drawn using the Kaplan-Meier method, and the log-rank test was used for comparison. $P < 0.05$ was considered statistically significant. All statistical analysis was performed with R Statistical Software (version 4.0.3).

RESULT

Patient Clinical Characteristics

The patient's condition and tumor characteristics are shown in **Table 1**. This is a real-world study of patients with GC (stage II-III) who underwent D2 gastrectomy and received adjuvant chemotherapy with SOX or XELOX regimen in Harbin Medical University Cancer Hospital from January 2007 to December 2017. We conducted a retrospective study of 470 patients who underwent D2 resection and received postoperative adjuvant chemotherapy at our hospital and completed at least four cycles of adjuvant chemotherapy with either XELOX or SOX regimens. There were 159 patients available for analysis of DFS and 203 patients available for analysis of OS. Postoperative pathological staging was stage II or stage III in 369 patients, of which 290 patients received six cycles of chemotherapy and 79 patients received eight cycles of chemotherapy. Following the administration of chemotherapy, 51 patients were excluded

based on the exclusion criteria. A total of 152 patients were included in the analysis according to the exclusion criteria.

The clinical characteristics of the 6-cycle and 8-cycle chemotherapy groups were similar. There were no significant differences in Lauren classification, tumor location, TNM staging, or WHO grade (P > 0.05). There was an obvious difference between these two groups in age distribution, with most patients under 65 years of age, but this difference was not statistically significant (P=0.063). Obvious differences in gender distribution (P = 0.05) and histological classification (P = 0.48) were observed (**Table 1**).

Survival Outcome for Stage II-III GC Patients Treated With Six or Eight Chemotherapy Cycles

All patients were followed up for at least 5 years. We conducted a comprehensive analysis of the data for patients with stage II and stage III, irrespective of whether they underwent XELOX or SOX regimens. Patient survival was then compared between groups. The number of patients receiving six and eight cycles of chemotherapy was 125 and 27, respectively. Patients receiving six or eight chemotherapy cycles had similar rates of DFS and OS. The Kaplan–Meier method was used for survival analysis and to draw DFS and OS survival curves. Median DFS time of patients receiving six and eight cycles of chemotherapy was 14.9 and 26.8 months (P = 0.08), respectively. Median OS time of patients receiving six and eight cycles of chemotherapy was 30.2 and 30.8 months (P = 0.5) (**Figures 1A, B**). The number of patients with stage II and stage III GC receiving six and eight cycles of XELOX regimen chemotherapy were 109 and 18, respectively. Median DFS time of patients receiving six and eight cycles of chemotherapy was 16 and 27 months (P = 0.07), respectively. The median OS times of patients receiving six and eight cycles of chemotherapy, respectively, were 30 and 31.9 months (P = 0.9. The number of patients receiving six and eight cycles of SOX regimen chemotherapy was 16 and 9, respectively. The median DFS times in these patient groups were 13.7 and 24.2 months (P = 0.6), respectively. The median OS times in these patient groups were 21.5 and 24.5 months (P = 0.5), respectively. Comprehensive analysis of DFS (P = 0.29) and OS (P = 0.61) between the XELOX and SOX groups revealed no statistical difference (**Figures 1C, D**). In patients receiving six chemotherapy cycles, DFS and OS did not differ between those receiving XELOX and SOX regimens (DFS, P = 0.97 and OS, P = 0.83) (**Figures 2A, B**). In patients receiving eight chemotherapy cycles, DFS and OS did not differ between those receiving the XELOX and the SOX regimens (DFS, P = 0.49 and OS, P = 0.084) (**Figures 2C, D**).

Among all patients with stage III GC, 92 and 19 received six and eight chemotherapy cycles, respectively. Overall DFS time in patients receiving six and eight cycles of chemotherapy were 14.6 and 23.2 months (P = 0.3), respectively. The median OS times in patients receiving six and eight cycles of chemotherapy were 26 and 30.6 months (P=0.9), respectively (**Figures 3A, B**).

In patients with stage III GC, 77 and 11 patients received six and eight cycles of the XELOX regimen chemotherapy, respectively. The median DFS times for patients receiving six and eight cycles of chemotherapy were 14.7 and 23.2 months (P = 0.6), respectively. The median OS times for patients receiving six and eight cycles of chemotherapy, 28 and 30.7 months (P = 0.6), respectively. the difference was not statistically significant. The number of people receiving six and eight cycles of SOX regimen chemotherapy was 15 and 8, respectively. The median DFS times for patients receiving six and eight cycles of chemotherapy were 13.7 and 26.8 months (P = 0.6), respectively. The median OS times for patients receiving six and eight cycles of chemotherapy were 21.5 and 24.5 months (P= 0.6), respectively. No differences in DFS (P = 0.73) and OS (P=0.6) were observed between the XELOX and SOX groups (**Figures 3C, D**). In patients receiving six chemotherapy cycles, DFS and OS did not significantly differ between the two treatment regimens (DFS, P = 0.7 and OS, P = 0.37) (**Figures 4A, B**). In patients receiving eight chemotherapy cycles, DSF and OS did not differ between the two treatment groups (DFS, P = 0.35 and OS, P = 0.25) (**Figures 4C, D**).

Results of the univariate Cox regression suggested that there is no difference in survival between patients receiving six or eight chemotherapy cycles in either of the treatment regimens examined (P>0.05) (**Figures 5A–D**). Patients receiving eight cycles of XELOX regimen chemotherapy appeared to have better OS than did those receiving eight cycles of SOX or XELOX regimen chemotherapy, but this difference was not statistically significant (OS: HR, 0.46; P = 0.086) (**Figure 5B**).

TABLE 1 | Clinical characteristics of patients with gastric cancer after D2 resection enrolled in this study.

Clinical characteristics	Cycle 6 (n=290)	Cycle 8 (n=79)	X-squared	p-value[a]
Age				
<=65	248	60	3.455	0.063
>65	42	19		
Gender				
Male	196	63	3.826	0.05
Female	94	16		
Lauren				
Intestinal type	60	14	1.678	0.642
Diffuse type	73	24		
Mixed type	43	14		
Unknown	114	27		
Tumor_size				
Cardia	9	2	1.540	0.463
Gastric body or Whole stomach	82	28		
Gastric antrum	199	49		
TNM				
II	127	34	<0.001	1
III	163	45		
WHO_grade				
Adenocarcinoma	155	42	0.111	0.991
Signet ring cell carcinoma	19	5		
Low adhesion carcinoma	19	6		
Mixed cancer	97	26		
Histological classification				
Poorly differentiated	142	27	7.914	0.048
Moderately differentiated	124	47		
Well differentiated	10	1		
Undifferentiated	14	5		

[a]*p-value was derived from the Chi-square test.*

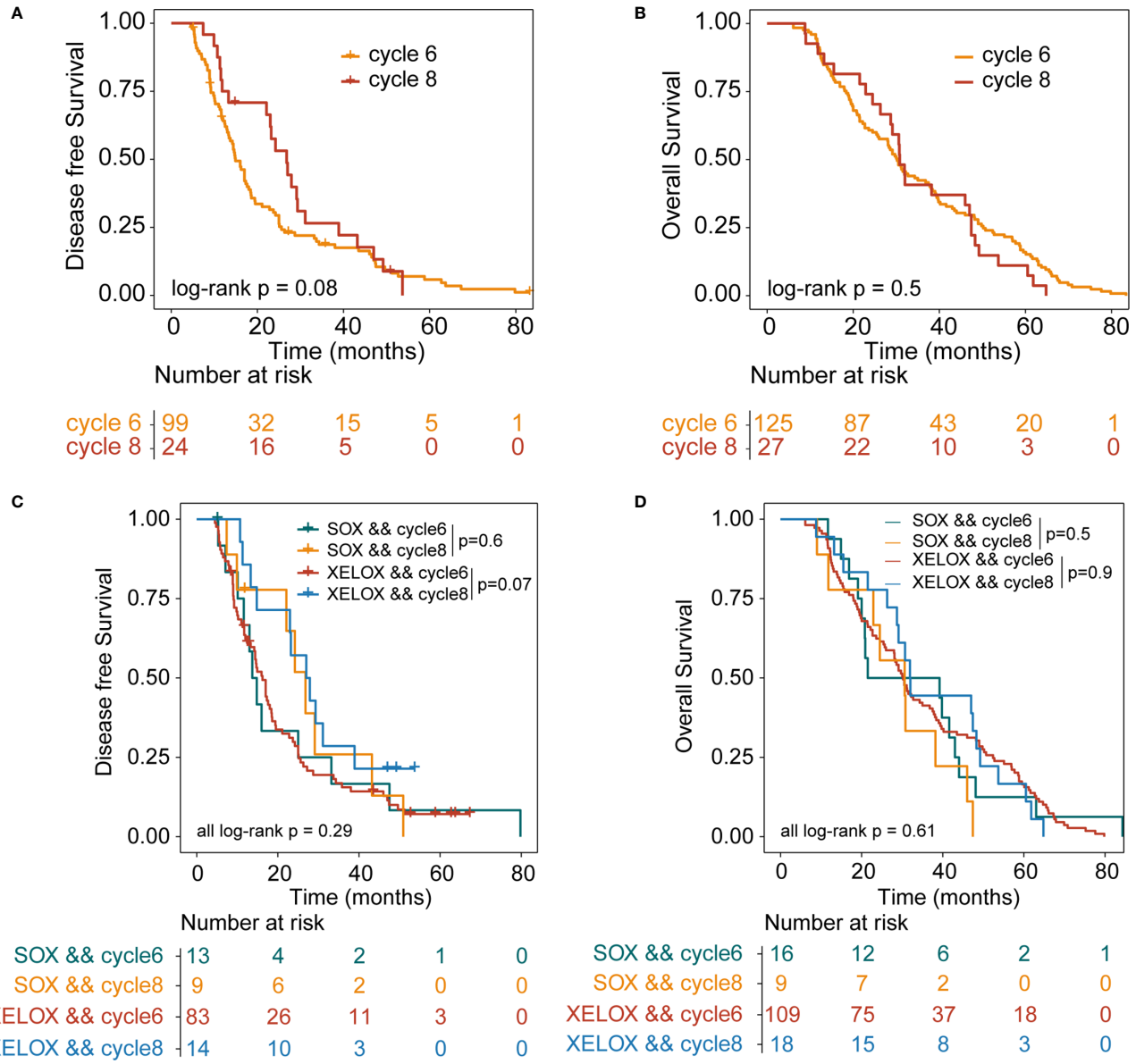

FIGURE 1 | Kaplan-Meier survival curves for disease-free survival (DFS) and overall survival (OS). DFS **(A)** and OS **(B)** analyses for stage II and stage III patients who received six or eight cycles of chemotherapy, irrespective of whether they underwent XELOX or SOX regimens. DFS **(C)** and OS **(D)** analyses for stage II and stage III patients who received six or eight cycles of chemotherapy, taking the specific regimen into account. XELOX, Capecitabine plus oxaliplatin; SOX, S-1 plus oxaliplatin.

Subgroup Analysis

Stratification by gender, age, Lauren classification, tumor location, TNM staging, WHO grade, and histological classification revealed similar DFS results for patients receiving six and eight cycles of chemotherapy (**Figure 6A**; P > 0.05). However, a significant difference was observed in DFS in patients classified as poorly differentiated histologically (P = 0.034), suggesting that six cycles of chemotherapy for patients with GC histologically classified as poorly differentiated should be sufficient. Stratification by gender, age, Lauren classification, tumor location, TNM staging, WHO grade, and histological classification revealed similar that OS for all patients irrespective of whether they received six or eight cycles of chemotherapy (**Figure 6B**; P>0.05).

DISCUSSION

GC is a highly invasive and highly heterogeneous disease. The survival rate of locally advanced or metastatic disease of GC has not been significantly improved. It is still a serious global health problem. GC passes through the lymphatic system, blood and

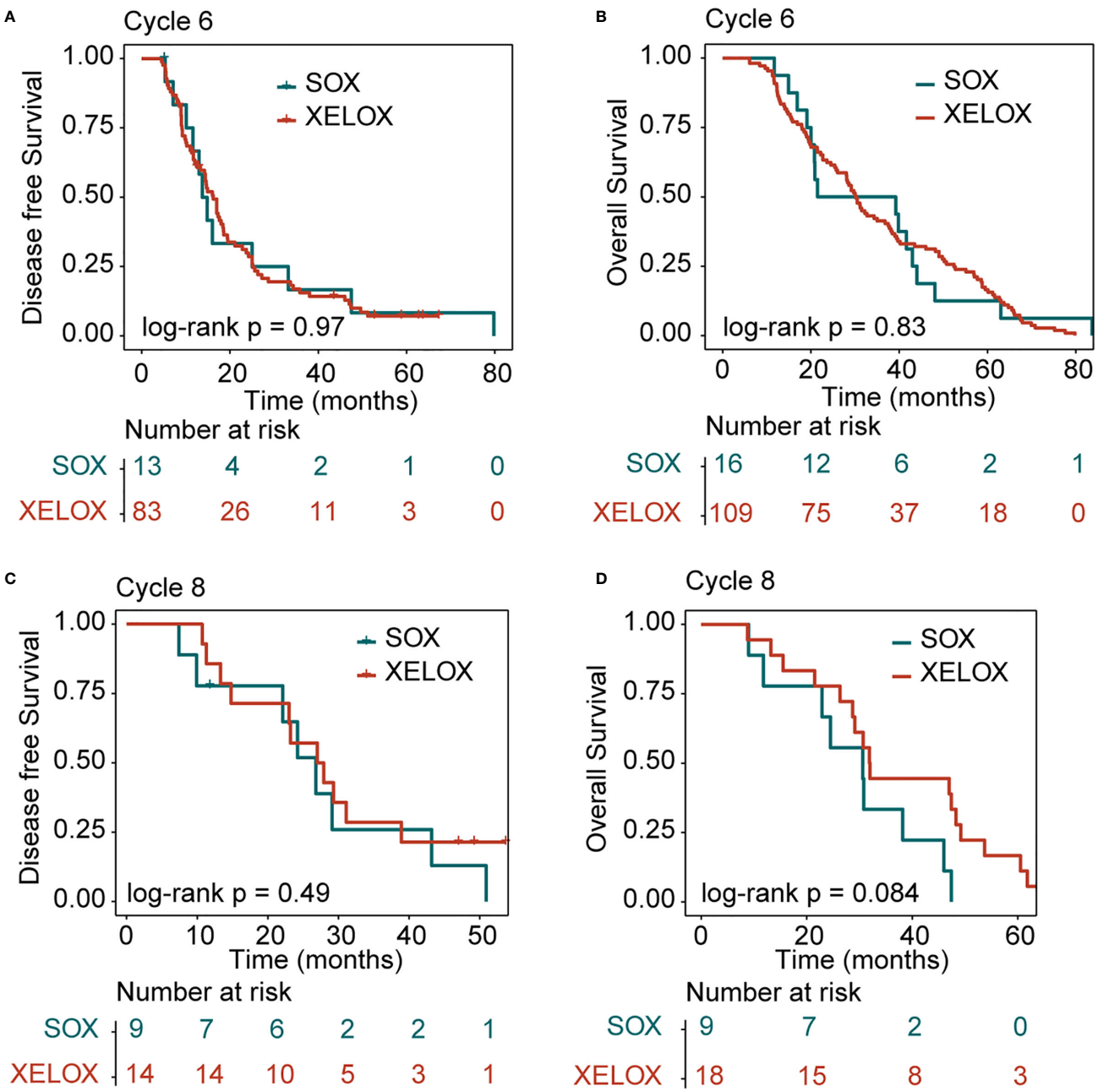

FIGURE 2 | Kaplan-Meier survival curves for disease-free survival (DFS) and overall survival (OS). DFS **(A)** and OS **(B)** analyses for the XELOX and SOX regimens for patients with stage II and stage III gastric cancer receiving six cycles of chemotherapy. DFS **(C)** and OS **(D)** analyses for the XELOX and SOX regimens for patients with stage II and stage III gastric cancer receiving eight cycles of chemotherapy. XELOX, Capecitabine plus oxaliplatin; SOX, S-1 plus oxaliplatin.

peritoneum in the early stage. Spread, recurrence after surgery is common, about 40% of patients relapse within 2 years after surgery (14–16). In order to reduce the rate of local recurrence and metastasis of GC and prolong the survival time of patients, we routinely perform postoperative adjuvant chemotherapy for patients. SOX regimen and XELOX regimen are the first-line treatment options for advanced GC, reducing cancer recurrence, improving the survival rate, and reducing the occurrence of adverse reactions, so that the survival of patients with advanced GC has obvious benefits (17–21). In recent years, a number of large randomized clinical studies have also confirmed the status of the two regimens in adjuvant chemotherapy after GC surgery. The purpose of our research is to compare the efficacy of patients receiving 6, and 8 cycles of SOX and XELOX adjuvant chemotherapy after D2 radical resection of GC, and to compare the prognosis of patients receiving different

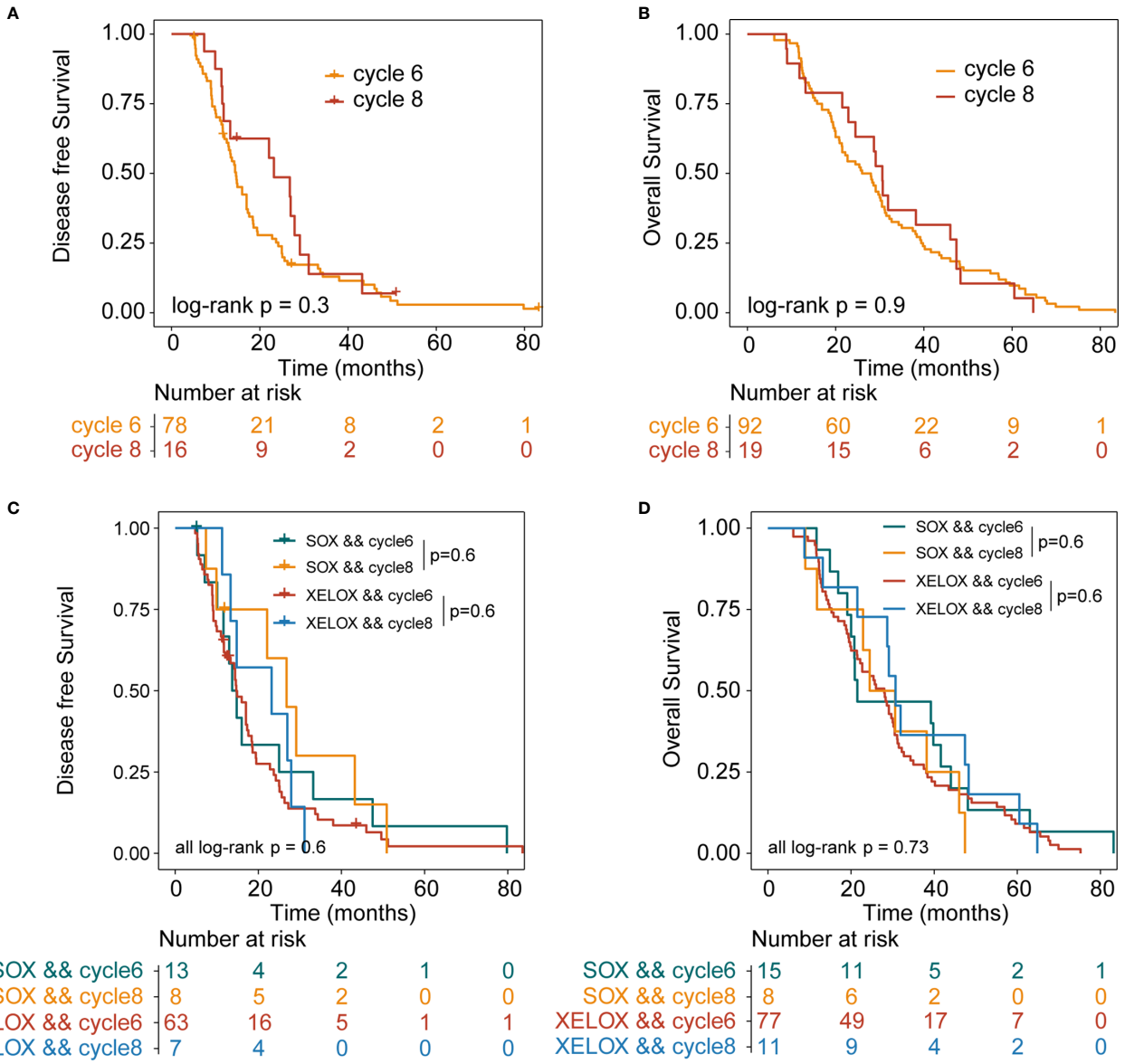

FIGURE 3 | Kaplan-Meier survival curves for disease-free survival (DFS) and overall survival (OS). DFS **(A)** and OS **(B)** analyses for patients with stage III gastric cancer who received six or eight cycles of chemotherapy, irrespective of whether they underwent XELOX or SOX regimens. DFS **(C)** and OS **(D)** analyses for patients with stage III gastric cancer who received six or eight cycles of chemotherapy, taking the specific regimen into account. XELOX, Capecitabine plus oxaliplatin; SOX, S-1 plus oxaliplatin.

chemotherapy cycles. As far as we know, this idea was proposed for the first time. Regardless of how many cycles of chemotherapy the patient received, we did not observe significant differences between the two regimens in DFS and OS. In all subgroup analyses, only the distribution of patients classified as poorly differentiated histologically in 6 and 8 chemotherapy cycles was significantly different (P=0.034).

Previous prospective studies on the adjuvant treatment of GC, the ACTS-GC, CLASSIC, and ARTIST II studies, showed that compared with surgery alone, S-1, SOX and XELOX regimens have better curative effects, but these studies did not directly compare the efficacy of SOX regimen and XELOX regimen. Therefore, the difference in the efficacy of these two regimens was still unknown at that time. A single-center retrospective study showed that there was no significant difference in the efficacy of S-1 and XELOX regimens in stage III patients, but XELOX regimen was more effective than S-1 in patients with stage IIIC GC (22). Another multi-center retrospective study showed that for patients with stage IIIB or IIIC GC after D2 lymph node dissection, XELOX regimen adjuvant chemotherapy is more effective than S-1 (23). For the comparison of the effects of SOX and XELOX, a Japanese study showed that XELOX and

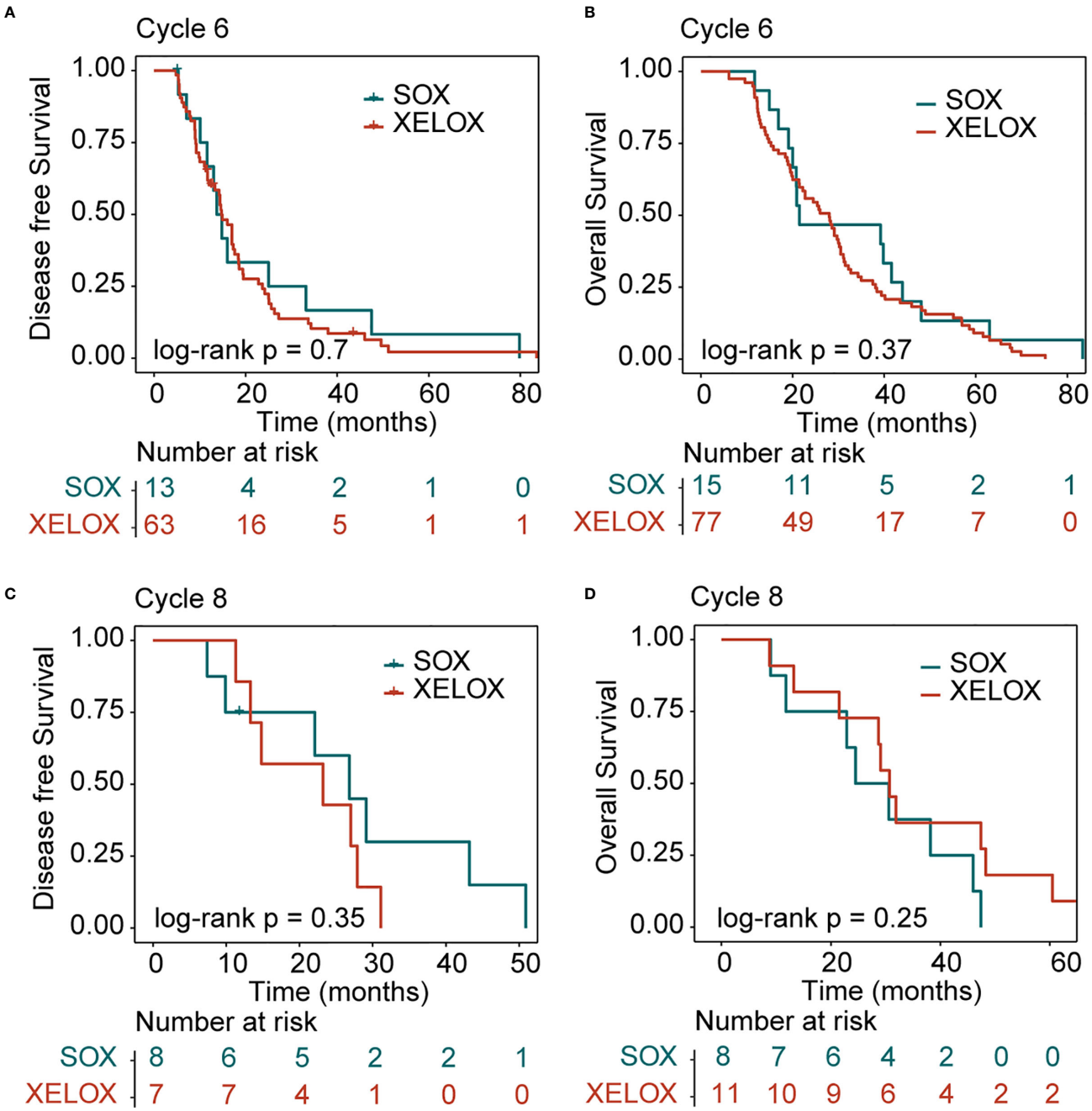

FIGURE 4 | Kaplan-Meier survival curves for disease-free survival (DFS) and overall survival (OS). DFS **(A)** and OS **(B)** analyses for XELOX and SOX regimens for patients with stage III gastric cancer receiving six cycles of chemotherapy. DFS **(C)** and OS **(D)** analyses for the XELOX and SOX regimens in stage III patients receiving eight cycles of chemotherapy. XELOX, Capecitabine plus oxaliplatin; SOX, S-1 plus oxaliplatin.

SOX treatments have similar effects in patients with stage III GC who underwent D2 resection (24). Subsequently, the RESOLVE study published by ESMO in 2019 showed that the SOX adjuvant chemotherapy for 8 cycles after radical resection of GC D2 is not inferior to XELOX (25). The results of a recent single-center retrospective study also showed that SOX is as effective as XELOX for patients with GC after radical resection and that there is no significant difference in survival rate in patients receiving the different treatments (13).

The limitations of this study should be taken into consideration when analyzing the results. First, this is a single-center retrospective study, and the data collected will inevitably have some deviations. Second, the number of patients included is small and the sample distribution is uneven. These factors may

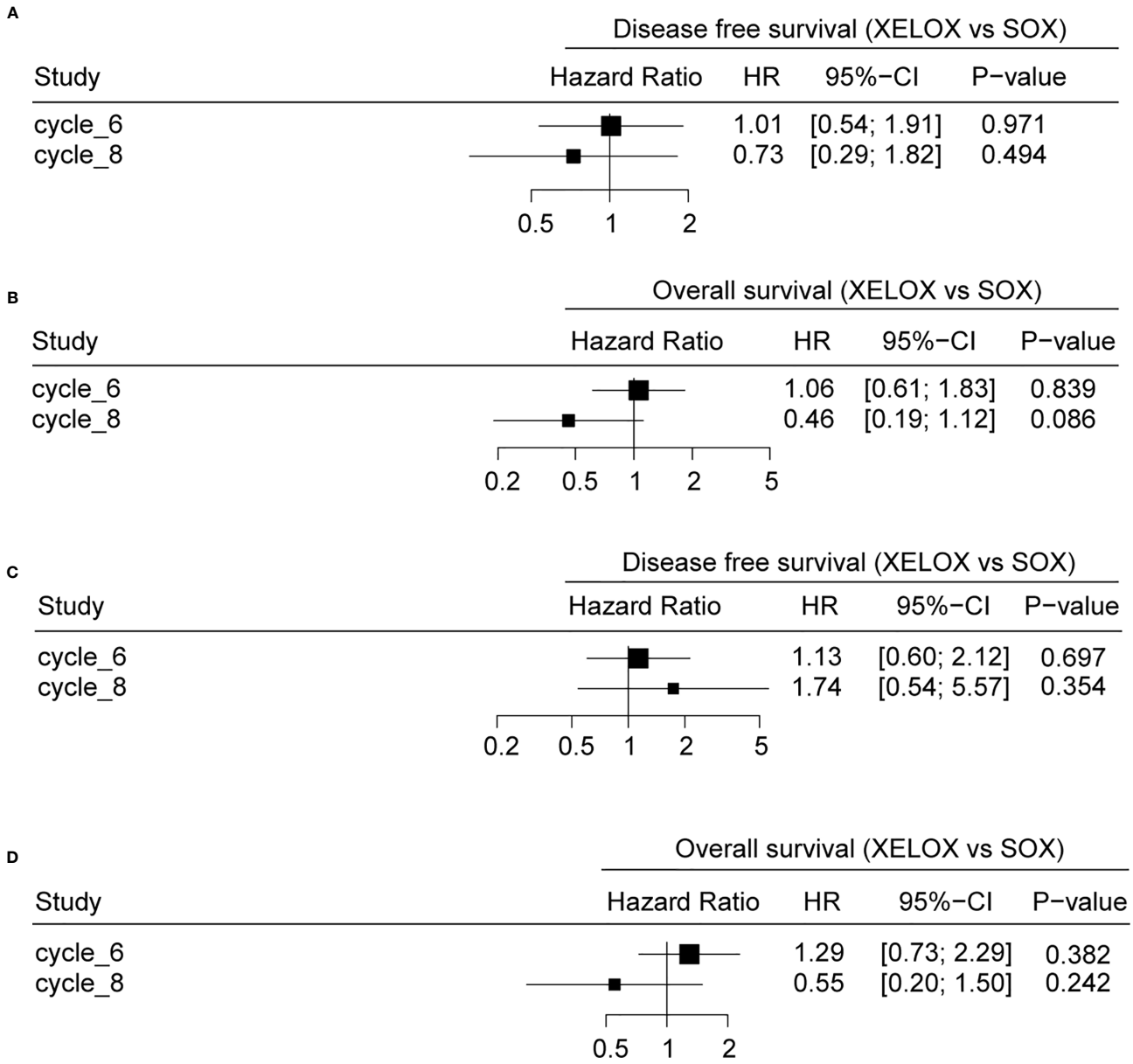

FIGURE 5 | The relationship between different chemotherapy cycles and disease-free survival (DFS) and overall survival (OS) of gastric cancer patients. DFS **(A)** and OS **(B)** analyses for patients with stage II and stage III gastric cancer. DFS **(C)** and OS **(D)** analyses for stage patients with stage III gastric cancer.

affect the experimental results. Therefore, to verify the accuracy of our results, it is necessary to conduct large-scale prospective clinical randomized controlled trials.

Together, these results and ours presented here show that the SOX chemotherapy regimen is not inferior to the XELOX regimen. Therefore, it is appropriate to compare the survival and prognosis of patients with GC receiving six and eight chemotherapy cycles, irrespective of whether they underwent SOX or XELOX regimens. Our results suggest that for patients with stage III GC, eight cycles of chemotherapy are not more effective than six cycles with regards to DFS and OS. We propose that clinically, for patients with stage III GC, six chemotherapy cycles are effective and decrease the occurrence of chemotherapy-related adverse reactions. This result needs to be verified, but may help patients with GC choose the number of adjuvant chemotherapy cycles after surgery, avoid unnecessary increased rounds of chemotherapy, improve the quality of life, and reduce family burdens.

CONCLUSION

Six chemotherapy cycles of SOX or XELOX are as effective as eight cycles in patients with TNM stage III GC after D2 radical resection.

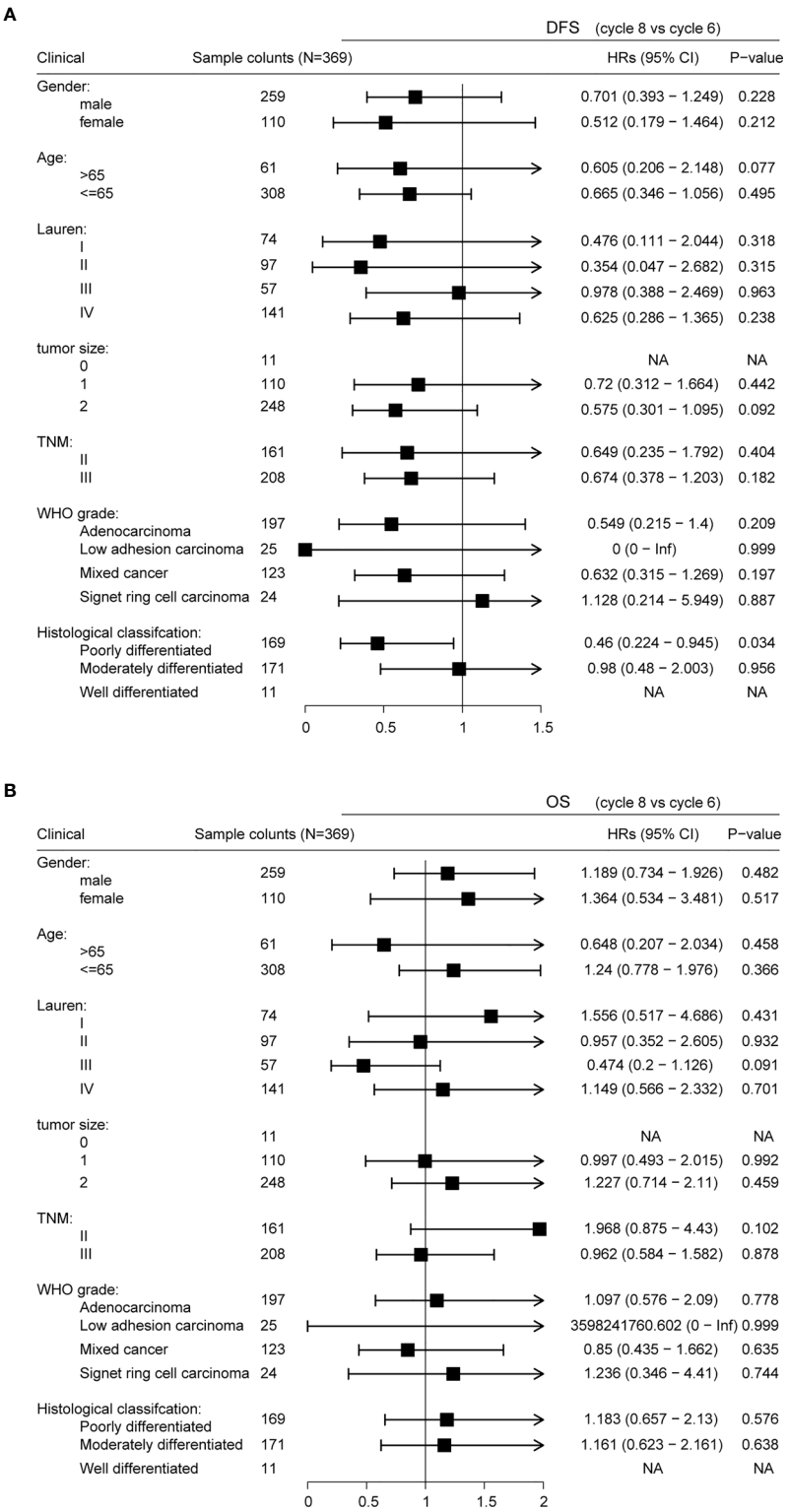

FIGURE 6 | Subgroup analyses of disease-free survival (DFS) **(A)** and of overall survival (OS) **(B)**.

DATA AVAILABILITY STATEMENT

The original contributions presented in the study are included in the article/supplementary material. Further inquiries can be directed to the corresponding authors.

AUTHOR CONTRIBUTIONS

GW and JS conceived the study. YY, ZZ and QM performed data analysis and wrote the manuscript. XF and YM provided technical guidance. YY and QM carried out data collection. GW finalized the research results and the final version of the manuscript. All authors contributed to the article and approved the submitted version.

FUNDING

This work was supported by grants from Haiyan Fund Key Project (JJZD2018-05).

REFERENCES

1. Sung H, Ferlay J, Siegel RL, Laversanne M, Soerjomataram I, Jemal A, et al. Global Cancer Statistics 2020: GLOBOCAN Estimates of Incidence and Mortality Worldwide for 36 Cancers in 185 Countries. *CA Cancer J Clin* (2021) 0:1–41. doi: 10.3322/caac.21660
2. Chen W, Zheng R, Baade PD, Zhang S, Zeng H, Bray F, et al. Cancer Statistics in China, 2015. *CA Cancer J Clin* (2016) 66(2):115–32. doi: 10.3322/caac.21338
3. Allemani C, Matsuda T, Di Carlo V, Harewood R, Matz M, Nikšić M, et al. Global Surveillance of Trends in Cancer Survival 2000-14 (Concord-3): Analysis of Individual Records for 37 513 025 Patients Diagnosed With One of 18 Cancers From 322 Population-Based Registries in 71 Countries. *Lancet* (2018) 391(10125):1023–75. doi: 10.1016/s0140-6736(17)33326-3
4. Sasako M, Sakuramoto S, Katai H, Kinoshita T, Furukawa H, Yamaguchi T, et al. Five-Year Outcomes of a Randomized Phase III Trial Comparing Adjuvant Chemotherapy With S-1 Versus Surgery Alone in Stage II or III Gastric Cancer. *J Clin Oncol* (2011) 29(33):4387–93. doi: 10.1200/jco.2011.36.5908
5. Bang YJ, Kim YW, Yang HK, Chung HC, Noh SH. CLASSIC Trail Investigators: Adjuvant Capecitabine and Oxaliplatin for Gastric Cancer After D2 Gastrectomy (CLASSIC): A Phase 3 Open-Label, Randomized Controlled Trail. *Lancet* (2012) 379(9813):315–21. doi: 10.1016/S0140-6736(11)61873-4
6. Noh SH, Park SR, Yang HK, Chung H, Chung IJ, Kim SW, et al. Adjuvant Capecitabine Plus Oxaliplatin for Gastric Cancer After D2 Gastrectomy (CLASSIC): 5-Year Follow-Up of an Open-Label, Randomised Phase 3 Trial. *Lancet Oncol* (2014) 15(12):1389–96. doi: 10.1016/s1470-2045(14)70473-5
7. Yasuhiro K, Kazuhiro Y, Mitsugu K, Wataru I, Yoshihiro K, Takeshi S, et al. A Randomized Phase III Study Comparing S-1 Plus Docetaxel With S-1 Alone as a Postoperative Adjuvant Chemotherapy for Curatively Resected Stage III Gastric Cancer (JACCRO GC-07 Trial). *J Clin Oncol* (2018) 36(15):4007. doi: 10.1200/JCO.18.o1138
8. Lee J, Lim DH, Kim S, Park SH, Park JO, Park YS, et al. Phase III Trial Comparing Capecitabine Plus Cisplatin Versus Capecitabine Plus Cisplatin With Concurrent Capecitabine Radiotherapy in Completely Resected Gastric Cancer With D2 Lymph Node Dissection: The ARTIST Trial. *J Clin Oncol* (2018) 30(3):268–73. doi: 10.1200/JCO.2011.39.1953
9. Prak SH, Zang DY, Han B, Ji JH, Kim TG, Oh SY, et al. ARTIST 2:Interm Result of a Phase III Trail Involving Adjuvant Chemotherapy and/or Chemoradiotherapy After D2 Gastrectomy in Stage II/III Gastric Cancer(GC). *J Clin Oncol* (2019) 37(15):4001. doi: 10.1200/JCO.2019.37.15_suppl.4001
10. Park SH, Lim DH, Sohn TS, Lee J, Zang DY, Kim ST, et al. A Randomized Phase III Trial Comparing Adjuvant Single-Agent S1, s-1 With Oxaliplatin, and Postoperative Chemoradiation With S-1 and Oxaliplatin in Patients With Node-Positive Gastric Cancer After D2 Resection: The ARTIST 2 Trial. *Ann Oncol* (2021) 32(3):368–74. doi: 10.1016/j.annonc.2020.11.017
11. Maehara Y. S-1 in Gastric Cancer: A Comprehensive Review. *Gastric Cancer* (2003) 6(1):2–8. doi: 10.1007/s10120-003-0232-9
12. Lee JL, Kang YK, Kang HJ, Lee KH, Zang DY, Ryoo BY, et al. A Randomised Multicentre Phase II Trial of Capecitabine vs S-1 as First-Line Treatment in Elderly Patients With Metastatic or Recurrent Unresectable Gastric Cancer. *Br J Cancer* (2008) 99(4):584–90. doi: 10.1038/sj.bjc.6604536
13. Ji J, Shen L, Li Z, Zhang X, Liang H, Xue Y, et al. Perioperative Chemotherapy of Oxaliplatin Combined With S-1 (SOX) Versus Postoperative Chemotherapy of SOX or Oxaliplatin With Capecitabine (XELOX) in Locally Advanced Gastric Adenocarcinoma With D2 Gastrectomy: A Randomized Phase III Trial (RESOLVE Trial). *Ann Oncol* (2019) 30(5):877. doi: 10.1093/annonc/mdz394.033
14. D'Angelica M, Gonen M, Brennan MF, Turnbull AD, Bains M, Karpeh MS. Patterns of Initial Recurrence in Completely Resected Gastric Adenocarcinoma. *Ann Surg* (2004) 240(5):808–16. doi: 10.1097/01.sla.0000143245.28656.15
15. Gao JP, Xu W, Liu WT, Yan M, Zhu ZG. Tumor Heterogeneity of Gastric Cancer: From the Perspective of Tumorinitiating Cell. *World J Gastroenterol* (2018) 24:2567–81. doi: 10.3748/wjg.v24.i24.2567
16. Wu CW, Lo SS, Shen KH, Hsieh MC, Chen JH, Chiang JH, et al. Incidence and Factors Associated With Recurrence Patterns After Intended Curative Surgery for Gastric Cancer. *World J Surg* (2003) 27(2):153–8. doi: 10.1007/s00268-002-6279-7
17. Hoff PM, Fuchs CS. The Experience With Oxaliplatin in the Treatment of Upper Gastrointestinal Carcinomas. *Semin Oncol* (2003) 30(4):54–61. doi: 10.1016/s0093-7754(03)00406-8
18. Hong YS, Song SY, Lee SI, Chung HC, Choi SH, Noh SH, et al. A Phase II Trial of Capecitabine in Previously Untreated Patients With Advanced and/or Metastatic Gastric Cancer. *Ann Oncol* (2004) 15(9):1344–7. doi: 10.1093/annonc/mdh343
19. Sumpter K, Harper-Wynne C, Cunningham D, Rao S, Tebbutt N, Norman AR, et al. Report of Two Protocol Planned Interim Analyses in a Randomised Multicentre Phase III Study Comparing Capecitabine With Fluorouracil and Oxaliplatin With Cisplatin in Patients With Advanced Oesophagogastric Cancer Receiving ECF. *Br J Cancer* (2005) 92(11):1976–83. doi: 10.1038/sj.bjc.6602572
20. Koizumi W, Narahara H, Hara T, Takagane A, Akiya T, Takagi M, et al. S-1 Plus Cisplatin Versus S-1 Alone for First-Line Treatment of Advanced Gastric Cancer (SPIRITS Trial): A Phase III Trial. *Lancet* (2008) 9(3):215–21. doi: 10.1016/S1470-2045(08)70035-4
21. Koizumi W, Takiuchi H, Yamada Y, Boku N, Fuse N, Muro K, et al. Phase II Study of Oxaliplatin Plus S-1 as First-Line Treatment for Advanced Gastric Cancer (G-SOX Study). *Ann Oncol* (2010) 21(5):1001–5. doi: 10.1093/annonc/mdp464
22. Cho JH, Lim JY, Cho JY. Comparison of Capecitabine and Oxaliplatin With S-1 as Adjuvant Chemotherapy in Stage III Gastric Cancer After D2 Gastrectomy. *PloS One* (2017) 12(10):e0186362. doi: 10.1371/journal.pone.0186362
23. Kim IH, Park SS, Lee CM, Kim MC, Kwon IK, Min JS, et al. Efficacy of Adjuvant s-1 Versus Xelox Chemotherapy for Patients With Gastric Cancer After D2 Lymph Node Dissection: A Retrospective, Multi-Center Observational Study. *Ann Surg Oncol* (2018) 25(5):1176–83. doi: 10.1245/s10434-018-6375-z
24. Nakamura Y, Yamanaka T, Chin K, Cho H, Katai H, Terashima M, et al. Survival Outcomes of Two Phase 2 Studies of Adjuvant Chemotherapy With S-1 Plus Oxaliplatin or Capecitabine Plus Oxaliplatin for Patients With Gastric Cancer After D2 Gastrectomy. *Ann Surg Oncol* (2019) 26(2):465–72. doi: 10.1245/s10434-018-7063-8
25. Jiang Z, Sun Y, Zhang W, Cui C, Yang L, Zhou A. Comparison of S-1 Plus Oxaliplatin (SOX) and Capecitabine Plus Oxaliplatin (XELOX) as Adjuvant Chemotherapies for Stage II and III Gastric Cancer After D2 Resection: A

Single-Center Retrospective Study. *Asia Pac J Clin Oncol* (2020) 16(3):180–6. doi: 10.1111/ajco.13321

Conflict of Interest: The authors declare that the research was conducted in the absence of any commercial or financial relationships that could be construed as a potential conflict of interest.

frontiers in Oncology

ORIGINAL RESEARCH
published: 03 June 2021
doi: 10.3389/fonc.2021.651644

Chrysin Induced Cell Apoptosis Through *H19*/let-7a/*COPB2* Axis in Gastric Cancer Cells and Inhibited Tumor Growth

Lin Chen[1†], *Qirong Li*[1†], *Ziping Jiang*[2†], *Chengshun Li*[1†], *Haobo Hu*[1], *Tiedong Wang*[1], *Yan Gao*[1] *and Dongxu Wang*[1*]

[1] Laboratory Animal Center, College of Animal Science, Jilin University, Changchun, China, [2] Department of Hand Surgery, The First Hospital of Jilin University, Changchun, China

OPEN ACCESS

Edited by:
Yue Hou,
Northeastern University, China

Reviewed by:
Yi Qin,
Fudan University, China
Jiang Pi,
Guangdong Medical University, China
Xiangyan Li,
Changchun University of Chinese Medicine, China
Chunmeng Sun,
China Pharmaceutical University, China

***Correspondence:**
Dongxu Wang
wang_dong_xu@jlu.edu.cn

[†]These authors have contributed equally to this work

Specialty section:
This article was submitted to Pharmacology of Anti-Cancer Drugs, a section of the journal Frontiers in Oncology

Received: 10 January 2021
Accepted: 10 May 2021
Published: 03 June 2021

Citation:
Chen L, Li Q, Jiang Z, Li C, Hu H, Wang T, Gao Y and Wang D (2021) Chrysin Induced Cell Apoptosis Through H19/let-7a/COPB2 Axis in Gastric Cancer Cells and Inhibited Tumor Growth. Front. Oncol. 11:651644. doi: 10.3389/fonc.2021.651644

Background: Chrysin is a natural flavone that is present in honey and has exhibited anti-tumor properties. It has been widely studied as a therapeutic agent for the treatment of various types of cancers. The objectives of this present study were to elucidate how chrysin regulates non-coding RNA expression to exert anti-tumor effects in gastric cancer cells.

Methods: Through the use of RNA sequencing, we investigated the differential expression of mRNAs in gastric cancer cells treated with chrysin. Furthermore, *COPB2, H19* and let-7a overexpression and knockdown were conducted. Other features, including cell growth, apoptosis, migration and invasion, were also analyzed. Knockout of the *COPB2* gene was generated using the CRISPR/Cas9 system for tumor growth analysis *in vivo*.

Results: Our results identified *COPB2* as a differentially expressed mRNA that is down-regulated following treatment with chrysin. Moreover, the results showed that chrysin can induce cellular apoptosis and inhibit cell migration and invasion. To further determine the underlying mechanism of COPB2 expression, we investigated the expression of the long non-coding RNA (lncRNA) *H19* and microRNA let-7a. Our results showed that treatment with chrysin significantly increased let-7a expression and reduced the expression of *H19* and *COPB2*. In addition, our results demonstrated that reduced expression of *COPB2* markedly promotes cell apoptosis. Finally, *in vivo* data suggested that *COPB2* expression is related to tumor growth.

Conclusions: This study suggests that chrysin exhibited anti-tumor effects through a *H19*/let-7a/*COPB2* axis.

Keywords: *H19*, let-7a, *COPB2*, chrysin, gastric cancer

INTRODUCTION

Currently, gastric cancer (GC) is the third most common cause of human mortality among malignant cancers (1). Although surgical treatment for GC has led to increased survival rates, the diagnosis of GC needs to improve (2). There are several potential biomarkers of GC, including many genes and cell signaling pathways that are involved in GC development, such as *BRCA2* and Ras-Raf-MAPK signaling (3, 4). Coatomer protein complex subunit beta 2 (COPB2) is a protein that functions to transport other proteins as vesicles from the endoplasmic reticulum to Golgi apparatus (5). Recently, numerous reports have indicated that *COPB2* is abnormally expressed in colorectal cancer (CRC), cholangiocellular carcinoma and lung cancer (6–8). Previous studies have indicated that the reduction of *COPB2* expression inhibited cell growth and induced apoptosis through the JNK/c-Jun signaling pathway in RKO and HCT116 cells (9). Moreover, miR4461 and miR335 were found to regulate *COPB2* expression, which subsequently inhibited cell growth in CRC and lung cancer cells (10, 11).

Increasing evidence suggests that non-coding RNAs (ncRNAs), such as miRNAs, can be applied to the classification of GC (12). As tumor suppressors, the let-7 family is down-regulated in GC (13). Increased expression of let-7a has been shown to inhibit cell migration and invasion in prostate cancer (14). Compared to the loss of let-7a expression, the long non-coding RNA (lncRNA) *H19* has been shown to be highly expressed in cancers, including GC (15). As a molecular sponge, *H19* was found to be related to let-7 in the context of breast cancer stem cells (16). Previous reports have suggested that *H19* expression suppressed endogenous let-7 while *H19* mutant was not related to let-7 (17). Additionally, reduced expression of *H19* induced cellular apoptosis and inhibited cell growth in HCC (18). However, there is little evidence to suggest that *COPB2* expression is associated with lncRNAs and miRNAs in GC.

As a traditional Chinese medicine, chrysin is a natural flavone that has anti-cancer function (19). Previous reports have indicated that chrysin induces cellular apoptosis and inhibits tumor glycolysis in HCC (20). Moreover, chrysin has been shown to inhibit cell migration and invasion in melanoma cells (21). In this study, chrysin was used to treat GC cells and we screened differentially expressed genes using RNA-seq. Additionally, we created a *COPB2* knockout (KO) cell line using the CRISPR/Cas9 system. Our findings indicate that chrysin can regulate *COPB2* expression through let-7, which is antagonized by *H19*.

MATERIALS AND METHODS

Cell Culture and Chrysin Treatment

Human GC cell lines (SGC7901, MKN45 and BGC823) and the human gastric epithelial cell line GES-1 were grown in Dulbecco's modified Eagle's (DMEM; Gibco) supplemented with 10% fetal bovine serum (Gibco), and cultured at 37°C in 5% CO_2. The human gastric epithelial cell GES1 served as control. Experiments were conducted by treating GES1, SGC7901, MKN45 and BGC823 cells with 40 μM of Chrysin (Yuanye Bio-Technology, Shanghai) for 48 h when they reached 80 to 90% confluence.

RNA Isolation and RNA-Seq Analysis

GC cells were treated with 40 μM chrysin for 48 h, after which total RNA was extracted. To remove and purify ribosomal RNA (rRNA), we used the RiboZero Magnetic Gold Kit (Epidemiology, USA). Then, RNA-seq (Sangon Biotech, Shanghai, China) was carried out on HiSeq2500 (Illumina, USA) to analyze raw reads, which were quality controlled by FastQC. Using the HISAT2 software, the sequenced-reads were aligned to the reference sequence. The gene expression analysis and differential gene expression analysis were determined using DEGseq and DESeq program, respectively, in HISAT2 (qValue <0.05, Fold Change >2). Using clusterProfiler, the enrichment analysis, including Kyoto Encyclopedia of Genes and Genomes (KEGG) pathway, of differential expressed genes was determined.

Knockdown and Overexpression of *COPB2, H19* and let-7a

The pcDNA3.1 (GenePharma, China) vector served as the backbone for the overexpression construct of *COPB2* (pcDNA3.1-COPB2) and *H19* (pcDNA3.1-H19). The cells were cultured without FBS once they reached a confluence of 80% over 12–16 h. Next, the pcDNA3.1-COPB2 (2 μg), pcDNA3.1-H19 (2 μg) and Lipofectamine 2000 (Invitrogen, USA) were utilized for transfection. After incubating for 48 h, G418 (400 mg/ml, Invitrogen, USA) was added to GC cells. The clones were grown and picked after 14 days.

The siRNAs of *COPB2* (si-COPB2) and *H19* (si-H19) were obtained from RiboBio (Guangzhou, China). The target sequences of small interfering RNAs (siRNAs) are listed in **Table S1**. The mimics and inhibitors of let-7a-3p, miR29b-3p and miR675-3p were obtained from RiboBio. The GC cells were transfected with knockdown (siRNA), let-7a-3p mimics, and let-7a-3p inhibitor for 48 h. The nonspecific siRNA (si-Nc) was transfected into control cells.

The COPB2-KO was generated using the CRISPR/Cas9 system (px459, Addgene, USA). The single guide RNAs (sgRNAs) were designed as previously reported (22). The sequences of sgRNAs are listed in **Table S2**. Transfection was conducting using COPB2-KO (5 μg) and Lipofectamine 2000 (Invitrogen, USA) for 48 h. Next, puromycin helped select the positive clones. After 14 days, the clones (COPB2-KO) were grown and picked for subsequent western blot, qPCR and sequencing analysis.

DNA Methylation Analysis

The Bisulfite Sequencing PCR (BSP) protocol was carried out as previously described (23). Using the TIANamp Genomic DNA Kit (TIANGEN, Beijing, China), the DNA of SGC7901 and BGC823 cells were extracted. The DNA was modified using CpGenome™ Turbo Bisulfite Modification Kit (Millipore, USA). The differentially methylated regions (DMRs) of *H19* were

amplified using nested PCR. The products, which included 10 positive clones, were analyzed using the BiQ Analyzer software (http://biq-analyzer.bioinf.mpi-inf.mpg.de/tools/MethylationDiagrams/index.php). The primers of *H19* DMR are listed in **Table S3**.

Gene Expression Analysis

The GC cells' RNA was extracted and cDNAs were generated using the cDNA first-strand synthesis kit (TIANGEN, China). Gene expression analysis was conducted using quantitative real-time PCR (qPCR). The conditions for qPCR included heating to 94°C for 3 min, and then denaturation at 94°C for 10 s after 35 cycles. The annealing was carried out at 59°C for 15 s. The products were extended at 72°C for 30 s. The internal controls included GAPDH and U6 for genes and miRNAs, respectively. The primers for qPCR are listed in **Table S4**. The sequences of *COPB2* exon 5 and exon 22 are listed in **Table S5**.

Cell Migration and Invasion Analysis

Wound healing assay was conducted to analyze cell migration of GC cells. In brief, 5×10^5 cells were cultured and seeded before treatment with chrysin, siRNAs, overexpression vectors, let-7a-3p mimics or let-7a-3p inhibitor. The cells were cultured after a scratched line was created with culture medium without serum. Cell migration was measured using the scratched area at 12, 24 and 48 h.

For cell invasion assays, GC cells (3×10^4) were cultured and seeded with 20 μl Matrigel prior to treatment with chrysin, siRNAs, overexpression vectors, let-7a-3p mimics and let-7a-inhibitor (BD Biosciences, USA). Next, 0.5 ml of medium, which contained 10% FBS, was added to the cells for 24 h. Then, 0.2% crystal violet dye (Solarbio, China) was used to stain cells after being fixed with 4% paraformaldehyde. The stained cells were assayed using the ImageJ software.

Cell Counting Kit-8 Assay

The GC cells (4×10^3) were cultured and seeded prior treatment with chrysin, siRNAs, overexpression vectors, let-7a-3p mimics and let-7a-3p inhibitors in order to conduct cell viability assay, as previously described (24). Then, Cell Counting Kit-8 (CCK-8) solution (10 μl, Dojindo, Kumamoto, Japan) was added to each well. After incubating for 2.5 h, the cells were measured using absorbance (OD) at 450 nm to analyze cell viability.

Cell Apoptosis Analysis

GC cells (1×10^6) were cultured prior to treatment with chrysin, siRNAs, overexpression vectors, let-7a-3p mimics and let-7a-inhibitor for detection of cellular apoptosis, as previously described (25). Then, Annexin V-FITC/PI reagent was added to cell to react for 30 min and flow cytometry (BD Biosciences, Franklin Lakes, NJ, USA) was used to detect fluorescent cells.

Western Blot Analysis

Total protein was extracted from GC cells using protein extraction buffer (Beyotime, China). Then, proteins were quantified utilizing the BCA protein assay kit (TIANGEN, Beijing, China). Sodium dodecyl sulfate-polyacrylamide gel electrophoresis was used to separate the proteins. After electrophoresis, proteins were transferred to the polyvinylidene difluoride (PVDF) membrane. The membrane was then incubated with primary antibodies, including anti-COPB2 (BETHYL, A304-522A-M-1, USA), anti-P53 (Abcam, ab131442, USA), anti-BAX (CST, D2E11, USA), anti-BCL2 (CST, D55G8, USA), anti-E-CADHERIN (Proteintech, 20874-1-AP,USA) and anti-GAPDH (Bioworld, AP0066, USA), overnight at 4°C. Subsequently, membranes were incubated with HRP-conjugated affiniPure goat antibodies IgG (BOSTER, China) for 1.5 h. The target bands were analyzed using ECL Super Signal (Pierce, USA).

Hematoxylin and Eosin (H&E) Staining

Tumor tissues from the control and chrysin groups were fixed in 4% paraformaldehyde for 48 h, embedded in paraffin wax and sliced into 5 μm sections. The slides were then stained with H&E and cancer cell infiltration was determined by observation under a light microscope.

Animals and Animal Care

For *in vivo* experiments, 17 female nude mice (6–8 weeks old) were utilized to determine the effect of chrysin treatment and *COPB2* KO on tumor growth. The mice were acquired and grouped-housed in the Laboratory Animal Center of Jilin University. All mice were provided *ad libitum* access to standard rodent food and tap water within the laboratory cages, as well as under specific pathogen-free (SPF) conditions. The BGC823, pcDNA3.1-COPB2 and COPB2-KO cell lines (3×10^6) were subcutaneously injected into the left flank of each mouse, and tumors were observed after seven days. The tumor length (L) and width (W) were calculated as $L \times W^2/2$.

Statistical Analysis

An unpaired Student's *t*-test was utilized in the present study. The SPSS 16.0 software (SPSS Inc., Chicago, IL, USA) helped conduct statistical analysis. All data was expressed as mean ± SD. A *p*-value of <0.05 was considered to be statistically significant. The website of http://ualcan.path.uab.edu/index.html was used for The Cancer Genome Atlas (TCGA) analysis. The TargetScan database was used to predict miRNA.

RESULTS

Screen of Differentially Expressed Gene of Chrysin-Treated GC Cells

In order to analyze gene expression patterns of chrysin treatment in gastric cancer cells, we performed RNA-Seq. Overall, 20,010 genes were identified as core genes (**Figure 1A**). Compared to the control group, 380 genes were significantly up-regulated while 2,071 were significantly down-regulated (**Figure 1B**). Data from heatmap and KEGG pathway suggests that the differentially expressed genes have functions in cell death and growth (**Figures 1C, D**). In order to confirm this data, six genes (*CAPN2*, *MXI1*, *HSPA9*, *RHBDD2*, *COPB2* and *GABAPAPL1*), which were related to cell growth and death, were further

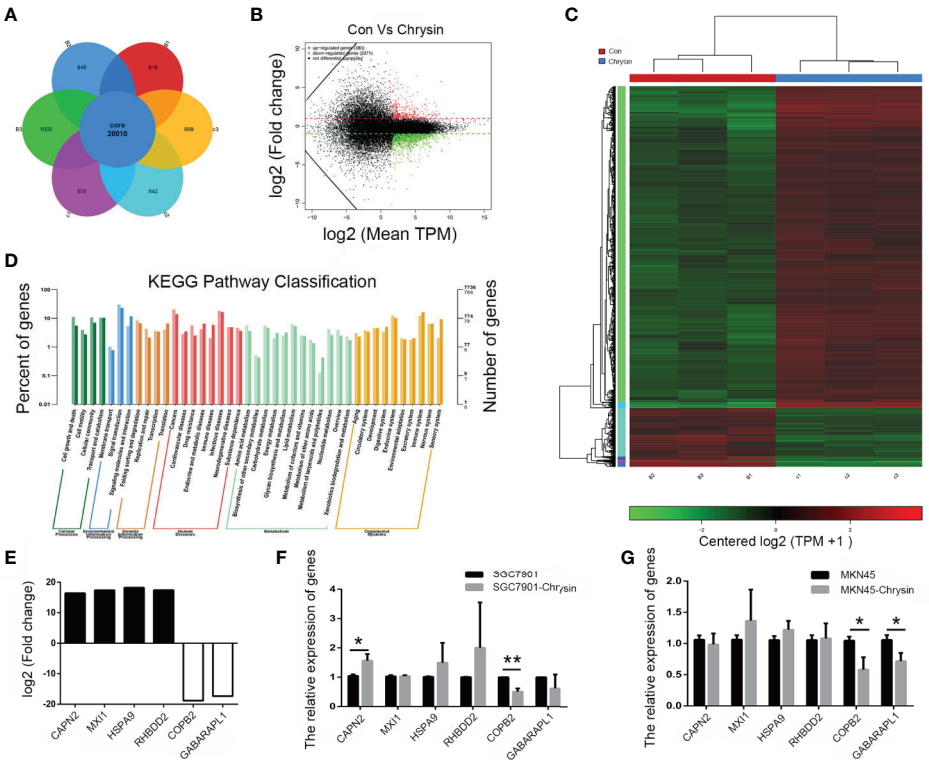

FIGURE 1 | Screening of differentially expressed genes by RNA-seq. Analysis of differential expressed genes after chrysin treatment **(A)**, Identification of different expressed genes **(B)**. The heatmap was drawn to show the differentially expressed genes **(C)**. KEGG pathway of the differentially expressed genes **(D)**. The expression of log2 fold change in six genes **(E)**. Relative expression of *CAPN2*, *MXI1*, *HSPA9*, *RHBDD2*, *COPB2* and *GABAPAPL1* were analyzed by qPCR after Chrysin treatment in SGC7901 **(F)** and MKN45 cells **(G)**. The data are represented as the mean ± SD (n = 3). * (p <0.05) and ** (p <0.01) indicate statistically significant differences.

validated (**Figure 1E**). The qPCR results indicated that *COPB2* expression was downregulated upon chrysin treatment in SGC7901 (**Figure 1F**) and MKN45 (**Figure 1G**) cells. These results indicate that *COPB2* expression is regulated by chrysin in GC cells.

Chrysin Increased let-7a and Inhibited *H19* and *COPB2* Expression in GC Cells

In order to further verify the expression levels of *COPB2* in GC, we utilized the TCGA database. Results indicated increased expression of *COPB2* in primary tumor of the stomach adenocarcinoma (STAD) patients (**Figure S1A**). Compared to GES1 cells, qPCR and western bolt results indicated increased expression of COPB2 in MKN45, SGC7901 and BGC823 cells (**Figures 2A, B**). To investigate which miRNAs were involved in *COPB2* expression, bioinformatics analysis was performed. The database suggested that let-7a targets *COPB2* (**Figures 2C**, **S2**). Furthermore, we analyzed let-7a levels in the TCGA database. Results indicated no differences between normal and tumor tissues (**Figure S1B**). However, qPCR results suggested that let-7a levels were reduced in GC cells, compared to GES1 cells (**Figure 2D**). Considering that let-7a is associated with expression of the lncRNA *H19*, we analyzed the expression pattern of *H19*. The TCGA database indicated increased expression of *H19* among STAD patients (**Figure S1C**). The qPCR results indicated increased expression of *H19* in GC cells (**Figure 2E**). DNA methylation results indicated the hypo-methylation profile of *H19* DMR in GC cells (**Figure S3**). The cell growth was analyzed after chrysin treatment. The CCK8 results indicated that 40 μM was the optimal dose for subsequent experiments (**Figure 2F**). Moreover, qPCR results indicated increased expression of let-7a, as well as reduced expression of *H19* after chrysin treatment in GC cells (**Figure 2G**). Besides, chrysin was able to induce cell apoptosis, as well as inhibit cell migration and invasion in GC cells (**Figures 3**, **S4**). These results indicate that chrysin has an anti-cancer role and regulates expression of *COPB2*, *H19* and let-7a in GC cells.

H19/let-7a Regulate *COPB2* Expression

Considering that *H19* has a role in let-7a expression, we analyzed the effect of *H19* knockdown and overexpression in GC cells. The results indicated reduced expression of let-7a in the *H19* overexpression group, as well as overexpression of let-7a in

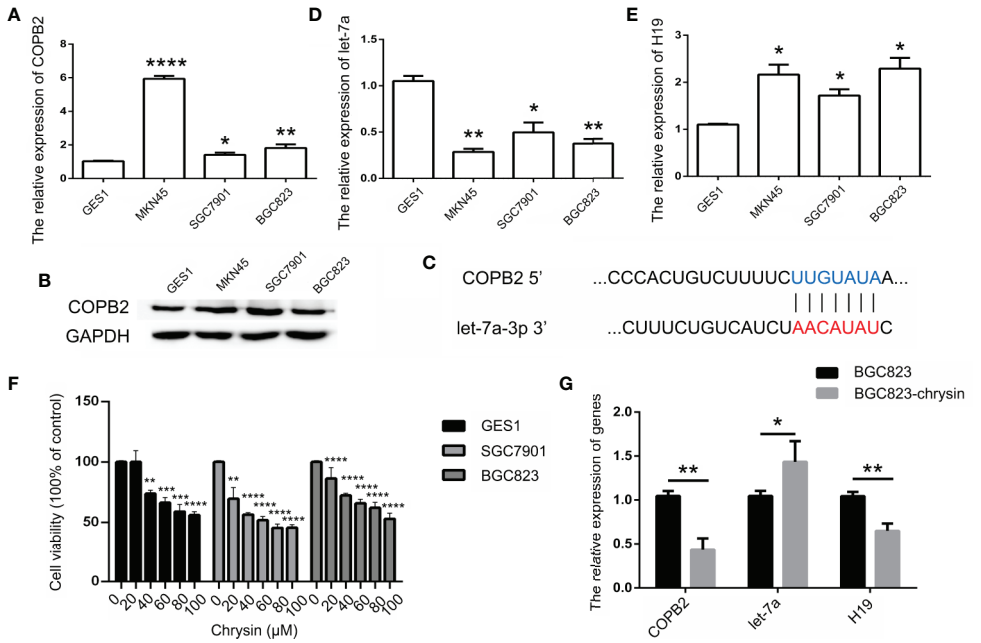

FIGURE 2 | Analysis of *COPB2*, let-7a and *H19* expression pattern. The expression of COPB2 in GC cells using qPCR **(A)** and western blot **(B)**. Schematic representations of *COPB2* and let-7a **(C)**. Relative expression of let-7a in GC ells **(D)**. Relative expression of *H19* in GC ells **(E)**. The cell growth was analyzed by CCK8 assay **(F)**. Relative expression of *COPB2*, let-7a and *H19* was analyzed by qPCR after chrysin treatment in GC cells **(G)**. The data are represented as the mean ± SD (n = 3). * (p <0.05), ** (p <0.01), *** (p <0.001) and **** (p <0.0001) indicate statistically significant differences.

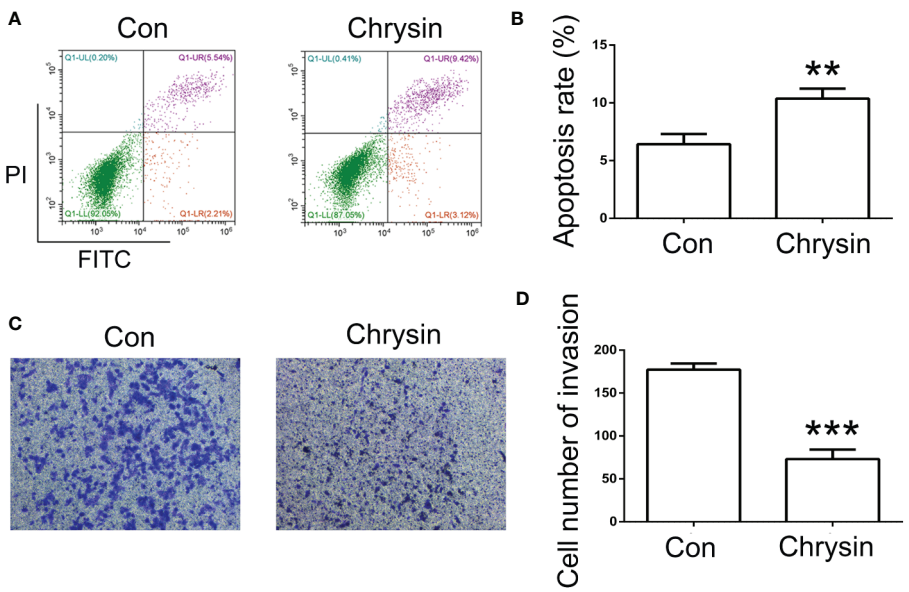

FIGURE 3 | Analysis of cell apoptosis and invasion after chrysin treatment. The cell apoptosis was analyzed between Con and chrysin group **(A)**. Statistical analysis of the percentage of cell apoptosis **(B)**. The cell invasion was analyzed **(C)**. Statistical analysis of the percentage of cell invasion **(D)**. The data are represented as the mean ± SD (n = 3). ** (p <0.01) and *** (p <0.001) indicate statistically significant differences.

the *H19* knockdown group (**Figures 4A–C**). In order to investigate the expression pattern of let-7a, we utilized miRNA mimics and inhibitors. The qPCR and western blot results demonstrated that let-7a mimics led to suppressed expression of *COPB2* (**Figures 4D–G**). These results confirm that *H19* acts as a sponge that competes with let-7a, thus regulating *COPB2* expression.

Reduced Expression of *COPB2* Induced Cell Apoptosis and Inhibited Cell Invasion

In order to analyze whether *COPB2* expression has an effect on cell death and growth, we transfected knockdown and overexpression vector of *COPB2* into GC cells. The CCK8 data demonstrates that reduced expression of *COPB2* and increased expression of let-7a inhibits cell growth (**Figure S5**). Moreover, our results suggested that reduced expression of *COPB2* induced cellular apoptosis (**Figures 5A, B**). In order to validate this, we analyzed markers of cell apoptosis. The results showed that increased expression of p53 was observed in the *COPB2* knockdown group (**Figure S6**). In addition, *COPB2* expression did not have an effect on cell migration in GC cells (**Figures 5C, D**). However, our data shows that reduced expression of *COPB2* inhibited cell invasion (**Figures 5E, F**). Next, we investigated the effect of chrysin about cell migration and invasion in the COPB2 overexpression group. This result demonstrated that chrysin induced cell apoptosis and inhibited cell migration and invasion (**Figures S7**, **S8**). In order to validate this finding, the overexpression and knockdown of *H19* and let-7a were used to analyze cell apoptosis. The results demonstrated that reduced expression of *H19* and increased expression of let-7a induced cell apoptosis (**Figure S9**). Overall, these results suggest that *COPB2* has a role in cell apoptosis and invasion.

Loss Expression of *COPB2* Inhibited Tumor Growth *In Vivo*

In order to assess the anti-cancer effect of chrysin *in vivo*, we utilized nude mice. The BGC823 cells were injected into nude mice and after seven days, mice were treated with chrysin (20 mg/kg) for two weeks. The results showed that chrysin is able to inhibit tumor growth and *COPB2* expression *in vivo* (**Figures 6A–D**). The H&E staining results confirm this data (**Figure S10**). Moreover, qPCR result indicated that chrysin inhibited the expression of *H19*, and increased let-7a *in vivo* (**Figure S11**). In order to determine the effect of loss expression of *COPB2 in vivo*, CRISPR/Cas9 system was used to edit the *COPB2* exon 5 (**Figure 6E**). The qPCR data showed lower expression of *COPB2* in the *COPB2* KO group compared to the control group (**Figure 6F**). Moreover, chrysin treatment reduced *COPB2* expression in overexpression and KO of *COPB2* cells (**Figure S12**). To further confirm the effect of *COPB2* expression, *COPB2* KO cells were injected into nude mice. Results suggested that loss of expression of *COPB2* inhibited tumor growth

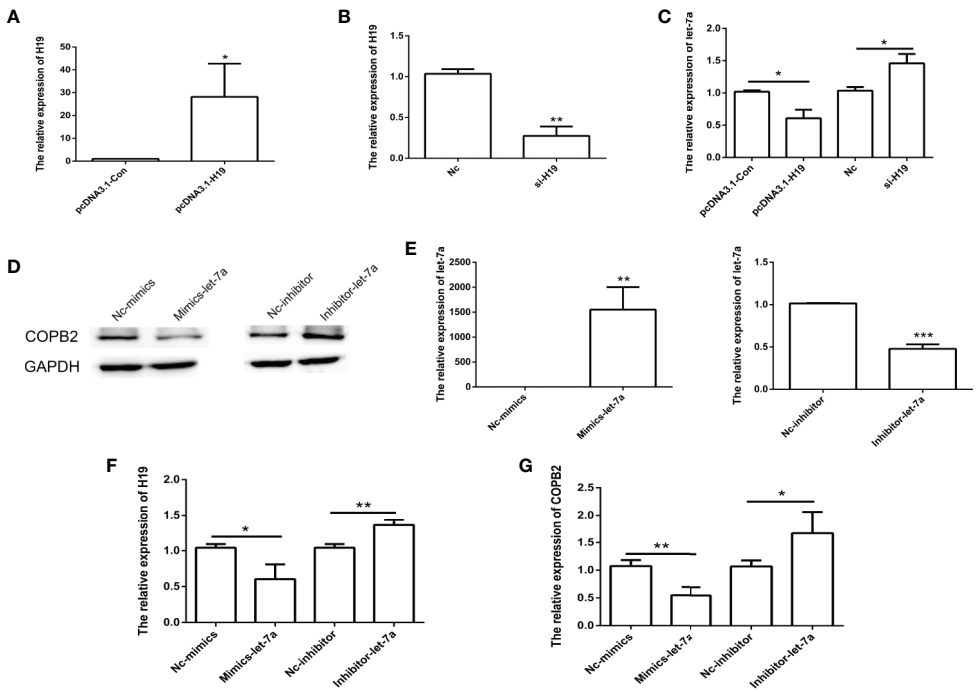

FIGURE 4 | Analysis of *COPB2* expression pattern through *H19*/let-7a in GC cells. Relative expression of *H19* and let-7a in pcDNA3.1-Con, pcDNA3.1-H19, Nc and si-H19 group using qPCR **(A–C)**. Expression of COPB2 protein in Nc-mimics, mimics-let-7a, Nc-inhibitor and inhibitor-let-7a group using Western blot **(D)**. Relative expression of let-7a, *H19* and *COPB2* in Nc-mimics, mimics-let-7a, Nc-inhibitor and inhibitor-let-7a group using qPCR **(E–G)**. The data are represented as the mean ± SD (n = 3). * (p <0.05), ** (p <0.01) and *** (p <0.001) indicate statistically significant differences.

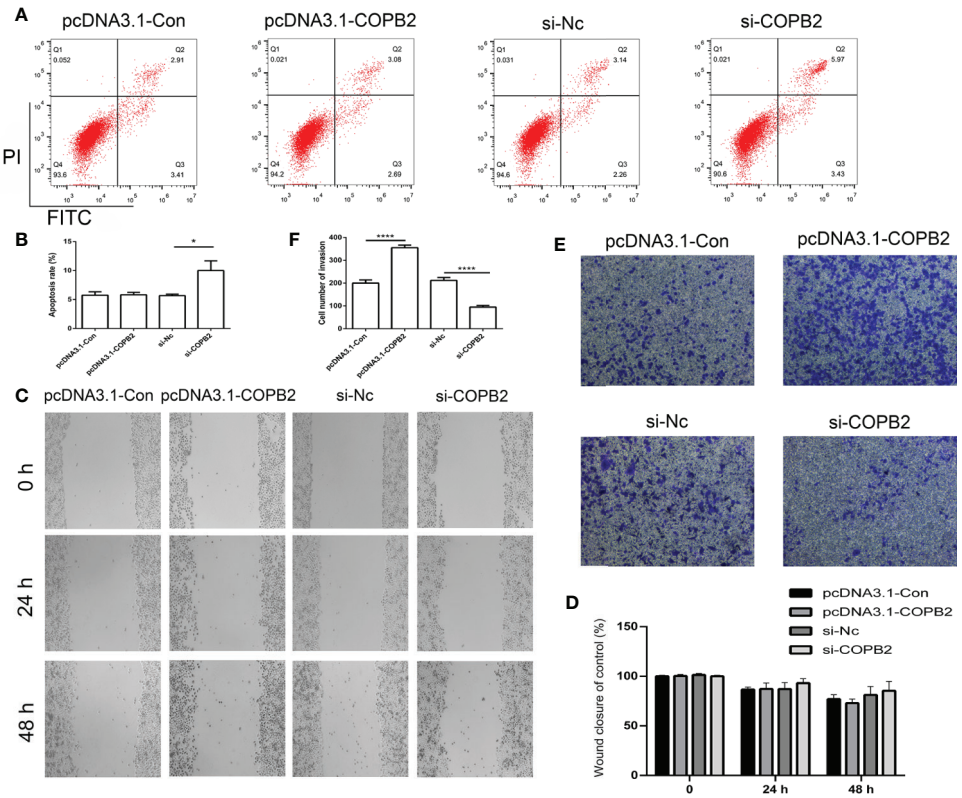

FIGURE 5 | Analysis of cell apoptosis, migration and invasion after knockdown and overexpression of *COPB2*. Cell apoptosis was analyzed in the pcDNA3.1-Con, pcDNA3.1-COPB2, si-Nc, and si-COPB2 group **(A, B)**. Cell migration was analyzed after si-COPB2 and pcDNA3.1-COPB2 were transfected **(C, D)**. The cell invasion was analyzed in pcDNA3.1-Con, pcDNA3.1-COPB2, si-Nc, and si-COPB2 group **(E, F)**. Statistical analysis of the percentage of cell invasion **(D)**. The data are represented as the mean ± SD (n = 3). * (p <0.05) and **** (p <0.0001) indicate statistically significant differences.

(**Figures 6G, H**). Overall, these results indicate that reduced expression of *COPB2* leads to anti-tumor effects.

DISCUSSION

Chrysin, a natural medicine, has anti-inflammatory and anti-cancer function and has been used to treat degenerative disorders and cancers in several Asian countries (26, 27). In this study, chrysin was used to treat GC cells in order to evaluate its effect on cellular apoptosis, growth, migration and invasion. Previous reports have indicated that chrysin induces cell apoptosis and inhibits cell growth, migration and invasion in glioblastoma cells (28), which was by validated by our results, which showed that chrysin has anti-cancer effects in SGC7901, MKN45 and BGC823 cells. Moreover, chrysin was found to increase expression of miR-9 and let-7a in GC cells, in accordance with previous data (29). Interestingly, our previous data suggested that chrysin inhibited cell migration and invasion in MKN45 cells through TET1, which regulates global DNA methylation (30). Previous reports have indicated abnormal DNA methylation in GC (31). Herein, our results suggested that *H19* DMR is hypomethylated in SGC7901 and BGC823 cell lines, which is related to increased expression of *H19*. In addition, chrysin functions to regulate the expression of *H19*, let-7a and *COPB2*. Furthermore, chrysin inhibited cell invasion which was overexpression of *COPB2*.

Recently, lncRNAs and miRNAs have been demonstrated to have roles in development of different types of cancer, including HCC (18). There is evidence that reduced expression of lncRNA *H19* leads to inhibition of tumor growth in breast cancer, bladder cancer and colorectal cancer (32). Moreover, *H19*, as a competitive endogenous RNA, is associated with miRNAs, such as miR-29 and let-7 (16, 33). Our results indicated that *H19* and let-7a have competitive regulation in GC cells, which has also been confirmed in a previous report (17). Emerging evidence suggested that loss of expression of let-7 correlates with poor prognosis in various cancer (34). Our data showed that chrysin increased expression of let-7a and inhibited cell migration and invasion. Previous reports indicated that silencing of let-7, which targets MDM4, promotes cell proliferation, migration and invasion (35). Further, reduced expression of *H19* and increased let-7a expression induced cell apoptosis in GC cells, which validated the previous report (36). These results suggested that the expression of *H19* and let-7a is involved in cell apoptosis, growth and invasion of GC cells.

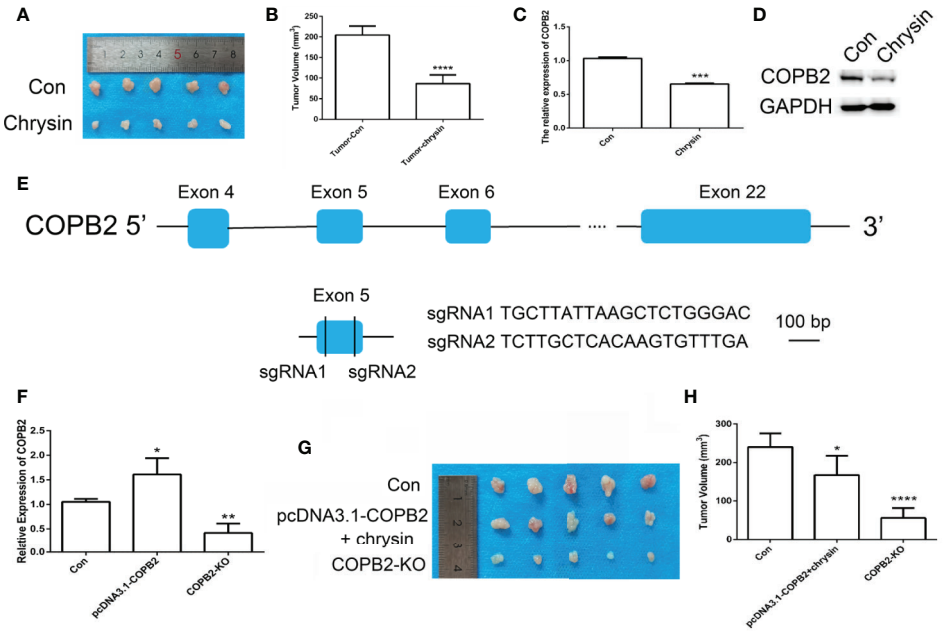

FIGURE 6 | CRISPR/Cas9-mediated gene targeting of *COPB2*. Morphological observation of mouse tumor tissue **(A)**. Analysis of tumor volume **(B)**. The expression pattern of *COPB2* in tumor of mice after chrysin treatment **(C, D)**. Schematic diagram of sgRNAs targeting the *COPB2* gene loci **(E)**. The expression of *COPB2* using qPCR **(F)**. The tumor morphology **(G)** and volume **(H)**. Blue indicated *COPB2*. * ($p < 0.05$), ** ($p < 0.01$), *** ($p < 0.001$) **** and ($p < 0.0001$) indicate statistically significant differences.

Previous reports indicated that let-7f targets HMGA2 in thyroid cancer (37). Compared to let-7f, *IL-6* and *CKIP-1* were reported to be targets of let-7a (38, 39). Our results suggest that let-7a targets *COPB2*, which leads to differential expression after chrysin treatment in GC cells. A previous study indicated that the expression of *COPB2* is associated with cell growth, apoptosis, migration and invasion, functioning through a miR-216a manner, in lung cancer (8). Our results suggested that

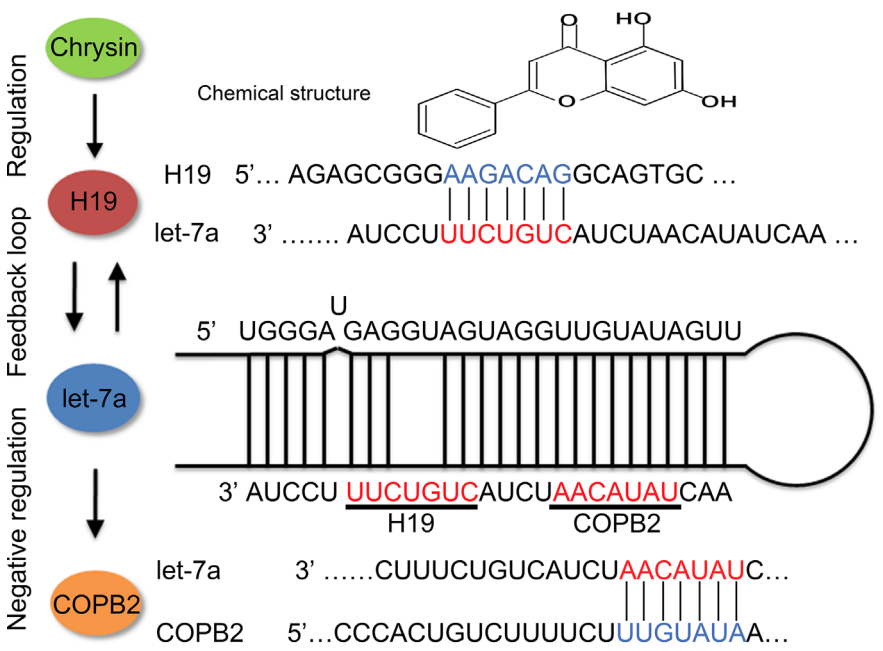

FIGURE 7 | Schematic diagram of *H19*/let-7a regulate *COPB2* expression.

expression of *COPB2* was regulated by *H19*/let-7 axis in GC cells (**Figure 7**). Moreover, reduced expression of *COPB2* induced cellular apoptosis and inhibited cell growth in prostate cancer (40). Our data showed reduced expression of *COPB2* increased p53 and E-cadherin expression. These results indicated that reduced expression of *COPB2* induced cell apoptosis and inhibited invasion through *H19*/let-7a.

In order to confirm the effect of *COPB2 in vivo*, a xenograft model using nude mice was established. The *in vivo* results suggested that chrysin led to reduced expression of *COPB2*, which further confirms our data in GC cells. Furthermore, chrysin inhibited tumor growth *in vivo*, which is in accordance with a previous report in melanomas (41). These data indicate that chrysin can regulate *COPB2* expression, which inhibits tumor growth *in vivo*. In order to further analyze the putative effect of *COPB2*, the KO and overexpression *COPB2* cell line were injected into nude mice. As a powerful gene editing tool, the CRISPR/Cas9 system was wildly used *in vitro* and *in vivo*. Our results indicated that *COPB2* KO suppressed tumor growth.

In summary, *COPB2* is a differentially expressed gene that was identified after chrysin treatment in GC cells. Our data indicated that *COPB2* is regulated by let-7a, which acts as a molecular sponge of *H19*. Moreover, reduced expression of *COPB2* induced cellular apoptosis and inhibited cell growth and invasion. Therefore, this present study revealed that *COPB2* is a potential molecular targeted therapy in GC.

DATA AVAILABILITY STATEMENT

The datasets presented in this study can be found in online repositories. The names of the repository/repositories and accession number(s) can be found in the article/ **Supplementary Material**.

ETHICS STATEMENT

The animal study was reviewed and approved by Laboratory Animal Center of Jilin University.

AUTHOR CONTRIBUTIONS

DW designed the experiments and wrote the manuscript. LC, QL, HH, and CL performed cell experiment and gene expression analysis. TW and ZJ contributed reagents and materials. YG and CL carried out animal experiment. DW analyzed the data and prepared figures. All authors contributed to the article and approved the submitted version.

FUNDING

This work was supported by the Jilin Health Commission Program under Grant 2020J05S, the Fundamental Research Funds for the Central Universities under Grant 2019JCKT-70, the Jilin Education Department Program under Grant JJKH20200950KJ, and the Jilin Scientific and Technological Development Program under Grant 20190103071JH.

SUPPLEMENTARY MATERIAL

The Supplementary Material for this article can be found online at: https://www.frontiersin.org/articles/10.3389/fonc.2021.651644/full#supplementary-material

Supplementary Figure 1 | Analysis of *COPB2*, let-7a and *H19* in TCGA database. Effect of *COPB2* **(A)**, let-7a **(B)** and *H19* **(C)** expression on GC patient survival in TCGA database.

Supplementary Figure 2 | Screen of miRNA which regulated by COPB2.

Supplementary Figure 3 | The DNA methylation status of *H19* DMR in MGC823 and SGC7901 using BSP.

Supplementary Figure 4 | Analysis of cell migration after chrysin treatment. The cell migration was analyzed between Con and chrysin group **(A)**. Statistical analysis of the percentage of cell migration **(B)**. **** ($p < 0.0001$) indicate statistically significant differences.

Supplementary Figure 5 | The CCK8 assay results in overexpression and knockdown of *COPB2*. The CCK8 assay in GES1 cells after chrysin treatment **(A)**. The CCK8 assay in pcDNA3.1-Con, pcDNA3.1-H19, Nc and si-H19 group **(B)**. The CCK8 assay in Nc-mimics, mimics-let-7a, Nc-inhibitor and inhibitor-let-7a group **(C)**. The mRNA expression of *COPB2* in the pcDNA3.1-Con, pcDNA3.1-COPB2, si-Nc, si-COPB2 group using qPCR **(D)**. The CCK8 assay in pcDNA3.1-Con, pcDNA3.1-COPB2, si-Nc, and si-COPB2 group **(E)**. ** ($p < 0.01$), *** ($p < 0.001$) and **** ($p < 0.0001$) indicate statistically significant differences.

Supplementary Figure 6 | Analysis of cell apoptosis markers. The protein expression of COPB2, BAX, BCL2, P53 and E-Cadherin were analyzed using western blot **(A)**. The relative mRNA expression of *BAX*, *BCL2* and *TP53* were analyzed using qPCR **(B)**. * ($p < 0.05$) and ** ($p < 0.01$) indicate statistically significant differences.

Supplementary Figure 7 | Cell apoptosis analysis. The cell apoptosis was analyzed after chrysin treatment in pcDNA3.1-COPB2 group **(A, B)**. *** ($p < 0.001$) indicate statistically significant differences.

Supplementary Figure 8 | The cell migration and invasion analysis. The cell migration was analyzed after chrysin treatment in pcDNA3.1-COPB2 group **(A, B)**. Cell invasion was analyzed after chrysin treatment in the pcDNA3.1-COPB2 group **(C, D)**. * ($p < 0.05$) and ** ($p < 0.01$) indicate statistically significant differences.

Supplementary Figure 9 | Cell apoptosis and cell growth analysis. The cell apoptosis was analyzed in pcDNA3.1-Con, pcDNA3.1-H19, Nc and si-H19 group **(A, B)**. Cell apoptosis was analyzed in the Nc-mimics, mimics-let-7a, Nc-inhibitor and inhibitor-let-7a group **(C, D)**. ** ($p < 0.01$) and *** ($p < 0.001$) indicate statistically significant differences.

Supplementary Figure 10 | Histopathological observation of tumor tissue.

Supplementary Figure 11 | Analysis of *H19* and let-7a levels after chrysin treatment using qPCR *in vivo*. * ($p < 0.05$) and **** ($p < 0.0001$) indicate statistically significant differences.

Supplementary Figure 12 | Analysis of chrysin treatment in overexpression and KO of *COPB2*. The genes expression in pcDNA3.1-COPB2 **(A)** and COPB2-KO **(B)** group after chrysin treatment using qPCR. The expression of COPB2 and P53 in pcDNA3.1-COPB2 **(C)** and COPB2-KO **(D)** group after chrysin treatment using western blot. * ($p < 0.05$) and ** ($p < 0.01$) indicate statistically significant differences.

REFERENCES

1. Global Burden of Disease Cancer C, Fitzmaurice C, Dicker D, Pain A, Hamavid H, Moradi-Lakeh M, et al. The Global Burden of Cancer 2013. *JAMA Oncol* (2015) 1(4):505–27. doi: 10.1001/jamaoncol.2015.0735
2. Chia NY, Tan P. Molecular Classification of Gastric Cancer. *Ann Oncol: Off J Eur Soc Med Oncol* (2016) 27(5):763–9. doi: 10.1093/annonc/mdw040
3. Chen K, Yang D, Li X, Sun B, Song F, Cao W, et al. Mutational Landscape of Gastric Adenocarcinoma in Chinese: Implications for Prognosis and Therapy. *Proc Natl Acad Sci USA* (2015) 112(4):1107–12. doi: 10.1073/pnas.1422640112
4. Huang Y, Yuan K, Tang M, Yue J, Bao L, Wu S, et al. Melatonin Inhibiting the Survival of Human Gastric Cancer Cells Under ER Stress Involving Autophagy and Ras-Raf-MAPK Signalling. *J Cell Mol Med* (2020) 25 (3):1480–92. doi: 10.1111/jcmm.16237
5. Beck R, Rawet M, Wieland FT, Cassel D. The COPI System: Molecular Mechanisms and Function. *FEBS Lett* (2009) 583(17):2701–9. doi: 10.1016/j.febslet.2009.07.032
6. Wang Y, Chai Z, Wang M, Jin Y, Yang A, Li M. COPB2 Suppresses Cell Proliferation and Induces Cell Cycle Arrest in Human Colon Cancer by Regulating Cell Cycle-Related Proteins. *Exp Ther Med* (2018) 15(1):777–84. doi: 10.3892/etm.2017.5506
7. Li ZS, Liu CH, Liu Z, Zhu CL, Huang Q. Downregulation of COPB2 by RNAi Inhibits Growth of Human Cholangiocellular Carcinoma Cells. *Eur Rev Med Pharmacol Sci* (2018) 22(4):985–92. doi: 10.26355/eurrev_201802_14380
8. Wang X, Shi J, Niu Z, Wang J, Zhang W. MiR-216a-3p Regulates the Proliferation, Apoptosis, Migration, and Invasion of Lung Cancer Cells *Via* Targeting COPB2. *Biosci Biotechnol Biochem* (2020) 84(10):2014–27. doi: 10.1080/09168451.2020.1783197
9. Wang Y, Xie G, Li M, Du J, Wang M. COPB2 Gene Silencing Inhibits Colorectal Cancer Cell Proliferation and Induces Apoptosis *Via* the JNK/c-Jun Signaling Pathway. *PloS One* (2020) 15(11):e0240106. doi: 10.1371/journal.pone.0240106
10. Chen HL, Li JJ, Jiang F, Shi WJ, Chang GY. MicroRNA-4461 Derived From Bone Marrow Mesenchymal Stem Cell Exosomes Inhibits Tumorigenesis by Downregulating COPB2 Expression in Colorectal Cancer. *Biosci Biotechnol Biochem* (2020) 84(2):338–46. doi: 10.1080/09168451.2019.1677452
11. Pu X, Jiang H, Li W, Xu L, Wang L, Shu Y. Upregulation of the Coatomer Protein Complex Subunit Beta 2 (COPB2) Gene Targets microRNA-335-3p in NCI-H1975 Lung Adenocarcinoma Cells to Promote Cell Proliferation and Migration. *Med Sci Monitor: Int Med J Exp Clin Res* (2020) 26:e918382. doi: 10.12659/MSM.918382
12. Alessandrini L, Manchi M, De Re V, Dolcetti R, Canzonieri V. Proposed Molecular and Mirna Classification of Gastric Cancer. *Int J Mol Sci* (2018) 19 (6):1683. doi: 10.3390/ijms19061683
13. Hu W, Chen Y, Lv K. The Expression Profiles of MicroRNA Let-7a in Peripheral Blood Mononuclear Cells From Patients of Gastric Cancer With Neoadjuvant Chemotherapy. *Clin Lab* (2018) 64(5):835–9. doi: 10.7754/Clin.Lab.2017.171213
14. Tang G, Du R, Tang Z, Kuang Y. MiRNALet-7a Mediates Prostate Cancer PC-3 Cell Invasion, Migration by Inducing Epithelial-Mesenchymal Transition Through CCR7/MAPK Pathway. *J Cell Biochem* (2018) 119(4):3725–31. doi: 10.1002/jcb.26595
15. Chen JS, Wang YF, Zhang XQ, Lv JM, Li Y, Liu XX, et al. H19 Serves as a Diagnostic Biomarker and Up-Regulation of H19 Expression Contributes to Poor Prognosis in Patients With Gastric Cancer. *Neoplasma* (2016) 63 (2):223–30. doi: 10.4149/207_150821N454
16. Peng F, Li TT, Wang KL, Xiao GQ, Wang JH, Zhao HD, et al. H19/let-7/LIN28 Reciprocal Negative Regulatory Circuit Promotes Breast Cancer Stem Cell Maintenance. *Cell Death Dis* (2017) 8(1):e2569. doi: 10.1038/cddis.2016.438
17. Kallen AN, Zhou XB, Xu J, Qiao C, Ma J, Yan L, et al. The Imprinted H19 lncRNA Antagonizes Let-7 Micrornas. *Mol Cell* (2013) 52(1):101–12. doi: 10.1016/j.molcel.2013.08.027
18. Zhong X, Huang S, Liu D, Jiang Z, Jin Q, Li C, et al. Galangin Promotes Cell Apoptosis Through Suppression of H19 Expression in Hepatocellular Carcinoma Cells. *Cancer Med* (2020) 9(15):5546–57. doi: 10.1002/cam4.3195
19. Xiang Y, Guo Z, Zhu P, Chen J, Huang Y. Traditional Chinese Medicine as a Cancer Treatment: Modern Perspectives of Ancient But Advanced Science. *Cancer Med* (2019) 8(5):1958–75. doi: 10.1002/cam4.2108
20. Xu D, Jin J, Yu H, Zhao Z, Ma D, Zhang C, et al. Chrysin Inhibited Tumor Glycolysis and Induced Apoptosis in Hepatocellular Carcinoma by Targeting Hexokinase-2. *J Exp Clin Cancer Res: CR* (2017) 36(1):44. doi: 10.1186/s13046-017-0514-4
21. Yufei Z, Yuqi W, Binyue H, Lingchen T, Xi C, Hoffelt D, et al. Chrysin Inhibits Melanoma Tumor Metastasis *Via* Interfering With the FOXM1/Beta-Catenin Signaling. *J Agric Food Chem* (2020) 68(35):9358–67. doi: 10.1021/acs.jafc.0c03123
22. Cong L, Ran FA, Cox D, Lin S, Barretto R, Habib N, et al. Multiplex Genome Engineering Using CRISPR/Cas Systems. *Science* (2013) 339(6121):819–23. doi: 10.1126/science.1231143
23. Clark SJ, Harrison J, Paul CL, Frommer M. High Sensitivity Mapping of Methylated Cytosines. *Nucleic Acids Res* (1994) 22(15):2990–7. doi: 10.1093/nar/22.15.2990
24. Ding C, Li L, Yang T, Fan X, Wu G. Combined Application of Anti-VEGF and Anti-EGFR Attenuates the Growth and Angiogenesis of Colorectal Cancer Mainly Through Suppressing AKT and ERK Signaling in Mice Model. *BMC Cancer* (2016) 16(1):791. doi: 10.1186/s12885-016-2834-8
25. William-Faltaos S, Rouillard D, Lechat P, Bastian G. Cell Cycle Arrest and Apoptosis Induced by Oxaliplatin (L-OHP) on Four Human Cancer Cell Lines. *Anticancer Res* (2006) 26(3A):2093–9.
26. Naz S, Imran M, Rauf A, Orhan IE, Shariati MA, Iahtisham Ul H, et al. Chrysin: Pharmacological and Therapeutic Properties. *Life Sci* (2019) 235:116797. doi: 10.1016/j.lfs.2019.116797
27. Kasala ER, Bodduluru LN, Madana RM, AK V, Gogoi R, Barua CC. Chemopreventive and Therapeutic Potential of Chrysin in Cancer: Mechanistic Perspectives. *Toxicol Lett* (2015) 233(2):214–25. doi: 10.1016/j.toxlet.2015.01.008
28. Wang J, Wang H, Sun K, Wang X, Pan H, Zhu J, et al. Chrysin Suppresses Proliferation, Migration, and Invasion in Glioblastoma Cell Lines *Via* Mediating the ERK/Nrf2 Signaling Pathway. *Drug Design Dev Ther* (2018) 12:721–33. doi: 10.2147/DDDT.S160020
29. Mohammadian F, Pilehvar-Soltanahmadi Y, Zarghami F, Akbarzadeh A, Zarghami N. Upregulation of miR-9 and Let-7a by Nanoencapsulated Chrysin in Gastric Cancer Cells. *Artif Cells Nanomed Biotechnol* (2017) 45 (6):1–6. doi: 10.1080/21691401.2016.1216854
30. Zhong X, Liu D, Jiang Z, Li C, Chen L, Xia Y, et al. Chrysin Induced Cell Apoptosis and Inhibited Invasion Through Regulation of TET1 Expression in Gastric Cancer Cells. *OncoTarg Ther* (2020) 13:3277–87. doi: 10.2147/OTT.S246031
31. Tahara T, Arisawa T. DNA Methylation as a Molecular Biomarker in Gastric Cancer. *Epigenomics-Uk* (2015) 7(3):475–86. doi: 10.2217/epi.15.4
32. Ghafouri-Fard S, Esmaeili M, Taheri M. H19 Lncrna: Roles in Tumorigenesis. *Biomed Pharmacother Biomed Pharmacother* (2020) 123:109774. doi: 10.1016/j.biopha.2019.109774
33. Lv M, Zhong Z, Huang M, Tian Q, Jiang R, Chen J. Lncrna H19 Regulates Epithelial-Mesenchymal Transition and Metastasis of Bladder Cancer by miR-29b-3p as Competing Endogenous RNA. *Biochim Biophys Acta Mol Cell Res* (2017) 1864(10):1887–99. doi: 10.1016/j.bbamcr.2017.08.001
34. Balzeau J, Menezes MR, Cao S, Hagan JP. The LIN28/let-7 Pathway in Cancer. *Front Genet* (2017) 8:31. doi: 10.3389/fgene.2017.00031
35. Zhang L, Wang K, Wu Q, Jin L, Lu H, Shi Y, et al. Let-7 Inhibits the Migration and Invasion of Extravillous Trophoblast Cell *via* Targeting MDM4. *Mol Cell Probes* (2019) 45:48–56. doi: 10.1016/j.mcp.2019.05.002
36. Zhu Y, Xu F. Up-Regulation of Let-7a Expression Induces Gastric Carcinoma Cell Apoptosis In Vitro. *Chin Med Sci J Chung-kuo I Hsueh K'o Hsueh Tsa Chih* (2017) 32(1):44–7. doi: 10.24920/j1001-9242.2007.006
37. Damanakis AI, Eckhardt S, Wunderlich A, Roth S, Wissniowski TT, Bartsch DK, et al. MicroRNAs Let7 Expression in Thyroid Cancer: Correlation With Their Deputed Targets HMGA2 and SLC5A5. *J Cancer Res Clin Oncol* (2016) 142(6):1213–20. doi: 10.1007/s00432-016-2138-z
38. Sun Y, Zhong L, He X, Wang S, Lai Y, Wu W, et al. Lncrna H19 Promotes Vascular Inflammation and Abdominal Aortic Aneurysm Formation by Functioning as a Competing Endogenous RNA. *J Mol Cell Cardiol* (2019) 131:66–81. doi: 10.1016/j.yjmcc.2019.04.004

39. Yang Z, Jiang X, Zhang J, Huang X, Zhang X, Wang J, et al. Let-7a Promotes Microglia M2 Polarization by Targeting CKIP-1 Following ICH. *Immunol Lett* (2018) 202:1–7. doi: 10.1016/j.imlet.2018.07.007
40. Mi YY, Yu ML, Zhang LF, Sun CY, Wei BB, Ding WH, et al. Copb2 Is Upregulated in Prostate Cancer and Regulates Pc-3 Cell Proliferation, Cell Cycle, and Apoptosis. *Arch Med Res* (2016) 47(6):411–8. doi: 10.1016/j.arcmed.2016.09.005
41. Sassi A, Maatouk M, El Gueder D, Bzeouich IM, Abdelkefi-Ben Hatira S, Jemni-Yacoub S, et al. Chrysin, a Natural and Biologically Active Flavonoid Suppresses Tumor Growth of Mouse B16F10 Melanoma Cells: In Vitro and In Vivo Study. *Chem-Biol Interact* (2018) 283:10–9. doi: 10.1016/j.cbi.2017.11.022

Conflict of Interest: The authors declare that the research was conducted in the absence of any commercial or financial relationships that could be construed as a potential conflict of interest.

frontiers in Oncology

ORIGINAL RESEARCH
published: 21 June 2021
doi: 10.3389/fonc.2021.652567

Analysis of Long Noncoding RNAs in Aila-Induced Non-Small Cell Lung Cancer Inhibition

Lin Chen[1,2†], Cui Wu[1†], Heming Wang[3,4†], Sinuo Chen[3,4], Danhui Ma[3,4], Ye Tao[5], Xingye Wang[1], Yanhe Luan[5], Tiedong Wang[2], Yan Shi[6], Guangqi Song[3,4], Yicheng Zhao[1], Xijun Dong[1,5*] and Bingmei Wang[1*]*

[1] College of Clinical Medicine, College of Integrated Traditional Chinese and Western Medicine, Changchun University of Chinese Medicine, Changchun, China, [2] College of Animal Science, Jilin University, Changchun, China, [3] Department of Gastroenterology and Hepatology, Zhongshan Hospital, Fudan University, Shanghai, China, [4] Department of Gastroenterology and Hepatology, Zhongshan Hospital of Fudan University, Shanghai, China, [5] Affiliated Hospital to Changchun University of Chinese Medicine, Changchun University of Chinese Medicine, Changchun, China, [6] School of Pharmacy, Jilin University, Changchun, China

OPEN ACCESS

Edited by:
Peng Qu,
National Institutes of Health (NIH), United States

Reviewed by:
Meng Xu,
Carnegie Mellon University, United States
Yafeng He,
National Heart, Lung, and Blood Institute (NHLBI), United States

***Correspondence:**
Yicheng Zhao
yichengzhao@live.cn
Xijun Dong
dongxijun1064@163.com
Bingmei Wang
bingmeiwang1970@163.com

†These authors have contributed equally to this work

Specialty section:
This article was submitted to Pharmacology of Anti-Cancer Drugs, a section of the journal Frontiers in Oncology

Received: 12 January 2021
Accepted: 21 May 2021
Published: 21 June 2021

Citation:
Chen L, Wu C, Wang H, Chen S, Ma D, Tao Y, Wang X, Luan Y, Wang T, Shi Y, Song G, Zhao Y, Dong X and Wang B (2021) Analysis of Long Noncoding RNAs in Aila-Induced Non-Small Cell Lung Cancer Inhibition. Front. Oncol. 11:652567. doi: 10.3389/fonc.2021.652567

Non-small cell lung cancer (NSCLC) has the highest morbidity and mortality among all carcinomas. However, it is difficult to diagnose in the early stage, and current therapeutic efficacy is not ideal. Although numerous studies have revealed that Ailanthone (Aila), a natural product, can inhibit multiple cancers by reducing cell proliferation and invasion and inducing apoptosis, the mechanism by which Aila represses NSCLC progression in a time-dependent manner remains unclear. In this study, we observed that most long noncoding RNAs (lncRNAs) were either notably up- or downregulated in NSCLC cells after treatment with Aila. Moreover, alterations in lncRNA expression induced by Aila were crucial for the initiation and metastasis of NSCLC. Furthermore, in our research, expression of *DUXAP8* was significantly downregulated in NSCLC cells after treatment with Aila and regulated expression levels of *EGR1*. In conclusion, our findings demonstrate that Aila is a potent natural suppressor of NSCLC by modulating expression of *DUXAP8* and *EGR1*.

Keywords: Ailanthone, non-small cell lung cancer, long noncoding RNA, *DUXAP8*, *EGR1*

INTRODUCTION

Lung cancer is the most widespread malignant tumor and has the highest mortality among all cancers. Based on one global cancer study conducted by the International Agency for Research on Cancer (IARC), there were approximately 4 million newly diagnosed and dead lung cancer patients in 2018 worldwide (1). Moreover, the number of people who are initially diagnosed with lung cancer is approximately 770,000, and those who die from lung cancer is nearly 700,000 annually in China (2). All of these data indicate that lung cancer is a tremendous threat to public health. Currently, lung cancer is classified into a variety of histological subtypes, among which NSCLC accounts for approximately 80-85% of all cases (3, 4). At present, the primary treatments for NSCLC include surgery, radiotherapy and pharmacotherapy, the latter including chemotherapy, targeted therapy, immunotherapy, etc. (5). However, due to the insidious onset of NSCLC, the majority of patients

have lost the optimal timing for radical surgery at the time of diagnosis (6). In addition, since chemoradiotherapy has nonnegligible deficiencies, such as side effects, drug resistance and narrow indications (7, 8). Drug resistance and metastasis may arise during the chemotherapy, thereby substantially compromising the therapeutic efficacy of cancer treatment (9). So its overall therapeutic efficacy for NSCLC is unsatisfactory, and the 5-year survival rate of patients is poor at less than 20% (10). Therefore, it is particularly important to identify novel treatment method to provide early diagnosis, improve treatment efficiency, and reduce the mortality rate of NSCLC.

Currently, natural products have become a focus of new anticancer drug development, accounting for approximately 3/4 of clinical applications of antitumor drugs (11). Chinese herbal medicine is considered a gift of nature and these compounds derived from herbs have the advantage with availability, efficacy, and relatively low toxicity (12). As the primary active compound isolated from the root bark of the traditional medicinal plant Ailanthus altissima, Aila (11β,20-Epoxy-1β,11,12α-trihydroxy picrasa-3,13 (21)-diene-2,16-dione) has been proven to have a robust anticancer effect and can inhibit various cancers, including those arising in the reproductive system, urinary system, digestive system, blood system, respiratory system and other systems, in recent years (13). In genitourinary cancer, Aila significantly inhibited MDA-MB-231 mammary cancer cell viability and invasion and led to apoptosis by upregulating expression of miR-148a, blocking the AMPK and Wnt/β-catenin signaling pathways (14). Additionally, Wang et al. found that Aila induces apoptosis and restrains proliferation in MCF-7 mammary cancer cells by upregulating proapoptotic caspase-3 and upregulating the antiapoptotic apoptosis regulator B-cell lymphoma-2 (15). In addition, He et al. observed that Aila inhibited the proliferation and migration of castration-resistant prostate cancer (CRPC) cells and prevented drug resistance of the androgen receptor (AR) antagonist MDV3100 by binding *p23* (16). Daga et al. found that Aila also significantly reduced expression of *Nrf2*, *YAP* and *c-Myc* in 253J and T24 bladder cancer cells. Since these proteins can increase the drug resistance of cisplatin (CDDP), Aila plays a role in limiting the proliferation and migration of bladder cancer cells, as well as reversing drug resistance (17). Moreover, Cucci found that Aila inhibits the growth of A2780/CP70 oophoroma cells and reverses resistance to CDDP (18). For alimentary system cancers, Aila causes Huh7 hepatocellular carcinoma cell cycle arrest and induces apoptosis by downregulating cyclins and CDKs and upregulating *p21* and *p27* (19). Furthermore, Aila induced G (2)/M cell cycle arrest and apoptosis in SGC-7901 human gastric carcinoma cells by decreasing *Bcl-2* and increasing *Bax* expression (20). In terms of hematologic cancers, Wei et al. discovered that Aila exerts a tumor suppressor effect on HL-60 human promyelocytic leukemia cells and dose-dependently increases *beclin-1* and *LC3-II* and decreases *LC3-I* and *p62* expression (21). By upregulating *miR-449a* to disturb the Notch and PI3K/AKT signaling pathways, Aila represses acute myeloid leukemia (AML) cell metastasis and invasion (22). In lung cancer, Aila restrains cell proliferation and promotes apoptosis and autophagy by upregulating expression of miR-195 alone and reducing phosphorylation of *PI3K*, *Akt*, *JAK* and *STAT3* (23). Aila also inhibits DNA duplication to curb NSCLC cell growth by downregulating *RPA1* (24). Moreover, Aila exhibits inhibitory effects on other types of cancers. Liu et al. observed that Aila causes B16 and A375 melanoma cell cycle arrest and induces apoptosis, exerting a tumor-suppressive effect (25). Furthermore, Aila inhibits vestibular schwannomas (VS) by controlling miR-21 to regulate the Ras/Raf/MEK/ERK and mTOR signaling pathways (26). Aila also hinders MG63 osteosarcoma cell proliferation, migration, and invasion and induces apoptosis by upregulating miR-126 and downregulating *VEGF-A* to block PI3K/AKT signaling pathways (27).

LncRNAs, a class of RNAs with more than 200 nucleotides that perform essential regulatory functions with respect to genetic expression (28), are involved in the occurrence and development of numerous diseases, particularly tumors (29). With the development of profound experimental and high-throughput sequencing technology, a variety of lncRNAs have been identified as aberrantly expressed in NSCLC (30). For example, *MALAT1* is more highly expressed than in normal tissues in NSCLC, and its aberrant upregulation enhances the migration and invasion of NSCLC cells (31), while this effect was suppressed after implementation of gene silencing (32). In addition, *MEG3* promotes NSCLC cell proliferation by aberrant downregulation, the levels of which are correlated with the course of lung cancer, tumor size, and prognostic status (33) and strengthen the sensitivity of lung cancer cells to chemotherapeutic agents (34). Double homeobox A pseudogene 8 (*DUXAP8*), derived from a pseudogene (35), is highly expressed in many cancers, such as hepatocellular carcinoma (36), colorectal cancer (37) and oral cancer (38). Recently, Yin et al. determined that overexpression of *DUXAP8* in NSCLC cells not only promotes cell proliferation and migration but was also related to the clinical grade and prognosis of NSCLC patients, and downregulation of *DUXAP8* remarkably inhibited cell growth and migration (39).

Human early growth response factor-1 (*EGR1*) is a nuclear transcription factor belonging to the EGR family and containing a highly conserved DNA binding domain that binds to a GC-rich consensus sequence (40). In recent years, *EGR1* was proven to directly or indirectly upregulate multiple tumor suppressors, such as *PTEN*, *TP53*, *fibronectin*, *BCL-2* and *TGFb1* (40, 41), and was expressed at low levels in a variety of cancers, such as colon cancer (42) and oophoroma (43).

In this study, we found that Aila inhibits A549 and H1299 cell viability and invasion and promotes cell cycle stagnation and apoptosis. Moreover, exploring its molecular mechanism, we determined that *DUXAP8* was significantly downregulated and *EGR1* expression was upregulated in Aila-treated NSCLC cells. Moreover, knockdown of *DUXAP8* enhanced Aila's antitumor effect, whereas its overexpression had the opposite effect. Consequently, these results indicate that Aila affects cell proliferation, cell cycle progression and apoptosis by reducing expression of *DUXAP8* to increase expression of *EGR1* in A549 and H1299 cells. Our research may provide new insight into therapeutic approaches for NSCLC.

MATERIALS AND METHODS

Cell Culture

Human NSCLC A549 and H1299 cell lines were obtained from Jilin University. A549 cells were cultured in high glucose DMEM (HyClone, Los Angeles, USA), and H1299 cells were incubated in RPMI-1640 (HyClone, Los Angeles, USA). All culture media were supplemented with 10% fetal bovine serum (tbd Science, Tianjin, China) and 100 units/mL penicillin and streptomycin (HyClone, Los Angeles, USA) and were then cultured in a humidified atmosphere of 5% CO_2 at 37°C.

MTT Assay

The MTT assay was applied to determine the effect of Aila on NSCLC cell proliferation. Aila was purchased from BioBioPha Co., Ltd. (Yunnan, China). Briefly, A549 and H1299 cells were collected and seeded in 96-well plates at a density of 1×10^4 cells per well. Following treatment with 1 μM Aila, MTT was added and incubated for another 4 h. The medium was changed to dimethyl sulfoxide (DMSO). A microplate reader was used to detect the optical density (OD) of the cells at 490 nm every 24 h until 72 hours.

Live/Dead Cell Staining

Live/dead cell staining was used to visualize the influence of Aila on the viability of NSCLC cells. The Live and Dead Cell Double Staining Kit was obtained from Abbkine (Abbkine, Beijing, China). A549 cells were cultured in 24-well plates at 8×10^4 cells per well. After administration of 1 μM Aila for 24 h, cells were stained for 15-30 min at room temperature in the dark according to the instructions. Subsequently, after washing cells with phosphate-buffered saline (PBS), they were imaged under a fluorescence microscope (Leica, Wetzlar, Germany) with appropriate filters as soon as possible.

Colony Formation Assay

To test the role of Aila in A549 and H1299 cell tumorigenicity, a colony formation assay was performed. First, 100 cells/well were seeded into 6-well plates. Then, 1 μM Aila was added to the trial group, while an equal volume of solvent was added to the control group. Cells were cultured for 7 to 10 days, and the medium was replaced every 3 to 4 days. Furthermore, after washing with PBS, cells were fixed in 4% paraformaldehyde and stained with crystal violet. Finally, colonies were imaged and counted under an inverted microscope (Leica, Wetzlar, Germany).

Wound Healing Assay

The wound healing assay was applied to assess the migration ability of NSCLC cells. Briefly, 7×10^4 cells/well were cultured in 24-well plates. When A549 and H1299 cells reached 90% confluence, a wound area was created using a 200 μL pipette tip. Afterward, at 0, 24 and 48 h, images of cellular migration were captured.

Transwell Assay

To evaluate the invasive capacity of A549 and H1299 cells, we performed a transwell assay. A total of 1×10^5 cells per well were seeded into the upper transwell chamber precoated with 40 μL Matrigel and cultured in serum-free medium. Subsequently, 500 μL medium containing 10% FBS was transferred into the lower chamber. Cells continued to be incubated for 24 h. Subsequently, the upper cells were wiped off, and the invaded cells were fixed with 4% paraformaldehyde and stained with crystal violet. Images of stained cells were collected using an inverted microscope.

Cell Cycle Analysis

We conducted cell cycle analysis using a Cell Cycle and Apoptosis Analysis Kit (Beyotime, Shanghai, China). In brief, A549 and H1299 cells were cultured in 6-well plates separately. Then, cells were treated with 1 μM Aila. Next, we fixed cells in 70% ethanol at 4°C for 12 to 24 h. Following washing and collection, cells were resuspended in 500 μL PI staining solution for 30 min in the dark. Ultimately, these dyed cells were detected using the PI signal detector of the flow cytometer (Beckman Coulter, USA), and the results were analyzed using ModFit LT.

Cell Apoptosis Analysis

An Annexin V-FITC Apoptosis Detection Kit (Beyotime, Shanghai, China) was used to perform the apoptosis analysis. First, A549 and H1299 cells were seeded into 6-well plates and treated with 1 μM Aila. Then, cells were harvested and resuspended in 195 μL binding buffer along with 5 μL Annexin V-FITC and 5 μL PI. Flow cytometry was used to measure cell apoptosis, and FlowJo (vX.0.7) was employed to analyze the data. An One Step TUNEL Apoptosis Kit (Beyotime, Shanghai, China) was also employed according to the manufacturer's instruction.

LncRNA-seq and Data Analysis

We performed high-throughput lncRNA sequencing to further explore the molecular mechanism of Aila in NSCLC. Initially, H1299 and A549 cells were evenly cultured in 10 cm dishes. When cells reached 80-90% confluence, 3 μM Aila was added for 24 h, and the control group was set up. Subsequently, collected cells were sent to GENEWIZ Biotech (GENEWIZ, Suzhou, China) to perform lncRNA sequencing. Total RNAs were isolated using TRIzol solution. Then, next-generation sequencing library preparations were constructed using ribosomal depleted RNA. Therefore, sequencing was implemented on an Illumina NovaSeq (Illumina, San Diego, CA, USA) using a 2x150 paired-end (PE) configuration. Clean data were obtained after removing adapters and QCs less than 25 in raw sequencing date using trim_galore (0.6.4). Then, data were analyzed using STAR (STAR_2.6.1a) to map clean data to a reference human genome (GRCh38). After that, transcripts were quantified and annotated (GENECODE v35) using stringtie (1.3.3), and the count for each transcript was obtained. Furthermore, transcripts were normalized, and differential expression analysis was performed using DESeq2. Moreover, GO and KEGG enrichment analyses were performed using clusterProfiler (44). The data of LUAD patients were obtained from TCGA. Sequencing data were submitted to the Sequence Read Archive (SRA) dataset under the accession number PRJNA (PRJNA690710).

Knockdown and Overexpression of *DUXAP8*

We knocked down and overexpressed *DUXAP8* to verify the regulatory role of lncRNAs in NSCLC. Si-*DUXAP8* was purchased

from RiboBio (RiboBio, Guangzhou, China), and pcDNA3.1-*DUXAP8* was constructed in the laboratory. A549 and H1299 cells were collected when the density was approximately 70-90%. Subsequently, cells were transfected using Lipofectamine™ 3000 Reagent (Thermo Fisher, Massachusetts, USA) following the manufacturer's instructions. Afterward, the medium was changed to serum-containing medium after 4 h of transfection. Moreover, RT-PCR was used to examine whether knockdown and overexpression were successfully established. The siRNA target sequences are listed in **Table S1**.

Real-Time PCR

A549 cells were incubated in 6 cm dishes, and one group was treated with 1 μM Aila, while the other was given an equal volume of DMSO. First, total RNA was extracted from A549 cells using TriPure isolation reagent (Roche, Basel, Switzerland). Then, cDNA was synthesized using Plus All-in-one 1st Strand cDNA Synthesis SuperMix (Novoprotein, Shanghai, China) according to the manufacturer's guidelines. Furthermore, quantitative real-time PCR was performed utilizing SYBR qPCR SuperMix Plus (Novoprotein, Shanghai, China) on a PIKOREAL 96 Real-Time PCR System. RT-PCR was conducted using the following parameters: predenaturation at 95°C for 1 min, followed by 40 cycles of denaturation at 95°C for 20 s, annealing at 60°C for 20 s, and extension at 72°C for 30 s. Moreover, GAPDH was used as an internal reference, and expression of related genes was calculated utilizing the $2^{-\Delta\Delta Ct}$ method. Primer sequences are listed in **Table S2**.

Western Blot Analysis

First, A549 cells were collected and lysed in RIPA buffer to isolate proteins. Protein concentrations were subsequently determined using a BCA protein reagent assay kit (Beyotime, Shanghai, China). Next, 10% sodium dodecyl sulfate-polyacrylamide gel electrophoresis (SDS-PAGE) was conducted, followed by transfer of proteins onto a membrane. Afterward, membranes were blocked in 5% nonfat milk and then probed with primary antibodies against anti-EGR1 (Affinity, BF0443) and anti-GAPDH (Proteintech, 60004-1-Ig) at 4°C overnight. Furthermore, membranes were washed and incubated with horseradish peroxidase (HRP) and incubated with conjugated polyclonal goat antimouse IgG (Beyotime, A0216) secondary antibody for 1 h at room temperature. Finally, Fusion FX Edge Spectra (VILBER LOURMAT, Paris France) was utilized for imaging after washing the membranes once again.

Mouse Xenograft Experiments

Female nude mice (4-5 weeks) were employed to perform the xenograft experiments. First, 10 mice were randomly divided into two groups, and each group was subcutaneously injected with 1×10^6 H1299 cells. One week after tumor induction, mice in the trial group were intraperitoneally injected with 2 mg/kg Aila daily, while controls were treated with an equal volume of saline. Treatments were continued for 2 weeks. Subsequently, mice were sacrificed with CO_2 asphyxiation.

Statistical Analysis

In all experiments, trial and control groups were set up, and at least three independent experiments were performed. Data are expressed as the mean ± standard deviation (SD). Statistical analyses were performed using GraphPad statistical software (GraphPad Software, La Jolla, CA). $P<0.05$ was considered statistically significant.

RESULTS

Aila Inhibits A549 and H1299 Cell Viability

To test the anticancer effect of Aila on NSCLC, we examined the cell growth and colony formation of A549 and H1299 cells. A549 cells were treatment with Aila and counted by blood counting chamber. We chose 1μM for subsequent experiments (**Figure 1A**). From the MTT assay, we could see that Aila significantly inhibited the proliferation of A549 and H1299 cells in a time-dependent manner ($P<0.01$) (**Figure 1B**). Additionally, Aila significantly restrained cell viability in live/dead cell staining (**Figure 1C**). Moreover, colony formation was reduced after treatment with Aila (**Figure 1D**).

Aila Restrains A549 and H1299 Migration and Invasion

Wound healing assays and transwell assays were performed to observe the influences of Aila on migration and invasion. Wound images were collected at 0, 24 and 48 h after the scratch was made. Results showed that Aila clearly slowed cell migration of A549 cells ($P<0.05$) (**Figures 2A, B**) and H1299 cells ($P<0.01$) (**Figures 2E, F**). Furthermore, compared to the control group, the inhibitory effect of Aila on cell invasion was significant of A549 cells ($P<0.001$) (**Figures 2C, D**) and H1299 cells ($P<0.05$) (**Figures 2G, H**).

Aila Induces A549 and H1299 Cell Cycle Arrest and Apoptosis

The uncontrollable growth of tumors is primarily related to cell cycle disturbances (45). Therefore, cell cycle analysis was performed to test whether Aila had a positive effect on the cell cycle arrest. Flow cytometry results showed that the S phase was decreased in A549 and H1299 cells after treatment with Aila ($P < 0.001$) (**Figures 3A, C**). Therefore, we concluded that Aila led to G1 stagnation in A549 and H1299 cells.

To further investigate whether Aila suppressed the growth of A549 and H1299 cells by triggering apoptotic signals, we used Annexin V/PI double staining to evaluate the apoptotic effects of Aila on A549 and H1299 cells. Results revealed that apoptosis of A549 and H1299 cells was increased in response to treatment with Aila ($P < 0.01$) (**Figures 3B, D**), implying that Aila significantly induces apoptosis.

Aila Downregulates *DUXAP8* in A549 Cells

To explore lncRNA expression patterns after treatment with Aila in NSCLC, lncRNA-seq was performed with Illumina NovaSeq in H1299 cells. A total of 489 lncRNAs in A549 cells and 339 lncRNAs

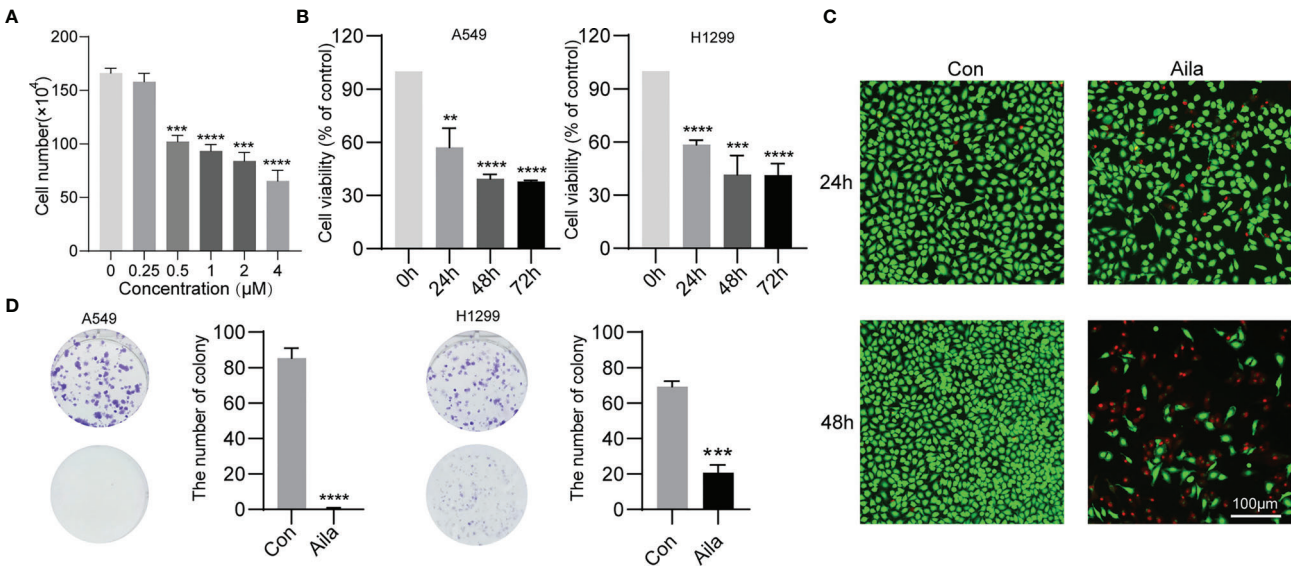

FIGURE 1 | Aila inhibits A549 and H1299 cell viability and colony formation. **(A)** Cells treated with different dosages of Aila (0, 0.25, 0.5, 2, 2 and 4 μM). **(B)** The proliferation of A549 and H1299 cells was analyzed by MTT assay at 24, 48 and 72 h. **(C)** Cell viability of A549 cells was detected by live/dead assay after the addition of 1 μM Aila with an established control group. **(D)** Colony formation of A549 and H1299 cells was performed after treatment with or without 1 μM Aila in 6-well plates. Data are represented as the mean ± SD (n = 3). **(P < 0.01), ***(P < 0.001) and ****(P < 0.0001) indicate statistically significant differences.

in A549 cells were differentially expressed between cells treated with Aila and untreated cells. From Venn diagrams, GARS1-DT, AL162595.1, DUXAP8, AC027627.1 and AC008735.2 were downregulated in two cell lines (**Figure 4A**). GSEA result show that genes involved in apoptosis were enriched after treatment with Alia in two cell lines (**Figures 4B, C**). Next, RT-PCR confirmed that DUXAP8 was significantly downregulated (**Figure 4D**). Moreover, The Cancer Genome Atlas (TCGA) database showed that *DUXAP8* in lung adenocarcinoma patients (LUAD) was significantly higher than in noncancerous tissue, and the level of *DUXAP8* upregulation was associated with poor prognosis and reduced survival (**Figures 4E, F**). The Cancer Cell Line Encyclopedia (CCLE) database revealed that *DUXAP8* in A549 and H1299 cells was significantly higher than in IMR-90 cells (**Figure 4G**). At present, one study has found that knockdown of *DUXAP8* inhibits growth of NSCLC cells (39). These data support our results, suggesting that Aila inhibits the growth of H1299 cells by downregulating *DUXAP8*.

Effects of Knockdown and Overexpression of *DUXAP8* on Cell Viability and Invasion

A549 and H1299 cells were transfected with si-*DUXAP8* and pcDNA3.1-*DUXAP8* expression vectors and treated with Aila to further elucidate the possible regulatory mechanism of *DUXAP8* in NSCLC. RT-PCR revealed that the expression of *DUXAP8* was decreased in response to si-*DUXAP8*, while that in pcDNA3.1-*DUXAP8* was increased, indicating that knockdown and overexpression were successfully established (**Figure 5B**). Next, we investigated the phenotypes of NSCLC after knockdown and overexpression of *DUXAP8* and Aila treatment. Compared to the control group, si-*DUXAP8* significantly attenuated cell viability (**Figures 5A, C**). Aila and si-*DUXAP8* treatment also significantly attenuated cell viability (**Figure 5E**). Besides, si-*DUXAP8* significantly reduced the number of invaded cells, while overexpression of *DUXAP8* has no significant effects (**Figure 5D**). Cells treated with Aila and si-*DUXAP8* and overexpression of *DUXAP8* has the same trend (**Figure 5F**).

Effects of Knockdown and Overexpression of *DUXAP8* on Cell Cycle and Apoptosis in A549 Cells

To further analyze the effect of expression of *DUXAP8* on the cell cycle and apoptosis, A549 cells was transfected with si-*DUXAP8* or pcDNA3.1-*DUXAP8* expression vectors and treated with Aila. Flow cytometry results showed that si-*DUXAP8* significantly decreased S phase, while pcDNA3.1-*DUXAP8* reversed this pattern in A549 cells (**Figures 6A, C**). Cells treated with Aila and si-*DUXAP8* also significantly decreased S phase and overexpression of *DUXAP8* and Aila treated reversed this pattern (**Figures 6E, G**). To investigate whether *DUXAP8* is associated with apoptosis in A549 cells, we used the Annexin V/PI double staining method. Results revealed that si-*DUXAP8* induced apoptosis of A549 cells, while pcDNA3.1-*DUXAP8* reversed this effect (**Figures 6B, D**). Cells treated with Aila and si-*DUXAP8* also induced apoptosis and overexpression of *DUXAP8* and Aila treated reversed this pattern (**Figures 6F, H**).

Knockdown and Overexpression of *DUXAP8* on Cell Cycle and Apoptosis in H1299 Cells

To further analyze the effect of expression of *DUXAP8* on the cell cycle and apoptosis, H1299 cells was transfected with si-*DUXAP8* or pcDNA3.1-*DUXAP8* expression vectors and treated

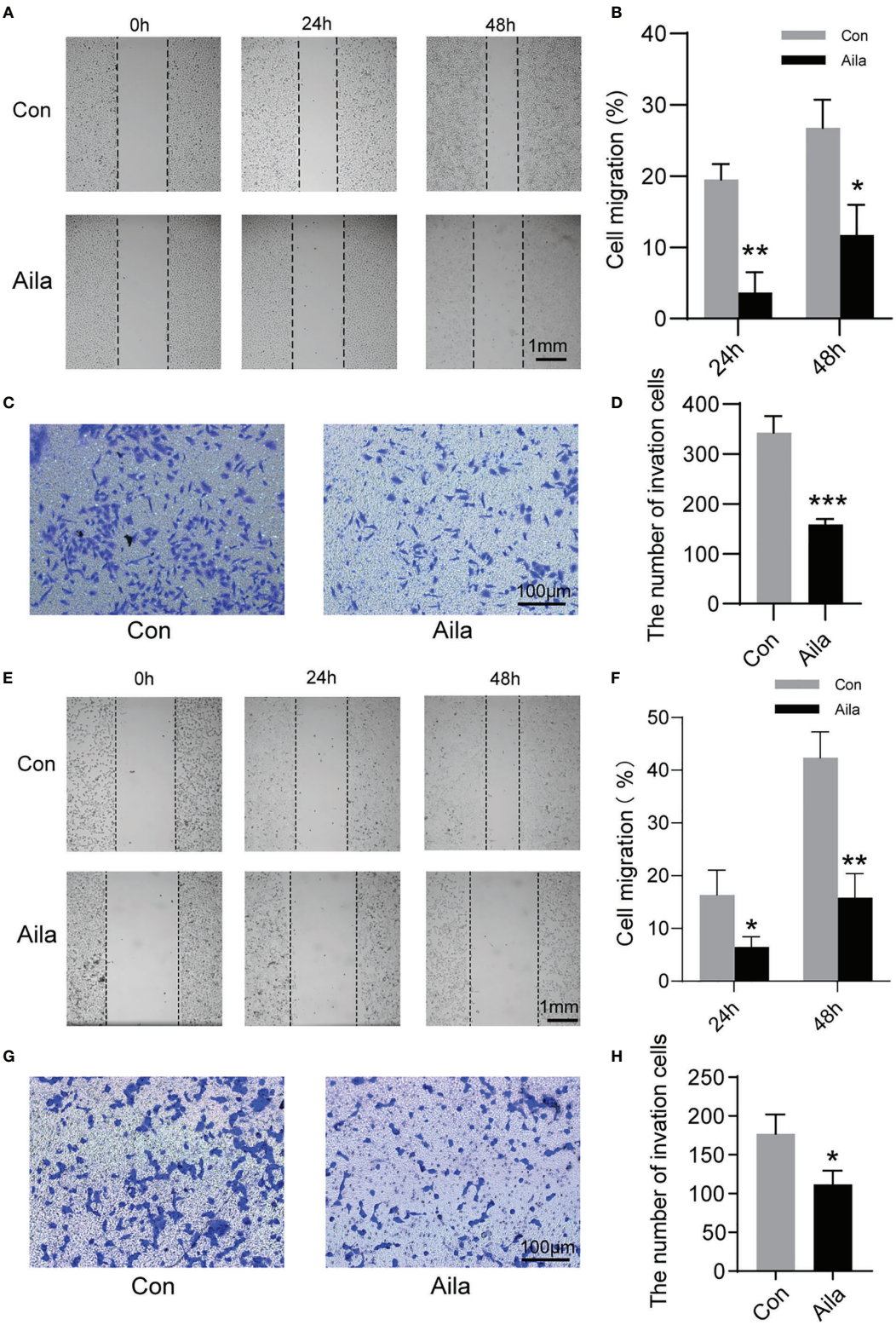

FIGURE 2 | Aila restrains A549 and H1299 cells migration and invasion. **(A, B)** Cell migration of A549 cells was tested by wound healing experiments between control and Aila groups. **(C, D)** Cell invasion was analyzed using the transwell assay of A549 cells. **(E, F)** Cell migration of H1299 cells was tested by wound healing experiments between control and Aila groups. **(G, H)** Cell invasion was analyzed using the transwell assay of H1299 cells. The data are represented as the mean ± SD (n = 3). *($P < 0.05$), **($P < 0.01$) and ***($P < 0.001$) indicate statistically significant differences.

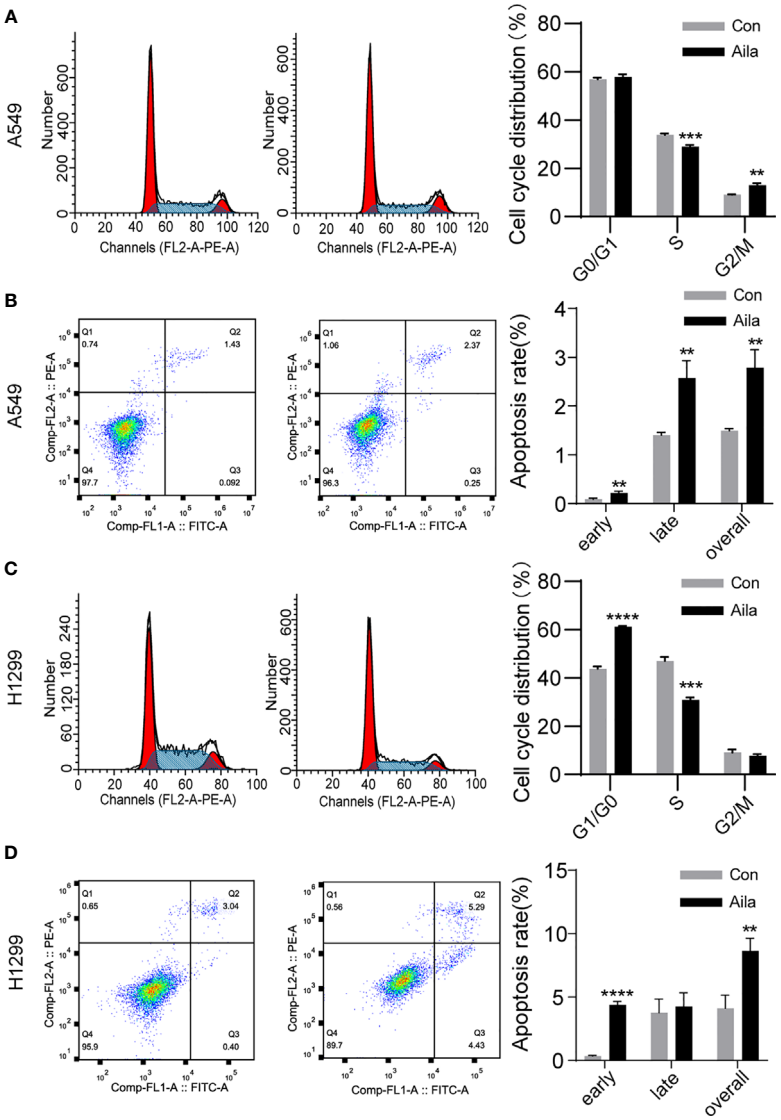

FIGURE 3 | Aila induces cell cycle arrest and apoptosis in A549 and H1299 cells. **(A, C)** The cell cycle of A549 and H1299 cells was examined by flow cytometry between control and Aila groups. **(B, D)** Apoptosis of A549 and H1299 cells was analyzed between control and Aila groups and the quantified apoptosis data refers to the total proportion of both early and late apoptosis. The results were analyzed using FlowJo and ModFit software. Data are represented as the mean ± SD (n = 3). **(P < 0.01), ***(P < 0.001) and ****(P < 0.0001) indicate statistically significant differences.

with Aila. Flow cytometry results showed that si-*DUXAP8* significantly decreased S phase, while pcDNA3.1-*DUXAP8* reversed this pattern in H1299 cells (**Figures 7A, C**). Cells treated with Aila and si-*DUXAP8* also significantly decreased S phase and overexpression of *DUXAP8* and Aila treated reversed this pattern (**Figures 7E, G**). To investigate whether *DUXAP8* is associated with apoptosis in H1299 cells, we used the Annexin V/PI double staining method. Results revealed that si-*DUXAP8* induced apoptosis of H1299 cells, while pcDNA3.1-*DUXAP8* reversed this effect (**Figures 7B, D**). Cells treated with Aila and si-*DUXAP8* also significantly induced apoptosis and overexpression of *DUXAP8* and Aila treated reversed this pattern (**Figures 7F, H**). These results were all consistent with our previous finding that *DUXAP8* was downregulated in NSCLC cells treated with Aila, indicating that downregulation of *DUXAP8* may represent a potential therapeutic strategy for the treatment of NSCLC.

Expression Patterns of *DUXAP8* and *EGR1*

We detected the effect of *DUXAP8* overexpression on cell apoptosis after Aila treatment *via* tunnel test. The results showed that overexpressing *DUXAP8* after Aila treatment can reduce the apoptosis (**Figure 8A**), indicating that *DUXAP8* may play an important role during the cell apoptosis. Based on the sequencing results, we screened *PTGS2*, *IRF1*, *EGR1*, *BIRC3* and

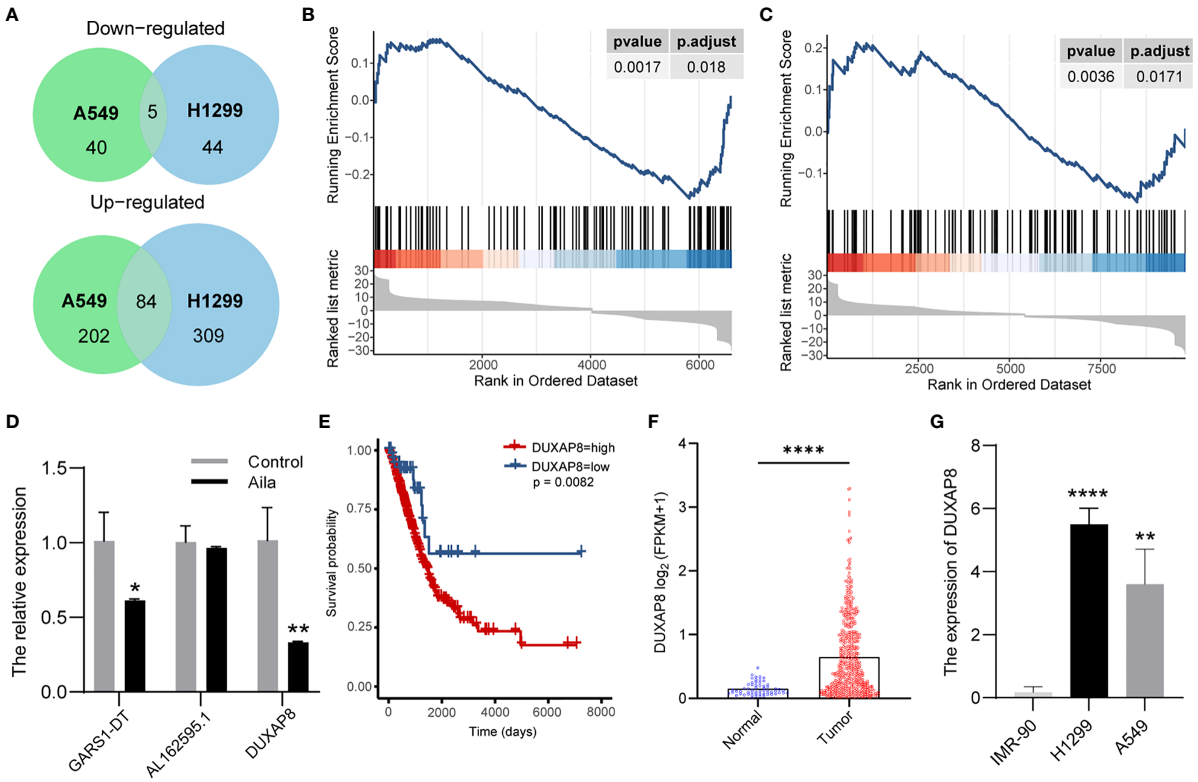

FIGURE 4 | LncRNA expression profiling by RNA-seq. **(A)** Venn diagrams of differentially expressed lncRNAs. Gene set enrichment analysis (GSEA) revealed that apoptosis was upregulated after treatment with Aila in A549 cells **(B)** and H1299 cells **(C)**. **(D)** Relative expression of GARS1-DT, AL162595.1, and DUXAP8 was analyzed by RT-PCR after Aila treatment in A549 cells. **(E)** The effect of DUXAP8 expression level on patient survival in TCGA database. **(F)** Expression of DUXAP8 in LUAD based on sample types. **(G)** The expression of DUXAP8 between IMR-90, A549 and H1299 cells in CCLE database. Data are shown as the mean ± SD (n = 3). *(P < 0.05), **(P < 0.01) and ****(P < 0.0001) indicate statistically significant differences.

CCL5 genes, which are closely related to cell proliferation, cell cycle progression and apoptosis. First, RT-PCR was used to detect mRNA expression of these genes after knockdown of *DUXAP8*, and *EGR1* was significantly upregulated (**Figure 8B**). Moreover, TCGA database revealed that *EGR1* in lung adenocarcinoma patients (LUAD) was significantly lower than in noncancerous tissue, and the downregulation level of *EGR1* was associated with poor prognosis and short survival inversely (**Figures 8C, D**). CCLE database revealed that *EGR1* in A549 and H1299 cells was significantly lower than in IMR-90 cells (**Figure 8E**). Next, we transfected the knockdown and overexpression vectors to detect the interaction mechanism between *DUXAP8* and *EGR1* at the mRNA and protein levels. The results revealed that after knockdown of *DUXAP8*, expression of *EGR1* was much higher than in the control group by both RT-PCR and western blot analysis; in contrast, expression levels of *EGR1* were significantly decreased in the overexpression group (**Figures 8F, H**). Compared to the control group, Aila group delay the growth of tumor xenografts in mouse models (**Figure 8G**). This finding demonstrates that *EGR1* expression is regulated by *DUXAP8* and is negatively correlated with its expression.

DISCUSSION

In recent years, lncRNAs have become an attractive research focus because lncRNAs have been found to be involved in important physiological and pathological processes in a variety of cells. By interacting with multiple DNAs, RNAs and proteins, lncRNAs exhibit tumor-suppressive or oncogenic effects and have enormous potential as cancer biomarkers (46). It has already been demonstrated that abnormal expression of lncRNAs is closely related to the occurrence, metastasis, diagnosis and treatment of lung cancer (47). For example, EPEL promotes lung cancer cell proliferation by activating E2F (48). Additionally, MetaLnc9 facilitates metastasis of lung carcinoma by sensitizing cells to the AKT/mTOR signaling pathway (49). Furthermore, Li et al. found that AFAP1-AS1 was easily detected *in vivo*, which may help in diagnosing carcinoma (50). In addition, MALAT1 directly reverses the resistance of NSCLC cells to chemotherapeutic agents (51).

In our study, high-throughput lncRNA sequencing was conducted. The results showed that *DUXAP8* was significantly downregulated in H1299 cells treated with Aila. Moreover, knockdown of *DUXAP8* greatly inhibited cell viability and

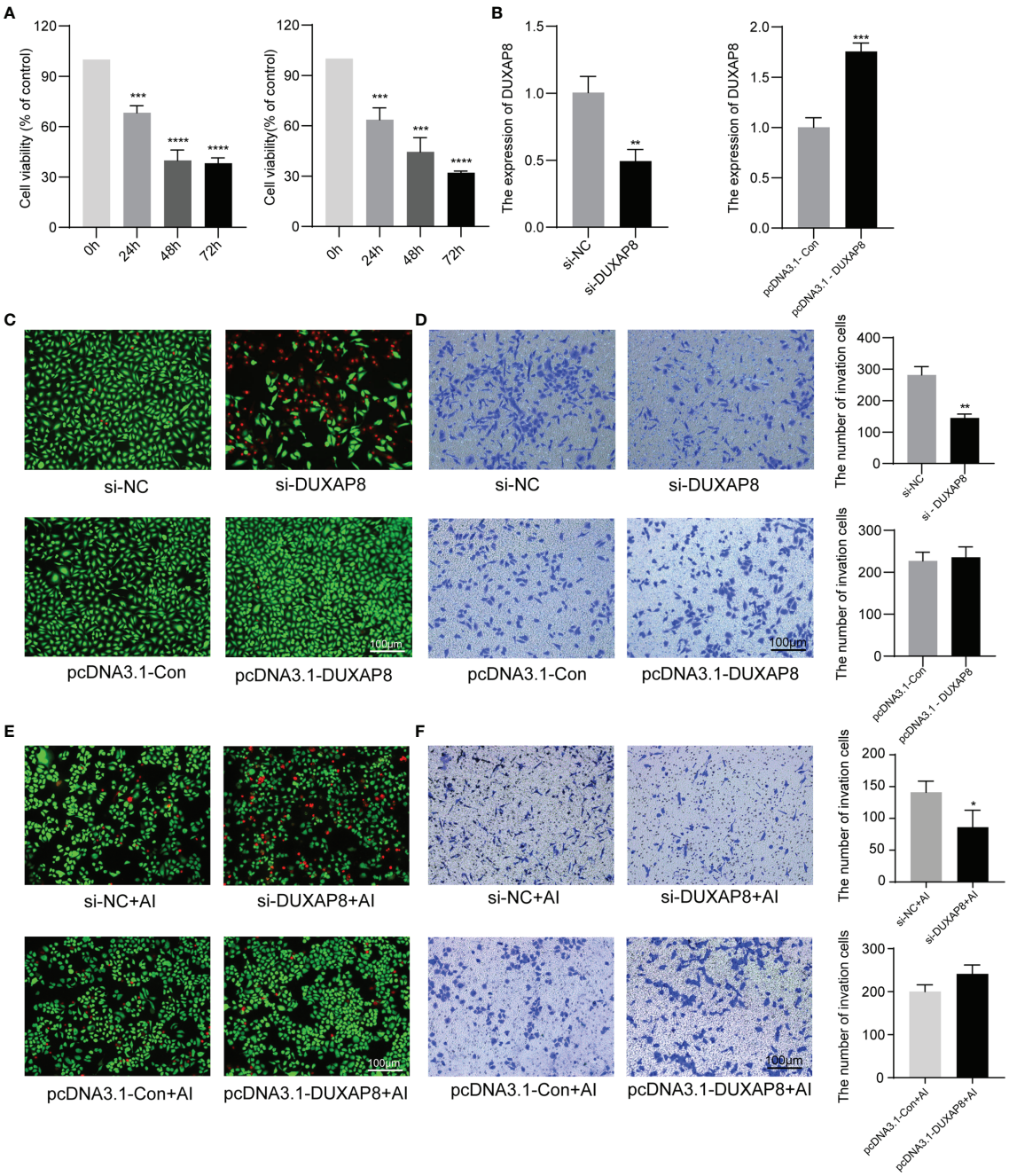

FIGURE 5 | Analysis of the effects of *DUXAP8* expression on the viability and invasion ability of A549 and H1299 cells. **(A)** Cell growth of A549 and H1299 cells was analyzed after si-*DUXAP8* transfection by MTT assay. **(B)** Relative expression of *DUXAP8* in the Nc, si-*DUXAP8*, pcDNA3.1-Con and pcDNA3.1-*DUXAP8* groups using RT-PCR. **(C)** Live/dead cell staining of A549 cells was analyzed after si-*DUXAP8* and pcDNA3.1-*DUXAP8* transfection. **(D)** The invasion assay of A549 cells was performed after si-*DUXAP8* and pcDNA3.1-*DUXAP8* transfection. **(E)** Live/dead cell staining of A549 cells was analyzed after si-*DUXAP8* and pcDNA3.1-*DUXAP8* transfection and Aila treatment. **(F)** The invasion assay of H1299 cells was performed after si-*DUXAP8* and pcDNA3.1-*DUXAP8* transfection and Aila treatment. Data are shown as the mean ± SD (n = 3). *($P < 0.05$), **($P < 0.01$), ***($P < 0.001$) and ****($P < 0.0001$) indicate statistically significant differences.

induced cell cycle arrest and apoptosis in A549 and H1299 cells, whereas overexpression of *DUXAP8* reversed these effects. Previous experiments reported that *DUXAP8* was overexpressed in cancers and that its aberrant upregulation promoted cancer cell growth (36), which is consistent with our results. Although the degree of apoptosis cycle arrest after overexpression and knockdown of *DUXAP8* was not completely consistent between A549 and H1299 cells, the Alia induced apoptosis and cell cycle

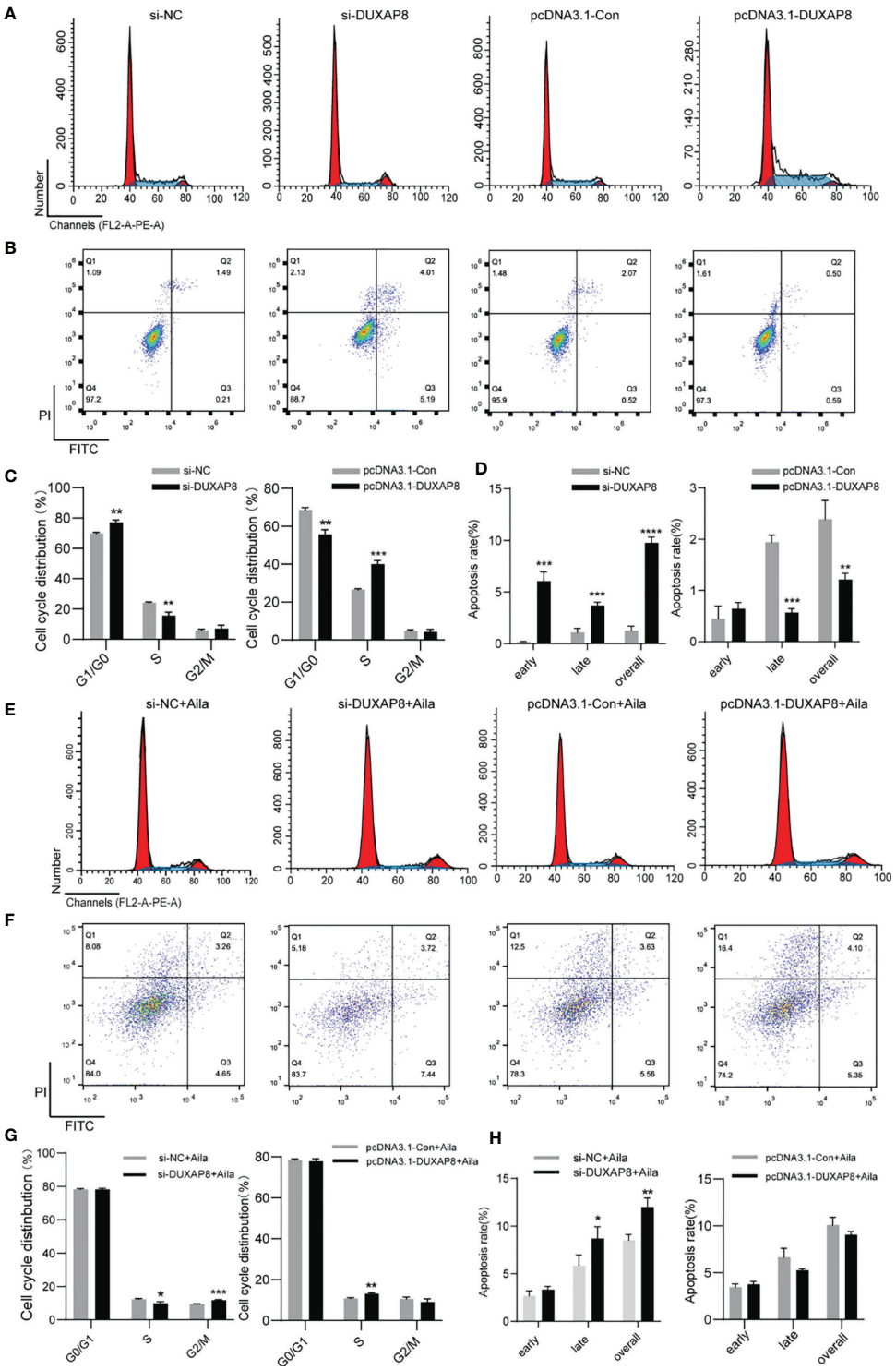

FIGURE 6 | Analysis of the effects of *DUXAP8* expression on the cell cycle and apoptosis of A549 cells. **(A)** The cell cycle was analyzed after si-*DUXAP8* and pcDNA3.1-*DUXAP8* transfection of A549 cells. **(B)** Apoptosis was detected after si-*DUXAP8* and pcDNA3.1-*DUXAP8* transfection of A549 cells. **(C)** Statistical analysis of the percentage of cell cycle distribution. **(D)** The quantified apoptosis data were calculated from the total proportion including both early and late apoptosis, the histogram represents the sum of Q2 and Q3. **(E)** The cell cycle was analyzed after si-*DUXAP8* and pcDNA3.1-*DUXAP8* transfection and treated with Aila. **(F)** Apoptosis was detected after si-*DUXAP8* and pcDNA3.1-*DUXAP8* and treated with Aila. **(G)** Statistical analysis of the percentage of cell cycle distribution. **(H)** The quantified apoptosis data were calculated from the total proportion including both early and late apoptosis, the histogram represents the sum of Q2 and Q3. The data are represented as the mean ± SD (n = 3). *($P < 0.05$), **($P < 0.01$), ***($P < 0.001$) and ****($P < 0.0001$) indicate statistically significant differences.

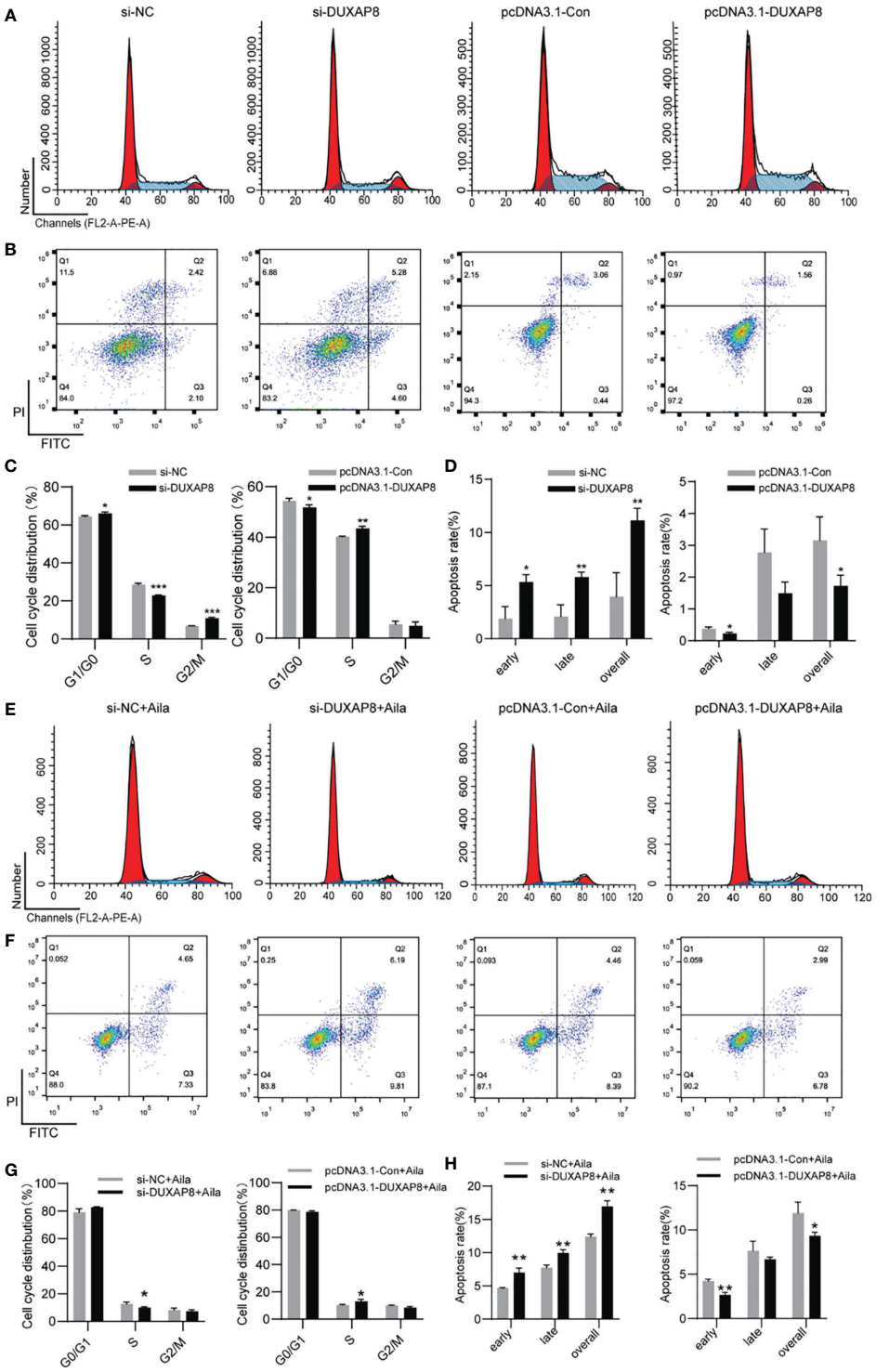

FIGURE 7 | Analysis of the DUXAP8 expression on the cell cycle and apoptosis of H1299 cells. **(A)** The cell cycle was analyzed after si-DUXAP8 and pcDNA3.1-DUXAP8 transfection of H1299 cells. **(B)** Apoptosis was detected after si-DUXAP8 and pcDNA3.1-DUXAP8 transfection of H1299 cells. **(C)** Statistical analysis of the percentage of cell cycle distribution. **(D)** The quantified apoptosis data were calculated from the total proportion including both early and late apoptosis, the histogram represents the sum of Q2 and Q3. **(E)** The cell cycle was analyzed after si-DUXAP8 and pcDNA3.1-DUXAP8 transfection and treated with Aila. **(F)** Apoptosis was detected after si-DUXAP8 and pcDNA3.1-DUXAP8 and treated with Aila. **(G)** Statistical analysis of the percentage of cell cycle distribution. **(H)** The quantified apoptosis data were calculated from the total proportion including both early and late apoptosis, the histogram represents the sum of Q2 and Q3. The data are represented as the mean ± SD (n = 3). *($P < 0.05$), **($P < 0.01$) and ***($P < 0.001$) indicate statistically significant differences.

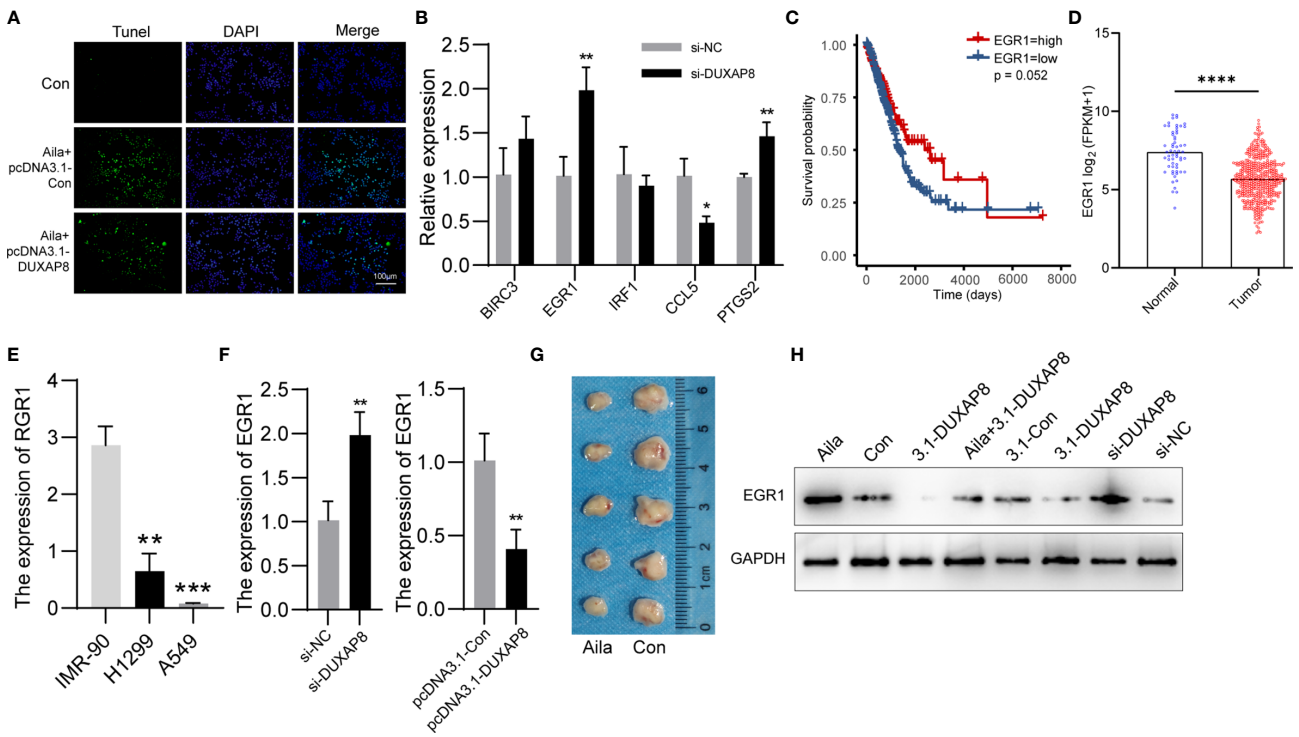

FIGURE 8 | Expression patterns of *DUXAP8* and EGR1 in A549 cells. **(A)** The effect of *DUXAP8* overexpression on cell apoptosis after Aila treatment by tunnel tests in A549 cells. **(B)** Relative expression of PTGS2, IRF1, EGR1, BIRC3 and CCL5 after si-*DUXAP8* transfection by RT-PCR in A549 cells. **(C)** The effect of EGR1 expression level on patient survival in TCGA database. **(D)** Expression of EGR1 in LUAD based on sample types. **(E)** The expression of ERG1 between IMR-90, A549 and H1299 cells in CCLE database. **(F)** Relative mRNA expression of EGR1 in the Nc, si-*DUXAP8*, pcDNA3.1-Con, and pcDNA3.1-*DUXAP8* groups determined by RT-PCR in A549 cells. **(G)** Tumor morphology of the control group (right) and Aila group (left). **(H)** Relative protein expression of EGR1 in the Nc, si-*DUXAP8*, pcDNA3.1-Con, pcDNA3.1-*DUXAP8* and Aila treatment groups using western blotting in A549 cells. The data are represented as the mean ± SD (n = 3). *(P < 0.05), **(P < 0.01) ***(P < 0.001), and ****(P < 0.0001) indicate statistically significant differences.

arrest was substantially similar. Therefore, reduced expression of *DUXAP8* plays a vital role in restraining NSCLC.

An increasing number of reports suggest that decreased expression of *EGR1* is involved in cancer progression (52). Downregulation of *EGR1* contributes to the proliferation of colorectal cancer (42). SUN et al. performed RIP assays, and showed that *DUXAP8* RNA could directly bind to EZH2 in H1299 cells. Additionally, they found that EZH2 could directly bind to *EGR1* promoter region, and *DUXAP8* was able to repress *EGR1* by interacting with EZH2 (53). Our results demonstrated that *EGR1* is upregulated in response to knockdown of *DUXAP8*, inhibiting lung cancer growth.

Currently, approximately 75% of NSCLC patients in the world are at an advanced stage when diagnosed, leading to a particularly short life expectancy (8). As a malignant tumor, NSCLC has a complicated pathogenesis. Although a large number of studies have developed drugs to combat NSCLC, such as PD-1 inhibitors and angiogenesis inhibitors (54, 55), they are far from meeting the clinical demands. Therefore, it remains urgent to explore novel regulators to identify new therapeutic strategies for NSCLC. Natural products have been proven to possess powerful anticancer ability by regulating multiple genes and proteins related to cancers. Aila, an active compound extracted from Ailanthus altissima, has been shown to have a powerful inhibitory effect on NSCLC (13). However, there have been no studies investigating the relationships between Aila and *DUXAP8*.

Aila can significantly decrease cell viability of both B16 and A375, with the IC50 values of 1.83 and 5.77 μM (25). Aila is able to repress the viability of SGC-7901 cells and the IC50 at 72 h was 2.47 μM (56) and Ni et al. found that Aila has ability to inhibit A549 cell proliferation at 1.25uM (24). Based on these previous data, we decided to employ Aila with a concentration at 1 μM for this study. In the present research, it was shown that Aila significantly inhibits A549 and H1299 cell proliferation both *in vitro* and induced cell cycle arrest and apoptosis. Meanwhile, sequencing results demonstrated that Aila markedly downregulated *DUXAP8* and upregulated *EGR1* in H1299 cells. Consequently, we conclude that Aila suppresses cell viability and induces cycle arrest and apoptosis in A549 and H1299 cells by downregulating *DUXAP8* and upregulating *EGR1* expression.

Altogether, this research verifies the antitumor effects of Aila in NSCLC and further illuminates its mechanism involving *DUXAP8* and *EGR1*. These data all suggest that *DUXAP8* has

great potential for the diagnosis, treatment, and prognosis of NSCLC, and our results provide a feasible theoretical basis for subsequent studies.

DATA AVAILABILITY STATEMENT

The datasets presented in this study can be found in online repositories. The names of the repository/repositories and accession number(s) can be found in the article/**Supplementary Material**.

AUTHOR CONTRIBUTIONS

Study concept and design: YZ, XD, and BW. Acquisition of data: LC, CW, DM, HW, and SC. Analysis and interpretation of data: LC, XW, YT, YL, and HW. Drafting of the manuscript: CW. Critical revision of the manuscript for important intellectual content: YZ, XD, BW, TW, and YS. Reagents and material support: YZ, XD, and BW. Administrative, technical, and supervision: YZ, XD, and BW. All authors contributed to the article and approved the submitted version.

FUNDING

This research was funded by the Jilin Scientific and Technological Development Program (grant number: 20200404085YY) and the Science and technology project of traditional Chinese medicine in Jilin Province (grant number: 2021139) to XD.

SUPPLEMENTARY MATERIAL

The Supplementary Material for this article can be found online at: https://www.frontiersin.org/articles/10.3389/fonc.2021.652567/full#supplementary-material

REFERENCES

1. Bray F, Ferlay J, Soerjomataram I, Siegel RL, Torre LA, Jemal A. Global Cancer Statistics 2018: GLOBOCAN Estimates of Incidence and Mortality Worldwide for 36 Cancers in 185 Countries. *Ca-a Cancer J Clin* (2018) 68:394–424. doi: 10.3322/caac.21492
2. Feng R-M, Zong Y-N, Cao S-M, Xu R-H. Current Cancer Situation in China: Good or Bad News From the 2018 Global Cancer Statistics? *Cancer Commun* (2019) 39. doi: 10.1186/s40880-019-0368-6
3. Travis WD, Brambilla E, Nicholson AG, Yatabe Y, Austin JHM, Beasley MB, et al. The 2015 World Health Organization Classification of Lung Tumors. *J Thoracic Oncol* (2015) 10:1243–60. doi: 10.1097/JTO.0000000000000630
4. Osmani L, Askin F, Gabrielson E, Li QK. Current WHO Guidelines and the Critical Role of Immunohistochemical Markers in the Subclassification of Non-Small Cell Lung Carcinoma (NSCLC): Moving From Targeted Therapy to Immunotherapy. *Semin Cancer Biol* (2018) 52:103–9. doi: 10.1016/j.semcancer.2017.11.019
5. Hirsch FR, Scagliotti GV, Mulshine JL, Kwon R, Curran WJ, Wu YL, et al. Lung Cancer: Current Therapies and New Targeted Treatments. *Lancet* (2017) 389:299–311. doi: 10.1016/S0140-6736(16)30958-8
6. Reck M, Rabe KF. Precision Diagnosis and Treatment for Advanced Non-Small-Cell Lung Cancer. *New Engl J Med* (2017) 377:849–61. doi: 10.1056/NEJMra1703413
7. Swanton C, Govindan R. Clinical Implications of Genomic Discoveries in Lung Cancer. *N Engl J Med* (2016) 374:1864–73. doi: 10.1056/NEJMra1504688
8. Folch E, Costa DB, Wright J, VanderLaan PA. Lung Cancer Diagnosis and Staging in the Minimally Invasive Age With Increasing Demands for Tissue Analysis. *Trans Lung Cancer Res* (2015) 4:392–403. doi: 10.3978/j.issn.2218-6751.2015.08.02
9. Huang Y, Yuan K, Tang M, Yue J, Bao L, Wu S, et al. Melatonin Inhibiting the Survival of Human Gastric Cancer Cells Under ER Stress Involving Autophagy and Ras-Raf-MAPK Signalling. *J Cell Mol Med* (2021) 25:1480–92. doi: 10.1111/jcmm.16237
10. Haddadin S, Perry MC. History of Small-Cell Lung Cancer. *Clin Lung Cancer* (2011) 12:87–93. doi: 10.1016/j.cllc.2011.03.002
11. Newman DJ, Cragg GM. Natural Products as Sources of New Drugs Over the Last 25 Years. *J Natural Products* (2007) 70:461–77. doi: 10.1021/np068054v
12. Xiang Y, Guo Z, Zhu P, Chen J, Huang Y. Traditional Chinese Medicine as a Cancer Treatment: Modern Perspectives of Ancient But Advanced Science. *Cancer Med* (2019) 8:1958–75. doi: 10.1002/cam4.2108
13. Mousavi F, Shahali Y, Pourpak Z, Majd A, Ghahremaninejad F. Year-to-Year Variation of the Elemental and Allergenic Contents of Ailanthus Altissima Pollen Grains: An Allergomic Study. *Environ Monit Assess* (2019) 191. doi: 10.1007/s10661-019-7458-4
14. Gao W, Ge S, Sun J. Ailanthone Exerts Anticancer Effect by Up-Regulating miR-148a Expression in MDA-MB-231 Breast Cancer Cells and Inhibiting Proliferation, Migration and Invasion. *Biomedicine Pharmacotherapy* (2019) 109:1062–9. doi: 10.1016/j.biopha.2018.10.114
15. Wang R, Lu Y, Li H, Sun L, Yang N, Zhao M, et al. Antitumor Activity of the Ailanthus Altissima Bark Phytochemical Ailanthone Against Breast Cancer MCF-7 Cells. *Oncol Lett* (2018) 15:6022–8. doi: 10.3892/ol.2018.8039
16. He Y, Peng S, Wang J, Chen H, Cong X, Chen A, et al. Ailanthone Targets p23 to Overcome MDV3100 Resistance in Castration-Resistant Prostate Cancer. *Nat Commun* (2016) 7. doi: 10.1038/ncomms13122
17. Daga M, Pizzimenti S, Dianzani C, Cucci MA, Cavalli R, Grattarola M, et al. Ailanthone Inhibits Cell Growth and Migration of Cisplatin Resistant Bladder Cancer Cells Through Down-Regulation of Nrf2, YAP, and c-Myc Expression. *Phytomedicine* (2019) 56:156–64. doi: 10.1016/j.phymed.2018.10.034
18. Cucci MA, Grattarola M, Dianzani C, Damia G, Ricci F, Roetto A, et al. Ailanthone Increases Oxidative Stress in CDDP-resistant Ovarian and Bladder Cancer Cells by Inhibiting of Nrf2 and YAP Expression Through a Post-Translational Mechanism. *Free Radical Biol Med* (2020) 150:125–35. doi: 10.1016/j.freeradbiomed.2020.02.021
19. Zhuo Z, Hu J, Yang X, Chen M, Lei X, Deng L, et al. Ailanthone Inhibits Huh7 Cancer Cell Growth *via* Cell Cycle Arrest and Apoptosis *In Vitro* and *In Vivo*. *Sci Rep-Uk* (2015) 5. doi: 10.1038/srep16185
20. Chen Y, Zhu L, Yang X, Wei C, Chen C, He Y, et al. Ailanthone Induces G(2)/M Cell Cycle Arrest and Apoptosis of SGC-7901 Human Gastric Cancer Cells. *Mol Med Rep* (2017) 16:6821–7. doi: 10.3892/mmr.2017.7491
21. Wei C, Chen C, Cheng Y, Zhu L, Wang Y, Luo C, et al. Ailanthone Induces Autophagic and Apoptotic Cell Death in Human Promyelocytic Leukemia HL-60 Cells. *Oncol Lett* (2018) 16:3569–76. doi: 10.3892/ol.2018.9101
22. Zhang Y, Zhang C, Min D. Ailanthone Up-Regulates miR-449a to Restrain Acute Myeloid Leukemia Cells Growth, Migration and Invasion. *Exp Mol Pathol* (2019) 108:114–20. doi: 10.1016/j.yexmp.2019.04.011
23. Hou S, Cheng Z, Wang W, Wang X, Wu Y. Ailanthone Exerts an Antitumor Function on the Development of Human Lung Cancer by Upregulating Microrna-195. *J Cell Biochem* (2019) 120:10444–51. doi: 10.1002/jcb.28329
24. Ni Z, Yao C, Zhu X, Gong C, Xu Z, Wang L, et al. Ailanthone Inhibits Non-Small Cell Lung Cancer Cell Growth Through Repressing DNA Replication Via Downregulating RPA1. *Br J Cancer* (2017) 117:1621–30. doi: 10.1038/bjc.2017.319

25. Liu W, Liu X, Pan Z, Wang D, Li M, Chen X, et al. Ailanthone Induces Cell Cycle Arrest and Apoptosis in Melanoma B16 and A375 Cells. *Biomolecules* (2019) 9. doi: 10.3390/biom9070275
26. Yang P, Sun D, Jiang F. Ailanthone Promotes Human Vestibular Schwannoma Cell Apoptosis and Autophagy by Downregulation of Mir-21. *Oncol Res* (2018) 26:941–8. doi: 10.3727/096504018X15149775533331
27. Kong D, Ying B, Zhang J, Ying H. Retracted ArticleThe Anti-Osteosarcoma Property of Ailanthone Through Regulation of miR-126/VEGF-A Axis. *Artif Cells Nanomedicine Biotechnol* (2019) 47:3913–9. doi: 10.1080/21691401.2019.1669622
28. Kopp F, Mendell JT. Functional Classification and Experimental Dissection of Long Noncoding Rnas. *Cell* (2018) 172:393–407. doi: 10.1016/j.cell.2018.01.011
29. Rafiee A, Riazi-Rad F, Havaskary M, Nuri F. Long Noncoding RNAs: Regulation, Function and Cancer. *Biotechnol Genet Eng Rev* (2018) 34:153–80. doi: 10.1080/02648725.2018.1471566
30. Chen ZY, Lei TY, Chen X, Gu JY, Huang JL, Lu BB, et al. Long Non-Coding RNA in Lung Cancer. *Clin Chim Acta* (2020) 504:190–200. doi: 10.1016/j.cca.2019.11.031
31. Li S, Mei Z, Hu HB, Zhang X. The Lncrna MALAT1 Contributes to Non-Small Cell Lung Cancer Development Via Modulating miR-124/STAT3 Axis. *J Cell Physiol* (2018) 233:6679–88. doi: 10.1002/jcp.26325
32. Tang Y, Xiao GM, Chen YJ, Deng Y. Lncrna MALAT1 Promotes Migration and Invasion of Non-Small-Cell Lung Cancer by Targeting miR-206 and Activating Akt/mTOR Signaling. *Anti-Cancer Drug* (2018) 29:725–35. doi: 10.1097/CAD.0000000000000650
33. Zhao YJ, Zhu ZX, Shi SM, Wang J, Li N. Long Non-Coding RNA MEG3 Regulates Migration and Invasion of Lung Cancer Stem Cells *via* miR-650/SLC34A2 Axis. *BioMed Pharmacother* (2019) 120. doi: 10.1016/j.biopha.2019.109457
34. Xia H, Qu XL, Liu LY, Qian DH, Jing HY. Lncrna MEG3 Promotes the Sensitivity of Vincristine by Inhibiting Autophagy in Lung Cancer Chemotherapy. *Eur Rev Med Pharmaco* (2018) 22:1020–7. doi: 10.26355/eurrev_201802_14384
35. Ma H, Xie M, Sun M, Chen T, Jin R, Ma T, et al. The Pseudogene Derived Long Noncoding RNA DUXAP8 Promotes Gastric Cancer Cell Proliferation and Migration *via* Epigenetically Silencing PLEKHO1 Expression. *Oncotarget* (2017) 8:52211–24. doi: 10.18632/oncotarget.11075
36. Hu Y, Zhang X, Zai H, Jiang W, Xiao L, Zhu Q. Lncrna DUXAP8 Facilitates Multiple Malignant Phenotypes and Resistance to PARP Inhibitor in HCC *via* Upregulating Foxm1. *Mol Ther Oncolytics* (2020) 19:308–22. doi: 10.1016/j.omto.2020.10.010
37. He W, Yu Y, Huang W, Feng G, Li J. The Pseudogene Duxap8 Promotes Colorectal Cancer Cell Proliferation, Invasion, and Migration by Inducing Epithelial-Mesenchymal Transition Through Interacting With EZH2 and H3k27me3. *Oncotargets Ther* (2020) 13:11059–70. doi: 10.2147/OTT.S235643
38. Chen M, Zheng Y, Xie J, Zhen E, Zhou X. Integrative Profiling Analysis Identifies the Oncogenic Long Noncoding RNA DUXAP8 in Oral Cancer. *Anti-Cancer Drug* (2020) 31:792–8. doi: 10.1097/CAD.0000000000000936
39. Yin D, Hua L, Wang J, Liu Y, Li X. Long Non-Coding Rna DUXAP8 Facilitates Cell Viability, Migration, and Glycolysis in Non-Small-Cell Lung Cancer *via* Regulating HK2 and LDHA by Inhibition of Mir-409-3p. *Oncotargets Ther* (2020) 13:7111–23. doi: 10.2147/OTT.S243542
40. Boone D, Qi Y, Li Z, Hann S. Egr1 Mediates p53-independent c-Myc-induced Apoptosis *via* a Noncanonical ARF-dependent Transcriptional Mechanism. *Proc Natl Acad Sci USA* (2011) 108:632–7. doi: 10.1073/pnas.1008848108
41. Zhang H, Chen X, Wang J, Guang W, Han W, Zhang H, et al. EGR1 Decreases the Malignancy of Human Non-Small Cell Lung Carcinoma by Regulating KRT18 Expression. *Sci Rep* (2014) 4:5416. doi: 10.1038/srep05416
42. Wei F, Jing H, Wei M, Liu L, Wu J, Wang M, et al. Ring Finger Protein 2 Promotes Colorectal Cancer Progression by Suppressing Early Growth Response 1. *Aging* (2020) 12:26199–220. doi: 10.18632/aging.202396
43. Shi S, Li F, Wu L, Zhang L, Liu L. Feasibility of BMSCs Mediated-Synthetic Radiosensitive Promoter Combined NIS for Radiogenetic Ovarian Cancer Therapy. *Hum Gene Ther* (2020). doi: 10.1089/hum.2020.214
44. Yu G, Wang LG, Han Y, He QY. clusterProfiler: An R Package for Comparing Biological Themes Among Gene Clusters. *Omics* (2012) 16:284–7. doi: 10.1089/omi.2011.0118
45. Uhl E, Wolff F, Mangal S, Dube H, Zanin E. Light-Controlled Cell-Cycle Arrest and Apoptosis. *Angewandte Chemie (International Ed English)* (2020) 60:1187–96. doi: 10.1002/anie.202008267
46. Iyer M, Niknafs Y, Malik R, Singhal U, Sahu A, Hosono Y, et al. The Landscape of Long Noncoding RNAs in the Human Transcriptome. *Nat Genet* (2015) 47:199–208. doi: 10.1038/ng.3192
47. Qiu MT, Feng DJ, Zhang HT, Xia WJ, Xu YT, Wang J, et al. Comprehensive Analysis of lncRNA Expression Profiles and Identification of Functional lncRNAs in Lung Adenocarcinoma. *Oncotarget* (2016) 7:16012–22. doi: 10.18632/oncotarget.7559
48. Park SM, Choi EY, Bae DH, Sohn HA, Kim SY, Kim YJ. The LncRNA Epel Promotes Lung Cancer Cell Proliferation Through E2F Target Activation. *Cell Physiol Biochem* (2018) 45:1270–83. doi: 10.1159/000487460
49. Yu T, Zhao YJ, Hu ZX, Li J, Chu DD, Zhang JW, et al. Metalnc9 Facilitates Lung Cancer Metastasis *via* a PGK1-Activated Akt/mTOR Pathway. *Cancer Res* (2017) 77:5782–94. doi: 10.1158/0008-5472.CAN-17-0671
50. Wei C-C, Nie F-Q, Jiang L-L, Chen Q-N, Chen Z-Y, Chen X, et al. The Pseudogene DUXAP10 Promotes an Aggressive Phenotype Through Binding With LSD1 and Repressing LATS2 and RRAD in Non Small Cell Lung Cancer. *Oncotarget* (2017) 8:5233–46. doi: 10.18632/oncotarget.14125
51. Jiang Y, Sun A, Zhao Y, Ying W, Sun H, Yang X, et al. Proteomics Identifies New Therapeutic Targets of Early-Stage Hepatocellular Carcinoma. *Nature* (2019) 567:257–61. doi: 10.1038/s41586-019-0987-8
52. Ma Z, Gao X, Shuai Y, Wu X, Yan Y, Xing X, et al. EGR1-Mediated linc01503 Promotes Cell Cycle Progression and Tumorigenesis in Gastric Cancer. *Cell proliferation* (2020) 54:e12922. doi: 10.1111/cpr.12922
53. Sun M, Nie FQ, Zang C, Wang Y, Hou J, Wei C, et al. The Pseudogene Duxap8 Promotes Non-Small-Cell Lung Cancer Cell Proliferation and Invasion by Epigenetically Silencing EGR1 and RHOB. *Mol Ther* (2017) 25:739–51. doi: 10.1016/j.ymthe.2016.12.018
54. Malapelle U, Rossi A. Emerging Angiogenesis Inhibitors for Non-Small Cell Lung Cancer. *Expert Opin Emerg Dr* (2019) 24:71–81. doi: 10.1080/14728214.2019.1619696
55. Liu TT, Ding SL, Dang J, Wang H, Chen J, Li G. First-Line Immune Checkpoint Inhibitors for Advanced Non-Small Cell Lung Cancer With Wild-Type Epidermal Growth Factor Receptor (EGFR) or Anaplastic Lymphoma Kinase (ALK): A Systematic Review and Network Meta-Analysis. *J Thorac Dis* (2019) 11:2899–+. doi: 10.21037/jtd.2019.07.45
56. Chen Y, Zhu L, Yang X, Wei C, Chen C, He Y, et al. Ailanthone Induces G2/M Cell Cycle Arrest and Apoptosis of SGC−7901 Human Gastric Cancer Cells. *Mol Med Rep* (2017) 16:6821–7. doi: 10.3892/mmr.2017.7491

Conflict of Interest: The authors declare that the research was conducted in the absence of any commercial or financial relationships that could be construed as a potential conflict of interest.

frontiers in Oncology

ORIGINAL RESEARCH
published: 25 June 2021
doi: 10.3389/fonc.2021.688195

The Antitumor Activity and Mechanism of a Natural Diterpenoid From *Casearia graveolens*

Ying Li, Jun Ma, Ziteng Song, Yinan Zhao, Han Zhang, Yeling Li, Jing Xu and Yuanqiang Guo**

State Key Laboratory of Medicinal Chemistry Biology, College of Pharmacy, Tianjin Key Laboratory of Molecular Drug Research, and Drug Discovery Center for Infectious Disease, Nankai University, Tianjin, China

OPEN ACCESS

Edited by:
Peng Qu,
National Institutes of Health (NIH), United States

Reviewed by:
Mingxiao Feng,
Johns Hopkins University, United States
Likui Feng,
The Rockefeller University, United States
Lin Jiang,
University of Cincinnati, United States

***Correspondence:**
Jing Xu
xujing611@nankai.edu.cn
Yuanqiang Guo
victgyq@nankai.edu.cn

Specialty section:
This article was submitted to Pharmacology of Anti-Cancer Drugs, a section of the journal Frontiers in Oncology

Received: *30 March 2021*
Accepted: *08 June 2021*
Published: *25 June 2021*

Citation:
Li Y, Ma J, Song Z, Zhao Y, Zhang H, Li Y, Xu J and Guo Y (2021) The Antitumor Activity and Mechanism of a Natural Diterpenoid From Casearia graveolens. Front. Oncol. 11:688195. doi: 10.3389/fonc.2021.688195

Casearlucin A, a diterpenoid obtained from *Casearia graveolens*, has been reported to possess strong cytotoxic activity. However, the *in vivo* anti-tumor effects and the action mechanism of casearlucin A remain poorly understood. Our study revealed that casearlucin A arrested cell cycle at G0/G1 stage and induced cell apoptosis in cell level. Additionally, casearlucin A inhibited HepG2 cell migration *via* regulating a few of metastasis-related proteins. Furthermore, it inhibited tumor angiogenesis in zebrafish *in vivo*. More importantly, casearlucin A significantly inhibited cell proliferation and migration in an *in vivo* zebrafish xenograft model. Collectively, these results are valuable for the further development and application of casearlucin A as an anticancer agent.

Keywords: cytotoxic activity, zebrafish xenograft model, apoptosis, cell cycle, FAK-MMPs, antiangiogenesis inhibitors

INTRODUCTION

Cancer is the leading cause of death in the world, and the incidence rate is high in many Asian countries including China (1, 2). Nowadays, the most common ways to treat cancer are the combination of chemotherapy, radiation therapy, and surgical interventions. However, there are still many problems in current clinical treatment, such as side effects and drug resistances, which urges researchers to develop new treatment strategies or find alternative treatments (3). As we all know, medicinal plants are a promising source for developing new pharmaceuticals, and many well-known drugs approved by FDA, such as paclitaxel, camptothecin, and artemisinin, have been derived from natural products or their derivatives (4). In the development of new drugs, the main role of natural products is to provide lead compounds, or provide clues for the discovery of lead compounds.

The genus *Casearia* Jacq. belonging to the family Flacourtiaceae, consists of about 160 species, which distributed widely in tropical Africa, Asia, northwest Australia, and South America. Recent phytochemical studies have revealed the presence of abundant diterpenoids, particularly clerdoane

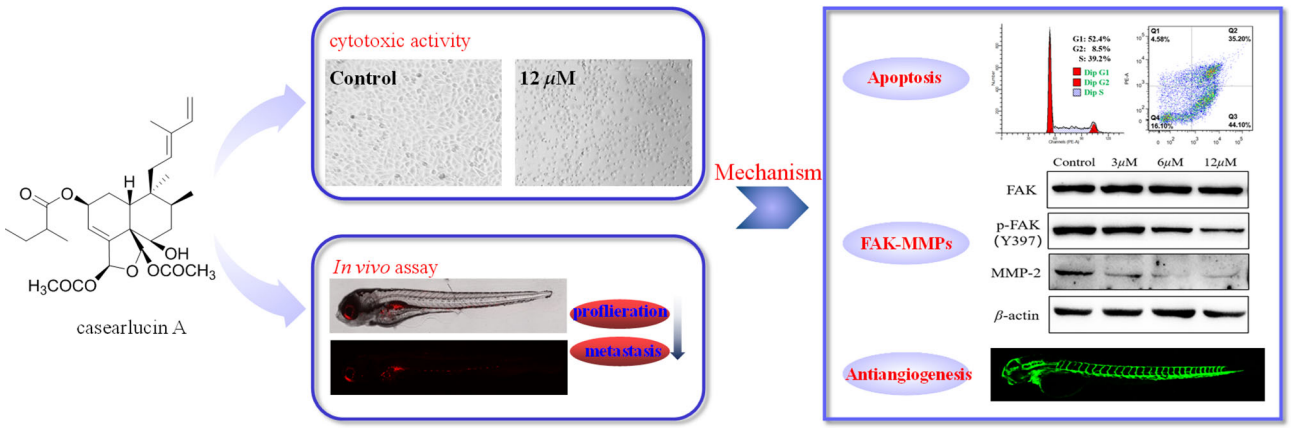

GRAPHICAL ABSTRACT |

diterpenoids, in *Casearia* plants, which showed extensive biological activities, including antimalarial, antimicrobial, antifungal, and cytotoxic activities (5–13). The plant *Casearia graveolens* evoked our interest, a phytochemical examination aiming to acquire biologically active compounds was thus carried out by our research group. In the previous chemical investigation conducted by our group, nine new clerodane diterpenoids (graveospenes A–I) and three known clerodane diterpenoids (casearlucin A, casearlucin F, and bucidarasin C) was obtained. A biological evaluation of the new compounds was performed, and graveospenes A was found to be cytotoxic (14). Therefore, three known compounds with similar structure to graveospenes A were screened for cytotoxic activity. The results revealed that all of the three compounds were cytotoxic against HepG2, A549, and Hela cell lines, and casearlucin A was the most active. According to the previous literature, there have been no reports on the mechanism of casearlucin A, especially the anti-tumor effects *in vivo*. The further research on casearlucin A with remarkable cytotoxicity may be potentially useful for the development of casearlucin A as an anticancer agent.

Casearlucin A with prominent cytotoxic activity attracted our interest, and there is no report on its action mechanism. So, this study aims to investigate the anti-tumor effects *in vivo* using a zebrafish tumor xenograft, and the anti-tumor mechanism, all of which are important and valuable for the further development and application of casearlucin A as an anticancer agent.

MATERIALS AND METHODS

Materials and Cell Culture

Dulbecco's modified Eagle's medium (DMEM), Fetal bovine serum (FBS, BI, Israel) were purchased from LABBIOTECH Co. Ltd. (Shandong, China). MTT and dimethyl sulfoxide (DMSO) were purchased from Solarbio (Beijing, China). Celltracker CM-DiI was obtained from Yeasen Biotechnology Co. Ltd (Shanghai, China). Annexin V-FITC Apoptosis Detection Kit, Cell Cycle and Apoptosis Kit, BCA protein assay kit were provided by Beyotime Biotechnology Co. Ltd (Shanghai, China). Rabbit monoclonal antibodies to Bax, Bcl-2, FAK, p-FAK (phospho Y397), MMP-2, β-actin were all purchased from Cell Signaling Technology (Danvers, MA, USA).

The three cancer cell lines (HepG2, Hela and A549 cells) were obtained from Shanghai Institutes for Biological Sciences, Chinese Academy of Sciences (Shanghai, China). The cells were cultured in DMEM containing 10% (v/v) fetal bovine serum and 100 U/mL penicillin/streptomycin under a water-saturated atmosphere of 95% air and 5% CO_2.

Cytotoxic Activity Assay

The cytotoxic activities were evaluated using MTT assay (15). Briefly, after reaching approximate 80% confluence, the cells were harvested and seeded in 96-well plates (1×10^4 cells/well) and allowed to adhere for 24 h at 37°C. Then, the cells were treated with the test samples dissolved in DMSO at different concentrations, including the positive. Etoposide was used as a positive control. After continuous incubation for 48 h, 20 μL MTT solution (5 mg/mL) was added in each well for 4 h incubation. Then, the medium was replaced with 150 μL DMSO and the absorbance was measured at 492 nm using microplate reader (Thermo Fisher Scientific Inc. America). The experiments were performed in triplicate, and the IC_{50} value was defined as the concentration of the compounds that inhibited cell proliferation by 50%.

Wound-Scratch Assay

The effects of casearlucin A on motility ability of HepG2 cells were assessed using wound scratch assay (16). Briefly, cells were seeded into 6-wells plate with a concentration of 5×10^5cells/well. After reaching 90% confluence, cells were scratched by a sterile pipette tip. Then, the cells were treated with various concentrations of casearlucin A. The wounded healing was observed using microscope at 0 and 48 h. The scratch distance value was measured by Image J software.

Cell Cycle Analysis

The distribution of cell cycle of HepG2 cells affected by casearlucin A was performed using Flow cytometric analysis (17). HepG2 cells in exponential growth phase were seeded in 12 well plate at the density of 2×10^5 cells/well for 24 h at 37 °C. Then, the cells were treated with different concentrations of casearlucin A (2, 4, and 8 μM). After an exposure to the test sample for 48 h, the cells were harvested, washed with PBS twice, and fixed in 70% ice-cold ethanol at 4°C overnight. Then, the cells were washed with PBS twice and treated with propidium iodide staining buffer containing RNase (Beyotime, C1052) for 30 minutes at 37°C in the dark, followed immediately by cellar DNA analysis using BDLSR Fortessa flow cytometry. Data were processed using ModFit LT Software.

Apoptosis Analysis by Flow Cytometry

The apoptosis analysis of HepG2 cells induced by the tested compound was accomplished by flow cytometry using Annexin V-FITC Apoptosis Detection Kit (Beyotime, C1062L) according to the manufacturer's instructions (18, 19). Briefly, HepG2 cells were harvested and seeded in 12-well plates (1×10^5 cells/well) and allowed to adhere for 24 h at 37°C. Then, the cells were treated with various concentrations (5, 10, and 15 μM) of casearlucin A. After 48 h incubation, the cells were washed twice with PBS and resuspended in the binding buffer (Beyotime, Shanghai, China). This suspension was incubated for 20 min at room temperature in the dark after adding 10 μL Annexin V-FITC and 5 μL PI. Then, cell apoptosis was examined by BD LSRFortessa flow cytometry (BD Biosciences). The cell apoptosis data were obtained with FLOWJO flow cytometry analysis software (FLOWJO LLC, Ashland, OR, USA).

Western Blot Analysis

HepG2 cells were seeded in 6-well plate at the density of 1×10^5 cells/well for 24 h. Then, the cells were treated with casearlucin A for 36 h, the cells were washed with cold PBS twice and collected. The cells were lysed with lysis buffer containing protease inhibitor cocktail and PMSF. Then, the lysates were centrifuged at 10,000 rpm for 10 min and the supernatants were collected to acquire the total protein. Protein concentrations were quantified using the BCA protein assay kit (Beyotime, P0012S). The proteins were separated by 10% SDS-PAGE and transferred to polyvinylidene difluoride. The membrane was blocked with 5% skim milk for 1 h at room temperature and then incubated (4°C, overnight) with primary antibodies against Bax (Cell Signaling Technology, 14796S), Bcl-2 (Cell Signaling Technology, 4223S), FAK (Cell Signaling Technology, 3285S), p-FAK (phospho Y397) (Cell Signaling Technology, 8556S), and MMP-2 (Cell Signaling Technology, 87809S). The membranes were subsequently incubated with horseradish peroxidase-conjugated secondary antibody for 1 h at room temperature. Lastly, the protein blots were visualized using an ECL detection kit (Beyotime, P0018AS). β-Actin protein (Cell Signaling Technology, 4970S)was used as an internal reference. Each band was quantified by Image J software (20).

Toxicity Screening of Zebrafish Embryos

Adult AB strain zebrafish were obtained from School of Medicine, Nankai University (Tianjin, China). Embryos were taken from adult zebrafish, which were placed in the breeding room overnight and mixed for 30 min to give fertilized eggs. Embryos were cultured in Holt buffer (NaCl 59.9 mM, KCl 0.7 mM, $NaHCO_3$ 0.3 mM, and $CaCl_2$ 0.9 mM) for further experiments.

The healthy zebrafish embryos were selected and treated with casearlucin A of 2.5, 5, 10, and 20 μM, to assess the toxicity of the compound on developing zebrafish embryos.The deformity rate and mortality rate were recorded every 24 h after continuous administration. All the procedures involving animals were approved by the Institutional Animal Care Committee of Nankai University (No. SYXK (JIN) 2019-0001).

Antiangiogenetic Assay Using Transgenic Zebrafish Model

The angiogenesis inhibitory activity of the selected compound was carried out using transgenic zebrafish *Tg (fli1: EGFP)*. Transgenic zebrafish were obtained from Shanghai FishBio Co., Ltd. The embryos were obtained from adult Tg zebrafish as reported previously (21, 22). Briefly, 6 hour post fertilization (hpf) embryos were grouped randomly and placed in the 24-well plate, and then the embryos were exposed to various concentrations of casearlucin A for 48 h at 28.5°C. After the treatment, embryos were anesthetized with 0.02% tricaine and photographed by a confocal microscopy (Leica, Germany). The development of intersegmental blood vessels (ISVs) and dorsal longitudinal anastomotic vessels (DLAVs) at 48 hpf were observed, and the length of ISV vessels was measured using Image J software.

In Vivo Anti-Tumor Assay Using Zebrafish Model

Embryos were obtained from adult AB zebrafish as reported previously (23). 48 hours post-fertilization (hpf) embryos were utilized to establish a xenograft tumor model (24). Prior to microinjection, HepG2 cells were labeled with 2 μM CM-DiI (Yeasen, 40718ES50). Then, the cells were resuspended in serum-free DMEM medium and adjusted to a density of 1×10^7 cells/mL. Subsequently, 48 hpf embryos were anesthetized and microinjected into the yolk with 5 nL stained cells. After 4 h incubation, tumor-bearing embryos were randomly divided into five groups (15/group) and treated with different concentrations of casearlucin A by soaking. The embryos were incubated continuously for 48 h at 28.5°C. Lastly, images were captured at 5 days post-fertilization using a confocal microscopy (Leica, Germany), and the density and focus number of red fluorescence was measured using Image J software.

Statistical Analysis

Data were analyzed by GraphPad Prism and presented as mean ± SD. Probabilities (P) less than 0.05 were determined to be significant by analysis of variance (ANOVA). The differences among three or more groups were analyzed by one-way ANOVA multiple comparisons. The experiments were repeated three times.

RESULTS

Casearlucin A Inhibited Cancer Cell Growth *In Vitro*

In recent years, the potential therapeutic effects of bioactive natural products for cancer treatment have attracted broad attention (4). Thus, we studied the anti-cancer effects of three clerodane diterpenoids (casearlucin A, casearlucin F and bucidarasin C) from *Casearia graveolens*. To assess the anti-proliferative activity of the compound, three human cancer cell lines (HepG2, A549, and Hela cells) were selected to test their toxicities by MTT assays (25, 26). Etoposide was used as a positive control (27, 28). Results showed that casearlucin A was the most active and reduced the cell growth in a dose-dependent manner (**Figure 1**). Their respective IC_{50} values on three cell lines were calculated and shown in **Table 1**, casearlucin A intensively inhibited the three tumor cell lines with lower IC_{50} values than etoposide, especially on HepG2 cells.

Next, we further investigated the inhibitory effects of casearlucin A on cell migration, the wounded healing assay was performed (29, 30). As shown in **Figure 2**, after 48 h treatment of different concentrations of casearlucin A, the migration of HepG2 cells were markedly inhibited.

Effects of Casearlucin A on Cell Cycle

In order to investigate whether casearlucin A inhibited the growth of HepG2 cells by regulating the cell cycle, we first detected its contribution to the induction of cell cycle arrest by flow cytometric analysis (31, 32). HepG2 cells were treated with various concentrations of casearlucin A and then were stained with PI for cell cycle analysis. With the concentrations of casearlucin A increasing from 2 μM to 8 μM, the percentage of cells in the G1 phase increased from 28.9% (control) to 34.7% (2 μM), 39.2% (4 μM), and 52.4% (8 μM), while the S and G2 phase decreased after treated with different concentrations (**Figure 3**). Collectively, these results implied that casearlucin A could induce G0/G1 cell cycle arrest in HepG2 cells.

Apoptosis Effects Induced by Casearlucin A

Then, the effects of casearlucin A on cell apoptosis were investigated in HepG2 cells. We analyzed the apoptosis by flow cytometry using Annexin V/PI double staining (33, 34). As shown in **Figure 4**, we found that the population of the early and late apoptotic cells increased dramatically. With the increase of concentrations of casearlucin A, the percentage of apoptotic cells rose from 8.0% (control) to 37.4% (5 μM), 67.2% (10 μM) and 79.3% (15 μM). The data indicated that the apoptosis of HepG2 cells induced by casearlucin A was dose-dependent. As a result, casearlucin A was proven to possess strong apoptotic induction abilities against HepG2 cells.

Moreover, since the Bcl-2 family proteins are the key regulators of mitochondrial membrane function, which have pivotal roles in the regulation of mitochondrial apoptosis. We examined the effects of casearlucin A on the expression of anti-apoptotic Bcl-2 protein, and pro-apoptotic Bax protein. As the results illustrated in **Figure 5**, casearlucin A treatment increased the protein levels of Bax, and decreased the protein levels of Bcl-2.

Casearlucin A Inhibited HepG2 Cell Metastasis *via* Regulating FAK/MMPs Signaling Pathway

In order to further reveal the mechanism of casearlucin A inhibiting cell metastasis, a few of metastasis-related proteins were detected after 36 h treatment (35, 36). Many studies have reported that matrix-metalloproteinases (MMPs) play key roles in tumor progression and metastasis, tumor cells usually have high expression levels of MMP. Our results revealed that the protein expression level of MMP-2 in HepG2 cells was obviously reduced in a dose-dependent manner after casearlucin A treatment (**Figure 6**). Then, the mechanism underlying casearlucin A-induced downregulation of MMP-2 expression in HepG2 cells was investigated, and accumulating evidence have demonstrated that the phosphorylation at Tyr 397 of FAK could promote the combination between FAK and PI3K, which in turn activated Akt, ultimately increased the MMPs. Thus, as shown in **Figure 6**, we further confirmed that the phosphorylation of FAK was decreased when HepG2 cells were treated with casearlucin A.

Toxicity Screening of Casearlucin A to Zebrafish Embryos

The zebrafish embryos were treated with casearlucin A (2.5 to 20 μM) for 48 h. As shown in **Figure 7**, the morphology of zebrafish was healthy without deformity, tail dysplasia, and yolk enlargement under the concentration of 2.5–20 μM. Hence,

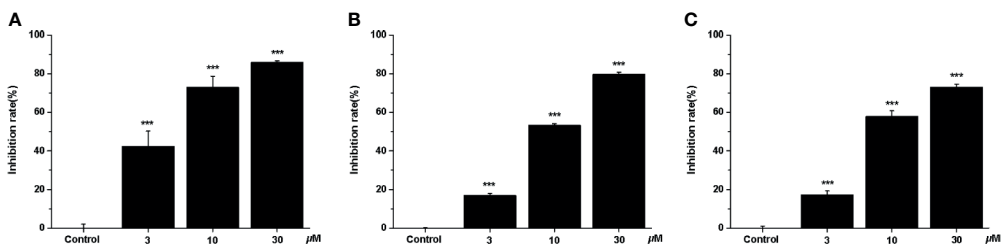

FIGURE 1 | Anti-proliferative effects of casearlucin A treatment on three cell lines. HepG2 **(A)**, A549 **(B)** and Hela **(C)** cells were treated with casearlucin A (3, 10, and 30 μM) for 48 h. Cell viability was examined using MTT assay. DMSO was used as a negative control. The results are presented as means ± SD. ***$p < 0.001$ *versus* control group.

TABLE 1 | Cytotoxicities of three compounds against three human cancer cell lines.

Compound	HepG2 (IC_{50}, μM)	A549 (IC_{50}, μM)	Hela (IC_{50}, μM)
Casearlucin A	3.8 ± 0.3	9.9 ± 0.1	10.5 ± 0.8
Casearlucin F	9.1 ± 0.9	17.1 ± 1.8	15.6 ± 1.1
Bucidarasin C	10.2 ± 1.0	16.6 ± 0.7	7.2 ± 0.2
Etoposide[a]	15.7 ± 1.6	42.7 ± 2.7	31.0 ± 0.7

[a]*Etoposide was used as a positive control. All results are expressed as mean ± SD.*

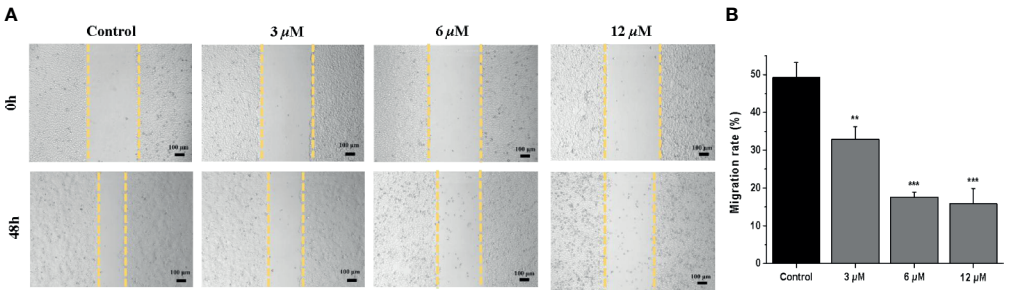

FIGURE 2 | Casearlucin A inhibited HepG2 cells in wounded healing assay. **(A)** HepG2 cells were photographed at 0 h and 48 h (scale bar: 100 μm). Data of Migration rate (%) were shown in **(B)**. DMSO was used as a negative control. The results are presented as means ± SD. $^{**}p < 0.01$, and $^{***}p < 0.001$ *versus* control group.

there was no toxicity to zebrafish after the treatment of casearlucin A (2.5–20 μM). Based on the results, the concentrations of 5, 10, 20 μM were selected for further *in vivo* research.

Antiangiogenetic Activity of Casearlucin A Using a Transgenic Zebrafish Model

In this study, the effects of casearlucin A on zebrafish intersegmental vessels formation were examined. Herein, we used the transgenic zebrafish embryos to directly visualize the effect of casearlucin A on the new vessel development (37, 38). As shown in **Figure 8**, in contrast with the blank control, the intersegmental vessels (ISVs) and dorsal longitudinal anastomotic vessels (DLAVs) were absent and broken after treatment with casearlucin A and the positive control, sunitinib malate. According to the satanical results, the average length of ISVs of the control group was 2654.9 μm, and the length decreased in a dose-dependent manner (2119.0 ± 137.7 μm at 5 μM, 1542.6 ± 126.4 μm at 10 μM, and 1232.0 ± 74.6 μm at 20 μM) with the increase of concentrations of casearlucin A.

In Vivo Anti-Tumor Activity of Casearlucin A Using a Zebrafish Model

Previous studies showed that casearlucin A exhibited cytotoxic activity to three human tumor cells *in vitro*, and markedly inhibited the migration of HepG2 cells. Thus, we examined whether the compound could block HepG2 cells proliferation in zebrafish xenograft tumor model (39, 40). HepG2 cells labeled with CM-DiI were microinjected into the yolk sac of 48 hpf embryos, and examined by fluorescence microscopy. As presented in **Figure 9**, treatment with casearlucin A significantly decreased cell proliferation and migration, and the compound showed inhibition effects in dose-dependent manners. The results showed that casearlucin A effectively blocked tumor cell invasion and metastasis, which was comparable to the positive control, etoposide.

CONCLUSION AND DISCUSSION

As numerous studies reported, because of its abnormal proliferation and high invasiveness, the treatment of cancer is very difficult. A key feature of tumor proliferation and metastasis processes is abnormal angiogenesis. Thus, the therapeutic agents targeting these characteristics will be more effective.

In our study, we have taken out a series of experiments to detect the effects of casearlucin A on cancer cell proliferation and migration *in vitro*. The results showed that casearlucin A exhibited the cytotoxicity against the selected cancer cell lines and possessed the most cytotoxic effects against HepG2 cells with an IC_{50} value of 3.8 μM. Meanwhile, the wound healing assay indicated that HepG2 cells showed a migration inhibition tendency after treated by casearlucin A. Furthermore, we used zebrafish as a powerful and reliable preclinical animal model to further study the inhibitory activity of casearlucin A on the proliferation and metastasis of HepG2 cells, which revealed the anti-tumor activity *in vivo* of casearlucin A. Taken together, the *in vitro* and *in vivo* promising results suggested that the mechanism of casearlucin A should be further assessed.

The subsequent preliminary mechanism investigation revealed that casearlucin A induced the apoptosis and arrested

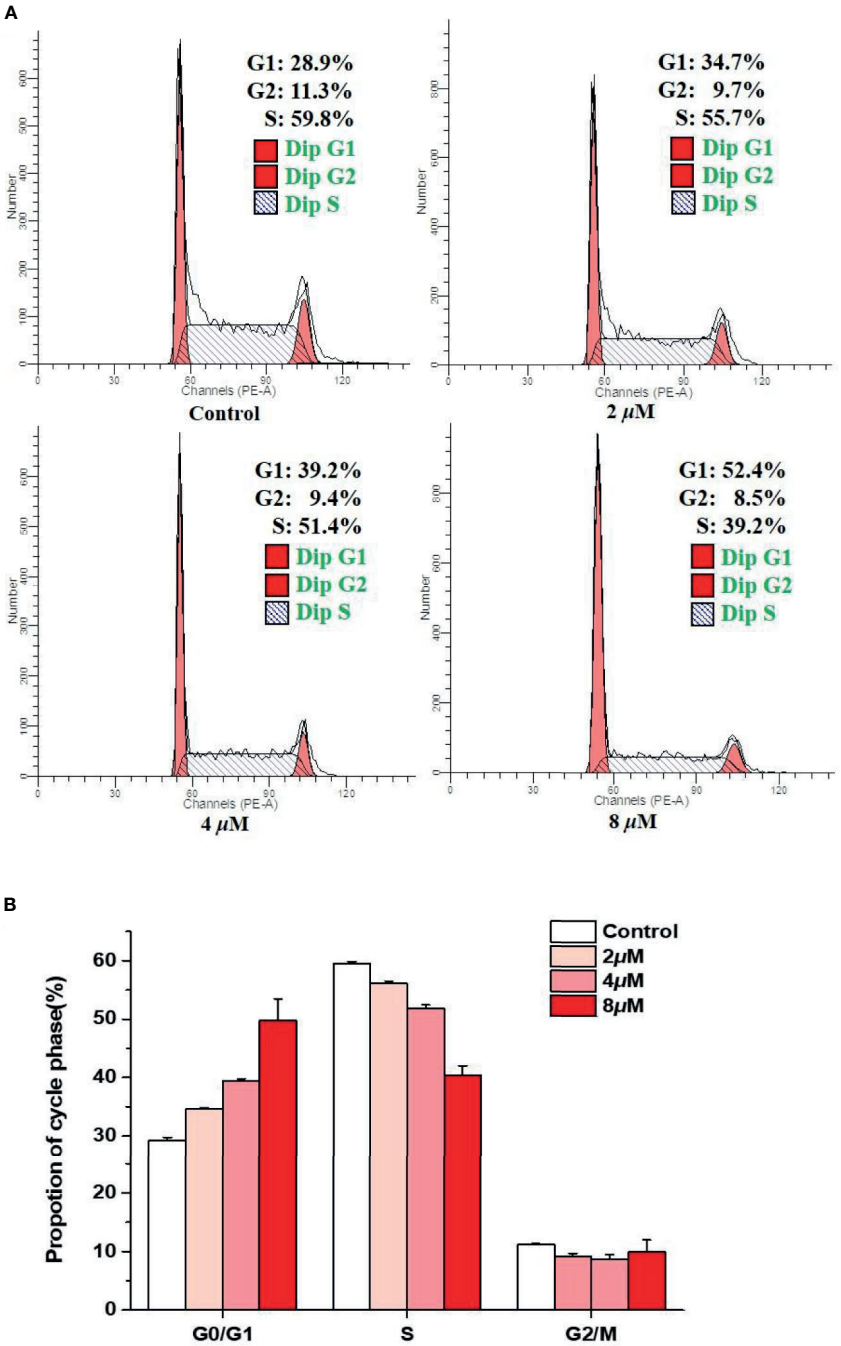

FIGURE 3 | Arrest effects of casearlucin A on HepG2 cell cycle. HepG2 cells were treated with different concentrations (2, 4, and 8 μM) of casearlucin A for 48 h. DMSO was used as a negative control. **(A)** The cells were harvested and stained with propidium iodide (PI), and the cell cycle distribution was analyzed using flow cytometry. **(B)** Data processing of cell cycle distribution. Data from three separate experiments are expressed as means ± SD.

the HepG2 cell cycle at the G0/G1 stage to exert cytotoxic effects. Moreover, we examined the expression levels of the representative proteins associated with cell apoptosis. It has been reported that the proteins of Bcl-2 family play a vital role in the mitochondria-mediated apoptosis pathway. In our study, the inhibition of Bcl-2 expression and the increase in Bax protein level by casearlucin A, demonstrated that the compound could promote apoptosis by targeting mitochondrial pathway.

In addition, FAK/MMPs signaling pathway had been proved to play critical roles in cancer cell migration and invasion. As we all know,, over-expressed FAK protein participates in the formation of focal adhesions and activates signaling pathways

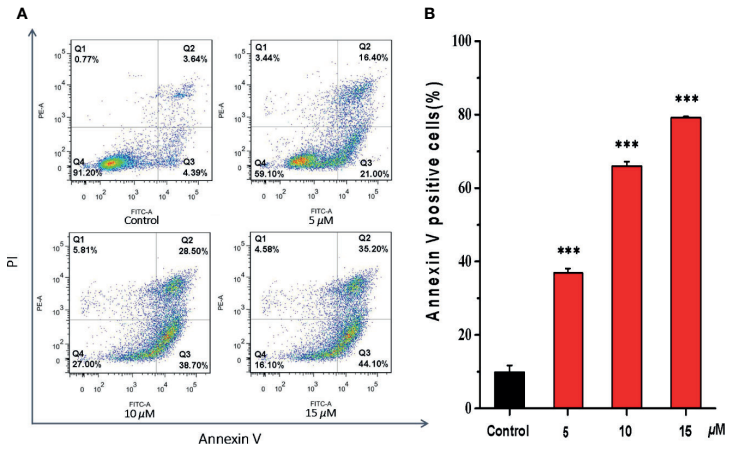

FIGURE 4 | Apoptosis effects of HepG2 cells induced by casearlucin A. HepG2 cells were treated with different concentrations (5, 10, and 15 μM) of casearlucin A for 48 h. DMSO was used as a negative control. Then, the cells were harvested, stained with Annexin V and propidium iodide (PI), and subsequently analyzed by flow cytometry. **(A)** Flow cytometric analysis of HepG2 cells after treated with different concentrations of casearlucin A. **(B)** Histogram of apoptotic cells at 48 h with the treatment of casearlucin A. Data from three separate experiments are expressed as means ± SD. ***$p < 0.001$ *versus* control group.

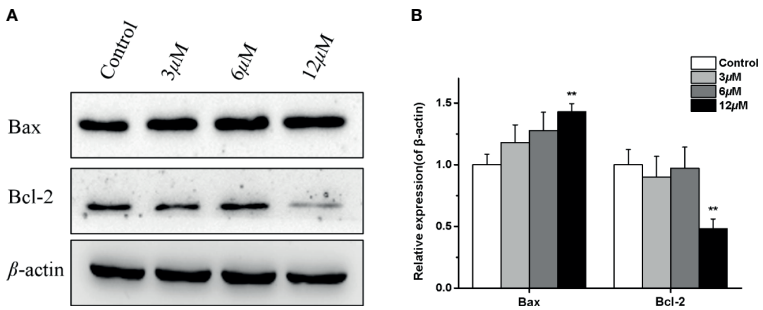

FIGURE 5 | Effects of casearlucin A on apoptosis related proteins expression in HepG2 cells. HepG2 cells were pre-treated with casearlucin A for 36 h, and western blotting analysis was performed. DMSO was used as a negative control. **(A)** Western blotting results of protein levels. **(B)** Quantitative analysis of apoptosis related proteins expression. β-Actin protein was used as internal reference. **$p < 0.01$ compared with control group cells. Data were obtained by at least three independent experiments.

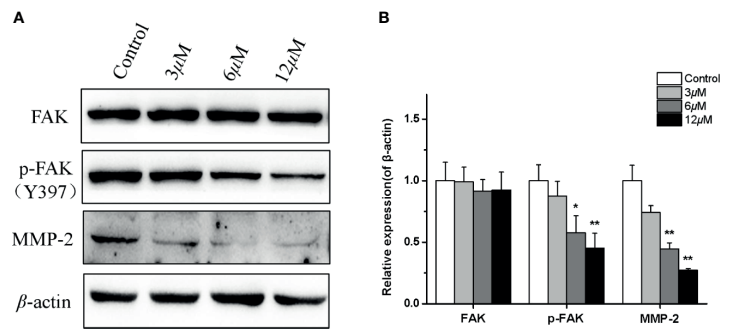

FIGURE 6 | Effects of casearlucin A on metastasis-related proteins expression in HepG2 cells. HepG2 cells were pre-treated with casearlucin A for 36 h, and western blotting analysis was performed. DMSO was used as a negative control. **(A)** Western blotting results of protein levels. **(B)** Quantitative analysis of metastasis-related proteins expression. β-Actin protein was used as an internal reference. *$p < 0.05$, and **$p < 0.01$ compared with control group cells. Data were obtained by at least three independent experiments.

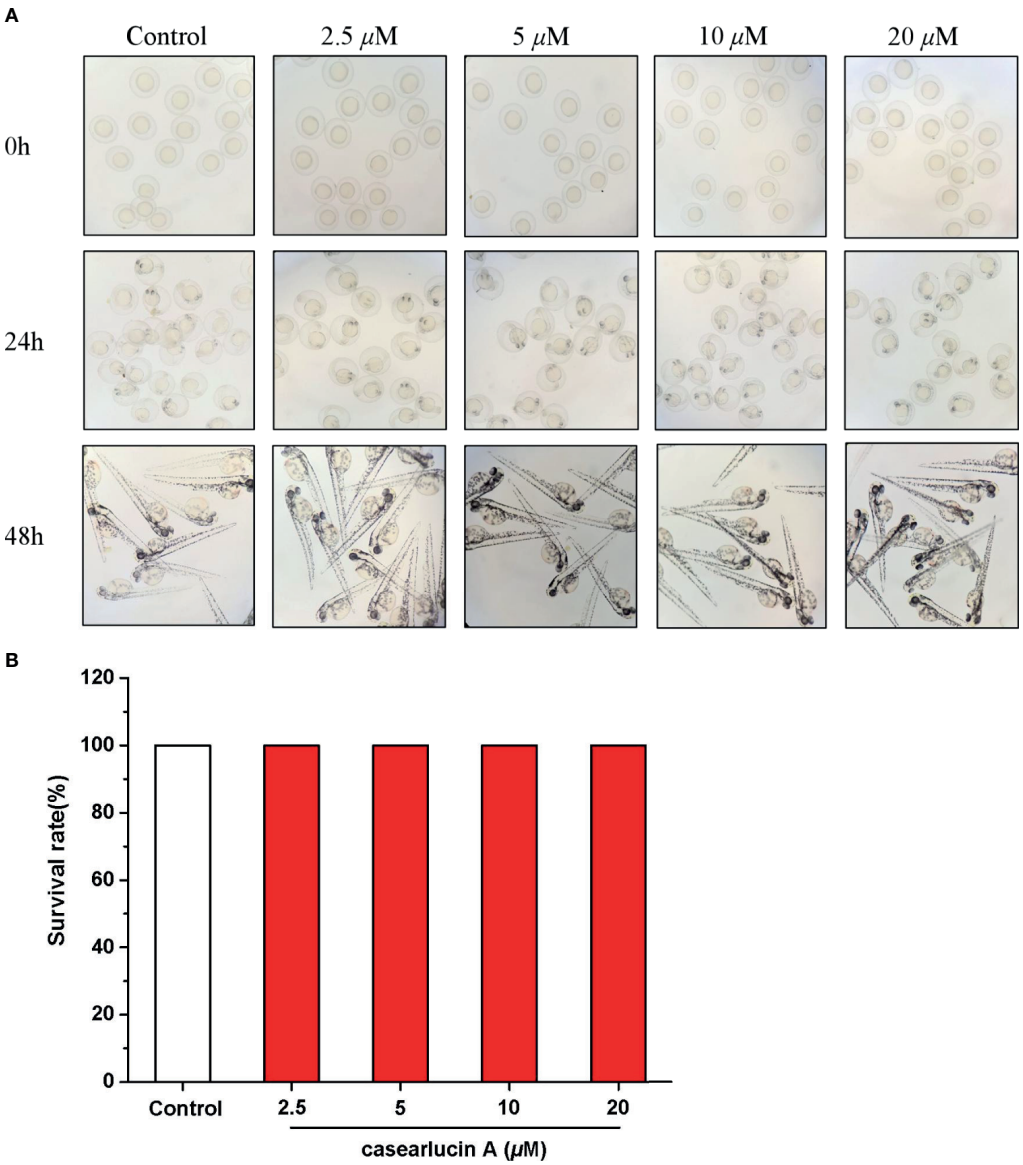

FIGURE 7 | Developmental toxicity of casearlucin A in Zebrafish Embryos. The zebrafish embryos were treated with casearlucin A (2.5, 5, 10, and 20 μM) for 48 h. **(A)** The morphology of zebrafish. **(B)** The survival rate of zebrafish. DMSO was used as a negative control.

related to proliferation, cell migration, and angiogenesis. Furthermore, many studies have reported that matrix-metalloproteinases (MMPs) are overexpressed in almost all cancer types of cancer, and play key roles in the cancer progression and aggression (41, 42). While, as a major kinase of focal adhesion, in this process, the phosphorylation at Tyr 397 of FAK could promote the combination between FAK and PI3K, ultimately increasing the MMPs (43). Our results revealed that casearlucin A treatment decreased the phosphorylation of FAK, and the protein expression level of MMP-2 was obviously reduced in a dose-dependent manner.

Moreover, the abnormal angiogenesis is a key feature of tumor proliferation and metastasis, and thus, angiogenesis is considered as an attractive target for cancer therapeutic strategy. In our study, we used the transgenic zebrafish embryos to directly demonstrate its anti-angiogenic *Tg (fli1: EGFP)* activity.

For a long time, the favorable efficacy and low side effect of phytochemicals promoted people to seek for anti-cancer drug candidates from natural source. In our study, casearlucin A had stronger cytotoxic activity than the positive control etoposide, and there was no toxicity to zebrafish embryo development under the concentration of 2.5–20 μM. With the in-depth research, the potential pharmacological effects and mechanism had been evaluated. In conclusion, casearlucin A may be a novel chemotherapeutic drug for cancer by inhibiting cell proliferation and migration and blocking angiogenesis.

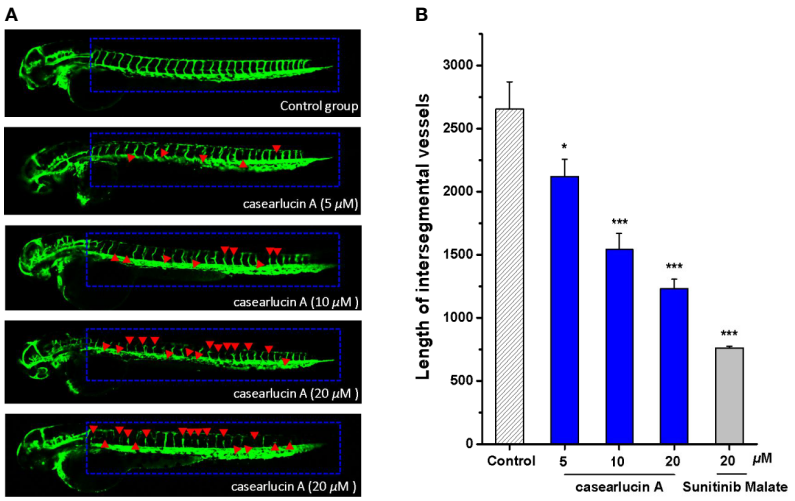

FIGURE 8 | Anti-angiogenesis activity of casearlucin A in transgenic zebrafish model. The embryos from transgenic zebrafish *Tg (fli1: EGFP)* were treated by the tested compound and the anti-angiogenetic compound, sunitinib malate (positive control). DMSO was used as a negative control. After exposure to the compounds for 48 h, the development of intersegmental vessels (ISVs) and dorsal longitudinal anastomotic vessels (DLAVs) were observed, and the length of ISV vessels was measured using ImageJ program. **(A)** Representative images of zebrafish embryos treated with vehicle, casearlucin A, and sunitinib malate. **(B)** The average length of ISVs of zebrafish after treated with different concentrations of casearlucin A (5, 10, and 20 μM). (n = 15 for each experimental group). $^{*}p < 0.5$, $^{***}p < 0.001$ *versus* control group.

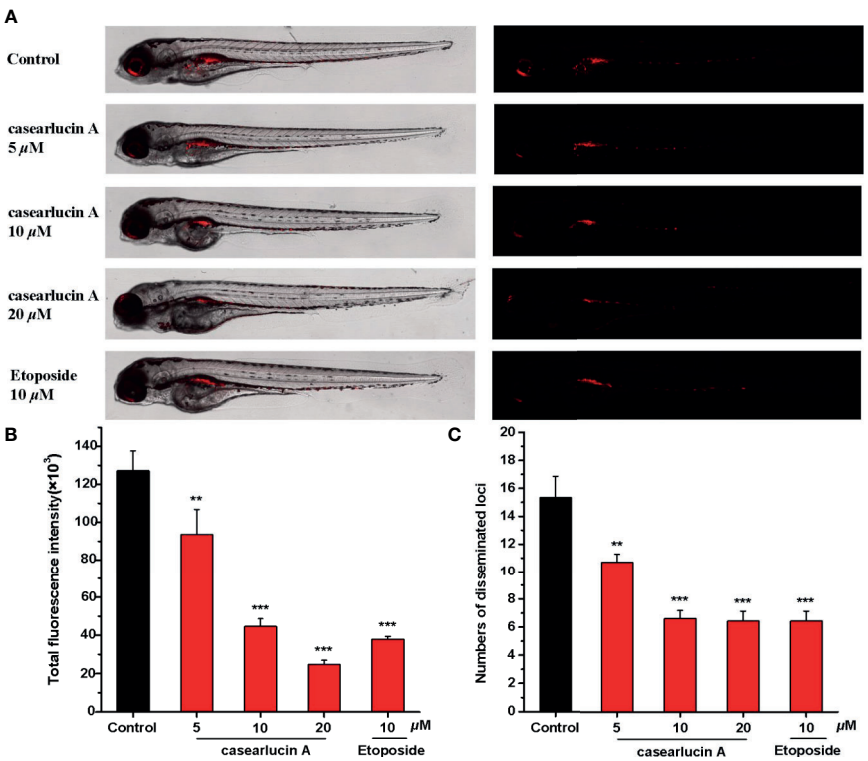

FIGURE 9 | *In vivo* anti-tumor effects of casearlucin A in zebrafish xenografts. CM-DiI stained HepG2 cells were transplanted into 2 dpf zebrafish embryos by microinjecting. 4 h later, tumor-bearing embryos were treated with casearlucin A (5, 10, and 20 μM) and etoposide (10 μM) for 48 h (n = 15/group). DMSO was used as a negative control. **(A)**Intensity and distribution of the red fluorescence were imaged under a confocal microscope. **(B)** Fluorescence intensity of the tumor xenografts, representing the number of HepG2 cells. **(C)** Quantification of the fluorescent area of the tumor xenografts, representing HepG2 cell metastasis. Results are expressed as means ± SD. $^{**}p < 0.01$ and $^{***}p < 0.001$ *versus* control group.

DATA AVAILABILITY STATEMENT

The original contributions presented in the study are included in the article/supplementary material. Further inquiries can be directed to the corresponding authors.

ETHICS STATEMENT

The animal study was reviewed and approved by Experimental animal ethics committee of Nankai University.

AUTHOR CONTRIBUTIONS

JX & YG: Designing the experiments and directing the study. YiL: Performing the experiments, analyzing the data, and writing the original draft preparation. JM: Performing the extraction, purification, and structure identification of casearlucin A. ZS, YZ, HZ & YeL: Reviewing and revising the manuscript. All authors contributed to the article and approved the submitted version.

FUNDING

This research was supported financially by the National Natural Science Foundation of China (Nos. 22077067 and U1801288), the Natural Science Foundation of Tianjin, China (No. 19JCYBJC28100), Hundred Young Academic Leaders Program of Nankai University, and the Fundamental Research Funds for the Central Universities, Nankai University (No. 63201236).

REFERENCES

1. Bray F, Ferlay J, Soerjomataram I, Siegel RL, Torre LA, Jemal A. Global Cancer Statistics 2018: GLOBOCAN Estimates of Incidence and Mortality Worldwide for 36 Cancers in 185 Countries. *CA: Cancer J Clin* (2018) 68:394–424. doi: 10.3322/caac.21492
2. Torre LA, Siegel RL, Ward EM, Jemal A. Global Cancer Incidence and Mortality Rates and Trends–An Update. *Cancer Epidem Biomar* (2016) 25:16–27. doi: 10.1158/1055-9965.EPI-15-0578
3. Lichota A, Gwozdzinski K. Anticancer Activity of Natural Compounds From Plant and Marine Environment. *Int J Mol Sci* (2018) 19:3533. doi: 10.3390/ijms19113533
4. Huang MY, Zhang LL, Ding J, Lu JJ. Anticancer Drug Discovery From Chinese Medicinal Herbs. *Chin Med UK* (2018) 13:35. doi: 10.1186/s13020-018-0192-y
5. Xia L, Guo Q, Tu PF, Chai XY. The Genus Casearia: A Phytochemical and Pharmacological Overview. *Phytochem Rev* (2015) 14:99–135. doi: 10.1007/s11101-014-9336-6
6. Ferreira PM, Militao GC, Lima DJ, Costa ND, Machado KC, Santos AG, et al. Morphological and Biochemical Alterations Activated by Antitumor Clerodane Diterpenes. *Chem Biol Interact* (2014) 222:112–25. doi: 10.1016/j.cbi.2014.10.015
7. Nguyen HT, Truong NB, Doan HT, Litaudon M, Retailleau P, Do TT, et al. Cytotoxic Clerodane Diterpenoids From the Leaves of Casearia Grewiifolia. *Pham J Nat Prod* (2015) 78:2726–30. doi: 10.1021/acs.jnatprod.5b00677
8. Vieira-Júnior GM, Dutra LA, Ferreira PM, de Moraes MO, Costa Lotufo LV, Pessoa Cdo O, et al. Cytotoxic Clerodane Diterpenes From Casearia Rupestris. *J Nat Prod* (2011) 74:776–81. doi: 10.1021/np100840w
9. Wang B, Wang XL, Wang SQ, Shen T, Liu YQ, Yuan HQ, et al. Cytotoxic Clerodane Diterpenoids From the Leaves and Twigs of Casearia Balansae. *J Nat Prod* (2013) 76:1573–9. doi: 10.1021/np400212d
10. Whitson EL, Thomas CL, Henrich CJ, Sayers TJ, Mcmahon JB, Mckee TC, et al. Clerodane Diterpenes From Casearia Arguta That Act As Synergistic TRAIL Sensitizers. *J Nat Prod* (2010) 73:2013–8. doi: 10.1021/np1004455
11. Xu J, Ji FF, Sun XC, Cao XR, Li S, Ohizumi Y, et al. Characterization and Biological Evaluation of Diterpenoids From Casearia Graveolens. *J Nat Prod* (2015) 78:2648–56. doi: 10.1021/acs.jnatprod.5b00583
12. Xu J, Kang J, Sun XC, Cao XR, Rena K, Lee D, et al. Di- and Triterpenoids From the Leaves of Casearia Balansae and Neurite Outgrowth Promoting Effects of PC12 Cells. *J Nat Prod* (2016) 79:170–9. doi: 10.1021/acs.jnatprod.5b00815
13. Xu JJ, Wu X, Li MM, Li GQ, Yang YT, Luo HJ, et al. Antiviral Activity of Polymethoxylated Flavones From "Guangchenpi", the Edible and Medicinal Pericarps of Citrus Reticulata 'Chachi'. *J Nat Prod* (2014) 77:2182–9. doi: 10.1021/jf404310y
14. Liu F, Ma J, Shi ZY, Zhang Q, Wang HM, Li DH, et al. Clerodane Diterpenoids Isolated From the Leaves of Casearia Graveolens. *J Nat Prod* (2020) 83:36–44. doi: 10.1021/acs.jnatprod.9b00515
15. Li DH, Li JY, Xue CM, Han T, Sai CM, Wang KB. Antiproliferative Dimeric Aporphinoid Alkaloids From the Roots of Thalictrum Cultratum. *J Nat Prod* (2017) 80:2893–904. doi: 10.1021/acs.jnatprod.7b00387
16. Fan ZJ, Xu Q, Wang CH, Lin XK, Zhang QB, Wu N. A Tropomyosin-Like Meretrix Meretrix Linnaeus Polypeptide Inhibits the Proliferation and Metastasis of Glioma Cells Via Microtubule Polymerization and FAK/Akt/MMPs Signaling. *Int J Biol Macromol* (2020) 145:154–64. doi: 10.1016/j.ijbiomac.2019.12.158
17. Guo LM, Cui J, Wang HR, Medina R, Zhang SL, Zhang XH, et al. Metformin Enhances Anti-Cancer Effect of Cisplatin in Meningioma Through AMPK-mTOR Signaling Pathways. *Mol Ther Oncolytics* (2021) 20:119–31. doi: 10.1016/j.omto.2020.11.004
18. Wei LY, Yang Y, Gupta P, Wang A, Zhao M, Zhao Y, et al. A Small Molecule Inhibitor, Ogp46, Is Effective Against Imatinib-Resistant Bcr-Abl Mutations *Via* the BCR-ABL/JAK-STAT Pathway. *Mol Ther Oncolytics* (2020) 18:137–48. doi: 10.1016/j.omto.2020.06.008
19. Wu Z, Li H, Wang YD, Yang DJ, Tan HJ, Zhan Y, et al. Optimization Extraction, Structural Features and Antitumor Activity of Polysaccharides From Z. Jujuba Cv. Ruoqiangzao Seeds. *Int J Biol Macromol* (2019) 135:1151–61. doi: 10.1016/j.ijbiomac.2019.06.020
20. Wang B, Ding YM, Fan P, Wang B, Xu JH, Wang WX. Expression and Significance of MMP2 and HIF-1alpha in Hepatocellular Carcinoma. *Oncol Lett* (2014) 8:539–46. doi: 10.3892/ol.2014.2189
21. Wang HL, Li YM, Shi G, Wang Y, Lin Y, Wang Q, et al. A Novel Antitumor Strategy: Simultaneously Inhibiting Angiogenesis and Complement by Targeting VEGFA/PIGF and C3b/C4b. *Mol Ther Oncolytics* (2020) 16:2029. doi: 10.1016/j.omto.2019.12.004
22. Hsu WJ, Lin MH, Kuo TC, Chou CM, Mi FL, Cheng CH, et al. Fucoidan From Laminaria Japonica Exerts Antitumor Effects on Angiogenesis and Micrometastasis in Triple-Negative Breast Cancer Cells. *Int J Biol Macromol* (2020) 149:600608. doi: 10.1016/j.ijbiomac.2020.01.256
23. Mazumder A, Lee JY, Talhi O, Cerella C, Chateauvieux S, Gaigneaux A, et al. Hydroxycoumarin OT-55 Kills CML Cells Alone or in Synergy With Imatinib or Synribo: Involvement of ER Stress and DAMP Release. *Cancer Lett* (2018) 438:197–218. doi: 10.1016/j.canlet.2018.07.041
24. Tseng CH, Chen YR, Tzeng CC, Liu W, Chou CK, Chiu CC, et al. Discovery of Indeno[1,2-B]Quinoxaline Derivatives as Potential Anticancer Agents. *Eur J Med Chem* (2016) 108:258–73. doi: 10.1016/j.ejmech.2015.11.031
25. Ma J, Cui Y, Cao T, Xu H, Shi Y, Xia J, et al. PDS5B Regulates Cell Proliferation and Motility *Via* Upregulation of Ptch2 in Pancreatic Cancer Cells. *Cancer Lett* (2019) 460:65–74. doi: 10.1016/j.canlet.2019.06.014
26. Yu JS, Lee D, Lee SR, Lee JW, Choi CI, Jang TS, et al. Chemical Characterization of Cytotoxic Indole Acetic Acid Derivative From Mulberry Fruit (Morus Alba L.) Against Human Cervical Cancer. *Bioorg Chem* (2018) 76:28–36. doi: 10.1016/j.bioorg.2017.10.015
27. Mirzaei H, Shokrzadeh M, Modanloo M, Ziar A, Riazi GH, Emami S. New Indole-Based Chalconoids as Tubulin-Targeting Antiproliferative Agents. *Bioorg Chem* (2017) 75:86–98. doi: 10.1016/j.bioorg.2017.09.005

28. Pertuit D, Larshini M, Brahim MA, Markouk M, Mitaine-Offer AC, Paululat T, et al. Triterpenoid Saponins From the Roots of Spergularia Marginata. *Phytochemistry* (2017) 139:81–7. doi: 10.1016/j.phytochem.2017.03.007
29. Liang CC, Park AY, Guan JL. In Vitro Scratch Assay: A Convenient and Inexpensive Method for Analysis of Cell Migration *In Vitro*. *Nat Protoc* (2007) 2:329–33. doi: 10.1038/nprot.2007.30
30. Lu WL, Yang T, Song QJ, Fang ZQ, Pan ZQ, Liang C, et al. Akebia Trifoliata (Thunb.) Koidz Seed Extract Inhibits Human Hepatocellular Carcinoma Cell Migration and Invasion *In Vitro*. *J Ethnopharmacol* (2018) 234:204–15. doi: 10.1016/j.jep.2018.11.044
31. Dong XD, Yu J, Feng YY, Ji HY, Yu SS, Liu AJ. Alcohol-soluble Polysaccharide From Castanea Mollissima Blume: Preparation, Characteristics and Antitumor Activity. *J Funct Foods* (2019) 63:103563. doi: 10.1016/j.jff.2019.103563
32. Hou Y, Pi C, Feng X, Wang Y, Fu S, Zhang X, et al. Antitumor Activity *In Vivo* and Vitro of New Chiral Derivatives of Baicalin and Induced Apoptosis *Via* the PI3K/Akt Signaling Pathway. *Mol Ther Oncolytics* (2020) 19:6778. doi: 10.1016/j.omto.2020.08.018
33. Hu X, Jiao RW, Li HN, Wang XH, Lyu HD, Gao X, et al. Antiproliferative Hydrogen Sulfide Releasing Evodiamine Derivatives and Their Apoptosis Inducing Properties. *Eur J Med Chem* (2018) 151:376–88. doi: 10.1016/j.ejmech.2018.04.009
34. Dong XD, Feng YY, Liu YN, Ji HY, Yu SS, Liu AJ, et al. A Novel Polysaccharide From Castanea Mollissima Blume: Preparation, Characteristics and Antitumor Activities *In Vitro* and *In Vivo*. *Carbohyd Polym* (2020) 240:116323. doi: 10.1016/j.carbpol.2020.116323
35. Shao M, Lou DD, Yang JB, Lin MT, Deng XH, Fan Q. Curcumin and Wikstroflavone B, a New Biflavonoid Isolated From Wikstroemia Indica, Synergistically Suppress the Proliferation and Metastasis of Nasopharyngeal Carcinoma Cells Via Blocking FAK/STAT3 Signaling Pathway. *Phytomedicine* (2020) 79:153341. doi: 10.1016/j.phymed.2020.153341
36. Zheng QQ, Diao S, Wang Q, Zhu C, Sun X, Yin B, et al. Il-17A Promotes Cell Migration and Invasion of Glioblastoma Cells *Via* Activation of PI3K/AKT Signalling Pathway. *J Cell Mol Med* (2019) 23:357–69. doi: 10.1111/jcmm.13938
37. Alqahtani AS, Nasr FA, Noman OM, Farooq M, Alhawassi T, Qamar W, et al. Cytotoxic Evaluation and Anti-Angiogenic Effects of Two Furano-Sesquiterpenoids From Commiphora Myrrh Resin. *Molecules* (2020) 25:1318. doi: 10.3390/molecules25061318
38. Petrović J, Glamočlija J, Ilić-Tomić T, Soković M, Robajac D, Nedić O, et al. Lectin From Laetiporus Sulphureus Effectively Inhibits Angiogenesis and Tumor Development in the Zebrafish Xenograft Models of Colorectal Carcinoma and Melanoma. *Int J Biol Macromol* (2020) 148:129–39. doi: 10.1016/j.ijbiomac.2020.01.033
39. Wu JQ, Fan RY, Zhang SR, Li CY, Shen LZ, Wei P, et al. A Systematical Comparison of Anti-Angiogenesis and Anti-Cancer Efficacy of Ramucirumab, Apatinib, Regorafenib and Cabozantinib in Zebrafish Model. *Life Sci* (2020) 247:117402. doi: 10.1016/j.lfs.2020.117402
40. Tu WM, Huang XC, Chen YL, Luo YL, Liau I, Hsu HY. Longitudinal and Quantitative Assessment Platform for Concurrent Analysis of Anti-Tumor Efficacy and Cardiotoxicity of Nano-Formulated Medication In Vivo. *Anal Chim Acta* (2020) 1095:129–37. doi: 10.1016/j.aca.2019.10.019
41. Lu PF, Weaver VM, Werb Z. The Extracellular Matrix: A Dynamic Niche in Cancer Progression. *J Cell Biol* (2012) 196:395–406. doi: 10.1083/jcb.201102147
42. Paw I, Carpenter RC, Watabe K, Debinski W, Lo HW. Mechanisms Regulating Glioma Invasion. *Cancer Lett* (2015) 362:1–7. doi: 10.1016/j.canlet.2015.03.015
43. Liu XJ, Wu X, Wang YM, Li YH, Chen XL, Yang WC, et al. CD47 Promotes Human Glioblastoma Invasion Through Activation of the PI3K/Akt Pathway. *Oncol Res* (2019) 27:415–22. doi: 10.3727/096504018x15155538502359

Conflict of Interest: The authors declare that the research was conducted in the absence of any commercial or financial relationships that could be construed as a potential conflict of interest.

frontiers in Oncology

ORIGINAL RESEARCH
published: 06 July 2021
doi: 10.3389/fonc.2021.651648

Cucurbitacin B Inhibits Cell Proliferation by Regulating X-Inactive Specific Transcript Expression in Tongue Cancer

Boqiang Tao[1,2,3†], Dongxu Wang[1,2†], Shuo Yang[2†], Yingkun Liu[1], Han Wu[1], Zhanjun Li[2], Lu Chang[1], Zhijing Yang[1] and Weiwei Liu[1]*

[1] Department of Oral and Maxillofacial Surgery, Hospital of Stomatology, Jilin University, Changchun, China, [2] Laboratory Animal Center, College of Animal Science, Jilin University, Changchun, China, [3] Jilin Provincial Key Laboratory of Oral Biomedical Engineering, Changchun, China

OPEN ACCESS

Edited by:
Peng Qu,
National Institutes of Health (NIH), United States

Reviewed by:
Xiaonan Zhang,
Bengbu Medical College, China
Guohao Wang,
National Institutes of Health (NIH), United States
Pentti Nieminen,
University of Oulu, Finland
Ibrahim O. Bello,
King Saud University, Saudi Arabia

***Correspondence:**
Weiwei Liu
liuweiw@jlu.edu.cn

[†]These authors have contributed equally to this work

Specialty section:
This article was submitted to Pharmacology of Anti-Cancer Drugs, a section of the journal Frontiers in Oncology

Received: 10 January 2021
Accepted: 18 June 2021
Published: 06 July 2021

Citation:
Tao B, Wang D, Yang S, Liu Y, Wu H, Li Z, Chang L, Yang Z and Liu W (2021) Cucurbitacin B Inhibits Cell Proliferation by Regulating X-Inactive Specific Transcript Expression in Tongue Cancer. Front. Oncol. 11:651648. doi: 10.3389/fonc.2021.651648

Cucurbitacin B (CuB), a natural product, has anti-tumor effects on various cancers. In order to investigate the expression of long non-coding RNAs (lncRNA), we carried out RNA sequencing (RNA-seq) and quantitative PCR (qPCR). The data indicated that CAL27 and SCC9 tongue squamous cell carcinoma (TSCC) cells had reduced expression of X-inactive specific transcript (XIST) after CuB treatment. Moreover, our results showed increased expression of *XIST* in human tongue cancer. In this study, CuB treatment inhibited proliferation, migration and invasion of SCC9 cells, and induced cellular apoptosis. Interestingly, knockdown of XIST led to inhibition of cell proliferation and induced apoptosis *in vitro*. In addition, reduced expression of *XIST* suppressed cell migration and invasion. MicroRNA 29b (miR-29b) was identified as a direct target of *XIST*. Previous reports indicated that miR-29b regulates p53 protein. Our results suggest that increased expression of miR-29b induces cell apoptosis through p53 protein. The clustered regularly interspaced short palindromic repeats (CRISPR)/CRISPR-associated protein 9 (CRISPR/Cas9) system validated the role of *XIST* knockout in tumor development *in vivo*. Together, these results suggest that CuB exerts significant anti-cancer activity by regulating expression of *XIST via* miR-29b.

Keywords: *XIST*, miRNA, cucurbitacin B, cell proliferation, tongue cancer

INTRODUCTION

Although significant advances have been made in the diagnosis and treatment of TSCC, a type of oral cancer, the 5-year overall survival remains low. The natural products, including traditional Chinese medicine, have been widely used to treat human cancer (1). Recently, CuB, which is derived primarily from *Trichosanthes cucumerina L.* fruits, has been shown to be effective across various cancers. There is evidence that the anti-cancer properties of CuB are through regulated cell death by altering cell cycle progression in osteosarcoma cells (2, 3). Moreover, CuB has the ability to induce cell apoptosis *via* the Janus kinase 2/signal transducer and activator of transcription 3 signaling pathway across human gastric carcinoma cells (4). In addition, CuB inhibits cell proliferation by

regulating focal adhesion kinase/p53 pathways in human cholangiocarcinoma cells (5). Previous reports indicated that CuB suppresses cell proliferation through lncRNAs and microRNAs (miRNAs) in pancreatic cancer cells (6). Results from these studies suggest that CuB plays an important role in cancer development.

A previous report suggested that numerous lncRNAs are aberrantly expressed in TSCC (7). *XIST*, a lncRNA, regulates X chromosome inactivation (XCI) (8), and plays a crucial role in the development of numerous cancers. The expression pattern of lncRNA *XIST* is associated with cellular apoptosis, proliferation, migration, and invasion in human colorectal cancer (CRC), as well as bladder cancer (9, 10). Compared to lncRNAs, miRNAs are small non-coding RNA molecules that are approximately 20 - 22 nucleotides in length. As a tumor suppressor, miR-29 inhibits cell growth and induces cell apoptosis (11). Moreover, miR-29 has a function in epithelial-mesenchymal transition (EMT) (12). There is evidence to indicate that the miR-29 family activates the p53 pathway in order to induce cell apoptosis in MCF-7 and HeLa cells (13). Indeed, lncRNAs work with miRNAs to participate in cancer development. However, the roles of *XIST* and miR-29b in TSCC have not yet been investigated.

Herein, we investigated *XIST* expression by RNA-seq in SCC9 cells after CuB treatment. Moreover, we examined the role of miR-29b as a potential target of *XIST*. In order to analyze the role of *XIST* and miR-29b in cell apoptosis, proliferation, migration and invasion, *XIST* and miR-29b were both overexpressed and knocked down. To validate the role of miR-29b in cell apoptosis, we investigated the expression of p53 protein. In addition, we evaluated the effects of CuB on tumor development in nude mice. Finally, we utilized the CRISPR/Cas9 system to knock out (KO) the *XIST* gene, and to evaluate its role in tumor development *in vivo* (14). Our findings have suggested that CuB exerts its anti-cancer effects by regulating *XIST* and miR-29b expression in TSCC.

MATERIALS AND METHODS

TSCC Samples

All TSCC samples were acquired from patients (N = 3) which underwent clinical surgery at the Hospital of Stomatology of Jilin University. The tumor samples were collected and stored in liquid nitrogen.

Cell Culture

CAL27 and SCC9 cells were cultured in Dulbecco's modified Eagle's medium (DMEM; Gibco, Gaithersburg, MD, USA), high glucose or DMEM/F12. The culture media was supplemented with 10% fetal bovine serum and 100 U/mL penicillin/streptomycin (Gibco). The cells were cultured in a 5% CO_2 incubator at 37°C.

RNA Isolation and RNA-Seq Analysis

In order to analyze the differential expression of lncRNAs after CuB treatment in SCC9 cells, we utilized RNA-seq. The SCC9 cells were grown to 70-90% confluency, and were seeded onto a 6-well plate and treated with CuB (Sigma, St. Louis, MO, USA) for 48 h. Next, total RNA was extracted from SCC9 cells through the use of a TRIzol reagent (Invitrogen, Carlsbad, CA, USA). Ribosomal RNA was removed and purified using the Ribo Zero Magnetic Gold Kit (Sangon Biotech, Shanghai, China). RNA-seq was performed using the Sequencing and Non-Coding RNA Program (Sangon Biotech, Shanghai, China). Next, the reads were aligned to the genome. Then, the reads were compared to known genes, and the raw counts were generated and calculated using various algorithms, including HISAT2, RSeQC, BEDTools and Qualimap.

Knockdown and Overexpression of *XIST* and miR-29b

For knockdown, the small interfering RNA (siRNA) target sequence of *XIST* (GCATGCATCTTGGACATTT) was purchased from RiboBio (Guangzhou, China), while pcDNA3.1-XIST was purchased from GenePharma (Shanghai, China) for overexpression. The miR-29b-3p-mimics and miR-29b-3p-inhibitor were purchased from RiboBio. The SCC9 cells were transiently transfected with pcDNA3.1-XIST, si-XIST, miR-29b-3p-inhibitor or miR-29b-3p-mimics for 48 h *in vitro*. A non-specific siRNA was transfected into control (Con) cells.

Construction of pcDNA3.1-XIST and XIST-KO Cells Lines by Stable Transfection

In order to construct the pcDNA3.1-XIST overexpression cell line, we utilized SCC9 cells. The SCC9 cells were cultured without FBS once cells reached a confluence of 80% for 12 – 16 h. Next, the pcDNA3.1-XIST (2 μg) and Lipofectamine 2000 (Invitrogen, USA) were utilized for transfection. After incubation for 48 h, G418 (400 mg/mL, Invitrogen, USA) was added into SCC9 cells. The clones were grown and picked after 14 days.

The CRISPR/Cas9 plasmid (px459; Addgene, Watertown, MA, USA) was utilized for gene editing of *XIST*. The design of a single guide RNA (sgRNA) has been previously described (14). The sgRNAs and primer sequences are listed in **Table S1**. Plasmid construction with sgRNA (XIST-KO) was validated *via* sequencing (Sangon, China). Transfection was conducted using XIST-KO (5 μg) and Lipofectamine 2000 (Invitrogen, USA) for 48 h. Next, puromycin was used to select the positive clones. After 14 days, the clones (XIST-KO) were grown and picked for subsequent western blot, qPCR and sequencing analysis.

Analysis of Gene Expression

Total RNA was isolated from CAL27 and SCC9 cells. Additionally, total RNA was extracted from human tumor and mouse tumor samples through the use of TRIzol reagents (Invitrogen, Carlsbad, CA, USA). Using the BioRT cDNA first-strand synthesis kit (Bioer Technology, Hangzhou, China), cDNA was generated as per the manufacturer's protocols. The qPCR was carried out to detect the expression of genes utilizing the BioEasy SYBR Green I Real-Time PCR Kit (Tiangen, Beijing, China). The qPCR reaction was carried out at 94°C for 3 min,

followed by 35 denaturation cycles at 94°C for 10 s, annealing at 59°C for 15 s, and extension at 72°C for 30 s. *GAPDH* was utilized as an internal reference. The $2^{-\Delta\Delta CT}$ method was used to assess relative gene expression. All experiments were conducted in triplicate.

Western Blot

The protein from TSCC cells was extracted utilizing the protein extraction buffer (Beyotime, China). In order to quantify the proteins from TSCC cells, we utilized the BCA protein assay kit (Tiangen, China). The proteins were then separated through the use of 10% SDS-PAGE gels. Next, these proteins were transferred onto the PVDF membranes. These membranes were then blocked (5% non-fat milk powder) and washed with TBST (0.1% Tween-20). The primary antibodies, including anti-p53 (Abcam, ab131442, USA), anti-E-cadherin (Proteintech, 20874-1-AP, USA) and anti-Gapdh (Bioworld, AP0066, USA), were incubated with the membrane overnight at 4°C. Subsequently, the membranes were incubated with HRP-conjugated affiniPure goat antibodies IgG (BOSTER, China) for 2 h. Finally, the proteins were identified using ECL Super Signal (Pierce; Thermo Fisher Scientific, USA).

The Colony Formation Assay

For the colony formation assay, the target cells (1×10^3) were seeded per well of a 60 mm plate. After 2 weeks, colonies were fixed with paraformaldehyde and stained with 0.1% (w/v) crystal violet. Photographs were acquired and the cell numbers were counted.

Cell Migration Analysis

Cell migration was measured through the use of a wound healing assay. In brief, 5×10^5 cells were seeded and cultured 48 h prior to transfection. A scraped line was created, and cells were cultured in a serum-free medium. The scratched area of cell migration was then visualized at 12, 24, and 48 h. Through the use of an inverted microscope and ImageJ software, the cell migration area was measured. All experiments were conducted in triplicate.

Cell Invasion Analysis

The cell invasion was analyzed through the use of a Transwell assay (15). In brief, SCC9 cells were treated with CuB or transfected with pcDNA3.1-XIST, si-XIST, miR-29b-3p-inhibitor or miR-29b-3p-mimics. Next, they were serum-starved for 24 h. Subsequently, cells (3×10^4) were added to the upper chamber of Transwell assay (Corning, New York, NY, USA), which contained 20 μL of Matrigel (BD Biosciences, Franklin Lakes, NJ, USA). This was then followed by the addition of 0.5 mL medium containing 10% FBS to the bottom chamber (Corning, New York, NY, USA). After incubation at 37°C for 24 h, cells on the bottom side were fixed in 4% paraformaldehyde and stained using a 0.1% crystal violet dye (Solarbio, Beijing, China). Using an inverted microscope and ImageJ software, the stained cells were counted. All experiments were conducted in triplicate.

Cell Counting Kit-8 Assay

Cell viability was determined through the use of a Cell Counting Kit-8 (CCK-8) assay (Dojindo, Kumamoto, Japan). In brief, cells (4×10^3) were seeded after they have undergone CuB treatment or were transfected with pcDNA3.1-XIST, si-XIST, miR-29b-3p-inhibitor, miR-29b-3p-mimics. Next, 10 μL of the CCK-8 solution was added to 96-well plates. The cells were then incubated at 37°C for 2.5 h. The absorbance (optical density) at 450 nm was utilized to measure cell viability. To analyze the CuB concentration in TSCC cells, half maximal inhibitory concentration (IC50) was performed using GraphPad Software (USA).

Cell Apoptosis Analysis

Cell apoptosis was assessed as previously described (16). In brief, SCC9 cells were treated with CuB or transfected with pcDNA3.1-XIST, si-XIST, miR-29b-3p-inhibitor or miR-29b-3p-mimics for 48 h. The cells were then washed twice with phosphate-buffered saline. Then, the cells (1×10^6 cells/mL) were harvested, and a mixture of Annexin V-FITC/PI reagent (Beyotime, China, Cat No. C1062L) was added to the cells and incubated for 30 min. Finally, cell fluorescence was analyzed through flow cytometry (BD Biosciences, USA).

Animals and Animal Care

Overall, 36 nude mice (half male half female, 8 weeks old) were utilized for this study. All mice were acquired from the Laboratory Animal Center of Jilin University. The mice were then grouped and housed in laboratory cages under specific pathogen-free conditions at a temperature of 24°C, with a relative humidity of 50 - 60%, and under a 12-h-light/12-h-dark schedule. Animals were then provided *ad libitum* access to standard rodent food and tap water. All mice were healthy and not infected during the experimental period. All surgical procedures were carried out under aseptic conditions. The SCC9 cell lines (8×10^6) were subcutaneously injected into the left flank of each mouse, and tumors were observed after seven or eight days. The mice were then used for CuB treatment when tumor volumes had reached 100 - 150 mm^3. The nude mice were treated with CuB (0.5 mg/kg, N = 6) each day for 14 days, while the Con group (N = 6) were treated with PBS. The pcDNA3.1-XIST and XIST-KO cells lines were acquired through a stable transfection. Then, the pcDNA3.1-Con, pcDNA3.1-XIST and XIST-KO cells lines (8×10^6) were inoculated into nude mice. Half of pcDNA3.1-XIST group (N = 6) was administered 0.5 mg/kg of CuB. The Con (N = 6), XIST-KO (N = 6) group and half of pcDNA3.1-XIST group (N = 6) received an equivalent volume of PBS. The tumor length (L) and width (W) were recorded and tumor volumes were calculated as $L \times W^2/2$.

Statistical Analysis

The unpaired Student's t-test was utilized to assess differences between the two groups (Con and experimental group) in CCK8 assay, cell apoptosis, migration, invasion, qPCR and tumor volumes. The measurement data were tested for normal distribution using the Kolmogorov Smirnov (K-S) test to compare cumulative distribution. Data conforming with the

normal distribution were summarized with mean values and standard deviations (SD). Statistical analysis was conducted using GraphPad Prism 5.0 (GraphPad Software, Inc). $P < 0.05$ was considered statistically significant.

RESULTS

Effects of CuB in Cell Apoptosis, Growth, Migration, and Invasion

In order to analyze the viability of SCC9 cells, the CCK-8 assay was conducted after CuB treatment. IC50 data indicated that 200 and 500 nM CuB had toxic effects on SCC9 cells (**Figure 1A**). Thus, 50 nM CuB was utilized for qPCR analysis. Moreover, compared to Con cells, CuB was able to induce apoptosis (**Figures 1B, C**), and inhibit cell migration (**Figures 1D, E**) and invasion (**Figures 1F, G**) in SCC9 cells. Overall, these results suggest that CuB exerts its anti-cancer effects by inhibiting the migratory and invasive potential of TSCC cells.

Expression Profile of lncRNAs

Next, we performed RNA-seq to determine the expression profile of lncRNAs in SCC9 cells. The results demonstrated that there were 90 upregulated and 87 downregulated lncRNAs in the CuB-treated group compared to the Con group (**Figure 2A**). Moreover, gene function classification indicated that the differentially expressed lncRNAs were more likely to be expressed during cell growth (**Figures 2B, C**). Specifically, we analyzed the role of five lncRNAs (*BBC3, STK11IP, XIST, FDFT1*, and *PRR14*), which are known to be related to cell growth and apoptosis in cancer development (**Figure S1**). The qPCR results demonstrated that *XIST* expression was reduced in both CAL27 and SCC9 cells after CuB treatment (**Figures 2D, E**). Hence, *XIST* was further analyzed in this study.

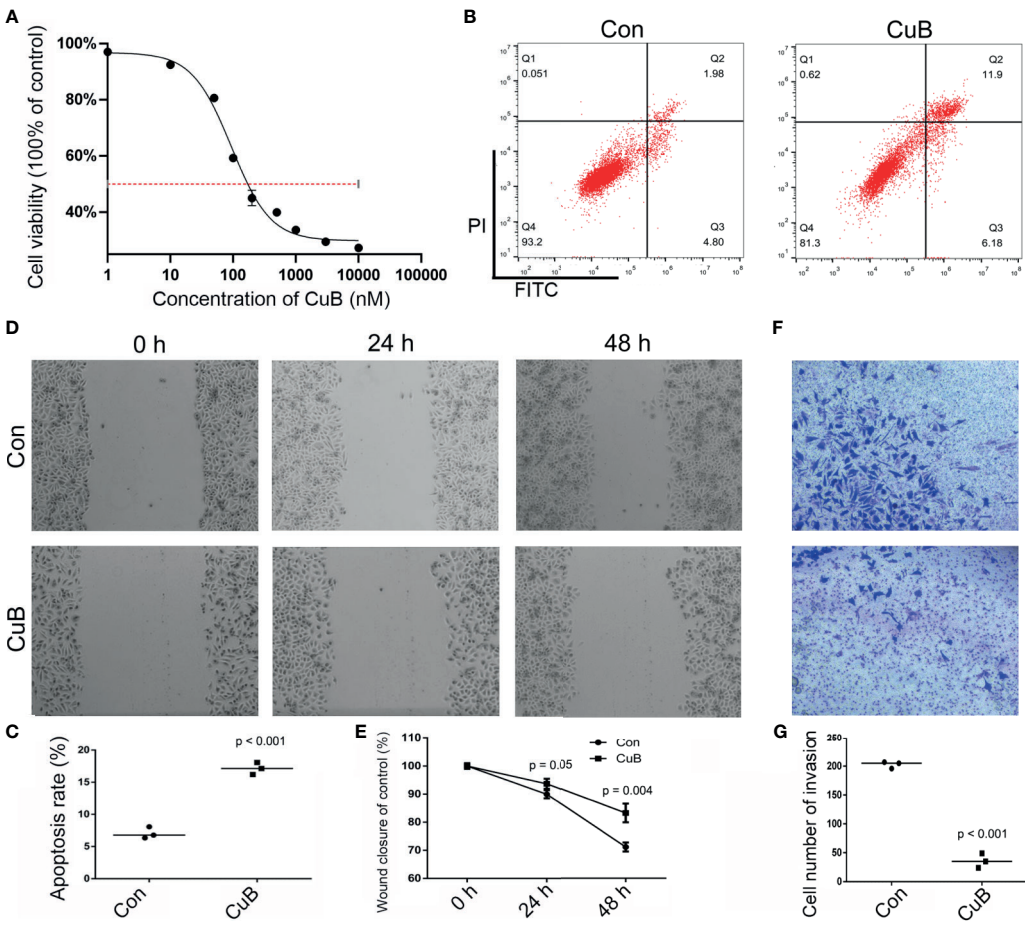

FIGURE 1 | Effects on cell growth, apoptosis, migration, and invasion after CuB treatment. **(A)** IC50 was assessed in SCC9 cells after CuB treatment to measure the proliferation of SCC9 using CCK8. **(B)** Cell apoptosis was analyzed in the Con and CuB groups (50 nM) in SCC9 cells to determine the effect of CuB on cell apoptosis. **(C)** Statistical analysis of the percentage of cell apoptosis among the two groups. **(D)** Analysis of cell migration in the Con and CuB groups in SCC9 cells to determine the effect of CuB on cell migration. **(E)** Statistical analysis of the percentage of cell migration between the Con and CuB groups. **(F)** Analysis of cell invasion in the SCC9 cells to determine the effect of CuB on cell invasion. **(G)** Statistical analysis of the percentage of cell invasion migration between the Con and CuB groups. Statistical significances between groups were evaluated using t-test for independent groups.

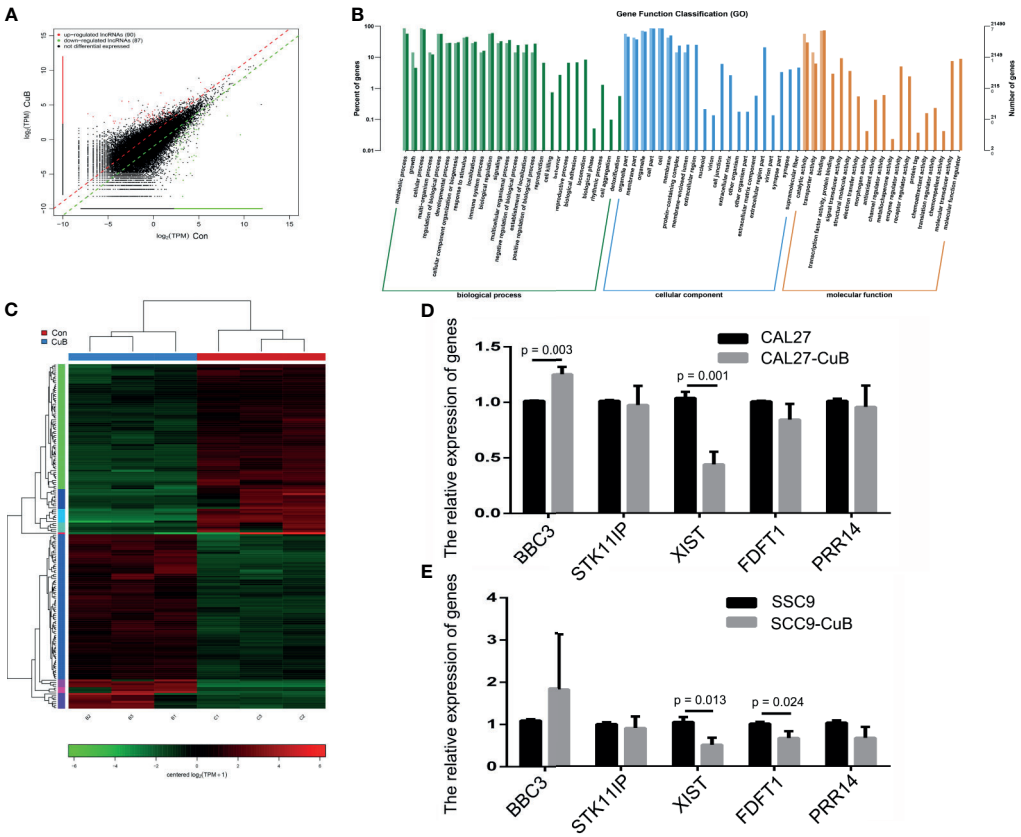

FIGURE 2 | LncRNA expression profile by RNA-seq. **(A)** Identification of differentially expressed lncRNAs in SCC9 cells. **(B)** KEGG pathways associated with the differentially expressed lncRNAs. **(C)** Heatmap depicts the differentially expressed lncRNAs. **(D)** Relative expression of *BBC3, STK11IP, XIST, FDFT1* and *PRR14* were analyzed *via* qPCR post-CuB treatment of CAL27 cells. **(E)** Relative expression of *BBC3, STK11IP, XIST, FDFT1* and *PRR14* were analyzed in SCC9 cells. Data are expressed as mean ± SD (n = 3). Statistical significances between groups were evaluated using t-test for independent groups.

CuB Reduced Expression of *XIST* in TSCC Cells

The Cancer Genome Atlas (TCGA) database showed that higher *XIST* expression is associated with a poorer prognosis for patients with head and neck squamous cell carcinoma (HNSCC) (**Figure S2**). The qPCR results revealed that *XIST* was significantly higher expressed in TSCC tissue compared to the paracancerous tissue (**Figure 3A**). Moreover, expression of *XIST* was reduced after CuB treatment (**Figure 3B**). Next, miR-29, which is located on exon 1 of *XIST*, was investigated as a potential target of *XIST* (**Figures 3C**, **S3**). The inhibited expression of miR-29 was observed in TSCC patients (**Figure 3D**). Additionally, CuB increased miR-29b expression in SCC9 cells (**Figure 3E**). These results indicate that CuB is able to regulate expression of *XIST* and miR-29b in TSCC cells.

Effects of *XIST* and miR-29b Expression on Cell Apoptosis, Growth, Migration, and Invasion

In order to further determine the effect of *XIST* on cell apoptosis, *XIST* was knocked down, as well as overexpressed, in SCC9 cells. As expected, the qPCR results demonstrated that *XIST* expression was inhibited in the si-XIST group, and overexpressed after the pcDNA3.1-XIST transfection (**Figures 4A, B**). The CCK-8 assay demonstrated that reduced expression of *XIST* led to an inhibition in the growth of SCC9 cells (**Figure 4C**) and induced apoptosis (**Figures 4D, E**). Next, we analyzed the effect of *XIST* expression on cell migration and invasion in SCC9 cells. The data indicated that overexpression of *XIST* is able to stimulate migration (**Figures 5A, B**) and invasion (**Figures 5C, D**), compared to the Con group. These results demonstrated that expression of *XIST* plays a role in cell growth, apoptosis, migration, and invasion. The role of miR-29b expression was also investigated in cell growth, apoptosis, migration, and invasion. The qPCR and CCK8 results revealed that increased expression of miR-29b led to inhibition of cell growth (**Figures 6A–C**) and induced cell apoptosis (**Figures 6D, E**). Considering that miR-29b positively regulates p53 protein, we investigated the expression of p53 (**Figure S4A**). Western blot and qPCR results validated that miR-29b mimics led to increased expression of p53 and E-cadherin (**Figure S4B, C**). In addition, increased expression of miR-29b led to inhibition of cell invasion (**Figures 7**, **S5**). In order to validate the role of miR-

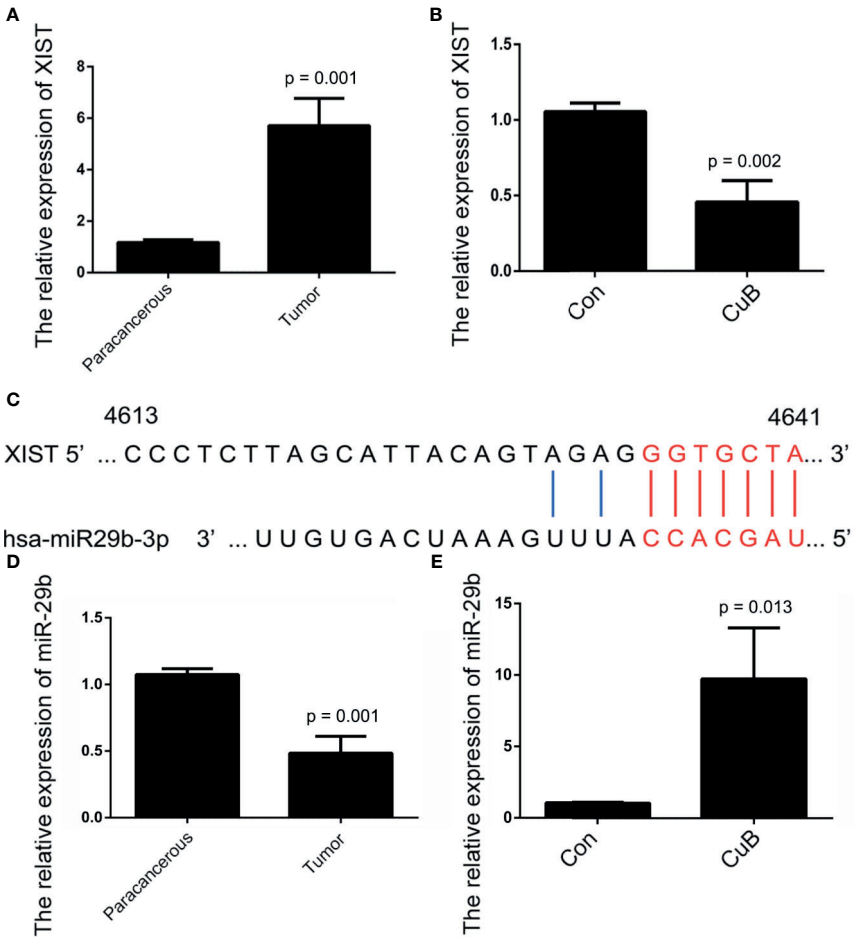

FIGURE 3 | Analysis of *XIST* and miR-29b expression after CuB treatment. **(A)** Relative expression of *XIST in* TSCC patients (N = 3) using qPCR. **(B)** The relative expression of *XIST*, analyzed by qPCR, after CuB treatment of SCC9 cells. **(C)** Schematic representations of the sequences of *XIST* and miR-29b. **(D)** Relative expression of miR-29b among TSCC patients (N = 3). **(E)** Relative expression of miR-29b, analyzed by qPCR, after CuB treatment of SCC9 cells. Data are expressed as mean ± SD (n = 3). Statistical significances between groups were evaluated using t-test for independent groups.

29b, a miR-29b inhibitor was transfected in the CuB group. The results demonstrated that miR-29b inhibitor promotes cell growth and inhibits apoptosis in SCC9 cells (**Figure S6**). Hence, our results validated that decreased expression of *XIST* induced apoptosis and suppressed cell growth through miR-29b in SCC9 cells.

Anti-Tumor Effects of CuB *In Vivo*

In order to analyze CuB-mediated regulation of *XIST* expression in nude mice, SCC9 cells were injected. Compared to the Con group, the nude mice were treated with CuB (0.5 mg/kg) after 11 days. Our results demonstrated that CuB treatment significantly suppressed tumor growth *in vivo* (**Figures 8A, B**). The qPCR results indicated that CuB suppressed expression of *XIST* (**Figure 8C**). In order to analyze the effect of reduced expression of *XIST* in SCC9 cells, we designed two sgRNAs of *XIST* exon 1 (**Figure 8D**). The results demonstrated that *XIST* expression was lost in XIST KO cells (**Figure 8E**). Sanger sequence data validated the effect of gene editing of *XIST* (**Figure S7**). In order to investigate the *XIST* expression profile, XIST KO cells were injected into nude mice. Our *in vivo* data suggested that compared to the Con group, suppressed tumor growth occurred in the XIST KO group. Additionally, treatment with CuB in the *XIST* overexpression group suppressed tumor growth (**Figures 8F, G**). These results suggest that CuB has a function in the biological processes of cancer cells by regulating *XIST* expression.

DISCUSSION

CuB is a tetracyclic triterpene compound found in the *Cucurbitaceae* family, and has anti-inflammatory and anti-tumor effects on cancers. Considering that CuB has potential

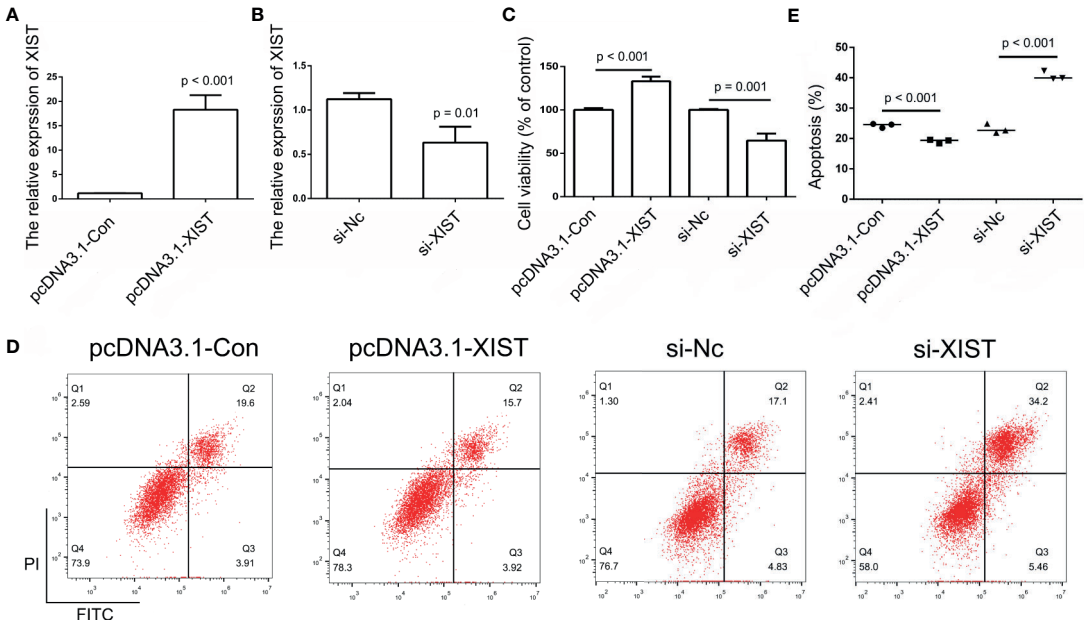

FIGURE 4 | Analysis of *XIST* expression. **(A, B)** Relative expression of *XIST* in pcDNA3.1-Con, pcDNA3.1-XIST, si-Nc, and si-XIST groups, respectively, using qPCR in SCC9 cells. Data are represented as mean ± SD (n = 3). **(C)** Cell growth was analyzed using the CCK-8 assay in SCC9 cells to determine the effect of XIST on cell proliferation. **(D)** Cell apoptosis was analyzed after transfection with pcDNA3.1-XIST and si-XIST in SCC9 cells to determine the effect of XIST on cell apoptosis. **(E)** Statistical analysis of the percentage of cells undergoing apoptosis in the four groups. Statistical significances between groups were evaluated using t-test for independent groups.

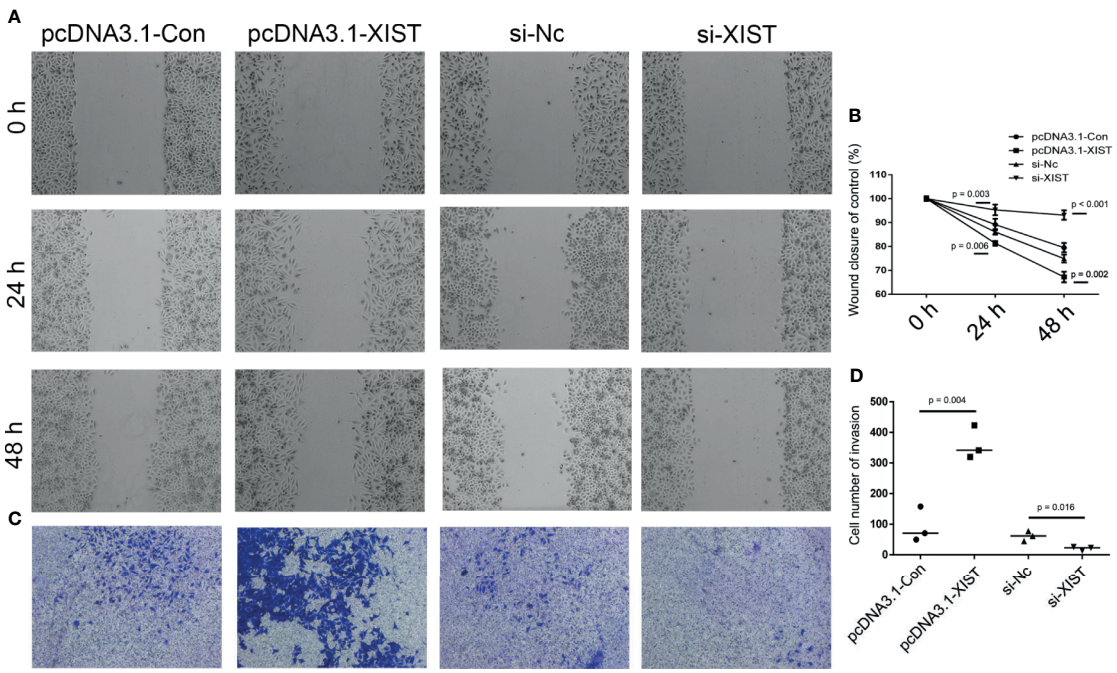

FIGURE 5 | Analysis of cell migration and invasion after *XIST* knockdown and overexpression. **(A)** Cell migration was assessed in the pcDNA3.1-Con, pcDNA3.1-XIST, si-Nc, and si-XIST groups in SCC9 cells to determine the effect of XIST on cell migration. **(B)** Statistical analysis of the percentage of cell migration among the four groups in 0 h, 24 h and 48 h. **(C)** Cell invasion was assessed in the pcDNA3.1-Con, pcDNA3.1-XIST, si-Nc, and si-XIST groups in SCC9 cells to determine the effect of XIST on cell invasion. **(D)** Statistical analysis of the percentage of cell invasion among the four groups. Statistical significances between groups were evaluated using t-test for independent groups.

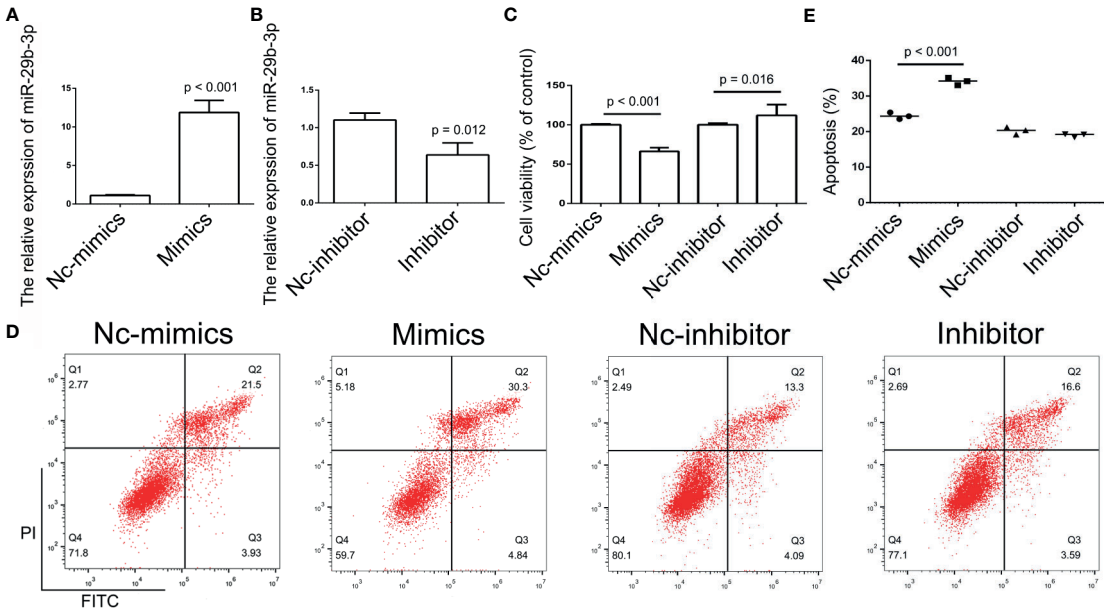

FIGURE 6 | Analysis of miR-29b-3p expression. **(A, B)** Relative expression of miR-29b in the Nc-mimics, miR-29b-3p-mimics, Nc-inhibitor, and miR-29b-3p-inhibitor groups, utilizing qPCR in SCC9 cells. Data are represented as mean ± SD (n = 3). **(C)** Cell growth was assessed by the CCK-8 assay in SCC9 cells to determine the effect of miR-29b-3p on cell proliferation. **(D)** Cell apoptosis was analyzed after transfection with miR-29b-3p-mimics and miR29b-3p-inhibitor in SCC9 cells to determine the effect of miR-29b-3p on cell apoptosis. **(E)** Statistical analysis of the percentage of cell apoptosis among the four groups. Statistical significances between groups were evaluated using t-test for independent groups.

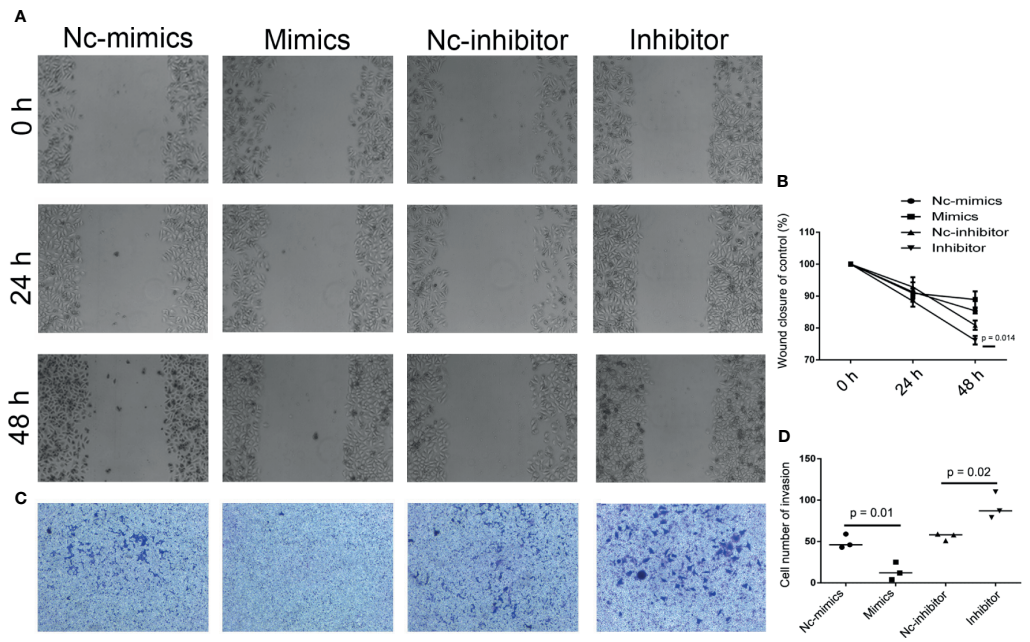

FIGURE 7 | Analysis of cell migration and invasion after miR-29b knockdown and overexpression. **(A)** To determine the effect of miR-29b-3p on cell migration, cell migration was analyzed in Nc-mimics, miR-29b-3p-mimics, Nc-inhibitor, and miR-29b-3p-inhibitor groups, respectively, in SCC9 cells. **(B)** Statistical analysis of the percentage of cell migration among the four groups. **(C)** To determine the effect of miR-29b-3p on cell invasion, Cell invasion was analyzed in Nc-mimics, miR-29b-3p-mimics, Nc-inhibitor, and miR-29b-3p-inhibitor groups, respectively, in SCC9 cells. **(D)** Statistical analysis of the percentage of cell invasion among the four groups. Statistical significances between groups were evaluated using t-test for independent groups.

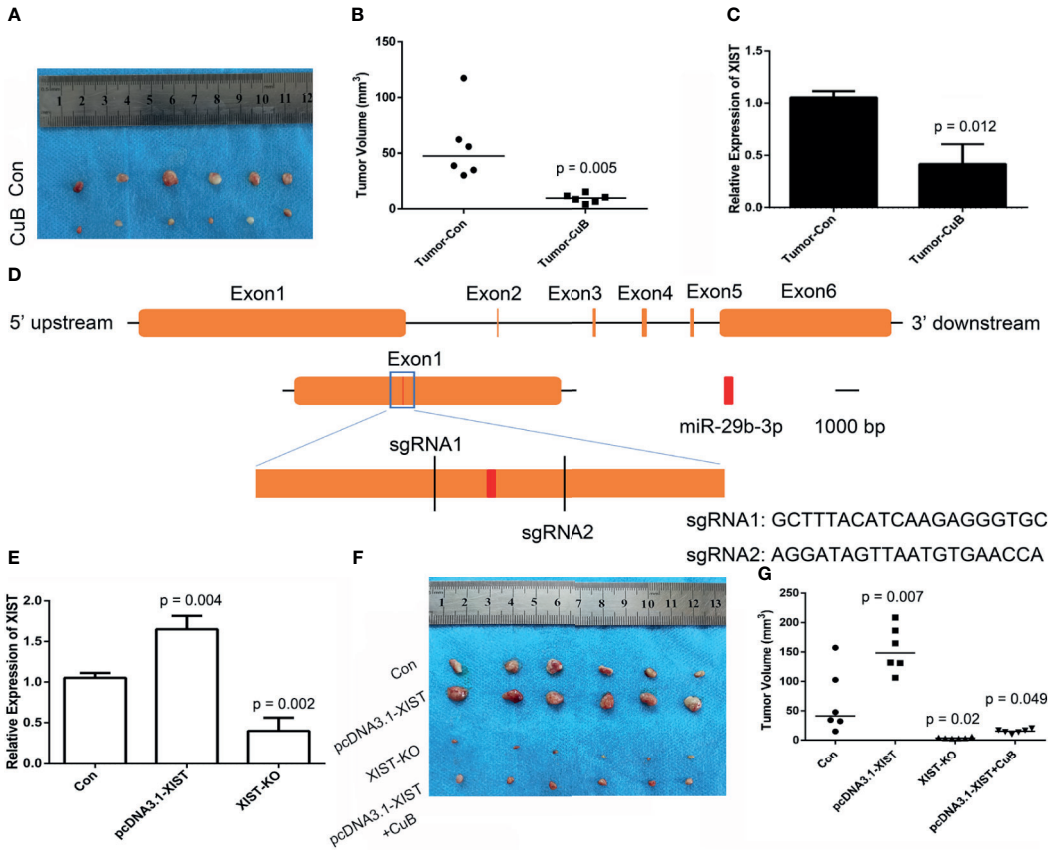

FIGURE 8 | CRISPR/Cas9-mediated gene targeting of *XIST*. **(A)** Morphological observation of the mouse TSCC tumor tissue (N = 6 in each group). **(B)** Analysis of tumor volume. **(C)** Expression pattern of *XIST in* mice tumors after CuB treatment. Data are represented as mean ± SD (n = 3). **(D)** Schematic diagram of sgRNAs targeting the *XIST* gene loci. **(E)** Expression of *XIST* using qPCR in SCC9 cells. Data are represented as mean ± SD (n = 3). **(F)** Tumor morphology and **(G)** volume (N = 6 in each group). Statistical significances between groups were evaluated using t-test for independent groups. Yellow indicates *XIST*, while red indicates exon of miR-29b-3p.

anti-cancer effects on breast cancer and CRC (17, 18), we analyzed cell invasion, migration, apoptosis and growth in TSCC cells that were treated with CuB. Our results demonstrated that CuB induced cell apoptosis and inhibited cell growth, migration and invasion in SCC9 cells. A previous study revealed that CuB inhibits cell growth by regulating expression of miR-146b-5p and the lncRNA *actin filament associated protein 1 antisense RNA1* in pancreatic cancer cells (6). In addition, CuB regulates the expression of the lncRNA *gastric cancer-associated transcript 3*, which induces apoptosis in gastric cancer cells (19). These results suggest that CuB may have a function in TSCC through a lncRNA-mediated mechanism.

Noncoding RNAs (ncRNAs) play significant roles in the development of various cancers. Specifically, lncRNAs are associated with being either tumor suppressors or oncogenes, and therefore, regulate the expression of genes and proteins in human cancer. In this study, RNA-seq revealed the presence of several differentially expressed lncRNAs that were associated with cell growth, apoptosis, migration and invasion after CuB treatment. Furthermore, the expression of *XIST* was found to be significantly reduced in both CAL27 and SCC9 cells. As an imprinted gene, *XIST* is crucial for embryo development and regulates XCI in mammals. However, *XIST* is abnormally expressed in various cancers, including hepatocellular carcinoma (HCC) (20). This indicates that the expression of *XIST* may be related to TSCC cancer development. A previous report demonstrated that reduced expression of *XIST* led to inhibition of tumor growth in thyroid cancer (21). Our results suggested that knockdown of *XIST* expression inhibited growth of SCC9 cells, which was validated from prior studies. Moreover, knockdown of *XIST* inhibited EMT in CRC (22). These data indicate that overexpression of *XIST* promotes cell migration and invasion. Furthermore, cellular apoptosis was induced by altered expression of *XIST* in HCC (23). The results of this study suggest that the expression of *XIST* has a function in cell apoptosis, growth, migration and invasion in TSCC.

Mounting evidence has revealed that miR-29b is a potential therapeutic candidate for CRC, HCC and lung cancer (24–26). In this study, bioinformatics analysis suggested that *XIST* has potentially competitive binding sites with miR-29b. Thus, miR-

29b may play a role in TSCC. A previous report indicated that overexpression of miR-29b led to a reduction in myeloid cell leukemia 1 expression and induced cell apoptosis in KMCH cholangiocarcinoma cells (27). Additionally, miR-29b was targeted to the folate receptor 1 (*FOLR1*) in order to inhibit cell growth in CRC (28). Interestingly, previous RNA-seq data demonstrated that *FOLR1*, which has high expression in ovarian cancer, is differentially expressed in TSCC (29, 30). Indeed, miR-29b activates p53 protein, which induces cell apoptosis (13). Our results demonstrate that *XIST* regulates miR-29b expression, which induces cell apoptosis through the p53 pathway in TSCC cells.

In order to confirm the effect of *XIST* on TSCC *in vivo*, a mouse tumor model in nude mice was established. The *in vivo* data demonstrates suppressed expression of *XIST* after CuB treatment, which was further validated by our data in SCC9 cells. Moreover, CuB inhibited tumor growth in mice, which is in accordance with previous data in breast cancer (31). These results suggest that CuB is able to regulate the expression of *XIST*, which inhibits tumor development. In order to further investigate the putative function of *XIST* and miR-29b in TSCC, we analyzed KO and overexpressed *XIST*. The CRISPR/Cas9 system is powerful for gene editing in HCC and GC cells (32, 33). Our study revealed that *XIST* KO *via* the CRISPR/Cas9 system is able to inhibit tumor growth. These results suggest that reduced the expression of *XIST* inhibits tumor growth.

In summary, we identified 177 differentially expressed lncRNAs in TSCC cells after CuB treatment. These results suggested that expression of *XIST* is regulated by CuB in TSCC. Furthermore, knockdown of *XIST* and overexpression of miR-29b led to an inhibition of cell growth and invasion, and induced apoptosis. Collectively, our results indicate that CuB plays a role in TSCC by regulating expression of *XIST* and miR-29b, which regulates the p53 protein.

DATA AVAILABILITY STATEMENT

The datasets presented in this study can be found in online repositories. The names of the repository/repositories and accession number(s) can be found in the article/ **Supplementary Material**.

ETHICS STATEMENT

The studies involving human participants were reviewed and approved by Ethics Committee of the Hospital of Stomatology, Jilin University. The patients/participants provided their written informed consent to participate in this study. The animal study was reviewed and approved by Laboratory Animal Center of Jilin University. Written informed consent was obtained from the individual(s) for the publication of any potentially identifiable images or data included in this article.

AUTHOR CONTRIBUTIONS

DW and WL designed the experiments and wrote the manuscript. BT, SY, LC, ZY, and YL performed cell experiment and gene expression analysis. WL contributed reagents and materials. BT and HW carried out animal experiment. DW analyzed the data and prepared figures. All authors contributed to the article and approved the submitted version.

FUNDING

Fundamental Research Funds for the Central Universities (no. 2019JCKT-70, 2020JCXK-45); Jilin Province Development and Reform Commission (no. 2019C051-5); Department of Finance of Jilin Province (no. JCSZ2019378-8); Jilin Scientific and Technological Development Program (no. 20190103071JH); Education Department of Jilin Province (no. JJKH20200950KJ).

SUPPLEMENTARY MATERIAL

The Supplementary Material for this article can be found online at: https://www.frontiersin.org/articles/10.3389/fonc.2021.651648/full#supplementary-material

Supplementary Figure 1 | Screen of cell growth related genes by RNA-seq. **(A)** LncRNAs were identified utilizing the CPC2, CNCI, Pfam and PLEK software. **(B)** LncRNAs on each chromosome. **(C)** The log2 fold change of lncRNAs.

Supplementary Figure 2 | Analysis of *XIST* and miR-29b in TCGA data base. **(A)** The effect of *XIST* expression on survival of HNSCC patients, as per analysis of the TCGA data. **(B)** Effect of miR-29 expression on HNSCC patient survival, according to analysis of TCGA data.

Supplementary Figure 3 | Screen of miRNA which was regulted by *XIST*.

Supplementary Figure 4 | Analysis the expression pattern of p53 and E-cadherin in SCC9 cells. **(A)** Schematic diagram of XIST and miR-29b regulated p53 expression. **(B)** The expression of p53 and E-cadherin using Western blot. (C) The relative expression of TP53 and CDH1 using qPCR. Data are represented as mean ± SD (n = 3). Statistical significances between groups were evaluated using t-test for independent groups.

Supplementary Figure 5 | Analysis of cell invasion by colony formation assay. **(A, B)** Cell invasion was analyzed using colony formation assay after CuB treatment in SCC9 cells **(C, D)** Cell invasion was analyzed after transfection with pcDNA3.1-XIST and si-XIST in SCC9 cells. **(E, F)** Cell invasion was analyzed after transfection with miR-29b-3p-mimics and miR29b-3p-inhibitor in SCC9 cells. Statistical significances between groups were evaluated using t-test for independent groups.

Supplementary Figure 6 | Analysis of cell growth and apoptosis after transfection of miR-29b inhibitor in CuB-treated cells. **(A)** Cell growth was analyzed using the CCK-8 assay after transfection with the miR-29b-3p-inhibitor in CuB-treated (50 nM) SCC9 cells. **(B)** Cell apoptosis was assessed after miR-29b-3p-inhibitor transfection in CuB-treated (50 nM) SCC9 cells. **(C)** Statistical analysis of the percentage of cell apoptosis among the two groups. Statistical significances between groups were evaluated using t-test for independent groups.

Supplementary Figure 7 | Analysis of XIST-KO by Sanger sequencing of SCC9 cells.

REFERENCES

1. Xiang Y, Guo Z, Zhu P, Chen J, Huang Y. Traditional Chinese Medicine as a Cancer Treatment: Modern Perspectives of Ancient But Advanced Science. *Cancer Med* (2019) 8(5):1958–75. doi: 10.1002/cam4.2108
2. Garg S, Kaul S C, Wadhwa R. Cucurbitacin B and Cancer Intervention: Chemistry, Biology and Mechanisms (Review). *Int J Oncol* (2018) 52(1):19–37. doi: 10.3892/ijo.2017.4203
3. Zhang Z-R, Gao M-X, Yang K. Cucurbitacin B Inhibits Cell Proliferation and Induces Apoptosis in Human Osteosarcoma Cells *via* Modulation of the JAK2/STAT3 and MAPK Pathways. *Exp Ther Med* (2017) 14(1):805–12. doi: 10.3892/etm.2017.4547
4. Xie Y-L, Tao W-H, Yang T-X, Qiao J-G. Anticancer Effect of Cucurbitacin B on MKN-45 Cells *via* Inhibition of the JAK2/STAT3 Signaling Pathway. *Exp Ther Med* (2016) 12(4):2709–15. doi: 10.3892/etm.2016.3670
5. Klungsaeng S, Kukongviriyapan V, Prawan A, Kongpetch S, Senggunprai L. Targeted Modulation of FAK/PI3K/PDK1/AKT and FAK/p53 Pathways by Cucurbitacin B for the Antiproliferation Effect Against Human Cholangiocarcinoma Cells. *Am J Chin Med* (2020) 48(6):1475–89. doi: 10.1142/S0192415X2050072X
6. Zhou J, Liu M, Chen Y, Xu S, Guo Y, Zhao L. Cucurbitacin B Suppresses Proliferation of Pancreatic Cancer Cells by ceRNA: Effect of miR-146b-5p and lncRNA-AFAP1-As1. *J Cell Physiol* (2019) 234(4):4655–67. doi: 10.1002/jcp.27264
7. Zhang S, Ma H, Zhang D, Xie S, Wang W, Li Q, et al. LncRNA KCNQ1OT1 Regulates Proliferation and Cisplatin Resistance in Tongue Cancer *via* miR-211-5p Mediated Ezrin/Fak/Src Signaling. *Cell Death Dis* (2018) 9(7):742. doi: 10.1038/s41419-018-0793-5
8. Loda A, Heard E. Xist RNA in Action: Past, Present, and Future. *PloS Genet* (2019) 15(9):e1008333. doi: 10.1371/journal.pgen.1008333
9. Hu B, Shi G, Li Q, Li W, Zhou H. Long Noncoding RNA XIST Participates in Bladder Cancer by Downregulating P53 *via* Binding to TET1. *J Cell Biochem* (2019) 120(4):6330–8. doi: 10.1002/jcb.27920
10. Yang X, Zhang S, He C, Xue P, Zhang L, He Z, et al. METTL14 Suppresses Proliferation and Metastasis of Colorectal Cancer by Down-Regulating Oncogenic Long non-Coding RNA XIST. *Mol Cancer* (2020) 19(1):46. doi: 10.1186/s12943-020-1146-4
11. Wang Y, Zhang X, Li H, Yu J, Ren X. The Role of miRNA-29 Family in Cancer. *Eur J Cell Biol* (2013) 92(3):123–8. doi: 10.1016/j.ejcb.2012.11.004
12. Cicchini C, de Nonno V, Battistelli C, Cozzolino AM, De Santis Puzzonia M, Ciafrè SA, et al. Epigenetic Control of EMT/MET Dynamics: HNF4α Impacts DNMT3s Through miRs-29. *Biochim Biophys Acta* (2015) 1849(8):919–29. doi: 10.1016/j.bbagrm.2015.05.005
13. Park S-Y, Lee JH, Ha M, Nam J-W, Kim VN. miR-29 miRNAs Activate P53 by Targeting P85 Alpha and CDC42. *Nat Struct Mol Biol* (2009) 16(1):23–9. doi: 10.1038/nsmb.1533
14. Cong L, Ran FA, Cox D, Lin S, Barretto R, Habib N, et al. Multiplex Genome Engineering Using CRISPR/Cas Systems. *Science* (2013) 339(6121):819–23. doi: 10.1126/science.1231143
15. Valster A, Tran NL, Nakada M, Berens ME, Chan AY, Symons M. Cell Migration and Invasion Assays. *Methods* (2005) 37(2):208–15. doi: 10.1016/j.ymeth.2005.08.001
16. William-Faltaos S, Rouillard D, Lechat P, Bastian G. Cell Cycle Arrest and Apoptosis Induced by Oxaliplatin (L-OHP) on Four Human Cancer Cell Lines. *Anticancer Res* (2006) 26(3A):2093–9.
17. Dandawate P, Subramaniam D, Panovich P, Standing D, Krishnamachary B, Kaushik G, et al. Cucurbitacin B and I Inhibits Colon Cancer Growth by Targeting the Notch Signaling Pathway. *Sci Rep* (2020) 10(1):1290. doi: 10.1038/s41598-020-57940-9
18. Liang J, Zhang X-L, Yuan J-W, Zhang H-R, Liu D, Hao J, et al. Cucurbitacin B Inhibits the Migration and Invasion of Breast Cancer Cells by Altering the Biomechanical Properties of Cells. *Phytother Res* (2019) 33(3):618–30. doi: 10.1002/ptr.6250
19. Lin Y, Li J, Ye S, Chen J, Zhang Y, Wang L, et al. LncRNA GACAT3 Acts as a Competing Endogenous RNA of HMGA1 and Alleviates Cucurbitacin B-Induced Apoptosis of Gastric Cancer Cells. *Gene* (2018) 678:164–71. doi: 10.1016/j.gene.2018.08.037
20. Dong Z, Yang J, Zheng F, Zhang Y. The Expression of lncRNA XIST in Hepatocellular Carcinoma Cells and Its Effect on Biological Function. *J BUON* (2020) 25(5):2430–7.
21. Liu H, Deng H, Zhao Y, Li C, Liang Y. LncRNA XIST/miR-34a Axis Modulates the Cell Proliferation and Tumor Growth of Thyroid Cancer Through MET-PI3K-AKT Signaling. *J Exp Clin Cancer Res* (2018) 37(1):279. doi: 10.1186/s13046-018-0950-9
22. Chen D-L, Chen L-Z, Lu Y-X, Zhang D-S, Zeng Z-L, Pan Z-Z, et al. Long Noncoding RNA XIST Expedites Metastasis and Modulates Epithelial-Mesenchymal Transition in Colorectal Cancer. *Cell Death Dis* (2017) 8(8):e3011. doi: 10.1038/cddis.2017.421
23. Mo Y, Lu Y, Wang P, Huang S, He L, Li D, et al. Long Non-Coding RNA XIST Promotes Cell Growth by Regulating miR-139-5p/PDK1/AKT Axis in Hepatocellular Carcinoma. *Tumour Biol* (2017) 39(2):1010428317690999. doi: 10.1177/1010428317690999
24. Avasarala S, Van Scoyk M, Wang J, Sechler M, Vandervest K, Brzezinski C, et al. Hsa-Mir29b, a Critical Downstream Target of Non-Canonical Wnt Signaling, Plays an Anti-Proliferative Role in Non-Small Cell Lung Cancer Cells *via* Targeting MDM2 Expression. *Biol Open* (2013) 2(7):675–85. doi: 10.1242/bio.20134507
25. Ding D, Li C, Zhao T, Li D, Yang L, Zhang B. LncRNA H19/miR-29b-3p/PGRN Axis Promoted Epithelial-Mesenchymal Transition of Colorectal Cancer Cells by Acting on Wnt Signaling. *Mol Cells* (2018) 41(5):423–35. doi: 10.14348/molcells.2018.2258
26. Yang J, Gong X, Yang J, Ouyang L, Xiao R, You X, et al. Suppressive Role of microRNA-29 in Hepatocellular Carcinoma *via* Targeting IGF2BP1. *Int J Clin Exp Pathol* (2018) 11(3):1175–85.
27. Mott JL, Kobayashi S, Bronk SF, Gores GJ. Mir-29 Regulates Mcl-1 Protein Expression and Apoptosis. *Oncogene* (2007) 26(42):6133–40. doi: 10.1038/sj.onc.1210436
28. Fu Q, Zhang J, Huang G, Zhang Y, Zhao M, Zhang Y, et al. microRNA-29b Inhibits Cell Growth and Promotes Sensitivity to Oxaliplatin in Colon Cancer by Targeting FOLR1. *Biofactors* (2020) 46(1):136–45. doi: 10.1002/biof.1579
29. Shivange G, Urbanek K, Przanowski P, Perry JSA, Jones J, Haggart R, et al. A Single-Agent Dual-Specificity Targeting of FOLR1 and DR5 as an Effective Strategy for Ovarian Cancer. *Cancer Cell* (2018) 34(2):331–45. doi: 10.1016/j.ccell.2018.07.005
30. Zhang HX, Liu OS, Deng C, He Y, Feng YQ, Ma JA, et al. Genome-Wide Gene Expression Profiling of Tongue Squamous Cell Carcinoma by RNA-Seq. *Clin Oral Investig* (2018) 22(1):209–16. doi: 10.1007/s00784-017-2101-7
31. Gupta P, Srivastava SK. Inhibition of Integrin-HER2 Signaling by Cucurbitacin B Leads to *In Vitro* and *In Vivo* Breast Tumor Growth Suppression. *Oncotarget* (2014) 5(7):1812–28. doi: 10.18632/oncotarget.1743
32. Zhong X, Huang S, Liu D, Jiang Z, Jin Q, Li C, et al. Galangin Promotes Cell Apoptosis Through Suppression of H19 Expression in Hepatocellular Carcinoma Cells. *Cancer Med* (2020) 9(15):5546–57. doi: 10.1002/cam4.3195
33. Zhong X, Liu D, Jiang Z, Li C, Chen L, Xia Y, et al. Chrysin Induced Cell Apoptosis and Inhibited Invasion Through Regulation of TET1 Expression in Gastric Cancer Cells. *Onco Targets Ther* (2020) 13:3277–87. doi: 10.2147/OTT.S246031

Conflict of Interest: The authors declare that the research was conducted in the absence of any commercial or financial relationships that could be construed as a potential conflict of interest.

frontiers in Oncology

ORIGINAL RESEARCH
published: 08 July 2021
doi: 10.3389/fonc.2021.696282

Wan-Nian-Qing, a Herbal Composite Prescription, Suppresses the Progression of Liver Cancer in Mice by Regulating Immune Response

Xinrui Zhang[1,2†], Xin Liu[2†], Yue Zhang[1,2], Anhui Yang[2], Yongfeng Zhang[2], Zhijun Tong[3], Yingwu Wang[2] and Ye Qiu[1*]*

[1] Department of Pharmacy, Changchun University of Chinese Medicine, Changchun, China, [2] School of Life Sciences, Jilin University, Changchun, China, [3] R&D Department, Jilin Tianlitai Pharmaceutical Co. Ltd, Baishan, China

The Wan-Nian-Qing prescription (WNQP), an herbal composite containing *Ornithogalum caudatum*, has been used in China for several years for cancer treatment. However, the mechanism of its pharmacological action against liver cancer is not clear. This study aimed to investigate the role of WNQP in inhibiting tumor growth in hepatocellular carcinoma model mice and determine its mechanism of action. We established HepG2- and SMMC-7721-xenografted tumor models in nude mice and BALB/c mice. The mice were administered WNQP for 2 weeks. The bodyweight of each mouse was monitored every day, and the tumor size was measured using vernier caliper before each round of WNQP administration. After the last dose, mice were sacrificed. The tumors were removed, lysed, and subjected to proteome profiling, enzyme-linked immunosorbent assay, and western blotting. The liver, spleen, and kidney were collected for histopathological examination. The effects of WNQP against liver cancer were first systematically confirmed in HepG2- and SMMC-7721-xenografted nude mice and BALB/c mice models. WNQP inhibited tumor growth, but failed to affect bodyweight and organ structures (liver and spleen), confirming that it was safe to use in mice. In BALB/c mice, WNQP regulated immune function, inferred from the modulation of immune-related cytokines such as interleukins, interferon, tumor necrosis factors, and chemokines. Further results confirmed that this regulation occurred *via* the regulatory effects of WNQP on Nrf2 signaling. WNQP can inhibit the growth of HepG2- and SMMC-7721-xenografted tumors in nude mice and BALB/c mice. This effect manifests at least partially through immunomodulation mediated apoptosis.

Keywords: Wan-Nian-Qing prescription, liver cancer, apoptosis, immune response, Nrf2

OPEN ACCESS

Edited by:
Peng Qu,
National Institutes of Health (NIH), United States

Reviewed by:
Ning Wang,
The University of Hong Kong, Hong Kong
Yuhuan Li,
Monash University, Australia

***Correspondence:**
Ye Qiu
ccyeqiu@163.com
Yingwu Wang
wyw@jlu.edu.cn

[†]These authors have contributed equally to this work

Specialty section:
This article was submitted to Pharmacology of Anti-Cancer Drugs, a section of the journal Frontiers in Oncology

Received: *16 April 2021*
Accepted: *08 June 2021*
Published: *08 July 2021*

Citation:
Zhang X, Liu X, Zhang Y, Yang A, Zhang Y, Tong Z, Wang Y and Qiu Y (2021) Wan-Nian-Qing, a Herbal Composite Prescription, Suppresses the Progression of Liver Cancer in Mice by Regulating Immune Response. Front. Oncol. 11:696282. doi: 10.3389/fonc.2021.696282

INTRODUCTION

Liver cancer is the sixth most common type of malignant tumor in the world and the second most common cause of tumor-related deaths (1). Epidemiological data from the United States in 2018 shows that between 2011 and 2015, the mortality of patients suffering from liver cancer increased by 2.7% per year among women and 1.6% per year among men (2). In China, the situation is even worse. Although treatment strategies have improved significantly, they mainly involve surgery, chemotherapy, radiotherapy, and immunotherapy (3). Unfortunately, most patients are not eligible for these curative treatments when they are at the advanced stages of the disease. To facilitate a breakthrough in the safety and efficacy of liver cancer treatment, there is an urgent need to develop new treatments to help increase patient life expectancy and the clinical benefits.

Oxidative stress is defined as the excessive production of reactive oxygen species (ROS) (4) and perturbation of the cell's redox balance (5) in a manner that cannot be counteracted by antioxidants. Oxidative stress factors can damage DNA and DNA repair enzymes, activate proto-oncogenes, disrupt cell signaling molecules, and ultimately lead to cancer. Nuclear factor-erythroid 2-related factor 2 (Nrf2) is a basic leucine zipper (bZIP) protein that regulates the expression of antioxidant proteins that protect against environmental oxidative stress (6, 7). In the nucleus, Nrf2 binds to the antioxidant response element (ARE), resulting in the transcription of antioxidant genes such as heme oxygenase-1 (HO-1) and superoxide dismutase (SOD) (8). The improvement of antioxidant capacity is contributed to improve the immune response of the host (9).

In China, traditional Chinese medicine has been used in clinics for a long time because of its wide efficacy and low side effects. The Wan-Nian-Qing-Prescription (WNQP) is a kind of compound traditional Chinese medicine commonly used in the treatment of malignant tumor, mainly composed of *Ornithogalum caudatum Jacq* (OC) (30%), *Scutellaria barbata D.Don* (SB) (15%), *Reynoutria japonica Houtt* (RJ) (6.70%), *Curcuma aromatica Salisb* (CAS) (7.50%), *Hedyotis diffusa Willd* (HD) (15%), *Panax ginseng C.A.Mey* (PG) (7.50%), *Salvia miltiorrhiza Bunge* (SMB) (7.50%), *Astragalus propinquus Schischkin* (APS) (15%), *Buthus martensii Karsch* (BMK) (3%), and *Scolopendra subspinipes* (SS) (3%) (**Table 1**). WNQP has been used in the combination of chemotherapy for liver cancer, lung cancer and gastric cancer for several years (10). In the theory of traditional Chinese medicine, OC and RJ both have the functions of dieresis and removing moisture of the body; SB has the function of clearing away heat; HD has the functions of detoxification and anti-cancer; CAS can enhance the function of the stomach; PG, SMB and APS can enhance human immunity; while BMK and SS have the function of killing cancer cells. Moreover, in the research results of modern pharmacy, OC is mainly composed of saponins, polysaccharides, terpenes and flavonoids and has a variety of pharmacological activities, such as anti-tumor, anti-inflammatory, and immunity-enhancing effects, as have been previously reported (11, 12). The total saponins present in the OC can inhibit the growth of HepG-2 cells by regulating mitochondrial function (13). HD can inhibit tumor growth *in vivo* and *in vitro* (14). APS combined with cisplatin can inhibit the growth of Lewis lung cancer cells and reduce the expression levels of CD44, CD62P and OPN protein in tumor tissue (15). WNQP has been shown to reduce the adverse reactions caused by mFOLFOX6 chemotherapy in patients with late-stage gall bladder cancer by improving their immune function (16, 17). However, the effects of WNQP against liver cancer and the mechanisms underlying the same have not been systematically reported, especially in animal models.

TABLE 1 | The English name, full botanical plant name and the ratio of the ingredients of Compound WNQP Capsule.

Full botanical plant name	English name	Ratio
Ornithogalum caudatum Aiton	*Ornithogalum caudatum*	33.40%
Scutellaria barbata D.Don	Half Lotus/Barbate Skullcap	15%
Reynoutria japonica Houtt.	*Polygonum cuspidatum*	6.70%
Curcuma aromatica Salisb.	*Radix curcumae*	7.50%
Hedyotis diffusa Willd.	Oldenlandia	15%
Panax ginseng C.A.Mey.	Ginseng	7.50%
Salvia miltiorrhiza Bunge	Salvia mill	7.50%
Astragalus propinquus Schischkin	*Astragalus membranaceus*	15%
Buthus martensii Karsch*	Scorpion	3%
*Scolopendra subspinipes**	Centipede	3%

*Not plants.

In this study, we systematically investigated the effects of WNQP against liver cancer on HepG2- and SMMC-7721-xenografted mouse models. We assessed the roles of WNQP in regulating the immune response *via* modulation of the oxidative stress response. We specifically focused on the regulation of Nrf2 signaling as a possible mechanism underlying the effects of WNQP against liver cancer. Based on our experiments, we provide novel evidence in support of the therapeutic formula WNQP in treating liver cancer patients.

MATERIALS AND METHODS

WNQP Information

The compound WNQP capsule, with national medicine approval number B20020717 and implemented in accordance with the China National Food and Drug Administration National Drug Standard (WS-5696 (B-0696)-2014Z), is a preparation comprising Chinese traditional medicines. We obtained the compound WNQP capsule with drug batch number 160301

Abbreviations: ARE, antioxidant response element; Bax, bcl2-associated X; Bcl-xL, B-cell lymphoma-extra-large; bZIP, basic leucine zipper; CCL, chemokine (C–C motif) ligand; ELISA, enzyme-linked immunosorbent assay; FADD, Fas-associated protein with death domain; GAPDH, glyceraldehyde-3-phosphate dehydrogenase; HO-1, heme oxygenase-1; HRP, horseradish peroxidase; HSP, heat shock protein; H&E, hematoxylin and eosin; IFN, interferon; IL, interleukin; MMP, matrix metalloproteinase; Nrf2, nuclear factor-erythroid 2-related factor 2; PFA, paraformaldehyde; ROS, reactive oxygenated species; SOD, superoxide dismutase; SPF, specific pathogen-free; TNF, tumor necrosis factor; WNQP, Wan-Nian-Qing-Prescription.

from the Jilin Tianlitai Pharmaceutical Co., Ltd. For the *in vitro* experiment, WNQP was extracted with double distilled (DD) water at the ratio of 1:10 at 60°C for 4 h and stored at 4°C.

Cell Culture

The liver cancer cells, HepG2 (American Type Culture Collection, USA) and SMMC-7721 (China Center for Type Culture Collection, China), were cultured in Dulbecco's Modified Eagle Media (DMEM; Gibco, Grand Island, NY) containing 10% fetal bovine serum (FBS; Zhejiang Tian hang bio Polytron Technologies Inc.), and 1% penicillin and streptomycin at 37°C under 95%/5% air/CO_2 conditions.

Animal Models

The mice used for experiments were housed in barrier facilities (temperature: 23 ± 1 °C and humidity: 50 ± 10%) under a 12 h/12 h light/dark cycle. They had free access to food and water. The animal experiments were carried out under the supervision of the Institutional Animal Care and Use Committee of Jilin University (NO. 2017SY0601).

HepG2- and SMMC-7721-Xenografted Tumor Models in BALB/c Nude Mice

Five-week-old male BALB/c nude mice (SCXK(JI)-2016-0003; purchased from Wei-tongli-hua Laboratory Animal Technology Company, Beijing, China) were injected subcutaneously with 3–4 × 10^6 cells of either the HepG2 or SMMC-7721 lineage. When the tumor volume reached 100 mm^3, the tumor-bearing mice were divided into three groups (n = 6/group) for both the HepG2- and SMMC-7721-xenografted tumor models; the first group was given physiological saline (n = 6), the second group was given 0.3 g/kg of WNQP (n = 6), and the third group was given 0.6 g/kg of WNQP (n = 6). All doses of saline/WNQP were administered orally, every day for 2 weeks. The bodyweight of each mouse was monitored every day, and the tumor size was measured using vernier calipers before each round of saline/WNQP administration. The tumor volume was calculated using the following formula:

$$V(mm^3) = 0.5 \times (\text{larger diameter} \times \text{smaller diameter}^2)$$

After the final dose, the mice were sacrificed. The tumors were then removed, lysed, and subjected to proteome profiling and western blotting. The liver, spleen, and kidney were collected and fixed in 4% paraformaldehyde (PFA) for histopathological examination.

HepG2- and SMMC-7721-Xenografted Tumor Models in BALB/c Mice

Male BALB/c mice (18–22 g, specific pathogen-free [SPF] grade) were purchased from the Yis Laboratory Animal Technology Co., Ltd., Changchun, China (SCXK(JING)2016-0011). After adaptive feeding, they were injected intraperitoneally with cyclophosphamide (CTX; 50 mg/kg) for three consecutive days. Fresh tumor samples obtained from the HepG2 and SMMC-7721 heterotopic tumor models in nude mice were cleaned and sliced with a scalpel to obtain 2 mm × 2 mm × 2 mm sections. The tumor masses were implanted in the right dorsum (near the hind leg) of the BALB/c mice, and tumor growth was monitored daily. When the tumors attained a certain volume, the mice were randomly divided into three groups (n = 6/group); the first group was given physiological saline (n = 6), the second group was given 0.3 g/kg of WNQP (n = 6), and the third group was given 0.6 g/kg of WNQP (n = 6). All doses of saline/WNQP were administered orally, every day for 4 weeks. To avoid the restoration of immune function in mice, CTX (50 mg/kg) was injected once a week. The day after the last administration, blood was collected from the hearts of the mice, after which the mice were anesthetized using sodium pentobarbital and photographed. After euthanasia of mice, the tumors were removed, lysed, and subjected to proteome profiling and western blotting. The liver, spleen, and kidney were collected and fixed in 4% PFA for histopathological examination.

Nrf2-siRNA Transfection of Spleen Cells

The primary culture of spleen cells was seeded onto 6-well plates, in accordance with previously described protocol (18). The cells were transfected with 20 nM Nrf2-siRNA (5′-GGATGAAG AGACCGGAGAA-3′; R100438, RiboBio, China) for 30 min using the riboFECT^{TM}CP Reagent (RiboBio), in accordance with the manufacturer's protocol. Following transfection, the cells were treated with 0.5 mg/mL of WNQP for 4 h and then harvested. The expression of Nrf2, HO-1, HO-2, SOD-1, and glyceraldehyde-3-phosphate dehydrogenase (GAPDH) was analyzed using western blots.

Histopathological Examination

Liver, spleen, and kidney tissues were washed with water and dehydrated using different concentrations of alcohol. We used xylene to clear the tissues and then embedded the samples in paraffin wax. After the paraffin solidified, sections were cut using a microtome (Leica, Wetzlar, Germany) and were stained with hematoxylin and eosin (H&E) (19). Images were captured using an Eclipse TE 2000-S fluorescence microscope (Nikon Corp., Tokyo, Japan).

Antibody Chip Analysis

The apoptotic factors expressed by the tumors were collected from BALB/c nude mice and detected using cytokine chip analysis. Briefly, total protein was extracted from tumor tissue and its amount was determined using a BCA Protein Assay Kit (Merck Millipore, Billerica, MA, USA). An Apoptosis Array Kit (ARY009, R&D Systems, Millipore, USA) was used to assess the presence of 35 factors in the total protein, following protocols outlined by the manufacturer.

The tumors obtained from the BALB/c mice were used to detect 308 mouse proteins. Total protein was extracted from tumor tissue using ice-cold tissue protein extraction reagent containing 0.5% protease inhibitor cocktail, phenylmethylsulfonyl fluoride, and phosphatase inhibitor cocktail. The total protein amount was determined using a BCA Protein Assay Kit. A RayBio® L-Series Mouse Antibody Array 308 Glass Slide Kit (RayBiotech, AAM-BLG-1, USA) was used to assess the presence of 308 factors in the total protein, in accordance with the manufacturer's protocols.

Immune Cytokine Detection

Blood from BALB/c mice was collected from the caudal vein before performing euthanasia. The serum levels of interleukin (IL)-2 (42903), IL-10 (CK-E20005), IL-31 (44865), interferon-γ (IFN-γ) (42918), tumor necrosis factor (TNF)-α (CK-E20220), TNF-β (42867), and chemokine (C-C motif) ligand 28 (CCL28) (44866) were detected using specific enzyme-linked immunosorbent assay (ELISA) kits, in accordance with the manufacture's protocol (The Source Leaf Biological Technology Co. Ltd., Shanghai, China).

Western Blot Analysis

The tumors from BALB/c nude mice and spleens from BALB/c mice were homogenized along with a tissue protein extraction reagent. The total protein content was determined using a BCA Protein Assay Kit (Merck Millipore, Billerica, MA, USA). We loaded 40 μg of protein per sample and separated them using sodium dodecyl sulfate-polyacrylamide gel electrophoresis. The separated proteins were then transferred onto polyvinylidene fluoride membranes (0.45 μm, Merck Millipore, Billerica, MA, USA). Subsequently, the membranes were blocked and incubated with the appropriate primary antibodies: bcl2-associated X (Bax) (21 kDa) (ab32503), B-cell lymphoma-extra-large (Bcl-xL) (26 kDa) (ab32370; Abcam, Cambridge, MA, USA), Nrf2 (97 kDa) (12721S; Cell Signaling Technologies, Danvers, MA, USA), heat shock protein 27 (HSP27) (27 kDa) (bs-0730R), heat shock protein 60 (HSP60) (58 kDa) (bs-0191R), heat shock protein 70 (HSP70) (70 kDa) (bs-0126R), HO-1 (32 kDa) (bs-2075R), HO-2 (36 kDa) (bs-1238R), SOD-1 (17 kDa) (bs-10216R), GAPDH (37 kDa) (bs-0755R; Bioss Antibodies, China), overnight at 4°C. The membranes were then incubated with the appropriate secondary antibody, either a horseradish peroxidase (HRP)-conjugated goat anti-rabbit immunoglobulin G antibody (SH-0032; Beijing Dingguo Changsheng Biotechnology Co., Ltd., Beijing, China) or an HRP-conjugated goat anti-mouse immunoglobulin G antibody (sc-2005; Santa Cruz Biotechnology, Inc., Texas, USA), for 4 h at a dilution of 1:2,000. Finally, the blots were visualized using electrochemiluminescence detection kits (Merck Millipore, Billerica, MA, USA) and quantified using ImageJ software (NIH, Bethesda, MD, USA).

Statistical Analysis

All data are presented as the mean ± standard deviation (SD). One-way analysis of variance and post-hoc multiple comparisons (Dunn's test) were performed where applicable using the Statistical Package for Social Sciences (SPSS) v16.0 software (IBM Corporation, Armonk, NY). The statistical significance threshold was set at $P < 0.05$.

RESULTS

WNQP Inhibits HepG2- and SMMC-7721-Xenografted Tumor Growth in Nude Mice

The nude mice with tumor xenografts were used to investigate the anti-tumor activity of WNQP. A 14-day treatment regimen of WNQP administered at either 0.3 or 0.6 g/kg significantly inhibited the growth of tumors, but more so for the latter dose (HepG2-xeongrafted tumors: P <0.001, 136.5 mm^3 *vs.* 357.0 mm^3, **Figures 1A, C, E**; SMMC-7721-xenografted tumors: P <0.001, 148.2 mm^3 *vs.* 323.3 mm^3, **Figures 1B, D, F**). WNQP showed no significant effects on the bodyweights (**Figures 1G, H**) and organ structures of the liver, spleen, and kidney (**Figures 1I, J**) in either HepG2- or SMMC-7721-xenografted nude mice.

To systematically investigate the possible mechanisms underlying the inhibitory effects of WNQP on HepG2- and SMMC-7721-xenografted tumor growth in nude mice, cell cytokines related to apoptosis and oxidation were detected using a Proteome Profiler Apoptosis Array Kit. When HepG2- and SMMC-7721-xenografted tumors from nude mice were assessed, WNQP at 0.6 g/kg was found to strongly regulate the levels of cytokines related to apoptosis and oxidation, including Bax, Bcl-2, Bcl-xL, cleaved caspase-3, cellular inhibitors of apoptosis (cIAP), clusterin, TNF-related apoptosis-inducing ligand (TRAIL) R2/death receptor (DR) 5, Fas-associated protein with death domain (FADD), Fas, hypoxia-inducible factor (HIF)-1α, HO-1, HSP60, high temperature requirement protein 2 (HtrA 2), livin, supramolecular activation complex (SMAC), survivn, and X-chromosome-linked inhibitor of apoptosis (XIAP) (**Figures 2A–D** and **Table S1**).

Western blot analysis revealed that WNQP increased the expression levels of Bax, and reduced the expression levels of Bcl-xL, HSP27, HSP60, and HSP70 in HepG2- (**Figure 2E**) and SMMC-7721-xenografted tumors in nude mice (**Figure 2F**).

WNQP Inhibits HepG-2 and SMMC-7721-Xenografted Tumor Growth in BALB/c Mice *via* Regulation of Immune Function

The BALB/c mice bearing tumor xenografts were used to investigate whether the effects of WNQP against liver cancer occur *via* the modulation of immune functions. A 28-day treatment regimen of WNQP administered at either 0.3 or 0.6 g/kg strongly inhibited the growth of HepG2-xenografted (**Figures 3A, C**) and SMMC-7721-xenografted tumors (**Figures 3B, D**), without any effects on bodyweights (**Figures 3E, F**) and organ structures of the liver, spleen, and kidney (**Figure 3G**).

A RayBio L-Series Mouse Antibody Array 308 Glass Slide Kit was used to detect 308 proteins in the tumor tissues. As compared to control mice, WNQP administered at 0.6 g/kg markedly affected the levels of 66 types of cytokines in the HepG2-xenografted tumors (**Figures 4A, C** and **Table S2**), and 57 types of cytokines in the SMMC-7721-xenografted tumors (**Figures 4B, D** and **Table S3**). Most of the cytokines were associated with immune functions.

Based on these results, seven types of immunological correlation factors were analyzed from the serum of BALB/c mice using ELISA. In BALB/c mice bearing HepG2- and SMMC-7721-xenografted tumors, WNQP enhanced the serum levels of TNF-α (P <0.05), TNF-β (P <0.05), IFN-γ (P <0.05), IL-2 (P <0.05), IL-10 (P <0.05), and CCL-28 (P <0.05), and reduced the serum levels of IL-31 (P <0.05) (**Table 2**).

Nrf2 Signaling Is Involved in WNQP-Mediated Inhibition of Tumor Growth

We used western blotting to analyze the changes in the expression of Nrf2 and its downstream factors in the spleen

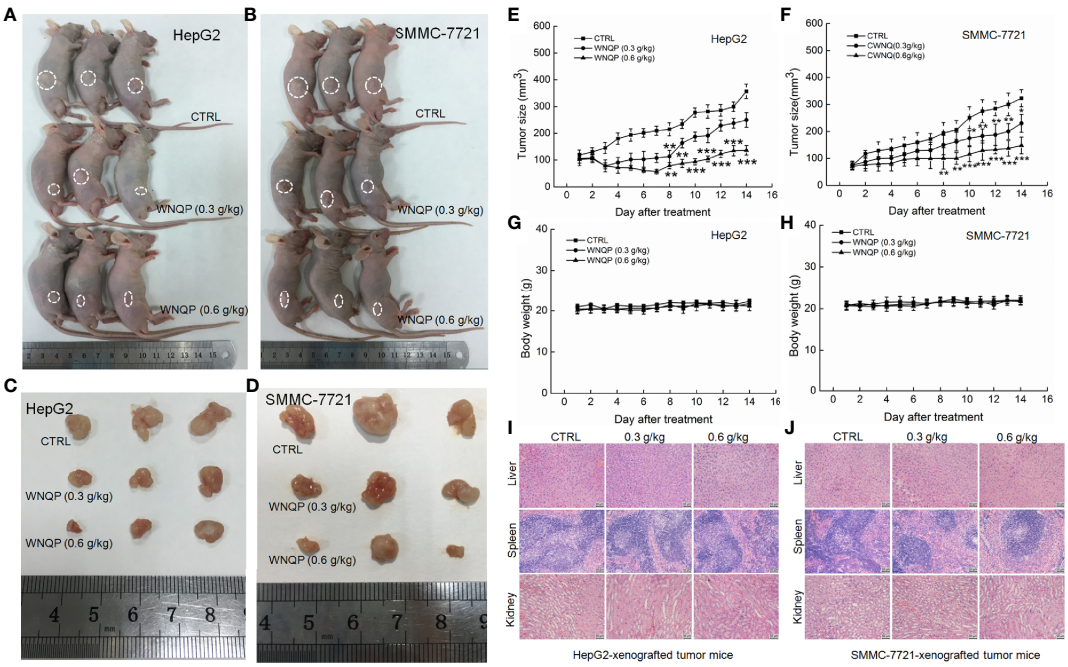

FIGURE 1 | WNQP inhibited HepG2- and SMMC-7721-xenograft tumor growth in BALB/c nude mice. BALB/c athymic nude mice inoculated with HepG2 and SMMC-7721 cells were treated with WNQP (0.3 and 0.6 g/kg dissolved in 0.9% saline solution) or vehicle solvent (0.9% saline solution) for 14 days. **(A, B)** Tumor-bearing nude mice and **(C, D)** tumor tissues collected from control (CTRL) and WNQP-treated groups (n = 3). **(E, F)** Tumor volumes were measured every day. Tumor sizes are expressed as the mean ± SD (n = 6). $^{*}P < 0.05$, $^{**}P < 0.01$ and $^{***}P < 0.001$ *versus* the control group. **(G, H)** Mean (± SD) bodyweights of mice in the WNQP-treated and CTRL groups (n = 6). **(I, J)** H&E staining of liver, spleen, and kidney tissues from nude mice (n = 3) (20× magnification, scale bar: 50 μm).

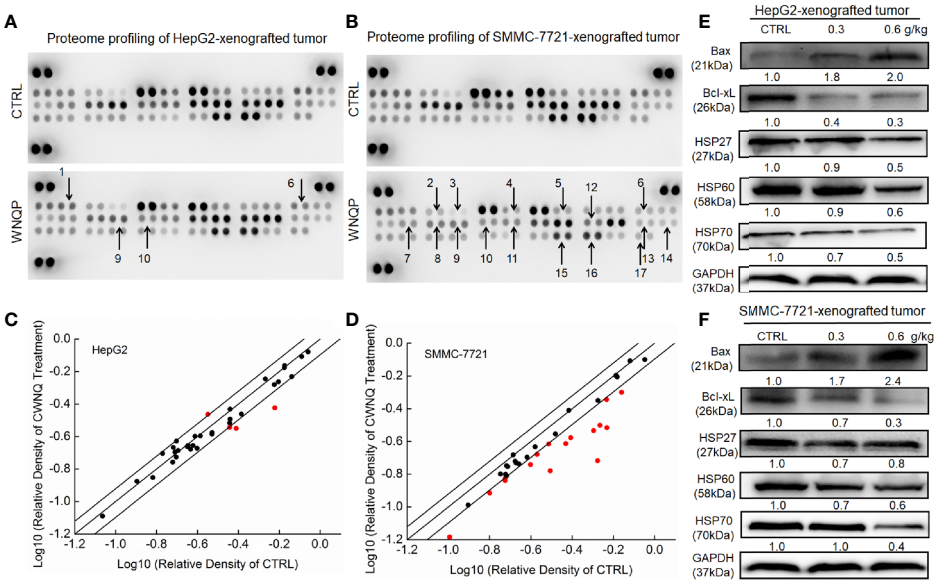

FIGURE 2 | The effects of WNQP on 35 types of cytokines in nude mice tumors, detected using an Apoptosis Array Kit (n = 3). The arrows indicate factors marked for further detection: 1. Bax, 2. Bcl-2, 3. Bcl-xL, 4. cleaved caspase-3, 5. cIAP, 6. clusterin, 7. TRAIL R2/DR5, 8. FADD, 9. Fas, 10. HIF-1α, 11. HO-1, 12. HSP 60, 13. HtrA2, 14. livin, 15. SMAC, 16. survivn, 17. XIAP. **(A, B)** Scatter diagram of 35 cytokines. The relative density is the ratio of the absolute value and reference spot value. The red dots indicate factors with a change of >20% relative to control mice. **(C, D)** WNQP strongly enhanced the expression levels of Bax and suppressed the expression levels of Bcl-xL, HSP27, HSP60, and HSP70 in tumor tissues. Quantitative protein expression data were normalized to the corresponding GAPDH levels, and the average fold changes in band intensity are marked **(E, F)** (n = 3).

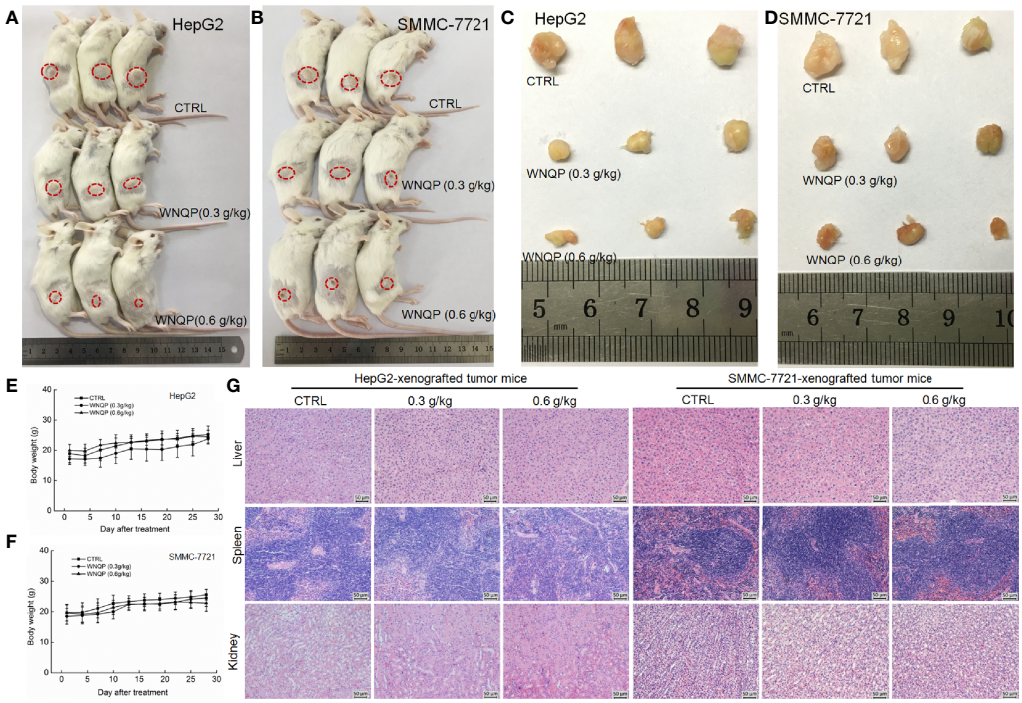

FIGURE 3 | WNQP inhibited HepG2- and SMMC-7721-xenograft tumor growth in BALB/c mice. After three consecutive CTX injections, BALB/c mice inoculated with HepG2 and SMMC-7721 cells were treated with WNQP (0.3 and 0.6 g/kg dissolved in 0.9% saline solution) or vehicle solvent (0.9% saline solution) for 28 days. **(A, B)** Tumor-bearing mice and **(C, D)** tumor tissues from control (CTRL) and WNQP-treated groups (n = 3). **(E, F)** Mean (± SD) bodyweights of mice in the WNQP-treated and CTRL groups (n = 6). **(G)** H&E staining of liver, spleen, and kidney tissues from BALB/c mice (n = 3) (20× magnification, scale bar: 50 μm).

tissue of BALB/c mice. A 28-day treatment regimen of WNQP administration strongly enhanced the expression levels of Nrf2, HO-1, HO-2, and SOD-1 in the spleens of BALB/c mice carrying xenografts of both HepG2- (P <0.05) (**Figures 5A, B**) and SMMC-7721 tumors (P <0.05) (**Figures 5C, D**).

In primary cultured spleen cells transfected with Nrf2-siRNA, the WNQP failed to increase in the expression levels of Nrf2, HO-1, HO-2, and SOD-1 (**Figures 5E, F**) This suggested an important role of Nrf2 in the improvement of immune function during WNQP-mediated inhibition on tumor growth.

DISCUSSION

In this study, we first systematically confirmed the inhibitory effects of the Traditional Chinese Medicine formula, WNQP, on the growth of HepG2- and SMMC-7721-xenografted tumors in nude mice and BALB/c mice models. WNQP effectively inhibited tumor growth, but had no effects on the bodyweights and organ structures, confirming that it was safe to use in mice. Traditional Chinese Medicine plays an important role in the treatment of tumors. When combined with chemotherapy, radiation therapy, or post-operative treatment, Traditional Chinese Medicine can help to reduce toxic side effects (20).

Cancers are usually associated with uncontrolled cell proliferation and oxidative stress (21). As a physiological and/or pathological process, apoptosis has been recognized as a therapeutic target for various types of cancers; these therapeutic strategies commonly require the regulation of cytokines (22). As members of the Bcl-2 family, Bcl-2 and Bax are usually present as heterodimers and regulate the initiation of apoptosis by modulating mitochondrial activity that in turn regulates the release of cytochrome C and the caspase cascade (21). HSPs are a large family of molecular chaperones, which participate in the folding and maturation of a variety of client proteins and protect them from degradation, oxidative stress, hypoxia and heat stress (23). Abnormally high levels of HSP have been noted in tumor tissues. They participate in the caspase-mediated apoptotic pathway to protect mitochondrial integrity. High levels of HSP also enhance the resilience of tumors, allowing them to evade immune-mediated apoptosis (24). We observed that the levels of HSP27 and HSP60 were strongly suppressed after WNQP administration in nude mice. HSP27 can inhibit p53-mediated induction of p21, resulting in unlimited proliferation of tumor cells and eventually leading to tumorigenesis (25). HSP60, an immunodominant antigen associated with cellular immunity and immune responses to certain infectious diseases, prevents cellular apoptosis by inhibiting the activation of pro-apoptotic factors (26). HSP60 binds to Bax and Bcl-2, preventing Bax activation and maintaining normal folding of Bcl-2 to prevent apoptosis (27). HSP70 can enhance the immunosuppressant function of T regulatory cells (Tregs) and downregulate the secretion of cytokines IFN-γ and TNF-α (28, 29) Data obtained from nude

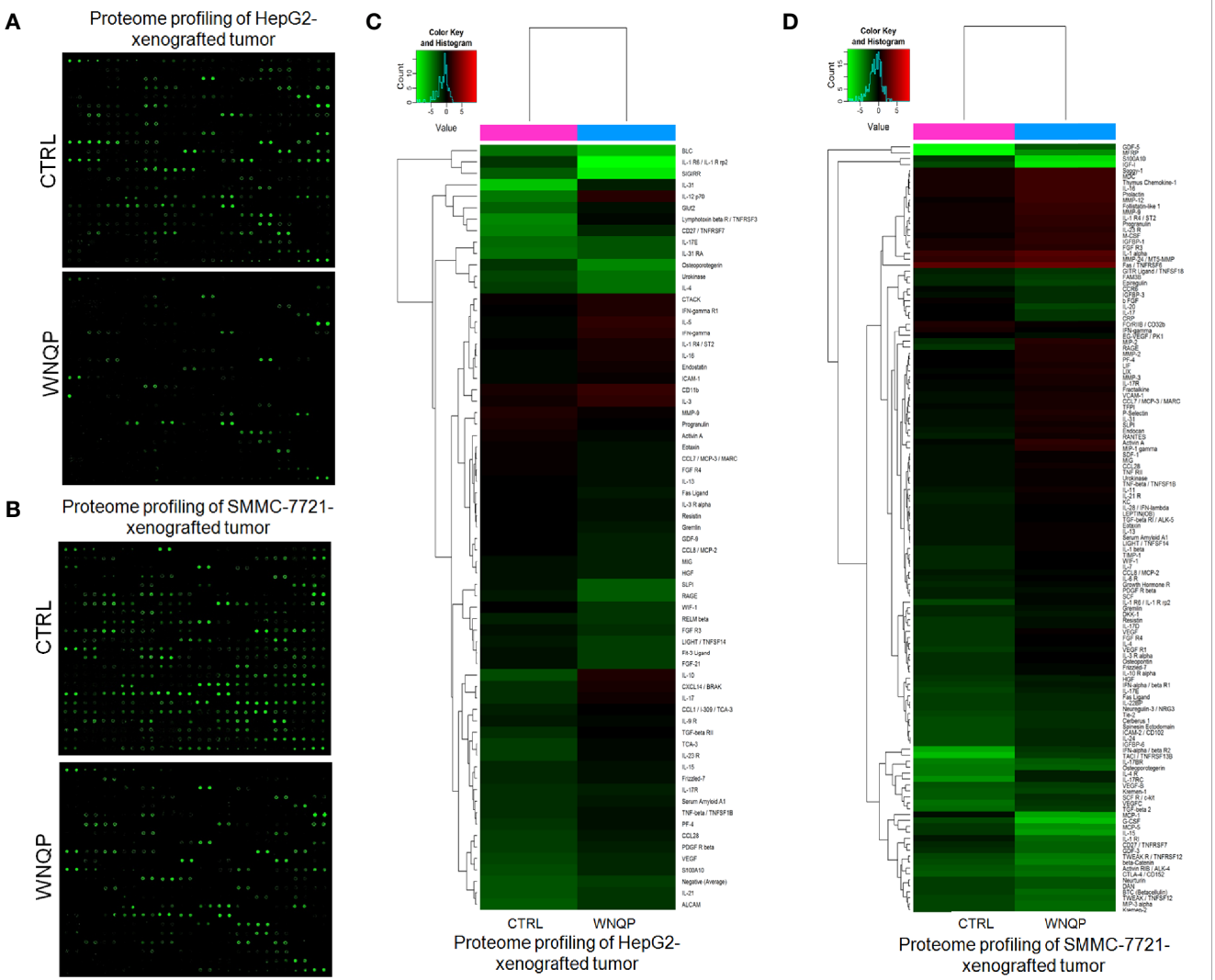

FIGURE 4 | **(A, B)** The effects of WNQP on 308 types of cytokines in mice tumors, detected using the L-Series Mouse Antibody Array 308 Glass Slide Kit (n = 3). **(C, D)** Proteomic profiling of HepG2- and SMMC-7721-xenografted tumors. When compared with CTRL mice, WNQP-treated mice showed regulated levels of 66 types of cytokines in HepG2-xenografted tumors and of 57 types of cytokines in SMMC-7721-xenografted tumors.

TABLE 2 | The effects of WNQP on the immune factors of serum in tumor-xenografted BALB/c mice.

Factors (pg/ml)	HepG2-xenografted tumor BALB/c mice			SMMC-7721-xenografted tumor BALB/c mice		
	CTRL	WNQP (0.3 g/kg)	WNQP (0.6 g/kg)	CTRL	WNQP (0.3 g/kg)	WNQP (0.6 g/kg)
TNF-α	784.7 ± 35.9	820.0 ± 27.8	858.1 ± 48.0*	773.8 ± 69.6	831.6 ± 18.0	850.8 ± 32.5*
TNF-β	297.3 ± 11.6	327.1 ± 29.1*	310.9 ± 12.5	251.2 ± 3.7	311.8 ± 16.3**	307.7 ± 38.9*
IFN-γ	249.2 ± 11.8	281.4 ± 18.8*	249.4 ± 16.8	257.5 ± 12.7	254.6 ± 21.5	260.6 ± 27.8
IL-2	421.7 ± 25.9	423.5 ± 43.1	413.2 ± 10.6	387.6 ± 12.1	430.9 ± 18.1*	468.5 ± 32.9*
IL-10	489.7 ± 39.8	545.5 ± 46.7*	589.7 ± 35.8*	417.2 ± 3.1	480.1 ± 36.2*	526.9 ± 54.5**
IL-31	50.1 ± 5.2	49.6 ± 3.2	41.9 ± 3.2*	51.7 ± 4.4	50.5 ± 6.1	49.2 ± 6.3
CCL-28 (*10^3)	48.5 ± 2.3	62.6 ± 10.7*	66.0 ± 6.8**	44.9 ± 9.3	49.4 ± 5.2	54.5 ± 5.9*

*Results are represented as means ± S.D. (n = 6). *P <0.05 and **P <0.01 vs. related control group, respectively.*

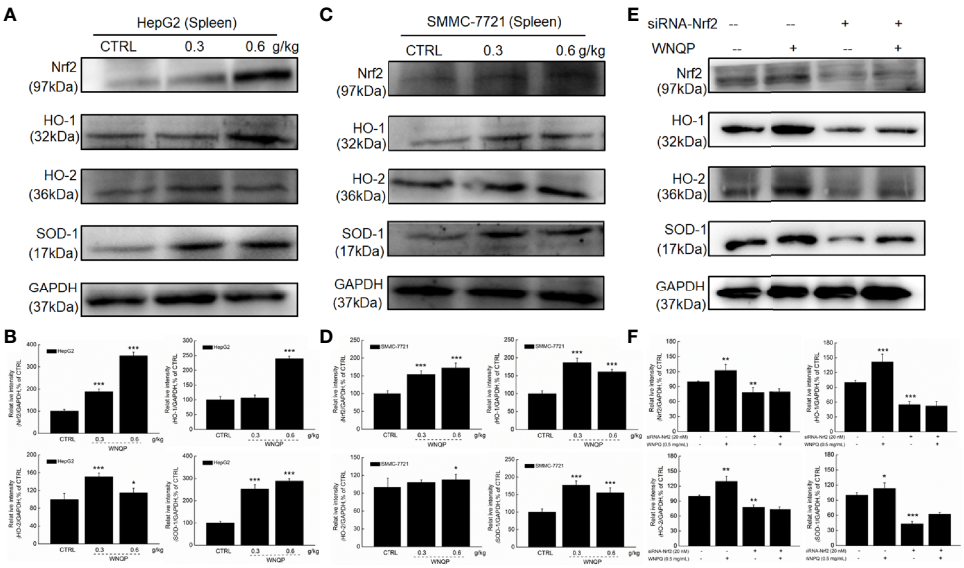

FIGURE 5 | Nrf2 signaling is involved in the improvement of immune function during WNQP-mediated inhibition of tumor growth. WNQP strongly enhanced the expression levels of Nrf2, HO-1, HO-2 and SOD-1 in the spleen tissues of BALB/c mice bearing **(A, B)** HepG2- and **(C, D)** SMMC-7721-xenograft tumors. **(E, F)** In Nrf2-siRNA-transfected primary cultured spleen cells, WNQP-induced increase in the levels of Nrf2, HO-1, HO-2 and SOD-1 were abolished. Quantitative protein expression data were normalized to the corresponding GAPDH levels, and the average fold changes in band intensity are marked. Data are expressed as the mean ± SD (n = 3). $^{*}P < 0.05$, $^{**}P < 0.01$ and $^{***}P < 0.001$ *versus* the control group.

mice bearing HepG2- and SMMC-7721-xenografted tumors confirmed that WNQP showed pro-apoptotic effects on liver cancers while inhibiting tumor growth. The apoptosis of tumor cells induced by WNQP has also been associated with immune regulation.

Carcinogenesis involves several important processes, including, but not limited to, migration, invasion, metastasis, and angiogenesis; all of these are dependent on the extracellular environment (30). The antibody chip array screen in immunosuppression BALB/c mice bearing a hepatoma showed that WNQP regulated the serum levels of interleukins and chemokines that can in turn regulate tumor progression. IL-10 has been shown to have anti-tumor effects, which are enhanced when combined with IL-2; these effects can potentially be harnessed for immunotherapy (31). IL-2 stimulates the growth of thymocytes and, as a result, induces T-cell differentiation and prompts the immune system to attack tumor cells (32). IL-2 can activate nature killer (NK) cells to secrete CCL28, thus enhancing the targeted killing of tumor cells. TNF can regulate immunity and enhance the anti-tumor cytolytic activity of NK cells and production of cytotoxicity-related proteins such as IFN-γ (33, 34). However, some cytokines can also promote tumor development (35). It has been reported that IL-31 can improve angiogenesis and promote tumor progression (36, 37). WNQP regulates these cytokines to form an immune regulatory network that inhibits the growth of tumor cells.

The activation of Nrf2 has been considered beneficial for the prevention of cancer, as Nrf2 is the main cellular defense mechanism against carcinogens, ROS, and other DNA-damaging factors (38). Activated Nrf2 can modulate cellular antioxidant regulators; it can upregulate the expression of HO-1, SOD-1, and other downstream genes in normal cells to maintain the intracellular redox balance and reduce tumorigenesis (39). Activated Nrf2 is involved in the regulation of immune factors (40, 41), which it achieves by inducing T lymphocytes to produce ILs, interferons, and TNF (42). In our previous experiments, we showed that *Antrodia cinnamomea* polysaccharides (APCS) enhance immune functions in mice by upregulating the expression of Nrf2 (43). Cumulatively, these results indicate that WNQP inhibits oxidative stress by regulating Nrf2 and its downstream proteins to counteract ROS generation and accumulation, increases SOD activity, regulates the levels of inflammatory factors and thus, further suppresses the growth of tumors in mice.

Some studies have reported that Nrf2 is frequently mutated in human cancer cells, leading to an increase in the expression of the corresponding protective genes and thereby giving these cells a growth advantage and anti-apoptotic ability (44). However, the activation of Nrf2 is a double-edged sword in the context of cancer (45). The expression of Nrf2 in cancer cells can promote tumor growth, while in the host cells it can limit tumor growth by maintaining a functional immune system (46, 47). Both Nrf2 inducers and inhibitors have been predicted to function as anti-cancer drugs, although their targets are different (48–51). Nrf2 inducers can protect normal cells from anticancer drugs during chemotherapy, implying that Nrf2 inducers in combination with anti-cancer drugs may help to overcome the limitations of traditional chemotherapy (44). This is consistent with our data showing that WNQP can be used for liver cancer treatment in combination with chemotherapeutics.

CONCLUSION

WNQP inhibited the tumor growth of HepG2- and SMMC-7721-xenografted tumor models in nude mice and BALB/c mice. This effect is at least partially due to the regulation of oxidative stress-mediated immunomodulation. However, the study has some limitations. We failed to identify the key ingredient in WNQP that mediated the inhibition of liver cancer growth. This aspect needs further investigation.

DATA AVAILABILITY STATEMENT

The original contributions presented in the study are included in the article/**Supplementary Material**. Further inquiries can be directed to the corresponding authors.

ETHICS STATEMENT

The experimental animal protocol was approved by the Institutional Animal Care and Use Committee of Jilin University.

AUTHOR CONTRIBUTIONS

YQ and YW designed the experiments, draft and revised the manuscript. XZ, XL, YuZ, and AY performed the experiments and analyzed the data. YoZ and ZT analyzed the data. All authors contributed to the article and approved the submitted version.

FUNDING

This work was supported by the Special Projects of Cooperation between Jilin University and Jilin Province in China (SXGJSFKT2020-1), Medical Health Project in Jilin Province of P. R. China (Grant No.20191102027YY, 20200708037YY and 20200708068YY).

SUPPLEMENTARY MATERIAL

The Supplementary Material for this article can be found online at: https://www.frontiersin.org/articles/10.3389/fonc.2021.696282/full#supplementary-material

REFERENCES

1. Bray F, Ferlay J, Soerjomataram I, Siegel RL, Torre LA, Jemal A. Global Cancer Statistics 2018: GLOBOCAN Estimates of Incidence and Mortality Worldwide for 36 Cancers in 185 Countries. *CA: A Cancer J Clin* (2018) 68 (6):394–424. doi: 10.3322/caac.21492
2. Siegel RL, Miller KD, Jemal A. Cancer Statistics, 2018. *CA: Cancer J Clin* (2018) 68(1):7–30. doi: 10.3322/caac.21442
3. Kulik L, El-Serag HB. Epidemiology and Management of Hepatocellular Carcinoma. *Gastroenterology* (2019) 156(2):477–91.e1. doi: 10.1053/j.gastro.2018.08.065
4. D'Autreaux B, Toledano MB. ROS as Signalling Molecules: Mechanisms That Generate Specificity in ROS Homeostasis. *Nat Rev Mol Cell Biol* (2007) 8 (10):813–24. doi: 10.1038/nrm2256
5. Apel K, Hirt H. Reactive Oxygen Species: Metabolism, Oxidative Stress, and Signal Transduction. *Annu Rev Plant Biol* (2004) 55:373–99. doi: 10.1146/annurev.arplant.55.031903.141701
6. Gold R, Kappos L, Arnold DL, Bar-Or A, Giovannoni G, Selmaj K, et al. Placebo-Controlled Phase 3 Study of Oral BG-12 for Relapsing Multiple Sclerosi. *N Engl J Med* (2012) 367(12):1098–107. doi: 10.1056/NEJMoa1114287
7. Li WG, Kong AN. Molecular Mechanisms of Nrf2-Mediated Antioxidant Response. *Mol Carcinog* (2009) 48(2):91–104. doi: 10.1002/mc.20465
8. Rushworth SA, Macewan DJ. The Role of Nrf2 and Cytoprotection in Regulating Chemotherapy Resistance of Human Leukemia Cells. *Cancers* (2011) 3(2):1605–21. doi: 10.3390/cancers3021605
9. Gostner JM, Becker K, Fuchs D, Sucher R. Redox Regulation of the Immune Response. *Redox Rep Commun Free Radical Res* (2013) 18(3):88–94. doi: 10.1179/1351000213Y.0000000044
10. Min Z, Yuhui H, Xia W. Determination of Emodin in Compound Wannianqing Capsules by High-Performance Liquid Chromatograph. *Chin J Public Health Eng* (2007) 6:1–39.
11. Gui W, Song X, Li Y, Jin Y. Clinical Observation of Wannianqing Capsules Combined With Morphine Sulfate Sustained-Release Tablets on 97 Cases of Lung Cancer Patients With Severe Pain. *J Hunan Univ Chin Med* (2017) 37:12–1408.
12. Li X, Gao L. Research Progress on Chemical Composition and Pharmacological Activities of Ornithogalum Caudatum Ai. *Asia-Pacific Traditional Med* (2016) 12(22):52–4.
13. Qu Z, Shi X, Zou X, Ji Y. Study on the Apoptotic Mechanisms of Human Liver Cancer HepG-2 Cells Induced by Total Saponins of Ornithogalum Caudatum. *J Chin Med Mater* (2016) 39:4–867.
14. Lu L, Zhan S, Liu X, Zhao X, Lin X, Xu H. Antitumor Effects and the Compatibility Mechanisms of Herb Pair Sclerotrion Diffusum (Willd.) R. J. Wang-Sculellaria Barbata D. Don. *Front Pharmacol* (2020) 11:292. doi: 10.3389/fphar.2020.00292
15. Liu D, Li Y, Wang X, Wang Y, Ma Y, Chen Y, et al. Astragalus Polysaccharide Combined With Cisplatin Inhibits Growth of Recurrent Tumor and Down-Regulats the Expression of CD44, CD62P and Osteopontin in Tumor Tissues in Mice Bearing Lewis Lung Cancer. *Chin J Cell Mol Immunol* (2018) 34 (12):1105–10.
16. Wang X, Li D, Zhang Y, Wu S, Tang F. Costus Root Granules Improve Ulcerative Colitis Through Regulation of TGF-β Mediation of the PI3K/AKT Signaling Pathway. *Exp Ther Med* (2018) 15(5):4477–84. doi: 10.3892/etm.2018.5946
17. Xing J, Zhang H, Yan K, Zhang Y. The Effects of Compound Wanningqing Capsule on Adverse Reaction of Advanced Gallbladder Carcinoma Treated by Mfolfox6 Method Chemotherapy. *Shaanxi J Tradit Chin Med* (2019) 40 (8):1010–3.
18. Meng T, Zhang M, Song JY, Dai YF, Duan HW. Development of a Co-Culture Model of Mouse Primary Hepatocytes and Splenocytes to Evaluate Xenobiotic Genotoxicity Using the Medium-Throughput Comet Assay. *Toxicol Vitro* (2020) 66:10. doi: 10.1016/j.tiv.2020.104874
19. Jiao C, Chen W, Tan X, Liang H, Li J, Yun H, et al. Ganoderma Lucidum Spore Oil Induces Apoptosis of Breast Cancer Cells *In Vitro* and *In Vivo* by Activating Caspase-3 and Caspase-9. *J Ethnopharmacol* (2020) 247:112256. doi: 10.1016/j.jep.2019.112256
20. Hong Z. Progress in the Study of TCMmedicine for the Treatment of Cancer. *Clin J Chin Med* (2014) 6(20):142–4.
21. Pei Y, Li Y, Yan CS, Wang H. Astragaloside-IV Induces Apoptosis in Human Breast Cancer MCF- 7 Cells via Modulating Bax/Bcl-2/Caspase-3 Signaling Pathway. *Tradit Chin Drug Res Clin Pharmacol* (2019) 30:9–1077.
22. Li PD, Wang YH, Xiao Y, Wen YY, Wan XF, Zheng D, et al. Effects of Hydroquinone on Apoptosis and Expression of Bcl-2, Bax and Caspase-3 in Human Leukemia Cells. *Mod Prev Med* (2018) 45:5–878.
23. Chatterjee S, Burns TF. Targeting Heat Shock Proteins in Cancer: A Promising Therapeutic Approach. *Int J Mol Sci* (2017) 18(9):39. doi: 10.3390/ijms18091978

24. Minowada G, Welch WJ. Clinical Implications of the Stress Response. *J Clin Invest* (1995) 95(1):3–12. doi: 10.1172/jci117655
25. Tsuruta M, Nishibori H, Hasegawa H. Heat Shock Protein 27 a Novel Regular of 5-Fluorouracil Resistance in Colon Cancer. *Oncol Rep* (2008) 20:5–1165. doi: 10.3892/or_00000125
26. Samali A, Holmberg C, Sistonen L. Thermotolerance and Cell Death are Distinct Cellular Responses to Stress:Despendence on Heat Shock Protein. *FEBS Lett* (1999) 461:3–306. doi: 10.1016/S0014-5793(99)01486-6
27. Chan JYH, Cheng HL, Chou JLJ, Li FCH, Dai KY, Chan SHH, et al. Heat Shock Protein 60 or 70 Activates Nitric-Oxide Synthase (NOS) I- and Inhibits NOSII-Associated Signaling and Depresses the Mitochondrial Apoptotic Cascade During Brain Stem Death. *J Biol Chem* (2007) 282(7):4585–600. doi: 10.1074/jbc.M603394200
28. Zaghloul MS, Abdelrahman RS. Nilotinib Ameliorates Folic Acid-Induced Acute Kidney Injury Through Modulation of TWEAK and HSP-70 Pathways. *Toxicology* (2019) 427:8. doi: 10.1016/j.tox.2019.152303
29. Wachstein J, Tischer S, Figueiredo C, Limbourg A, Falk C, Immenschuh S, et al. HSP70 Enhances Immunosuppressive Function of $CD4^{(+)}CD25^{(+)}FoxP3^{(+)}$ T Regulatory Cells and Cytotoxicity in $CD4^{(+)}CD25(-)$ T Cell. *PLoS One* (2012) 7(12):e51747. doi: 10.1371/journal.pone.0051747
30. Gialeli C, Theocharis AD, Karamanos NK. Roles of Matrix Metalloproteinases in Cancer Progression and Their Pharmacological Targeting. *FEBS J* (2011) 278(1):16–27. doi: 10.1111/j.1742-4658.2010.07919.x
31. Mannino MH, Zhu ZW, Xiao HP, Bai Q, Wakefield MR, Fang YJ. The Paradoxical Role of IL-10 in Immunity and Cancer. *Cancer Lett* (2015) 367 (2):103–7. doi: 10.1016/j.canlet.2015.07.009
32. Hemmers S, Schizas M, Azizi E, Dikiy S, Zhong Y, Feng YQ, et al. IL-2 Production by Self-Reactive CD4 Thymocytes Scales Regulatory T Cell Generation in the Thymus. *J Exp Med* (2019) 216(11):2466–78. doi: 10.1084/jem.20190993
33. Vujanovic NL. Role of TNF Family Ligands in Antitumor Activity of Natural Killer Cells. *Int Rev Immunol* (2001) 20(3–4):415–37. doi: 10.3109/08830180109054415
34. Mocellin S, Rossi CR, Pilati P, Nitti D. Tumor Necrosis Factor, Cancer and Anticancer Therapy. *Cytokine Growth Factor Rev* (2005) 16(1):35–53. doi: 10.1016/j.cytogfr.2004.11.001
35. Schiffer L, Worthmann K, Haller H. CXCL13 as a New Biomarker of Systemic Lupus Erythematosus and Lupus Nephritis - From Bench to Bedside? *Clin Exp Immunol* (2015) 179:1–89. doi: 10.1111/cei.12439
36. Ferretti E, Corcione A, Pistoia V. The IL-31/IL-31 Receptor Axis: General Features and Role in Tumor Microenvironment. *J Leukocyte Biol* (2017) 102 (3):711–7. doi: 10.1189/jlb.3MR0117-033R
37. Li Q, Tang T, Zhang P, Liu C, Pu Y, Zhang Y, et al. Correlation of IL-31 Gene Polymorphisms With Susceptibility and Clinical Recurrence of Bladder Cancer. *Familial Cancer* (2018) 17(4):577–85. doi: 10.1007/s10689-017-0060-4
38. Li H, Wang X, Chen J, Zhou X, Xu C, Huang J, et al. Expression and Significance of Nrf2 and Caspase-3 in non-Small Cell Lung Cancer. *J Chin Physician* (2019) 21(5):688–91.
39. Fu L, ZHAO Y, CHEN M, Xu F, ZHU J, AN Y. Dual Roles of Nrf2 in Tumorigenesis. *Chin J Endemiol* (2016) 35:1–75.
40. Feng J, Kong R, Xie L, Lu W, Zhang Y, Dong H, et al. Clematichinenoside Protects Renal Tubular Epithelial Cells From Hypoxia/Reoxygenation Injury *In Vitro* Through Activating the Nrf2/HO-1 Signaling Pathway. *Clin Exp Pharmacol Physiol* (2019) 47(3):495–502. doi: 10.1111/1440-1681.13219
41. Chen Z, Xiao J, Liu H, Yao K, Hou X, Cao Y, et al. Astaxanthin Attenuates Oxidative Stress and Immune Impairment Ind-Galactose-Induced Aging in Rats by Activating the Nrf2/Keap1 Pathway and Suppressing the NF-Kappa B Pathway. *Food Funct* (2020) 11(9):8099–111. doi: 10.1039/d0fo01663b
42. Xiang W, Jia-jia M, Peng Z, Hui S, Jinling H. Effect of Traditional Chinese Medicine and Its Active Ingredients on Cardiovascular Disease Based on Nrf2/HO-1 Signaling Pathway. *Chin J Exp Tradit Med Formulae* (2020) 26 (10):227–34. doi: 10.13422/j.cnki.syfjx.20200405
43. Liu YG, Yang AH, Qu YD, Wang ZQ, Zhang YQ, Liu Y, et al. Ameliorative Effects of Antrodia Cinnamomea Polysaccharides Against Cyclophosphamide-Induced Immunosuppression Related to Nrf2/HO-1 Signaling in BALB/c Mice. *Int J Biol Macromol* (2018) 116:8–15. doi: 10.1016/j.ijbiomac.2018.04.178
44. Taguchi K, Yamamoto M. The KEAP1-NRF2 System in Cance. *Front Oncol* (2017) 7:85. doi: 10.3389/fonc.2017.00085
45. Furfaro AL, Piras S, Domenicotti C, Fenoglio D, De Luigi A, Salmona M, et al. Role of Nrf2, HO-1 and GSH in Neuroblastoma Cell Resistance to Bortezomi. *PloS One* (2016) 11(3):17. doi: 10.1371/journal.pone.0152465
46. Rojo de la Vega M, Chapman E, Zhang DD. NRF2 and the Hallmarks of Cance. *Cancer Cell* (2018) 34(1):21–43. doi: 10.1016/j.ccell.2018.03.022
47. Zhu J, Wang H, Chen F, Fu J, Xu Y, Hou Y, et al. An Overview of Chemical Inhibitors of the Nrf2-ARE Signaling Pathway and Their Potential Applications in Cancer Therapy. *Free Radical Biol Med* (2016) 99:544–56. doi: 10.1016/j.freeradbiomed.2016.09.010
48. Yu D, Liu Y, Zhou YQ, Ruiz-Rodado V, Larion M, Xu GW, et al. Triptolide Suppresses IDH1-Mutated Malignancy via Nrf2-Driven Glutathione Metabolism. *Proc Natl Acad Sci U S A* (2020) 117(18):9964–72. doi: 10.1073/pnas.1913633117
49. Cai SJ, Liu Y, Han S, Yang CZ. Brusatol, an NRF2 Inhibitor for Future Cancer Therapeutic. *Cell Biosci* (2019) 9:3. doi: 10.1186/s13578-019-0309-8
50. Tang XY, Fu X, Liu Y, Yu D, Cai SJ, Yang CZ. Blockade of Glutathione Metabolism in IDH1-Mutated Glioma. *Mol Cancer Ther* (2020) 19(1):221–30. doi: 10.1158/1535-7163.mct-19-0103
51. Liu Y, Lu Y, Celiku O, Li A, Wu Q, Zhou Y, et al. Targeting IDH1-Mutated Malignancies With NRF2 Blockade. *Jnci-J Natl Cancer Inst* (2019) 111 (10):1033–41. doi: 10.1093/jnci/djy230

Conflict of Interest: Author ZT was employed by Jilin Tianlitai Pharmaceutical Co. Ltd.

The remaining authors declare that the research was conducted in the absence of any commercial or financial relationships that could be construed as a potential conflict of interest.

Advantages of publishing in Frontiers

OPEN ACCESS
Articles are free to read for greatest visibility and readership

FAST PUBLICATION
Around 90 days from submission to decision

HIGH QUALITY PEER-REVIEW
Rigorous, collaborative, and constructive peer-review

TRANSPARENT PEER-REVIEW
Editors and reviewers acknowledged by name on published articles

Frontiers
Avenue du Tribunal-Fédéral 34
1005 Lausanne | Switzerland

Visit us: www.frontiersin.org
Contact us: frontiersin.org/about/contact

REPRODUCIBILITY OF RESEARCH
Support open data and methods to enhance research reproducibility

DIGITAL PUBLISHING
Articles designed for optimal readership across devices

FOLLOW US
@frontiersin

IMPACT METRICS
Advanced article metrics track visibility across digital media

EXTENSIVE PROMOTION
Marketing and promotion of impactful research

LOOP RESEARCH NETWORK
Our network increases your article's readership